Novel Porphyrin Amino Acids as Building Blocks for Artificial Photosynthetic Reaction Centers: Photoinduced Energy and Electron Transfer

Dissertation

zur Erlangung des Grades
“Doktor der Naturwissenschaften“
im Promotionsfach Chemie

am Fachbereich Chemie, Pharmazie und Geowissenschaften
der Johannes Gutenberg-Universitat Mainz

Jascha Melomedov
geboren in Kiew

Mainz, 2014

Die vorliegende Arbeit wurde unter der Betreuung von [redacted] in der Zeit vom Januar 2009 bis Juni 2014 am Institut für Anorganische Chemie und Analytische Chemie der Johannes Gutenberg-Universität Mainz angefertigt.

Mainz, 13.06.2014

Dekan: [redacted]
Erster Berichterstatter: [redacted]
Zweiter Berichterstatter: [redacted]

Tag der mündlichen Prüfung: 13.06.2014

Abstract

Dioxygen we breathe, food we eat and oil derivatives we use to fuel our cars, heat our houses and to manufacture manifold day-to-day goods, are products of photosynthesis. Photosynthesis is hence the guarantor of existence of human civilisation. To get insight into essential processes like conversion of solar energy into chemical energy in the photosynthetic reaction centers (RC = reaction centers) is one important task of modern photosynthesis research. The complexity of energy transfer (EnT) in the light-harvesting antenna complexes (LHC = light-harvesting antenna complex) with the following charge separation (CS, PET = photoinduced electron transfer) and electron transfer (ET) within the RC caused the need to design and prepare donor-acceptor model compounds to mimic the mentioned processes.

This thesis reports on the synthesis and characterisation of *trans*-AB_2C *meso*-substituted porphyrin amino acid esters with tunable electron donating and electron withdrawing Ar substituents at B positions (Ar = 4-$C_6H_4O^nBu$, 4-C_6H_4OMe, 2,4,6-$C_6H_2Me_3$, 4-C_6H_4Me, C_6H_5, 4-C_6H_4F, 4-$C_6H_4CF_3$, C_6F_5). These porphyrin amino acids were used as key building blocks for photosynthetic LHC and RC model compounds. Their *N*-acetylated free-base derivatives and zinc(II) complexes were used as reference compounds for electrochemical, optical and EPR investigations. The porphyrin amino acid esters with unsubstituted and *para* substituted phenyl rings were synthesized according to the Lindsey type 2 + 2 condensation approach using nitro and ester substituted phenyl dipyrromethanes and corresponding substituted carbonyl compounds. Reduction of the nitro functional group was carried out in hydrochloric acid using tin(II) chloride dihydrate as reducing agent. Porphyrin amino acid esters with Ar = 2,4,6-$C_6H_2Me_3$ or C_6F_5 were prepared by condensation of corresponding aryl dipyrromethanes with methyl 4-formylbenzoate to *trans*-A_2B_2 diester porphyrins followed by hydrolysis of one ester group under acidic reaction conditions. The acid functionality was transformed to the Boc protected amine (Boc = *tert*-butoxy carbonyl) by a Curtius reaction using diphenylphosphoryl azide (DPPA) and *tert*-butanol. Cleavage of the protecting Boc group gives the porphyrin amino acid ester. Zinc(II) porphyrins were obtained from the corresponding free-base compounds by metalation with zinc(II) acetate dihydrate. Absorption and emission spectra of porphyrin amino acid esters and their derivatives show a slight hypsochromic shift of Soret and Q bands and anodic shift of redox potentials with increasing of electron withdrawing power of the Ar substituents at B position.

Based on free-base or zinc(II) porphyrin amino acid esters and porphyrin acids several amide linked free-base bis(porphyrins) P^{Ar1}-P^{Ar2} (Ar^1 = 2,4,6-$C_6H_2Me_3$, C_6F_5 and Ar^2 = 2,4,6-$C_6H_2Me_3$, 4-C_6H_4F, 4-$C_6H_4CF_3$, C_6F_5) and mono metallated bis(porphyrin) P^{Ar1}-(Zn)P^{Ar2} (Ar^1 = 2,4,6-$C_6H_2Me_3$ and

Ar^2 = 4-C_6H_4F) with adjustable electron withdrawing power at each porphyrin site were prepared. Doubly zincated complexes ((Zn)P^{Ar1}-(Zn)P^{Ar2}) were obtained by subsequent reaction of mono-metallated bis(porphyrin) with zinc(II) acetate dihydrate. The absorption spectra and redox potentials of bis(porphyrins) are not significantly altered by linking the two porphyrins compared to reference compounds indicating only weak interactions between chromophores in the ground state. In the fluorescence spectra of free-base bis(porphyrins) the porphyrin with the strongest electron donating power of Ar substituents at B positions is the light emitting unity. The emission of mono metallated bis(porphyrin) occurs only from the free-base porphyrin building block. This phenomenon is caused by an efficient energy transfer likely via the Dexter through-bond mechanism. The EPR spectra of chemicaly oxidized and reduced bis(porphyrins) exhibited a charge localization corresponding to the redox potentials of individual porphyrin building blocks. These results were also confirmed by DFT/PCM calculations (DFT = density functional theory, PCM = polarizable continuum model).

Linking of anthraquinone (Q) as electron acceptor (A) to the *N*-terminus of porphyrin amino acid esters (P^{Ar}) via an amide bond gave Q-P^{Ar} dyads (Ar = 4-$C_6H_4O^nBu$, 4-C_6H_4OMe, 2,4,6-$C_6H_2Me_3$, 4-C_6H_4Me, C_6H_5, 4-C_6H_4F, 4-$C_6H_4CF_3$, C_6F_5). After ester hydrolysis under basic conditions aminoferrocene (Fc) as an electron donor (D) was attached via amid linkage to the *C*-terminus of the porphyrin resulting in Q-P^{Ar}-Fc triads with tunable electron density at the porphyrin chromophore. Further modification of the porphyrins’ first excited singlet state energy (S_1) and energies of CS states was achieved by metalation of triads with zinc(II) acetate dihydrate to Q-(Zn)P^{Ar}-Fc triads. Using the same synthetic route used for triad synthesis, a tetrad Q-P^{Ar1}-P^{Ar2}-Fc with Ar^1 = C_6H_5 and Ar^2 = 4-C_6H_4Me was prepared. In the ground state of the arrays only weak interactions between chromophors Q, P^{Ar} and Fc were observed. However, the emission of Q-P^{Ar} dyads is quenched by oxidative PET. In the Q-(M)P^{Ar}-Fc triads with M = 2H or Zn and the Q-P^{Ar1}-P^{Ar2}-Fc tetrad a reductive PET pathway additionally contributes to the emission quenching. The efficiency of the PET pathways is controlled by the specific porphyrin electron density. Whilst in model compounds with electron donating Ar substituents at B positions the oxidative pathway contributes most to the PET, in conjugates with strong withdrawing Ar substituents at B positions the reductive PET pathway is favoured. In the Q-(Zn)P^{Ar} triads with electron rich substituents both pathways have very similar driving force ($-\Delta G_{ET}$). All metallated conjugates are almost non-fluorescent suggesting an efficient PET.

Amide-linked conjugates P^{Ar}-Fc (Ar = 2,4,6-$C_6H_2Me_3$, C_6F_5) and Fmoc-Fc-P^{Ar1} (Ar^1 = C_6H_5, 4-C_6H_4F, 4-$C_6H_4CF_3$, C_6F_5) as well as hinges P^{Ar2}-Fc-P^{Ar1} (Ar^1 = C_6H_5, 4-C_6H_4F and Ar^2 = 2,4,6-

$C_6H_2Me_3$) were studied with respect to the reductive PET. The dyads were synthesized by coupling of porphyrin acids (P^{Ar}) with aminoferrocene (Fc) and by linking of porphyrin amino acid esters (P^{Ar1}) with *N*-Fmoc protected 1,1'-ferrocene amino acid (Fmoc-Fc, Fmoc= 9-Fluorenylmethoxycarbonyl). After cleavage of the Fmoc protecting group a further porphyrin was attached by an amide bond giving hinges P^{Ar2}-Fc-P^{Ar1}. The corresponding zinc(II) complexes were obtained by metalation with zinc(II) acetate dihydrate. The PET driving force ($-\Delta G_{ET}$) in dyads increases with the increasing electron withdrawing character of Ar substituents. Additionally, intramolecular energy transfer between porphyrins P^{Ar1} and P^{Ar2} is feasible in the hinges via the Förster mechanism.

Kurzzusammenfassung

Sauerstoff, den wir atmen, Nahrungsmittel, die wir zu uns nehmen und Erdölprodukte, die wir zum Tanken unserer Autos und zur Herstellung von Kunststofferzeugnissen nutzen, die unerläßlich für unser Alltagsleben sind, sind Produkte der Photosynthese. Photosynthese ist deshalb der Garant der Existenz der menschlichen Zivilisation. Einen tiefen Einblick in die grundlegenden Prozesse wie die Umwandlung der Sonnenenergie in chemische Energie in den photosynthetischen Reaktionszentren (RC = reaction center) zu erhalten, ist eine wichtige Aufgabe der modernen Photosyntheseforschung. Die Komplexität des Energietransfers (EnT) in den Lichtsammelkomplexen (LHC = light-harvesting antenna complex) mit der darauf folgenden Ladungstrennung CS (CS = charge separation, PET = photoinduced electron transfer) und dem Elektronentransfer (ET) im RC erfordert das Design und die Herstellung von Donor-Akzeptor-Modellverbindungen, mit deren Hilfe die o.g. Prozesse nachgeahmt werden können.

In dieser Arbeit wird vom Aufbau eines Pools aus *trans*-AB_2C *meso*-Ar-substituierten Porphyrin-Aminosäure-Estern mit einstellbaren elektronenschiebenden und elektronen-ziehenden Ar-Substituenten an den B-Positionen (Ar = 4-$C_6H_4O^nBu$, 4-C_6H_4OMe, 2,4,6-$C_6H_2Me_3$, 4-C_6H_4Me, C_6H_5, 4-C_6H_4F, 4-$C_6H_4CF_3$, C_6F_5) berichtet. Die Porphyrin-Aminosäuren wurden als Schlüsselbausteine für photosynthetische LHC- und RC- Modelverbindungen eingesetzt. Ihre *N*-acetylierten „free-base“-Derivate und Zink(II)-Komplexe wurden als Referenzverbindungen in elektrochemischen, optischen und EPR-Untersuchungen verwendet. Porphyrin-Aminosäure-Ester mit unsubstituierten und nur in *para*-Stellung substituierten Aryl-Resten an den B-Positionen wurden durch eine 2 + 2 Kondensation nach Lindsey von Nitro- und Ester-substituierten Aryldipyromethanen mit entsprechend substituierten aktivierten Carbonylverbindungen hergestellt. Die Reduktion der Nitrogruppe zur Aminofunktion wurde in Salzsäure mit Zinn(II)-chlorid-Dihydrat als Reduktionsmittel durchgeführt. Porphyrin-Aminosäure-Ester mit Ar = 2,4,6-$C_6H_2Me_3$ und C_6F_5 lassen sich durch die Kondensation des entsprechenden Aryldiphyrromethanes mit 4-Formylbenzoesäuremethylester zu A_2B_2 Porphyrin-Diestern, anschließender Hydrolyse einer der Estergruppen unter sauren Bedingungen, gefolgt von einer Curtius-Umlagerung der Säure-Funktionalität mit Phosphorsäurediphenylesterazid (DPPA) und *tert*-Butanol zum Boc geschützten Amin herstellen (Boc = *tert*-Butoxycarbonyl). Die Abspaltung der Boc-Schutzgruppe liefert den Porphyrin-Aminosäure-Ester. Die Zink(II)-Porphyrin-Komplexe wurden durch Metallierung der entsprechenden freien Porphyrinbasen mit Zink(II)-Acetat-Dihydrat erhalten. Die Absorptions- und Emissionsspektren der Porphyrin-Aminosäuren-Ester und ihrer Derivate zeigten eine leichte hypsochrome Verschiebung der Soret- und Q-Banden und eine anodische Verschiebung der

Redoxpoteniale mit zunehmender elektronenziehender Kraft der Ar-Substituenten an den B-Positionen.

Basierend auf den „free-base“ oder Zink(II)-Porphyrin-Aminosäure-Estern und Porphyrin-Monoestern wurden mehrere amidverknüpfte „free-base“ Bisporphyrine P^{Ar1}-P^{Ar2} (Ar^1 = 2,4,6-$C_6H_2Me_3$, C_6F_5 und Ar^2 = 2,4,6-$C_6H_2Me_3$, 4-C_6H_4F, 4-$C_6H_4CF_3$, C_6F_5) oder monometalliertes Bisporphyrin P^{Ar1}-(Zn)P^{Ar2} (Ar^1 = 2,4,6-$C_6H_2Me_3$ und Ar^2 = 4-C_6H_4F) mit einstellbaren elektronischen Eigenschaften an jedem Porphyrin-Baustein hergestellt. Der doppelt metallierte Komplex ((Zn)P^{Ar1}-(Zn)P^{Ar2}) wurde durch anschließende Reaktion des monometallierten Bisporphyrins mit Zink(II)-Acetat-Dihydrat erhalten. Die Absorptionsspektren und Redoxpotentiale der Porphyrin-Bausteine ändern sich nicht wesentlich durch die Verknüpfung der Porphyrine zum Bisporphyrin verglichen mit Referenzverbindungen. Dies deutet auf nur schwache Wechselwirkungen der Chromophore im Grundzustand hin. In den Fluoreszenzspektren der „free-base“ Bisporphyrine ist der Porphyrinbaustein mit den elektronenreichsten Ar-Substituenten an den B-Positionen die Licht-emittierende Einheit. In dem monometallierten Bisporphyrin findet die Emission nur aus dem „free-base“ Porphyrinbaustein statt. Dieses Phänomen ist auf einen effizienten Energietransfer „durch die Brücke“ wahrscheinlich nach dem Dexter-Mechanismus zurückzuführen. Die EPR-Spektren der chemisch oxidierten und reduzierten Bisporphyrine zeigten eine Ladungslokalisierung entsprechend den Redoxpotentialen der einzelnen Porphyrin-Bausteine. Diese Ergebnisse wurden auch durch DFT/PCM-Berechnungen bestätigt (DFT = density functional theory, PCM = polarizable continuum model).

Anbindung von Anthrachinon (Q) als Elektronenakzeptor (A) an den *N*-Terminus des Porphyrin-Aminosäure-Esters (P^{Ar}) über eine Amidbindung lieferte Q-P^{Ar}-Dyaden (Ar = 4-$C_6H_4O^nBu$, 4-C_6H_4OMe, 2,4,6-$C_6H_2Me_3$, 4-C_6H_4Me, C_6H_5, 4-C_6H_4F, 4-$C_6H_4CF_3$, C_6F_5). Die Esterhydrolyse unter basischen Bedingungen und Anbindung von Aminoferrocen (Fc) als Elektronendonor (D) über eine Amidbindung an den *C*-Terminus ergab Q-P^{Ar}-Fc-Triaden mit einer einstellbaren Elektronendichte an den Porphyrinen. Eine weitere Modifikation der Energie des ersten angeregten Porphyrin-Singulettzustandes (S_1) und der Energien der CS-Zustände wurde durch Metallierung der Triaden mit Zink(II)-Acetat-Dihydrat erreicht. Diese ergab Q-(Zn)P^{Ar}-Fc-Triaden. Die Tetrade Q-P^{Ar1}-P^{Ar2}-Fc mit Ar^1 = C_6H_5 und Ar^2 = 4-C_6H_4Me wurde nach der gleichen Kopplungsmethode wie die Triaden Q-P^{Ar}-Fc hergestellt. Im Grundzustand der Arrays wurden nur schwache Wechselwirkungen zwischen den Chromophoren Q, P^{Ar} und Fc beobachtet. Die Emission der Q-P^{Ar}-Dyaden ist jedoch durch oxidativen PET gelöscht. In den Q-P^{Ar}-Fc- / Q-(Zn)P^{Ar}-Fc-Triaden und der Q-P^{Ar1}-P^{Ar2}-Fc-Tetrade trägt zusätzlich der reduktive PET zur Löschung der Emission bei. Die Effizienz der PET-Kanäle wird dabei durch die Elektronendichte am Porphyrin bestimmt. Während in den Modelverbindungen mit elektronenschiebenden Substituenten der oxidative Kanal einen großen Anteil hat, ist in den Konjugaten mit stark elektronenziehenden Substituenten der reduktive PET-Kanal sehr stark favorisiert. In den Q-(Zn)P^{Ar}-Triaden mit elektronenschiebenden Substituenten haben beide PET-Kanäle sehr ähnliche Triebkraft ($-\Delta G_{ET}$). Alle metallierten Konjugate sind aufgrund des effizienten PET nicht fluoreszent.

Die Untersuchung des reduktiven PET erfolgte an amidverknüpften P^{Ar}-Fc- (Ar = 2,4,6-$C_6H_2Me_3$, C_6F_5) und Fmoc-Fc-P^{Ar1}-Konjugaten (Ar^1 = C_6H_5, 4-C_6H_4F, 4-$C_6H_4CF_3$, C_6F_5) sowie P^{Ar2}-Fc-P^{Ar1}-Scharnieren (Ar^1 = C_6H_5, 4-C_6H_4F und Ar^2 = 2,4,6-$C_6H_2Me_3$). Die Dyaden wurden durch Kupplung von Porphyrin-Monosäuren (P^{Ar}) mit Aminoferrocen (Fc) und durch Anbringen der Porphyrin-Aminosäureester (P^{Ar1}) an *N*-Fmoc geschützte Ferrocen-Aminosäure synthetisiert (Fmoc-Fc, Fmoc = 9-Fluorenylmethoxycarbonyl). Die Abspaltung der Fmoc-Schutzgruppe und die Anknüpfung eines weiteren Porphyrins über eine Amidbindung ergab Scharniere P^{Ar2}-Fc-P^{Ar1}. Die entsprechenden Zink(II)-Komplexe wurden durch Metallierung mit Zink(II)-Acetat-Dihydrat erhalten. Die Triebkraft ($-\Delta G_{ET}$) des PET in Dyaden steigt mit der Zunahme des elektronenziehenden Charakters der Ar-Substituenten an den B-Positionen an. In den Scharnieren ist zusätzlich ein intramolekularer Energietransfer zwischen P^{Ar1} und P^{Ar2} nach dem Förster-Mechanismus möglich.

Contents

Abbreviations

°C	degree Celsius
$\Delta G^{\ddagger}$	activation energy
ΔG^{o}	Gibbs free energy
δ	chemical shift (NMR) [ppm]
ε	molar extinction coefficient [M^{-1} cm^{-1}]
λ	wavelength or reorganization energy depending on the context
$\tilde{\nu}$	wavenumber
Φ	quantum yield
τ	fluorescence lifetime
A	acceptor or relative amplitude depending on the context
Ac	acetyl
Ar	aryl substituent
ATP	adenosine triphosphate
a.u.	arbitrary units
B	bridge
Boc	*tert*-butyloxycarbonyl
Bu	butyl
cal.	calculated
$CDCl_3$	deuterated chloroform
Cc	cobaltocenium carboxylic acid
COSY	correlated spectroscopy
CR	charge recombination
CS	charge separation
CV	cyclic voltammetry
Cp	cyclopentadienyl
D	donor
DDQ	2,3-dichloro-5,6-dicyano-1,4-benzoquinone
d_8-THF	deuterated tetrahydrofuran
DFT	density functional theory
DPPA	diphenoxyphosphoryl azide
$E_{\frac{1}{2}}$	halfwave potential
e.g.	*exempli gratia* (for example)

EnT	energy transfer
eq.	equivalent
EPR	electron paramagnetic resonance
ESI	electrospray ionization (mass spectrometry)
ET	electron transfer
eV	electron volt
Fc	ferrocene, 1-ferrocenyl, 1,1’-ferrocene amino acid or 1,1’-ferrocenyl
$(Fc)_2$	1,1’-biferrocene or 1,1’-biferrocenyl
FD	field desorption (mass spectrometry)
Fmoc	9-Fluorenylmethyloxycarbonyl
g	gram
G	Gauss
g	g-value (EPR)
h	hour
HATU	2-(7-aza-1H-benzotriazole-1-yl)-1,1,3,3-tetramethyluronium hexafluorophosphate
HOMO	highest occupied molecular orbital
HMBC	heteronuclear multiple bond correlation (NMR)
HSQC	heteronuclear single quantum coherence (NMR)
HR	high resolution (mass spectrometry)
IC	internal conversion
IHB	intramolecular hydrogen bond
IR	infrared spectroscopy
ISC	intersystem crossing
^{n}J	coupling constant (NMR)
k	rate constant
K	Kelvin
k_B	Boltzmann constant = 1.381×10^{-23} [J/K]
L	liter
LHC	light-harvesting antenna complex
LUMO	lowest unoccupied molecular orbital
m	milli
M	molarity or metal depending on the context
M^{x+}	metal cation or base peak depending on the context

Me	methyl
Mes	mesityl
MS	mass spectrometry
m/z	mass-to-charge ratio
$NADP^+$	nicotinamide adenine dinucleotide phosphate
NADPH	reduced form of $NADP^+$
NIR	near infrared
NMR	nuclear magnetic resonance spectroscopy
ns	nanosecond
P	porphyrin or product depending on the context
P_1-^{t}Bu	*tert*-butylimino-tris(dimethylamino)phosphorane
P_2-^{t}Bu	1-*tert*-butyl-2,2,4,4,4-pentakis (dimethyl-amino)-2λ^5,4λ^5-catenadi(phosphazene)
PCM	polarizable continuum model
PET	photoinduced electron transfer
Ph	phenyl
ppm	parts per million
q	reaction coordinate
Q	quinone
R	reactant
RC	reaction center
S	singlet state
SP	“special pair”
SWV	squarewave voltammetry
t	triplet
T	triplet state
T	temperature
TCNQ	7,7,8,8-tetracyano-quinodimethane
TEA	triethylamine
TFA	trifluoroacetic acid
THF	tetrahydrofuran
UV	ultra-violet (light)
V	electronic coupling matrix element
Vis	visible (light)

1 Introduction

Many essential processes in nature covering living organisms and plants are based on porphyrins, metalloporphyrins or their derivatives. In photosynthesis porphyrins as building blocks of chlorophylls and bacteriochlorophylls are not only responsible for light-harvesting but are also involved in charge separation und transport.[1-18] In hemoglobin and myoglobin an iron porphyrin plays a key role in oxygen binding, its transport and storage.[19,21] Corrin, a porphyrin derivative with only three *meso*-carbons between the four pyrrole rings, was found in vitamin B12.[20,21] So it is not surprising that porphyrins are called “pigments of life”[22] since the green color of leaves and the red color of blood are caused by porphyrins and their complexes. Thus porphyrin studies embrace a variety of major disciplines including preparative organic and inorganic chemistry, biochemistry, physical chemistry, chemical engineering and medicine.

Designing porphyrin-based compounds for a particular purpose requires a targeted modification of structural and electronic parameters. To tune these parameters, it is indispensable to understand the structural and photophysical characteristics of the porphyrin macrocycle.

1.1 Structure and Properties of Porphyrins

The porphyrin skeleton can be described as a macrocycle consisting of four pyrrolic rings linked by methine bridges (Figure 1a).[23] It has a planar structure (Figure 1b). The free-base porphyrin, porphyrin without a metal ion in the cavity, exhibits D_{2h} symmetry and the metalloporphyrins are of higher symmetry (D_{4h}). Substitution of porphyrins on the periphery can be performed at four *meso* and eight β positions. The four α positions are accessible only after reduction of the porphyrin skeleton. The size of the internal N4-cavity in porphyrins is remarkably invariant upon four fold symmetrical substitutions at the *meso* position.[23]

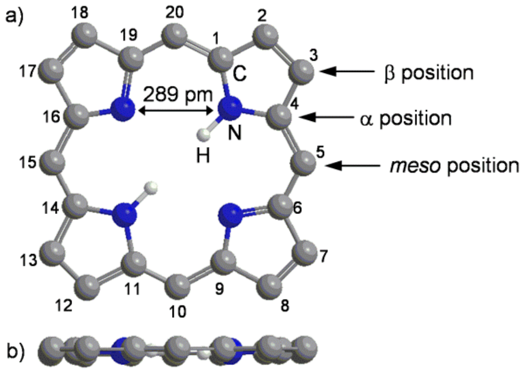

Figure 1. a) Porphyrin skeleton structure with possible substitution positions; b) Side view of the porphyrin molecule.

Porphyrins’ aromaticity is covered by the (4n+2)-Hückel rule. The porphyrin macrocycle has 22 π electrons but only 18 of them are delocalized. Thus porphyrins satisfy the [18]annulene model proposed by E. Vogel and are diaza[18]annulenes.[24]

1.2 *Cis-Trans* Tautomerism

Porphyrins H_2P are amphotheric compounds. Free-base porphyrins, as the name suggests, are bases and can be doubly protonated to $[H_4P]^{2+}$. The acidic character of the porphyrins is given by losing of the inner NH pyrrole protons $[P]^{2-}$and subsequent metalation.

The distribution of the two inner pyrrole NH protons in H_2P between the four nitrogen atoms can occur in different ways. In the *trans* structure the protons are positioned at the opposite pyrrole rings, while in the *cis* form the protons are located at adjacent pyrroles’ nitrogen atoms (Figure 2). The *trans* tautomers are 32.7 kJ mol^{-1} thermodynamically more stable than their *cis* isomers.[23] For the porphyrin two chemically equivalent *trans* isomers (**Ia'** and **Ia''**) and four equivalent *cis* tautomers (**Ib' - Ib''''**) are predicted.

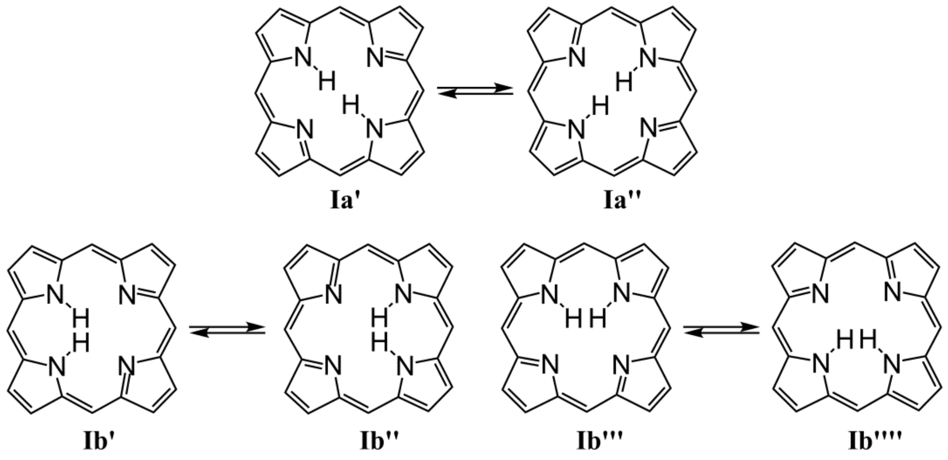

Figure 2. *Trans* (bottom) and *cis* (top) tautomers of porphyrin.[23]

For the transformation **Ib'** to **Ib''** and **Ib'''** to **Ib''''** the same energy barrier is assumed. However, for the transformation from **Ib'** to **Ib'''** this not the case if the former processes are concerted. The conversion **Ib'** to **Ib'''** requires a stepwise mechanism involving one of the *trans* forms **Ia** as an intermediate.[23]

The rapid tautomerisation of the inner NH protons at room temperature causes only one characteristic resonance for the NH groups. But at lower temperatures, it is possible to "freeze out" the individual tautomers on the NMR time scale.[25-27] The presence of the extended delocalised π-electron system of the porphyrin macrocycle causes a strong ring current in the molecules placed in the magnetic field. The protons of NH groups are exocyclic regarding to the local ring current which leads to a strong shielding of these protons. They are observed at a very high field $\delta = -1.4$ - – 4.4 ppm.[26]

1.3 Optical Features of Porphyrins

Free-base porphyrins, *e.g.* *meso*-tetraphenylporphyrin (H_2TPP), show a characteristic UV/Vis absorption pattern in solution: a very intense B or so-called Soret band ($\varepsilon \approx 46.9 \times 10^4$ M^{-1} cm^{-1}) and four weaker Q bands (($\varepsilon \approx 0.18 \times 10^4 - 1.87 \times 10^4$ M^{-1} cm^{-1}) (Figure 3b).[27-29] The absorption spectra of metalloporphyrins *e.g.* *meso*-tetraphenylporphyrinato zinc(II) ((Zn)TPP) exhibit a reduced number of Q bands (Figure 3a).[27-29] Both, Soret and Q bands, have their origin in π-π* electronic transitions. The general absorption features were described by Gouterman in his four-orbital model.[28,29] In this model the Soret and Q bands are described considering the transition between the ground state S_0 and the two lowest excited singlet states S_1 and S_2 in metalloporphyrins with D_{4h} symmetry. The orbitals a_{2u}, a_{1u} and 2 × e_g are the porphyrin frontier orbitals HOMO−1, HOMO, LUMO and LUMO+1. The electronic transitions are interpreted as a linear combination of the $^1(a_{2u}e_g)$ and $^1(a_{1u}e_g)$ configurations. The e_g orbitals in metalloporphyrins with D_{4h} symmetry are degenerate, while free-base porphyrins with D_{2h} symmetry feature two non-degenerate LUMOs. In both cases, the one-electron excited states with the same or nearly the same symmetry interact with each other resulting in the aforementioned Soret and Q bands. The transition moments of both pairs $^1(a_{2u}e_g)$ and $^1(a_{1u}e_g)$ are orthogonal and lie in the porphyrin plane. This was accounted for abbreviations Q_x and Q_y implying the polarisation along the NH-NH direction (Q_x) and the one orthogonal to that (Q_y). The Q_x transitions of most porphyrins are of lower energy than the Q_y one. In all porphyrin absorption spectra a strong vibronic component located between the Q_x and Q_y bands is observed. The notation Q(0,0) and Q(1,0) differ between the vibronic transitions. To sum up, metalloporphyrins with D_{4h} symmetry show one Soret and two Q bands (Q(0,0) and Q(1,0)) (Figure 3a), whereas one Soret and four Q bands (Q_x(0,0), Q_x(1,0), Q_y(0,0), Q_y(1,0)) are observed for free-base porphyrins with D_{2h} symmetry (Figure 3b).

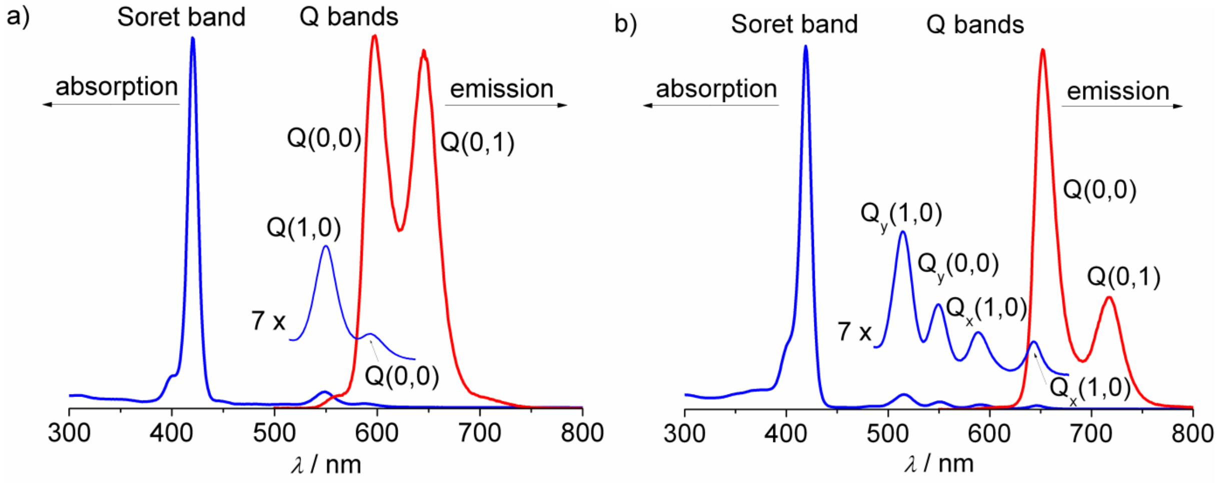

Figure 3. a) Absorption and normalized emission spectra of (Zn)TPP. b) Absorption and normalized emission spectra of H_2TPP. All spectra were measured in CH_2Cl_2 at room temperature.

The main channels of the porphyrins S_1 decay is intersystem crossing (ISC) to the triplet state T_1, internal conversion to S_0 (IC) and fluorescence to S_0.[23,30] The emission spectra of free-base and metalloporphyrins feature two intense bands resulting from the transitions from the first excited state S_1 to the vibronic ground state Q(0,0) and to the first vibronic excited state Q(0,1) of S_0 (Figure 3).The fluorescence quantum yields amount to $\Phi = 10 – 15\%$ and the decays are about 10 ns for free-base porphyrins.[30] The complexation with heavy atoms like zinc(II) leads to an increase in the triplet formation which resulsts in lower quantum yields $\Phi = 2 - 11\%$ and a fluorescence decay is about 2 ns.[30-32] Gold(III) porphyrins are even non-fluorescent but phosphorescent.[33-35] Absorption and emission properties of porphyrins render them suitable for photochemical studies.

1.4 The Marcus Theory of Electron Transfer

Published by Rudolph A. Marcus in 1957, the theory of electron transfer (ET) is the basis of a rational design of photosynthetic reaction models (Chapter 2.2.2).[36-38] In 1992, he was awarded with the Nobel Prize in chemistry for his outstanding scientific work in the field of ET reactions.[38] Marcus explored the ET between two solvated species. No chemical bonds are broken during an ET reaction and thus the reactants and products retain their respective chemical composition. However the bond lengths and angles differ from the initial state due to the generation of the CS state. Intersection of the potential energy profiles of reactants and products is the prerequisite for the ET reaction. (Figure 4). At the intersection of the profiles the reaction coordinates and the energy of product and reactants before and after an ET are identical. The Frank-Condon principle is also taken in into account in this process.

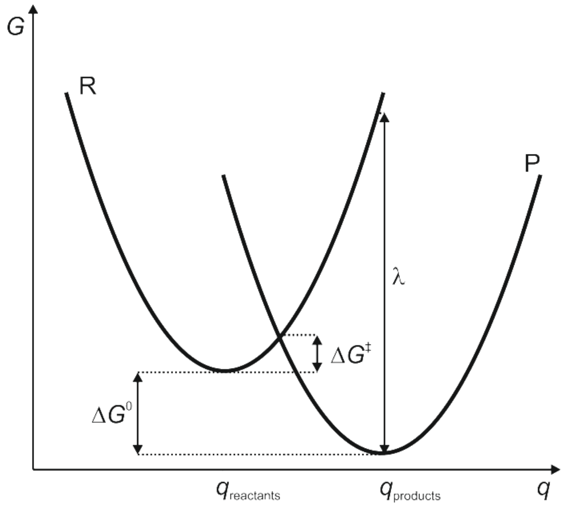

Figure 4. Plot of the Gibbs free energy G of reactants (R) and products (P) *vs.* reactions coordinate q.[38]

Marcus distinguishes between adiabatic reactions, where the ET occurs with every passage of crossing point and nonadiabatic ET reactions, where the system passes the parabola intersection with high velocity so the ET cannot occur with every passage. The rate constant of the ET k_{ET} is expressed as given in Equation 1, where A is specific for the kind of reaction (*e.g.* inter- or intramolecular), $\Delta G^{\ddagger}$ is the activation energy or the free energy barrier for ET, k_B is the Boltzmann constant and T is the temperature.[36-38]

$$k_{ET} = A\exp(-\frac{\Delta G^{\ddagger}}{k_B T}) \qquad (1)$$

The activation energy $\Delta G^{\ddagger}$ is depending on the standard Gibbs free energy ΔG^0, the driving force of the ET reaction, and λ, the reorganization energy, the energy required for the transformation of the reactants' nuclear coordinates in those of the products (Equation 2).

$$\Delta G^{\ddagger} = \frac{\lambda}{4}(1+\frac{\Delta G^0}{\lambda})^2 \qquad (2)$$

The reorganization energy λ is composed of solvational (λ_o) and vibrational (λ_i) terms. It considers the reorganization of the solvent molecules outside the reactants as well as the inner changes with respect to molecule geometry modification from the initial to the ET state (Equation 3).

$$\lambda = \lambda_o + \lambda_i \qquad (3)$$

With

$$A = \left(\frac{4\pi^3}{h^2 \lambda k_B T}\right)^{\frac{1}{2}} V^2 \qquad (4)$$

as the rate constant for activation-free ET ($-\Delta G^0 = \lambda$) where V is the electronic coupling matrix element, the following expression for the rate constant k_{ET} can be formulated (Equation 5).

$$k_{ET} = \left(\frac{4\pi^3}{h^2 \lambda k_B}\right)^{\frac{1}{2}} V^2 \exp\left[\frac{(\lambda + \Delta G^0)^2}{4\lambda k_B T}\right] \qquad (5)$$

The quadratic dependence of k_{ET} on the sum (λ + ΔG^0) in Equation (5) results in the normal and inverted region of ET (Figure 5).

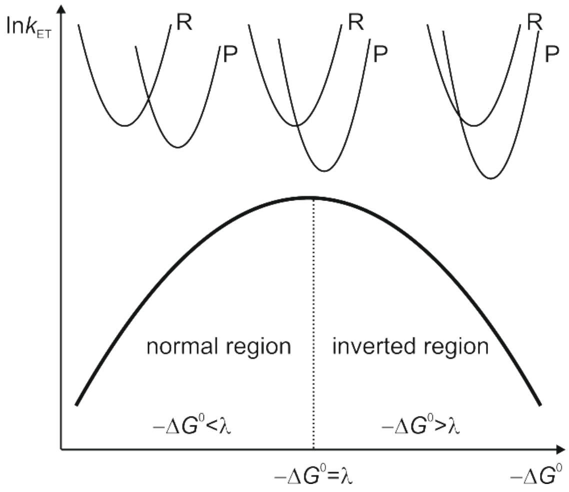

Figure 5. Plot of $\ln k_{ET}$ *vs.* $-\Delta G^0$.[35]

In the normal region ($-\Delta G^0 < \lambda$), the increase of $-\Delta G^0$ or decrease of λ leads to reduction of $\Delta G^\ddagger$ and consequently to an increase of k_{ET}. In case $-\Delta G^0 = \lambda$ the activation energy $\Delta G^\ddagger = 0$ and k_{ET} reaches the maximum value (*vide supra*). In the highly exothermic inverted region ($-\Delta G^0 > \lambda$) Marcus *et al*. predicted and determined that the rise of driving force $-\Delta G^0$ leads to an increase of $\Delta G^\ddagger$ and thus to a decrease of k_{ET}.[23, 36-38]

In summary: efficient artificial photosynthetic constructs should have small reorganization energies λ attained by use of building blocks with delocalized π electron systems, optimal electronic coupling V attained by *e.g.* small distances between components, which reduces λ as well. The life time of CS states can be extended also by lowering the temperature to reduce diffusion and collision with the solvent molecules.

1.5 Theory of Energy Transfer

The study of excitation energy transfer (EnT) between chromophores is a very interesting field as a basis for the development of molecular scale electronic devices[39-45] and the rational design of artificial photosynthesis systems.[46-62] Two terms describe the electronic coupling for EnT in good approximation: the Coulomb interaction and the electron exchange interaction. The electron exchange interaction explored by Dexter[63,64] requires an orbital overlap und occurs thus at distances less than 10 Å, whilst the Coulomb interaction is active at distances up to 100 Å and was investigated by Förster.[65,66] For thorough investigation of EnT a series of donor-bridge-acceptor systems (D-B-A) was proposed.[46-57,59-62] Free-base and metallated porphyrins with different substitution patterns often act as donors and acceptors.[46-62] The bridge is an inert spacer between them. For the electron transfer devised superexchange (through-bond) mechanism can be applied also for explanation of energy transfer.[67] The electronic coupling between donor and acceptor can be expressed as in Equation 6.[52]

$$V_{\mathrm{DA}} = \frac{V_{\mathrm{DB}} V_{\mathrm{BA}}}{\Delta E_{\mathrm{DB}}} \tag{6}$$

V_{DB} and V_{BA} are the corresponding electronic coupling between B and D or B and A, ΔE_{DB} is respectively the energy splitting (HOMO's$_{\mathrm{D}}$ − LUMO's$_{\mathrm{B}}$) between D and B. The dependence of V_{DA} on the D-A distance is given by Equation 7.[52]

$$V_{\mathrm{DA}} = A_0 \exp\left(-\frac{\beta}{2} R_{\mathrm{DA}}\right) \tag{7}$$

R_{DA} is the distance between D and A and β is a bridge specific attenuation factor.

An EnT in artificial RCs is often an undesirable process reducing the life time of the CS state. This can be suppressed by sophisticated optimization of the redox gradient.

1.6 Research on the Primary Processes of Photosynthesis

The investigation of primary steps of photosynthesis can be divided into two fields.[68] The first one focuses on the isolation and crystallisation of natural bacterial and plant RCs (Chapter 1.6.1). The second possibility to get insights into photosynthetic key reactions is to mimic these processes by means of design and preparation of model compounds (Chapter 1.6.2).

1.6.1 Natural Photosynthetic Reaction Centres

Photosynthesis is one of the most important biological phenomenon on Earth. The harvesting of sunlight by plants to combine water with atmospheric carbon dioxide producing organic biomass and dioxygen is the fundament of the existence of living organisms, giving them food and oxygen to breathe. Photosynthesis is not only the heart of plant biogenetics. Also the photosynthetic bacteria, so-called purple bacteria, use sunlight as a source of their energy.[1-18] These bacteria have proved to be outstanding model systems for the investigation of primary processes of photosynthesis, namely, the conversion of light into chemical energy. These processes start with the absorption of light quanta by the light harvesting complex antenna (LHC) and cause an effective energy transfer by the Förster mechanism[65,66] to the "special pair" (SP, $BChl_2$) of the photosynthetic reaction center (RC). The LHC consists of bacteriochlorophyl molecules (BChl) linked noncovalently to surrounding proteins and form a stoichiometric complex with the RC. The best characterized RC is that of *Rhodopseudomonas viridis* (*R. viridis*) (Figure 6).[1-6,69] It consists of four protein subunits H (heavy), M (medium) and L (light) with different weights and cytochromes (not shown in Figure 6) and 14 cofactors. The RC has a total length of about 130 Å and a cross section of 70 Å. The core of the complex is formed by protein subunits L and M and their cofactors: four BChl molecules, two bacteriopheophytin molecules (BPh), two quinones (menaquinone (Q_A) and ubiquinone (Q_B)) and a non-heme iron atom. The role of the protein subunits in stabilizing the redox species is essential to ensure high forward ET rates and to prevent charge recombinations (CR) to occur faster than CS. Proteins L and M ensure that the chemically identical Q_A and Q_B have different behaviour. Whilst Q_A is bound to the M subunit in a hydrophobic pocket, it acts as a one electron acceptor and is never protonated, Q_B is attached to the L subunit and is surrounded by charged and polar residues. It behaves as a two electron acceptor and receives two protons from the cytoplasm.

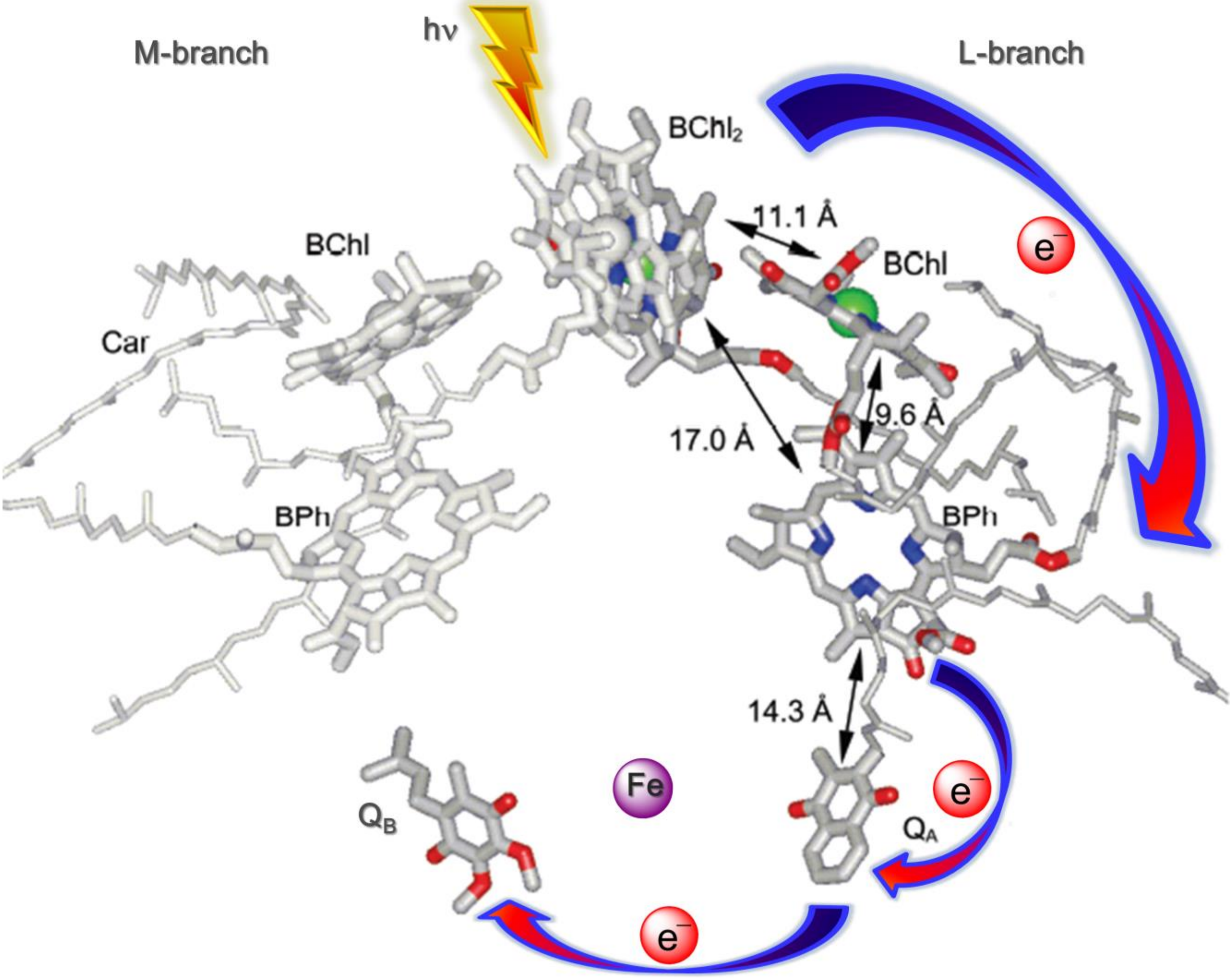

Figure 6. X-ray crystal structure of RC of *R. Viridis*.[69]

The activation by light or energy transfer from LHC (*vide supra*) to the "special pair" (primary electron donor) put it to its first excited singlet state S_1. The photoexcited pair reduces the metal free BPh at the L-brunch within approximately 3 ps. From the BPh the electron is transferred to the primary acceptor Q_A within ca. 200 ps and to the secondary acceptor Q_B within 100 μs. The non-heme iron is not relevant in this step. Q_B picks up two electrons via this way and two protons from the cytoplasmic water molecules or amino acid residues during or after the CS steps. Doubly reduced and protonated ubiquinol (Q_BH_2) leaves the RC which initiates a refilling of the Q_B pocket from a pool of quinones dissolved in the RC surrounding plasma membrane. The back electron and proton transfer to the RC's cytochrom c, from which the $BChl_2$ will be reduced, is much slower than the CS steps. The reduction of $BChl_2$ occurs *e.g.* within 270 ns.[2] Thus the efficiency of CT at the RC is nearly 100 %.[69]

The formation of a proton gradient across the plasma membrane drives the reduction of $NADP^+$ to NADPH, the reducing agent for CO_2 in the Calvin cycle and initiates the synthesis of the energy transporter adenosine triphosphate (ATP).[3]

In photosynthetic reaction centers the fast CS and ET occur in the Marcus normal region ($-\Delta G^0 < \lambda$), while the slow CR proceeds in the Marcus inverted region, where the CR driving force is larger than λ of the ET ($-\Delta G^0 > \lambda$).

1.6.2 Artificial Light Harvesting Antenna, Special Pair and Photosynthetic Reaction Centers

To learn from nature is a common way of modern science development. A great deal of technological wonders like robots is based on the model of snakes[70] or scorpions[71], which are very difficult to bring out of balance or intelligent paints based on self-cleaning of the lotus leaf[72], are innovative products with great potential.

The design of synthetic LHCs, SPs and RCs with the same quantum yield of EnT and the same rates and time scales of CS and ET found in nature, is a major challenge of modern photosynthesis research with the goal to better understand the common processes in the natural special pairs and reactions centres. Even if the photochemical water splitting could not be established as a near future energy source, practical perspectives of model compounds are extremely promising in the multidisciplinary field of research involving for instance molecular electronic devices[39-45], organic solar cells[73-83] and redox catalysts[85-88].

Using Marcus theory and information about components, distances between them and their orientation found in the natural LHC and RC, a rational design of artificial model compounds is possible, which are able to lossless energy transfer and its conversion to a chemical potential.

Many models utilizing porphyrins[32,46-57,59-62,87-144,146-164,170,171], quinones[32,89-106], fullerenes[87,88,107-135], ferrocenes[107-117,136-145] and carotenoids[47,48,58,94,101,171] as suitable building blocks for artificial RC were prepared with respect to the above-mentioned features. The artificial light harvesting and energy transferring antennas and SP as part of RC are generally built up of porphyrin arrays[46,51,52-57,59-62], while ET capable RC models are often P-A, P-D or D-P-A systems (P = porphyrin)[87,88-164]. The ensembles in the models are covalenty[32,89-124,127-129,131-144,146-154,171] and noncovalently[125,126,130,155-164] linked to each other. In following a few of them are presented.

1.6.2.1 Cofacial Porphyrin Dimers as Artificial "Special Pair"

The SP is, as mentioned above, a bacteriochlorophyll dimer ($BChl_2$) with the mean distances between chromophors of around 3.5 Å.[167] This results in a strong π-π interaction between the bacteriochlorophylls. After one electron oxidation to the radical cation the interaction is intensified due to radical stabilisation and is detectable in the doubling of hyperfine splitting in the EPR spectrum.[23] The study of this interaction and the role of SPs' dimer structure were examined by the synthesis of cofacial porphyrin dimers with tuneable distances between the porphyrins upon variation of the spacers.[51,53,60,168-170] In the dimers **ZnZn-II** with 1,8-bis[5-(2,8,13,17-tetraethyl-3,7,12,18-tetramethylporphyrinyl)]biphenylene (DPB) and **ZnZn-III** with 4,6-bis[5-(2,8,13,17-tetraethyl-3,7,12,18-tetramethylporphyrinyl)] dibenzofuran (DPO) as a rigid spacer the P-P distances are approximately 3.8 Å and 7.8 Å, respectively (Figure 7a and 7b).[170] 2,2'-bis[5-(2,8,13,17-tetraethyl-3,7,12,18-tetramethy-lporphy-rinyl)]diphenyl-ether (DPOx) was used as flexible spacer in dimer **ZnZn-IV** (Figure 7c).[170]

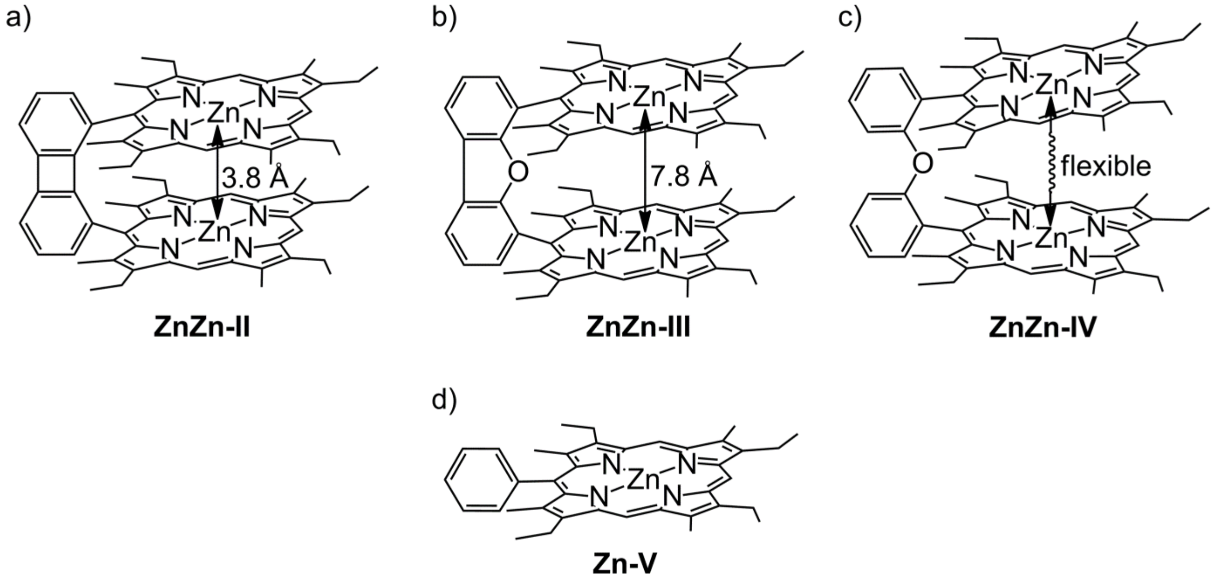

Figure 7. a) Artificial SP **ZnZn-II** with rigid spacer DPB. b) Artificial SP **ZnZn-III** with rigid spacer DPO. c) Artificial SP **ZnZn-IV** with flexible spacer DPOx. d) Reference porphyrin **Zn-V**.[170]

The strength of the π-π interaction in these compounds was investigated by cyclic voltammetry. The first oxidation potential of **ZnZn-II** is 140 mV lower than that of the reference porphyrin **Zn-V** (720 mV *vs.* SCE) (Figure 7d). The better stabilisation of the radical cation **ZnZn-II**$^{\cdot+}$ compared with **Zn-V**$^{\cdot+}$ is caused by π-π interactions between the two porphyrin macrocycles. With increasing of the porphyrin center to porphyrin center distance the π-π interaction becomes weaker and the stabilisation of radical cations **ZnZn-III**$^{\cdot+}$ (110 mV *vs.* SCE) and **ZnZn-IV**$^{\cdot+}$ (40 mV *vs.* SCE) decreases relative to the reference porphyrin radical **Zn-V**$^{\cdot+}$.

Based on these results a through space singlet EnT (Dexter mechanism) of the cofacial dyads with mono metallated zinc(II) porphyrin as D and free-base porphyrinas A (**Zn2H-II**, **Zn2H-III** and **Zn2H-IV**) upon excitation of both porphyrins was studied with respect to the D-A distance (Figure 8).[51,53]

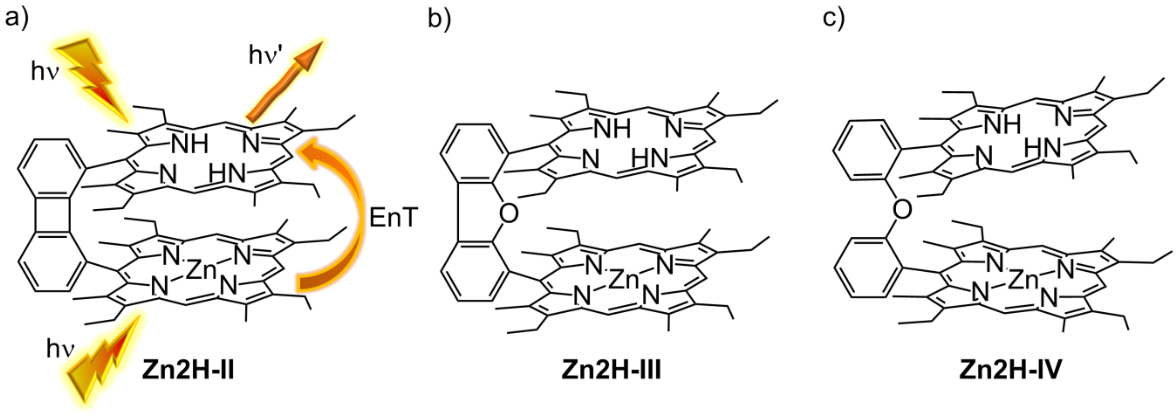

Figure 8. a) Artificial SP **Zn2H-II** with rigid spacer DPB. b) Artificial SP **Zn2H-III** with rigid spacer DPO. c) Artificial SP **Zn2H-IV** with flexible spacer DPOx.[51,53]

Due to EnT the fluorescence spectra of these artificial SPs exhibit a strong decrease in relative intensity for the zincated porphyrin moiety compared with free base porphyrin. Also the fluorescence lifetimes and quantum yield of monometallated dyads decrease. Here, the bismetallated dimers (**ZnZn-II**, **ZnZn-III** and **ZnZn-IV**) depicted in Figure 7 served as reference compounds. The most efficient EnT was observed in **Zn2H-II** with the smallest distance between both porphyrins ($k_{\mathrm{EnT}} = 20.8\times10^{-9}\mathrm{s}^{-1}$) and the slowest one in **Zn2H-IV** ($k_{\mathrm{EnT}} = 5.0\times10^{-9}\mathrm{s}^{-1}$) because of twisting in this dyad.[53]

1.6.2.2 Extended Bis(porphyrins) as Artificial LHCs

Albinsson and coworkers investigated singlet excitation energy transfer in D-B-A systems **VI** with respect to variation of bridge length and the D-B energy gap in D-A dyads connected by π-conjugated bridges (Figure 9).[52] The exchange interaction in such conjugates is mediated by low lying bridge LUMOs and a clear distinction between Förster and Dexter (superexchange) mechanism is lost. In conjugates **VI** both mechanisms are involved in EnT and contribute significantly to EnT rates. A series of *p*-phenyleneethynylene with variable length were used as bridges between D (zinc(II) porphyrin) and A (free-base porphyrin).

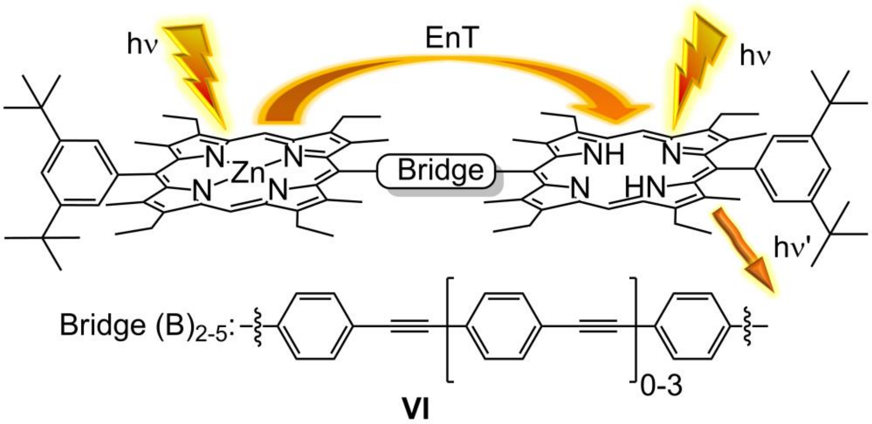

VI

Figure 9. Structures of (Zn)P-(B)$_{2-5}$-P with bridges of variable length.[52]

The absorption spectra of **VI** show a complete electronic isolation of chromophores. But a decrease of donor and an increase of acceptor emission intensity are observed, compared to a D-B reference compound, due to EnT depending on the bridge length. The most efficient EnT with $\Phi_{(\mathrm{EnT})}$ = 81% was observed for the (Zn)P-(B)$_2$-P system with $k_{\text{Förster}} = 1.5\times10^9$ s^{-1}and $k_{\text{Dexter}} = 1.9\times10^9$ s^{-1} and the weakest one for (Zn)P-(B)$_5$-P with $\Phi_{(\mathrm{EnT})}$= 5% ($k_{\text{Förster}} = 2.0\times10^7$ s^{-1} and $k_{\text{Dexter}} = 3.2\times10^7$ s^{-1}). The contribution of these two mechanisms (Förster *vs.* Dexter) is of the same magnitude and the relative contribution is practically independent on the bridge length. The estimated energy difference between the singlet excited states of the donor and bridge (ΔE_{DB}) correlates with these observations (see Chapter 1.5). It is maximal for (Zn)P-(B)$_2$-P (ΔE_{DB} = 15800 cm^{-1}) and minimal for (Zn)P-(B)$_5$-P (ΔE_{DB} = 9700 cm^{-1}) in the investigated dyad series.

The DFT optimised geometries for the dyads show, that the HOMO (a_{2u}) exhibits electron density at the bridge attachment site. According to this, electronic coupling between donor, bridge and acceptor is given and the Dexter through-bond mechanism is probable.

In all systems **VI** no evidence for radical bands in transient absorption spectra was detected which would be expected for PET, thus the EnT is a dominant S_1 state deactivation channel of the donor.

1.6.3 Rational Design of RC Model Compounds

The complexity of the PET mechanism in photosynthesis (Chapter 1.6.1) requires the design and preparation of model compounds, which can mimic PET processes in the RC. In these arrays specific properties of RC building blocks can be adopted and tuned by synthesis of suitable compounds. In general, they consist of covalently and noncovalently linked electron donor(s) (D), bridge(s) (B) and electron acceptor(s) (A). These models should show a rapid and efficient CS (forward PET) and preferably slow back ET reactions resulting in long-lived CS states. In the following, different strategies of artificial RC construction to achieve a long-lived CS state upon a sequence of one or several short range ET reactions along a sophisticated designed redox gradient will be presented.

1.6.3.1 Bis(porphyrin) RC Model Compounds

The most suitable building blocks for model compounds are porphyrin derivatives[32,46-57,59-62,87-144,146-164,170], due to their important role in the PET in photosynthetic RC[1-18]. Their absorption features are unique and allow the efficient use of the solar spectrum.[23] The extensively conjugated two dimensional π-electron system of porphyrins (Chapter 1.1) and hence the minimal structural and solvatational changes due to ET result in a low reorganization energy λ (Chapter 1.4). Due to these features, porphyrins are excellent electron donors, electron acceptors and bridges in PET reactions.

Because of the weak electron donor character of zinc porphyrins and electron acceptor character of free-base porphyrins, an ET in bis(porphyrin) systems between zinc(II) and free-base porphyrins is hampered (Chapters 1.6.2.1 and 1.6.2.2). By modifying the porphyrin skeleton by means of substitution with strongly electron withdrawing substituents or complexation with high oxidation state metal ions an ET can be facilitated.

For this approach Gust and coworkers synthesized a bis(porphyrin) **VII** consisting of bispentafluorophenyl porphyrin (P^{F6}) as electron donor and tetracyano substituted porphyrin (P^{TCNP}) at β positions as electron acceptor (Figure 9).[118] A further enlargement of **VII** will be not discussed here.

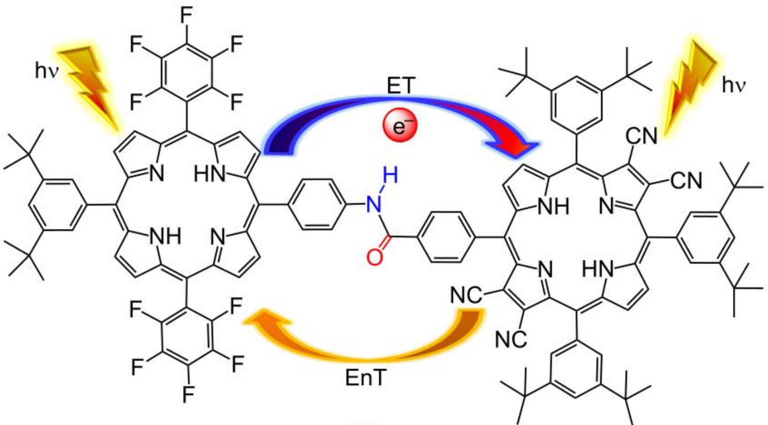

VII

Figure 10. Structure of P^{F6}-P^{TCNP} dyad **VII**.[118]

The absorption spectrum of **VII** is a linear combination of the individual spectra of its two photoactive units. Thus no strong ground state electronic interactions between them are present. Apart from EnT from P^{F6} to P^{TCNP} observed in fluorescence experiments, the CS state P$^{F6.+}$-P$^{TCNP.-}$ generated by PET with characteristic absorption of P$^{F6.+}$at 650 nm and a decay of 12 ps was detected by transient absorption techniques in benzonitrile. The PET features a quantum yield of Φ_{ET} = 77%.

The synthesis of (M)P-(Au^{III})P bis(porphyrins) with M = 2H or Zn is another way to design ET capable D-A systems.[147-155] Porphyrin metalation with Au^{III} leads to a dramatic increase of the first porphyrin reduction potential (E((Au)P)$_{1/2}$(red^1) ≈ −1.10 V *vs.* Fc/Fc$^+$)[149] compared with the corresponding free base (E(P)$_{1/2}$(red^1) ≈ −1.60 V *vs.* Fc/Fc$^+$)[32,136] or zinc(II) porphyrins (E((Zn)P)$_{1/2}$(red^1) ≈ −1.70 V *vs.* Fc/Fc$^+$)[149] and consequently to an increase of the ET driving force ($-\Delta G_{ET}$). It renders Au^{III} porphyrins suitable electron acceptors in porphyrin arrays. Mårtensson *et al.* synthesized a series of (Zn)P-B-(Au)P$^+$ constructs (**VIII**) with geometrically similar but electronically variable bridge structures and investigated the quenching of the S$_1$ state of the donor porphyrin due to EnT (Förster mechanism), ET in the Marcus normal region and intersystem crossing (ISC) by the heavy-atom effect of gold (Figure 11).[149]

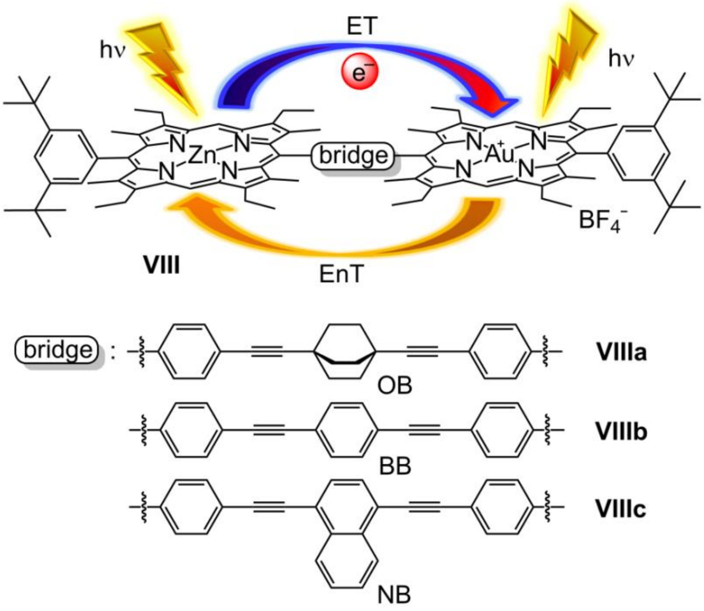

Figure 11. Structures of (Zn)P-B-(Au)P$^+$ dyad **VIII** with different bridges B.[149]

In these dyad series the life time of the S_1 state of the zinc(II) porphyrin is strongly reduced when the gold(III) porphyrin is covalently linked. The emission quenching for fully conjugated bridges 1,4-bis(phenylethynyl)benzene (BB) (**VIIIb**) and 1,4-bis(phenyl-ethynyl)naphthalene (NB) (**VIIIc**) is larger than that for the bridge with the disturbed π conjugation 1,4-bis(phenylethynyl)bicyclo[2.2.2]octane (OB) (**VIIIa**). As the lowest S_1 state of (Au)P$^+$ is of higher energy (ΔE = 0.12 eV) than that of (Zn)P, the EnT from (Zn)P to (Au)P$^+$ is much slower than that for dyads (Zn)P-B-P (Chapter 1.6.2.2). EnT from (Au)P$^+$ to (Zn)P is not possible as (Au)P$^+$ is non fluorescent and its S_1 life time is too short for an EnT. In **VIIIa** Förster EnT is the main decay pathway. In dyads **VIIIb** and **VIIIc** with conjugation within the bridges the quenching rate constant of the donor is dramatically higher and corresponds to the expected PET rates. While for **VIIIa** no evidence of existence of CS state (Zn)P$^{\cdot+}$-B-(Au)P$^{\cdot}$ was found, the characteristic absorption band of (Zn)P$^{\cdot+}$ at around 680 nm was observed for the fully conjugated dyads **VIIIb** and **VIIIc** in transient absorption spectra. In these dyads PET is the main decay pathway for ^{1}(Zn)P depopulation. The deactivation processes of excited (Zn)P in **VIIIb** and **VIIIc** are summarized in the energy level diagram in Figure 12.

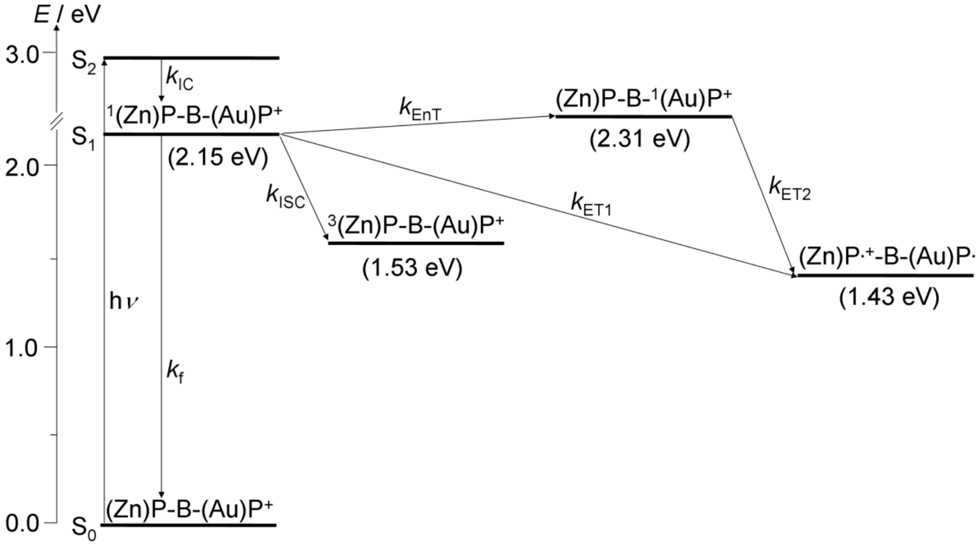

Figure 12. Energy level diagram for (Zn)P-B-(Au)P^+ dyads **VIIIb** and **VIIIc**.[149]

1.6.3.2 Porphyrin-Quinone RC Model Compounds

Quinones (Q) are the most common electron acceptors in artificial RCs[32,89-108] because of their acceptor function in natural photosynthesis[1-18]. Their predestination as electron acceptor is based on their suitable redox potentials, their stepwise reduction to stable products (semiquinones after first reduction and hydroquinones after second reduction and protonation), their ability to form hydrogen bonds and to undergo protonation and deprotonation. Thus, as small mobile molecules they are perfect charge transporters. Porphyrins attached covalently or noncovalently to quinones are the most extensively studied model compounds for PET.[32,89-108] In the following some of them will be presented.

In 1984, Wasielewski *et al.* published a detailed report of PET in (M)P-Q dyads **IX** (M = 2H and Zn) with different quinones 1,4-benzoquinone (BQ) **IXa**, 1,4-naphthoquinone (NQ) **IXb** and 9,10-anthraquinone (AQ) **IXc** (Figure 13) using fluorescence and transient absorption measurements.[32] The redox potentials of porphyrins and quinones as well as ground state absorption spectra are not altered by linking the two molecules but the fluorescence quantum yield of the porphyrins is diminished up to 96% due to PET in the respective dyads. The most dramatic porphyrin emission quenching in these dyad series was observed for **IXa** with M = 2H and Zn.

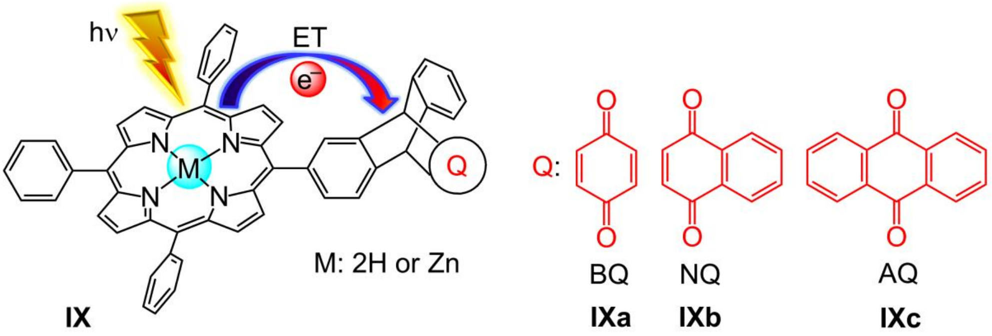

Figure 13. Structures of (M)TPP-Q model compounds **IX** with M = 2H or Zn and different quinones Q (BQ (**IXa**), NQ (**IXb**) and AQ (**IXc**)).[32]

Transient absorption measurements showed evidence for the formation of the CS state. For selected compounds, only bands of (Zn)TPP$^{\cdot+}$ at around 650 nm and no bands of Q$^{\cdot-}$ because of the very low absorptivity of these radical anions could be detected in transient absorption experiments. The PET quantum yield amounted to 79% for the generation of (Zn)TPP$^{\cdot+}$-BQ$^{\cdot-}$ in **IXa**.

Stepwise sequential PET from porphyrin to quinone similar to PET in photosynthetic natural RC was studied on P-Q^1-(Q^2)$_2$ model **X** containing multiple quinones for enhancement of the CS life time.[99] In this construct, free base porphyrin is linked via an amide bond to a triquinone moiety which consists of a naphthoquinone (NQ) bearing two equivalent benzoquinone moieties (BQ$_2$) (Figure 14).

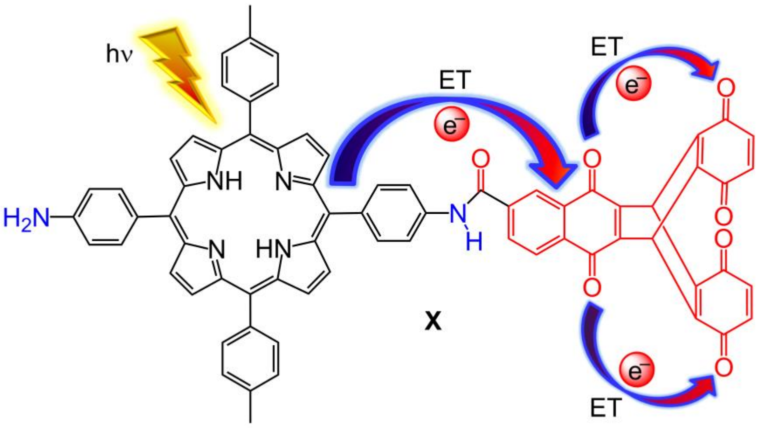

Figure 14. Structure of P-Q^1-(Q^2)$_2$ model compound **X** with Q^1 = NQ and Q^2 = BQ$_2$.[99]

In analogy to other P-Q biomimetic model compounds[32,89-98,100-108] the porphyrin fluorescence of the **X** is drastically quenched compared to a porphyrin reference compound and transient absorption measurements confirmed the generation of CS state. The lifetime of the observed porphyrin radical cation of P$^{\cdot+}$-NQ$^{\cdot-}$-BQ$_2$ CS state in acetonitrile was 300 fs while that of P$^{\cdot+}$-NQ-BQ$_2$$^{\cdot-}$ amounted to

52 ps. The sequential electron transfer from the photoexcited porphyrin to the naphthoquinone and benzoquinones is shown in Figure 15.

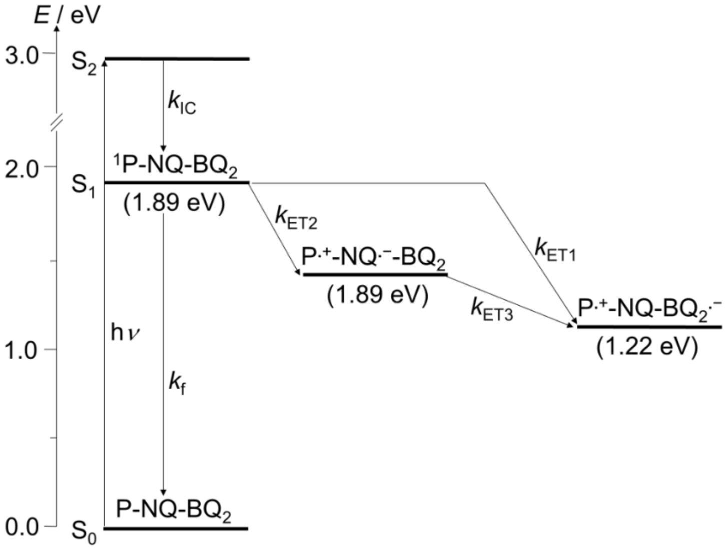

Figure 15. Energy level diagram for P-NQ-BQ$_2$ model architecture **X**.[99]

1.6.3.3 Porphyrin-Ferrocene RC Model Compounds

Ferrocene (Fc) substituted porphyrins are of great interest as photochemical devices and photosynthetic model compounds.[107-117,133,134,136-145] Due to reversible redox features and the ability to reduce the S_1 state of the porphyrin moiety, ferrocene is a suitable electron donor for the mimicry of photosynthetic processes in RC at a molecular level, in which porphyrins act as electron acceptors.

Whereas only weak electronic interactions between chromophores in the ground state of P-Fc model compound **XI** (Figure 16) can be observed by UV/Vis spectroscopy and cyclic voltammetry, the porphyrin fluorescence is quenched by 62% for the dyad with a vinylidene spacer (mixture of *cis* (73%) and *trans* (27%)) (**XIa**) and by 16% for the dyad with an ethylene spacer (**IXb**) compared to the porphyrin reference compound.[136] This emission diminution was attributed to intramolecular reductive PET from ferrocene to porphyrin generating $P^{\cdot-}$-$Fc^{\cdot+}$. The ET rate constants for both compounds were given as $\kappa_{ET} \approx 10^8\ s^{-1}$.

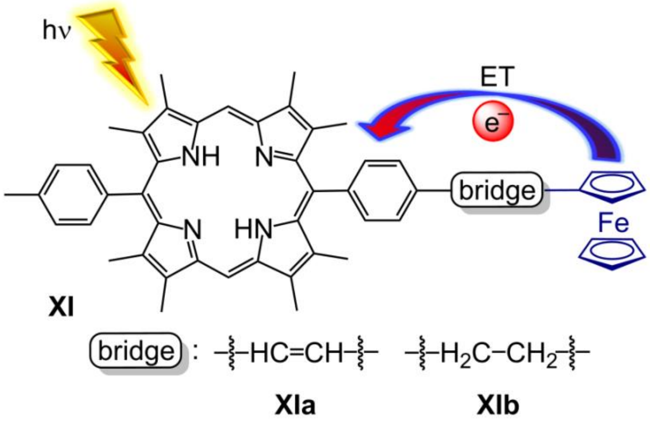

Figure 16. Structure of P-Fc dyad **XI** with vinylidene (**XIa**) and ethylene (**XIb**) as bridge.[136]

In order to extend the CS state lifetime of P-Fc dyads Fukuzumi *et al.* proposed a series of ferrocene-porphyrin-fullerene ensembles (Fc-(M)P_n-C_{60}) with n = 1-3 and M = 2H or Zn.[108-117,133] In contrast to (M)P-Fc dyads the two dimensional primary electron acceptor porphyrin is replaced by the 3D acceptor fullerene (C_{60}) in these triads, tetrads and pentads. Electron transfer to C_{60} is very efficient due to minimal changes of structure and solvation sphere resulting in a minimal reorganization energy λ associated with ET and generation of $C_{60}^{\cdot-}$.

In the triads Fc-(M)P-C_{60} **XII** with M = 2H or Zn and edge-to-edge distance between Fc and C_{60} R_{ee} = 30.3 Å (Figure 17) two constructive ET steps yielding the CS states Fc-(M)$P^{\cdot+}$-$C_{60}^{\cdot-}$ and $Fc^{\cdot+}$-(M)$P^{\cdot-}$-C_{60} are feasible.[112] Both CS states lead to the final CS state $Fc^{\cdot+}$-(M)P-$C_{60}^{\cdot-}$ in the Marcus normal region. Transient absorption spectroscopy revealed the characteristic $C_{60}^{\cdot-}$ band at ca. 1000 nm *e.g.* for Fc-(Zn)P-C_{60} but none for the (Zn)$P^{\cdot+}$ due to the subsequent and rapid ET from Fc-(Zn)$P^{\cdot+}$-$C_{60}^{\cdot-}$ to the final CS state $Fc^{\cdot+}$-(Zn)P-$C_{60}^{\cdot-}$. Because of the very small molar absorption of the ferrocenium ion ($\varepsilon \approx 1000$ M^{-1} at $\lambda_{max} \approx 800$ nm) this species was not detectable in the transient absorption measurements.[113] The rate constant k_{ET1} of the ET from Fc to (Zn)P generating $Fc^{\cdot+}$-(Zn)$P^{\cdot-}$-C_{60} is 20 times slower (estimated from the fluorescence lifetime measurements of Fc-(Zn)P reference compound) than every CS process involving C_{60} (k_{ET3}, k_{ET4}, k_{ET5}) and is thus negligible. Figure 18 depicts the possible ET pathways leading to formation of $Fc^{\cdot+}$-(Zn)P-$C_{60}^{\cdot-}$ CS final state. The CS quantum yield is Φ_{ET} = 82% and the lifetime of the final CS in frozen benzonitrile is 16 μs.

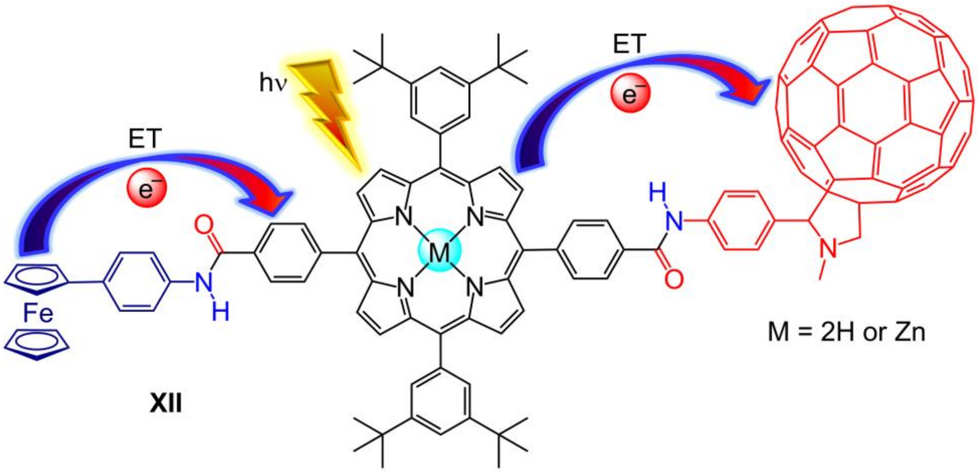

Figure 17. Structure of Fc-(M)P-C_{60} triad **XII** with M = 2H or Zn.[112]

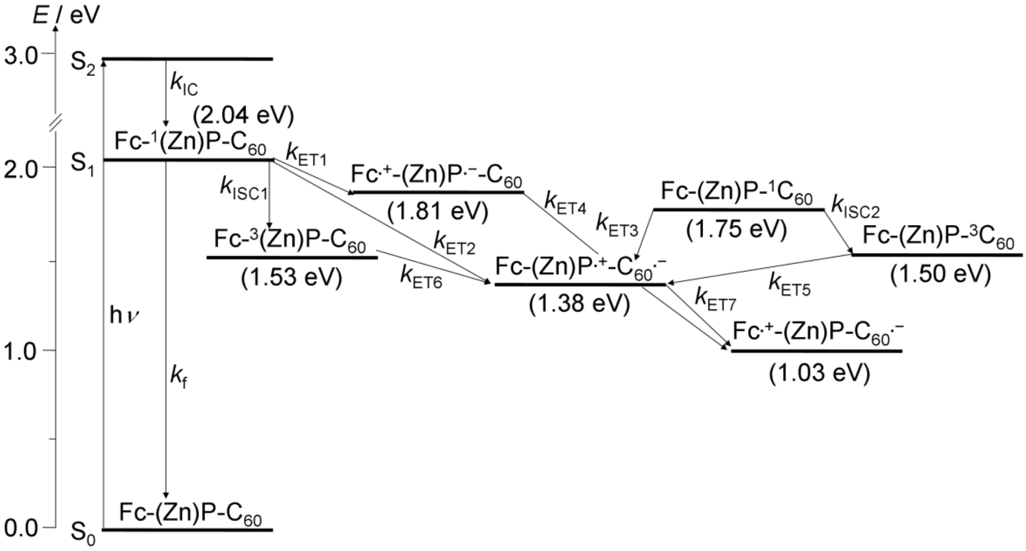

Figure 18. Energy level diagram for Fc-(Zn)P-C_{60} triad **XII**.[112]

One of the best molecule mimicking multi-step ET processes in the photosynthetic RC is a ferrocene-*meso*,*meso*-linked porphyrin trimer-fullerene pentad Fc-$(ZnP)_3$-C_{60} **XIII** (Figure 19).[116] In this molecule, Fc and C_{60} are attached at opposite ends of the porphyrin triad with an edge-to-edge distance of R_{ee} = 46.9 Å. Transient absorption spectra of the pentad are virtually identical to those of triad **XII**. They exhibited the formation of $C_{60}^{\cdot-}$ band at ca. 1000 nm and disappearance of the (Zn)P$^{\cdot+}$ band at around 650 nm. The latter could be observed due to the relatively slow charge migration within the porphyrin trimer in comparison with ET from Fc to (Zn)P$^{\cdot+}$ in **XII**.

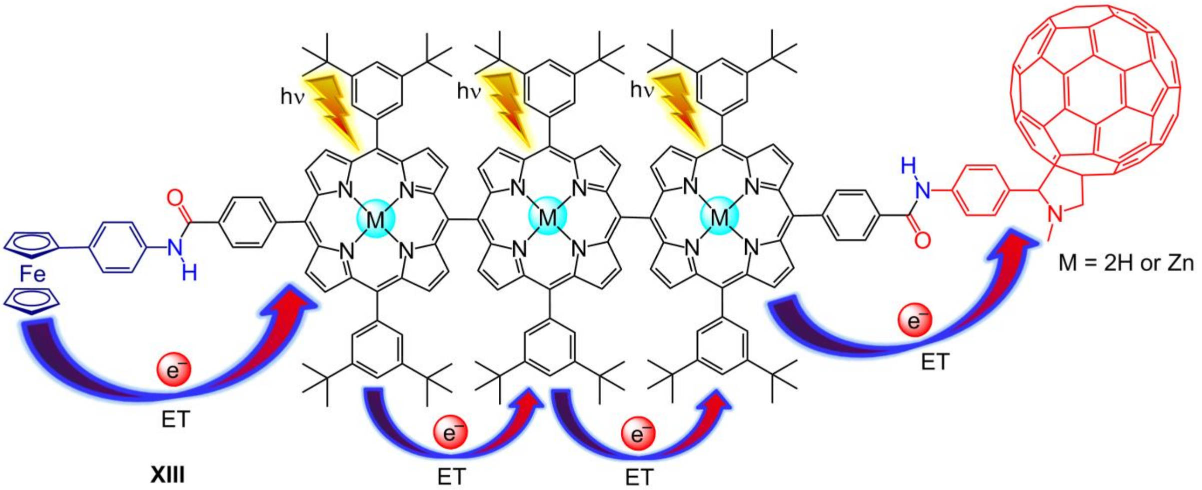

XIII

Figure 19. Structure of Fc-(M)P-C_{60} pentad **XIII** with M = 2H or Zn.[116]

The initial ET occurs from the excited $^1(ZnP)_3$ to the C_{60} moiety generating Fc-$(ZnP)_3^{\cdot+}$-$C_{60}^{\cdot-}$. The fluorescence life time measurement for Fc-$(ZnP)_3$ reference compound showed that an initial ET occurs from the Fc to the $^1(ZnP)_3$ producing $Fc^{\cdot+}$-$(ZnP)_3^{\cdot-}$-C_{60}. However, this ET is 20 times slower than any ET pathways involving C_{60} and thus it is negligible. The energies of CS states and ET pathways are widely equivalent to those depicted in the energy diagram in Figure 18. The CS quantum yield is Φ_{ET} = 83%. The lifetime of the final CS state in frozen benzonitrile τ = 0.53 s is one of the highest ever reported for intramolecular ET in artificial RC and comparable with that (≈ 1 s) of the bacteriochlorophyl dimer radical cation- secondary quinone radical anion CS state ($Bchl_2^{\cdot+}$-$Q_B^{\cdot-}$) in bacterial RC.[116] However, such long CS state lifetime could be determined only in frozen polar media like benzonitrile. The dynamics of the intramolecular ET in model RC in solution are still dominated by the back ET.

1.6.3.4 Porphyrin Tweezer Electron Acceptor Sandwich Complexes as RC Model Compounds

Various cofacial bis(porphyrin) systems were prepared and extensively studied with regard to π-π interactions and excited EnT between the two macrocycles due to their structural similarity to photosynthetic SP (Chapter 1.6.1). Reports of efficient PET in such porphyrin tweezers by encapsulation of electron acceptors into the bis(porphyrin) cavity are very rare.[159,162,164]

Chaudhary and Rath studied PET by encapsulation of 7,7,8,8-tetracyanoquinodimethane (TCNQ) as electron acceptor within a diethylpyrrole-bridged bis(porphyrin) cavity (Figure 20).[164]

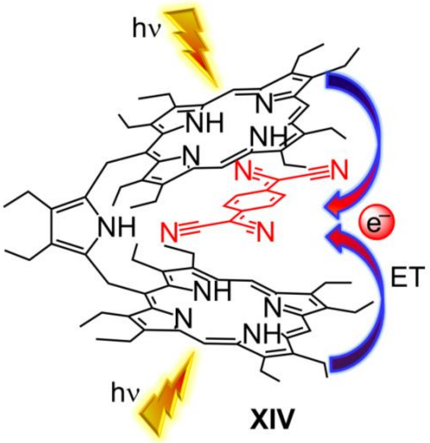

XIV

Figure 20. Structure of 4HDEP$^{\cdot}$TCNQ sandwich complex **XIV**.[164]

The formation of the π-π sandwich complex **XIV** was followed by absorption, fluorescence and EPR spectroscopy studies. The complexation of the tweezer with up to one equivalent TCNQ leads to an increase of the Soret band intensity and a decrease of the Q band intensity. Additionally new CT bands at λ_{max} = 769 nm and 851 nm appeared in the UV/Vis spectra. These bands are characteristic for porphyrin radical cations ($P^{\cdot+}$)[32,110,112-116] and tetracyanoquinodimethane radical anions ($TCNQ^{\cdot-}$)[156,164] as well. Due to ET the emission intensity of porphyrins in the 4HDEP$^{\cdot}$TCNQ complex was reduced by 65% compared to the untreated porphyrin tweezer.

An EPR measurement of the isolated 1 : 1 host-guest complex **XIV** exhibited a radical signal with resonance at g = 2.005, which is characteristic for both $P^{\cdot+}$ and $TCNQ^{\cdot-}$ radicals showing that ET has already partially occurred in the ground state.

2 Aim of Work

The aim of this work is to investigate essential steps of photosynthesis: light harvesting, energy transfer (EnT), charge separation (CS) and electron transfer (ET). For this purpose biomimetic model compounds for light harvesting antenna complexes (LHC) and artificial reaction centers (RC) are to develop and to prepare. It was focussed on model compounds that are similar to natural pigments in the LHCs and RCs.

As key building blocks for such model compounds porphyrin amino acids are especially suitable. Therefore, ester protected *trans*-AB_2C-*meso*-substituted porphyrin amino acids with tunable electronical features by means of electron donating and electron withdrawing power of Ar substituents at B positions should be synthesized.

Based on free-base or zinc(II) porphyrin amino acid esters amide-linked free-base, mono and doubly metallated bis(porphyrins) with adjustable electron density at each porphyrin site should be prepared and an EnT along the energy gradient at these artificial LHCs should be investigated. The greatest synthetic challenge herein is to elaborate the activation reagent for a successful preparation of monometallated bis(porphyrins). This reagent must not demetallate the acid-labile zinc porphyrin complex and the reaction should give only monometallated product.

As discussed in the introduction (Chapter 1.4) the design of efficient artificial photosynthetic systems for the conversion and storage of light energy is based on the Marcus theory. A series of PET-capable amide-bridged anthraquinone-porphyrin-ferrocene triads Q-(M)P^{Ar}-Fc (M = 2H or Zn) with Q as electron acceptor (A) and Fc as electron donor (D) should be prepared. Furthermore, efficiencies of the initial oxidative PET pathway (excited porphyrin to quinone) *vs.* reductive PET pathway (ferrocene to excited porphyrin) at conjugates with tunable electron density at porphyrin moiety shall be examined. To investigate the effect of A-D distance enlargement a tetrad Q-P^{Ar1}-P^{Ar2}-Fc shall be synthesized and investigated with respect to EnT between porphyrin entities and possible PET pathways.

The preparation of amide-linked P^{Ar}-Fc conjugates with different Fc donors and P^{Ar2}-Fc-P^{Ar1} hinges shall give insight into the reductive PET pathway. Additionally, the efficiency of PET should be checked in these conjugates by variation of the Ar substituents at B positions and complexation of the porphyrin chromophor with zinc(II) to give (Zn)P^{Ar}-Fc and (Zn)P^{Ar2}-Fc-(Zn)P^{Ar1}. From the

$(M)P^{Ar2}$-Fc-$(M)P^{Ar1}$ hinges with M = 2H and Zn further artificial RCs with a nature-related noncovalently attached electron acceptor between the porphyrin chromophors are to construct.

The EnT and PET should be investigated by electrochemical measurements (cyclic voltammetry and square-wave voltammetry), UV/Vis spectroscopy, steady-state emission and time resolved fluorescence measurements. The CS states at conjugates should be examined by means of time-resolved transient absorption spectroscopy. Associated DFT calculations should facilitate interpretation of the experimental results.

3 Results and Discussion

In the following the synthesis and properties of ester protected *trans*-AB_2C *meso*-substituted porphyrin amino acid esters with tunable electronical features (Chapter 3.1) as well as artificial LHCs and RCs constructed of these building blocks (Chapter 3.2 – 3.4) will be presented. The research work can be categorized into three different but closely related projects. They are schematically represented in Scheme 1.

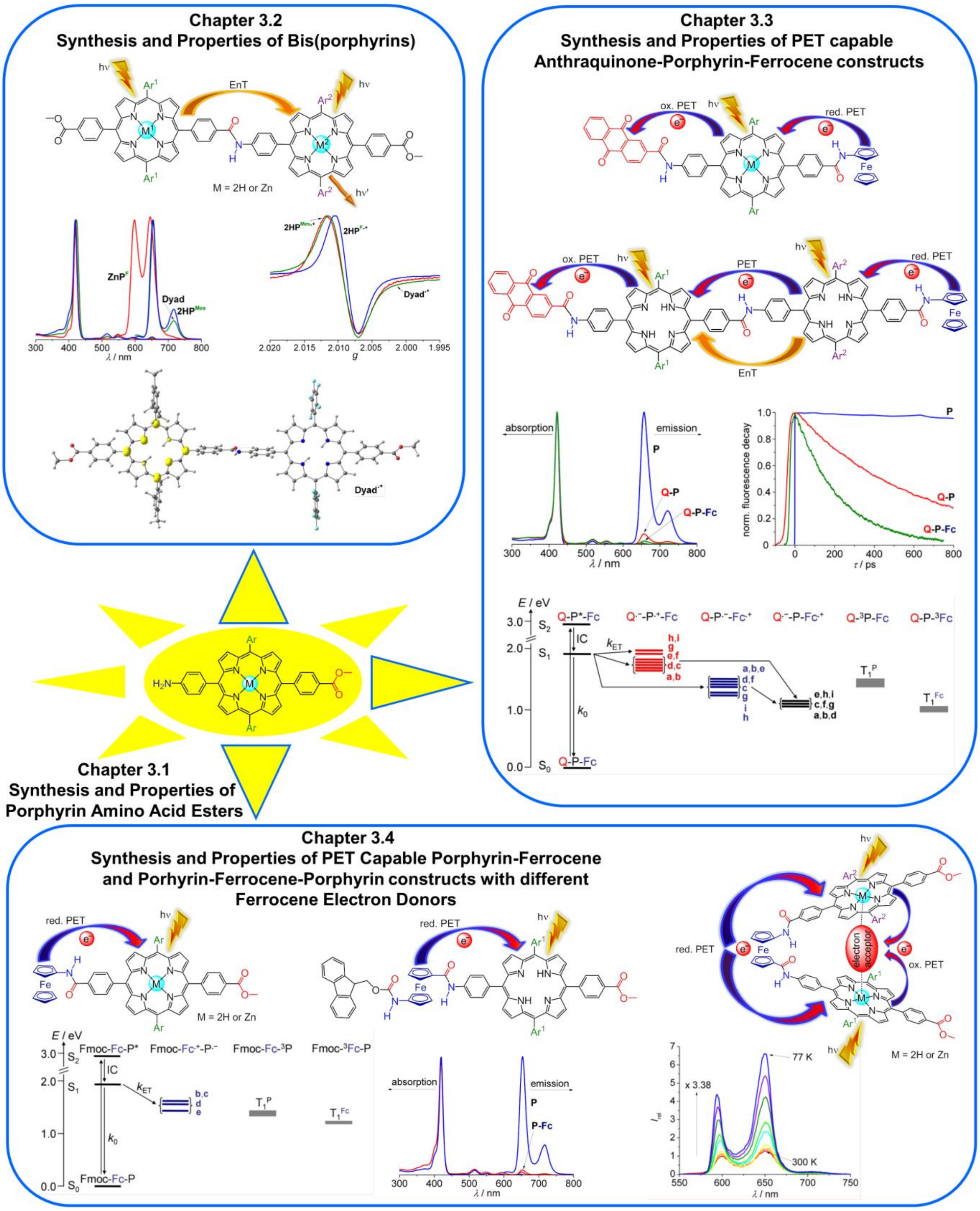

Scheme 1. Schematic representation of the research work projects.

3.1 Synthesis and Properties of Porphyrin Amino Acid Esters

In this chapter the synthesis and properties of *trans*-AB_2C porphyrin amino acid esters are presented. Figure 21 shows the structure of the *trans*-AB_2C porphyrin amino acid esters **3a** − **3h**.

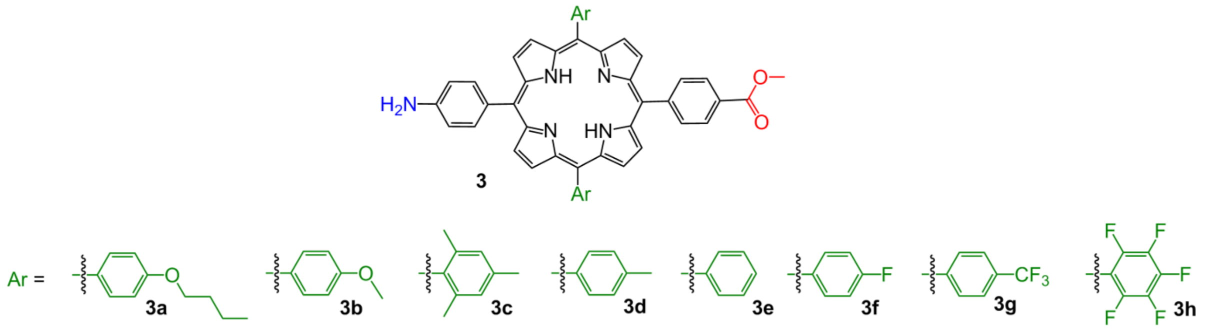

Figure 21. Porphyrin amino acid ester building blocks **3a** − **3h**.

The synthesis of well-defined AB_2C porphyrins in good yields is still a challenge. A rational route to prepare *trans*-AB_2C porphyrin amino acids with A = *p*-C_6H_4-NH_2, B = C_6H_5 and C = *p*-C_6H_4-COOH was reported by Heinze *et al.*[30] Using this established method a pool of porphyrin amino acid esters with Ar substituents of variable electron donating and withdrawing power at B positions was synthesized (Ar = 4-$C_6H_4O^nBu$ (**3a**), 4-C_6H_4OMe (**3b**), 4-C_6H_4Me (**3d**), C_6H_5[30] (**3e**), 4-C_6H_4F (**3f**), 4-$C_6H_4CF_3$ (**3g**)). These substituents cover a wide range of electron affinities. However, this route is only applicable for *p*-substituted Ar substituents at B positions (Scheme 2, route A).

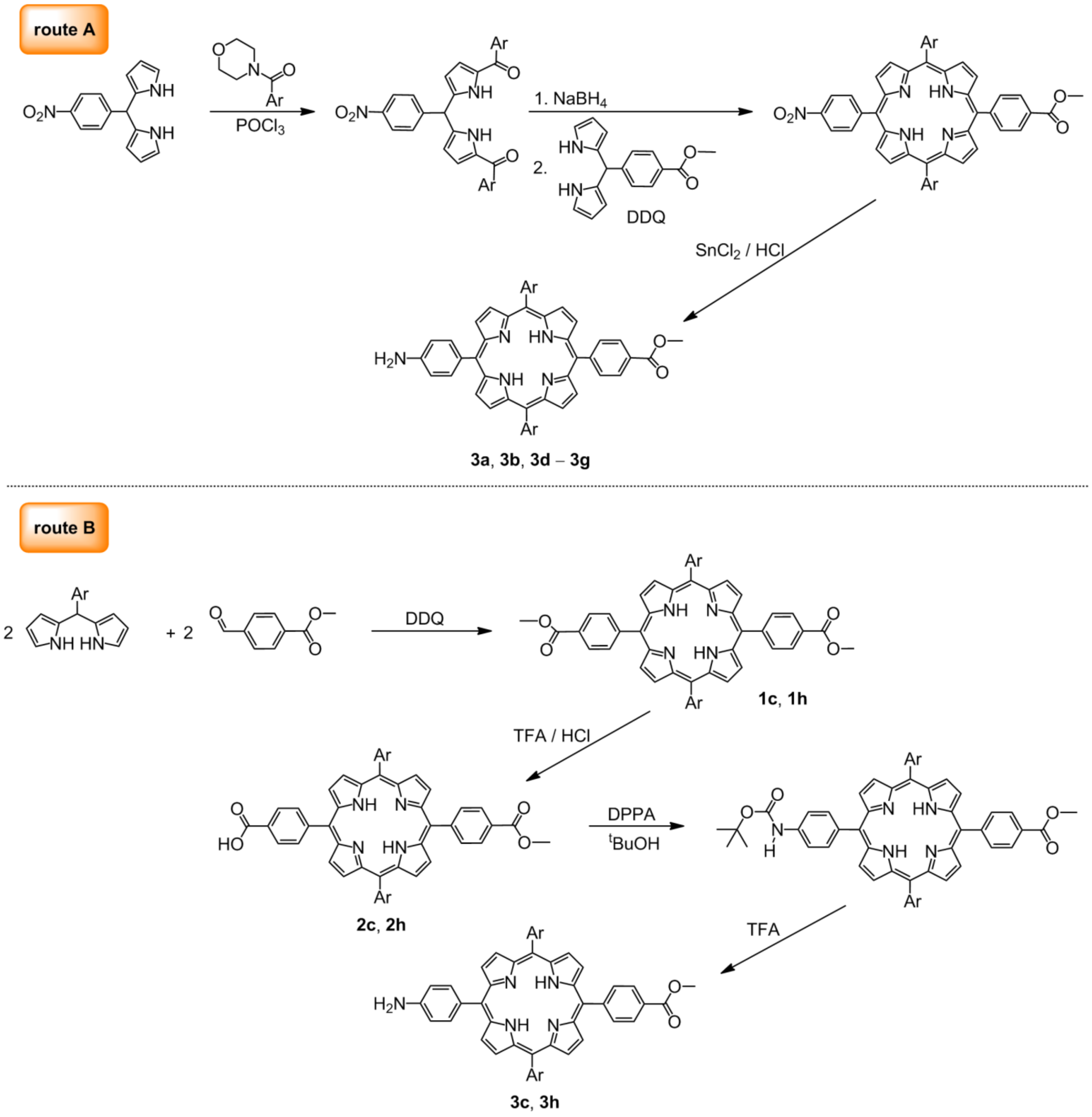

Scheme 2. Synthesis of porphyrin amino acids **3a**, **3b**, **3d** – **3g** (route A)[30] and **3c**, **3h** (route B)[171].

All attempts to synthesize porphyrins with Ar = 2,4,6-$C_6H_2Me_3$ (**3c**) and C_6F_5 (**3h**) via this method were unsuccessful. Whether the *in situ* activation of the corresponding *N*-benzoyl morpholine with phosphorous(V) oxychloride ($POCl_3$) forming an iminium salt (“Vilsmeier reagent”) due to sterical hindrance of *o*-phenyl substituents or the subsequent reaction of the iminium salt with 4-nitrophenyldipyrromethane giving corresponding 1,9-bis(benzoyl)-5-(4-nitrophenyl) dipyrromethane are responsible for failure, is not clear. A test reaction with an extended reaction time of 48 h instead of 3 h to the iminium salt and prolongation of the following acylation reaction to 6 h instead of 2 h did not yield the expected product. In these reactions the *N*-benzoyl morpholine could be isolated unspent. Therefore, both *trans*-AB_2C porphyrin amino acid esters (**3c** and **3h**) were obtained according to an established route by Moore *et al.* for porphyrin amino acid ester preparation with Ar = 2,4,6-$C_6H_2Me_3$ at B positions (**3c**).[171] This synthetic route is however much more time consuming than the first one. It requires repeated desymmetrization of a *trans*-A_2B_2 porphyrin diester (**1c** and **1h**) to get high yields of porphyrin mono acids **2c** and **2h** (Scheme 2, route B).

Linkage of the porphyrin amino acid building blocks via amide bonds to give artificial LHC and RC enables not only vectorial design of well-defined rigid multicomponent conjugates and simple extension of devices with a further chromophor but also the synthesis of such oligopeptides on solid-phase in the future.

Figure 22 depicts the emission data of *N*-Acetyl (Ac) protected reference free-base **Ac-3** (Figure 22 a) and zinc(II) metallated **Zn-Ac-3** (Figure 22 b) compounds. A slight hypsochromic shift is observed for the free-base porphyrin series **Ac-3a→Ac-3h** with increasing electron withdrawing power of the B-Ar-substituents due to enlargement of the HOMO−LUMO energy gap. In zinc(II) complexes, the situation is less clear. Although the blue shift of the emission bands for compounds with fluorine-free substituents is observable here, but for the porphyrins with Ar = 4-C_6H_4F (**3f**) and C_6F_5 (**3h**) this trend is not followed. This discrepancy from the expected trend might be explained by intermolecular F···Zn interactions. The first excited singlet state (S_1) of the porphyrin zinc complexes is energetically higher than that of free-base porphyrins by ca. 0.15 eV, hence zinc derivatives are better electron donors than their free-base analogous.

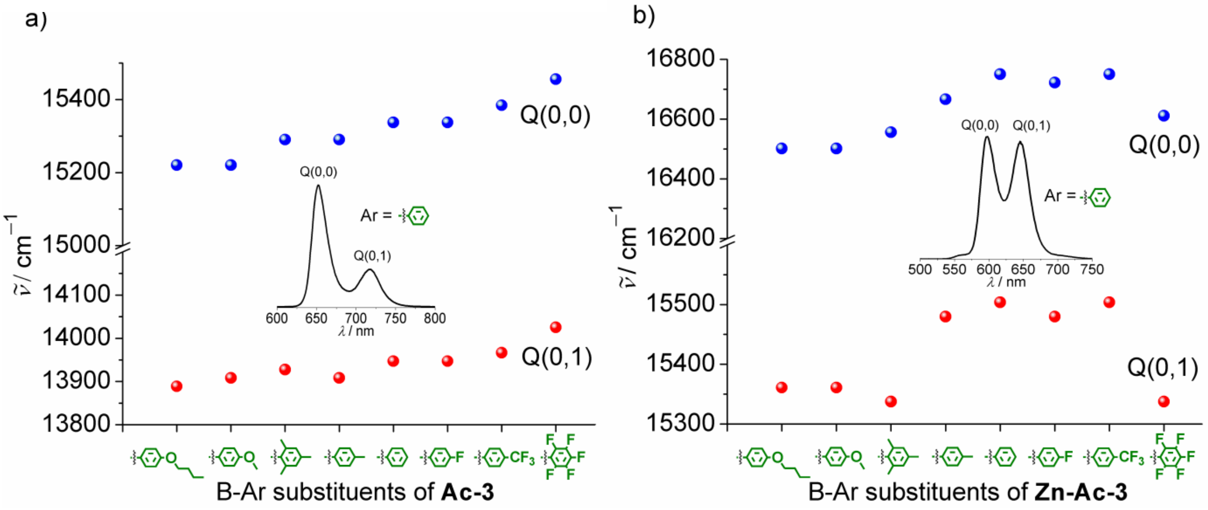

Figure 22. a) Emission data of **Ac-3a** − **Ac-3h**. Inset: emission spectrum of **Ac-3e**. b) Emission data of **Zn-Ac-3a** − **Zn-Ac-3h**. Inset: emission spectrum of **Zn-Ac-3e**. All spectra were measured in CH_2Cl_2 at room temperature.

The cyclic voltammograms of porphyrin amino acid esters often show irreversible oxidation peaks due to an electrochemical polymerisation via the amino function.[172,173] Thus, the electrochemical measurements of reference compounds are indispensable for estimation of the ET driving force. The cyclic voltammograms of *N*-acetyl protected building blocks show four reversible redox waves (Figure 23 insets). The influence of Ar substituents on the porphyrin first oxidation and reduction potentials is depicted in Figure 23. The redox waves are shifted to higher potentials with increasing electron withdrawing character of Ar substituents for free-base as well as for zinc(II) compounds. The redox potentials of zinc(II) complexes are shifted to lower values by ca. 0.2 V compared to the free-base porphyrins. Hence, they are better electron donors and worse electron acceptors than the corresponding free-base porphyrins (*vide supra*).

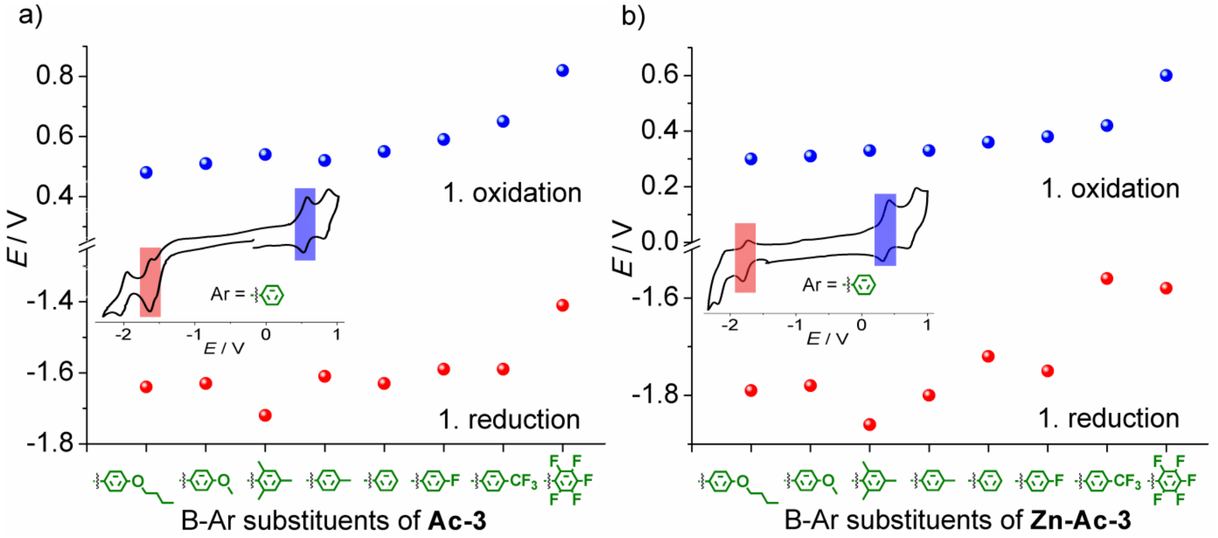

Figure 23. a) First Oxidation and first reduction potentials of **Ac-3a** – **Ac-3h**. Inset: cyclic voltam-mogram of **Ac-3e**. b) First Oxidation and first reduction potentials of **Zn-Ac-3a** – **Zn-Ac-3h**. Inset: cyclic voltammogram of **Zn-Ac-3e**. All measurements were performed in $(n\mathrm{Bu}_4\mathrm{N})(\mathrm{PF}_6)/\mathrm{CH}_2\mathrm{Cl}_2$ at room temperature. Potentials are given *vs.* $\mathrm{Fc/Fc}^+$.

3.2 Synthesis and Properties of Bis(porphyrins)

In project 3.2 the synthesis and electronic communication within ground and excited states in amide bridged free-base, monometallated and fully metallated bis(porphyrins) ($(M)P^{Ar1}$-$(M)P^{Ar2}$) with M = 2H and / or Zn (**4a** – **4d**, **Zn^2-4d** and **Zn^{1}Zn^2-4d**) are presented.

The porphyrin amino acid esters with varying electron donating and electron withdrawing Ar substituents at B positions (**3c** and **3f** − **3h**) were coupled to porphyrin acids with Ar = 2,4,6-$C_6H_2Me_3$ (**2c**) or C_6F_5 (**2h**) leading to **4a** – **4d**. As activation reagent for the porphyrin acids Ghosez's reagent[174] (1-(chloro-2,*N*,*N*-trimethyl-1-propene-1-amine) was used. As no free HCl is formed during the amide synthesis, this route is also applicable with the acid-labile zinc complex **(Zn)-3f** as the amine component giving the monometallated bis(porphyrin) **Zn^2-4d**. The derivative **Zn^{1}Zn^2-4d** was successfully synthesized by metalation of **Zn^2-4d**. Figure 24 shows the synthesized bis(porphyrins) **4a – 4d**, **Zn^2-4d** and **Zn^{1}Zn^2-4d**.

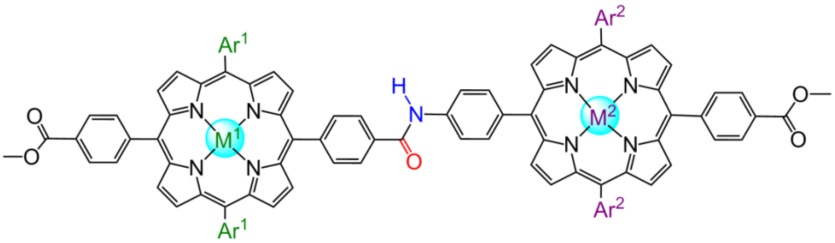

4a: Ar^1 = 2,4,6-$C_6H_2Me_3$ / Ar^2 = C_6F_5 / M^1 = M^2 = 2H
4b: Ar^1 = C_6F_5 / Ar^2 = 2,4,6-$C_6H_2Me_3$ / M^1 = M^2 = 2H
4c: Ar^1 = C_6F_5 / Ar^2 = 4-$C_6H_4CF_3$ / M^1 = M^2 = 2H
4d: Ar^1 = 2,4,6-$C_6H_2Me_3$ / Ar^2 = 4-C_6H_4F / M^1 = M^2 = 2H
Zn^2-4d: Ar^1 = 2,4,6-$C_6H_2Me_3$ / Ar^2 = 4-C_6H_4F / M^1 = 2H / M^2 = Zn
Zn^{1}Zn^2-4d: Ar^1 = 2,4,6-$C_6H_2Me_3$ / Ar^2 = 4-C_6H_4F / M^1 = M^2 = Zn

Figure 24. Structures of bis(porphyrins) **4a – 4d**, **Zn^2-4d** and **Zn^{1}Zn^2-4d**.

Attempts to synthesize monometallated bis(porphyrin) **Zn^1-4d** by amide coupling from the zincated porphyrin acid with Ar^1 = 2,4,6-$C_6H_2Me_3$ (**Zn-2c**) and porphyrin amino acid ester with Ar^2 = 4-C_6H_4F (**3f**) were unsuccessful because of the high acid instability of the respective zinc porphyrin complex. Activation of the zinc porphyrin acid by Ghosez's reagent led to porphyrin demetalation and only yielded the bis(free-base porphyrin) **4d** (Scheme 3, attempt 1). Dyade coupling by activation with Ghosez's reagent under basic conditions prevents demetalation of **Zn-2c** but no amide bond was formed at all (Scheme 3, attempt 1). Similarly, no bis(porphyrin) was obtained after activation of **Zn-2c** by 2-(7-aza-1H-benzotriazole-1-yl)-1,1,3,3-tetramethyluronium hexafluorophosphate (HATU) (Scheme 3, attempt 2).

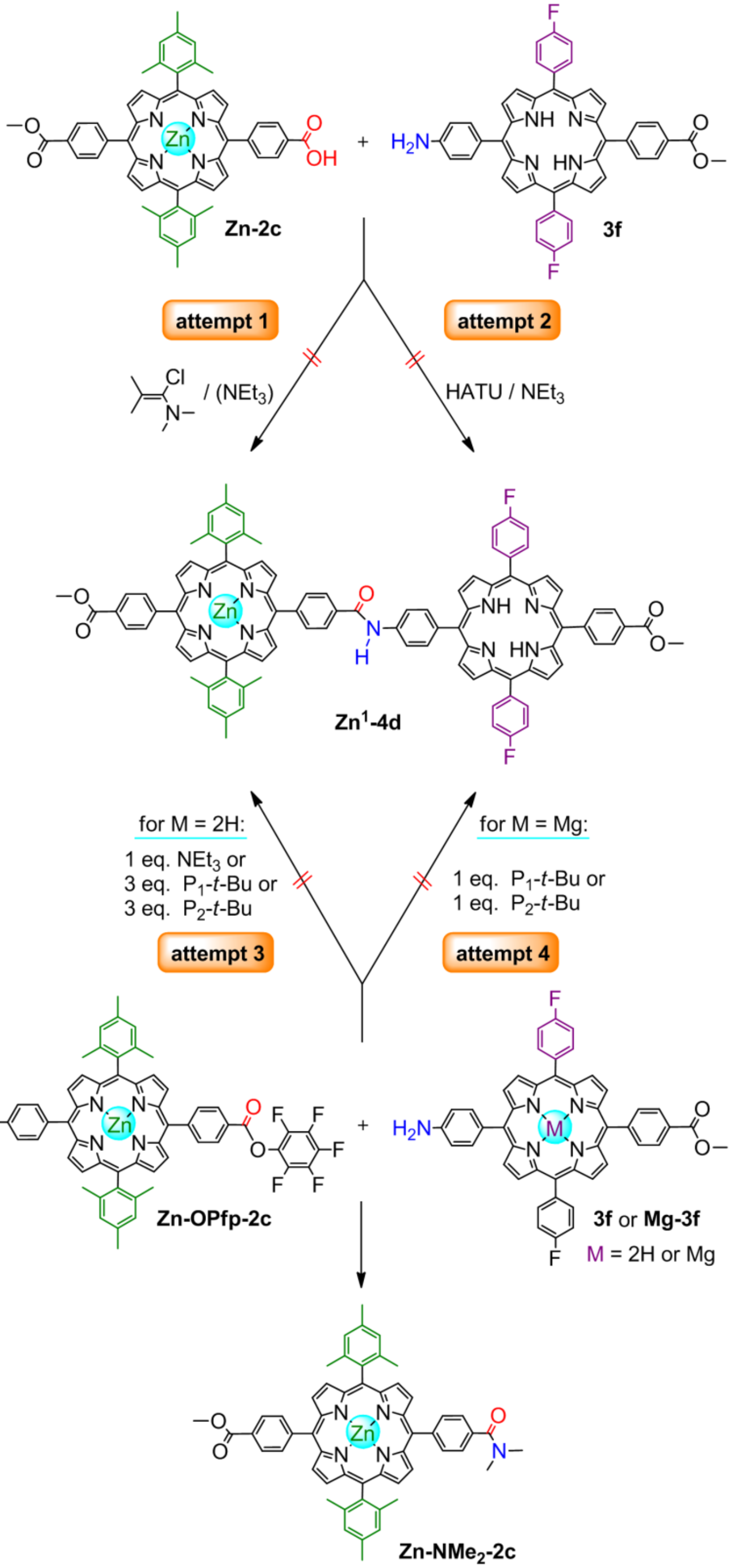

Scheme 3. Synthesis attempts for **Zn^1-4d**.

Reaction of the pentafluorophenyl ester activated zinc porphyrin acid (**Zn-OPfp-2c**) with **3f** deprotonated by three equivalents of *tert*-butylimino-tris(dimethylamino)phosphorane (P_1-*t*-Bu)[175] or three equivalents of 1-*tert*-butyl-2,2,4,4,4-pentakis(dimethylamino)-2λ^5,4λ^5-catenadi (phosphazene) (P_2-*t*-Bu)[175] (three equivalents of phosphazene base are necessary due to deprotonation of inner pyrrole protons) led to the formation of [5-(4-(*N*,*N*-dimethylcarbonylphenyl))-10,20-bis(2,4,6-trimethylphenyl)-15-(4-(methoxycarbonylphenyl)) porphyrinato] zinc(II) (**Zn-NMe$_2$-2c**) and **3f** which could be re-isolated from the reaction mixture (Scheme 3, attempt 3). To reduce the amount of phosphazene bases to one equivalent magnesium(II) protected derivate of **3f** (**Mg-3f**) was prepared. Magnesium porphyrin complexes are less stable under acid condition then zinc (II) complexes und magnesium can be easily removed by stirring of a magnesium porphyrin solution with silica gel.[176,177] However, the amide coupling reaction under these conditions also gave only [5-(4-(*N*,*N*-dimethylcarbonylphenyl))-10,20-bis(2,4,6-trimethylphenyl)-15-(4-(methoxycarbonylphenyl)) porphyrinato] zinc(II) (**Zn-NMe$_2$-2c**) as the product and **Mg-3f** could be re-isolated (Scheme 3, attempt 4). Hence, the isomer of **Zn^2-4d Zn^1-4d** could not be obtained.

A comparison of absorption data of bis(porphyrins) with those of the reference porphyrin derivatives indicates only weak electronic interaction between the two chromophores in the ground state. The absorption spectrum *e.g.* of **Zn^2-4d** is interpreted as simple superposition of the absorption spectra of the two constituent chromophores. However, this is not the case for the emission spectra of the conjugates due to efficient excitation energy transfer between the building blocks (Figure 25a). Fluorescence is almost exclusively observed from the porphyrin unit with the lowest energy S_1 state which is shown exemplarily for **4b** in Figures 25b and 25c. The fluorescence spectrum of **Zn^{1}Zn^2-4d** neither matches with those of its components nor a superposition of them. DFT calculation for this bis(porphyrin) shows pairwise degenerate frontier orbitals and delocalization of its local HOMOs. This could explain the differing excited state feature of **Zn^{1}Zn^2-4d**.

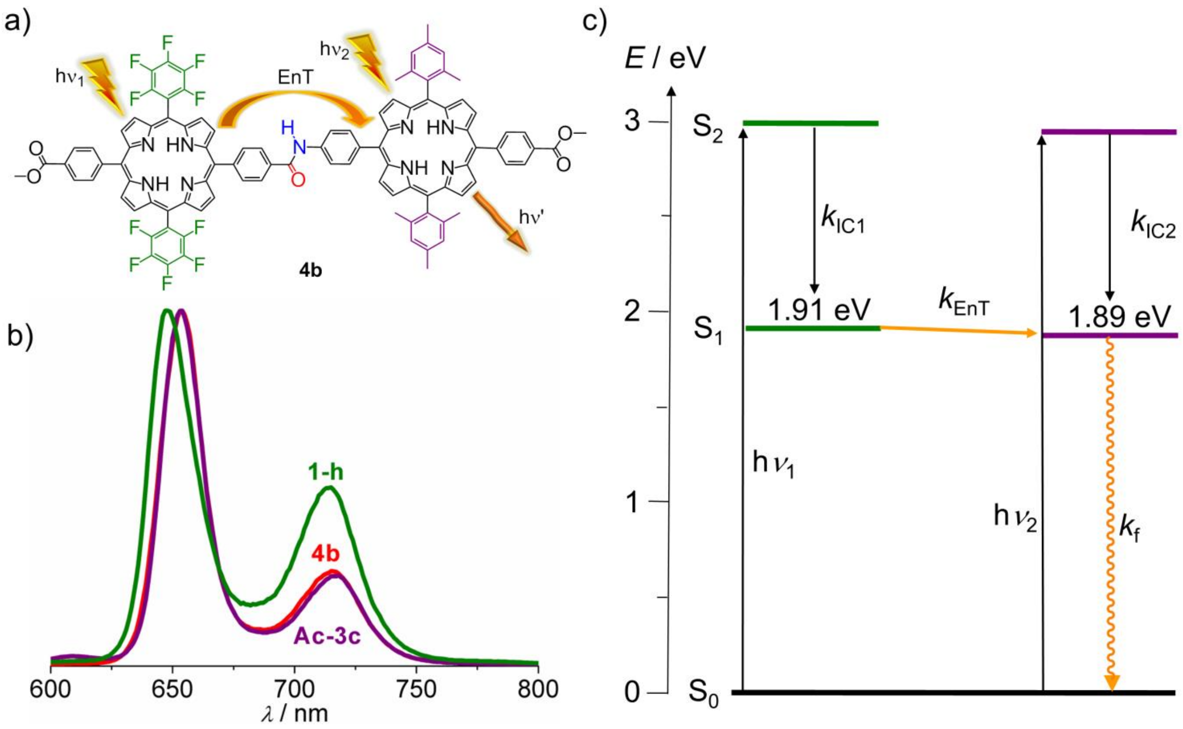

Figure 25. a) Schematical depiction of EnT in **4b**. b) Normalized emission spectra of **4b** and its constituent porphyrins in CH_2Cl_2 at room temperature. c) Energy level diagram for **4b**.

Oxidation and reduction of bis(porphyrins) occurs at the respective building block sites as predicted by electrochemical measurements, EPR studies and by DFT calculations. For example, in compound **4b** the positive charge after oxidation is located at the porphyrin unit with 2,4,6-$C_6H_2Me_3$ substituents and the negative charge after reduction at the building block with C_6F_5 residues.

The results of this research regarding substituent effects on porphyrin electron density are very important for the modular design of electron transfer (ET) capable artificial RC model compounds, which will be discussed in Chapters 3.3 and 3.4.

Publication 6.1: J. Melomedov, A. Wünsche von Leupoldt, M. Meister, F. Laquai, K. Heinze, *Dalton. Trans.* **2013**, *42*, 9727-9739.

3.3 Synthesis and Properties of PET Capable Anthraquinone-Porphyrin-Ferrocene Constructs

In Chapter 3.3 novel and versatile bioinspired electron-transfer systems based on *trans*-AB_2C porphyrin amino acid esters (P^{Ar}) are presented. Besides porphyrins, these multi-step ET arrays (**6**) are composed of anthraquinone (Q) as electron acceptor (A) and aminoferrocene[178] (Fc) moiety as electron donor (D). To increase the porphyrin S_1 state energy, zinc(II) derivatives (**Zn-6**) of amide bridged Q-P^{Ar}-Fc triads were prepared. The extension of the triad was achieved by introducing a further porphyrin entity giving the tetrad Q-P^{Ar1}-P^{Ar2}-Fc (**7**) with $Ar^1 = C_6H_5$ and $Ar^2 = 4\text{-}C_6H_4Me$. These compounds with tunable electron density at the porphyrin moiety are developed to mimic essential steps in photosynthetic RC (Chapter 1.1). Figure 26 depicts the structures of the ET triads **6** and **Zn-6**.

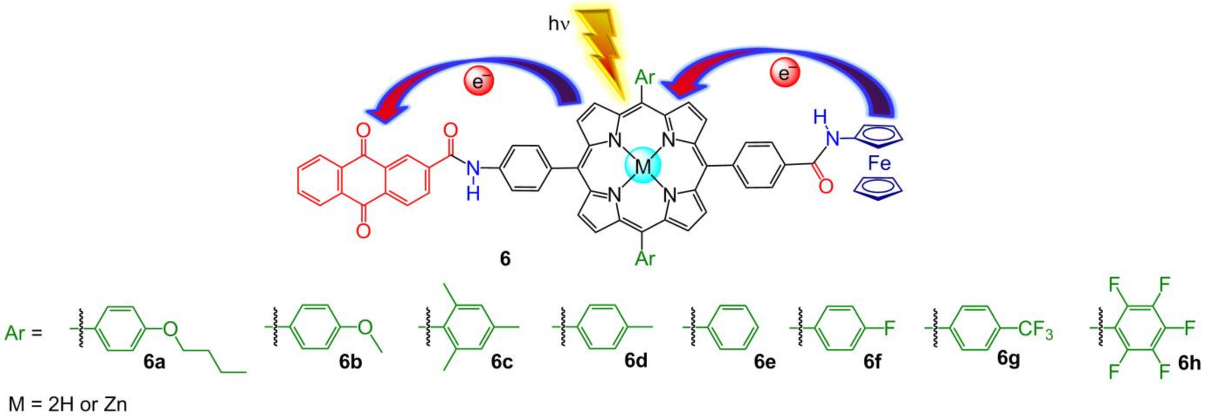

Figure 26. Structure of Q-(M)P^{Ar}-Fc triads **6** with M = 2H or Zn.

The electronic absorption spectra of Q-P^{Ar} dyads (**5**) (precursor for the triad preparation), Q-(M)P^{Ar}-Fc triads **6**, **Zn-6** and Q-P^{Ar1}-P^{Ar2}-Fc tetrad **7** are dominated by the porphyrin absorption bands. The bands of anthraquinone ((λ_{max}(*N*-ethyl-anthraquinone-2-carboxylic acid amide) = 328 nm, $\varepsilon = 5300$ M^{-1} cm^{-1}) and ferrocene (λ_{max}(1-(acetylamino)ferrocene) = 441 nm, $\varepsilon = 215$ M^{-1} cm^{-1}) [180] moieties are not discernible in the absorption spectra of the arrays. The absorption and electrochemical data suggest only weak ground state electronic interactions between the building blocks. However, the linking of quinone and ferrocene to porphyrin leads to a decrease of the porphyrin fluorescence intensity and, hence, indicates the presence of a new non-radiative decay channel (PET). The emission quenching efficiency strongly depends on the electron density of the porphyrin moiety (Figure 27). The oxidative PET pathway (porphyrine to quinone) is most efficient in compounds with electron donating Ar substituents at B positions, whilst the reductive PET pathway (ferrocene to porphyrine) is favorable in triads with a strong electron withdrawing character of Ar substituents. The PET quantum yields of triads are almost 100%.

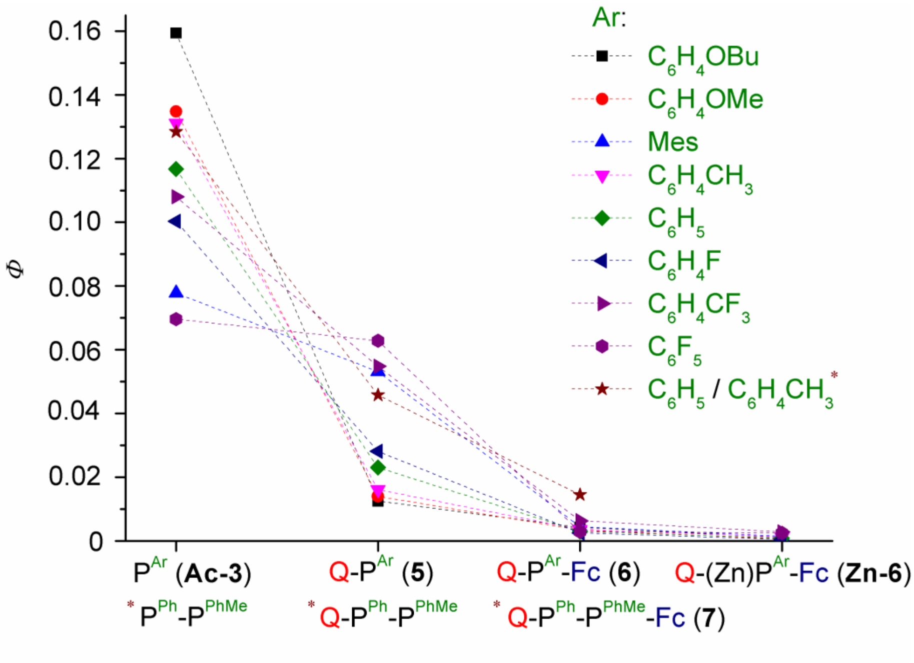

Figure 27. Fluorescence quenching in the Q-P dyads (**5**), Q-(M)P^{Ar}-Fc triads (**6** and **Zn-6**), Q-P^{Ph}-P^{PhMe} triads and Q-P^{Ph}-P^{PhMe}-Fc tetrad (**7**) compared with corresponding porphyrin reference compounds Ac-P^{Ar} (**Ac-3**) and P^{Ph}-P^{PhMe}.

The presented dyads, triads and tetrad can function not only as artificial multi-redox photosystems with efficient intramolecular ET, they are also potentially capable of molecular sensing or switching applications.

Publication 6.2: J. Melomedov, J. R. Ochsmann, M. Meister, F. Laquai, K. Heinze, *Eur. J. Inorg. Chem.* **2014**, 1984-2001.

3.4 Synthesis and Properties of PET Capable Porphyrin-Ferrocene and Porhyrin-Ferrocene-Porphyrin Constructs with Different Ferrocene Electron Donors

The focus of Chapter 3.4 is the detailed investigation of the reductive ET (ferrocene to excited porphyrin) at novel porphyrin-ferrocene conjugates with different ferrocene electron donors and porphyrin electron acceptors with tunable electron density at Ar substituents at B positions. Aminoferrocene (Fc)[178] (Chapter 3.3) and *N*-Fmoc protected 1,1'-ferrocene amino acid[179] (Fmoc-Fc-CO_2H) were used as electron donors and attached to the porphyrin moieties via an amide bond giving the corresponding dyads P^{Ar}-Fc with Ar = 2,4,6-$C_6H_2Me_3$ and C_6F_5 (**8c** and **8h**) and Fmoc-Fc-P^{Ar1} conjugates with Ar^1 = C_6H_5, 4-C_6H_4F, 4-$C_6H_4CF_3$, C_6F_5 (**9e − 9h**). The latter ferrocene derivatives allow the extension of the Fmoc-Fc-P^{Ar1} constructs to the hinges P^{Ar2}-Fc-P^{Ar1} (**10e** and **10f**) with Ar^2 = 2,4,6-$C_6H_2Me_3$. Dyads **8** and hinges **10** were metallated with zinc(II) to the corresponding zinc complexes (Zn)P^{Ar}-Fc (**Zn-8c** and **Zn-8h**) and (Zn)P^{Ar2}-Fc-(Zn)P^{Ar1} (**Zn-10e** and **Zn-10f**). Figure 28 gives an overview over the prepared model compounds.

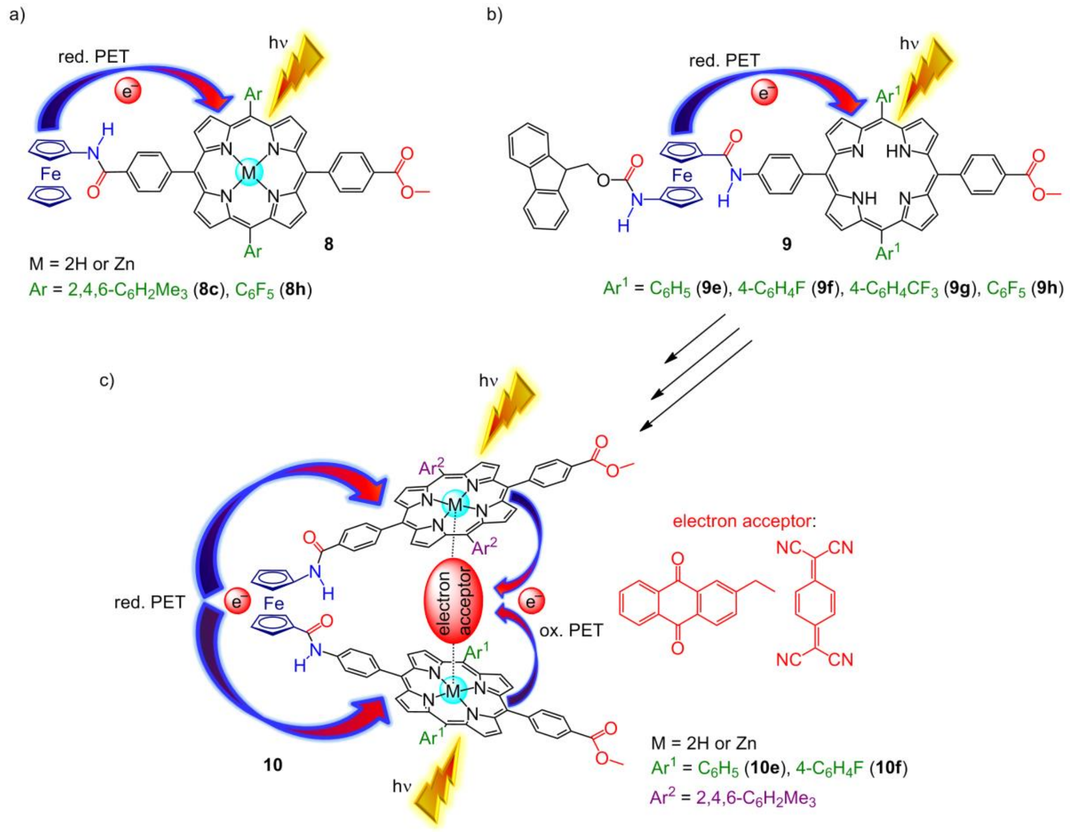

Figure 28. a) Structure of (M)P-Fc dyads **8c** and **8h** with M = 2H or Zn. b) Structure of Fmoc-Fc-P^{Ar1} conjugates **9e** − **9h**. c) Structure of (M)P^{Ar2}-Fc-(M)P^{Ar1} hinges **10e** and **10h** with M = 2H or Zn.

As discussed for the absorption spectra of Q-(M)P-Fc triads in Chapter 3.3, no absorption bands of ferrocene entities could be observed for porphyrin-ferrocene dyads and hinges. The porphyrin emission in the compound series **8**, **Zn-8** and **9** is strongly quenched by reductive PET. The decrease of the fluorescence quantum yields for arrays with the electron withdrawing substituents C_6F_5 is the strongest. Attachment of the second porphyrin in **10** leads to an increase of fluorescence intensity compared to the corresponding Fmoc-Fc-P^{Ar1} precursors.

DFT calculations show the alignment of the local porphyrin frontier orbital energies for the hinges. Thus, it is assumed that the generation of P^{Ar2}-$Fc^{\cdot+}$-$P^{Ar1\cdot-}$ or $P^{Ar2\cdot-}$-$Fc^{\cdot+}$-P^{Ar1} CS states after excitation is equally probable. IR measurements of **Zn-10e** in CH_2Cl_2 demonstrated that besides the “open hinge” structure an intramolecular hydrogen-bonded (IHB) ring “closed hinge” (V-shape) coexists which is characteristic for 1,1’ disubstituted ferrocene amides in weakly coordinating solvents.[179,180] According to a DFT optimization the V-shaped structure is only 7 kJ mol^{-1} less stable than the extended one. Based on these results host-guest complexes of **10e** and **Zn-10e** with *N*-ethyl-anthraquinone-2-carboxylic amide (Q) and 7,7,8,8-tetracyanoquinodimethane (TCNQ) as electron acceptors were targeted and PET from ferrocene via porphyrin entities to the noncovalently bonded guest was investigated. The binding between electron acceptor and hinges was studied by UV/Vis and fluorescence titrations.

Treatment of **Zn-10e** with various amounts of quinone neither results shifts, significant band-width or intensity changes of the Soret or Q bands, nor in CT bands in the UV/Vis spectra. Such changes would have been expected by the potential formation of the host-guest sandwich π-complex **Zn-10e·Q** by bonding of Q between the two porphyrins with a molar ratio of hinge: Q = 1 : 1 (Figure 29a). Only the expected increase of the quinone’s absorption bands intensity at 258 and 327 nm during the titration is observed. Even in the presence of a 1600-fold excess of Q-guest, no changes in the porphyrin absorption features or the appearance of zinc(II) porphyrin radical cation bands is detected. This observation was confirmed by fluorescence spectroscopy. Addition of Q led only to a marginal porphyrin emission quenching below 1% compared with the host emission (Figure 29b).

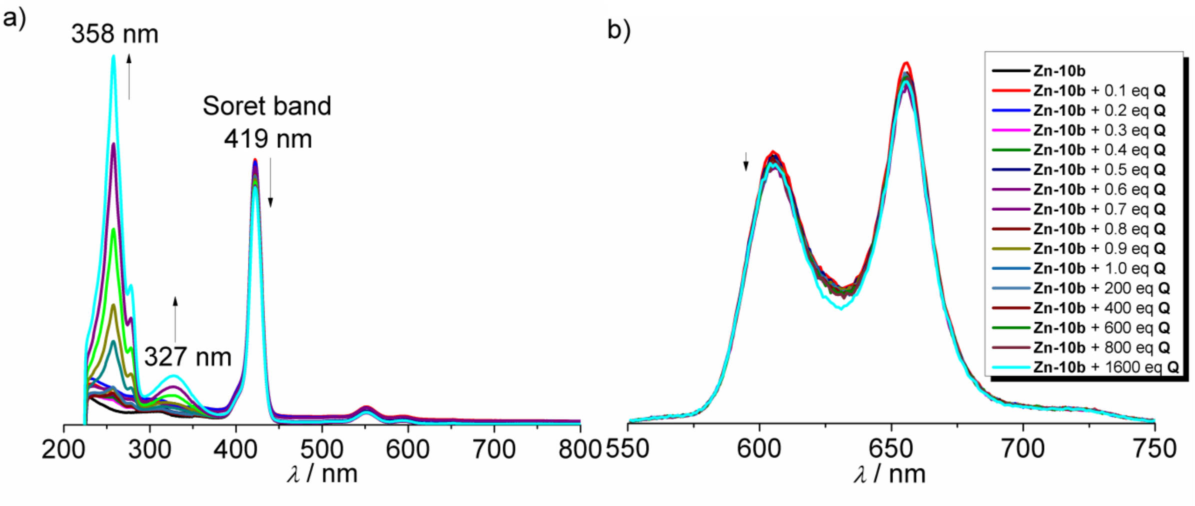

Figure 29. a) Absorption spectra of **Zn-10e** with different concentration of Q. b) Emission spectra of **Zn-10e** with different concentration of Q.

For a further attempt to design a charge-transfer complex with hinges, a quinone-related 7,7,8,8-tetracyanoquinodimethane (TCNQ) was used as strong electron acceptor.[155-158,160,164] However, Figure 30a shows no absorption spectral changes characteristic for the formation of a 1:1 host-guest complex of **10e·TCNQ**. Also no CT bands are detected during titration of **10e** with TCNQ by absorption spectroscopy with this molar ratio as well as with great excess of TCNQ. Only the expected increase of the TCNQ absorption band intensity at 403 nm during titration is observed. In the fluorescence spectra for the hinge-acceptor system only a slight intensity reduction of 8% was observed after addition of 1400 eq. TCNQ compared to fluorescence of untreated **10e** (Figure 29b), which excludes an efficient PET process from porphyrins to TCNQ.

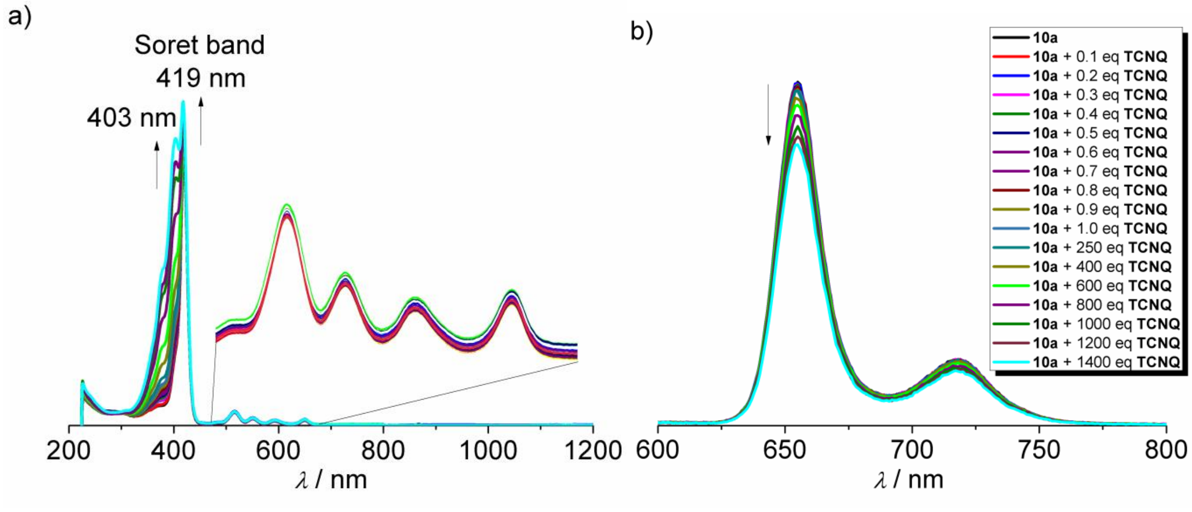

Figure 30. a) Absorption spectra of **10e** with different concentrations of TCNQ. b) Emission spectra of **10e** with different concentrations of TCNQ.

Similar observations were made after the treatment of **Zn-10e** with TCNQ. The emission quenching after the addition of 1400 eq. TCNQ to **Zn-10e** was even less than for **10e**. It amounts to 4% in comparison with untreated **Zn-10e**.

In summary, no evidence could be observed for a formation of **Zn-10e·Q** or **M-10e·TCNQ** (M = 2H or Zn) sandwich complexes or PET capable supramolecular architectures in the presence of an excess of the electron acceptors Q or TCNQ. This can be explained by a low affinity of **M-10** to the guests via uncharged quinone oxygen atoms to porphyrin's zinc, a too rapid energy transfer to the Fc moiety, a non-optimal cavity size or steric effects of 2,4,6-$C_6H_2Me_3$ substituents, which hinders the guest inclusion into the cavity and formation of higher order assemblies.

Publication 6.3: J. Melomedov, J. R. Ochsmann, M. Meister, F. Laquai, K. Heinze, *Eur. J. Inorg. Chem.* **2014**, accepted.

4 Outlook

Design and fabrication of photosynthetic RCs is an innovative and promising field of photosynthesis research. Based on the presented preparative, electrochemical, spectroscopic and theoretical results novel artificial RC systems with *trans*-AB_2C substituted porphyrin amino acids as building blocks with a long-living CS state can be designed.

As a highly efficient electron acceptor C_{60} ($E_{½} \approx -100$ mV in THF *vs.* Fc/Fc^+)[87,88,107-135] may be utilized due to a small reorganization energy (Chapter 1.4 and 1.6.3.3). In contrast to the $Q^{\cdot -}$ radical anion the $C_{60}^{\cdot -}$radical anion is also ascertainable by transient absorption techniques.[109,110,112-135]

For further development of ET capable architectures, aminobiferrocene or *C*-protected 1’-aminobiferrocene-1’’’-carboxylic acid $(Fc)_2$[181] can be proposed as a suitable electron donors. Oxidation of the first ferrocene unit of *C*-protected 1’-aminobiferrocene-1’’’-carboxylic acid is at about $E_{½} \approx -200$ mV in CH_2Cl_2 *vs.* Fc/Fc^+[181] and that one of aminobiferrocene is expected to be below this value. Hence, both biferrocenes are highly suitable electron donors and even more favourable than aminoferrrocene. Since the mixed-valent radical cation $(Fc)_2^{\cdot +}$ absorbs in the spectral region between 1400 and 1700 nm[181], where no overlay with porphyrin and fullerenene signals are possible, it might be amenable to transient absorption measurements despite of its low extinction coefficient ($\varepsilon < 1000\ M^{-1}cm^{-1}$).[181]

In order to extend the CS life time, the distance between electron acceptor and electron donor can be increased by introducing a directional porphyrin chromophor bridge consisting of three porphyrin unities (*e.g.* C_6F_5, 4-C_6H_4F and 4-C_6H_4OMe). A targeted metalation of the porphyrin with electron rich B-Ar subtituents (4-C_6H_4OMe) with zinc(II) ensures the multi-step downhill ET along the redox gradient in the C_{60}-P^{C6F5}-P^{C6H4F}-(Zn)$P^{C6H4OMe}$-$(Fc)_2$ pentad. Figure 31 depicts the proposed structure of an artificial RC.

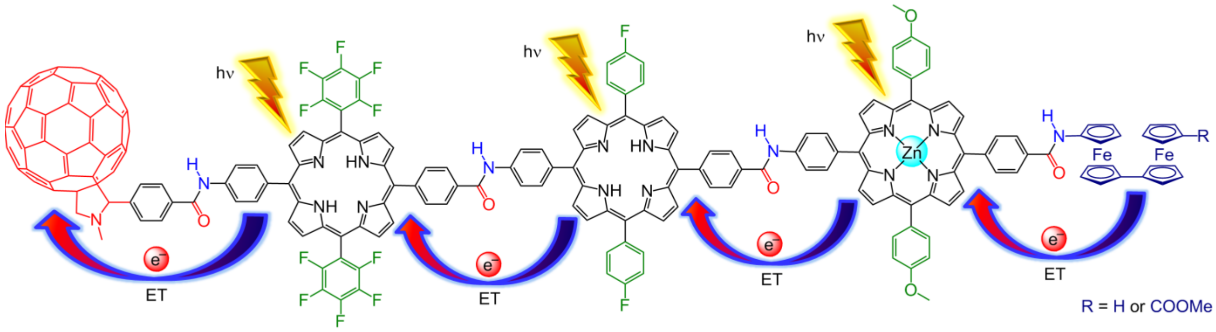

Figure 31. Structure of proposed sophisticated artificial RC C_{60}-P^{C6F5}-P^{C6H4F}-(Zn)$P^{C6H4OMe}$-$(Fc)_2$.

Au^{III} porphyrins are very efficient electron acceptors in (Au^{III})P-(M)P bisporphyrins (M = 2H or Zn) due to a low first porphyrin reduction potential of (Au^{III})P in comparison to the (M)P.[146-154]

Also an energy transfer between the porphyrin entities is not feasible or at least strongly hampered (Chapter 1.6.3.1).[146-154] Combining the Au^{III} accepting properties with directional porphyrin chromophor bridge and electron donating features of ferrocene derivatives in the (Au^{III})P^{C6F5}-P^{C6H4F}-(Zn)P^{C6H4OMe}-Fc array (Figure 32) should give an excellent model compound with long-lived final CS state.

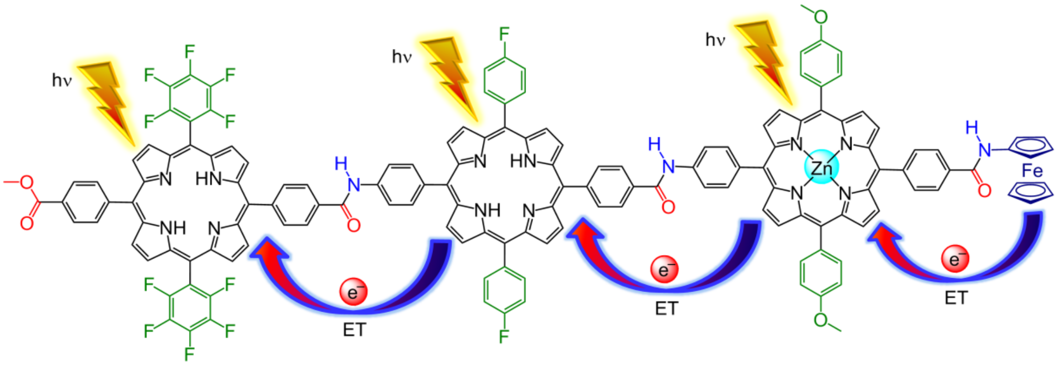

Figure 32. Structure of proposed sophisticated artificial RC (Au^{III})P^{C6F5}-P^{C6H4F}-(Zn)P^{C6H4OMe}-Fc.

In the tetrad (Au^{III})P^{C6F5}-P^{C6H4F}-(Zn)P^{C6H4OMe}-Fc the preferred initial PET pathways ((Au^{III})P^{C6F5}←P^{C6H4F} *vs.* (Zn)P^{C6H4OMe}←Fc) and the location of the negative charge (Au^{III}/Au^{II}) *vs.* P^{C6F5}/ P$^{C6F5\cdot -}$) after ET are to investigate by means of EPR spectroscopy.

Artificial RCs can be further modified by using cobaltocenium carboxylic acid (Cc^{+}) as suitable electron acceptor with $E_{½} \approx -1.15$ V in CH_3CN *vs.* Fc/Fc^{+}[182] to give [Cc-P^{C6H4F}-(Zn)P^{C6H4OMe}-Fc]$^{+}$ tetrad with two different metallocenes and a directional porphyrin chromophor bridge between them. (Figure 33).

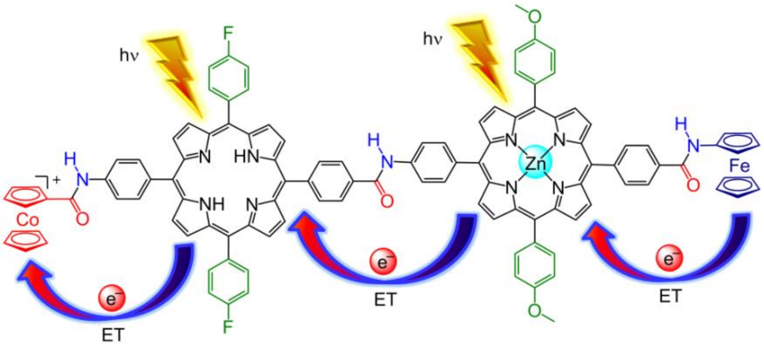

Figure 33. Structure of proposed sophisticated artificial RC [Cc-P^{C6H4F}-(Zn)P^{C6H4OMe}-Fc]$^{+}$.

This work lays the foundation for such advanced photosynthetic RCs.

5 References

[1] H. Michel, *J. Mol. Biol.* **1982**, *158*, 567-572.
[2] J. Deisenhofer, *J. Mol. Biol.* **1984**, *180*, 385-398.
[3] J. Deisenhofer, O. Epp, K. Mikki, R. Huber, H. Michel, *Science* **1985**, *318*, 618-624.
[4] J. Deisenhofer, H. Michel, *EMBO J.* **1989**, *8*, 2149-2170.
[5] J. Deisenhofer, O. Epp, I. Sinning, H. Michel, *J. Mol. Biol.* **1995**, *246*, 429-457.
[6] C. Roy D. Lancaster, H. Michel, *J. Mol. Biol.* **1999**, *286*, 883-898.
[7] J. Deisenhofer, H. Michel, *Science* **1989**, *245*, 1463-1473.
[8] C.-H. Chang, O. El-Kabbani, D. Tiede, J. Norris, M. Schiffer, *Biochemistry*, **1991**, *30*, 5353-5360.
[9] A. J. Chirino, E. J. Lous, M. Huber, J. P. Allen, A. C. C. Schenck, M. L. Paddock, G. Feher, D. C. Rees, *Biochemistry* **1994**, *33*, 4584-4593.
[10] B. Arnoux, J.-F. Gaucher, A. Ducrnaud, *Acta Cryst.* **1995**, *51*, 368-379.
[11] M. H. B. Stowell, T. M. McPhillips, D. C. Rees, S. M. Soltis, E. Abresch, G. Feher, *Science* **1997**, 276, 812-816.
[12] J. Tandori, P. Maroti, E. Alexov, P. Sebban, L. Baciou, *PNAS* **2002**, *99*, 6702-6706.
[13] A. W. Roszak, T. D. Howard, J. Southall, A. T. Gardiner, C. J. Law, N. W. Isaacs, R. J. Cogdell, *Science* **2003**, *302*, 1463-1972.
[14] R. J. Cogdell, A. Gall, J. Köhler, *Quart. Rev. Biophys.* **2006**, *39*, 227-324.
[15] I. McConnell, G. Li, G. W. Brudvig, *C & B* **2010**, 434-447.
[16] B. Neupane, P. Jaschke, R. Saer, J. T. Beatty, M. Reppert, R. Jankowiak, *J. Phys. Chem. B* **2012**, *116*, 3457-3466.
[17] J. Pan, S. Lin, N. W. Woodbury, *J. Phys. Chem. B* **2012**, *116*, 2014-2022.
[18] P. Lanciano, B. Khalfaoui-Hassani, N. Selamoglu, F. Daldal, *Biochemistry* **2013**, *52*, 7196-7206.
[19] F. Schmidt, *Biochemistry I*, IDG Books Worldwide, Inc. **2000**.
[20] F. Schmidt, *Biochemistry II*, IDG Books Worldwide, Inc. **2000**.
[21] H. R. Horton,L. A. Moran, K. G. Scrimgeour, M. D. Perry, J. David Rawn, *Principles of biochemistry*, Pearson Education, Inc., 4th ed. **2006**.
[22] A. R. Battersby, C. J. R. Fookes. G. W. J. Matcham, E. McDonald, *Nature* **1980**, *285*, 17-21.
[23] K. M. Kadish, K. M. Smith, R. Guilard, *Handbook of Porphyrin Science*, World Scientific Publishing Co. Pte. Ltd. **2010**.
[24] E. Vogel, *Pure Appl. Chem*. **1993**, *65*, 143-152.
[25] K. M. Kadish, K. M. Smith, R. Guilard, *The Porphyrin Handbook*, Academic Press **2000**.
[26] N. Z. Mamardashvili, O. A. Golubchikov, *Russ. Chem. Rev.* **2001**, *70*, 577-606.
[27] E. B. Fleischer, *Porphyrins and Metalloporphyrins*, Elsevier Publishing Co. **1964**.
[28] M. Gouterman, *J. Chem. Phys*. **1959**, *30*, 1139-1161.
[29] M. Gouterman, *J. Mol. Spectrosc*. **1961**, *6*, 138-163.
[30] K. Heinze, A. Reinhart, *Dalton Trans*. **2008**, 469-480.
[31] C.-Y. Huang, Y. O. Su, *Dalton Trans.* **2010**, *39*, 8306-8312.
[32] M. R. Wasielewski, M. P. Niemczyk, *J. Am. Chem. Soc.* **1984**, *106*, 5046-5045.
[33] E. B. Fleischer, A. Laszlo, *Inorg. Nucl. Chem. Letters* **1969**, *5*, 373-376.
[34] M. E. Jamin, R. T. Iwamoto, *Inorg. Chim. Acta* **1978**, *27*, 135-143.
[35] A. Antipas, D. Dolphin, M. Gouterman, E. C. Johnson, *J. Am. Chem. Soc.* **1978**, *100*, 7705-7709.
[36] R. A. Marcus, *J. Chem. Phys*. **1956**, *24*, 979-989.
[37] R. A. Marcus, *Annu. Rev. Phys. Chem.* **1964**, *15*, 155-196.
[38] R. A. Marcus, *Angew. Chem.* **1996**, *105*, 1161-1172; *Angew. Chem. Int. Ed.* **1993**, *32*, 1111-1121.

[39] R. W. Wagner, J. S. Lindsey, *J. Am. Chem. Soc.* **1994**, *116*, 9759-9760.

[40] A. Tsuda, A. Osuka, *Science* **2001**, *293*, 79-82.

[41] D. Holten, D. F. Bocian, J. S. Lindsey, *Acc. Chem. Res.* **2002**, *35*, 57-69.

[42] Z. Liu, A. A. Yasseri, J. S. Lindsey, D. F. Bocian, *Science* **2003**, *302*, 1543-1545.

[43] M. Jurowa, A. E. Schuckmanb, J. D. Batteasb, C. M. Drain, *Coord. Chem. Rev*. **2010**, *254*, 2297-2310.

[44] J. S. Lindsey, D. F. Bocian, *Acc. Chem. Res.* **2011**, *44*, 638-650.

[45] M. H. Hoang, Y. Kim, M. Kim, K. H. Kim, T. W. Lee, D. N. Nguyen, S.-J. Kim, K. Lee, S. J. Lee, D. H. Choi, *Adv. Mater.* **2012**, *24*, 5363-5367.

[46] M. R. Wasielewski, *Chem. Rev.* **1992**, *92*, 435-461.

[47] D. Gust, T. A. Moore, A. L. Moore, C. Devadoss, P. A. Liddell, R. Hermant, R. A. Nieman, L. J. Demanche, J. M. DeGraziano, I. Gouni, *J. Am. Chem. Soc.* **1992**, *114*, 3590-3603.

[48] D. Gust, T. Moore, A. Moore, *Acc. Chem. Res.* **1993**, *26*, 198-205.

[49] C. A. Hunter, R. K. Hyde, *Angew. Chem.* **1996**, *108*, 2064-2067; *Angew. Chem. Int. Ed.* **1996**, *35*, 1936-1939.

[50] M. D. Ward, *Chem. Soc. Rev.* **1997**, *26*, 365-375.

[51] S. Faure, C. Stern, R. Guilard, P. D. Harvey, *J. Am. Chem. Soc.* **2004**, *126*, 1253-1261.

[52] K. Pettersson, A. Kyrychenko, E. Rönnow, T. Ljungdahl, J. Mártensson, B. Albinsson, *J. Phys. Chem. A* **2006**, *110*, 310-318.

[53] C. P. Gros, F. Brisach, A. Meristoudi, E. Espinosa, R. Guilard, P. D. Harvey, *Inorg. Chem.* **2007**, *46*, 125-135.

[54] P. Kim, J. M. Lim, M.-C. Yoon, J. Aimi, T. Aida, A. Tsuda, D. Kim, *J. Phys. Chem. B* **2010**, *114*, 9157-9164.

[55] F. Brégier, S. M. Aly, C. P. Gros, J.-M. Barbe, Y. Rousselin, P. D. Harvey, *Chem. Eur. J.* **2011**, *17*, 14643-14662.

[56] M. S. Asano, K. Yamashita, M. Kitabayashi, K. Kusama, D. Kagota, K. Sugiura, *Phys. Chem. Chem. Phys.* **2011**, *13*, 12712-12715.

[57] G. Duvanel, J. Grilj, E. Vauthey, *J. Phys. Chem. A* **2013**, *117*, 918-928.

[58] M. Vengris, D. S. Larsen, L. Valkunas, G. Kodis, C. Herrero, D. Gust, T. Moore, A. Moore, R. van Grondelle, *J. Phys. Chem. B* **2013**, *117*, 11372-11382.

[59] J.-M. Camus, A. Langlois, S. M. Aly, R. Guilard, P. D. Harvey, *Chem. Commun.* **2013**, *49*, 2228-2230.

[60] J.-M. Camus, S. M. Aly, D. Fortin, R. Guilard, P. D. Harvey, *Inorg. Chem.* **2013**, *52*, 8360-8368.

[61] X.-L. Zeng, K. Tang, N. Zhou, M. Zhou, H. J. M. Hou, H. Scheer, K.-H. Zhao, D. Noy, *J. Am. Chem. Soc.* **2013**, *135*, 13479-13487.

[62] H. Yoon, J. M. Lim, H.-C. Gee, C.-H. Lee, Y.-H. Jeong, D. Kim, W.-D. Jang, *J. Am. Chem. Soc.* **2014**, *136*, 1672-1679.

[63] D. L. Dexter, *J. Chem. Phys.* **1953**, *21*, 836-850.

[64] S. H. Lin, W. Z. Xiao, *Phys. Rev. E* **1993**, *47*, 3698-3706.

[65] T. Förster, *Naturwissenschaften* **1946**, *33*, 166-175.

[66] T. Förster, *Ann. Phys.* **1948**, *2*, 55-75.

[67] H. M. McConnell, *J. Chem. Phys.* **1961**, *35*, 508-515.

[68] H. Kurreck, M. Huber, *Angew. Chem.* **1995**, *107*, 929-941; *Angew. Chem. Int. Ed.* **1995**, *34*, 849-866.

[69] http://www.rcsb.org/; ID = "1PRC" (accessed on 24.04.2014).

[70] http://www.snakerobots.com (accessed on 24.04.2014).

[71] http://www.nasa.gov/centers/ames/research/exploringtheuniverse/scorpion_robot.html (accessed on 24.04.2014).

[72] http://www.lotusan.de (accessed on 24.04.2014).

[73] A. C. Khazraji, S. Hotchandani, S. Das, P. V. Kamat, *J. Phys. Chem. B* **1999**, *103*, 4693-4700.

[74] H. Imahori, S. Fukuzumi, *Adv. Funct. Mater*. **2004**, *14*, 525-536.

[75] T. Hasobe, H. Imahori, P. V. Kamat, T. K. Ahn, D. Kim, T. Hanada, T. Hirakawa, S. Fukuzumi, *J. Am. Chem. Soc.* **2005**, *127*, 1216-1228.

[76] H. Imahori, T. Umeyama, *J. Phys. Chem. C* **2009**, *113*, 9029-9039.

[77] C.-W. Lee, H.-P. Lu, C.-M. Lan, Y.-L. Huang, Y.-R. Liang, W.-N. Yen, Y.-C. Liu, Y.-S. Lin, E. W.-G. Diau, C.-Y. Yeh, *Chem. Eur. J.* **2009**, *15*, 1403-1412.

[78] Y.-J. Cheng, S.-H. Yang, C.-S Hsu, *Chem. Rev.* **2009**, *109*, 5868-5923.

[79] T. Bessho, S. M. Zakeeruddin, C.-Y. Yeh, E. W.-G. Diau, M. Grätzel, *Angew. Chem.* **2010**, *122*, 6796-6799; *Angew. Chem. Int. Ed.* **2010**, *49*, 6646-6649.

[80] Y.-C. Chang, C.-L. Wang, T.-Y. Pan, S.-H. Hong, C.-M. Lan, H.-H. Kuo, C.-F. Lo, H.-Y. Hsu, C.-Y. Lin, E. W.-G. Diau, *Chem. Commun.* **2011**, *47*, 8910-8912.

[81] D. K. Panda, F. S. Goodson, S. Ray, R. Lowell S. Saha, *Chem. Commun.* **2012**, *48*, 8775-8777.

[82] G. Di Carlo, A. O. Biroli, M. Pizzotti, F. Tessore, V. Trifiletti, R. Ruffo, A. Abbotto, A. Amat, F. De Angelis, P. R. Mussini, *Chem. Eur. J.* **2013**, *19*, 10723-10740.

[83] S. M. Pratik, A. Datta, *Phys. Chem. Chem. Phys.* **2013**, *15*, 18471-18481.

[84] J. P. Collman, P. Denisevich, Y. Konai, M. Marrocco, C. Koval, F. C. Anson, *J. Am. Chem. Soc.* **1980**, *102*, 6027-6036.

[85] M. Grätzel, *Acc. Chem. Res.* **1981**, *14*, 376-384.

[86] J. P. Collman, P. S. Wagenknecht, J. E. Hutchison, *Angev. Chem.* **1994**. *106*, 1620-1639; *Angew. Chem. Int. Ed.* **1995**, *34*, 849-866.

[87] D. Gust, T. A. Moore, A. L. Moore, *Acc. Chem. Res.* **2009**, *42*, 1890-1898.

[88] F. D'Souza, O. Ito, *Chem. Commun.* **2009**, 4913-4928.

[89] M. R.Wasielewski, M. P. Niemczyk, W. A. Svec, E. B. Pewitt, *J. Am. Chem. Soc.* **1985**, *107*, 5563-5565.

[90] A. N. Macpherson, P. A. Liddell, S. Lin, L. Noss, G. R. Seely, J. M. DeGraziano, A. L. Moore, T. A. Moore, D. Gust, *J. Am. Chem. Soc.* **1995**, *117*, 7202-7212.

[91] F. Pollinger, C. Musewald, H. Heitele, M. E. Michel-Beyerle, C. Anders, M. Futscher, G. Voit, H. A. Staab, *Ber. Bunsenges. Phys. Chem.* **1996**, *100*, 2076-2080.

[92] M. Fuchs, J. von Gersdofl, H. Dieks, H. Kurreck, K. Möbius, T. Prisner, *J. Chem. Soc. Faraday Trans.* **1996**, *92*, 949-955.

[93] Y. Sakata, H. Imahori H. Tsue, S. Higashida, T. Akiyama, E. Yoshizawa, M. Aoki, K. Yamada, K. Hagiwara, S. Taniguchi, T. Okadab, *Pure Appl. Chem.* **1997**, *69*, 1951-1956.

[94] D. Kuciauskas, P. A. Liddell, S.-C. Hung, S. Lin, S. Stone, G. R. Seely, A. L. Moore, T. A. Moore, D. Gust, *J. Phys. Chem. B* **1997**, *101*, 429-440.

[95] M. Speck, H. Kurreck, M. O. Senge, *Eur. J. Org. Chem.* **2000**, 2303-2314.

[96] H. Tsue, H. Imahori, T. Kaneda, Y. Tanaka, T. Okada, K. Tamaki, Y. Sakata, *J. Am. Chem. Soc.* **2000**, *122*, 2279-2288.

[97] A. Wiehe, M. O. Senge, A. Schäfer, M. Speck, S. Tannert, H. Kurreck, B. Röder, *Tetrahedron* **2001**, *57*, 10089-10110.

[98] Y. K. Kang, I. V. Rubtsov, P. M. Iovine, J. Chen, M. J. Therien, *J. Am. Chem. Soc.* **2002**, *124*, 8275-8279.

[99] J. Springer, G. Kodis, L. de la Garza, A. L. Moore, T. A. Moore, D. Gust, *J. Phys. Chem. A* **2003**, *107*, 3567-3575.

[100] P. P. Kumar, G. Premaladha, B. G. Maiya, *J. Chem. Sci.* **2005**, *117*, 193-201.

[101] M. R. Wasielewski, *J. Org. Chem.* **2006**, *71*, 5051-5066.

[102] T. Nagasawa, S. I. Allakhverdiev, Y. Kimura T. Nagata, *Photochem. Photobiol. Sci.* **2009**, *8*, 174-180.

[103] R. Borrelli, W. Domcke, *Chem. Phys. Lett.* **2010**, *498*, 230-234.

[104] Y. K. Kanga, P. M. Iovine, M. J. Therien, *Coord. Chem. Rev.* **2011**, *255*, 804-824.

[105] O. Cramariuc, P. J. Aittala, T. I. Hukka, *J. Mol. Model.* **2013**, *19*, 697-704.

[106] A. O. Kichigina, V. N. Ionkin, A. I. Ivanov, *J. Phys. Chem. B* **2013**, *117*, 7426-7435.

[107] H. Imahori, H. Yamada, S. Ozawa, K. Ushida, Y. Sakata, *Chem. Commun.* **1999**, 1165-1166.

[108] H. Imahori, H. Yamada, Y. Nishimura, I. Yamazaki, Y. Sakata, *J. Phys. Chem. B* **2000**, *104*, 2099-2108.

[109] S. Fukuzumi, H. Imahori, H. Yamada, M. E. El-Khouly, M. Fujitsuka, O. Ito, D. M. Guldi, *J. Am. Chem. Soc.* **2001**, *123*, 2571-2575.

[110] H. Imahori, D. M. Guldi, K. Tamaki, Y. Yoshida, C.Luo, Y. Sakata, S. Fukuzumi, *J. Am. Chem. Soc.* **2001**, *123*, 6617-6628.

[111] H. Imahori, H. Norieda, H. Yamada, Y. Nishimura, I. Yamazaki, Y. Sakata, S. Fukuzumi, *J. Am. Chem. Soc.* **2001**, *123*, 100-110.

[112] H. Imahori, K. Tamaki, D. M. Guldi, C. Luo, M. Fujitsuka, O. Ito, Y. Sakata, S. Fukuzumi, *J. Am. Chem. Soc.* **2001**, *123*, 2607-2617.

[113] H. Imahori, K. Tamaki, Y. Araki, Y. Sekiguchi, O. Ito, Y. Sakata, S. Fukuzumi, *J. Am. Chem. Soc.* **2002**, *124*, 5165-5174.

[114] D. M. Guldi, *Pure. Appl. Chem.* **2003**, *75*, 1069-1075.

[115] D. M. Guldi, H. Imahori, K. Tamaki, Y. Kashiwagi, H. Yamada, Y. Sakata, S. Fukuzumi, *J. Phys. Chem. A* **2004**, *108*, 541-548.

[116] H. Imahori, Y. Sekiguchi, Y. Kashiwagi, T. Sato, Y. Araki, O. Ito, H. Yamada, S. Fukuzumi, *Chem. Eur. J.* **2004**, *10*, 3184-3196.

[117] S. Fukuzumi, *Bull. Chem. Soc.* **2006**, *79*, 177-195.

[118] J. D. Megiatto Jr., D. I. Schuster, S. Abwandner, G. de Miguel, D. M. Guldi, *J. Am. Chem. Soc.* **2010**, *132*, 3847-3861.

[119] M. E. El-Khouly, K.-J. Han, K.-Y. Kay, S. Fukuzumi, *Chem. Phys. Chem.* **2010**, *11*, 1726-1734.

[120] J.-Y. Liu, M. E. El-Khouly, S. Fukuzumi, D. K. P. Ng, *Chem. Eur. J.* **2011**, *17*, 1605-1613.

[121] F. D’Souza, A. N. Amin, M. E. El-Khouly, N. K. Subbaiyan, M. E. Zandler, S. Fukuzumi, *J. Am. Chem. Soc.* **2012**, *134*, 654-664.

[122] A. H. Al-Subi, M. Niemi, N. V. Tkachenko, H. Lemmetyinen, *J. Phys. Chem. A* **2011**, *115*, 3263-3271.

[123] S. Fukuzumi, K. Saito, K. Ohkubo, T. Khoury, Y. Kashiwagi, M. A. Absalom, S. Gadde, F. D’Souza, Y. Araki, O. Ito, M. J. Crossley, *Chem. Commun.* **2011**, *47*, 7980-7982.

[124] A. Tolkki, K. Kaunisto, A. Efimov, H. Kivistö, L. Storbacka, R. Savikoski, K. Huttunen, S. Lehtimäki, H. Lemmetyinen, *Phys. Chem. Chem. Phys.* **2012**, *14*, 3498-3504.

[125] D. Pal, A. Ray, S. Bhattacharya, *Spectrochim. Acta Part A*, **2012**, *95*, 317-330.

[126] M. E. El-Khouly, C. A. Wijesinghe, V. N. Nesterov, M. E. Zandler, S. Fukuzumi, F. D. Souza, *Chem. Eur. J.* **2012**, *18*, 13844-13853.

[127] M. Urbani, K. Ohkubo, D. M. S. Islam, S. Fukuzumi, F. Langa, *Chem. Eur. J.* **2012**, *18*, 7473-7485.

[128] A. H. Al-Subi, M. Niemi, N. V. Tkachenko, H. Lemmetyinen, *J. Phys. Chem. A* **2012**, *116*, 9653-9661.

[129] R. F. Enes, J.-J. Cid, A. Hausmann, O. Trukhina, A. Gouloumis, P. Vázquez, J. A. S. Cavaleiro, A. C. Tomé, D. M. Guldi, T. Torres, *Chem. Eur. J.* **2012**, *18*, 1727-1736.

[130] R. R. Zope, M. Olguin, T. Baruah, *J. Chem. Phys.* **2012**, *137*, 84317-84325.

[131] S. Pillai, J. Ravensbergen, A. Antoniuk-Pablant, B. D. Sherman, R. van Grondelle, R. N. Frese, T. A. Moore, D. Gust, A. L. Moore, J. T. M. Kennis, *Phys. Chem. Chem. Phys.* **2013**, *15*, 4775-4784.

[132] M. Olguin, R. R. Zope, T. Baruah, *J. Chem. Phys.* **2013**, *138*, 74306-74314.

[133] C. A. Wijesinghe, M. E. El-Khouly, M. E. Zandler, S. Fukuzumi, F. D'Souza, *Chem. Eur. J.* **2013**, *19*, 9629-9638.

[134] G. de la Torre, G. Bottari, M. Sekita, A. Hausmann, D. M. Guldi, T. Torres, *Chem. Soc. Rev.* **2013**, *42*, 8049-8105.

[135] S. Kuhri, G. Charalambidis, P. A. Angaridis, T. Lazarides, G. Pagona, N. Tagmatarchis, A. G. Coutsolelos, D. M. Guldi, *Chem. Eur. J.* **2014**, *20*, 2049-2057.

[136] R. Ciasson, E. J. Lee, X. Zbao, M. S. Wrighton, *J. Phys. Chem.* **1993**, *97*, 2596-2601.

[137] N. B. Thornton, H. Wojtowicz, T. Netzel, D. W. Dixon, *J. Phys. Chem. B* **1998**, *102*, 2101-2110.

[138] V. A. Nadtochenko, N. N. Denisov, V. Y. Gak, N. V. Abramova, N. M. Loim, *Russ. Chem. Bull.* **1999**, *48*, 1900-1903.

[139] M. Kubo, Y. Mori, M. Otani, M. Murakami, Y. Ishibashi, M. Yasuda, K. Hosomizu, H. Miyasaka, H. Imahori, S. Nakashima, *Chem. Phys. Lett.* **2006**, *429*, 91-96.

[140] H. Mansour, M. E. El-Khouly, S. Y. Shaban, O. Ito, N. Jux, *J. Porphyrins Phthalocyanines* **2007**, *11*, 719-728.

[141] J. H. Jang, H. J. Kim, H.-J. Kim, C. H. Kim, T. Joo, D. W. Cho, M. Yoon, *Bull. Korean Chem. Soc.* **2007**, *28*, 1967-1972.

[142] B. M. J. M. Suijkerbuijk, R. J. M. Klein Gebbink, *Angew. Chem.* **2008**, *120*, 7506-7532; *Angew. Chem. Int. Ed.* **2008**, *47*, 7396-7421.

[143] A. K. Burrell, W. Campbell, D. L. Officer, *Tetrahedron Lett.* **1997**, *38*, 1249-1252.

[144] M. A. Bakar, N. N. Sergeeva, T. Juillard, M. O. Senge, *Organometallics* **2011**, *30*, 3225-3228.

[145] K. Heinze, K. Hempel, M. Beckmann, *Eur. J. Inorg. Chem.* **2006**, 2040-2050.

[146] A. M. Brun, A. Harriman, V. Heitz, J.-P. Sauvage, *J. Am. Chem. Soc.* **1991**, *113*, 8657-8663.

[147] V. Heitz, S. Chardon-Noblat, J.-P. Sauvage, *Tetrahedron Lett.* **1991**, *32*, 197-198.

[148] E. K. L. Yeow, P. J. Sintic, N. M. Cabral, J. N. H. Reek, M. J. Crossley, K. P. Ghiggino, *Phys. Chem. Chem. Phys.* **2000**, *2*, 4281-4291.

[149] K. Kilså, J. Kajanus, A. N. Macpherson, J. Mårtensson, B. Albinsson, *J. Am. Chem. Soc.* **2001**, *123*, 3069-3080.

[150] S. Fukuzumi, K. Ohkubo, W. E. Z. Ou, J. Shao, K. M. Kadish, J. A. Hutchison, K. P. Ghiggino, P. J. Sintic, M. J. Crossley, *J. Am. Chem. Soc.* **2003**, *125*, 14984-14985.

[151] E. Göransson, J. Boixel, J. Fortage, D. Jacquemin, H.-C. Becker, E. Blart, L. Hammarström, F. Odobel, *Inorg. Chem.* **2012**, *51*, 11500-11512.

[152] J. Fortage, J. Boixel, E. Blart, L. Hammarström, H. C. Becker, F. Odobel, *Chem. Eur. J.* **2008**, *14*, 3467-3480.

[153] J. Fortage, A. Scarpaci, L. Viau, Y. Pellegrin, E. Blart, M. Falkenström, L. Hammarström, I. Asselberghs, R. Kellens, W. Libaers, K. Clays, M. P. Eng, F. Odobel, *Chem. Eur. J.* **2009**, *15*, 9058-9067.

[154] J. Fortage, J. Boixel, E. Blart, H. C. Becker, F. Odobel, *Inorg. Chem.* **2009**, *48*, 518-526.

[155] L. J. Pace, A. Ulman,, J. A. Ibers, *Znorg. Chem.* **1982**, *21*, 199-207.

[156] M. Yamaji, Y. Hama, S. Arai, M. Hoshino, *Inorg. Chem.* **1987**, *26*, 4375-4378.

[157] H. A. Staab, J. Weikard, A. Rückemann, A. Schwögler, *Eur. J. Org. Chem.* **1998**, 2703-2712.

[158] W. Hibbs, A. M. Arif, M. Botoshansky, M. Kaftory, J. S. Miller, *Inorg. Chem.* **2003**, *42*, 2311-2322.

[159] M. Tanaka, K. Ohkubo, C. P. Gros, R. Guilard, S. Fukuzumi, *J. Am. Chem. Soc.* **2006**, *128*, 14625-14633.

[160] Y.-J. Li, Y.-J. Zhao, A. H. Flood, C. Liu, H.-B. Liu, Y.-L. Li, *Chem. Eur. J.* **2011**, *17*, 7499-7505.

[161] J.-M. Barbe, B. Habermeyer, T. Khoury, C. P. Gros, P. Richard, P. Chen, K. M. Kadish, *Inorg. Chem.* **2010**, *49*, 8929-8940.

[162] B. Habermeyer, A. Takai, C. P. Gros, M. El Ojaimi , J.-M. Barbe, S. Fukuzumi, *Chem. Eur. J.* **2011**, *17*, 10670-10681.

[163] A. Chaudhary, S. P. Rath, *Chem. Eur. J.* **2011**, *17*, 11478-11487.

[164] A. Chaudhary, S. P. Rath, *Chem. Eur. J.* **2012**, *18*, 7404-7417.

[165] H. Yoon, C.-H. Lee, W.-D. Jang, *Chem. Eur. J.* **2012**, *18*, 12479-12486.

[166] S. Brahma, S. A. Ikbal, S. P. Rath, *Inorg. Chem.* **2014**, *53*, 49-62.

[167] A. A. Pascal, Z. Liu, K. Broess, B. van Oort, H. van Amerongen, C. Wang, P. Horton, B. Robert, W. Chang, A. Ruban, *Nature* **2005**, *436*, 134-137.

[168] R. Guilard, S. Brandes, A. Tabard, N. Bouhmaida, C. Lecomte, P. Richard, J.-M. Latour, *J. Am. Chem. Soc.* **1994**, *116*, 10202-10211.

[169] Y. Deng, C. J. Chang, D. G. Nocera, *J. Am. Chem. Soc.* **2000**, *122*, 410-411.

[170] A. Takai, C. P. Gros, J.-M. Barbe, R. Guilard, S. Fukuzumi, *Chem. Eur. J.* **2009**, *15*, 3110-3122.

[171] S. L. Gould, G. Kodis, R. E. Palacios, L. de la Garza, A. Brune, D. Gust, T. A. Moore, A. L. Moore, *J. Phys. Chem. B* **2004**, *108*, 10566-10580.

[172] A. Bettelheim, B. A. White, S. A. Raybuck, R. W. Murray, *Inorg. Chem.* **1987**, *26*, 1009-1017.

[173] C.-Y. Lin, Y.-C. Hung, C.-M. Liu, C.-F. Lo, Y.-C. Lin, C-L. Lin, *Dalton Trans.* **2005**, 396-401.

[174] A. Devos, J. Remion, A.-M. Frisque-Hesbain, A. Colens, L. Ghosez, *J. Chem. Soc. Chem. Commun.* **1979**, 1180-1181.

[175] T. Ishikawa, *Supberbases for Organic Synthesis*,Wiley*& Sons* Ltd: Chichester, U.K., **2009**, 145-185.

[176] J. S. Lindsey, J. N. Woodford, *Inorg. Chem.* **1995**, *34*, 1063-1069.

[177] D. F. O’Shea, M. A. Miller, H. Matsueda, J. S. Lindsey, *Inorg. Chem.* **1996**, *35*, 7325-7338.

[178] K. Heinze, M. Schlenker, *Eur. J. Inorg. Chem.* **2004**, 2974-2988.

[179] K. Heinze, D. Siebler, *Z. Anorg. Allg. Chem.* **2007**, *633*, 2223-2233

[180] D. Siebler, M. Linseis, T. Gasi, L. M. Carrella, R. F. Winter, C. Förster, K. Heinze, *Chem. Eur. J.* **2011**, *17*, 4540-4551.

[181] D. Siebler, C. Förster, T. Gasi, K. Heinze, *Organometallics* **2011**, *30*, 313-327.

[182] H. Huesmann, C. Förster, D. Siebler, T. Gasi, K. Heinze, *Organometallics* **2012**, *31*, 413-427.

6 Publications

In the following the publications that contribute to this thesis are given:

6.1. J. Melomedov, A. Wünsche von Leupoldt, M. Meister, F. Laquai and K. Heinze, *Dalton. Trans.* **2013**, *42*, 9727-9739. Porphyrin Amino Acids – Amide Coupling, Redox and Photophysical Properties of Bis(porphyrin) amides
[DOI: 10.1039/c3dt50711d]

6.2. J. Melomedov, J. R. Ochsmann, M. Meister, F. Laquai and K. Heinze, *Eur. J. Inorg. Chem.* **2014**, 1984-2001. Tuning Reductive and Oxidative Photoinduced Electron Transfer in Amide-Linked Anthraquinone-Porphyrin-Ferrocene Architectures
[DOI:10.1002/ejic.201400118]

6.3. J. Melomedov, J. R. Ochsmann, M. Meister, F. Laquai and K. Heinze, *Eur. J. Inorg. Chem.* **2014**, accepted. Aminoferrocene and Ferrocene Amino Acid as Electron Donors in Modular Porphyrin-Ferrocene and Porphyrin-Ferrocene-Porphyrin Conjugates
DOI:10.1002/ejic.201402138

6.1 Porphyrin Amino Acids−Amide Coupling, Redox and Photophysical Properties of Bis(porphyrin) amides

Jascha Melomedov, Anica Wünsche von Leupoldt, Michael Meister, Frédéric Laquai and Katja Heinze, *Dalton. Trans.* **2013**, *42*, 9727-9739.

DOI: 10.1039/c3dt50711d

Manuscript received: 15.03.2013

Manuscript accepted: 30.04.2013

Article first published online: 17.05 2013

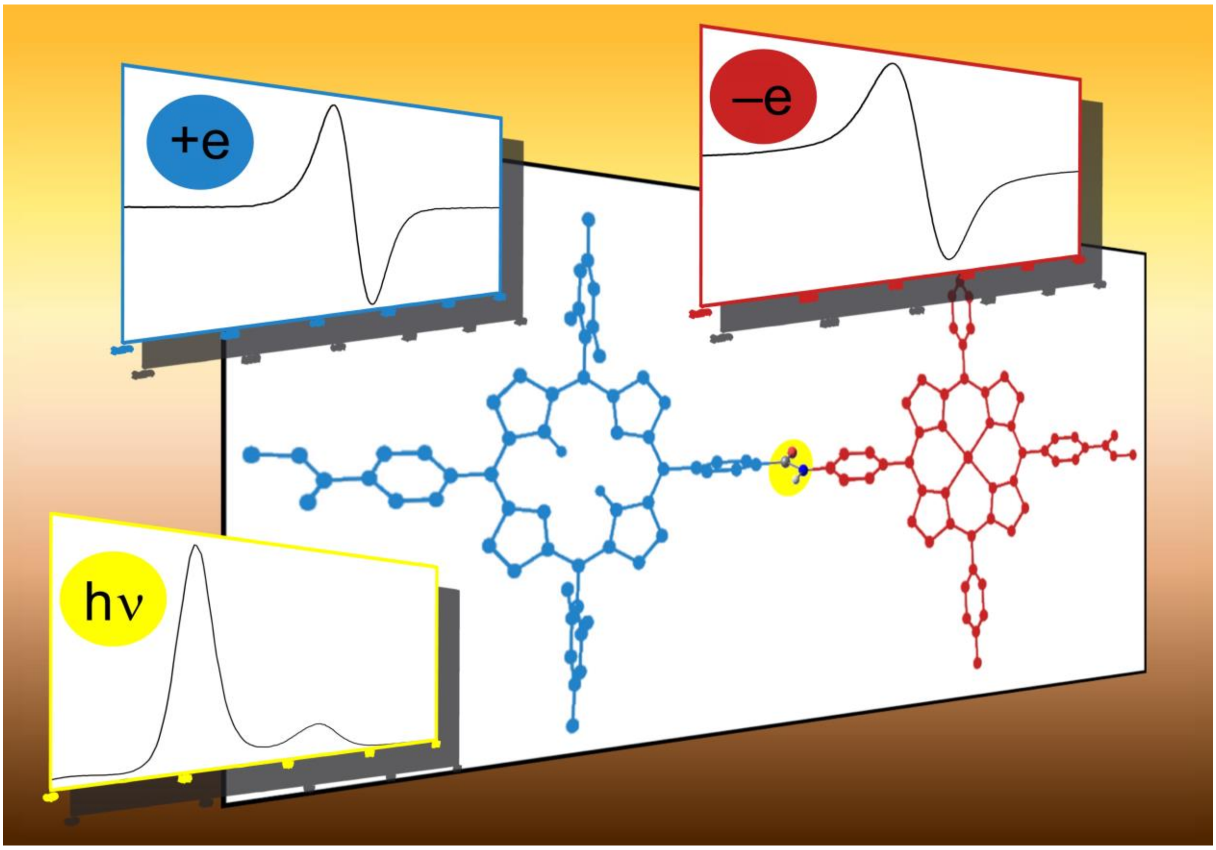

Dalton Transactions

RSC Publishing

PAPER

View Article Online
View Journal | View Issue

Cite this: *Dalton Trans.*, 2013, **42**, 9727

Porphyrin amino acids–amide coupling, redox and photophysical properties of bis(porphyrin) amides†

Jascha Melomedov,[a] Anica Wünsche von Leupoldt,[a] Michael Meister,[b] Frédéric Laquai[b] and Katja Heinze*[a]

Received 15th March 2013,
Accepted 30th April 2013

DOI: 10.1039/c3dt50711d

www.rsc.org/dalton

New *trans*-AB$_2$C *meso*-substituted porphyrin amino acid esters with *meso*-substituents of tunable electron withdrawing power (B = mesityl, 4-C$_6$H$_4$F, 4-C$_6$H$_4$CF$_3$, C$_6$F$_5$) were prepared as free amines **3a–3d**, as *N*-acetylated derivatives **Ac-3a–Ac-3d** and corresponding zinc(II) complexes **Zn-Ac-3a–Zn-Ac-3d**. Several amide-linked bis(porphyrins) with a tunable electron density at each porphyrin site were obtained from the amino porphyrin precursors by condensation reactions (**4a–4d**) and mono- and bis(zinc(II)) complexes **Zn^2-4d** and **Zn^{1}Zn^2-4d** were prepared. The electronic interaction between individual porphyrin units in bis(porphyrins) **4** is probed by electrochemical experiments (CV, EPR), electronic absorption spectroscopy, steady-state and time-resolved fluorescence spectroscopy in combination with DFT/PCM calculations on diamagnetic neutral bis(porphyrins) **4** and on respective charged mixed-valent radicals **4$^{+/-}$**. The interaction *via* the –C$_6$H$_4$–NHCO–C$_6$H$_4$– bridge, the site of oxidation and reduction and the lowest excited singlet state S$_1$, is tuned by the substituents on the individual porphyrins and the metalation state.

Introduction

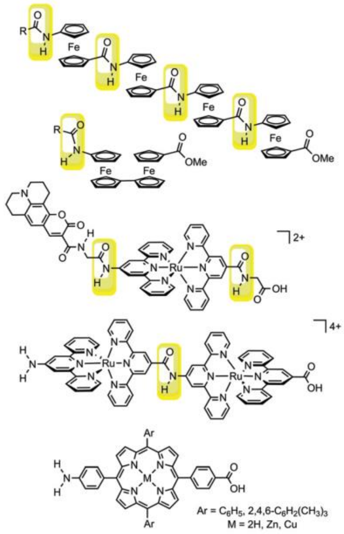

Scheme 1 Selection of inorganic and organometallic amino acids and of derived conjugates and oligomers.[5,6,8–21,28]

Amino acids are among the most versatile ingredients in functional materials, in natural peptides and proteins as well as in artificial synthetic materials, such as Nylon-6, Kevlar or switchable amide based foldamers to name a few.[1–6] Most of the functionality arises from the secondary (helices and sheets) and tertiary structures and the side chain functional groups. In our approach we incorporate functionalities like specialised redox, photo, magnetic or mechanical properties into the backbone of an oligoamide.[7] To this end we have designed inorganic and organometallic amino acids featuring stable redox centres (*e.g.* ferrocene[5,6,8–14] or biferrocene[15]), chromophores (*e.g.* ruthenium(II) oligopyridine complexes[16–20]) and (metallo)-porphyrins[21] which can be integrated into the backbone of peptides (Scheme 1). In addition to the functionality from the metal complex itself the folding to stable secondary structures *via* hydrogen bonding has been shown to be highly important, *e.g.* for the site-selective oxidation and the folding-induced resulting macrodipole moment.[5,6] A potential synthetic advantage of using amides as linkers between functional building

---

[a] *Johannes Gutenberg-University of Mainz, Duesbergweg 10-14, 55128 Mainz, Germany. E-mail: katja.heinze@uni-mainz.de; Fax: +49-6131-3927277*

[b] *Max Planck Institute for Polymer Research, Max Planck Research Group for Organic Optoelectronics, Ackermannweg 10, 55128 Mainz, Germany*

† Electronic supplementary information (ESI) available: Synthetic procedures and analytical data, ^{19}F NMR spectrum of **4c**, spin density plots of **4c$^+$** and **4c$^-$**, molecular orbitals of **4b**, **4c** and **Zn^2-4d**, EPR spectra of **4b$^{+/-}$**, **Zn^2-4d$^{+/-}$** and reference compounds at 77 K, EPR spectra of **Zn^{1}Zn^2-4d$^{+/-}$** and reference compounds at 295 K, normalised Soret bands of **4a–4d**, **Zn^2-4d** and **Zn^{1}Zn^2-4d** and reference porphyrins, emission spectra of **Ac-3a–Ac-3d**, fluorescence decays of **Zn^{1}Zn^2-4d**, **Zn-1a** and **Zn-Ac-3c**, Cartesian coordinates (DFT). See DOI: 10.1039/c3dt50711d

blocks is the application of solid-phase synthesis methods to construct well-defined larger arrays.[7,22,23]

Highly elaborated push–pull amino acids featuring a tetrapyrrole macrocycle have been employed as chromophores in dye-sensitised solar cells by Diau and Grätzel[24–27] as well as in systems for fundamental studies of photoinduced charge separation on a molecular level by Gust, Moore and Moore[28] and in molecular binary switches and Boolean logic gates.[29,30]

In this report we

(i) expand the diversity of *meso*-tetraphenyl amino acid porphyrin building blocks by installing substituents of tunable electron withdrawing power (4-C_6H_4F, 4-$C_6H_4CF_3$, C_6F_5) at the porphyrin amino acid,

(ii) elaborate amide coupling conditions which permit the selective formation of amide bridged bis(free-base porphyrins) as well as zincated bis(porphyrins),

(iii) study the mixed-valent radicals derived from one-electron oxidation and reduction of bis(porphyrins) by electrochemical and EPR spectroscopic analyses and by DFT/PCM calculations, and finally,

(iv) extract information on singlet excited state energies (S_1) and excited state communication within the dyads from absorption and emission spectroscopy.

These results will pave the way for the design of energy and redox gradients within multiporphyrin arrays based on amide linkers useful for light-harvesting and electron transfer applications. A special feature of the amide linker is its inherent asymmetry in contrast to commonly used CH═CH, C≡C and *p*-C_6H_4 bridges and thus careful design of the electronic situations on both sides is required in order to optimise electronic communication and energy/electron transfer directions. The aim of this study is to empirically extract correlations from a selected set of bis(porphyrins) and to underpin the experimental data by DFT/PCM calculations which will allow a future DFT guided rational design of energy and redox gradients in amide-linked oligoporphyrins.

Experimental

General considerations

The mesityl substituted porphyrins (Ar^1 = 2,4,6-$C_6H_2(CH_3)_3$) **1a**, **2a**, **Boc-3a** and **3a** were prepared according to reported methods.[28,31] The electrochemical and spectroscopic data of these porphyrins are reported in this paper in Tables 1–5 and in the ESI.† 5-(4-Nitrophenyl)dipyrromethane, 5-(pentafluorophenyl)dipyrromethane, 5-(4-(methoxycarbonylphenyl))dipyrromethane[32–34] and *N*-(4-(trifluoromethyl)benzoyl)morpholine[35] were prepared according to reported methods. Solvents were dried by standard methods. Other reagents were used as received from commercial suppliers (Acros, Sigma-Aldrich). NMR spectra were recorded on a Bruker Avance DRX 400 spectrometer at 400.31 MHz (^{1}H), 100.05 MHz (^{13}C{^{1}H}) and 367.67 MHz (^{19}F). Resonances are reported in ppm *versus* the solvent signal as an internal standard. $CDCl_3$ (^{1}H: δ = 7.24 ppm; ^{13}C: δ = 77.0 ppm), d_8-THF (^{1}H: δ = 1.73, 3.58 ppm; ^{13}C: δ = 25.5, 67.7 ppm) or *versus* external $CFCl_3$ (^{19}F: δ = 0 ppm); (s) = singlet, (pt) = pseudo triplet (unresolved doublet

Table 1 Redox potentials of relevant monoporphyrins in V *vs.* Fc/Fc$^+$ in (nBu$_4$N)(PF$_6$)–CH$_2$Cl$_2$ at room temperature

	M	Ar^1	C_6H_4-R′	$E_{1/2}$ (ox^1)	$E_{1/2}$ (ox^2)	$E_{1/2}$ (red^1)	$E_{1/2}$ (red^2)
1a	2H	Mes	COOMe	0.600	1.030	−1.670	−2.020
3a	2H	Mes	NH_2	0.455[b]	0.600[b]	−1.760	−2.100
Ac-3a	2H	Mes	NHAc	0.540	0.960	−1.710	−2.060
Zn-1a	Zn	Mes	COOMe	0.440	0.740	−1.780	−2.150
Zn-Ac-3a	Zn	Mes	NHAc	0.335	0.750	−1.860	n.o.
1b	2H	C_6F_5	COOMe	0.890	1.140	−1.350	−1.750
3b	2H	C_6F_5	NH_2	0.65[a]	0.79[a]	−1.390[b]	−1.820[b]
Ac-3b	2H	C_6F_5	NHAc	0.820	1.030	−1.410	−1.810
Zn-Ac-3b	Zn	C_6F_5	NHAc	0.600	0.940	−1.580	−1.980
3c	2H	C_6H_4F	NH_2	0.51[a]	n.o.	−1.650	−1.980
Ac-3c	2H	C_6H_4F	NHAc	0.590	0.870	−1.590	−1.920
Zn-Ac-3c	Zn	C_6H_4F	NHAc	0.380	0.780	−1.750	−2.110
3d	2H	$C_6H_5CF_3$	NH_2	0.53[a]	n.o.	−1.560	−1.900
Ac-3d	2H	$C_6H_5CF_3$	NHAc	0.640	0.890	−1.550	−1.900
Zn-Ac-3d	Zn	$C_6H_5CF_3$	NHAc	0.420	0.850	−1.560	−2.010

[a] Irreversible, peak potential given. [b] Quasi-reversible.

Table 2 Redox potentials of bis(porphyrins) **4** in V *vs.* Fc/Fc$^+$ in (nBu$_4$N)(PF$_6$)–CH$_2$Cl$_2$ at room temperature

	$E_{1/2}$ (ox^1)	$E_{1/2}$ (ox^2)	$E_{1/2}$ (ox^3)	$E_{1/2}$ (ox^4)	$E_{1/2}$ (red^1)	$E_{1/2}$ (red^2)	$E_{1/2}$ (red^3)	$E_{1/2}$ (red^4)
4a	0.570	0.880	1.001	1.161	−1.360	−1.691(2e)		−2.040
4b	0.589	0.838	1.049	n.o.	−1.380	−1.661	−1.800	−2.031
4c	0.650	0.900(2e)		1.140	−1.360	−1.541	−1.760	−1.871
4d	0.601(2e)		0.870	1.040	−1.621(2e)		−1.970(2e)	
Zn^2-4d	0.451	0.611	0.751	1.030	−1.710(2e)		−2.090(2e)	
Zn^{1}Zn^2-4d	0.459(2e)		0.779(2e)		−1.760(2e)		−2.151(2e)	

Table 3 EPR data of selected bis(porphyrins) and reference compounds[58] in CH_2Cl_2 at 295 K and at 77 K

	g	$\Delta H/G$	g	$\Delta H/G$
	295 K		77 K	
4b$^+$	2.0055	8.5	2.0051	7.1
1b$^+$	2.0051	6.6	2.0064	8.9
Ac-3a$^+$	2.0055	9.0	2.0058	9.7
4b$^-$	2.0049	5.1	2.0057	4.7
1b$^-$	2.0048	4.7	2.0053	4.8
Ac-3a$^-$	2.0045	5.2	2.0052	7.4
Zn^2-4d$^+$	2.0049	7.3	2.0049	6.9
1a$^+$	2.0047	8.6	2.0051	8.5
Zn-Ac-3c$^+$	2.0045	5.9	2.0050	7.4
Zn2-4d$^-$	2.0047	5.3	2.0044	7.4
1a$^-$	2.0045	5.0	2.0047	6.1
Zn-Ac-3c$^-$	silent	—	2.0028	7.4
Zn^{1}Zn^2-4d$^+$	2.0045	5.4	n.d.	n.d.
Zn-1a$^+$	2.0043	5.8	n.d.	n.d.
Zn-Ac-3c$^+$	2.0045	5.9	2.0050	7.4
Zn^{1}Zn^2-4d$^-$	2.0050	9.1	n.d.	n.d.
Zn-1a$^-$	2.0054	7.6	n.d.	n.d.
Zn-Ac-3c$^-$	silent	—	2.0028	7.4

Table 4 Emission data of relevant monoporphyrins in CH_2Cl_2 at room temperature

	M	Ar^1	C_6H_4-R′	Q(0,0)/nm	Q(0,1)/nm	Φ	τ/ns^a
1a	2H	Mes	COOMe	654	716	0.0774	9.87
3a	2H	Mes	NH_2	654	719	0.0882	n.d.^{b}
Ac-3a	2H	Mes	NHAc	654	718	0.0778	10.90
Zn-1a	Zn	Mes	COOMe	598	647	0.1001	2.53
Zn-Ac-3a	Zn	Mes	NHAc	604	652	0.1343	2.17
1b	2H	C_6F_5	COOMe	645	711	0.0520	10.05
3b	2H	C_6F_5	NH_2	654	717	0.0802	n.d.^{b}
Ac-3b	2H	C_6F_5	NHAc	647	713	0.0696	9.83
Zn-Ac-3b	Zn	C_6F_5	NHAc	602	652	0.0771	1.94
3c	2H	C_6H_4F	NH_2	656	719	0.1405	n.d.^{b}
Ac-3c	2H	C_6H_4F	NHAc	652	717	0.1003	9.64
Zn-Ac-3c	Zn	C_6H_4F	NHAc	598	646	0.0569	1.85
3d	2H	$C_6H_5CF_3$	NH_2	656	719	0.1189	n.d.^{b}
Ac-3d	2H	$C_6H_5CF_3$	NHAc	650	716	0.1080	9.98
Zn-Ac-3d	Zn	$C_6H_5CF_3$	NHAc	597	645	0.0838	2.07

[a] All decays are monoexponential; excitation wavelength λ_{exc} = 400 and 550 nm. [b] n.d. = not determined.

Table 5 Emission data of relevant bis(porphyrins) **4** in CH_2Cl_2 at room temperature

	Q(0,0)/nm	Q(0,1)/nm	Φ	τ/ns^a
4a	653	714	0.1125	9.92
4b	652	714	0.0846	10.16
4c	652	714	0.0783	10.18
4d	654	717	0.1880	10.33
Zn^2-4d	654	717	0.1564	10.88
Zn^{1}Zn^2-4d	598	653	0.1402	2.08

[a] All decays are monoexponential.

of doublets), (br. s) = broad singlet. IR spectra were recorded with a BioRad Excalibur FTS 3100 spectrometer as CsI disks; (vs) = very strong, (s) = strong, (m) = medium, (w) = weak. ESI mass spectra were recorded on a Micromass Q-TOF-Ultima spectrometer. FD mass spectra were recorded on an FD Finnigan MAT90 spectrometer. Electrochemical experiments were carried out on a BioLogic SP-50 voltammetric analyzer using a glassy carbon working electrode, a platinum wire as the counter electrode and a 0.01 m Ag/$AgNO_3$ electrode as the reference electrode. The measurements were carried out at a scan rate of 100 mV s^{-1} for cyclic voltammetry experiments and for square wave voltammetry experiments using 0.1 m ($n$$Bu_4N$)($PF_6$) as the supporting electrolyte in CH_2Cl_2. Potentials are given relative to the ferrocene/ferrocenium couple. X-band CW EPR spectra were measured on a Miniscope MS 300 (Magnettech GmbH, Germany). g-Values are referenced to external Mn^{2+} in ZnS (g = 2.118, 2.066, 2.027, 1.986, 1.946, 1.906). Simulations were performed with the program package EasySpin.[36] UV/Vis/NIR spectra were recorded on a Varian Cary 5000 spectrometer using 1.0 cm cells (Hellma, suprasil). Emission spectra were recorded on a Varian Cary Eclipse spectrometer. Quantum yields Φ were determined by comparing the areas under the emission spectra on an energy scale [cm^{-1}] recorded for optically matched solutions of the samples and the reference {$\Phi(H_2TPP) = 0.13$ in benzene}[37a] using the equation[37b] $\Phi = \Phi_{ref} \times I/I_{ref} \times \eta^2/\eta^2_{ref}$ with η(benzene) = 1.5011 and $\eta(CH_2Cl_2)$ = 1.4242; experimental uncertainty 15%. Kinetics were recorded using a Hamamatsu Streak Camera system. There were two time modes available for the measurements presented in this work: one with a resolution down to a few picoseconds and a maximum time range of two nanoseconds (fast sweep, mononuclear zinc(II) porphyrins and **Zn^{1}Zn^2-4d**), and a second time mode with a time resolution down to a few hundred picoseconds and a maximum time range limited by the repetition rate of the excitation source (slow sweep, all other porphyrins including **Zn^2-4d**). Excitation was provided depending on the measuring mode. For fast sweep experiments a Ti:sapphire ultrafast laser system (Coherent Mira 900-Dual fs-ps-Oscillator) with a repetition rate of 80 MHz and a pulse length of 100 fs pumped by a diode pumped solid-state laser (Coherent Verdi V8) was used. The 800 nm output was frequency doubled using a BBO crystal to achieve the excitation wavelength of 400 nm. For the slow sweep measurements, a Fianium fiber laser supercontinuum source (SC450-2) was used, which provides a white laser light (460–2200 nm) with a pulse width of 6 ps and a fundamental repetition rate of 20 MHz, which was typically derated by an implemented pulse picker to 1 MHz. The desired excitation wavelength (550 nm) was filtered out of the white-light using an acousto-optical modulator (AOM, Fianium AOTF).[38]

Density functional calculations were carried out with the Gaussian09/DFT series[39] of programs. The B3LYP formulation of density functional theory was used employing the LANL2DZ basis set. To include solvent effects the integral equation formalism polarisable continuum model (IEFPCM, CH_2Cl_2) was employed. No symmetry constraints were imposed on the molecules. The presence of energy minima of the ground states was checked by analytical frequency calculations. Syntheses and analytical properties of all new porphyrins are compiled in the ESI.

EPR measurements of radical anions

Under an inert atmosphere a solution of the porphyrin ($c = 5 \times 10^{-3}$ M) in CH_2Cl_2 was treated with one equivalent of decamethylcobaltocene $CoCp^*_2$.[40] The EPR spectrum of the sample was measured immediately at room temperature or after freezing to 77 K.

EPR measurements of radical cations

Under an inert atmosphere a solution of the porphyrin ($c = 5 \times 10^{-3}$ M) in CH_2Cl_2 was treated with one equivalent of tungsten hexachloride WCl_6 [40] and the solution was filtered. The EPR spectrum of the sample was measured immediately at room temperature or after freezing to 77 K.

Results and discussions

Synthesis and characterisation of mono- and bis(porphyrins)

Three novel *trans*-AB_2C substituted porphyrin[41–44] amino acid esters[21,28] with electron withdrawing *meso*-substituents B = C_6F_5, 4-C_6H_4F and 4-$C_6H_4CF_3$ were prepared by two different approaches. Route A encompasses desymmetrization of a *trans*-A_2B_2 diester porphyrin[45] **1a** → **2a** and **1b** → **2b** by partial hydrolysis of the ester group followed by a Curtius rearrangement using diphenylphosphoryl azide (DPPA) and *tert*-butanol to give the *N*-Boc protected derivatives **Boc-3a**/**Boc-3b** (Scheme 2, route A, Boc = *tert*-butoxy carbonyl). Boc deprotection using trifluoroacetic acid gives amino acid esters **3a** and **3b**. Route B is based on a selective synthesis of the nitro and ester substituted AB_2C porphyrins **2c**/**2d** according to a Lindsey-type 2 + 2 condensation approach[42] using the respective nitro and ester substituted phenyl dipyrromethanes[32–34] followed by reduction of the nitro functionality using tin(II) chloride/hydrochloric acid (Scheme 2, route B), to give amino acid esters **3c**/**3d** similar to the literature procedure for Ar^2 = C_6H_5.[21] Attempts to prepare **3a** and **3b** with *ortho* substituted aryl substituents Ar = 2,4,6-$C_6H_2(CH_3)_3$ and C_6F_5 by the preferred route B which avoids the tedious chromatographic separation of the monoacid/ester porphyrin from the diester and diacid failed.

N-Acetyl protected reference compounds **Ac-3a–Ac-3d** were prepared by acetylating amines **3a–3d** with acetyl chloride/iodine (Scheme 2, bottom).[46] Zinc(II) porphyrins **Zn-1a, Zn-Ac-3a–Zn-Ac-3d** were obtained from the corresponding free-base porphyrins and zinc acetate dihydrate after chromatographic workup. All monoporphyrins were fully characterised by multinuclear NMR spectroscopy (^{1}H, ^{13}C, ^{19}F), IR spectroscopy and (high-resolution) mass spectrometry. All data obtained confirm their identity and purity (see the ESI†).

Electron-rich mesityl substituted amino acid **3a** and electron-poor amino acids **3b–3d** are coupled to the electron-rich and electron-poor acids **2a** or **2b** (after the formation of the corresponding acid chlorides by Ghosez's reagent (1-(chloro-2,*N*,*N*-trimethyl-1-propene-1-amine))[6,15,47,48] giving amides **4a–4d** with a defined porphyrin sequence Ar^1/Ar^2, respectively (Scheme 3). The employed amide coupling procedure is even compatible using the metalated amino acid derivative **Zn-3c** as exemplified in the synthesis of the selectively monometalated bis(porphyrin) **Zn^2-4d** (Scheme 3). Double metalation of **4d** using zinc acetate dihydrate gives the fully metalated bis-

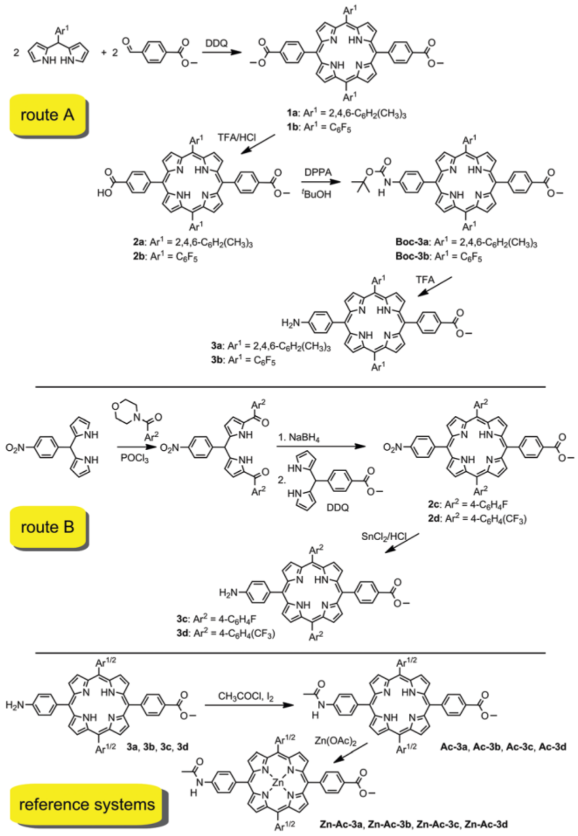

Scheme 2 Syntheses of porphyrin amino acid esters **3a**, **3b** (top) and **3c**, **3d** (center), *N*-acetylation to reference compounds **Ac-3a–Ac-3d** and metalation to **Zn-Ac-3a–Zn-Ac-3d** (bottom).

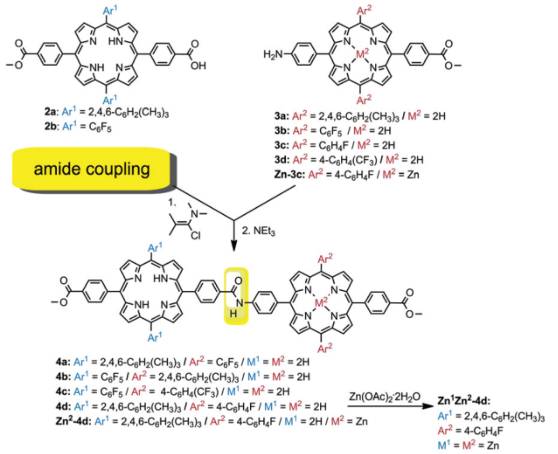

Scheme 3 Syntheses of bis(porphyrins) **4a**, **4b**, **4c**, **4d**, **Zn^2-4d** and **Zn^{1}Zn^2-4d**.

(porphyrin) **Zn^{1}Zn^2-4d** (Scheme 3). Attempts to prepare the monometalated bis(porphyrin) isomer **Zn^1-4d** by amide coupling from the metalated acid component **Zn-2a** (activation by Ghosez's reagent, by 2-(7-aza-1*H*-benzotriazole-1-yl)-1,1,3,3-tetramethyluronium hexafluorophosphate (HATU) or as pentafluorophenyl ester) and amino acid ester **3a** were unsuccessful due to the high lability of Zn^{2+} in **Zn-2a** and the poor reactivity of the amino group (even after activation with phosphazene bases[49,50]).

All bis(porphyrins) **4a–4d**, **Zn^2-4d** and **Zn^{1}Zn^2-4d** show correct molecular ion peaks in their FD and ESI mass spectra confirming the successful amide formation. NMR spectra of bis(porphyrins) **4a–4d** are 1 : 1 superpositions of the spectra of their respective constituents except for the replacement of the amine resonances around δ = 4.1 ppm by amide resonances around δ = 8.5 ppm (see the ESI†).

Redox processes – electron transfer

Two sequential one-electron reductions of porphyrins typically lead to the π anion radical and the porphyrin dianion whereas oxidation leads to the π cation radical and the porphyrin dication. However, oxidations of amine substituted porphyrins **3a–3d** are often irreversible or quasi-reversible likely due to the following polymerisation *via* the amine substituent (Table 1).[21,51,52] On the other hand, *N*-protected porphyrin amino acid esters feature reversible oxidations and reductions, and these are employed as reference compounds in the following. The redox potentials of *N*-acetylated free-base porphyrins **Ac-3a–Ac-3d** and their corresponding zinc(II) porphyrins **Zn-Ac-3a–Zn-Ac-3d** shift towards more positive values by 280–300 mV from Ar = mesityl, Ar = 4-C_6H_5F, Ar = 4-$C_6H_4CF_3$ to Ar = C_6F_5 according to the increasing electron-withdrawing nature of the substituent[53,54] (Table 1). As expected zinc(II) porphyrins **Zn-Ac-3a–Zn-Ac-3d** are easier to oxidise and more difficult to reduce than their corresponding free-base porphyrins **Ac-3a–Ac-3d**.

The electrochemistry of all bis(porphyrins) **4** is essentially represented by the sum of the individual porphyrins within the resolution of the CV and SWV experiments (Table 2). This is exemplarily depicted in Fig. 1 showing the cyclic voltammograms of **4c** and of its "components" **1b** and **Ac-3d**.

Oxidation of **4a** to **4a$^+$** and of **4b** to **4b$^+$** occurs at the mesityl substituted porphyrin while reduction to **4a$^-$** and **4b$^-$** occurs at the C_6F_5 substituted porphyrins as judged from the redox potentials of the reference porphyrins (Tables 1 and 2). Thus, the positive charge is located at porphyrin 1 in **4a$^+$** and at porphyrin 2 in **4b$^+$** while the negative charge is located at porphyrin 2 in **4a$^-$** and at porphyrin 1 in **4b$^-$**. This is also nicely reflected in the DFT (B3LYP/LANL2DZ, PCM CH_2Cl_2) optimised radical cations **4a$^+$**/**4b$^+$** and radical anions **4a$^-$**/**4b$^-$** as shown pictorially by their spin density distribution (Fig. 2).

Electronic discrimination between the porphyrins is also seen in **4c**. In the radical cation **4c$^+$** the positive charge is localised on the least electron-poor porphyrin which is the porphyrin with the 4-$C_6H_4CF_3$ substituent while reduction to **4c$^-$** takes place at the C_6F_5 substituted porphyrin (see the ESI† for spin density plots). Thus, radical ions **4a$^{+/-}$**, **4b$^{+/-}$** and **4c$^{+/-}$** are well described as valence localised redox-asymmetric mixed-valent species (Robin-Day class I[55,56]) based on electrochemical and DFT/PCM data.

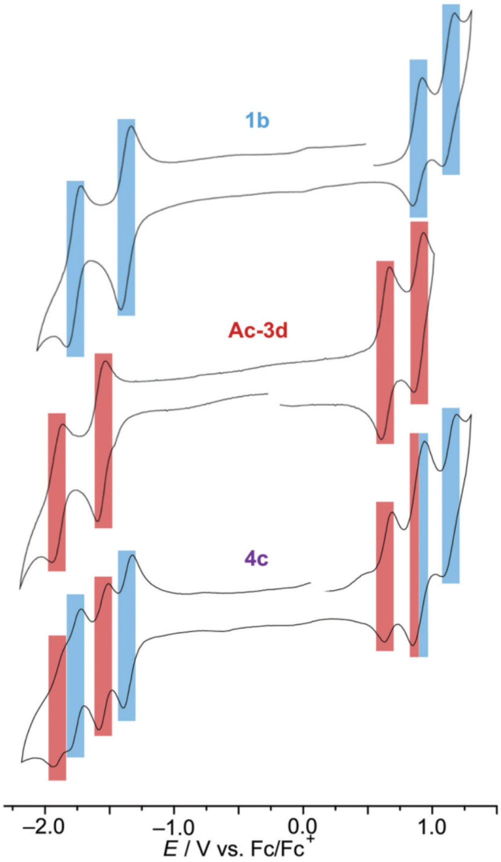

Fig. 1 Cyclic voltammograms of **1b**, **Ac-3d** and **4c** in CH_2Cl_2.

As electron-donating mesityl groups in combination with electron withdrawing 4-C_6H_5-CONHR groups act in total similarly to the 4-C_6H_5F/4-C_6H_5-NHCOR/4-C_6H_5-COOMe substitution pattern, the site discrimination is less pronounced in bis(porphyrin) **4d**. Indeed, both individual porphyrin subunits in **4d** are oxidised at a similar potential and also reduced at a similar potential in quasi-two-electron processes (Table 2). For cation **4d$^+$** the data of the corresponding reference components **1a$^{0/+}$** and **Ac-3c$^{0/+}$** suggest a marginal preference of the 4-C_6H_5F/4-C_6H_5-NHCOR site by 10 mV. Analogous arguments apply to the bis-metalated cation **Zn^{1}Zn^2-4d$^+$** again with a slight preference of the 4-C_6H_5F/4-C_6H_5-NHCOR site by 60 mV (Tables 1 and 2). In cation **Zn^2-4d$^+$** the zincated porphyrin is in the oxidised site as expected (favoured by 220 mV from reference compounds, Table 1) and predicted by DFT calculations (Fig. 3).

The situation is even less clear-cut for the radical anions **4d$^-$**, **Zn^2-4d$^-$** and **Zn^{1}Zn^2-4d$^-$**. The differences in redox potentials of the respective reference compounds amount to only 80 mV, 80 mV and 30 mV, respectively. According to the respective reference compounds the C_6H_4F radical site is

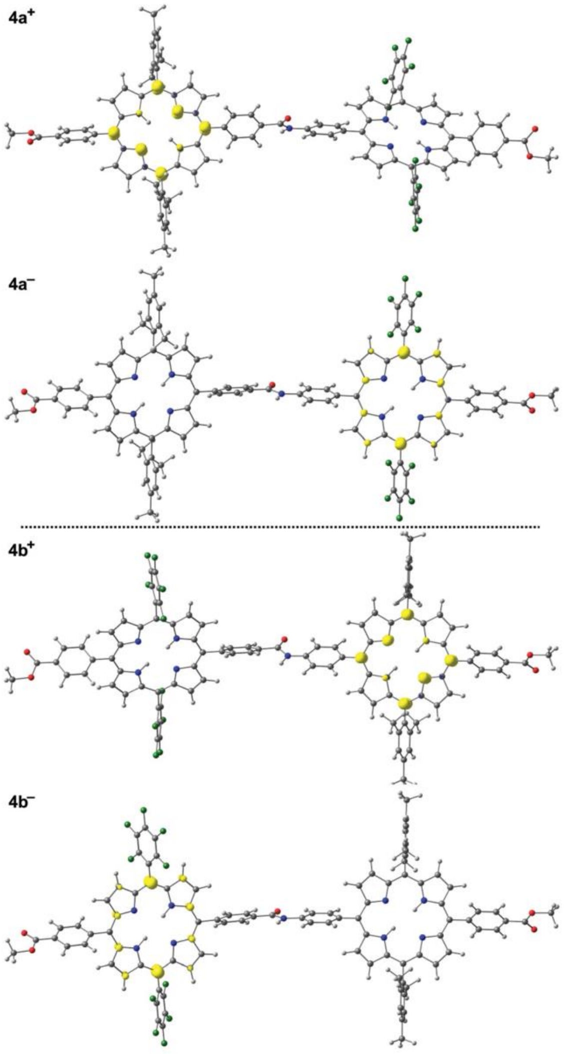

Fig. 2 DFT calculated spin densities of radical ions $\mathbf{4a}^{+/-}$ and $\mathbf{4b}^{+/-}$ (isosurface value at 0.01 a.u.; B3LYP/LANL2DZ, PCM CH_2Cl_2).

slightly preferred in $\mathbf{4d}^-$ and $\mathbf{Zn^1Zn^2}$-$\mathbf{4d}^-$ while in $\mathbf{Zn^2}$-$\mathbf{4d}^-$ the mesityl site is slightly favoured (Table 1). DFT/PCM calculations suggest that the unpaired electron localises on the C_6H_4F substituted porphyrin in $\mathbf{4d}^-$ and $\mathbf{Zn^1Zn^2}$-$\mathbf{4d}^-$ while it prefers the mesityl substituted porphyrin in the monometalated $\mathbf{Zn^2}$-$\mathbf{4d}^-$ in agreement with the electrochemical estimations (Fig. 3). At this point it should be stressed that DFT optimizations for the open-shell species derived from **4d** with electronically similar sites $\mathbf{4d}^{+/-}$, $\mathbf{Zn^2}$-$\mathbf{4d}^{+/-}$ and $\mathbf{Zn^1Zn^2}$-$\mathbf{4d}^{+/-}$ in the gas phase lead to different (and likely erroneous) results with the spin density delocalised over both sites, while the spin densities for the unambiguously localised redox asymmetric radicals $\mathbf{4a}^{+/-}$, $\mathbf{4b}^{+/-}$ and $\mathbf{4c}^{+/-}$ are correctly assigned already by gas-phase DFT calculations. Obviously, small energy differences between the redox sites in bis(porphyrins) require the inclusion of solvent models in theoretical treatments.

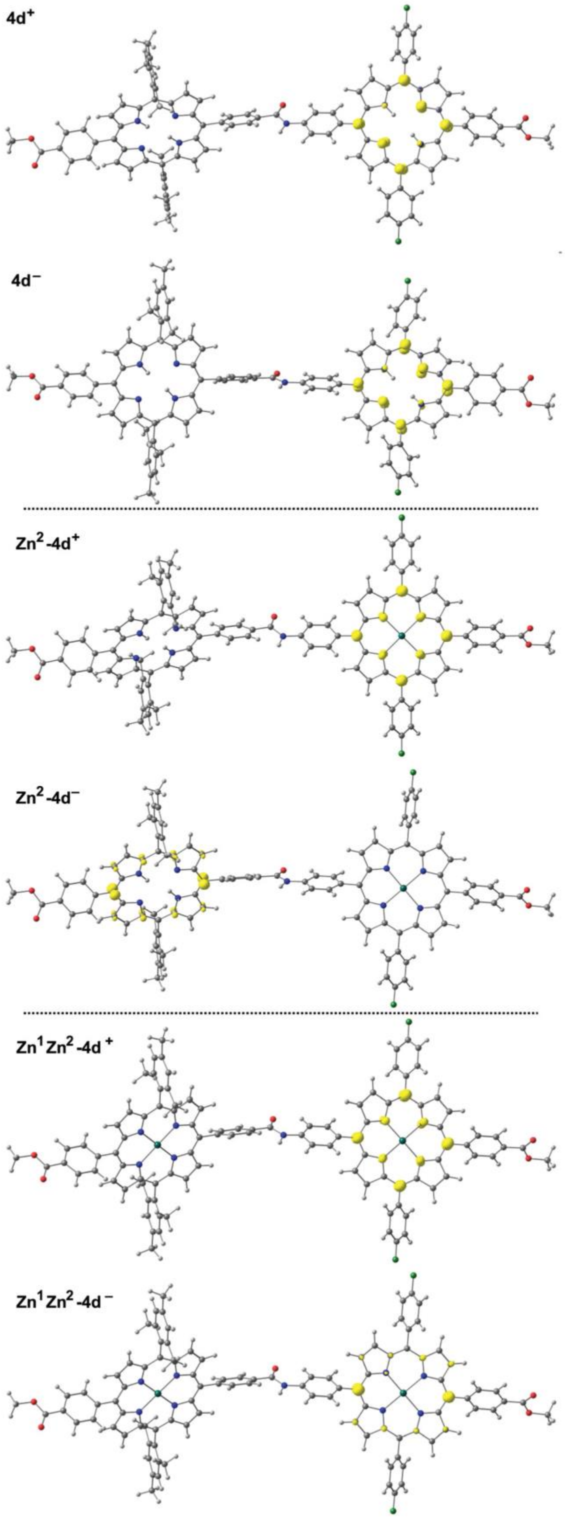

Fig. 3 DFT calculated spin densities of radical ions $\mathbf{4d}^{+/-}$, $\mathbf{Zn^2}$-$\mathbf{4d}^{+/-}$ and $\mathbf{Zn^1Zn^2}$-$\mathbf{4d}^{+/-}$ (isosurface value at 0.01 a.u.; B3LYP/LANL2DZ, PCM CH_2Cl_2).

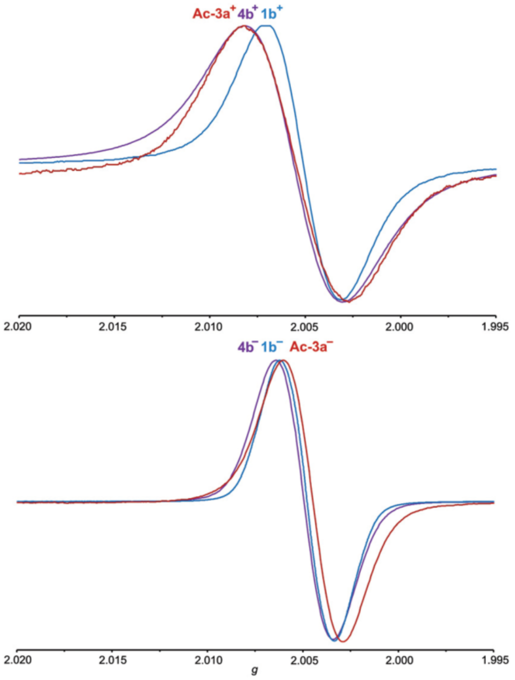

Fig. 4 X-band EPR spectra of radical ions $\mathbf{4b}^{+/-}$ and reference radicals in CH_2Cl_2 at 295 K (9.4 GHz).

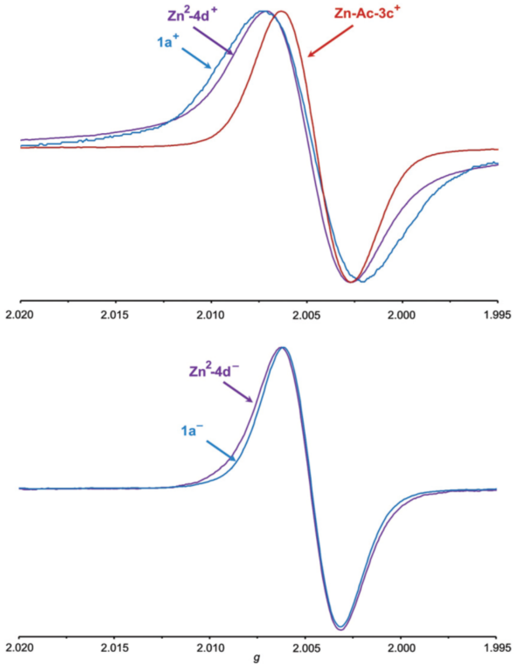

Fig. 5 X-band EPR spectra of radical ions $\mathbf{Zn^2\text{-}4d}^{+/-}$ and reference radicals in CH_2Cl_2 at 295 K (9.4 GHz).

To further corroborate the redox and DFT data, selected radical ions were prepared by chemical oxidation or reduction and probed by EPR spectroscopy (Table 3).[58–62] Exemplarily, the radical ions $\mathbf{4b}^+$ and $\mathbf{4b}^-$ were generated in CH_2Cl_2 by oxidation of **4b** with tungsten hexachloride ($E_{1/2}$ = 1.1 V in CH_2Cl_2 [40,57]) and by reduction of **4b** with decamethylcobaltocene ($E_{1/2}$ = −1.94 V in CH_2Cl_2 [40]), respectively, and the corresponding X-band EPR spectra were recorded both at 295 K and at 77 K. For comparison the spectra of the reference radical species were obtained in an analogous fashion (Fig. 4 and ESI†).

The shape (Gaussian/Lorentzian) and width of the EPR signal of radical anions are expected to be related to the (non-)degeneracy of the LUMO. Lifting the degeneracy by asymmetric substitution should lead to smaller line widths.[63] The type of aryl substituents (mesityl, 4-C_6H_4F, 4-$C_6H_4CF_3$, C_6F_5) modifies the number of electron-nuclear hyperfine coupling interactions (hfcs) present in the organic π radicals and hence influences the EPR line width.[63] Thus, we hoped to detect significant EPR differences in the differently substituted radical ions. Owing to the large number of hfcs present in the organic π radicals all EPR spectra at 295 K display resonances at $g \approx 2$ broadened into single unresolved lines (Fig. 4 and 5).[63] The isotropic g-value of $\mathbf{4b}^+$ closely resembles that of mesityl substituted $\mathbf{Ac\text{-}3a}^+$ and is significantly different from that of the pentafluorophenyl substituted radical $\mathbf{1b}^+$. Furthermore, the line width ΔH of $\mathbf{4b}^+$ matches that of $\mathbf{Ac\text{-}3a}^+$. This fully corroborates the assignment based on electrochemical and DFT data (Tables 1 and 2, Fig. 2). Similarly, the g-value of the anion radical $\mathbf{4b}^-$ compares favourably with that of $\mathbf{1b}^-$ but differs from that of $\mathbf{Ac\text{-}3a}^-$ underpinning the localization of the unpaired electron at the C_6F_5 substituted site. In both cases the difference in redox potentials as derived from the reference compounds is >350 mV (Table 1) suggesting that the equilibrium is essentially on one side[40] and only a single localised mixed-valent species is expected for the radical cation and the radical anion of **4b**.

The high difference in redox potentials is no longer fully valid for the radicals $\mathbf{Zn^2\text{-}4d}^{+/-}$ (Tables 1 and 2). Thus, the presence of both valence isomers is conceivable for the mixed-valent bis(porphyrin) radical ions $\mathbf{Zn^2\text{-}4d}^+$ and $\mathbf{Zn^2\text{-}4d}^-$, respectively. Indeed, the EPR spectrum of $\mathbf{Zn^2\text{-}4d}^+$ neither matches sufficiently well that of $\mathbf{Zn\text{-}Ac\text{-}3c}^+$ nor that of $\mathbf{1a}^+$ (Fig. 5, top). The different line shape suggests the presence of both valence isomers of $\mathbf{Zn^2\text{-}4d}^+$ with the hole residing either on the zinc(II) site or on the free-base porphyrin site. Furthermore, the EPR line shape of mixed-valent systems depends on the electron hopping rates between (redox similar) sites.[64] Wasielewski *et al.* have shown that intramolecular hole hopping is rapid even in *meso–meso meta*-phenylene linked mixed-valent oligoporphyrins.[65] Activated hole transfer is hence conceivable also within $\mathbf{Zn^2\text{-}4d}^+$ with not too strongly differing sites *via* the *para*-phenylene-amide–*para*-phenylene linker. Spin density at the bridging *meso* carbon atoms is found in mesityl substituted porphyrin radical cations (see *e.g.* $\mathbf{4a}^+$, Fig. 2) as well as in 4-C_6H_4F substituted zinc porphyrin radical cations (see *e.g.* $\mathbf{Zn^2\text{-}4d}^+$, Fig. 3). This corresponds to local a_{2u} orbital symmetries of the HOMOs of both sites in $\mathbf{Zn^2\text{-}4d}$ with large coefficients at the bridging *meso* carbon atoms which should favour hole transfer in **Zn^2-4d$^+$** (*vide infra*).

As the anionic reference radical **Zn-Ac-3c$^-$** is EPR-silent in our hands at room temperature (or the signal is too broad to be observed), a detailed comparison with **Zn^2-4d$^-$** is precluded. The EPR spectrum of **Zn^2-4d$^-$** matches that of the reference radical **1a$^-$** suggesting the presence of the valence isomer with the unpaired electron residing at the mesityl substituted free-base porphyrin in accordance with the electrochemical and DFT data (Fig. 5, bottom). Electron transfer between the similar sites is also possible in the mixed-valent system **Zn^2-4d$^-$** but definitive experimental facts cannot be extracted from the EPR data.[56] Mesityl substituted porphyrin radical anions feature high spin densities at the bridging *meso* carbon atom (see **Zn^2-4d$^-$**, Fig. 3) as do 4-C_6H_4F substituted zinc porphyrin radical anions (see *e.g.* **Zn^1Zn^2-4d$^-$**, Fig. 3) which should enable intramolecular electron transfer. This is also reflected in the MO description of **Zn^2-4d** showing that the LUMOs of both sites feature large coefficients at the bridging *meso* carbon atoms (*vide infra* and ESI†).

In the bis(zinc) complex **Zn^1Zn^2-4d** the first oxidation and reduction potentials are again very similar (Table 2) and both valence isomers are conceivable for the radical cation **Zn^1Zn^2-4d$^+$** and radical anion **Zn^1Zn^2-4d$^-$**, respectively. The isotropic EPR spectrum of **Zn^1Zn^2-4d$^+$** resembles that of **Zn-Ac-3c$^+$** and is distinct from that of **Zn-1a$^+$** (ESI, Fig. S10†) suggesting that the C_6H_4F substituted porphyrin is oxidised instead of the mesityl substituted porphyrin which is in full agreement with the DFT calculations (Fig. 3). The peak-to-peak line width of the EPR signal of **Zn^1Zn^2-4d$^+$** is slightly smaller than that of the constituent reference radicals suggesting rapid hole hopping on the EPR time scale.[65] This is also supported by orbital symmetry considerations (*vide infra*). As the EPR signals of the radical anions **Zn^1Zn^2-4d$^-$** and **Zn-Ac-1a$^-$** are very weak and the reference **Zn-Ac-3c$^-$** is even EPR silent a definitive conclusion as to the preferred site of the unpaired electron in the radical anion **Zn^1Zn^2-4d$^-$** cannot be reached (ESI, Fig. S10†).

The EPR spectra of the radical species obtained in a frozen solution at 77 K suffer from line broadening and anisotropy effects possibly due to aggregation or ion pairing of the mixed-valent cations and anions under these conditions (see the ESI†). Unfortunately, this precludes further reliable assignment to individual redox sites. In summary, the EPR spectra support the description of **4b$^{+/-}$** as valence asymmetric radicals with unambiguous assignments of formal oxidation states to the individual porphyrin sites and the description of the **Zn^2-4d$^{+/-}$** and **Zn^1Zn^2-4d$^+$** radical ions as more valence symmetric mixed-valent systems.

Photophysical properties – energy transfer

The absorption spectra of the bis(porphyrins) **4a–4d** are similar to the respective monoporphyrins showing Soret and Q bands at typical energies (Fig. 6 and 7). A slight bathochromic shift of the Soret band of a few nm is observed in all bis(porphyrins) as compared to the monomeric reference porphyrins indicating a weak excitonic coupling between the porphyrin subunits (see the ESI† for a graphical comparison, Fig. S7) independent of the concentration (between 4×10^{-6} M^{-1} and 5×10^{-8} M^{-1}). For the metalated bis(porphyrin) **Zn^1Zn^2-4d** the expected reduction of the number of Q bands from four to two in metalated porphyrins is observed (Fig. 7, bottom). In the mixed free-base/zinc(II) bis(porphyrin) **Zn^2-4d** the absorption spectrum is a superposition of a free-base porphyrin (four Q bands) and a zinc(II) porphyrin (two Q bands) (Fig. 7, center and inset). Thus, in the ground states of the bis(porphyrins) the individual porphyrins are essentially unperturbed and the porphyrins are only weakly electronically coupled.[66] Nevertheless, it has been shown that the weak ground state interaction does not prevent efficient charge injection of bis(porphyrins) *e.g.* into TiO_2.[67]

The emission data of relevant monoporphyrins and bis(porphyrins) are summarised in Tables 4 and 5, respectively. Fluorescence spectra of the monoporphyrin series **Ac-3a–Ac-3d**

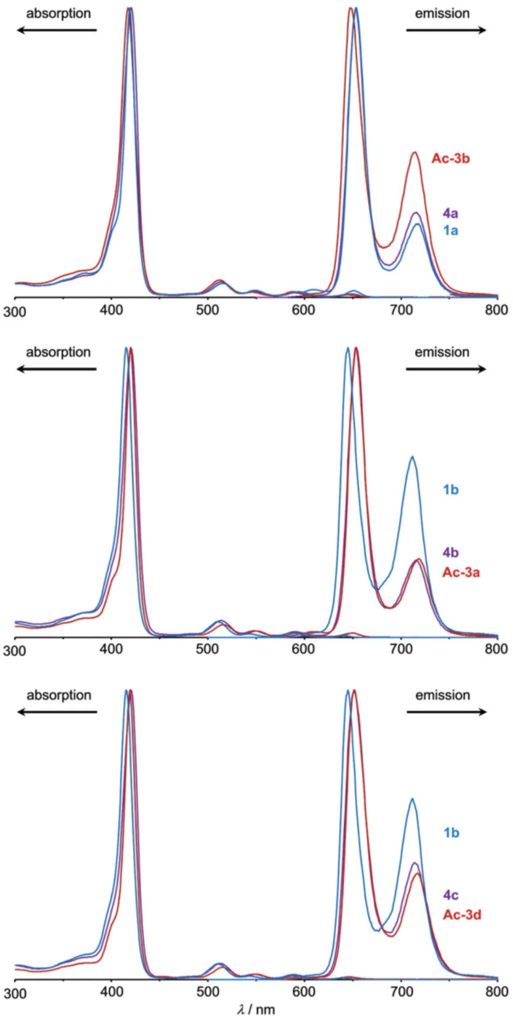

Fig. 6 Normalised absorption and emission spectra of **4a**, **4b** and **4c** and their constituent porphyrins in CH_2Cl_2.

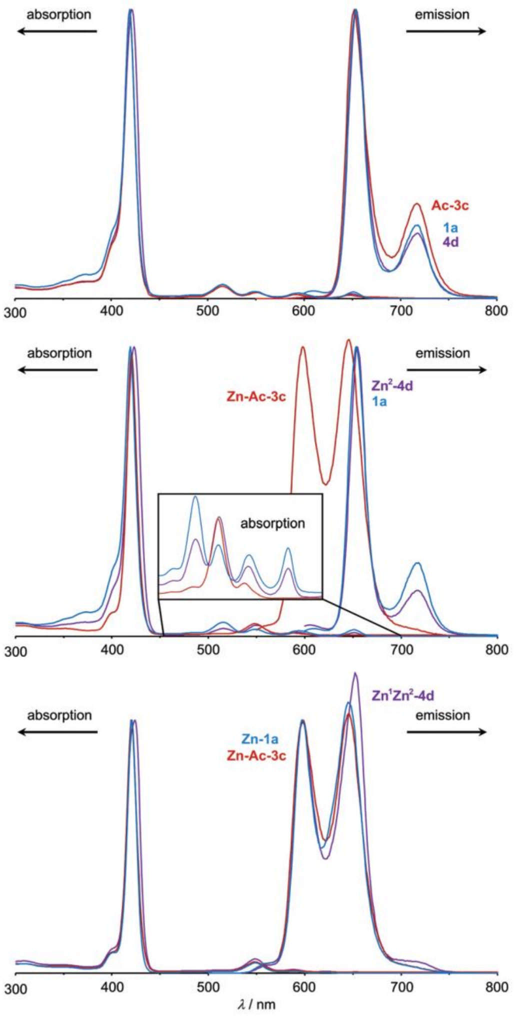

Fig. 7 Normalised absorption and emission spectra of **4d**, **Zn^2-4d** and **Zn^{1}Zn^2-4d** and their constituent porphyrins in CH_2Cl_2.

are displayed in Fig. S8 (ESI†). A slight hypsochromic shift of the Q(0,0) band is observed in the series **Ac-3a** → **Ac-3c** → **Ac-3d** → **Ac3b**. More pronounced than energy shifts are diagnostic intensity differences of the Q(0,0) and Q(0,1) emission bands (ESI, Fig. S8†).

Thus, from the shape and position of the vibronic progression of the emission band we can phenomenologically deduce the localisation of the lowest emitting state in the pentafluorophenyl derivatives **4a–4c**. The C_6F_5 substituted porphyrins **1b** and **Ac-3b** feature characteristic intense Q(0,1) emission bands (relative intensity with respect to Q(0,0) > 0.5) whereas all other relevant constituent porphyrins **1a**, **Ac-3a**, **Ac-3c** and **Ac-3d** display a lower relative intensity for the Q(0,1) emission band (<0.4). Thus, emission of **4a–4c** is easily assigned to the mesityl substituted porphyrins (**4a**, **4b**) and to the 4-$C_6H_4CF_3$ substituted porphyrin in **4c** (Fig. 6). For bis(porphyrin) **4d** emission is again assigned to the mesityl substituted porphyrin as deduced from the emission intensity signature which compares well to that of **1a** (Fig. 7, top). The lowest emitting state in **Zn^2-4d** is clearly associated with the free-base porphyrin (Fig. 7, center). Excited state lifetimes are also collected in Tables 4 and 5 with free-base porphyrins having $\tau \approx 10$ ns and zinc(II) porphyrins featuring $\tau \approx 2$ ns. The lifetime of τ = 10.88 ns of the mixed porphyrin **Zn^2-4d** fully corroborates emission from the free-base porphyrin subunit. Interestingly, a free-base/zinc(II) bis(porphyrin) with a short –CH═CH– *meso*-bridge shows dual emission of both subunits and, hence, points to less efficient energy transfer to the free-base porphyrin.[68] The fact that emission occurs essentially from a single porphyrin subunit in all bis(porphyrins) **4a-Zn^2-4d** points to an efficient energy transfer *via* the –C_6H_4–NHCO–C_6H_4– bridge with a center-to-center distance of the porphyrins of *ca.* 19 Å. Efficient energy transfer in similar systems featuring –C_6H_4–C≡C–C_6H_4– and –C_6H_4–CH═CH–C_6H_4– bridges and even hydrogen bonds has been previously observed and assigned to a predominantly Dexter through-bond mechanism.[66,69–74] A through-bond mechanism is also conceivable in dyads **4** *via* the –C_6H_4–NHCO–C_6H_4– bridge as all (local) HOMOs are of local a_{2u} symmetry (*vide infra*, Fig. 8–11 and ESI Fig. S3 and S4†) which promotes energy transfer in *meso–meso* linked porphyrins. The a_{2u} HOMO symmetry is even calculated for porphyrins possessing two C_6F_5 substituents instead of the a_{1u} symmetry (with a node at the linking *meso* position) reported for the HOMO of porphyrins with three C_6F_5 substituents.[66,70] As the considered porphyrins are highly unsymmetric the degeneracy of the e_g LUMOs of truly D_{4h} symmetric porphyrins is substantially lifted and the node structure of the lowest empty orbitals also becomes relevant

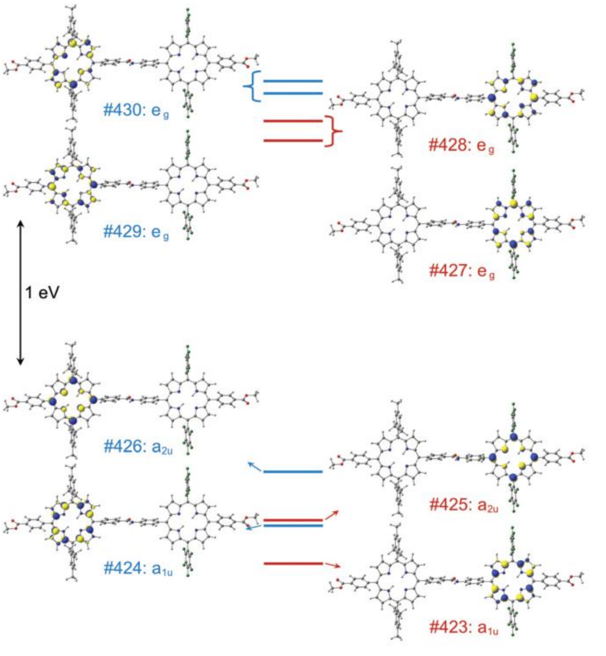

Fig. 8 Frontier molecular orbitals of **4a** (isosurface value at 0.05 a.u.; B3LYP/LANL2DZ, PCM CH_2Cl_2).

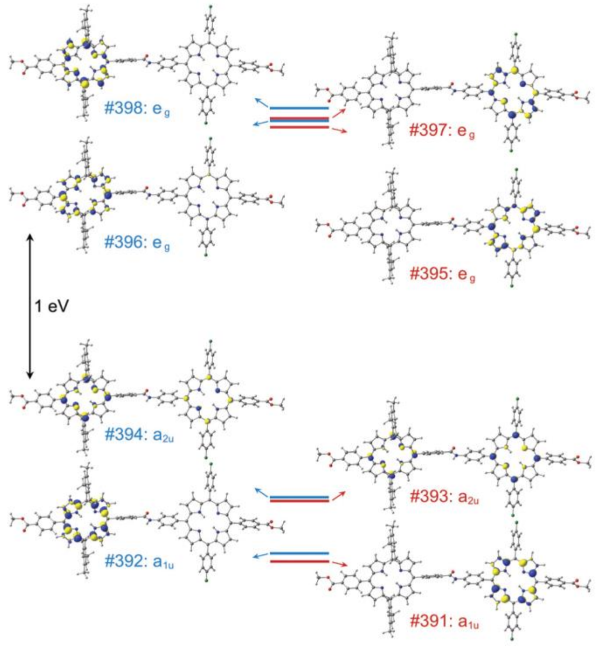

Fig. 9 Frontier molecular orbitals of **4d** (isosurface value at 0.05 a.u.; B3LYP/LANL2DZ, PCM CH_2Cl_2).

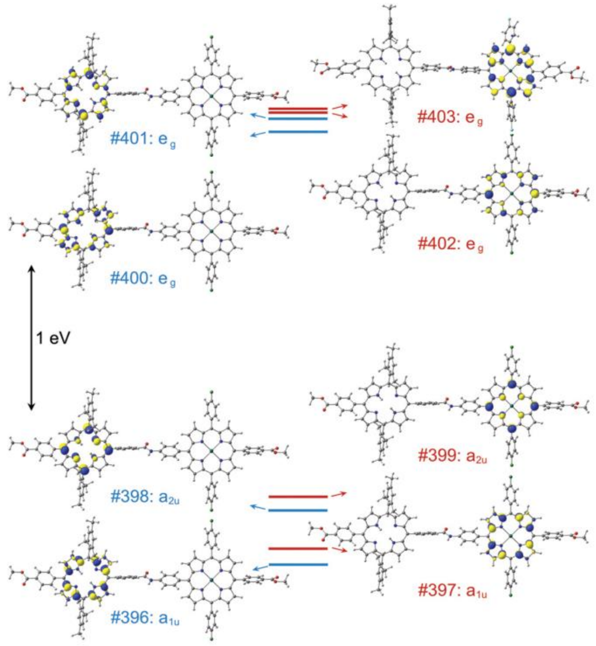

Fig. 11 Frontier molecular orbitals of **Zn^2-4d** (isosurface value at 0.05 a.u.; B3LYP/LANL2DZ, PCM CH_2Cl_2).

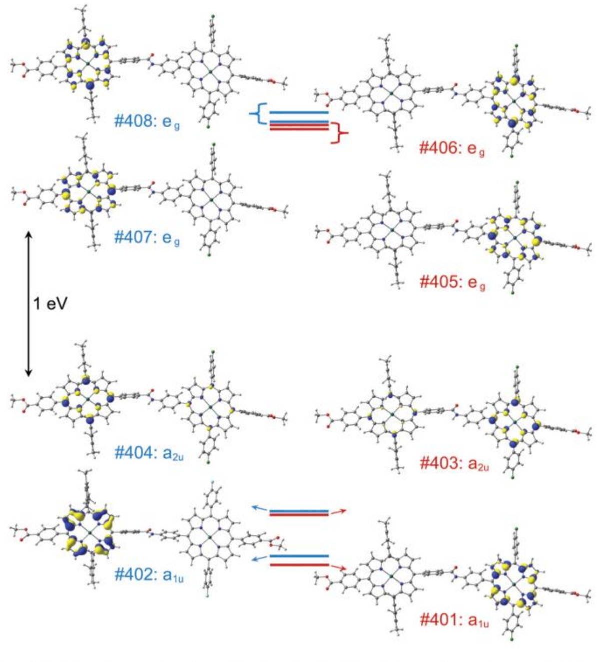

Fig. 10 Frontier molecular orbitals of **Zn^{1}Zn^2-4d** (isosurface value at 0.05 a.u.; B3LYP/LANL2DZ, PCM CH_2Cl_2).

for Dexter energy transfer processes. The LUMOs of the C_6F_5 and 4-$C_6H_4CF_3$ substituted porphyrins feature a node at the bridging *meso* carbon atoms while the LUMOs of mesityl and 4-C_6H_4F substituted porphyrins have large coefficients at the bridging *meso* carbon atoms which should further promote Dexter energy transfer.

The fluorescence spectrum of the bis(metalated) derivative **Zn^{1}Zn^2-4d** neither corresponds to that of an individual reference porphyrin **Zn-1a** or **Zn-Ac-3c** nor to a superposition of the individual fluorescence spectra of **Zn-1a** and **Zn-Ac-3c** (Fig. 7, bottom). Furthermore, the fluorescence lifetime is also distinct from that of the reference compounds **Zn-1a** and **Zn-Ac-3c** (Tables 4 and 5, ESI, Fig. S9†).

As a simple guide to the design of the electronic communication and interaction of the amide-linked porphyrins the 2 × 4 “Gouterman orbitals”[75] (the filled a_{2u}, a_{1u} and unoccupied e_g frontier orbitals in the nomenclature of an idealised local D_{4h} symmetry) of **4a–4d** have been calculated from the DFT/PCM optimised geometries. For bis(porphyrins) **4a–4c** the frontier orbitals of individual sites are rather unperturbed by the presence of the partner porphyrin (Fig. 8 and ESI, Fig. S3 and S4†).

In **4a–4c** the orbitals of the C_6F_5 substituted porphyrins are lower in energy than those of the respective mesityl and 4-$C_6H_4CF_3$ substituted porphyrins, respectively, underscoring the large electronic difference between the individual porphyrins. All HOMOs are of local a_{2u} symmetry favourable for electron transfer in radical cations and excited energy transfer. The LUMOs of the C_6F_5 and 4-$C_6H_4CF_3$ substituted porphyrins feature a nodal plane through the bridging *meso* carbon atoms while the mesityl substituted porphyrins have large coefficients at this *meso* position which should disfavour electron transfer in radical anions and singlet excited state energy transfer (Fig. 8 and Fig. S3 and S4, ESI†).

In **4d** the individual frontier orbitals are nearly pairwise degenerate with respect to the different sites (Fig. 9). The HOMOs are basically the in-phase and out-of-phase combination of the local a_{2u} orbitals (Fig. 9, #393, #394). The LUMOs of both the mesityl and 4-C_6H_4F substituted porphyrins possess large coefficients at the bridging *meso* position (Fig. 9, #395, #396). Hence, orbital energies and orbital symmetries should facilitate hole/electron transfer in **4d**$^{+/-}$ and energy transfer in **4d**.

A fully analogous description applies to the HOMOs and LUMOs of the bis(metalated) system **Zn**^{1}**Zn**^{2}**-4d** (Fig. 10, #403, #404 and #405, #407). The more delocalised electronic situation might also explain the different excited state behaviour of **Zn**^{1}**Zn**^{2}**-4d** as compared to that of its individual components **Zn-1a** and **Zn-Ac-3c** in terms of emission and singlet excited state lifetime (*vide supra*).

The frontier orbitals of **Zn**^{2}**-4d** obtained by DFT/PCM calculations (Fig. 11, #398, #399, #400, #402) suggest oxidation of the Zn-porphyrin site and reduction at the mesityl substituted free-base porphyrin which is in accordance with the experiments. Again, gas-phase DFT calculations predict a wrong oxidation site with the HOMO being located at the mesityl substituted porphyrin which is at odds with the experiment (ESI, Fig. S5†). Thus, for these close-lying orbitals gas-phase calculations are less reliable even in closed-shell systems. From orbital symmetry considerations hole transfer should be feasible in **Zn**^{2}**-4d**$^+$ (HOMOs #398, #399 of a_{2u} symmetry), electron transfer should be possible in **Zn**^{2}**-4d**$^-$ (LUMOs #400, #402 with large coefficients at the bridging *meso* carbon atoms) and thus bridge-mediated singlet energy transfer should be possible in the excited state of **Zn**^{2}**-4d** as found experimentally.

Conclusions

New *trans*-AB_2C *meso*-substituted porphyrin amino acid esters with *meso*-substituents of tunable electron withdrawing power B = 4-C_6H_4F, 4-$C_6H_4CF_3$ and C_6F_5 were prepared as free amines **3a–3d**, as *N*-acetylated derivatives **Ac-3a–Ac-3d** and as acetylated zinc(II) complexes **Zn-Ac-3a–Zn-Ac-3d**. Amide-linked bis(porphyrins) with tunable electron density at each porphyrin site were obtained from the amines (**4a–4d**) by amide formation and mono- and bis(zinc) complexes were prepared (**Zn**^{2}**-4d** and **Zn**^{1}**Zn**^{2}**-4d**).

In the ground states the properties of the individual porphyrins are largely preserved as judged from careful comparisons of the redox and UV/Vis absorption data with those of suitable reference compounds (weak ground state interaction).

In the mixed-valent radical anions and cations of bis(porphyrins) featuring similar local redox potentials **4d**$^{+/-}$, **Zn**^{2}**-4d**$^-$ and **Zn**^{1}**Zn**^{2}**-4d**$^{+/-}$ orbital symmetry, *i.e.* large coefficients at the bridging *meso* carbon atoms, permit hole and electron transfer *via* the phenyl–amide–phenyl bridge. A valence isomeric system with even three distinct charge and spin distributions has been recently reported with *meso*-vinylruthenium-modified zinc(II) porphyrin radical cations.[77] Charge and spin (de)localization in longer arrays of amide-bridged porphyrin radical ions will be addressed in the future.

The fluorescence spectra of bis(porphyrins) **4** reveal emission from the lowest energy S_1 state assigned to the mesityl (**4a**, **4b**, **4d**) and to the 4-$C_6H_4CF_3$ substituted porphyrin (**4c**). In the mixed bis(porphyrin) **Zn**^{2}**-4d** emission solely occurs from the free-base porphyrin. Thus, energy transfer across the phenyl–amide–phenyl linker is efficient in **4a–4d** and **Zn**^{2}**-4d** and Kasha's rule is obeyed.[76] Emission and lifetime data of **Zn**^{1}**Zn**^{2}**-4d** suggest a stronger electronic interaction between the individual porphyrin sites which can be traced back to more delocalised frontier orbitals over both sites.

Both substituent effects and (the site of) metalation affect the electronic situation in the reported amide linked bis(porphyrins) which is a fundamentally required knowledge for the rational design of energy transfer and electron transfer arrays based on amide-linked porphyrins. Arrays featuring these tunable porphyrin amino acids as chromophores and including electron donor and electron acceptor moieties for photoinduced electron transfer processes will be reported in due course.

Acknowledgements

We thank the Deutsche Forschungsgemeinschaft for supporting our work (He 2778/6-1) and the International Research Training Group (IRTG 1404, Self Organized Materials for Optoelectronics) also supported by the Deutsche Forschungsgemeinschaft. M.M. thanks the Max Planck Graduate Center for support. F.L. thanks the Max Planck Society for funding a Max Planck Research Group. We are grateful to the graduate student Steffy Becht for preparative assistance (Johannes Gutenberg-University of Mainz).

Notes and references

1 H. Vogler, *Chem. Unserer Zeit*, 2010, **44**, 308–309.

2 S. L. Kwolek, *U.S. patent*, 3 819 587 A (Dupont) 1974.

3 S. Hecht and I. Huc, *Foldamers*, Wiley-VCH, 2007.

4 E. Kolomiets, V. Berl and J.-M. Lehn, *Chem.–Eur. J.*, 2007, **13**, 5466–5479.

5 D. Siebler, M. Linseis, T. Gasi, L. M. Carrella, R. F. Winter, C. Förster and K. Heinze, *Chem.–Eur. J.*, 2011, **17**, 4540–4551.

6 D. Siebler, C. Förster and K. Heinze, *Dalton Trans.*, 2011, **40**, 3558–3575.

7 K. Heinze, M. Beckmann and K. Hempel, *Chem.–Eur. J.*, 2008, **14**, 9468–9480.

8 K. Heinze and M. Schlenker, *Eur. J. Inorg. Chem.*, 2004, 2974–2988.

9 K. Heinze and M. Schlenker, *Eur. J. Inorg. Chem.*, 2005, 66–71.

10 K. Heinze and M. Beckmann, *Eur. J. Inorg. Chem.*, 2005, 3450–3457.

11 K. Heinze, U. Wild and M. Beckmann, *Eur. J. Inorg. Chem.*, 2007, 617–623.

12 K. Heinze and D. Siebler, *Z. Anorg. Allg. Chem.*, 2007, **633**, 2223–2233.

13 M. Cakić Semenćić, D. Siebler, K. Heinze and V. Rapić, *Organometallics*, 2009, **28**, 2028–2037.

14 D. Siebler, C. Förster and K. Heinze, *Eur. J. Inorg. Chem.*, 2010, 523–527.

15 D. Siebler, C. Förster, T. Gasi and K. Heinze, *Organometallics*, 2011, **30**, 313–327.

16 K. Heinze, K. Hempel and M. Beckmann, *Eur. J. Inorg. Chem.*, 2006, 2040–2050.

17 K. Heinze and K. Hempel, *Chem.–Eur. J.*, 2009, **15**, 1346–1358.

18 K. Heinze, K. Hempel, S. Tschierlei, M. Schmitt, J. Popp and S. Rau, *Eur. J. Inorg. Chem.*, 2009, 3119–3126.

19 J. Dietrich, U. Thorenz, C. Förster and K. Heinze, *Inorg. Chem.*, 2013, **52**, 1248–1264.

20 (*a*) K. Heinze, K. Hempel and A. Breivogel, *Z. Anorg. Allg. Chem.*, 2009, **635**, 2541–2549; (*b*) A. Breivogel, K. Hempel and K. Heinze, *Inorg. Chim. Acta*, 2011, **374**, 152–162.

21 K. Heinze and A. Reinhart, *Dalton Trans.*, 2008, 469–480.

22 N. Metzler-Nolte, *Chimia*, 2007, **61**, 736–741.

23 G. Dirscherl and B. König, *Eur. J. Org. Chem.*, 2008, 597–634.

24 C.-W. Lee, H.-P. Lu, C.-M. Lan, Y.-L. Huang, Y.-R. Liang, W.-N. Yen, Y.-C. Liu, Y.-S. Lin, E. W.-G. Diau and C.-Y. Yeh, *Chem.–Eur. J.*, 2009, **15**, 1403–1412.

25 T. Bessho, S. M. Zakeeruddin, C.-Y. Yeh, E. W.-G. Diau and M. Grätzel, *Angew. Chem.*, 2010, **122**, 6796–6799, (*Angew. Chem., Int. Ed.*, 2010, **49**, 6646–6649).

26 Y.-C. Chang, C.-L. Wang, T.-Y. Pan, S.-H. Hong, C.-M. Lan, H.-H. Kuo, C.-F. Lo, H.-Y. Hsu, C.-Y. Lin and E. W.-G. Diau, *Chem. Commun.*, 2011, **47**, 8910–8912.

27 A. Yella, H.-W. Lee, H. N. Tsao, C. Yi, A. K. Chandiran, M. K. Nazeeruddin, E. W.-G. Diau, C.-Y. Yeh, S. M. Zakeeruddin and M. Grätzel, *Science*, 2011, **334**, 629–634.

28 S. L. Gould, G. Kodis, R. E. Palacios, L. de la Garza, A. Brune, D. Gust, T. A. Moore and A. L. Moore, *J. Phys. Chem. B*, 2004, **108**, 10566–10580.

29 (*a*) S. D. Straight, J. Andréasson, G. Kodis, S. Bandyopadhyay, R. H. Mitchell, T. A. Moore, A. L. Moore and D. Gust, *J. Am. Chem. Soc.*, 2005, **127**, 9403–9409; (*b*) D. Gust, T. A. Moore and A. L. Moore, *Chem. Commun.*, 2006, 1169–1178.

30 J. Andréasson, S. D. Straight, S. Bandyopadhyay, R. H. Mitchell, T. A. Moore, A. L. Moore and D. Gust, *Angew. Chem.*, 2007, **119**, 976–979, (*Angew. Chem., Int. Ed.*, 2007, **46**, 958–961).

31 C. M. Carcel, J. K. Laha, R. S. Loewe, P. Thamyongkit, K.-H. Schweikart, V. Misra, D. F. Bocian and J. S. Lindsey, *J. Org. Chem.*, 2004, **69**, 6739–6750.

32 T. Rohand, E. Dolusic, T. H. Ngo, W. Maes and W. Dehaen, *ARKIVOC*, 2007 (x), 307–324.

33 B. J. Littler, M. A. Miller, C.-H. Hung, R. W. Wagner, D. F. O'Shea, P. D. Boyle and J. S. Lindsey, *J. Org. Chem.*, 1999, **64**, 1391–1396.

34 K. Heinze and A. Reinhart, *Z. Naturforsch., B: Chem. Sci.*, 2005, **60**, 758–762.

35 D. T. Gryko, M. Tasior and B. Koszarna, *J. Porphyrins Phthalocyanines*, 2003, **7**, 239–248.

36 S. Stoll and A. Schweiger, *J. Magn. Reson.*, 2006, **178**, 42–55.

37 (*a*) A. Rosa, G. Ricciardi, E. J. Baerends, A. Romeo and L. Monsù Scolaro, *J. Phys. Chem. A*, 2003, **107**, 11468–11482; (*b*) J. R. Lakowicz, *Principles of Fluorescence Spectroscopy*, Springer, 3rd edn, 2006.

38 F. Etzold, I. A. Howard, N. Forler, D. M. Cho, M. Meister, H. Mangold, J. Shu, M. Ryan Hansen, K. Müllen and F. Laquai, *J. Am. Chem. Soc.*, 2012, **134**, 10569–10583.

39 M. J. Frisch, G. W. Trucks, H. B. Schlegel, G. E. Scuseria, M. A. Robb, J. R. Cheeseman, G. Scalmani, V. Barone, B. Mennucci, G. A. Petersson, H. Nakatsuji, M. Caricato, X. Li, H. P. Hratchian, A. F. Izmaylov, J. Bloino, G. Zheng, J. L. Sonnenberg, M. Hada, M. Ehara, K. Toyota, R. Fukuda, J. Hasegawa, M. Ishida, T. Nakajima, Y. Honda, O. Kitao, H. Nakai, T. Vreven, J. A. Montgomery Jr., J. E. Peralta, F. Ogliaro, M. Bearpark, J. J. Heyd, E. Brothers, K. N. Kudin, V. N. Staroverov, R. Kobayashi, J. Normand, K. Raghavachari, A. Rendell, J. C. Burant, S. S. Iyengar, J. Tomasi, M. Cossi, N. Rega, J. M. Millam, M. Klene, J. E. Knox, J. B. Cross, V. Bakken, C. Adamo, J. Jaramillo, R. Gomperts, R. E. Stratmann, O. Yazyev, A. J. Austin, R. Cammi, C. Pomelli, J. W. Ochterski, R. L. Martin, K. Morokuma, V. G. Zakrzewski, G. A. Voth, P. Salvador, J. J. Dannenberg, S. Dapprich, A. D. Daniels, O. Farkas, J. B. Foresman, J. V. Ortiz, J. Cioslowski and D. J. Fox, *GAUSSIAN 09 (Revision A.02)*, Gaussian, Inc., Wallingford CT, 2009.

40 N. G. Connelly and W. E. Geiger, *Chem. Rev.*, 1996, **96**, 877–910.

41 K. M. Smith, Porphyrins, in *Comprehensive Coordination Chemistry II*, ed. J. A. Mc Cleverty and T. J. Meyer, Elsevier, Oxford, UK, 2004, vol. 1, pp. 493–506.

42 J. S. Lindsey, *Acc. Chem. Res.*, 2010, **43**, 300–311.

43 (*a*) M. O. Senge, *Chem. Commun.*, 2011, **47**, 1943–1960; (*b*) M. O. Senge, Y. M. Shaker, M. Pintea, C. Ryppa, S. S. Hatscher, A. Ryan and Y. Sergeeva, *Eur. J. Org. Chem.*, 2010, 237–258.

44 A. K. Burrell, D. L. Officer, P. G. Plieger and D. C. W. Reid, *Chem. Rev.*, 2001, **101**, 2751–2796.

45 B. J. Littler, Y. Ciringh and J. S. Lindsey, *J. Org. Chem.*, 1999, **64**, 2864–2872.

46 K. Phukan, M. Ganguly and N. Devi, *Synth. Commun.*, 2009, **39**, 2694–2701.

47 A. Devos, J. Remion, A.-M. Frisque-Hesbain, A. Colens and L. Ghosez, *J. Chem. Soc., Chem. Commun.*, 1979, 1180–1181.

48 D. Siebler, C. Förster and K. Heinze, *Eur. J. Inorg. Chem.*, 2010, 3986–3992.

49 R. Schwesinger, C. Hasenfratz, H. Schlemper, L. Walz, E.-M. Peters, K. Peters and H. G. von Schnering, *Angew.*

Chem., 1993, **105**, 1420–1422, (*Angew. Chem., Int. Ed.*, 1993, **32**, 1361–1363).

50 R. Schwesinger, *Nachr. Chem. Technol. Lab.*, 1990, **38**, 1214–1226.

51 A. Bettelheim, B. A. White, S. A. Raybuck and R. W. Murray, *Inorg. Chem.*, 1987, **26**, 1009–1017.

52 C.-Y. Lin, Y.-C. Hung, C.-M. Liu, C.-F. Lo, Y.-C. Lin and C.-L. Lin, *Dalton Trans.*, 2005, 396–401.

53 T. Korenaga, K. Kadowaki, T. Ema and T. Sakai, *J. Org. Chem.*, 2004, **69**, 7340–7343.

54 K. M. Kadish and M. M. Morrison, *J. Am. Chem. Soc.*, 1976, **98**, 3326–3328.

55 M. B. Robin and P. Day, *Adv. Inorg. Chem. Radiochem.*, 1968, **10**, 247–422.

56 A. Heckmann and C. Lambert, *Angew. Chem.*, 2012, **124**, 334–404, (*Angew. Chem., Int. Ed.*, 2012, **51**, 326–392).

57 M. Gilet, A. Mortreux, J.-C. Folest and F. Petit, *J. Am. Chem. Soc.*, 1983, **105**, 3876–3881.

58 A. Klein in *Spectroelectrochemistry*, ed. W. Kaim and A. Klein, Royal Society of Chemistry, 2008, pp. 91–122.

59 M. Ohtani, K. Saito and S. Fukuzumi, *Chem.–Eur. J.*, 2009, **15**, 9160–9168.

60 R. H. Felton and H. Linschitz, *J. Am. Chem. Soc.*, 1966, **88**, 1113–1116.

61 J. Seth and D. F. Bocian, *J. Am. Chem. Soc.*, 1994, **116**, 143–153.

62 M. Huber, H. Kurreck, B. von Maltzan, M. Plato and K. Möbius, *J. Chem. Soc., Faraday Trans.*, 1990, **86**, 1087–1094.

63 M. Huber, *Eur. J. Org. Chem.*, 2001, 4379–4389.

64 S. Fukuzumi, Y. Endo and H. Imahori, *J. Am. Chem. Soc.*, 2002, **124**, 10974–10975.

65 T. M. Wilson, T. Hori, M.-C. Yoon, N. Aratani, A. Osuka, D. Kim and M. R. Wasielewski, *J. Am. Chem. Soc.*, 2010, **132**, 1383–1388.

66 D. Holten, D. F. Bocian and J. S. Lindsey, *Acc. Chem. Res.*, 2002, **35**, 57–69.

67 A. J. Mozer, M. J. Griffith, G. Tsekouras, P. Wagner, G. G. Wallace, S. Mori, K. Sunahara, M. Miyashita, J. C. Earles, K. C. Gordon, L. Du, R. Katoh, A. Furube and D. L. Officer, *J. Am. Chem. Soc.*, 2009, **131**, 15621–15623.

68 O. Locos, B. Bašić, J. C. McMurtrie, P. Jensen and D. P. Arnold, *Chem.–Eur. J.*, 2012, **18**, 5574–5588.

69 H. Song, M. Taniguchi, J. R. Diers, C. Kirmaier, D. F. Bocian, J. S. Lindsey and D. Holten, *J. Phys. Chem. B*, 2009, **113**, 16483–16493.

70 J.-P. Strachan, S. Gentemann, J. Seth, W. A. Kalsbeck, J. S. Lindsey, D. Holten and D. F. Bocian, *J. Am. Chem. Soc.*, 1997, **119**, 11191–11201.

71 J.-S. Hsiao, B. P. Krueger, R. W. Wagner, T. E. Johnson, J. K. Delaney, D. C. Mauzerall, G. R. Fleming, J. S. Lindsey, D. F. Bocian and R. J. Donohoe, *J. Am. Chem. Soc.*, 1996, **118**, 11181–11193.

72 A. Osuka, N. Tanabe, S. Kawabata, I. Yamazaki and Y. Nishimura, *J. Org. Chem.*, 1995, **60**, 7177–7185.

73 J. Otsuki, Y. Kanazawa, A. Kaito, D.-M. Shafiqul Islam, Y. Araki and O. Ito, *Chem.–Eur. J.*, 2008, **14**, 3776–3784.

74 J. Otsuki, K. Iwasaki, Y. Nakano, M. Itou, Y. Araki and O. Ito, *Chem.–Eur. J.*, 2004, **10**, 3461–3466.

75 M. Gouterman, *J. Chem. Phys.*, 1959, **30**, 1139–1161.

76 M. Kasha, *Faraday Discuss.*, 1950, **9**, 14–19.

77 J. Chen, E. Wuttke, W. Polit, T. Exner and R. F. Winter, *J. Am. Chem. Soc.*, 2013, **135**, 3391–3394.

6.2 Tuning Reductive and Oxidative Photoinduced Electron Transfer in Amide Linked Anthraquinone-Porphyrin-Ferrocene Architectures

Jascha Melomedov, Julian Robert Ochsmann, Michael Meister, Frédéric Laquai and Katja Heinze,

Eur. J. Inorg. Chem. **2014**, 1984-2001.

DOI: 10.1002/ejic.201400118

Manuscript received: 28.01.2014

Article first published online:27.02.2014

Issue published online: 10.04.2014

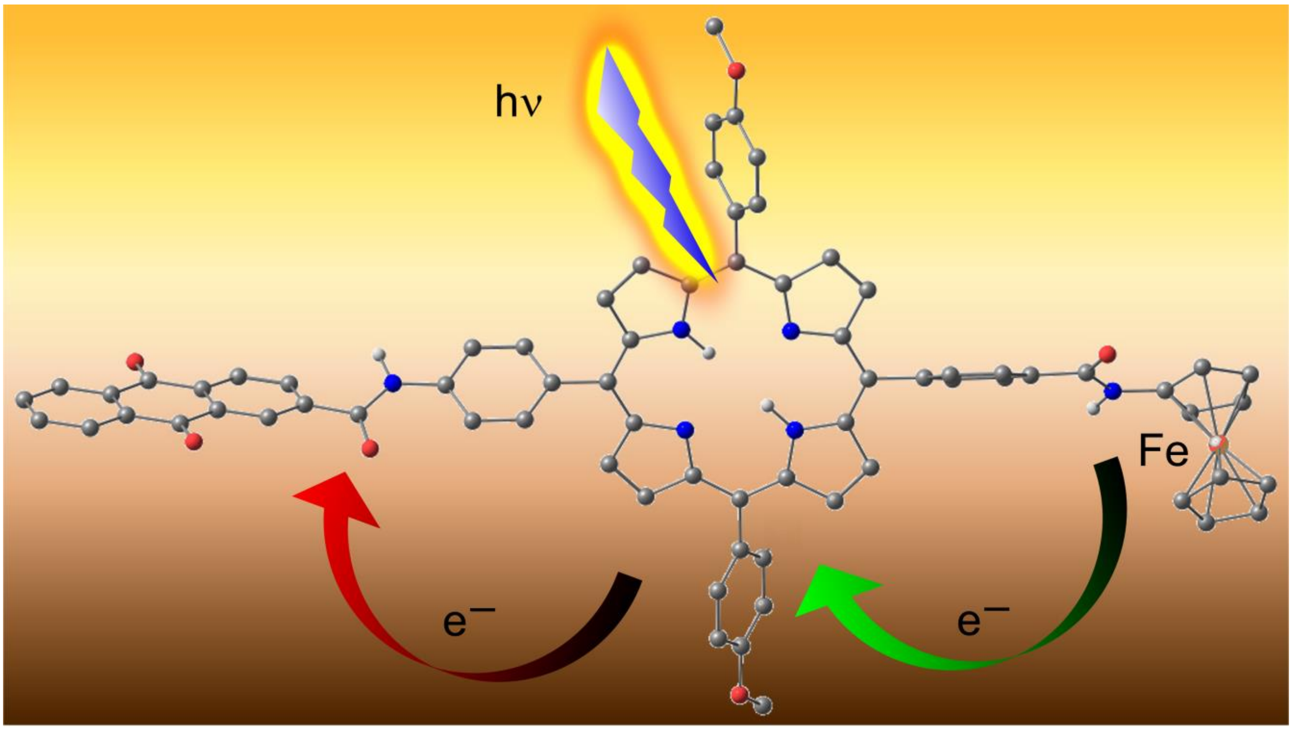

EurJIC European Journal of Inorganic Chemistry
ChemPubSoc Europe
FULL PAPER

DOI:10.1002/ejic.201400118

Tuning Reductive and Oxidative Photoinduced Electron Transfer in Amide-Linked Anthraquinone–Porphyrin–Ferrocene Architectures

Jascha Melomedov,[a] Julian Robert Ochsmann,[b] Michael Meister,[b] Frédéric Laquai,[b] and Katja Heinze*[a]

Keywords: Electron transfer / Density functional calculations / Substituent effects / Porphyrinoids / Quinones

Porphyrin amino acids **3a**–**3h** with *meso* substituents Ar of tunable electron-donating power (Ar = 4-C_6H_4OnBu, 4-C_6H_4OMe, 4-C_6H_4Me, Mes, C_6H_5, 4-C_6H_4F, 4-$C_6H_4CF_3$, C_6F_5) have been linked at the N terminus to anthraquinone Q as electron acceptor through amide bonds to give Q-P^{Ar} dyads **4a**–**4h**. These were conjugated to ferrocene Fc at the C terminus as electron donor to give the acceptor-chromophore-donor Q-P^{Ar}-Fc triads **6a**–**6h**. To further modify the energies of the electronically excited and charge-separated states, the triads **6a**–**6h** were metallated with zinc(II) to give the corresponding Q-(Zn)P^{Ar}-Fc triads **Zn-6a**–**Zn-6h**. The Q-P^{Ar1} dyad (Ar^1 = C_6H_5) was further extended with a second porphyrin P^{Ar2} (Ar^2 = 4-C_6H_4Me) as well as appended to a ferrocene to give the tetrad Q-P^{Ar1}-P^{Ar2}-Fc **9**. Almost all the conjugates show strongly reduced fluorescence quantum yields and excited-state lifetimes, which has been interpreted as photoinduced electron transfer (PET) either from the excited porphyrin to the quinone (oxidative PET) or from the ferrocene to the excited porphyrin (reductive PET). Electrochemical data, absorption spectroscopy, steady-state emission, time-resolved fluorescence, transient absorption pump-probe spectroscopy as well as DFT calculations have been used to elaborate the preferred PET pathway (reductive vs. oxidative PET) in these architectures with systematically varied electron-donating substituents at the central chromophore.

Introduction

Photoinduced electron transfer (PET) is a key step in natural photosynthesis.[1] For a deeper understanding of photosynthetic processes such as sunlight energy collection, light-energy storage, light-to-chemical energy conversion, electron-transport pathways and finally the efficient utilisation of sunlight, a number of elegant functional artificial reaction centres have been designed and intensively investigated to gain an increasingly clear picture of the important processes.[2–7] The rational design of reaction centres to mimic the multistep downhill electron transfer is theoretically based on the Marcus theory of electron transfer (ET)[8] and experimentally relies on the availability of suitable building blocks that can be assembled at will. Artificial reaction centres consist of non-covalently or covalently linked donor–acceptor units with quinones (natural acceptors),[3] porphyrins[4] or fullerenes[5] acting as electron acceptors and porphyrins,[6] ferrocene[5e–5i,7] or carotenoid polyenes[6] acting as electron donors. A variety of quinone–porphyrin[3] (Q-P) and porphyrin–ferrocene (P-Fc) systems[5e–5i,7] have been investigated with respect to PET, proving very useful for fundamental PET research and potential applications. Furthermore, several other metal complexes have been attached to porphyrins as electron-accepting units.[9] Variation of Q has allowed the effect of exothermicity on the rates of electron transfer to be studied in considerable detail[3c,3e] and variation of Fc substituents has shown that energy- and electron-transfer pathways depend on the oxidation potential of the ferrocene.[10] Elaborated C_{60}-P_n-Fc architectures feature long-lived charge-separated states.[5e–5h] In C_{60}-(Zn)P_n-Fc conjugates with C_{60} as the electron acceptor, the first PET typically is the thermodynamically favourable oxidative quenching of the excited porphyrin by the fullerene followed by a thermal shift of charge from the ferrocene to the central porphyrin.[5e–5h] The effect of the number of porphyrins sandwiched between C_{60} and ferrocene has also been thoroughly investigated.[5e–5h] In systems containing both Fc and Q, the preference of the initial photoinduced electron-transfer step is ambiguous as the free energies for both steps are of a similar magnitude.

To the best of our knowledge, systems combining the electron-accepting features of quinones, the light-absorbing properties of porphyrin chromophores and the electron-donating properties of ferrocene derivatives have not yet been studied with respect to either the preferred PET pathways

---

[a] Institute of Inorganic and Analytical Chemistry, Johannes Gutenberg University of Mainz,
Duesbergweg 10–14, 55128 Mainz, Germany
E-mail: katja.heinze@uni-mainz.de
http://www.ak-heinze.chemie.uni-mainz.de/
[b] Max Planck Institute for Polymer Research,
Ackermannweg 10, 55128 Mainz, Germany

Supporting information for this article is available on the WWW under http://dx.doi.org/10.1002/ejic.201400118.

or the tuning of PET pathways by modifying the excited-state energies of the central chromophore in a systematic manner with Fc donor and Q acceptor levels held at a fixed energy.

Linking reaction centre components through amide bonds has considerable advantages, namely a rather rigid connectivity of the building blocks,[11,12] a defined directional design in linear arrays (N terminus → C terminus) and a simple orthogonal modification at the termini with electron donors and acceptors. Furthermore, oligoamide synthesis can be conveniently accomplished by using solid-phase synthesis methods.[13]

We have previously reported suitable building blocks for directional oligoporphyrin amides, namely porphyrin amino acids with a *trans*-AB_2C substitution pattern (Scheme 1).[11,14] These porphyrin amino acids feature electron-donating mesityl, phenyl and electron-withdrawing fluorinated aryl groups at the *meso* positions (Ar = Mes, C_6H_5, 4-C_6H_4F, 4-$C_6H_4CF_3$, C_6F_5).[6c,11,14] More strongly electron-donating substituents such as Ar = 4-C_6H_4OR have not been studied. The key building blocks used in this study are porphyrin amino acids P^{Ar} and their esters with a full range of Ar substituents, anthraquinone-2-carboxylic acid Q as the electron acceptor and aminoferrocene Fc-NH_2 as the electron donor.[15]

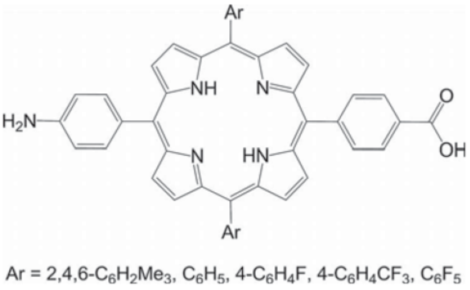

Scheme 1. Porphyrin amino acid building blocks.

Herein we report 1) the synthesis and properties of new *trans*-AB_2C-substituted porphyrin amino acid esters with electron-donating *meso* substituents Ar = 4-C_6H_4O*n*Bu, 4-C_6H_4OMe, 4-C_6H_4Me and C_6H_5[14] (**3a**, **3b**, **3d**, **3e**) and their corresponding *N*-acetyl-protected derivatives (**Ac-3a**, **Ac-3b**, **Ac-3d**, **Ac-3e**) as building blocks and reference compounds, 2) the coupling of eight *trans*-AB_2C-substituted porphyrin amino acid building blocks P^{Ar} with varying electron-withdrawing power (Ar = 4-C_6H_4O*n*Bu, 4-C_6H_4OMe, 4-C_6H_4Me, Mes, C_6H_5, 4-C_6H_4F, 4-$C_6H_4CF_3$, C_6F_5) to anthraquinone-2-carboxylic acid Q to give Q-P^{Ar} dyads (**4a**–**4h**), 3) the amide coupling of Fc-NH_2 to Q-P^{Ar} to give Q-P^{Ar}-Fc triads (**6a**–**6h**) and metallation with zinc(II) to give Q-(Zn)P^{Ar}-Fc triads (**Zn-6a**–**Zn-6h**), 4) the (formal) extension of the triad Q-P^{Ar1}-Fc (Ar^1 = C_6H_5) with an additional porphyrin amino acid P^{Ar2} (Ar^2 = 4-C_6H_4Me) to furnish the tetrad Q-P^{Ar1}-P^{Ar2}-Fc (**9**) and 5) the examination of initial charge separation pathway preferences in dyads **4**, triads **6** and **Zn-6** as well as in tetrad **9** with fixed acceptor (Q) and donor (Fc) levels, namely oxidative (P^{Ar} to Q) versus reductive (Fc to P^{Ar}) PET with respect to the substituent Ar, by electrochemical methods, absorption spectroscopy, steady-state emission, time-resolved fluorescence, transient absorption spectroscopy as well as by DFT calculations.

The results of this work will be of considerable value to the rational design of artificial photosynthetic systems that feature multistep electron transfer by well-defined efficient single-electron transfer and charge-shift steps. Through our design strategy it is easy to tune the individual energy levels of the chromophore radical ions relative to the acceptor and donor levels. This versatile modular design will allow the construction of even larger arrays with predefined sequences and excited-state energy levels.

Results and Discussion

Synthesis and Characterisation of Building Blocks 3, Dyads 4, Triads 6 and Zn-6, and Tetrad 9

In addition to the recently reported *trans*-AB_2C porphyrin amino acids P^{Ar}[11,14] with Ar = Mes (**3c**), C_6H_5 (**3e**), 4-C_6H_4F (**3f**), 4-$C_6H_4CF_3$ (**3g**) and C_6F_5 (**3h**), substituents with a greater electron-donating power are required for a comprehensive study. Hence, three novel *trans*-AB_2C-substituted porphyrin[16] amino acid esters[11,14] with electron-releasing *meso* substituents [Ar = 4-C_6H_4O*n*Bu (**3a**), 4-C_6H_4OMe (**3b**), 4-C_6H_4Me (**3d**)] were synthesised following a Lindsey-type 2+2 condensation procedure[17] employing nitro- and ester-substituted phenyldipyrromethanes.[18] The nitro functional group was reduced to the amine by reduction with tin(II) chloride in hydrochloric acid to obtain the porphyrin amino acid esters **3a**, **3b** and **3d** (see the Supporting Information). As the optical properties of amines are strongly pH-dependent and the oxidation of amines is often irreversible, *N*-acetyl-protected reference compounds **Ac-3a**, **Ac-3b**, **Ac-3d** and **Ac-3e** as well as their corresponding Zn^{II} complexes **Zn-Ac-3a**, **Zn-Ac-3b**, **Zn-Ac-3d** and **Zn-Ac-3e** were synthesised following established procedures (see the Supporting Information).[11,19]

The eight porphyrin amino acid esters **3a**–**3h**, with Ar exhibiting increasing electron-withdrawing power, were coupled to anthraquinone-2-carboxylic acid (as electron acceptor) after activating the latter as the acid chloride by reaction with thionyl chloride to give the Q-P^{Ar} dyads **4a**–**4h** (Scheme 2). Cleavage of the methyl ester by using aqueous KOH in methanol/THF delivered the quinone-porphyrin acids **5a**–**5g**, respectively (Scheme 2). The base-catalysed cleavage of dyad **4h** also led to the nucleophilic aromatic substitution of fluoride in the electron-poor aryl substituents by methoxide (Ar = C_6F_5 → Ar = 4-C_6F_4OMe) to give acid **5i**. Therefore to obtain **5h** from **4h**, an acid-catalysed hydrolysis protocol needed to be employed (Scheme 2). Quinone-porphyrin-ferrocene triads Q-P^{Ar}-Fc (**6a**–**6i**) were assembled by activation of the acid groups in **5a**–**5i** as acid chlorides by using thionyl chloride and coupling with aminoferrocene[15] (as electron donor). The quin-

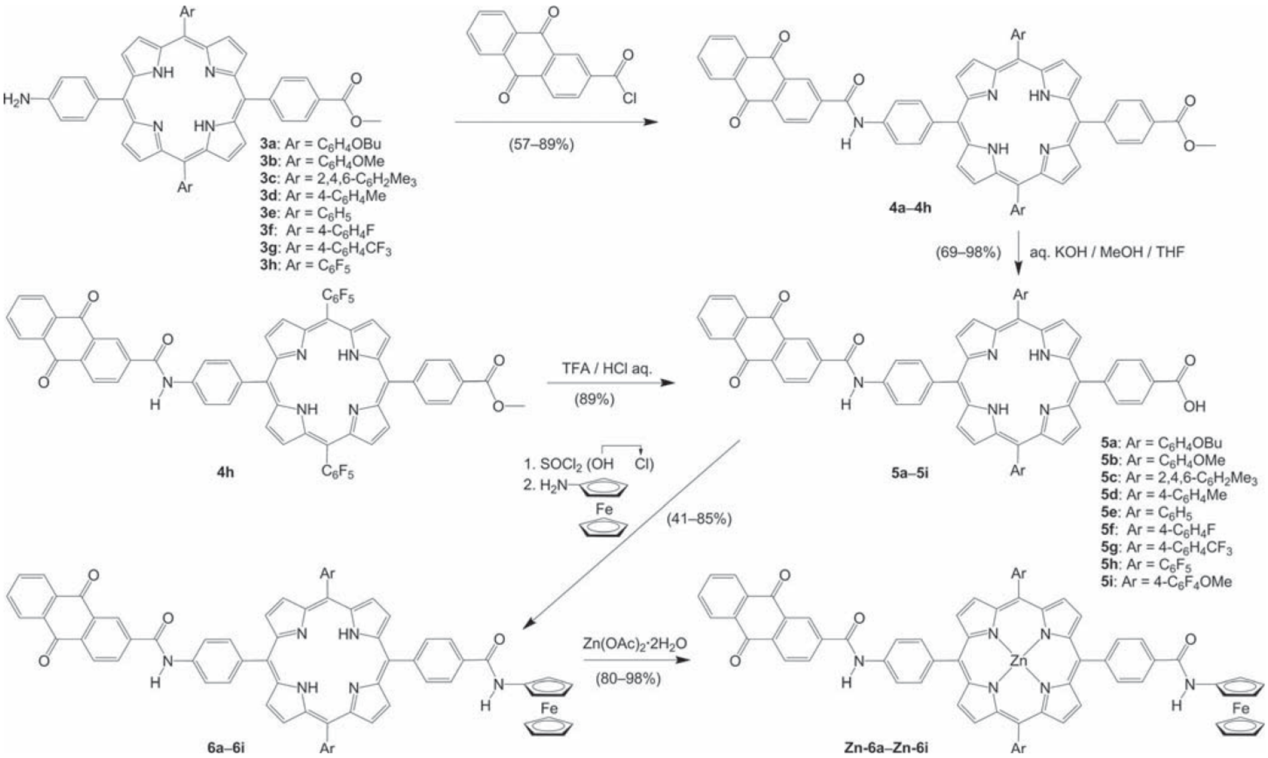

Scheme 2. Synthesis of dyads **4a**–**4h** and triads **6a**–**6i** and **Zn-6a**–**Zn-6i**.

one-(Zn)porphyrin-ferrocene triads Q-(Zn)P^{Ar}-Fc (**Zn-6a**–**Zn-6i**) were obtained from the free base triads **6a**–**6i** by metallation with zinc(II) acetate dihydrate (Scheme 2).

The construction of the Q-P^{C6H5}-P^{C6H4Me}-Fc tetrad **9** is depicted in Scheme 3. Q-P acid **5e** was coupled to porphyrin amino acid ester **3d** (activated as the acid chloride by using thionyl chloride) to give the Q-P^{C6H5}-P^{C6H4Me} triad **7**. The ferrocene entity was attached to **7** through an amide bond after base-catalysed methyl ester cleavage (to give free acid **8**, see the Supporting Information). Subsequent formation of the acid chloride and coupling with aminoferrocene gave the target tetrad **9**. The quinone reference *N*-ethylanthraquinone-2-carboxylic acid amide **10** as well as the bis(porphyrin) reference P^{C6H5}-P^{C6H4Me} **11** were synthesised as described in the Supporting Information.

The correct formation of all monoporphyrins **3**, the dyads **4**, the triads **6**, **Zn-6** and **7**, the tetrad **9**, the quinone reference compound **10** and the bis(porphyrin) reference **11** was substantiated by multinuclear NMR spectroscopy (^{1}H, ^{13}C, ^{19}F), IR and UV/Vis spectroscopy as well as (high-resolution) mass spectrometry (see the Supporting Information). In all cases the mass spectra show the signals expected for the intact porphyrin and porphyrin conjugates. In the ^{1}H NMR spectra, successful amide formation is clearly indicated by the disappearance of the amine proton resonances of **3a**–**3h** at δ = 4.99 ppm and the appearance of the amide resonances of dyads **4a**–**4h** at δ = 10.30–10.40 ppm. The covalent attachment of the ferrocene by amide coupling to the dyads **4** was confirmed by observing a second amide proton resonance at δ = 9.19–9.29 ppm in the ^{1}H NMR spectra of **6a**–**6h**. The presence of three NH amide resonances at δ = 9.21, 10.21 and 10.33 ppm demonstrates the successful synthesis of tetrad **9**. The resonances corresponding to the quinone and ferrocene moieties in the dyads, triads and tetrads further prove the integrity of the oligoamides. Metallation of triads **6** with Zn^{II} resulted in the expected changes in the porphyrin resonances, such as the disappearance of the pyrrole NH resonances. For the Q-(Zn)P dyads featuring an azomethine linker, the quinone proton resonances are reported to be shifted to a higher field. This has been rationalised by the coordination of the quinone carbonyl oxygen atom to the Zn^{II} centre.[3m] The Q proton resonances of the Q-Zn(P)-Fc triads **Zn-6** are not shifted, and hence a Zn···O=C interaction in **Zn-6** can be excluded. Possibly for the reported Q-Zn(P) dyads, a Zn···N$_{azomethine}$ interaction seems to be more likely than Zn···OC$_{quinone}$ coordination.[3m]

Absorption and Emission of Dyads 4, Triads 6 and Zn-6, and Tetrad 9

The absorption data for the dyads, triads, tetrad and reference compounds are presented in Table 1. The absorption spectra of **4a**–**4h**, **6a**–**6h** and **Zn-6a**–**Zn-6h** are essentially identical to those of the corresponding reference porphyrins **Ac-3a**–**Ac-3h** and **Zn-Ac-3a**–**Zn-Ac-3h**. As a result of the low extinction coefficients of *N*-ethylanthraquinone-2-carb-

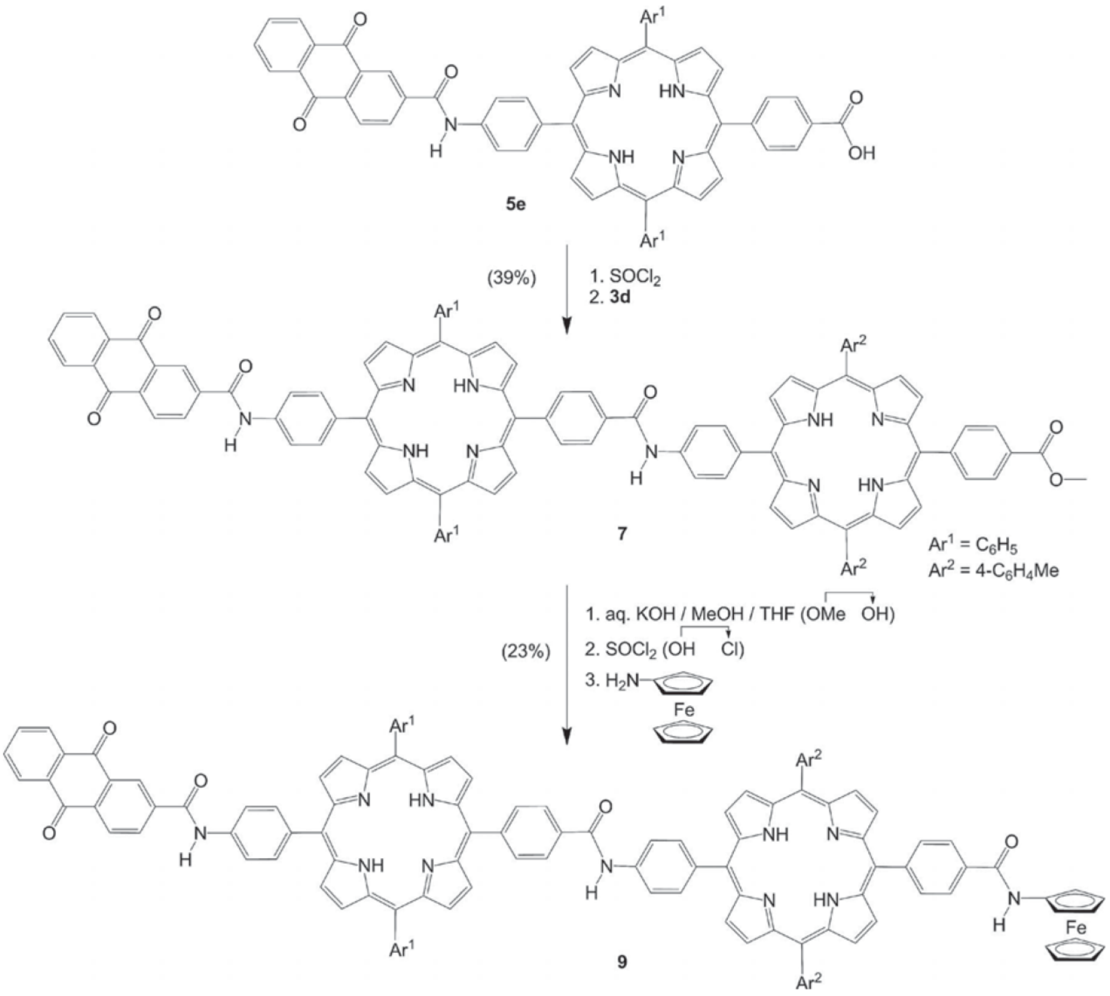

Scheme 3. Synthesis of tetrad **9**.

oxylic acid amide **10** (λ_{max} = 328 nm, ε = 5300 $\text{M}^{-1}\text{cm}^{-1}$) and 1-(acetylamino)ferrocene (Fc-NHAc; λ_{max} = 441 nm, ε = 215 $\text{M}^{-1}\text{cm}^{-1}$),[15] no absorption bands from these chromophores are discernible in the absorption spectra of the dyads and triads. The shapes and intensities of the Soret bands relative to their Q bands remain unaffected after the linking of quinone and ferrocene to the porphyrin core (Figure 1 and the Supporting Information). A slight blue shift of the porphyrin Soret and porphyrin Q bands is observed within the Q-P series **4a**→**4h** and Q-P-Fc series **6a**→**6h** due to the increasing electron-withdrawing character of *meso*-aryl substituents Ar. Neither new charge-transfer bands[20] nor perturbations of the porphyrin absorption bands were detected, which indicates only a weak ground-state electronic interaction between the quinone or the ferrocene with the central porphyrin. The Q-(Zn)P^{Ar}-Fc triads **Zn-6a–Zn-6h** show a small bathochromic shift (1–4 nm) of porphyrin absorbance bands in comparison with the corresponding reference porphyrins **Zn-Ac-3a**–**Zn-Ac-3h** (Figure 1 and Table 1).

Figure 2 shows the absorption spectra of triad Q-P^{C6H5}-P^{C6H4Me} (**7**), tetrad Q-P^{C6H5}-P^{C6H4Me}-Fc (**9**) and reference dyad P^{C6H5}-P^{C6H4Me} (**11**). Appending a quinone or a ferrocene to the bis(porphyrin) core does not alter the absorption spectrum, similarly to the monoporphyrin conjugates. Furthermore, the absorption spectra of the bis(porphyrins) **7**, **9** and **11** are nearly identical to those of the constituent porphyrins **Ac-3d** and **Ac-3e** and exhibit no splitting of the Soret or Q bands.[11] In summary, the absorption spectra are essentially a superposition of the individual unperturbed spectra of the building blocks.

The fluorescence data, quantum yields and the exited-state lifetimes of the new porphyrin amino acid esters **3a**, **3b**, **3d** and **3e**, and the reference porphyrins **Ac-3a**, **Ac-3b**, **Ac-3d**, **Ac-3e**, **Zn-Ac-3a**, **Zn-Ac-3b**, **Zn-Ac-3d**, **Zn-Ac-3e** and bis(porphyrin) **11** are collected in Table 2. As discussed previously[11] for related porphyrins, a small hypsochromic shift of the emission band is observed in the series **Ac-3a**→**Ac-3b**→**Ac-3d**→**Ac-3e** and **Zn-Ac-3a**→**Zn-Ac-3b**→**Zn-Ac-3d**→**Zn-Ac-3e**.

Table 1. Absorption data for **Ac-3a**–**Ac-3h**, **Zn-Ac-3a**–**Zn-Ac-3h**, **4a**–**4h**, **6a**–**6i**, **Zn-6a**–**Zn-6i**, **7**, **9** and **11** in CH_2Cl_2 at room temperature.

	Ar	λ [nm] (ε [10^{-4} M^{-1} cm^{-1}])				
		Soret	$Q_y(1,0)$	$Q_y(0,0)$	$Q_x(1,0)$	$Q_x(0,0)$
Ac-3a	C_6H_4OnBu	422 (30.03)	517 (1.14)	555 (0.73)	593 (0.63)	649 (0.65)
4a	C_6H_4OnBu	422 (32.44)	518 (1.36)	555 (0.84)	593 (0.49)	649 (0.47)
6a	C_6H_4OnBu	422 (36.31)	518 (1.35)	555 (0.89)	593 (0.36)	650 (0.39)
Zn-Ac-3a	C_6H_4OnBu	424 (40.10)	552 (1.75)	594 (0.65)	–	–
Zn-6a	C_6H_4OnBu	425 (47.78)	552 (1.33)	594 (0.78)	–	–
Ac-3b	C_6H_4OMe	421 (35.40)	517 (1.38)	554 (0.87)	593 (0.45)	648 (0.42)
4b	C_6H_4OMe	421 (39.59)	517 (1.40)	554 (0.89)	593 (0.33)	649 (0.35)
6b	C_6H_4OMe	422 (39.19)	518 (1.67)	554 (1.11)	593 (0.69)	649 (0.53)
Zn-Ac-3b	C_6H_4OMe	424 (48.62)	551 (1.90)	593 (0.63)	–	–
Zn-6b	C_6H_4OMe	424 (51.07)	552 (1.96)	594 (0.73)	–	–
Ac-3c	Mes	420 (36.29)	516 (1.24)	550 (0.37)	593 (0.28)	652 (0.55)
4c	Mes	421 (36.33)	516 (1.55)	551 (0.68)	592 (0.34)	651 (0.56)
6c	Mes	421 (36.18)	516 (1.51)	552 (0.60)	592 (0.30)	648 (0.25)
Zn-Ac-3c	Mes	423 (45.12)	551 (1.92)	592 (0.45)	–	–
Zn-6c	Mes	424 (49.71)	552 (1.88)	594 (0.18)	–	
Ac-3d	C_6H_4Me	420 (33.60)	516 (1.27)	552 (0.71)	592 (0.39)	647 (0.35)
4d	C_6H_4Me	420 (39.00)	517 (1.93)	552 (1.26)	591 (0.85)	647 (0.82)
6d	C_6H_4Me	420 (44.69)	517 (1.72)	553 (1.57)	591 (1.12)	647 (0.61)
Zn-Ac-3d	C_6H_4Me	421 (45.15)	549 (1.82)	588 (0.46)	–	–
Zn-6d	C_6H_4Me	423 (47.02)	551 (2.02)	593 (0.75)	–	–
Ac-3e	C_6H_5	419 (32.60)	515 (1.34)	551 (0.68)	591 (0.43)	646 (0.34)
4e	C_6H_5	419 (32.25)	515 (1.34)	551 (0.69)	591 (0.42)	646 (0.36)
6e	C_6H_5	419 (35.06)	516 (1.56)	551 (0.84)	591 (0.49)	646 (0.42)
Zn-Ac-3e	C_6H_5	420 (36.10)	549 (1.63)	589 (0.48)	–	–
Zn-6e	C_6H_5	423 (38.89)	551 (1.63)	592 (0.46)	–	–
Ac-3f	C_6H_4F	419 (50.42)	515 (2.16)	551 (1.07)	591 (0.72)	647 (0.61)
4f	C_6H_4F	419 (46.25)	515 (1.96)	551 (0.98)	591 (0.59)	647 (0.45)
6f	C_6H_4F	419 (41.79)	515 (2.22)	551 (1.38)	589 (1.00)	646 (0.86)
Zn-Ac-3f	C_6H_4F	420 (41.45)	548 (1.87)	587 (0.50)	–	–
Zn-6f	C_6H_4F	422 (47.69)	551 (2.05)	593 (0.63)	–	–
Ac-3g	$C_6H_4CF_3$	419 (41.40)	515 (1.78)	550 (0.79)	590 (0.57)	646 (0.40)
4g	$C_6H_4CF_3$	419 (31.57)	515 (1.45)	549 (0.69)	591 (0.47)	649 (0.41)
6g	$C_6H_4CF_3$	419 (32.42)	515 (1.54)	551 (0.78)	590 (0.53)	646 (0.41)
Zn-Ac-3g	$C_6H_4CF_3$	420 (28.30)	548 (1.17)	588 (0.21)	–	–
Zn-6g	$C_6H_4CF_3$	423 (34.13)	552 (1.59)	593 (0.48)	–	–
Ac-3h	C_6F_5	418 (39.31)	512 (2.38)	545 (0.84)	587 (0.93)	642 (0.56)
4h	C_6F_5	418 (34.69)	512 (2.15)	546 (0.70)	588 (0.79)	642 (0.44)
6h	C_6F_5	417 (41.02)	511 (2.20)	545 (0.42)	588 (0.49)	642 (0.48)
Zn-Ac-3h	C_6F_5	422 (51.09)	552 (2.01)	593 (0.36)	–	–
Zn-6h	C_6F_5	422 (47.51)	551 (1.68)	594 (0.65)	–	–
6i	C_6F_4OMe	419 (37.03)	512 (1.87)	546 (0.45)	589 (0.48)	644 (0.11)
Zn-6i	C_6F_4OMe	423 (43.97)	552 (1.86)	592 (0.32)	–	–
11	C_6H_5/C_6H_4Me	422 (73.50)	516 (3.53)	552 (2.05)	591 (1.19)	647 (1.06)
7	C_6H_5/C_6H_4Me	422 (76.62)	516 (3.57)	552 (2.06)	591 (1.15)	647 (1.04)
9	C_6H_5/C_6H_4Me	422 (77.48)	517 (3.74)	553 (2.14)	591 (1.14)	647 (1.02)

The emission spectra of selected dyads, triads, tetrad **9** and reference porphyrins are shown in Figures 1 and 2. Linking anthraquinone to porphyrins **3** and **Zn-3** as well as to (bis)porphyrin **11** leads to a significant decrease in the fluorescence intensity of quinone conjugates **4** and **7** (see Tables 2 and 3). The quenching efficiency varies between 10 and 92%, which indicates the presence of a new non-radiative decay channel in the dyads, namely oxidative PET. The strongest decrease in fluorescence intensity is found for dyad **4a** with Ar = 4-C_6H_4OnBu (92%, Figure 1), whereas almost no quenching at all is seen for dyad **4h** with Ar = C_6F_5 (10%, Table 2 and Table 3). As anticipated, the nature of the *meso*-aryl substituent Ar controls the efficiency of fluorescence quenching by oxidative PET. Electron-rich substituents induce stronger quenching than electron-withdrawing substituents. Only dyad **4c** with sterically demanding mesityl groups (Ar = Mes) at the *meso* positions deviates from the described trend. DFT geometry optimisations of **4c** revealed a 90° dihedral angle between the mesityl and porphyrin planes in contrast to the smaller angles observed for all other substituents (Ar = C_6F_5: 79°; all other Ar: 63–66°; see the Supporting Information). Furthermore, full rotation of a mesityl group connected to a porphyrin has an activation barrier of around 74 kJ mol^{-1} in solu-

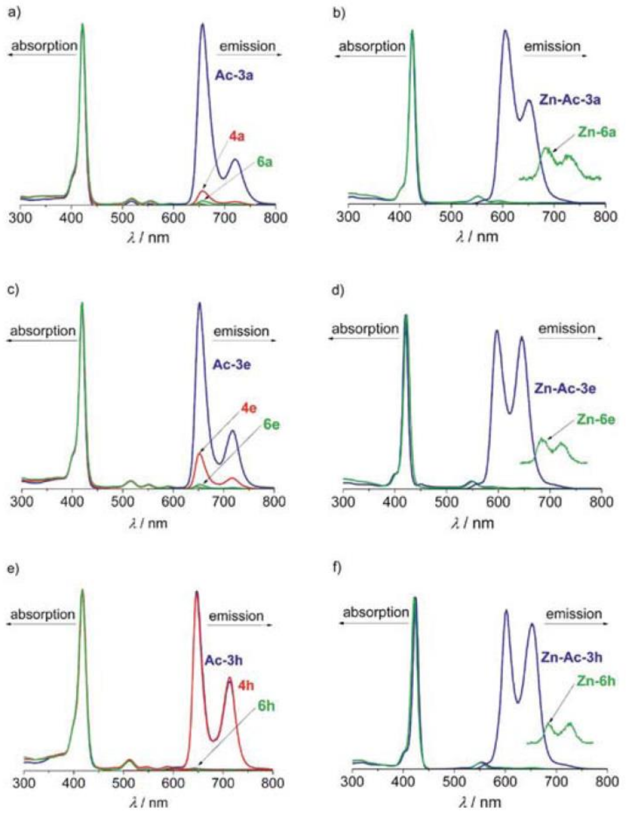

Figure 1. Normalised absorption and emission spectra of a) **Ac-3a**, **4a**, **6a**, b) **Zn-Ac-3a**, **Zn-6a**, c) **Ac-3e**, **4e**, **6e**, d) **Zn-Ac-3e**, **Zn-6e**, e) **Ac-3h**, **4h**, **6h** and f) **Zn-Ac-3h**, **Zn-6h** in CH_2Cl_2 at room temperature.

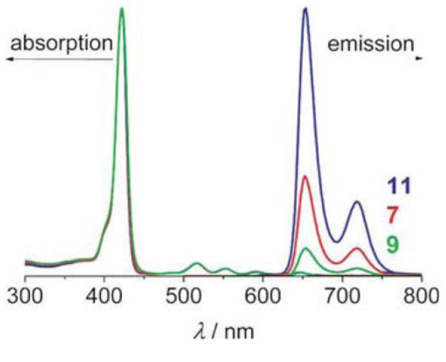

Figure 2. Normalised absorption and emission spectra of the reference compound P^{C6H5}-P^{C6H4Me} (**11**), triad Q-P^{C6H5}-P^{C6H4Me} (**7**) and tetrad Q-P^{C6H5}-P^{C6H4Me}-Fc (**9**) in CH_2Cl_2 at room temperature.

Table 2. Emission data for porphyrins **3** and bisporphyrin **11** in CH_2Cl_2 at room temperature.

	Ar	λ [nm]		Φ	τ [ns] [a]
		Q(0,0)	Q(0,1)		
3a	C_6H_4O*n*Bu	660	723	0.1631	n.d.[b]
Ac-3a	C_6H_4O*n*Bu	657	720	0.1594	9.28
Zn-Ac-3a	C_6H_4O*n*Bu	606	651	0.1003	1.71
3b	C_6H_4OMe	659	721	0.1448	n.d.[b]
Ac-3b	C_6H_4OMe	657	719	0.1348	9.49
Zn-Ac-3b	C_6H_4OMe	606	651	0.0940	1.81
3d	C_6H_4Me	657	721	0.0878	n.d. [b]
Ac-3d	C_6H_4Me	654	719	0.1311	9.69
Zn-Ac-3d	C_6H_4Me	600	646	0.0884	1.91
Ac-3e	C_6H_5	652	717	0.1167	9.88
Zn-Ac-3e	C_6H_5	597	645	0.1037	1.99
11	C_6H_5/C_6H_4Me	654	718	0.1284	9.70

[a] All decays are monoexponential; excitation wavelength λ_{exc} = 400 or 550 nm. [b] n.d.: not determined.

tion,[21] which also prevents the population of intermediate more co-planar conformations. Therefore the rather fixed orthogonal arrangement of the Mes substituent precludes the strong electronic influence expected from the trialkylated aryl group.

In quinone-bis(porphyrin) **7**, the emission is quenched by only 64% due to the attached quinone. From the extinction coefficients of the constituent porphyrins **Ac-3d** and **Ac-3e** (Table 1), it is reasonable to assume that both porphyrins in **7** are excited with nearly equal probability [ε(**Ac-3d**)/ε(**Ac-3e**) ≈ 1.03:1.00]. If energy transfer between the two porphyrins was absent, approximately 80%(**4e**)/2 = 40% quenching would be expected. The larger quenching observed suggests rapid energy transfer from the Ar = C_6H_4Me-substituted porphyrin to the Ar = C_6H_5-substituted porphyrin in **7**. The latter excited porphyrin undergoes oxidative PET to the appended quinone.

The fluorescence studies of the ferrocene conjugates **6** and **Zn-6** revealed an even stronger reduction of the emission quantum yield compared with the corresponding reference compounds **Ac-3** and **Zn-Ac-3** (Figure 1, Tables 2 and 4). The quenching of triads **6a**–**6h** and metallated triads **Zn-6a**–**Zn-6h** is almost quantitative and most of them are essentially non-fluorescent. Therefore a further efficient non-radiative decay pathway is enabled, namely reductive PET with ferrocene acting as electron donor and/or triplet energy transfer to the ferrocene.[7a,10]

To distinguish between electron and energy transfer, the emission spectra of **Ac-3a**, **4a** and **6a** (Figure 3) as well as **Ac-3h**, **4h** and **6h** were exemplarily recorded at low temperatures (300→77 K). Indeed, upon cooling, the integrated emission intensity of **6a** (×5.0) increases much more strongly than that of **Ac-3a** (×1.3) or **4a** (×1.7) (Figure 3). A similar trend is observed for the **Ac-3h** (×1.8), **4h** (×1.4), **6h** (×3.3) series. Even more pronounced is the gain in fluorescence intensity in the zinc triads **Zn-6a** (×17.5) and **Zn-6h** (×16.4) at low temperature. This supports the existence of PET pathways in triads **6** and **Zn-6** that are impeded at low temperatures.[3i] However, some residual quenching by energy transfer to ferrocene cannot be fully excluded on the basis of these data alone.

Tetrad **9** essentially shows similar emission behaviour to the triads **6**. The quantum yield of the Q-P^{C6H5}-P^{C6H4Me}-Fc conjugate **9** is decreased by 89% with respect to the

Table 3. Emission data for Q-P^{Ar} dyads **4a**–**4h** and triad **7** in CH_2Cl_2 at room temperature.

	Ar	λ [nm]		Φ	τ [ns][a]	Quenching [%]	k_{ET} [10^9 s^{-1}][d]	$Φ_{ET}$[e]
		Q(0,0)	Q(0,1)					
4a	C_6H_4OnBu	657	720	0.0125	0.613	92[b]	1.524	0.93
4b	C_6H_4OMe	656	720	0.0140	0.700	90[b]	1.323	0.93
4c	Mes	653	719	0.0532	1.820	32[b]	0.458	0.83
4d	C_6H_4Me	654	719	0.0161	0.942	78[b]	0.958	0.90
4e	C_6H_5	652	717	0.0230	1.370	80[b]	0.629	0.86
4f	C_6H_4F	652	717	0.0281	2.970	72[b]	0.233	0.69
4g	$C_6H_4CF_3$	652	717	0.0548	4.810	49[b]	0.108	0.52
4h	C_6F_5	647	712	0.0628	9.550	10[b]	0.003	0.03
7	C_6H_5/C_6H_4Me	653	718	0.0458	4.070	64[c]	0.143	0.58

[a] All decays are monoexponential; excitation wavelength $λ_{exc}$ = 400 or 550 nm. [b] Relative to reference compound **Ac-3**. [c] Relative to reference compound **11**. [d] $k_{ET} = 1/τ - 1/τ_{ref}$. [e] $Φ = k_{ET}τ$.

Table 4. Emission data for triads **6a**–**6i**, **Zn-6a**–**Zn-6i** and tetrad **9** in CH_2Cl_2 at room temperature.

	Ar	λ [nm]		Φ	$τ_1$ [ps] (A_1 [%]);	Quenching [%]	k_{ET} [10^9 s^{-1}][d]	$Φ_{ET}$[e]
		Q(0,0)	Q(0,1)		$τ_2$ [ps] (A_2 [%])[a,b]			
6a	C_6H_4OnBu	656	720	0.0042	214.99 (100)	97	4.544	0.98
6b	C_6H_4OMe	657	720	0.0034	240.54 (100)	97	4.052	0.97
6c	Mes	652	718	0.0041	272.83 (100)	94	3.574	0.97
6d	C_6H_4Me	655	720	0.0036	229.37 (100)	97	4.247	0.98
6e	C_6H_5	651	717	0.0030	164.02 (86); 644.23 (14)	97	5.996	0.98
6f	C_6H_4F	652	718	0.0025	148.07 (94); 586.62 (6)	98	6.650	0.98
6g	$C_6H_4CF_3$	652	717	0.0063	94.96 (86); 467.65 (14)	94	10.43	0.99
6h	C_6F_5	648	712	0.0029	26.39 (96); 274.57 (4)	96	37.79	1.00
6i	C_6F_4OMe	650	714	0.0006	39.30 (93); 398.03 (7)	n.d.[c]	n.d.[c]	n.d.[c]
Zn-6a	C_6H_4OnBu	607	652	0.0011	23.04 (87); 139.15 (13)	99	42.82	0.99
Zn-6b	C_6H_4OMe	606	651	0.0005	33.34 (92); 182.80 (8)	99	29.39	0.98
Zn-6c	Mes	604	653	0.0014	25.92 (77); 184.51 (13)	98	38.12	0.99
Zn-6d	C_6H_4Me	607	653	0.0012	27.13 (83); 189.38 (17)	99	36.34	0.99
Zn-6e	C_6H_5	601	647	0.0009	29.53 (88); 107.63 (12)	99	33.36	0.99
Zn-6f	C_6H_4F	602	649	0.0049	133.53 (73); 281.39 (27)	99	6.948	0.93
Zn-6g	$C_6H_4CF_3$	605	653	0.0028	35.20 (75); 285.80 (25)	97	27.93	0.98
Zn-6h	C_6F_5	602	654	0.0025	20.65 (94); 215.88 (6)	96	47.91	0.99
Zn-6i	C_6F_4OMe	602	651	0.0020	15.33 (90); 142.73 (10)	n.d.[c]	n.d.[c]	n.d.[c]
9	C_6H_5/C_6H_4Me	654	718	0.0145	361.77 (67); 2152.55 (33)	89	2.661; 0.363	

[a] Decays are mono- or biexponential; excitation wavelength $λ_{exc}$ = 400 or 550 nm. [b] The relative amplitudes A were calculated from fitting the data by the equations $Y = A_1e^{-k/τ1} + A_2e^{-k/τ2}$ and $A_1 + A_2 = 100\%$. [c] n.d.: not determined. [d] $k_{ET} = 1/τ - 1/τ_{ref}$. [e] $Φ_{ET} = k_{ET}τ$; $τ = τ_1$ with the largest amplitude used in the equations.

bis(porphyrin) reference **11**. When we neglect interporphyrin energy transfer, approximately 50% of the decay should occur oxidatively through Q-P^{C6H5} and 50% reductively through P^{C6H4Me}-Fc. The observed intermediate quenching of **9** (89%) between that of **4e** (80%) and **6d** (97%) is in accord with the concept of two decay pathways. Therefore both PET pathways appear possible in **9**.

Kinetics of Photoinduced Electron Transfer by Time-Resolved Fluorescence Decay

The fluorescence lifetimes τ of dyads, triads, tetrad **9** and reference compounds are presented in Tables 2–4 and the fluorescence decay curves of selected conjugates and reference porphyrins are shown in Figure 4.

The fluorescence lifetimes of the free-base reference porphyrins and P^{Ph}-P^{PhMe} (**11**) are $τ \approx 10$ ns and those of the zinc(II) porphyrins are $τ \approx 2$ ns, as expected.[11] All the excited states of the reference porphyrins **Ac-3**, **Zn-Ac-3**, reference dyad **11** and Q-P dyads **4a**–**4h** decay with a single rate constant. The PET from the porphyrin to the anthraquinone in the Q-P dyads **4** opens a new deactivation pathway for the excited singlet state and reduces its lifetime generating the $Q^{\cdot-}$-$P^{\cdot+}$ charge-separated state (CS state). Other pathways (e.g., originating from adventitiously reduced anthraquinone to the hydroquinone[31]) are not detected in dyads **4**. The fluorescence lifetimes of **4** are in the range of $τ = 0.613$ ns (**4a**, Ar = 4-C_6H_4OnBu) to $τ = 9.55$ ns (**4h**, Ar = C_6F_5). A clear trend (with the exception of **4c**, Ar = Mes, see above) is observed with the more electron-rich porphyrins featuring shorter lifetimes (Table 3). From these data, rate constants k_{ET} for oxidative PET were calculated (Table 3). The rate constants of the electron-rich porphyrins **4a**, **4b** and **4d** (1.5×10^9–0.9×10^9 s^{-1}) are fully compatible with those of the reported Q-P dyads consisting of electron-rich porphyrins and quinones.[3] The much lower rates of

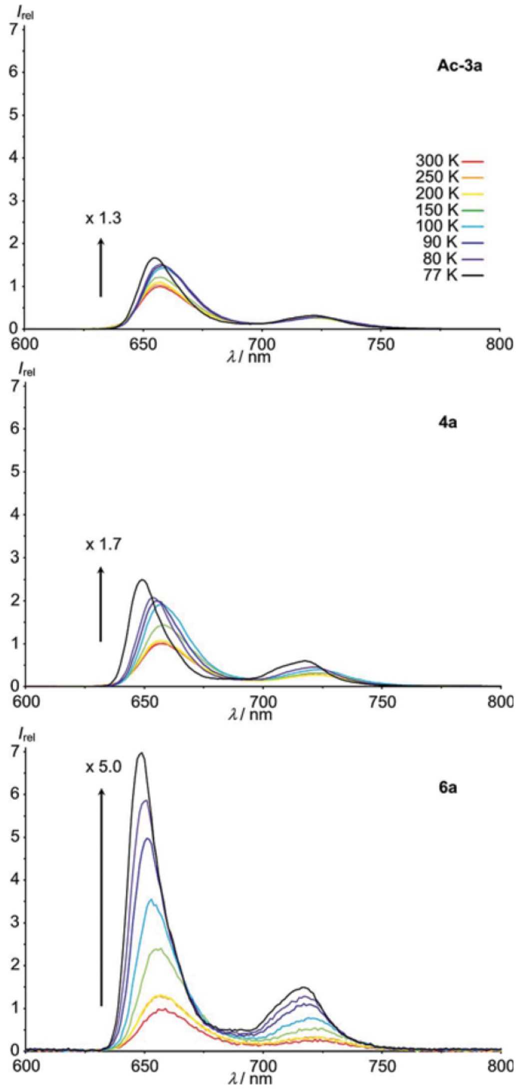

Figure 3. Normalised emission spectra of **Ac-3a**, **4a** and **6a** in 2-methyltetrahydrofuran at T = 300→77 K.

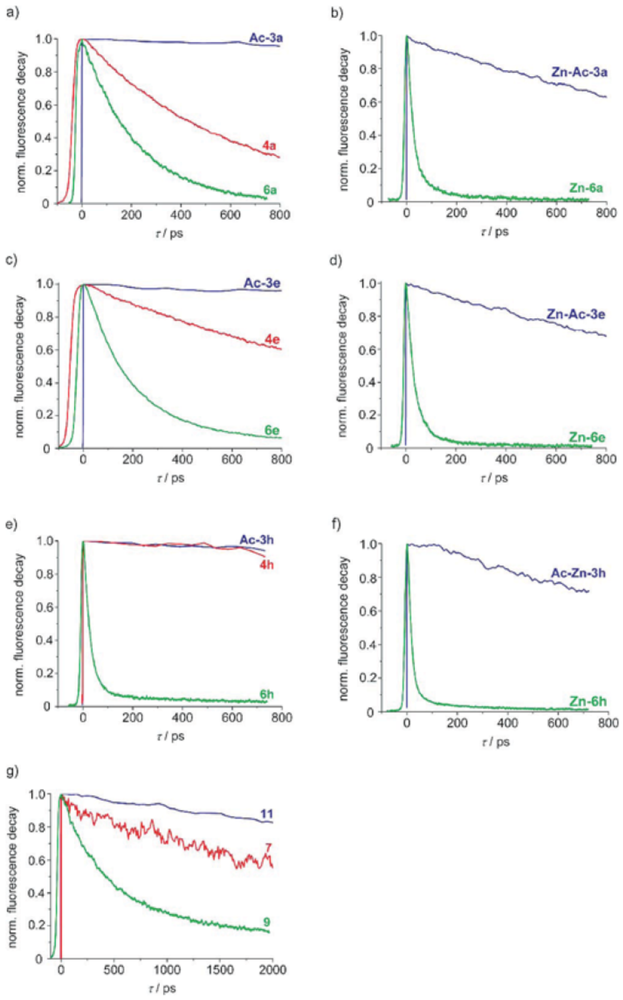

Figure 4. Fluorescence decay profiles of a) **Ac-3a**, **4a**, **6a**, b) **Zn-Ac-3a**, **Zn-6a**, c) **Ac-3e**, **4e**, **6e**, d) **Zn-Ac-3e**, **Zn-6e**, e) **Ac-3h**, **4h**, **6h**, f) **Zn-Ac-3h**, **Zn-6h** and g) **11**, **7**, **9** in CH_2Cl_2 (λ_{exc} = 400 and 550 nm).

ET observed for the electron-withdrawing porphyrin dyads **4f**–**4h** are related to the lower thermodynamic driving force for the ET (see Electrochemical Studies below).

Triads **6a**–**6d** feature a monoexponential decay whereas the decays of all other dyads have to be fitted by biexponential decay curves (Table 4). The minor component (τ_2, A_2) could be due to additional quenching by the heavy-atom effect of the ferrocene,[7c] population of the ferrocene triplet state,[10] the presence of ferrocene/amide conformations that are less suitable for ET or intermolecular Zn···O=C(quinone) interactions in **Zn-6**.[3m] The latter path, however, seems to be less pronounced based on NMR spectroscopic data for **Zn-6** (see above). Rate constants were estimated from the fluorescence lifetimes with the largest amplitude (τ_1, A_1; Table 4). These rate constants for **6a**–**6h** are larger than those of the corresponding **4a**–**4h** lacking ferrocene (Table 3 and Table 4). Whereas k_{ET} decreases for Q-P^{Ar} dyads **4** with electron-withdrawing substituents (Table 3), the reverse trend is observed for Q-P^{Ar}-Fc triads **6** (Table 4). The latter observation would be expected for reductive PET from ferrocene to the excited porphyrin as the dominant pathway. Indeed, k_{ET} is minimal for **6b**–**6d**, increases slightly for electron-rich **6a** favouring PET to the quinone and increases dramatically for electron-poor **6e**–**6h** favouring PET from ferrocene. Hence reductive PET seems to be favourable in **6e**–**6h** whereas oxidative and reductive pathways are both accessible in **6a**–**6d**.

In the zinc(II) porphyrin triads **Zn-6**, the rate constants k_{ET} are large (30×10^9–40×10^9 s^{-1}; except for **Zn-6f**, which is unexplained at the moment) and ET is basically quantitative. No clear correlation between k_{ET} and the nature of the porphyrin substituents can be discerned (Table 4). This might be explained by the larger driving force [$\Delta(\Delta G_{ET}) \approx$ 0.17 eV] of both PET pathways in zinc(II) porphyrin donor/acceptor assemblies due to the higher energy of the singlet excited state of zinc(II) porphyrins and the lower oxidation potential of zinc(II) porphyrins relative to free-base porphyrins (Table 4; see Electrochemical Studies below). Other scenarios would be accelerated quenching via ^{3}ZnP states due to the heavy-atom effect of ferrocene[7c] or via ferrocene triplet states.[10]

As suggested from the quantum yield data, the singlet excited states of tetrad **9** can be quenched by PET from the C_6H_5-substituted porphyrin to its adjacent quinone and/or by PET from ferrocene to its adjacent C_6H_4Me-substituted porphyrin. The two fluorescence lifetimes of **9** [τ_1 = 362 ps (67%) and τ_2 = 2153 ps (33%)] roughly correspond to the lifetimes of Q-P^{C6H4Me}-Fc **6d** (τ = 229 ps) and Q-P^{C6H5} **4e** (τ = 1370 ps). This suggests that indeed both initial PET pathways are conceivable in **9** with the reductive PET being more probable than the oxidative PET. On the basis of this interpretation, the rate constants were estimated to be 2.66×10^9 s^{-1} (reductive PET) and 0.36×10^9 s^{-1} (oxidative PET). The thermodynamic feasibility of reductive and oxidative PET will be discussed in the next sections.

Electrochemical Studies

Cyclic voltammograms of porphyrins typically show two reversible oxidation and two reversible reduction waves. Porphyrins **3a**–**3h** with amine substituents are only quasi-reversibly or even irreversibly oxidised.[11,14] As the amino porphyrins do not qualify as references, their *N*-acetylated analogues **Ac-3a**–**Ac-3h** were used instead. The redox potentials of the new amino porphyrins **3a**, **3b**, **3e** and **3d** and the porphyrin reference compounds **Ac-3a**, **Ac-3b**, **Ac-3d** and **Ac-3e** are presented in Table 5. As described previously, the *meso*-aryl substituents cause a stepwise anodic shift of porphyrin oxidation and reduction.[11] The new *N*-acetylated porphyrins **Ac-3a**, **Ac-3b**, **Ac-3d** and **Ac-3e** confirm and complete the trend in the full series Ar = 4-$C_6H_4OnBu \rightarrow$ 4-$C_6H_4OMe \rightarrow$ 4-$C_6H_4Me \rightarrow$ Mes $\rightarrow C_6H_5 \rightarrow$ 4-$C_6H_4F \rightarrow$ 4-$C_6H_4CF_3 \rightarrow C_6F_5$. The shifts observed amount to 0.34 V for the first oxidation and 0.25 V for the first reduction from **Ac-3a** (Ar = C_6H_4OnBu) to **Ac-3h** (Ar = C_6F_5[11]).

In Q-P dyads **4a**–**4h** an additional redox event at a rather constant potential of $E_{1/2}$ = –1.20 V corresponding to the first reversible reduction of the quinone to the semiquinonate is observed. For dyad **4c** even the second reduction of anthraquinone at $E_{1/2}$ = –1.72 V has been detected. The individual redox potentials of the porphyrins **Ac-3** are essentially unperturbed by the appended quinone in **4** (Table 6 and Figure 5).

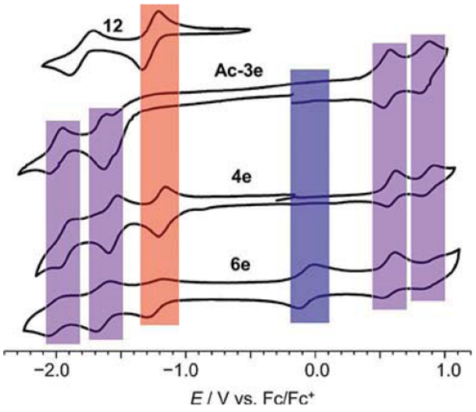

Figure 5. Cyclic voltammograms of quinone reference **12**, porphyrin **Ac-3e**, dyad **4e** and triad **6e** in (nBu$_4$N)(PF$_6$)/CH$_2$Cl$_2$.

Attachment of a ferrocene unit (**6a**–**6h**, **Zn-6a**–**Zn-6h**) yields a further oxidation process at a rather constant potential of $E_{1/2}$ = –0.08 V corresponding to the oxidation of ferrocene to ferrocenium (Table 6 and Figure 5). Only minor effects of ferrocene on the porphyrin and anthraquinone redox potentials are observed. Likewise only minor effects of the Ar substituent on the Fc and Q potentials are noted, which indicates a weak interchromophore interaction in the ground state. The quinone in the zinc porphyrins **Zn-6** is slightly easier to reduce than in the free-base porphyrins **6** (Table 6).

The redox data for bis(porphyrins) **11**, **7** and **9** are presented in Table 6. The additional porphyrin superimposes its redox waves onto those of the respective partner mono-

Table 5. Redox potentials of monoporphyrins **3**, **Ac-3**, **Zn-Ac-3** and (bis)porphyrin **11** vs. Fc/Fc$^+$ in (nBu$_4$N)(PF$_6$)/CH$_2$Cl$_2$ at room temperature.

	Ar	C_6H_4–R′	$E_{1/2}$(ox^1) [V]	$E_{1/2}$(ox^2) [V]	$E_{1/2}$(red^1) [V]	$E_{1/2}$(red^2) [V]
3a	C_6H_4OnBu	NH_2	0.420	0.590	–1.660[a]	–2.010[a]
Ac-3a	C_6H_4OnBu	NHAc	0.480	0.730	–1.640	–1.980
Zn-Ac-3a	C_6H_4OnBu	NHAc	0.300	0.720	–1.790	–2.160
3b	C_6H_4OMe	NH_2	0.540[a]	n.o.[b]	–1.660	–1.990
Ac-3b	C_6H_4OMe	NHAc	0.510	0.750	–1.630	–1.970
Zn-Ac-3b	C_6H_4OMe	NHAc	0.310	0.710	–1.780	n.o.[b]
3d	C_6H_4Me	NH_2	0.440	0.550	–1.640[a]	–1.980[a]
Ac-3d	C_6H_4Me	NHAc	0.520	0.830	–1.610	–1.950
Zn-Ac-3d	C_6H_4Me	NHAc	0.361	0.800	–1.720	–2.090
Ac-3e	C_6H_5	NHAc	0.550	0.840	–1.630	–2.000
Zn-Ac-3e	C_6H_5	NHAc	0.360	0.780	–1.750	–2.110
11	C_6H_5/C_6H_4Me	NHAc	0.540 (2e)	0.860	–1.660 (2e)	–2.010

[a] Irreversible. [b] n.o.: not observed.

Table 6. Redox potentials of **4**, **6**, **Zn-6**, **11**, **7** and **9** in V vs. Fc/Fc$^+$ in (nBu$_4$N)(PF$_6$)/CH$_2$Cl$_2$ at room temperature.

	Ar	$E(P)_{1/2}(ox^1)$ [V]	$E(P)_{1/2}(ox^2)$ [V]	$E(Fc)_{1/2}(ox)$ [V]	$E(Q)_{1/2}(red)$ [V]	$E(P/Q)_{1/2}(red^1)$ [V]	$E(P)_{1/2}(red^2)$ [V]
4a	C_6H_4OnBu	0.500	0.750	–	–1.230	–1.640	–2.000
4b	C_6H_4OMe	0.500	0.760	–	–1.230	–1.660	–1.990
4c	Mes	0.560	0.960	–	–1.230	–1.720 (2e)	–2.070
4d	C_6H_4Me	0.540	0.840	–	–1.210	–1.600	–1.980
4e	C_6H_5	0.580	0.870	–	–1.190	–1.560	–1.940
4f	C_6H_4F	0.600	0.880	–	–1.210	–1.580	–1.930
4g	$C_6H_4CF_3$	0.670	0.960	–	–1.200	–1.530	–1.870
4h	C_6F_5	0.830	1.050	–	–1.240	–1.420	–1.850
6a	C_6H_4OnBu	0.510	0.770	–0.070	–1.210	–1.650	–2.010[a]
6b	C_6H_4OMe	0.500	0.770	–0.079	–1.220	–1.650	–2.010[a]
6c	Mes	0.560	0.990	–0.070	–1.230	–1.710 (2e)	–2.070
6d	C_6H_4Me	0.550	0.855	–0.075	–1.190	–1.605	–1.965
6e	C_6H_5	0.560	0.925	–0.090	–1.260	–1.670	–2.060
6f	C_6H_4F	0.585	0.945[a]	–0.085	–1.235	–1.625	–2.015[a]
6g	$C_6H_4CF_3$	0.640	0.990	–0.080	–1.230	–1.570	–1.930
6h	C_6F_5	0.800	1.040	–0.100	–1.270	–1.430	–1.900
6i	C_6F_4OMe	0.770	1.075	–0.050	–1.240	–1.420	–1.890
Zn-6a	C_6H_4OnBu	0.370	0.670	–0.070	–1.170	–1.620	–2.200[a]
Zn-6b	C_6H_4OMe	0.360	0.670	–0.080	–1.150	–1.590[a]	n.o.[b]
Zn-6c	Mes	0.410	0.750	–0.060	–1.180[c]	–1.620[a]	–2.220[a]
Zn-6d	C_6H_4Me	0.390	0.710	–0.089	–1.190[c]	–1.630[a]	–2.230[a]
Zn-6e	C_6H_5	0.430	0.740	–0.080	–1.120	–1.580[a]	–2.190[a]
Zn-6f	C_6H_4F	0.440	0.750	–0.080	–1.120	–1.590	–2.180[a]
Zn-6g	$C_6H_4CF_3$	0.480	0.770	–0.100	–1.240[a]	–1.610[a]	n.o.[b]
Zn-6h	C_6F_5	0.630	0.910	–0.090	–1.180	n.o.[b]	–2.000[a]
Zn-6i	C_6F_4OMe	0.600	0.880	–0.090	–1.160	–1.610[a]	–2.040[a]
11	C_6H_5/C_6H_4Me	0.540 (2e)	0.860 (2e)	–	–	–1.650 (2e)	–2.010 (2e)
7	C_6H_5/C_6H_4Me	0.570 (2e)	0.890	–	–1.200	–1.600 (2e)	–1.970
9	C_6H_5/C_6H_4Me	0.590 (2e)	0.870	–0.060	–1.190	–1.600 (2e)	–1.980

[a] Irreversible, E_p given. [b] n.o.: not observed. [c] Quasi-reversible.

porphyrin, and two-electron reversible redox waves for the first oxidation and first reduction of both porphyrins at around –0.59 and –1.60 V are detected. Tetrad **9** additionally shows the one-electron reduction of the quinone at $E_{1/2}$ = –1.190 V and the one-electron oxidation of the ferrocene at $E_{1/2}$ = –0.060 V.

Thermodynamic Driving Force for Photoinduced Electron Transfer

The energies of the porphyrin first excited singlet states $E(S_0\rightarrow S_1)$ of **4a**–**4h** were obtained from the average values of the $Q_x(0,0)$ absorption and Q(0,0) emission bands (Tables 1–4). The energies of the CS states $Q^{\cdot-}$-$P^{\cdot+}$ were evaluated from the first oxidation potential of the porphyrin $E_{1/2}(P/P^{\cdot+})$, the first reduction potential of the quinone $E_{1/2}(Q/Q^{\cdot-})$ and the Coulomb term $e_0^2/[4\pi\varepsilon_0\varepsilon(CH_2Cl_2)r_{AD}]$ (Table 6). From these data the thermodynamic driving forces for PET were calculated according to the Rehm–Weller equation:[22] $\Delta G_{ET} = E_{1/2}(D/D^{\cdot+}) - E_{1/2}(A/A^{\cdot-}) - e_0^2/[4\pi\varepsilon_0\varepsilon(CH_2Cl_2)r_{AD}] - E(S_0\rightarrow S_1)$ with $\varepsilon_0 = 8.85519\times10^{-12}$ F m^{-1}, $\varepsilon(CH_2Cl_2) = 8.93$ and r_{AD} = 15.5 Å, as determined by DFT models (see below), to give a Coulomb term of 0.104 eV in CH$_2$Cl$_2$. The data are presented in Table 7. Figure 6 shows the energy level diagram for all Q-P dyads **4a**–**4h**. This series of compounds displays a $k_{ET}/\Delta G_{ET}$ correlation in the normal Marcus region (Table 3 and Table 7) with k_{ET} increasing the more negative ΔG_{ET} is (except for the mesityl derivative **4c**, see above). For **4h**, the ET is even calculated to be slightly endergonic, which accounts for the observed weak fluorescence quenching.

Table 7. Energies of the porphyrin S$_1$ and CS states for dyads **4a**–**4h** and the driving forces ΔG_{ET}.

	Ar	$E(S_0\rightarrow S_1)$ [eV]	$E(Q^{\cdot-}$-$P^{\cdot+})$[a] [eV]	ΔG_{ET} [eV]
4a	C_6H_4OnBu	1.89	1.63	–0.26
4b	C_6H_4OMe	1.89	1.63	–0.26
4c	Mes	1.90	1.69	–0.21
4d	C_6H_4Me	1.90	1.65	–0.25
4e	C_6H_5	1.91	1.67	–0.24
4f	C_6H_4F	1.91	1.71	–0.20
4g	$C_6H_4CF_3$	1.91	1.77	–0.14
4h	C_6F_5	1.93	1.97	+0.04

[a] Including Coulomb term of 0.104 eV.

As suggested above, two different PET pathways exist in triads **6a**–**6h** and **Zn-6a**–**Zn-6h**. The first one is the oxidative pathway, as is also found in Q-P dyads **4**, leading to the $Q^{\cdot-}$-$P^{\cdot+}$-Fc and $Q^{\cdot-}$-(Zn)$P^{\cdot+}$-Fc CS states, respectively (Table 8, Figures 7 and 8). The second one is the reductive pathway leading to the Q-$P^{\cdot-}$-$Fc^{\cdot+}$ and Q-(Zn)$P^{\cdot-}$-$Fc^{\cdot+}$ CS states, respectively (Table 8, Figures 7 and 8). The final CS states are described by $Q^{\cdot-}$-P-$Fc^{\cdot+}$ and $Q^{\cdot-}$-(Zn)P-$Fc^{\cdot+}$, respectively. The free energies of the initial and final CS states were estimated from the Rehm–Weller equation[22] and are

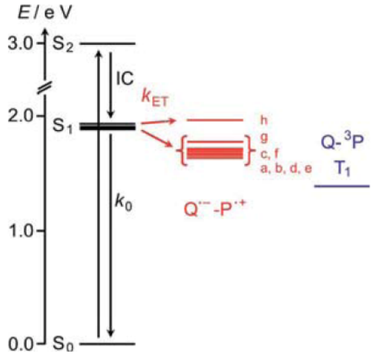

Figure 6. Energy level diagram for Q-P dyads **4a**–**4h** (IC = internal conversion; the porphyrin triplet state T_1 is estimated to be 1.43 eV[3f]).

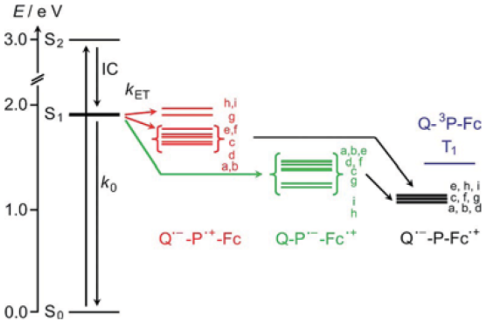

Figure 7. Energy level diagram for Q-P-Fc triads **6a**–**6i** (the porphyrin triplet state T_1 is estimated to be 1.43 eV[3f]).

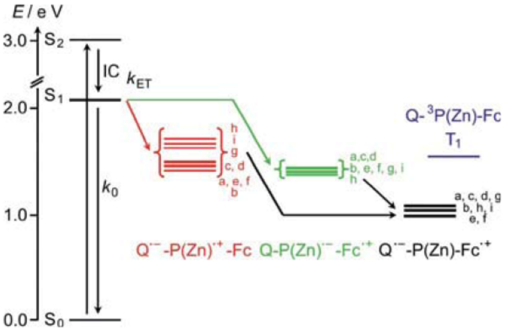

Figure 8. Energy level diagram for Q-(Zn)P-Fc triads **Zn-6a**–**Zn-6i** (the zinc porphyrin triplet state T_1 is estimated to be 1.53 eV.[5b]).

given in Table 8 (quinone-porphyrin centre-to-centre distance r_{AD} = 15.5 Å; Coulomb term for $Q^{\cdot-}$-$P^{\cdot+}$-Fc 0.104 eV; porphyrin centre to iron distance r_{AD} = 13.0 Å; Coulomb term for Q-$P^{\cdot-}$-$Fc^{\cdot+}$ 0.124 eV; quinone-centre to iron distance r_{AD} = 28.3 Å; Coulomb term for $Q^{\cdot-}$-P-$Fc^{\cdot+}$ 0.057 eV).

In the free-base porphyrin triads **6a**–**6i**, the reductive PET to give Q-$P^{\cdot-}$-$Fc^{\cdot+}$ as the initial CS state is clearly favoured over the oxidative PET that gives the $Q^{\cdot-}$-$P^{\cdot+}$-Fc initial CS state (Figure 7). This is especially pronounced in **6g**–**6i** with strongly electron-withdrawing substituents. In the zinc(II) porphyrin triads **Zn-6**, oxidative PET becomes competitive with reductive PET with respect to the driving force ΔG_{ET} (Table 8 and Figure 8). The final $Q^{\cdot-}$-(Zn)P-$Fc^{\cdot+}$ CS states of **Zn-6** are slightly lower than the final $Q^{\cdot-}$-P-$Fc^{\cdot+}$ CS states of **6** due to the slightly preferred reduction of Q in the zinc porphyrins **Zn-6** (see above, Table 6).

In bis(porphyrin) **11**, the conceivable $P_1^{\cdot+}$-$P_2^{\cdot-}$ and $P_1^{\cdot-}$-$P_2^{\cdot+}$ CS states are located 0.15 and 0.16 eV (including the Coulomb term of 0.08 eV; porphyrin-porphyrin centre-to-centre distance 19.3 Å) above the excited singlet state S_1 and are thus less relevant for excited-state decay (Figure 9 and Table 9). This is also reflected in the unchanged lifetime of **11** (τ = 9.70 ns) with respect to reference porphyrins **Ac-3d** (τ = 9.69 ns) and **Ac-3e** (τ = 9.88 ns). The thermodynamic driving forces for ET in tetrad **9** were again calculated from the Rehm–Weller equation[22] (see above) and are given in

Table 8. Energies of porphyrin S_1 and CS states for **6** and **Zn-6** and driving forces ΔG_{ET}.

	Ar	$E(S_0 \rightarrow S_1)$ [eV]	$E(Q^{\cdot-}$-$P^{\cdot+}$-Fc)[a] [eV]	E(Q-$P^{\cdot-}$-$Fc^{\cdot+}$)[b] [eV]	$E(Q^{\cdot-}$-P-$Fc^{\cdot+}$)[c] [eV]	$\Delta G_{ET}(Q^{\cdot-}$-$P^{\cdot+}$-Fc) [eV]	ΔG_{ET}(Q-$P^{\cdot-}$-$Fc^{\cdot+}$) [eV]	$\Delta G_{ET}(Q^{\cdot-}$-P-$Fc^{\cdot+}$) [eV]
6a	C_6H_4OnBu	1.90	1.62	1.46	1.08	–0.28	–0.44	–0.82
6b	C_6H_4OMe	1.90	1.62	1.45	1.08	–0.28	–0.45	–0.82
6c	Mes	1.91	1.69	1.39	1.10	–0.22	–0.52	–0.81
6d	C_6H_4Me	1.91	1.64	1.41	1.06	–0.27	–0.50	–0.84
6e	C_6H_5	1.91	1.72	1.46	1.11	–0.19	–0.45	–0.79
6f	C_6H_4F	1.91	1.72	1.42	1.09	–0.19	–0.49	–0.82
6g	$C_6H_4CF_3$	1.91	1.77	1.37	1.09	–0.04	–0.54	–0.82
6h	C_6F_5	1.92	1.97	1.21	1.11	+0.05	–0.71	–0.81
6i	C_6F_4OMe	1.92	1.91	1.25	1.13	–0.01	–0.67	–0.79
Zn-6a	C_6H_4OnBu	2.07	1.44	1.43	1.04	–0.63	–0.64	–1.03
Zn-6b	C_6H_4OMe	2.07	1.41	1.39	1.01	–0.66	–0.66	–1.06
Zn-6c	Mes	2.07	1.49	1.44	1.06	–0.58	–0.63	–1.01
Zn-6d	C_6H_4Me	2.07	1.48	1.42	1.04	–0.59	–0.65	–1.03
Zn-6e	C_6H_5	2.08	1.45	1.38	0.98	–0.63	–0.70	–1.10
Zn-6f	C_6H_4F	2.08	1.46	1.39	0.98	–0.62	–0.69	–1.10
Zn-6g	$C_6H_4CF_3$	2.07	1.62	1.39	1.08	–0.45	–0.68	–0.99
Zn-6h	C_6F_5	2.07	1.71	1.37[d]	1.03	–0.36	–0.70	–1.04
Zn-6i	C_6F_4OMe	2.08	1.66	1.40	1.01	–0.42	–0.68	–1.07

[a] Including Coulomb term of 0.104 eV. [b] Including Coulomb term of 0.124 eV. [c] Including Coulomb term of 0.057 eV. [d] Calculated with $E(P)_{1/2}(red^1)$ = –1.58 eV from reference porphyrin **Ac-3h**, see ref.[10].

Table 9. Reductive PET (ΔG_{ET} = –0.48 eV) to give $Q–P_1–P_2^{\cdot-}-Fc^{\cdot+}$ is thermodynamically favoured in **9** over oxidative PET (ΔG_{ET} = –0.26 eV) similarly to **6d** and **6e** (Tables 8, 9 and Figure 9). This excellently supports the kinetic analysis of ET in **9** (see above). The shift of charge from P_2 to P_1 to give $Q-P_1^{\cdot-}-P_2-Fc^{\cdot+}$ is slightly endergonic (0.09 eV) whereas the following thermal ET to give $Q^{\cdot-}-P_1-P_2-Fc^{\cdot+}$ is again exergonic by 0.42 eV (Figure 9).

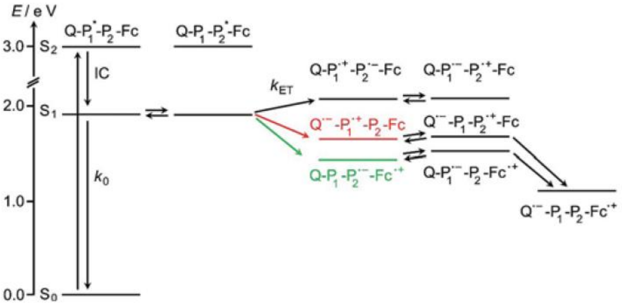

Figure 9. Energy level diagram for $Q–P_1–P_2-Fc$ tetrad **9**.

Table 9. Energies of porphyrin S_1 and CS states for **9** and driving forces ΔG_{ET}.

State	E [eV][a]	r_{AD} [Å]	Coulomb term [eV]
$E_{P1}(S_0 \rightarrow S_1)$	1.91	–	–
$E_{P2}(S_0 \rightarrow S_1)$	1.91	–	–
$E(Q-P_1^{\cdot+}-P_2^{\cdot-}-Fc)$ or $E(Q-P_1^{\cdot-}-P_2^{\cdot+}-Fc)$[b,c,d,e]	2.07/2.08	19.3	0.084
$E(Q^{\cdot-}-P_1^{\cdot+}- P_2-Fc)$[b]	1.65	15.5	0.104
$E(Q^{\cdot-}-P_1-P_2^{\cdot+}-Fc)$[c]	1.67	34.8	0.046
$E(Q-P_1-P_2^{\cdot-}-Fc^{\cdot+})$[d]	1.43	13.0	0.124
$E(Q-P_1^{\cdot-}-P_2-Fc^{\cdot+})$[e]	1.52	32.3	0.050
$E(Q^{\cdot-}-P_1-P_2-Fc^{\cdot+})$	1.10	47.8	0.033
Driving force	ΔG_{ET} [eV]		
$\Delta G_{ET}(Q^{\cdot-}-P_1^{\cdot+}-P_2-Fc)$	–0.26		
$\Delta G_{ET}(Q^{\cdot-}-P_1-P_2^{\cdot+}-Fc)$	–0.24		
$\Delta G_{ET}(Q–P_1-P_2^{\cdot-}-Fc^{\cdot+})$	–0.48		
$\Delta G_{ET}(Q-P_1^{\cdot-}-P_2-Fc^{\cdot+})$	–0.39		
$\Delta G_{ET}(Q^{\cdot-}-P_1-P_2-Fc^{\cdot+})$	–0.81		

[a] Including Coulomb terms. [b] Calculated with $E(P_1)_{1/2}(ox^1)$ = 0.550 V from reference porphyrin **Ac-3e**. [c] Calculated with $E(P_2)_{1/2}(ox^1)$ = 0.520 V from reference porphyrin **Ac-3d**. [d] Calculated with $E(P_1)_{1/2}(red^1)$ = –1.630 V from reference porphyrin **Ac-3e**. [e] Calculated with $E(P_2)_{1/2}(red^1)$ = –1.610 V from reference porphyrin **Ac-3d**.

Densitiy Functional Calculations on Ground and CS States

To estimate distances between redox sites (Q–P centre-to-centre; P centre to Fe, Q centre to Fe, P–P centre-to-centre) and to visualise frontier molecular orbitals, the ground states of dyads and triads with electron-donating and -withdrawing substituents were optimised by DFT (B3LYP/LANL2DZ, PCM, CH_2Cl_2)[23] methods (see the Supporting Information). Figure 10 exemplarily depicts the frontier molecular orbitals of dyads **4b** and **4h** showing the typical Gouterman four orbital scheme for porphyrins (nomenclature adopted from D_{4h} local point symmetry to describe the node structure of the orbitals[24]) and the lowest π* orbital of the quinone located between the HOMOs and LUMOs of the porphyrin. Two points are immediately evident: 1) electron-withdrawing Ar substituents reduce the energy gap between the LUMO of the porphyrin and the π* orbital of the quinone (Figure 11), which disfavours oxidative PET, and 2) the symmetry of the local porphyrin LUMO in **4h** (Figure 10, b; LUMO+1; Ar = C_6F_5) is different to that in all the other dyads and features a node at the *meso* carbon atoms in the amide direction. This orbital inversion is typically observed in porphyrins with strongly electron-withdrawing substituents.[11,25] Naturally, small orbital coefficients at the bridging unit between redox centres

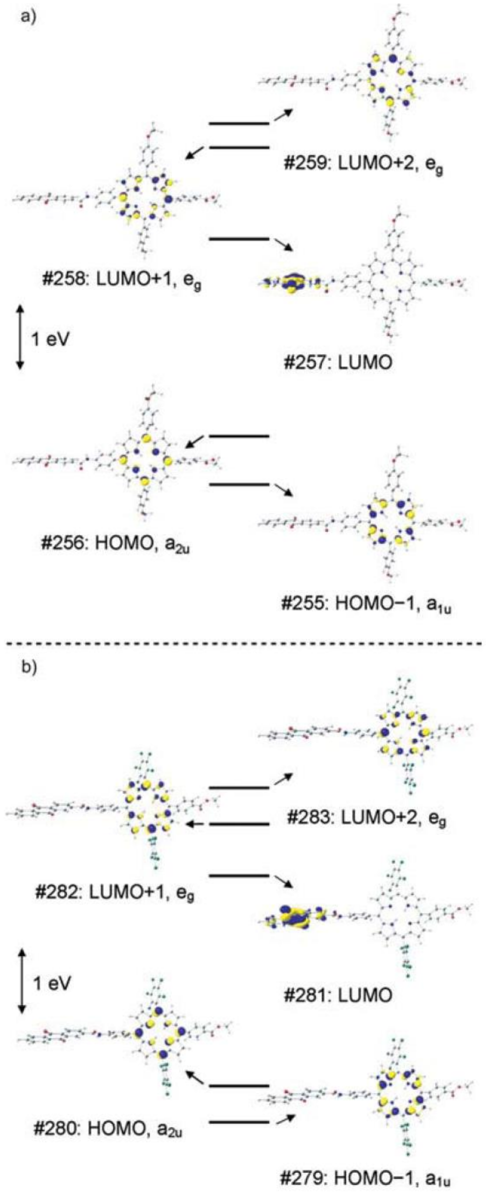

Figure 10. B3LYP/LANL2DZ, PCM-calculated frontier orbitals for a) **4b** and b) **4h** (isosurface value 0.05 a.u.).

disfavours ET. Hence, PET in **4h** is not only thermodynamically slightly uphill (Figure 6), but probably also kinetically hindered due to the unfavourable orbital symmetry.

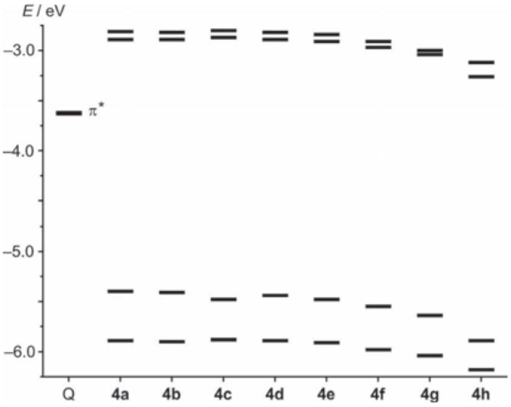

Figure 11. B3LYP/LANL2DZ, PCM-calculated molecular orbital energy diagram for dyads **4**.

A similar picture with respect to the quinone π* orbital arises for the triads **6** (Figure 12) and **Zn-6**. The porphyrin LUMO inversion is also observed for **6g** (Figure 13) and **6h**. In addition, the occupied ferrocene-based δ orbitals (d_{xy}, $d_{x^2-y^2}$) are close in energy to the local porphyrin HOMOs (Figure 12). For electron-rich **6a**–**6f**, the δ(Fc) orbitals are below the porphyrin a_{2u} orbital, in **6g** the a_{2u} orbital is lowered in energy and mixes with a δ(Fc) orbital (Figure 13, HOMO) and in **6h** the porphyrin a_{2u} orbital is located even below the δ(Fc) orbitals. Naturally, this simple orbital picture cannot account for quantitative relationships, but it clearly demonstrates the lowering of the porphyrin HOMOs relative to the essentially constant ferrocene HOMOs (Figure 12), which should favour reductive PET in triads with electron-withdrawing substituents (see Tables 4 and 8). The near degeneracy of porphyrin and ferrocene HOMOs in terms of energy also allows for orbital mixing (Figure 13) and mixing of states, which should also allow energy-transfer processes between porphyrin and ferrocene. These energy-transfer processes might be assigned to the second decay (τ_2, A_2) in **6e**–**6i** and **Zn-6a**–**Zn-6i** (Table 4; for the molecular orbitals of **Zn-6**, see the Supporting Information).

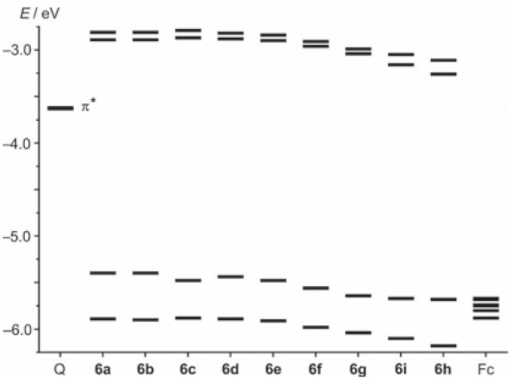

Figure 12. B3LYP/LANL2DZ, PCM-calculated molecular orbital energy diagram for triads **6**.

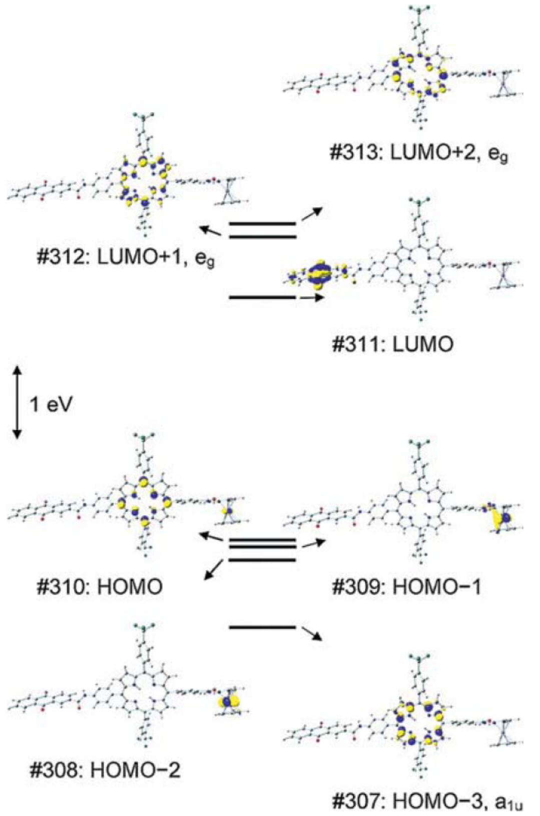

Figure 13. B3LYP/LANL2DZ, PCM-calculated frontier orbitals for triad **6g** (isosurface value 0.05 a.u.).

Tetrad **9** features a double nearly degenerate set of Gouterman orbitals as well as the quinone π* and the occupied ferrocene d orbitals, as expected from the constituent building blocks (see the Supporting Information). The porphyrin HOMOs are of local a_{2u} symmetry with large coefficients at the connecting *meso* carbon atoms. This should allow for energy and electron transfer between the two porphyrins[11] based on orbital symmetry arguments, as suggested in Figure 9.

For dyad **4b** (Ar = 4-C_6H_4OMe) we succeeded in optimising the $Q^{\cdot-}$-$P^{\cdot+}$ CS triplet state by DFT methods (Figure 14, a). The calculated spin density is clearly distributed over the porphyrin radical cation and quinone radical anion, as expected from the molecular orbital scheme (Figure 10). The quinone CO bond lengths were calculated to be 1.26 Å in the ground state and 1.30 Å in the CS state, clearly reflecting the semiquinone character. The analogous DFT optimisation of **4d** (Ar = 4-C_6H_4Me) resulted in the porphyrin triplet state T_1 (Figures 6 and 14, b), which suggests a close proximity of the CS (1.65 eV, Table 7) and local triplet states in terms of energy. Indeed, the porphyrin triplet state of H_2TPP has been reported to have an energy of 1.43 eV.[3f]

To gain an impression of the spin density and charge distribution in the final $Q^{\cdot-}$-P-$Fc^{\cdot+}$ and $Q^{\cdot-}$-(Zn)P-$Fc^{\cdot+}$ CS

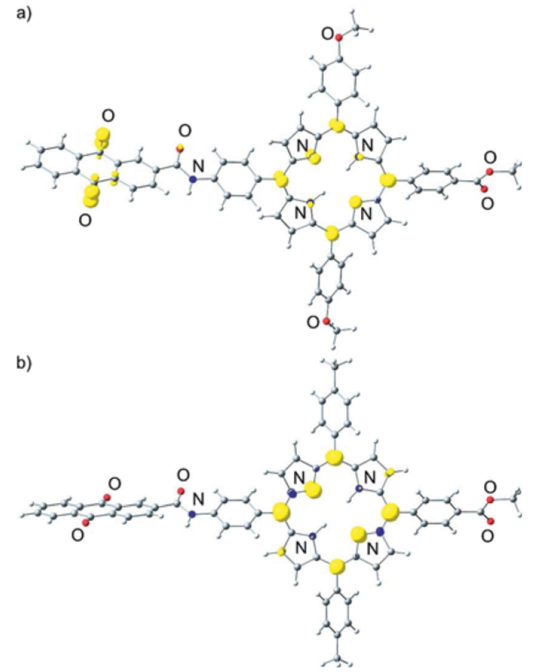

Figure 14. DFT-calculated spin density of a) the $Q^{\cdot -}$-$P^{\cdot +}$ CS triplet state of **4b** and b) the porphyrin triplet state of **4d** (isosurface value 0.01 a.u.).

states of the triads we tried to optimise this (triplet) state, but all attempts yielded only the optimised ferrocene triplet state with a Mulliken spin density of 2.03 at the iron centre (Figure 15, a). The calculated Fe···Cp(centroid) distances are increased significantly from 1.73 to 1.91 Å. The energy of the triplet state of unsubstituted ferrocene has been reported to be 1.16 eV,[10] which is clearly close to the energies of the $Q^{\cdot -}$-P-$Fc^{\cdot +}$ and $Q^{\cdot -}$-(Zn)P-$Fc^{\cdot +}$ CS states (cf. Table 8). To artificially stabilise the $Q^{\cdot -}$-P-$Fc^{\cdot +}$ and $Q^{\cdot -}$-(Zn)P-$Fc^{\cdot +}$ CS states relative to the ferrocene triplet we placed two Lewis acidic[26] BF_3 molecules at the quinone oxygen atoms, which allowed optimisation of the CS states of **6e**($\cdot 2BF_3$) and **Zn-6e**($\cdot 2BF_3$) as the lowest-energy triplet states (Figure 15, b,c). The calculated spin densities are clearly at both the ferrocenium and semiquinonato radicals. Again, the quinone CO bond lengths are elongated from 1.26 to 1.30 Å. Furthermore, the Fe···Cp(centroid) distances are elongated from 1.73 to 1.80 Å, which indicates the ferrocenium state.

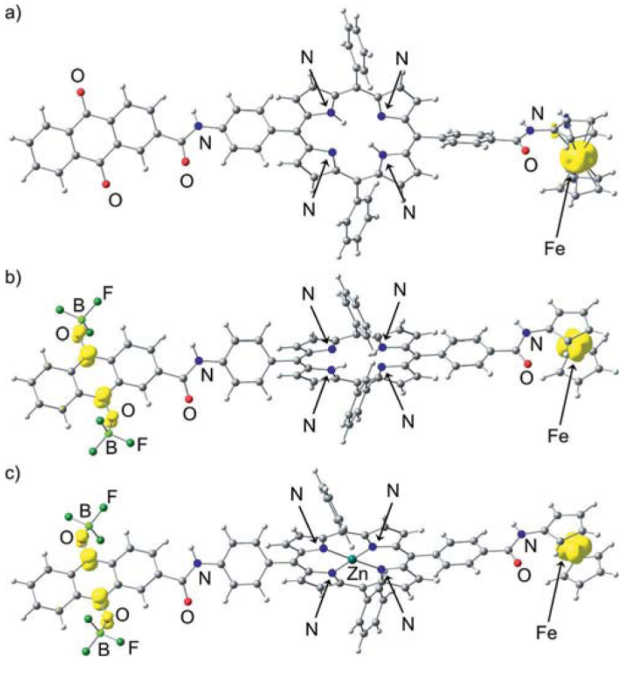

Figure 15. DFT-calculated spin densities of a) the ferrocene triplet state of **6e**, b) the $Q^{\cdot -}$-P-$Fc^{\cdot +}$ triplet CS state of **6e**($\cdot 2BF_3$) and c) the $Q^{\cdot -}$-(Zn)P-$Fc^{\cdot +}$ triplet CS state of **Zn-6e**($\cdot 2BF_3$) (isosurface value 0.01 a.u.).

Transient Absorption Spectroscopy of Selected Compounds

Compared with the porphyrin bands, the absorptions of the semiquinone radical anion $Q^{\cdot -}$ and ferrocenium cation $Fc^{\cdot +}$ are rather weak. Chemical reduction of the reference *N*-ethylanthraquinone-2-carboxylic acid amide with decamethylcobaltocene [$CoCp^*_2$][27] (see the Supporting Information) generated the semiquinone radical anion $Q^{\cdot -}$ with an absorption maximum at 618 nm and ε_{618} = 750 $\mathrm{M}^{-1}\,\mathrm{cm}^{-1}$ (THF). The ferrocenium reference $[\mathrm{Fc\text{-}NHAc}]^+$ absorbs at 759 nm with ε_{759} = 350 $\mathrm{M}^{-1}\,\mathrm{cm}^{-1}$ (CH_2Cl_2).[28] Owing to the low extinction coefficients, that is, small absorption cross-sections, these bands are difficult to detect in transient absorption (TA) pump-probe experiments as they are overwhelmed by the excited-state absorptions of the strongly absorbing porphyrin excited states. Hence all transient absorption spectra are largely dominated by features of the porphyrin radical(s) and porphyrin triplet states.

The pico- to nanosecond TA spectra of compounds **4a** and **6a** in THF are presented in Figure 16. The spectra show multiple peaked features that correspond to ground-

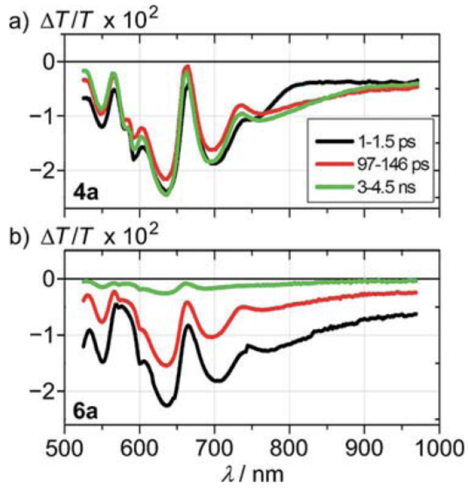

Figure 16. ps–ns transient absorption spectra of a) **4a** and b) **6a** in THF after excitation at λ_{exc} = 420 nm. Note the significantly faster decay of the TA signal for compound **6a**.

state bleaching and stimulated emission overlapped by the excited-state absorption of the porphyrin. The spectra do not change much during the observed period of time, except for compound **4a**, for which there is an increase in the intensity of the photoinduced absorption in the spectral region between 750–900 nm. This spectral evolution may be related to electron transfer from the porphyrin to the quinone, but a clear assignment is difficult.

As a consequence of the superposition of several bands corresponding to porphyrin radical ions, namely the excited-state absorption, the ground-state bleaching and stimulated emission bands, and the low extinction coefficients of the $Q^{\cdot-}$ and $Fc^{\cdot+}$ radicals, the transient spectra of intermediate CS states are not observed for dyad **4a** and triad **6a**. However, very clearly a much more rapid decay of the entire TA spectrum is observed for the ferrocenyl derivative **6a**. The decay is well fitted by a single exponential with an inverse rate of 220 ps, which is essentially the same as the 215 ps determined for the fluorescence lifetime of **6a**. This fast decay is likely due to the fast reductive quenching of the porphyrin excited state by the ferrocene, parallel oxidative quenching by the quinone (Figure 7) and/or heavy atom quenching by the ferrocene to give the porphyrin triplet state. For the two PET pathways, porphyrin radical anions and radical cations could be simultaneously present and would create superimposed excited-state absorption spectra that are difficult to analyse. After charge transfer from $P^{\cdot-}$ to Q or from Fc to $P^{\cdot+}$, the final CS state should show no features arising from porphyrin, but only weak bands corresponding to $Q^{\cdot-}$ and $Fc^{\cdot+}$ radicals. These latter would be difficult to detect, especially if the final CS state is only formed in low yields. However, the significant decrease in the TA signal intensity on the nanosecond timescale observed for **6a** in comparison with **4a** indicates that in the former a large fraction of the porphyrin excited states are rapidly quenched and that the ground state of the porphyrin in **6a** is quickly recovered after photoexcitation. This is in line with the experimentally observed faster photoluminescence decay of **6a**, the much lower fluorescence quantum yield and the predicted higher driving force for photoinduced electron transfer from the ferrocene to the porphyrin in comparison with electron transfer from the porphyrin to the quinone moiety, all of which indicate that the charge-transfer process from ferrocenium to the porphyrin is efficient.

As the pico- to nanosecond TA spectra are rather difficult to interpret due to the multitude of features and potentially parallel photophysical processes, we had a closer look at the nano- to microsecond spectra and dynamics. On the nanosecond timescale, the shapes of the transient absorption spectra of **Ac-3a**, **4a** and **6a** are rather similar (see the Supporting Information). The decay of the TA signals on this timescale should largely reflect the recombination dynamics of the triplet and CS states in these compounds. In fact, the dynamics of the TA signals of all three compounds **Ac-3a**, **4a** and **6a** can be well described by the sum of two exponentials with a nano- and microsecond component indicating two processes, as shown in Figure 17. In the case of the reference porphyrin **Ac-3a**, we obtained inverse rate constants of 12 ns and 7 µs.

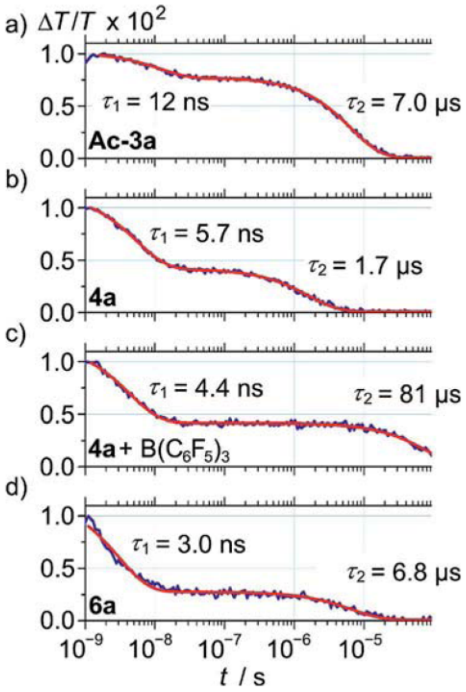

Figure 17. ns–µs transient absorption dynamics of a) **Ac-3a**, b) **4a**, c) **4a** plus 100 equiv. $B(C_6F_5)_3$ and d) **6a** in THF solution after excitation at λ_{exc} = 532 nm. The dynamics were monitored in the spectral region 550–620 nm. The solid red lines represent exponential fits to the data and the inverse decay rates are also shown. Note the significantly slower TA signal decay for compound **4a** plus additive indicating the stabilisation of the CS state by the Lewis acid.

The nanosecond lifetime τ_1 corresponds approximately to the measured fluorescence lifetime of around 10 ns within the error that can be expected between the two different experimental techniques. The microsecond lifetime τ_2 can be assigned to the decay of the porphyrin triplet T_1 state generated by intersystem crossing from the porphyrin singlet S_1 state due to its significantly longer lifetime in the range typical for the decay of triplets. Fitting the signal dynamics of **4a** yields inverse rate constants of 5.7 ns and 1.7 µs. The former is shorter than the lifetime observed for the reference porphyrin **Ac-3a**, indicating additional decay channels, but longer than the observed fluorescence lifetime of compound **4a** (in CH_2Cl_2), which might be a solvent effect. However, in this case we most probably approached the temporal resolution of our ns–µs TA set-up, which is about several nanoseconds. The second longer-lived component has a considerably shorter lifetime than the porphyrin triplet-state lifetime observed for compound **Ac-3a** and thus appears to originate from a state other than the T_1 triplet. Given that the efficiency of ET obtained by analysis of the fluorescence quenching is Φ_{ET} = 0.93, we assign this component to the decay of the $Q^{\cdot-}$-$P^{\cdot+}$ CS state, which is formed in high yield in the case of compound **4a**. The dynamics of the TA signals of compound **6a** can be fitted with inverse rates of τ_1 = 3 ns and τ_2 = 6.8 µs. Although the former is certainly limited by the temporal resolution of our set-up and represents the sub-nanosecond dynamics of the PET processes, the latter component is close to the triplet lifetime observed for compound **Ac-3a**. This appears reasonable as in this compound no features of porphyrin radicals should be observed from the final $Q^{\cdot-}$-P-$Fc^{\cdot+}$ CS state after electron transfer to Q and from Fc are complete. Therefore we observe the decay of a fraction of porphyrin triplet states created either by ISC from the porphyrin singlet state directly after photoexcitation or, which is more likely, by a transition of the initial Q-$P^{\cdot-}$-$Fc^{\cdot+}$ CS state (1.46 eV, Table 8 and Figure 7) into the T_1 state of the porphyrin (1.43 eV[3f]).

As suggested by the DFT calculations, a CS state involving the quinone can be stabilised by coordinating a Lewis acid to the quinone carbonyl groups. Excess tris(pentafluorophenyl)boron was added to **4a** and **6a** in THF and the ps–ns as well as ns–µs transient absorption spectra and dynamics were studied (see Figure 17 and the Supporting Information). Some spectral but mostly temporal differences were observed with respect to the spectra and dynamics of **4a** and **6a** in the absence of the Lewis acid. The most striking observation is a pronounced decrease in the decay rate, in other words, increase in the lifetime of the $Q^{\cdot-}$-$P^{\cdot+}$ CS state observed for compound **4a**. In fact, the ns–µs TA experiments showed that the lifetime of the CS state is significantly increased from τ_2 = 1.7 µs to τ_2 = 80 µs upon addition of $B(C_6F_5)_3$ (cf. Figure 17, b,c). This suggests that the $Q^{\cdot-}$-$P^{\cdot+}$ CS state is significantly stabilised by the Lewis acid, as suggested by the DFT calculations, and further supports our assignment of the dynamics to the recombination of the charge-separated state. Although the effect is pronounced for **4a**, it is much less obvious for **6a**. This appears reasonable as we assigned the dynamics in the latter to the recombination of the porphyrin triplet state, which should not be affected by the presence of the Lewis acid.

Conclusions

Anthraquinone–porphyrin dyads (Q-P, **4**), anthraquinone–porphyrin–ferrocene triads (Q-P-Fc, **6**) and zincated triads [Q-(Zn)P-Fc, **Zn-6**] with *meso* substituents Ar of increasing electron-withdrawing character in the porphyrin component have been designed and synthesised by amide coupling (Ar = 4-C_6H_4O*n*Bu, 4-C_6H_4OMe, Mes, 4-C_6H_4Me, C_6H_5, 4-C_6H_4F, 4-$C_6H_4CF_3$ and C_6F_5). Based on this modular amide-coupling approach, a Q-P^{C6H5}-P^{C6H4Me}-Fc tetrad (**9**) was constructed. In the ground states of **4**, **6**, **Zn-6** and **9**, only marginal interactions between the individual building blocks Q, P and Fc are observed, and energy transfer between the two porphyrins in **9** is possible. The fluorescence of dyads **4** is quenched by oxidative photoinduced electron transfer (PET). The rate of ET increases by several orders of magnitude with increasing electron-donating power of the *meso* substituent Ar ($k_{ET} = 0.003 \times 10^9$ to 1.5×10^9 s^{-1}) due to the increased driving force $\Delta(\Delta G_{ET})$ = –0.3 eV. In triads **6** an additional reductive PET pathway is thermodynamically feasible. This ET pathway is favoured by electron-withdrawing *meso* substituents Ar [k_{ET} = 4×10^9 to 38×10^9 s^{-1}; $\Delta(\Delta G_{ET})$ = –0.2 eV]. Comparable rates and driving forces for reductive and oxidative quenching are found for Ar = 4-C_6H_4O*n*Bu, 4-C_6H_4OMe and 4-C_6H_4Me in triads **6**. The zinc porphyrins **Zn-6** are basically non-fluorescent. If the major deactivation in zinc conjugates indeed occurs by PET, both pathways feature similar driving forces for Ar = 4-C_6H_4O*n*Bu, 4-C_6H_4OMe, Mes, 4-C_6H_4Me and C_6H_5. In tetrad **9**, both pathways are also feasible, although reductive PET (ΔG_{ET} = –0.48 eV; k_{ET} = 2.66×10^9 s^{-1}) is preferred over oxidative PET (ΔG_{ET} = –0.26 eV; k_{ET} = 0.363×10^9 s^{-1}). With these preparative, spectroscopic, electrochemical and theoretical results in hand, more complex architectures with well-defined excited-state energies in a structurally precisely organised manner can be envisaged.

Supporting Information (see footnote on the first page of this article): Experimental and analytical details, normalised absorption and emission spectra of selected Q-P dyads, Q-P-Fc triads and reference porphyrins in CH_2Cl_2n DFT (B3LYP/LANL2DZ, PCM) calculated frontier orbitals of **Zn-6b**, **Zn-6g**, **Zn-6h** and **9**, absorption spectra of *N*-ethylanthraquinone-2-carboxamide treated with $CoCp^*_2$ in THF; ns to µs transient absorption spectra of **Ac-3a**, **4a**, **4a** + $B(C_6F_5)_3$, **6a** and **6a** + $B(C_6F_5)_3$ in THF; after excitation at λ_{exc} = 532 nm, energies (eV) of relevant frontier molecular orbitals of the Q-P dyads **4a**–**4h** determined by DFT (B3LYP/LANL2DZ, PCM), energies (eV) of relevant frontier molecular orbitals of the Q-P-Fc triads **6a**–**6i** and Q-P-Fc triads **Zn-6a**–**Zn-6i** determined by DFT (B3LYP/LANL2DZ, PCM), Cartesian coordinates of DFT-optimised geometries.

Acknowledgments

This work was supported by the Deutsche Forschungsgemeinschaft (DFG) (He 2778-6/1). J. R. O. and M. M. thank the Max Planck Graduate Center for support and F. L. (all Max Planck Institute for Polymer Research of Mainz, Germany) thanks the Max Planck Society for funding the Max Planck Research group.

---

[1] a) M. G. Rockley, M. W. Windsor, R. J. Cogdellt, W. W. Parsont, H. Neurath, *Proc. Natl. Acad. Sci. USA* **1975**, *72*, 2251–2255; b) K. J. Kaufmann, P. L. Dutton, T. L. Netzel, J. S. Leigh, P. M. Rentzepis, *Science* **1975**, *188*, 1301–1304; c) J. J. Katz, J. R. Norris, L. L. Shipman, M. C. Thurnauer, M. R. Wasielewski, *Ann. Rev. Biophys. Bioeng.* **1978**, *7*, 393–434; d) J. Deisenhofer, O. Epp, K. Miki, R. Huber, H. Michel, *J. Mol. Biol.* **1984**, *180*, 385–398.

[2] a) M. R. Wasielewski, *Chem. Rev.* **1992**, *92*, 435–461; b) A. Harriman, J.-P. Sauvage, *Chem. Soc. Rev.* **1996**, *25*, 41–48; c) D. Gust, T. A. Moore, A. L. Moore, *Acc. Chem. Res.* **2001**, *34*, 40–48; d) L. Sun, L. Hammarström, B. Åkermark, S. Styring, *Chem. Soc. Rev.* **2001**, *30*, 36–49; e) S. Fukuzumi, *Org. Biomol. Chem.* **2003**, *1*, 609–620.

[3] a) A. R. McIntosh, A. Siemiarczuk, J. R. Bolton, M. J. Stillman, T.-F. Ho, A. C. Weedon, *J. Am. Chem. Soc.* **1983**, *105*, 7215–7223; b) A. Siemiarczuk, A. R. McIntosh, T.-F. Ho, M. J. Stillman, K. J. Roach, A. C. Weedon, J. R. Bolton, J. S. Connolly, *J. Am. Chem. Soc.* **1983**, *105*, 7224–7230; c) M. R. Wasielewski, M. P. Niemczyk, W. A. Svec, E. B. Pewitt, *J. Am. Chem. Soc.* **1985**, *107*, 1080–1082; d) D. Gust, T. A. Moore, P. A. Liddell, G. A. Nemeth, L. R. Makings, A. L. Moore, D. Barrett, P. J. Pessiki, R. V. Bemasson, M. Rougée, C. Chachaty, F. C.

De Schryver, M. Van der Auweraer, A. R. Holzwarth, J. S. Connolly, *J. Am. Chem. Soc.* **1987**, *109*, 846–856; e) A. D. Joran, B. A. Leland, P. M. Felker, A. H. Zewail, J. J. Hopfield, P. B. Dervan, *Nature* **1987**, *327*, 508–511; f) J. A. Schmidt, A. R. McIntosh, A. C. Weedon, J. R. Bolton, J. S. Connolly, J. K. Hurley, M. R. Wasielewski, *J. Am. Chem. Soc.* **1988**, *110*, 1733–1740; g) J. von Gersdorff, M. Huber, H. Schubert, D. Niethammer, B. Kirste, M. Plato, K. Möbius, H. Kurreck, R. Eichberger, R. Kietzmann, F. Willig, *Angew. Chem. Int. Ed. Engl.* **1990**, *29*, 670–672; *Angew. Chem.* **1990**, *102*, 690–692; h) J. Zimmermann, J. Von Gersdorff, H. Kurreck, B. Ridder, *J. Photochem. Photobiol. B: Biology* **1997**, *40*, 209–217; i) J. P. Sumida, P. A. Liddell, S. Lin, A. N. Macpherson, G. R. Seely, A. L. Moore, T. A. Moore, D. Gust, *J. Phys. Chem. A* **1998**, *102*, 5512–5519; j) O. Korth, A. Wiehe, H. Kurreck, B. Röder, *Chem. Phys.* **1999**, *246*, 363–372; k) Y. K. Kang, I. V. Rubtsov, P. M. Iovine, J. Chen, M. J. Therien, *J. Am. Chem. Soc.* **2002**, *124*, 8275–8279; l) J. Springer, G. Kodis, L. De Garza, A. L. Moore, T. A. Moore, D. Gust, *J. Phys. Chem. A* **2003**, *107*, 3567–3575; m) P. P. Kumar, G. Premaladha, B. G. Maiya, *J. Chem. Sci.* **2005**, *117*, 193–201.

[4] a) A. M. Brun, A. Harriman, V. Heitz, J.-P. Sauvage, *J. Am. Chem. Soc.* **1991**, *113*, 8657–8663; b) V. Heitz, S. Chardon-Noblat, J.-P. Sauvage, *Tetrahedron Lett.* **1991**, *32*, 197–198; c) E. K. L. Yeow, P. J. Sintic, N. M. Cabral, J. N. H. Reek, M. J. Crossley, K. P. Ghiggino, *Phys. Chem. Chem. Phys.* **2000**, *2*, 4281–4291; d) K. Kilså, J. Kajanus, A. N. Macpherson, J. Mårtensson, B. Albinsson, *J. Am. Chem. Soc.* **2001**, *123*, 3069–3080; e) S. Fukuzumi, K. Ohkubo, W. E. Z. Ou, J. Shao, K. M. Kadish, J. A. Hutchison, K. P. Ghiggino, P. J. Sintic, M. J. Crossley, *J. Am. Chem. Soc.* **2003**, *125*, 14984–14985; f) J. H. Jang, H. J. Kim, H.-J. Kim, C. H. Kim, T. Joo, D. Won Cho, M. Yoon, *Bull. Korean Chem. Soc.* **2007**, *28*, 1967–1972; g) J. Fortage, J. Boixel, E. Blart, L. Hammarström, H. C. Becker, F. Odobel, *Chem. Eur. J.* **2008**, *14*, 3467–3480; h) J. Fortage, A. Scarpaci, L. Viau, Y. Pellegrin, E. Blart, M. Falkenstrçm, L. Hammarström, I. Asselberghs, R. Kellens, W. Libaers, K. Clays, M. P. Eng, F. Odobel, *Chem. Eur. J.* **2009**, *15*, 9058–9067; i) J. Fortage, J. Boixel, E. Blart, H. C. Becker, F. Odobel, *Inorg. Chem.* **2009**, *48*, 518–526.

[5] a) D. Kuciauskas, S. Lin, G. R. Seely, A. L. Moore, T. A. Moore, T. Drovetskaya, C. A. Reed, P. D. W. Boyd, *J. Phys. Chem.* **1996**, *100*, 15926–15932; b) C. Luo, D. M. Guldi, H. Imahori, K. Tamaki, Y. Sakata, *J. Am. Chem. Soc.* **2000**, *122*, 6535–6551; c) H. Imahori, N. V. Tkachenko, V. Vehmanen, K. Tamaki, H. Lemmetyinen, Y. Sakata, S. Fukuzumi, *J. Phys. Chem. A* **2001**, *105*, 1750–1756; d) V. Vehmanen, N. V. Tkachenko, H. Imahori, S. Fukuzumi, H. Lemmetyinen, *Spectrochim. Acta Part A* **2001**, *57*, 2229–2244; e) H. Imahori, D. M. Guldi, K. Tamaki, Y. Yoshida, C. Luo, Y. Sakata, S. Fukuzumi, *J. Am. Chem. Soc.* **2001**, *123*, 6617–6628; f) H. Imahori, K. Tamaki, Y. Araki, Y. Sekiguchi, O. Ito, Y. Sakata, S. Fukuzumi, *J. Am. Chem. Soc.* **2002**, *124*, 5165–5174; g) H. Imahori, Y. Sekiguchi, Y. Kashiwagi, T. Sato, Y. Araki, O. Ito, H. Yamada, S. Fukuzumi, *Chem. Eur. J.* **2004**, *10*, 3184–3196; h) M. U. Winters, E. Dahlstedt, H. E. Blades, C. J. Wilson, M. J. Frampton, H. L. Anderson, B. Albinsson, *J. Am. Chem. Soc.* **2007**, *129*, 4291–4297; i) C. Wijesinghe, M. E. El-Khouly, M. E. Zandler, S. Fukuzumi, F. D′Souza, *Chem. Eur. J.* **2013**, *19*, 9629–9638.

[6] a) D. Gust, T. A. Moore, A. L. Moore, F. Cao, D. Luttrul, J. M. Degraziano, X. C. Ma, L. R. Makings, S. Lee, T. T. Trier, E. Bittersmann, G. R. Seely, S. Woodward, R. V. Bensasson, M. Roug, F. C. De Schryver, M. Van der Auweraer, *J. Am. Chem. Soc.* **1991**, *113*, 3638–3649; b) D. Gust, T. A. Moore, A. L. Moore, A. N. Macpherson, A. Lopez, J. M. DeGraziano, I. Gouni, E. Bittersmann, G. R. Seely, F. Gao, R. A. Nieman, X. C. Ma, L. J. Demanche, S. Hung, D. K. Luttrull, S. Lee, P. K. Kerrigan, *J. Am. Chem. Soc.* **1993**, *115*, 11141–11152; c) S. L. Gould, G. Kodis, R. E. Palacios, L. De La Garza, A. Brune, D. Gust, T. A. Moore, A. L. Moore, *J. Phys. Chem. B* **2004**, *108*, 10566–10580.

[7] a) R. Ciasson, E. J. Lee, X. Zbao, M. S. Wrighton, *J. Phys. Chem.* **1993**, *97*, 2596–2601; b) M. Kubo, Y. Mori, M. Otani, M. Murakami, Y. Ishibashi, M. Yasuda, K. Hosomizu, H. Miyasaka, H. Imahori, S. Nakashima, *Chem. Phys. Lett.* **2006**, *429*, 91–96; c) H. Mansour, M. E. El-khouly, S. Y. Shaban, O. Ito, N. Jux, *J. Porphyrins Phthalocyanines* **2007**, *11*, 719–728; d) V. S. Shetti, M. Ravikanth, *Eur. J. Org. Chem.* **2010**, 494–508.

[8] a) R. A. Marcus, *J. Chem. Phys.* **1956**, *24*, 979–989; b) R. A. Marcus, *Annu. Rev. Phys. Chem.* **1964**, *15*, 155–196; c) R. A. Marcus, *Angew. Chem. Int. Ed. Engl.* **1993**, *32*, 1111–1121; *Angew. Chem.* **1993**, *105*, 1161–1172.

[9] a) S. Fukuzumi, K. Ohkubo, W. E. Z. Ou, J. Shao, K. M. Kadish, *J. Am. Chem. Soc.* **2003**, *125*, 14984–14985; b) M. Linke-Schaetzel, C. E. Anson, A. K. Powell, G. Buth, E. Palomares, J. D. Durrant, T. Silviu Balaban, J.-M. Lehn, *Chem. Eur. J.* **2006**, *12*, 1931–1940; c) B. M. J. M. Suijkerbuijk, R. J. M. Klein Gebbink, *Angew. Chem.* **2008**, *120*, 7506–7532; d) J. Fortage, J. Boixel, E. Blart, L. Hammarström, *Chem. Eur. J.* **2008**, *14*, 3467–3480; e) K. Kiyosawa, N. Shiraishi, T. Shimada, D. Masui, H. Tachibana, *J. Phys. Chem. C* **2009**, *113*, 11667–11673; f) J. Fortage, A. Scarpaci, L. Viau, Y. Pellegrin, E. Blart, M. Falkenström, L. Hammarström, I. Asselberghs, R. Kellens, W. Libaers, K. Clays, M. P. Eng, F. Odobel, *Chem. Eur. J.* **2009**, *15*, 9058–9067; g) A. C. Benniston, A. Harriman, P. Li, *J. Am. Chem. Soc.* **2010**, *132*, 26–27; h) H. Kon, T. Nagata, *Chem. Eur. J.* **2012**, *18*, 1781–1788.

[10] Y. Araki, Y. Yasumura, O. Ito, *J. Phys. Chem. B* **2005**, *109*, 9843–9848.

[11] J. Melomedov, A. Wünsche Von Leupoldt, M. Meister, F. Laquai, K. Heinze, *Dalton Trans.* **2013**, *42*, 9727–9739.

[12] a) A. Breivogel, K. Hempel, K. Heinze, *Inorg. Chim. Acta* **2011**, *374*, 152–162; b) D. Siebler, M. Linseis, T. Gasi, L. M. Carrella, R. F. Winter, C. Förster, K. Heinze, *Chem. Eur. J.* **2011**, *17*, 4540–4551; c) J. Dietrich, U. Thorenz, C. Förster, K. Heinze, *Inorg. Chem.* **2013**, *52*, 1248–1264; d) J. Dietrich, A. Wünsche von Leupoldt, M. Grabolle, U. Resch-Genger, K. Heinze, *Eur. J. Inorg. Chem.* **2013**, 3009–3019.

[13] a) K. Heinze, U. Wild, M. Beckmann, *Eur. J. Inorg. Chem.* **2007**, 617–623; b) K. Heinze, M. Beckmann, K. Hempel, *Chem. Eur. J.* **2008**, *14*, 9468–9480; c) K. Heinze, K. Hempel, *Chem. Eur. J.* **2009**, *15*, 1346–1358; d) G. Dirscherl, B. König, *Eur. J. Org. Chem.* **2008**, 597–634; e) D. Siebler, C. Förster, K. Heinze, *Dalton Trans.* **2011**, *40*, 3558–3575.

[14] K. Heinze, A. Reinhart, *Dalton Trans.* **2008**, 469–480.

[15] a) B. Bildstein, M. Malaun, H. Kopacka, K. Wurst, M. Mitterböck, K. Ongania, G. Opromolla, P. Zanello, *Organometallics* **1999**, *18*, 4325–4336; b) K. Heinze, M. Schlenker, *Eur. J. Inorg. Chem.* **2004**, 2974–2988.

[16] a) P. D. Rao, S. Dhanalekshmi, B. J. Littler, J. S. Lindsey, *J. Org. Chem.* **2000**, *65*, 7323–7344; b) A. K. Burrell, D. L. Officer, P. G. Plieger, D. C. W. Reid, *Chem. Rev.* **2001**, *101*, 2751–2796; c) J. S. Lindsey, *Acc. Chem. Res.* **2010**, *43*, 300–311; d) M. O. Senge, *Chem. Commun.* **2011**, *47*, 1943–1960.

[17] C. M. Carcel, J. K. Laha, R. S. Loewe, P. Thamyongkit, K. Schweikart, V. Misra, D. F. Bocian, J. S. Lindsey, N. Carolina, *J. Org. Chem.* **2004**, *69*, 6739–6750.

[18] a) B. J. Littler, Y. Ciringh, J. S. Lindsey, *J. Org. Chem.* **1999**, *64*, 2864–2872; b) K. Heinze, A. Reinhart, *Z. Naturforsch. B* **2005**, *60*, 758–762; c) T. Rohand, E. Dolusic, T. H. Ngo, W. Maes, W. Dehaen, *ARKIVOC* **2007**, *x*, 307–324.

[19] K. Phukan, M. Ganguly, N. Devi, *Synth. Commun.* **2009**, *39*, 2694–2701.

[20] S. B. Colbran, S. T. Lee, D. G. Lonnon, F. J. D. Maharaj, A. M. McDonagh, K. A. Walker, R. D. Young, *Organometallics* **2006**, *25*, 2216–2224.

[21] P. Heier, C. Förster, D. Schollmeyer, N. Boscher, P. Choquet, K. Heinze, *Dalton Trans.* **2013**, *42*, 906–917.

[22] A. Weller, *Z. Phys. Chem. (Muenchen Ger.)* **1982**, *133*, 93–98.
[23] M. J. Frisch, G. W. Trucks, H. B. Schlegel, G. E. Scuseria, M. A. Robb, J. R. Cheeseman, G. Scalmani, V. Barone, B. Mennucci, G. A. Petersson, H. Nakatsuji, M. Caricato, X. Li, H. P. Hratchian, A. F. Izmaylov, J. Bloino, G. Zheng, J. L. Sonnenberg, M. Hada, M. Ehara, K. Toyota, R. Fukuda, J. Hasegawa, M. Ishida, T. Nakajima, Y. Honda, O. Kitao, H. Nakai, T. Vreven, J. A. Montgomery Jr., J. E. Peralta, F. Ogliaro, M. Bearpark, J. J. Heyd, E. Brothers, K. N. Kudin, V. N. Staroverov, R. Kobayashi, J. Normand, K. Raghavachari, A. Rendell, J. C. Burant, S. S. Iyengar, J. Tomasi, M. Cossi, N. Rega, J. M. Millam, M. Klene, J. E. Knox, J. B. Cross, V. Bakken, C. Adamo, J. Jaramillo, R. Gomperts, R. E. Stratmann, O. Yazyev, A. J. Austin, R. Cammi, C. Pomelli, J. W. Ochterski, R. L. Martin, K. Morokuma, V. G. Zakrzewski, G. A. Voth, P. Salvador, J. J. Dannenberg, S. Dapprich, A. D. Daniels, O. Farkas, J. B. Foresman, J. V. Ortiz, J. Cioslowski, D. J. Fox, *Gaussian 09*, revision A.02, Gaussian, Inc., Wallingford, CT, **2009**.
[24] M. Gouterman, *J. Chem. Phys.* **1959**, *30*, 1139–1161.
[25] D. Holten, D. F. Bocian, J. S. Lindsey, *Acc. Chem. Res.* **2002**, *35*, 57–69.
[26] For the use of Lewis acidic metal ions to stabilise a CS state, see: a) S. Fukuzumi, K. Okamoto, H. Imahori, *Angew. Chem. Int. Ed.* **2002**, *41*, 620–622; *Angew. Chem.* **2002**, *114*, 642–644; b) S. Fukuzumi, K. Okamoto, Y. Yoshida, H. Imahori, Y. Araki, O. Ito, *J. Am. Chem. Soc.* **2003**, *125*, 1007–1013.
[27] N. G. Connelly, W. E. Geiger, *Chem. Rev.* **1996**, *96*, 877–910.
[28] D. Siebler, C. Förster, K. Heinze, *Eur. J. Inorg. Chem.* **2010**, 3986–3992.

Received: January 28, 2014

6.3 Aminoferrocene and Ferrocene Amino Acid as Electron Donors in Modular Porphyrin-Ferrocene and Porphyrin-Ferrocene-Porphyrin Conjugates

Jascha Melomedov, Julian Robert Ochsmann, Michael Meister, Frédéric Laquai and Katja Heinze, *Eur. J. Inorg. Chem.* **2014**, accepted (ejic.201402138).

Manuscript received: 05.03.2014
Article first published online:26.05.2014

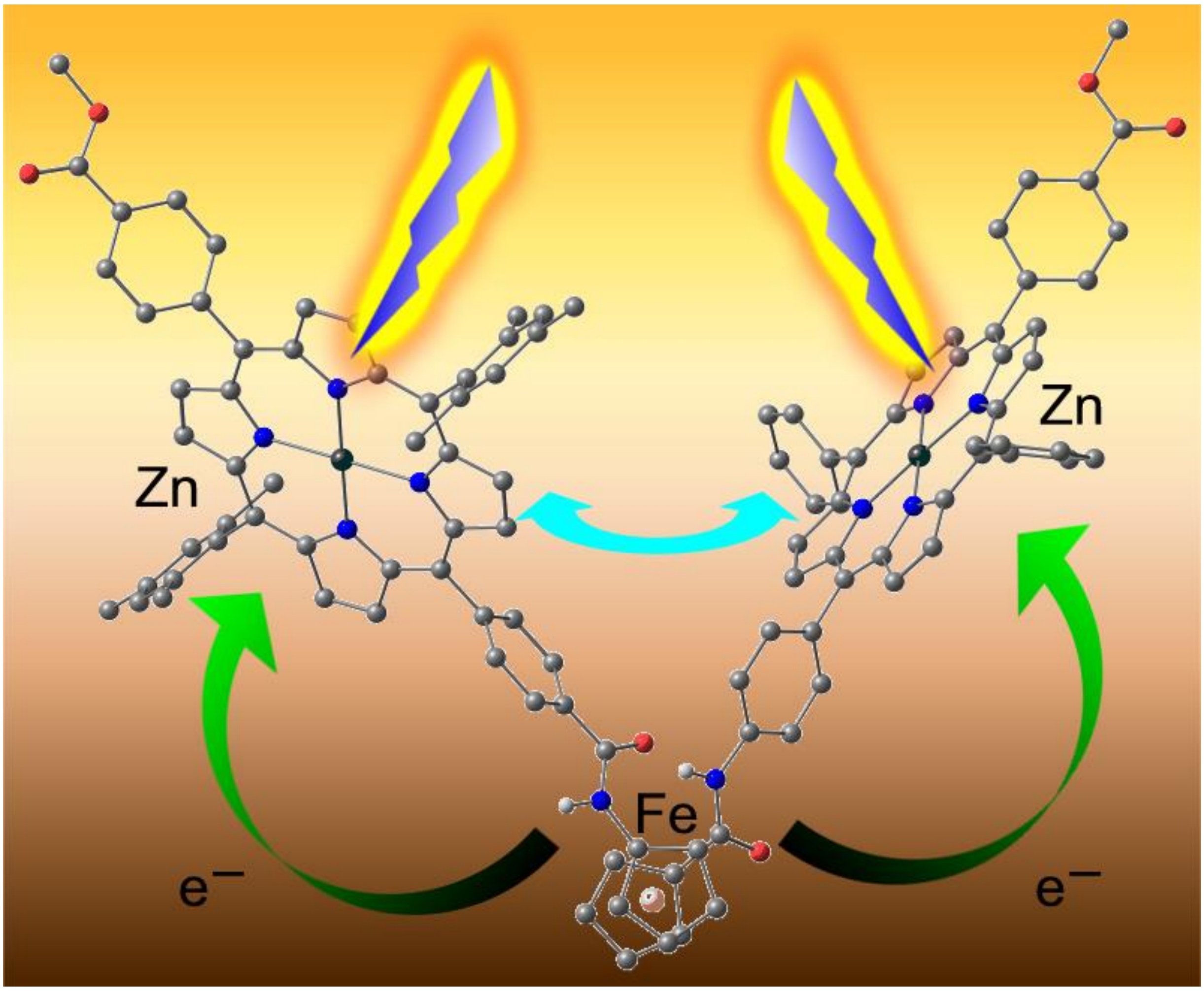

Aminoferrocene and Ferrocene Amino Acid as Electron Donors in Modular Porphyrin-Ferrocene and Porphyrin-Ferrocene-Porphyrin Conjugates

Jascha Melomedov,[a] Julian Robert Ochsmann,[b] Michael Meister,[b] Frédéric Laquai[b] and Katja Heinze*[a]

Keywords: Artificial photosynthesis / Energy transfer / Ferrocene / Photoinduced electron transfer / Porphyrin

[a] Institute of Inorganic Chemistry and Analytical Chemistry, Johannes Gutenberg-University of Mainz,
Duesbergweg 10–14, 55128 Mainz, Germany
Fax: +49-6131-39-27277
E-mail: katja.heinze@uni-mainz.de
Homepage: http://www.ak-heinze.chemie.uni-mainz.de/
[b] Max Planck Institute for Polymer Research, Ackermannweg 10, 55128 Mainz, Germany

Supporting information for this article is available on the WWW under http://www.eurjic.org/

Novel amide-linked porphyrin-ferrocene conjugates $M(P^{Ar})$-Fc were prepared from aminoferrocene and a carboxy-substituted *meso*-tetraaryl porphyrin (M = 2H, Zn; Ar = Mes, C_6F_5: **3a**, **3e**, **Zn-3a**, **Zn-3e**). A further porphyrin building block was attached to the second cyclopentadienyl ring of the ferrocene moiety giving the metallopeptides $M(P^{Mes})$-Fc-$M(P^{Ar})$ (M = 2H, Zn; Ar = C_6H_5, 4-C_6H_4F: **6b**, **6c** and **Zn-6b**, **Zn-6c**). The effects of the substituents Ar, the porphyrin central atom M and the presence of the second porphyrin at the ferrocene hinge on the excited state dynamics is studied by optical absorption spectroscopy, electrochemistry, steady-state emission, time resolved fluorescence measurements and transient absorption pump-probe spectroscopy in addition to Density Functional Theory calculations. In the ground state only weak interactions were revealed between ferrocene and porphyrin units by optical absorption spectroscopy and electrochemical measurements. However, the porphyrin emission is strongly quenched with respect to reference porphyrins lacking the ferrocene moieties. Fluorescence is partially recovered at lower temperatures suggesting an activated excited state decay process. All excited state lifetimes are reduced with respect to reference porphyrins. Quantum yields and lifetimes correlate with porphyrin and ferrocene redox potentials. All observations point to photoinduced electron transfer from ferrocene to the porphyrin in the normal Marcus region as dominant excited state reactivity. The resulting charge-separated state of selected conjugates was studied by ns-µs transient absorption pump-probe spectroscopy.

Hints for the feasibility of singlet-singlet energy transfer between cofacial porphyrins were found in tweezers **6** and **Zn-6**.

Introduction

To mimic the light harvesting and charge separating processes in natural photosynthesis a plethora of model compounds was deliberately designed and thoroughly investigated.[1-4,6] These artificial photosynthetic reaction centres typically consist of electron donor and electron acceptor units combined with a chromophore. Porphyrins and metalloporphyrins are highly suited and well established building elements for biomimetic model compounds[1-4,6] due to their favourable photophysical properties and their outstanding role in plant and bacterial photosynthesis. In artificial reaction centres porphyrins can act as electron donors[2] or acceptors[3]. Typically, in porphyrin-ferrocene arrays M(P)-Fc porphyrins function as electron acceptor and the organometallic ferrocene (Fc) acts as electron donor.[4,6]

Many ferrocene derivatives are stable, feature well defined Fc/Fc$^+$ redox states and are able to reduce the S$_1$ excited state of the porphyrin.[4,5]This renders ferrocene highly suitable as electron donor in model compounds for artificial charge separation and molecular electronic devices.[1,4,6,7]

Recently, we reported a modular synthetic strategy for amide-linked architectures constituting of porphyrin amino acids as chromophores, quinones as electron acceptors and ferrocenes as electron donors. In these conjugates both oxidative photoinduced electron transfer (PET), i.e. excited porphyrin to quinone and reductive PET pathways, namely ferrocene to excited porphyrin have been identified (Scheme 1).[1f]

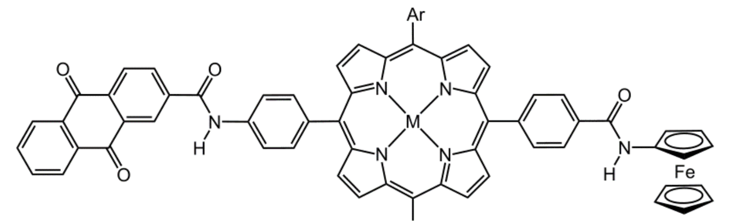

M = 2H, Zn
Ar = 4-$C_6H_4O^nBu$, 4-C_6H_4OMe, 2,4,6-$C_6H_2(CH_3)_3$, 4-C_6H_4Me, C_6H_5, 4-C_6H_4F, 4-$C_6H_4CF_3$, C_6F_5

Scheme 1. Artificial photosynthetic reaction centres assembled by amide bonds and based on *trans*-AB$_2$C substituted porphyrin amino acids, anthraquinone carboxylic acid and aminoferrocene.[1f]

The core building block of these artificial reaction centres is a *trans*-AB$_2$C substituted *meso*-tetraaryl porphyrin amino acid[9,10] with different aryl groups Ar of varying electron donating/withdrawing power at the *meso* positions which dictate the preferred PET pathway. In order to specifically focus on the reductive pathway, novel porphyrin-ferrocene conjugates and porphyrin-ferrocene-porphyrin tweezers[6] with tunable electronic properties of the porphyrin electron acceptor as well as of the ferrocene electron donor have been designed in the present study. Aminoferrocene[5a] and (*N*-Fmoc protected) ferrocene amino acid (Fmoc = 9-fluorenylmethoxycarbonyl)[5a] are employed as electron donors with different redox potentials. Furthermore, the orthogonal amine/acid substitution pattern of the latter allows straightforward access to unsymmetric 1,1'-disubstituted ferrocenes with two different porphyrines. We report the synthesis of M(P^{Ar})-Fc dyads (M = 2H, Zn; Ar = Mes, C_6F_5: **3a**, **3e**, **Zn-3a**, **Zn-3e**) by amide coupling of a porphyrin mono acid with aminoferrocene. *N*-Fmoc protected conjugates *N*-Fmoc-Fc-P^{Ar} (Ar = C_6H_5, 4-C_6H_4F, 4-$C_6H_4CF_3$, C_6F_5: **5b** − **5e**) are introduced as versatile building blocks by coupling of porphyrin amino acid esters with *N*-Fmoc-protected ferrocene amino acid. Finally, bis(porphyrin) tweezers P^{Mes}-Fc-P^{Ar} (**6b**, **6c**) are accessible from building blocks **5b** and **5c** and a porphyrin acid by amide coupling. Metalation yields the corresponding zinc(II) porphyrins Zn(P^{Mes})-Fc-Zn(P^{Ar}) (**Zn-6b**, **Zn-6c**). All new compounds are fully characterised by standard techniques in addition to detailed photophysical and redoxchemical characterisation. Density Functional calculations are employed to further underscore the experimental results.

Results and Discussion

Porphyrin starting materials and reference compounds **1a**, **2a**, **Zn-1a**, **1e**, **2e**, **4b** − **4e**, **Ac-4b** − **Ac-4e**, **Zn-Ac-4b** and **Zn-Ac-4c** were prepared according to literature procedures.[8,10] The synthesis and characterization of reference porphyrin 10,20-bis(pentafluorophenyl)-5,15-bis(4-methoxycarbonylphenyl) porphyrinato] zinc(II) **Zn-1e** is described in the Experimental Section. All analytical data are collected in the Supporting Information.

The novel porphyrin-ferrocene conjugates P^{Ar}-Fc **3a** and **3e** were prepared in a two-step procedure from *trans*-A_2B_2 porphyrin diesters **1a**/**1e** (Ar = Mes[1f,2d,8,10], C_6F_5[1f,10]) by partial hydrolysis giving monoacids **2a**/**2e**, *in situ* acid activation by thionyl chloride and coupling with aminoferrocene[5a]. Metalation of dyads **3** with zinc(II) acetate dihydrate gave the corresponding ferrocenyl zinc(II) porphyrins Zn(P^{Ar})-Fc **Zn-3a** and **Zn-3e** (Scheme 2).[1f,9,10]

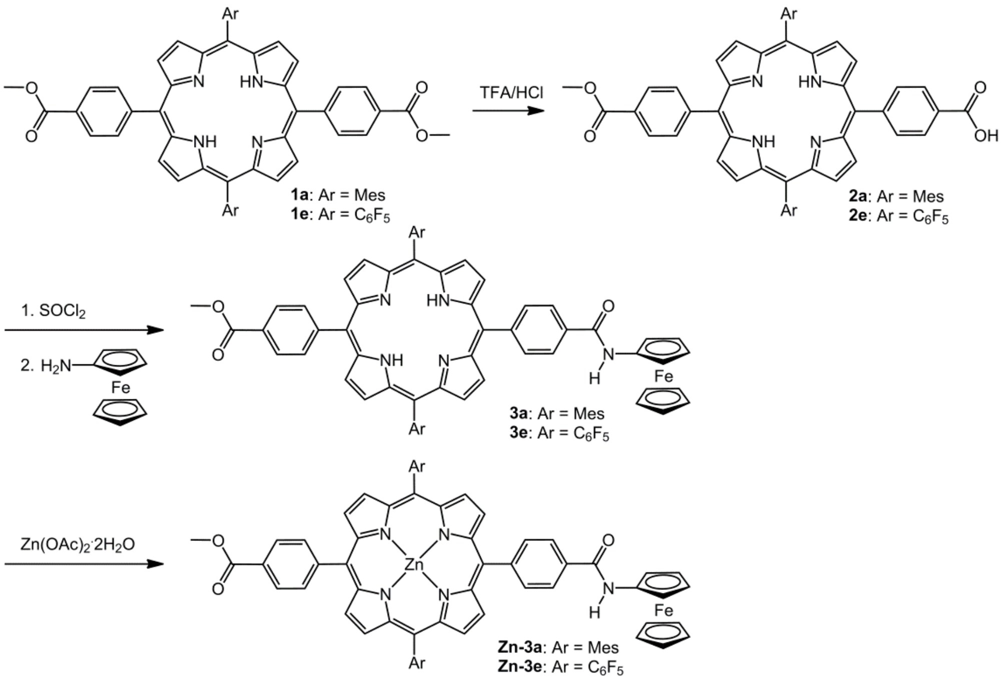

Scheme 2. Syntheses of **3** and **Zn-3** from aminoferrocene.

Key building block of 1,1'-ferrocenylene-bis(porphyrins) **6** is the *N*-Fmoc-protected ferrocene amino acid.[5a] It was found convenient to first couple a porphyrin amino ester **4b** – **4e**[1f,9,10] to the *C*-terminus of the central ferrocene to give *N*-Fmoc-Fc-P^{Ar} (Ar = C_6H_5, 4-C_6H_4F, 4-$C_6H_4CF_3$, C_6F_5: **5b** – **5e**). To prove the synthetic concept of adding a further porphyrine to **5** the *N*-Fmoc protecting groups of **5b** and **5c** were removed by tris(2-aminoethyl)amine and finally the second porphyrin was attached to the *N*-terminus after activation of the porphyrin acid **2a** with Ghosez's reagent (1-chloro-*N*,*N*,2-trimethyl-1-propenylamine[11]) similar to the synthesis of conjugates **3** (Scheme 3). Again metalation of **6b** or **6c** with zinc(II) acetate dihydrate yielded the corresponding trimetallic Zn-Fe-Zn complexes **Zn-6b** and **Zn-6c**.[1f,9,10]

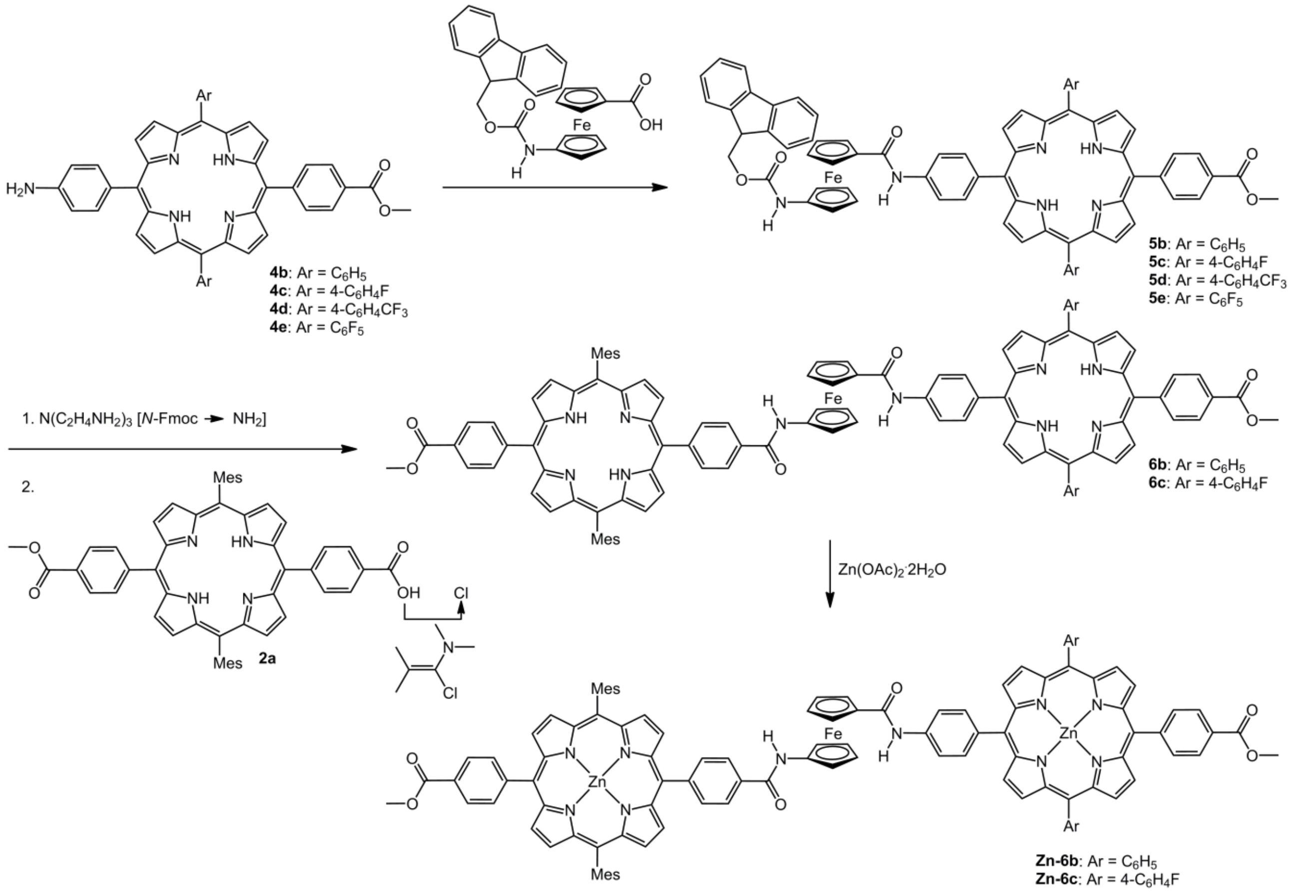

Scheme 3. Syntheses of **5**, **6** and **Zn-6** from *N*-Fmoc-protected ferrocene amino acid.

The correct composition of all novel compounds **3**, **Zn-3**, **5**, **6** and **Zn-6** was established by multinuclear NMR spectroscopy (^{1}H, ^{13}C, ^{19}F), IR and UV/Vis spectroscopy as well as (high-resolution) mass spectrometry. The appearance of amide proton resonances of **3**, **Zn-3** and **5** at about $\delta = 9.20$ ppm in $CDCl_3$ indicates the successful formation of the amide bonds. For tweezers **6** two amide proton resonances were found in d$_8$-THF at about $\delta = 9.75$ ppm for the FcNH amide proton and between $\delta = 10.21 – 10.42$ ppm for the P^{Ar}NH amide proton suggesting NH$^{\cdots}$O hydrogen bonds to the THF solvent. Interestingly, all tweezers **6** display only a single amide resonance in $CDCl_3$ at $\delta > 9$ ppm indicating that only one NH group forms hydrogen bonds while the second NH group is not involved in hydrogen bonding. This finding suggests that an intramolecular hydrogen bond (IHB) across the ferrocene moiety might be present in $CDCl_3$ solution. Such IHBs have been frequently observed in 1,1'-disubstituted ferrocenes with amide arms in weakly coordinating solvents.[5] IR spectra of **Zn-6b** were measured in CH_2Cl_2 solution and indeed two NH absorption bands were found at 3430 and 3299 cm^{-1} clearly indicating the simultaneous presence of free and hydrogen bonded NH groups, respectively. The intramolecular nature of the hydrogen bond is shown by diluting the sample while retaining the NH$_{free}$: NH$_{bonded}$ ratio (Figure 1a). An optimised

DFT model of **Zn-6b** (B3LYP, LANL2DZ, IEFPCM CH_2Cl_2) is displayed in Figure 1b illustrating the proposed NH···O IHB. This IHB type with an 8-membered ring is the most stable one according to literature precedence for other amide substituents at the 1,1'-disubstituted ferrocene.[5] The IHB results in a V-shape of the tweezers (Figure 1b).

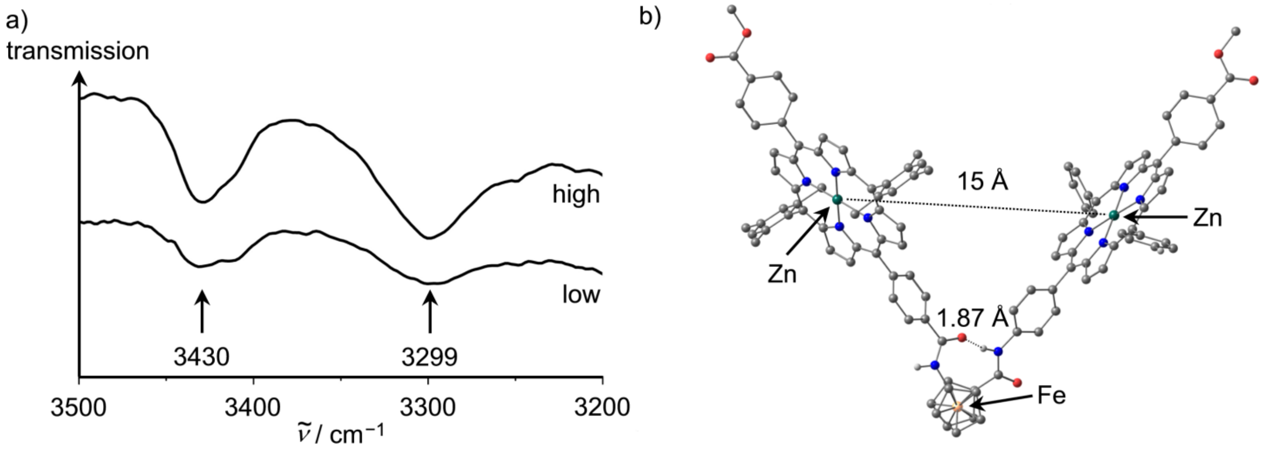

Figure 1. a) IR spectra of **Zn-6b** at high and low concentrations in CH_2Cl_2 at room temperature; b)B3LYP/LANL2DZ, IEFPCM calculated V-shape structure of **Zn-6b** featuring an NH···O IHB (CH hydrogen atoms omitted for clarity).

All cyclic voltammograms of dyads **3**, **Zn-3** and **5** exhibit two reversible oxidation and two reversible reduction processes of the porphyrin moieties and a reversible wave for the ferrocene/ferrocenium couple. For instance, Figure 2 depicts the cyclic voltammograms of **3a** and **Zn-3a** and of their corresponding ferrocene-free reference porphyrins **1a** and **Zn-1a**. Hence, the Fc-P conjugates **3**, **Zn-3** and **5** can store and release up to five electrons. With increasing electron withdrawing power of the *meso*-aryl substituents Ar an anodic shift of the porphyrin redox potentials was detected for **3**, **5** and **Zn-3** as expected (Table 1).[1f,10] The ferrocene/ferrocenium wave in **3** and **Zn-3** was detected at $E_{½} \approx -0.09$ V, whereas the oxidation of the ferrocene amino acid building block in **5** is shifted by ≈230 mV to $E_{½}$ = 0.13 – 0.14 V, as expected from the additional carbonyl substituent at the ferrocene hinge (Figure 2a/b).[5b]

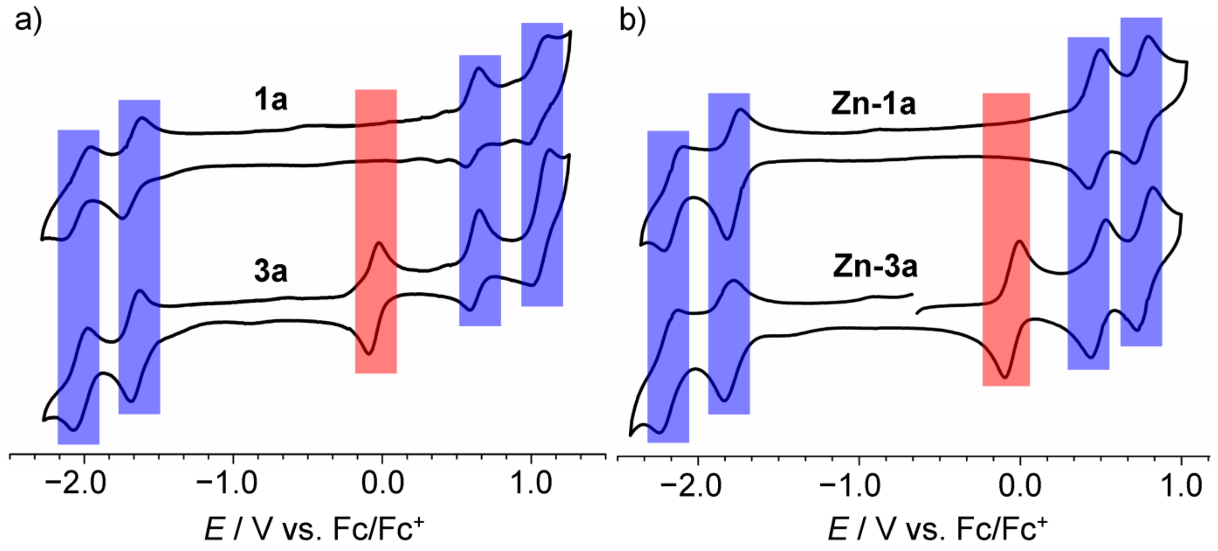

Figure 2. Cyclic voltammograms of **3a** and **Zn-3a** and reference porphyrins **1a** and **Zn-1a** in (nBu$_4$N)(PF$_6$)/CH$_2$Cl$_2$.

Table 1. Redox potentials [V] of **3**, **Zn-3**, **5**, **6** and **Zn-6** *vs.* Fc/Fc$^+$ in (nBu$_4$N)(PF$_6$)/CH$_2$Cl$_2$ at room temperature.

	Ar	$E_{½}$(P, ox^3)	$E_{½}$(P, ox^2)	$E_{½}$(P, ox^1)	$E_{½}$(Fc, ox)	$E_{½}$(P, red^1)	$E_{½}$(P, red^2)
3a	Mes	–	1.040	0.590	−0.090	−1.690	−2.060
3e	C_6F_5	–	n.o.	0.890	−0.090	−1.430	−1.820
Zn-3a	Mes	–	0.730	0.440	−0.090	−1.830	−2.230
Zn-3e	C_6F_5	–	0.920	0.680	−0.100	−1.570	−1.980
5b	C_6H_5	–	0.890	0.580	0.140	−1.610	−1.980
5c	4-C_6H_4F	–	0.880	0.590	0.130	−1.620	−1.960
5d	4-$C_6H_4CF_3$	–	0.940	0.660	0.140	−1.570	−1.900
5e	C_6F_5	–	1.050	0.820	0.130	−1.400	−1.820
6b	C_6H_5	1.070[a]	0.880	0.600 (2e)	0.160	−1.640 (2e)	−2.000
6c	4-C_6H_4F	1.080[a]	0.880	0.610 (2e)	0.150	−1.630 (2e)	−1.960
Zn-6b	C_6H_5	–	0.740 (2e)	0.420 (2e)	0.160	−1.830	n.o.[b]
Zn-6c	4-C_6H_4F	–	0.730 (2e)	0.400 (2e)	0.150	−1.910	n.o.[b]

[a] Only clearly observed in the square-wave voltammogram. [b] n.o.: not observed.

In tweezers **6** and **Zn-6** the redox waves of both porphyrins and the ferrocene unit ($E_{½}$ = 0.15 – 0.16 V) are superimposed (Table 1). In all cases reversible two-electron waves are observed for the first oxidations of the porphyrins. Zinc porphyrins **Zn-6** show a further 2e oxidation wave while in free-base bis(porpyhrins) **6** this wave is split into two 1e waves. In the reductive region free-base conjugates **6** show a 2e and a further 1e wave while **Zn-6** feature only a single 1e reduction under our conditions. The Fc/Fc$^+$ potential remains essentially unaffected by appending the second porphyrinto **5**. *Vice versa* the influence of ferrocene moiety on the porphyrin's redox features is marginal.[1f] In essence the redox properties are essentially described by the properties of the individual building blocks and the electronic interaction in the ground state between the building blocks in dyads and tweezers is considered as very weak. This is exemplified in Figure 3 with the cyclic voltammograms of **5c** and **6c** and of their corresponding ferrocene-free reference porphyrins **1a** and **Ac-4c**. Bis(porphyrins) **6** and **Zn-6** can store / release up to eight and six electrons, respectively ($[\mathbf{6}]^{3-}$···$[\mathbf{6}]^{5+}$; $[\mathbf{Zn\text{-}6}]^{-}$···$[\mathbf{Zn\text{-}6}]^{5+}$) and hence, these polyamides can be considered as multi-electron stores.

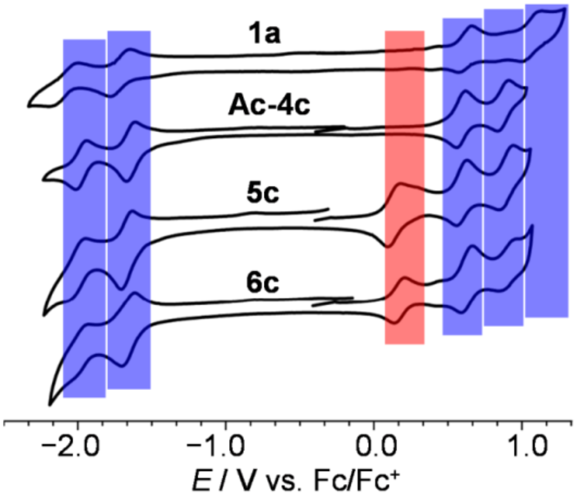

Figure 3. Cyclic voltammograms of **5c** and **6c** and reference porphyrins **1a** and **Ac-4c** in (nBu$_4$N)(PF$_6$)/CH$_2$Cl$_2$.

The electronic absorption spectra of **3**, **Zn-3**, **5**, **6** and **Zn-6** are essentially superpositions of the electronic transitions of the porphyrin constituents (Table 2). Figure 4 shows the absorption spectra of selected compounds and their references. Fully analogous observations were made previously concerning the absorption data of amide-linked porphyrins[10] and of anthraquinone-porphyrin-ferrocene triads.[1f] The characteristic absorption bands of the ferrocene moieties are not detectable in the absorption spectra of dyads and tweezers because of the much lower absorptivity of acetylamino ferrocene (λ_{max} = 441 nm, ε = 215 M^{-1}cm^{-1})[5a] and 1-(acetylamino)-ferrocene-1'-carboxylic acid (λ_{max} = 441 nm, ε = 350 M^{-1}cm^{-1})[5a] as compared to porphyrins (ε = 4×10^5 – 10×10^5 M^{-1}cm^{-1}). A comparison of absorption spectra of dyads and tweezers with those of corresponding reference porphyrins indicates neither new bands nor appreciable shifts of porphyrin bands and thus a very weak electronic interaction between the chromophores in the ground state.[1f,10]

Table 2. Absorption data of **3**, **5**, **6** and **Zn-6** in CH_2Cl_2 at room temperature.

	Ar	Soret λ_{max} / nm (ε /$M^{-1}cm^{-1}$)	$Q_y(1,0)$ λ_{max} / nm (ε / $10^4M^{-1}cm^{-1}$)	$Q_y(0,0)$ λ_{max} / nm (ε / $10^4M^{-1}cm^{-1}$)	$Q_x(1,0)$ λ_{max} / nm (ε / $10^4M^{-1}cm^{-1}$)	$Q_x(0,0)$ λ_{max} / nm (ε / $10^4M^{-1}cm^{-1}$)
3a	Mes	420 (44.69)	516 (1.77)	550 (0.79)	591 (0.61)	647 (0.57)
3e	C_6F_5	416 (33.50)	511 (1.69)	544 (0.30)	587 (0.42)	642 (0.54)
Zn-3a	Mes	424 (30.18)	552 (1.03)	594 (0.38)	–	–
Zn-3e	C_6F_5	421 (50.07)	552 (2.65)	583 (1.03)	–	–
5b	C_6H_5	420 (38.93)	516 (1.68)	552 (0.88)	591 (0.53)	647 (0.43)
5c	4-C_6H_4F	420 (39.89)	516 (1.56)	552 (0.97)	591 (0.56)	647 (0.46)
5d	4-$C_6H_4CF_3$	420 (29.14)	516 (1.46)	551 (0.77)	592 (0.51)	649 (0.43)
5e	C_6F_5	417 (66.61)	512 (4.26)	546 (1.37)	588 (1.45)	643 (0.73)
6b	C_6H_5	419 (78.60)	516 (3.99)	551 (2.09)	592 (1.30)	650 (1.46)
6c	4-C_6H_4F	420 (53.00)	516 (2.83)	552 (1.44)	591 (0.94)	647 (0.97)
Zn-6b	C_6H_5	422 (109.44)	551 (5.48)	593 (1.62)	–	–
Zn-6c	4-C_6H_4F	420 (82.95)	549 (5.68)	588 (2.81)	–	–

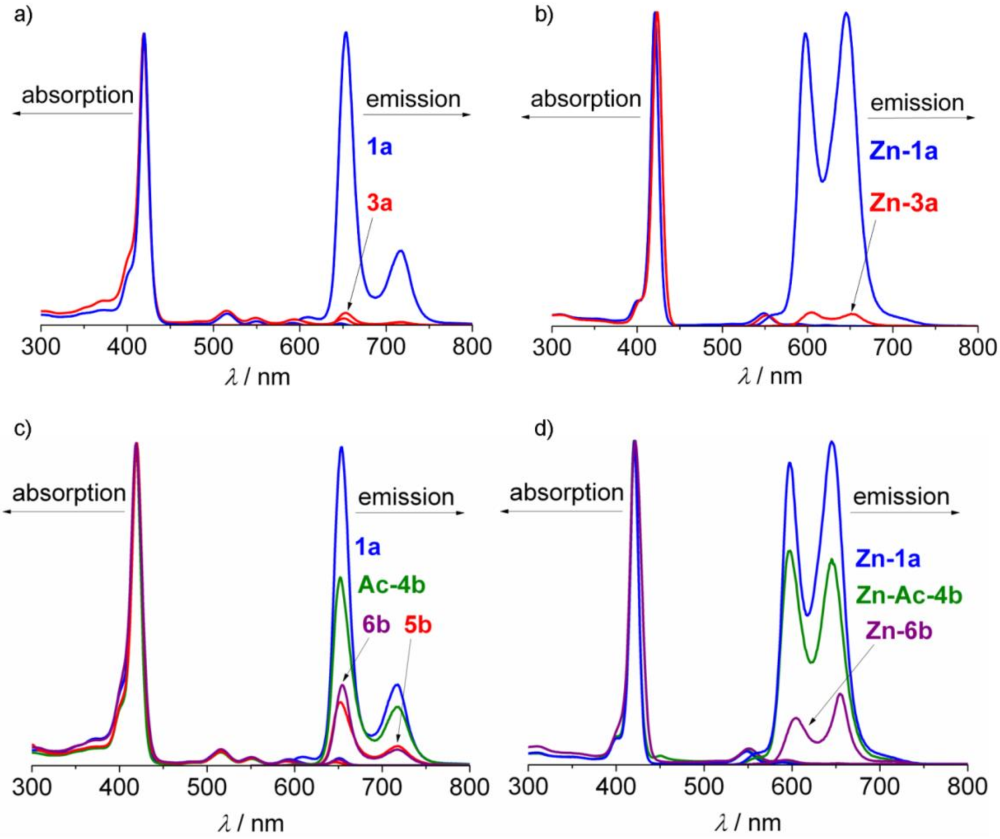

Figure 4. Normalised absorption and emission spectra of a) **1a**, **3a**, b) **Zn-1a**, **Zn-3a**, c) **1a**, **Ac-4b**, **5b**, **6b** d) **Zn-1a**, **Zn-Ac-4b**, **Zn-6b** in CH_2Cl_2 at room temperature.

Emission spectral data of dyads and tweezers are summarised in Table 3. The typical porphyrin fluorescence is strongly quenched in ferrocene porphyrins **3**, **Zn-3**, **5**, **6** and **Zn-6** relative to the respective reference compounds (Figure 4). Thus, the presence of ferrocene opens up new non-radiative pathways for the first excited singlet state (S_1) decay of the porphyrins. Particularly, electron transfer from ferrocene to porphyrin should account for this observation but also energy transfer to ferrocene[4e,12] is feasible. Notably, the most efficient fluorescence quenching in the series **3**, **Zn-3** and **5** was observed in dyads **3e**, **Zn-3e** and **5e** with the strongly electron withdrawing C_6F_5 substituent, while the weakest decrease of fluorescence intensity was detected in dyads with less electron withdrawing substituents Mes, 4-C_6H_4F and C_6H_5 (Table 3). Similarly, the lower Fc/Fc$^+$ potential of **3e** ($E_{½}$ = –0.09 V) compared to **5e** ($E_{½}$ = +0.13 V) results in a stronger fluorescence quenching in **3e** (Φ = 0.0014) than in **5e** (Φ = 0.0094). These electronic influences already clearly point to a significant contribution of the reductive PET pathway to the excited state decay.

Table 3. Emission data of **3**, **Zn-3**, **5**, **6** and **Zn-6** in CH_2Cl_2 at room temperature.

	Ar	Q(0,0) / nm	Q(0,1) / nm	Φ	τ / ns (A_1 / %); τ / ns (A_2 / %) [a]	quenching / % [b]	k_{ET} / $10^9 s^{-1}$ [c][d]	Φ_{ET} [e][f]
3a	Mes	653	717	0.0122	0.201 (80%); 3.52 (20%)	84	4.87	98
3e	C_6F_5	646	714	0.0014	0.022 (91%); 2.00 (9%)	97	45.36	100
Zn-3a	Mes	605	651	0.0096	0.139 (82%); 1.56 (18%)	90	6.80	95
Zn-3e	C_6F_5	598	649	0.0006	0.013 (84%); 1.11 (16%)	99	76.41	99
5b	C_6H_5	652	717	0.0416	2.00 (75%); 5.97 (25%)	64	0.40	80
5c	4-C_6H_4F	652	717	0.0449	2.05 (76%); 5.48 (24%)	55	0.39	80
5d	4-$C_6H_4CF_3$	655	716	0.0255	1.87 (100%)	76	0.43	80
5e	C_6F_5	649	716	0.0094	0.332 (72%); 1.49 (28%)	87	2.91	97
6b	C_6H_5	654	717	0.0475	3.17 (100%)	59[g]; 37[h]	0.43; 0.42	82; 80
6c	4-C_6H_4F	655	718	0.0451	3.07 (100%)	55[i]; 42[h]	0.23; 0.22	71; 68
Zn-6b	C_6H_5	603	655	0.0198	0.63 (84%); 1.87 (16%)	81[j]; 81[k]	1.08; 1.19	68; 75
Zn-6c	4-C_6H_4F	597	653	0.0203	0.74 (73%); 3.23 (27%)	64[l]; 80[k]	0.87; 0.95	64; 70

[a] The relative amplitudes A were calculated from fitting the data by the equations $Y = A_1 e^{-k/\tau 1} + A_2 e^{-k/\tau 2}$ and $A_1 + A_2 = 100\%$. [b] Φ_{ref} = 0.0774 (**1a**), 0.1001 (**Zn-1a**), 0.0520 (**1e**), 0.0788 (**Zn-1e**), 0.1003 (**Ac-4c**), 0.0569 (**Zn-Ac-4c**), 0.1167 (**Ac-4b**), 0.1037 (**Zn-Ac-4b**), 0.1080 (**Ac-4d**), 0.0696 (**Ac-4e**).[10] [c] $k_{ET} = 1/\tau - 1/\tau_{ref}$. [d] τ_{ref} / ns = 9.87 (**1a**), 2.53 (**Zn-1a**), 10.05 (**1b**), 1.95 (**Zn-1b**), 9.88 (**4b**), 1.99 (**Ac-Zn-4b**), 9.98 (**Ac-4c**), 2.07 (**Ac-Zn-4c**), 9.64 (**Ac-4d**), 9.83 (**Ac-4e**).[10] [e] $\Phi_{ET} = k_{ET}\tau$. [f] For calculating Φ_{ET} τ_1 with the largest amplitude was used. [g] Relative to **Ac-4b**. [h] Relative to **1a**. [i] Relative to **Ac-4c**. [j] Relative to **Zn-Ac-4b**. [k] Relative to **Zn-1a**. [l] Relative to **Zn-Ac-4c**.

Linkage of the second porphyrin unit to dyads **5b** and **5c** leads to no significant change of fluorescence quantum yield in **6b** and **6c** (Table 3). Both porphyrin components in **6b** and **6c** feature similar extinction coefficients at the excitation wavelength resulting in essentially equal excitation probability. The reduction potentials of the different porphyrins in the tweezers **6b** and **6c** (references **1a**/**Ac-4b**; **1a**/**Ac-4c**) are rather similar and hence a similar PET rate to both excited porphyrins might be expected. Complexation of tweezers **6** with zinc(II) leads to a further reduction of the porphyrin fluorescence quantum yield in **Zn-6** by enhancing the intersystem crossing (ISC) rate to the porphyrin triplet state T_1(P).

To substantiate that the emission quenching essentially results from PET rather than from energy transfer to ferrocene, low temperature fluorescence spectra for **1e**, **3e**, **Zn-1e** and **Zn-3e** were measured (Figure 5). Cooling 2-methyltetrahydrofuran solutions of references **1e** and **Zn-1e** to 77 K result in small increases of the integrated fluorescence intensity by factors of 1.83 and 1.29. On the other hand the ferrocene dyads **3e** and **Zn-3e** enjoy a fluorescence increase by factors of 2.88 and 3.38, respectively. Upon cooling the corresponding absorption bands of **1e** and **3e** sharpen and the Soret bands increase by a factor of 1.7 in both cases (see the Supporting Information). Hence, one part of the fluorescence increase is due to the increase of absorptivity (**1e**, **3e**) while for the ferrocenyl porphyrin **3e** an additional process is present. These results support an activated process in ferrocenyl porphyrins such as electron transfer requiring inner and outer sphere reorganization energy[13] as major decay path for the porphyrin S_1 states in addition to fluorescence, internal conversion (IC) to the ground state, ISC to the T_1(P) state promoted by the heavy atom effect and energy transfer to give the ferrocene triplet state T_1(Fc).[4e,12]

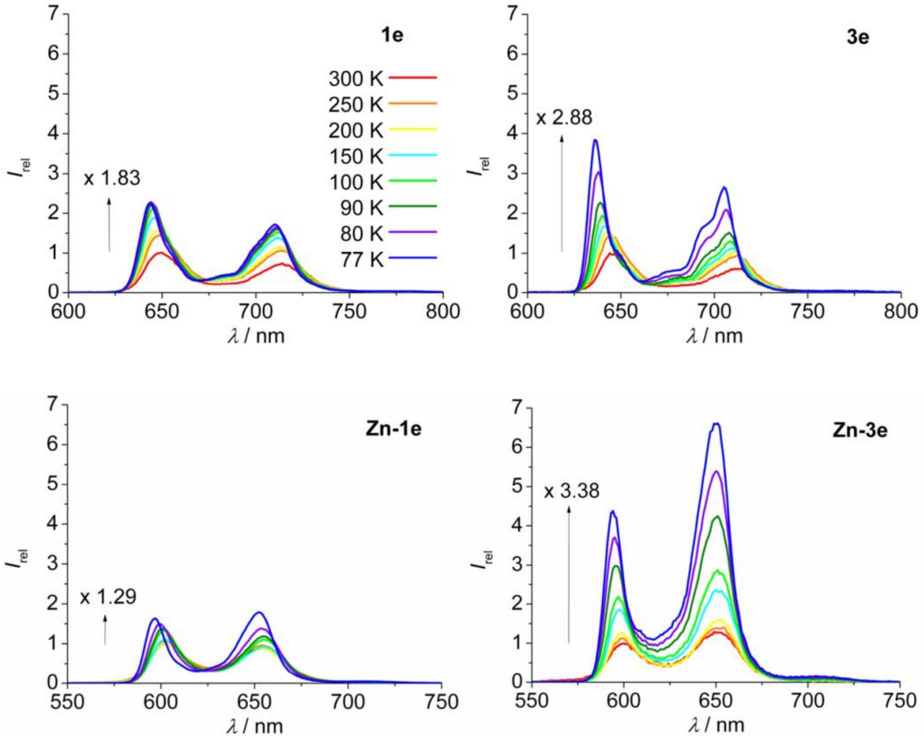

Figure 5. Normalised emission spectra of **1e**, **3e**, **Zn-1e** and **Zn-3e** in 2-methyltetrahydrofuran at T = 300 → 77 K (λ_{exc} = 420 nm)

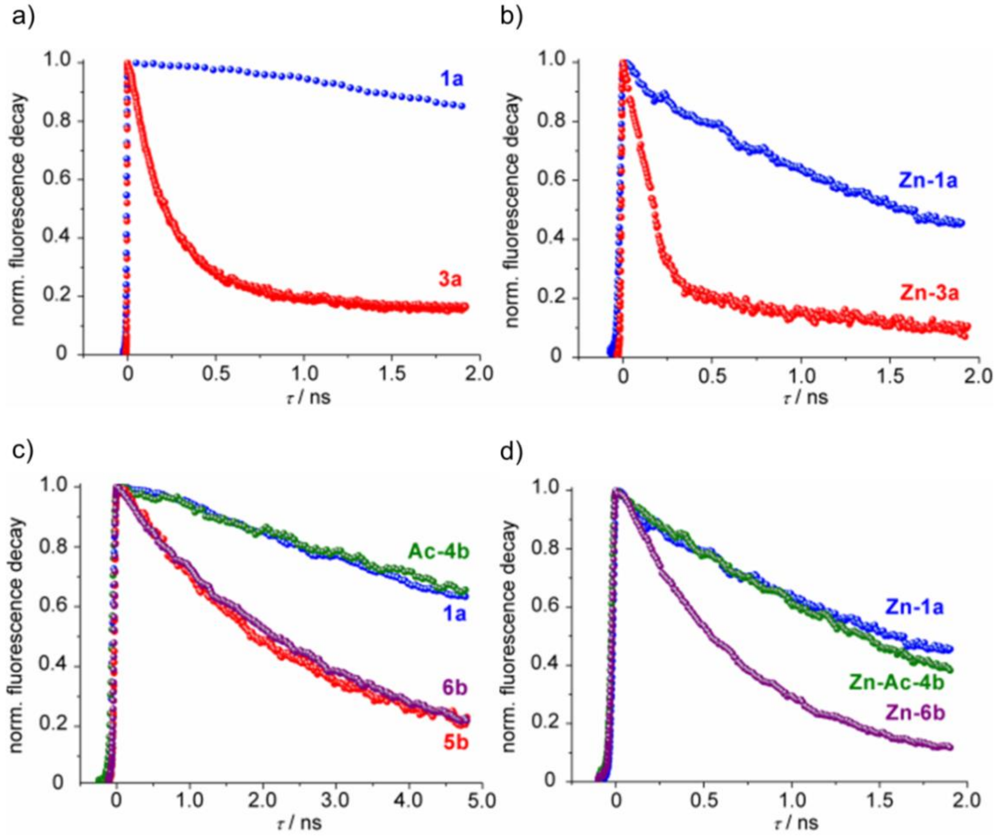

Figure 6. Fluorescence decay profiles of a) **1a, 3a**, b) **Zn-1a**, **Zn-3a**, c) **1a**, **Ac-4b**, **5b**, **6b**, d) **Zn-1a**, **Zn-Ac-4b**, **Zn-6b** in CH_2Cl_2 (λ_{exc} = 400 and 550 nm).

The results of fluorescence lifetime measurements in CH_2Cl_2 are summarised in Table 3 and representative decay profiles of dyads and tweezers are displayed in Figure 6. Dyad **5d** features a monoexponential decay, while all decays of dyads **3** and **5** were best fitted by biexponential rate laws (Figure 4). We assign the major component (τ_1, A_1) to the PET pathway, while the minor component (τ_2, A_2) is probably caused by ISC to $T_1(P)$ or energy transfer to generate $T_1(Fc)$[4e, 12] (*vide supra*). All lifetimes τ_1 are significantly reduced as compared to reference compounds. Similar to the quantum yields Φ the lifetimes τ_1 clearly depend on the electron withdrawing power of the porphyrin substituents Ar (Table 3, *e.g.* **3a** / **3e**; **Zn-3a** / **Zn-3e**; **5b** / **5e**) and the Fc/Fc^+ potential in **3e** (τ_1 = 0.022 ns) and **5e** (τ_1 = 0.332 ns).[1f]

Depending on the initial excitation at either the *N*-terminal mesityl or *C*-terminal aryl-substituted porphyrin (Ar = 4-C_6H_5, 4-C_6H_4F: **6b**, **6c**) the reductive PET in **6** and **Zn-6** can occur from the central ferrocene to the *N*- or to the *C*-terminus. In free-base tweezers **6** the decays are monoexponential with lifetimes around τ = 3 ns. This fact suggests that both PET paths $P^{Mes}\leftarrow Fc$ / $Fc\rightarrow P^{C6H5F}$ (**6d**) and $P^{Mes}\leftarrow Fc$ / $Fc\rightarrow P^{C6H4F}$ (**6d**) are conceivable with nearly the same rates or rapid singlet-singlet energy transfer between the porphyrins before ET (Table 3). Both are consistent with the quantum yields of **5b**/**6b** and **5c**/**6c** (Table 3). The zincated tweezers **Zn-6** feature biexponential decays. The dominant component (τ_1 = 0.63 ns for **Zn-6b** and τ_1 = 0.74 ns for **Zn-6c**) is again assigned to reductive PET to the *N*- and *C*-terminal porphyrins and the minor one (τ_2) is due to ISC giving the porphyrin triplet state $T_1(P)$ or energy transfer to give the ferrocene triplet state $T_1(Fc)$. From the lifetimes τ the rate constants for the electron transfer k_{ET} and quantum efficiencies Φ_{ET} were estimated (Table 3). To correlate the rates with thermodynamic driving forces the energies of the $P^{\cdot-}$-$Fc^{\cdot+}$ and *N*-Fmoc-$Fc^{\cdot+}$-$P^{\cdot-}$ charge-separated (CS) states were estimated from the oxidation potential of the ferrocene $E_{½}(\text{Fc,ox})$ and the first reduction potential of the porphyrin moiety $E_{½}(\text{P,red}^1)$ including the Coulomb term $e_0^2/(4\pi\varepsilon_0\varepsilon(CH_2Cl_2)r_{AD})$. The energies of the porphyrin S_1 excited states $E(S_0 \rightarrow S_1)$ were estimated as the average value of the $Q_x(0,0)$ absorption and Q(0,0) emission bands (Tables 2 and 3). The thermodynamic driving forces ΔG_{ET} were then estimated according to the Rehm-Weller equation[14] $\Delta G_{ET} = E_{½}(\text{Fc,ox}) - E_{½}(\text{P,red}^1) - e_0^2/(4\pi\varepsilon_0\varepsilon(CH_2Cl_2)r_{AD}) - E(S_0 \rightarrow S_1)$ with $\varepsilon_0 = 8.85519 \times 10^{-12}$ Fm^{-1}; $\varepsilon(CH_2Cl_2) = 8.93$; r_{AD} = 13.0 Å for **3a**, **3e**, **Zn-3a**, **Zn-3e**, **5e** and r_{AD} = 12.9 Å for **5b** – **5d** (Table 4). The Coulomb terms in CH_2Cl_2 are 0.124 eV for **3a**, **3e**, **Zn-3a**, **Zn-3e**, **5e** and 0.125 eV for **5b** – **5d**. The centre-to-centre distances (r_{AD}) were obtained from geometry optimised DFT models (*vide supra*). With $\Delta G_{ET} \approx 0.27 - 0.72$ eV the PET in the dyads occurs in the normal Marcus region.[15] As expected from Marcus theory the electron transfer rate increases with increasing driving force in dyads **3** and **5** (Tables 3 and 4, Figures 7 and 8).

Table 4. Energies [eV] of porphyrin S_1 and CS states for **3**, **Zn-3**, **5**, **6** and **Zn-6** and driving forces ΔG_{ET}.

	Ar	$E(S_0 \rightarrow S_1)$	$E(P^{\cdot-}\text{-}Fc^{\cdot+})$ or $(P^{Mes.-}\text{-}Fc^{\cdot+}\text{-}P^{Ar})$ / $(P^{Mes}\text{-}Fc^{\cdot+}\text{-}P^{Ar.-})$	$\Delta G_{ET}(P^{\cdot-}\text{-}Fc^{\cdot+})$ or $(P_{Mes}{}^{\cdot-}\text{-}Fc^{\cdot+}\text{-}P^{Ar})$ / $(P_{Mes}\text{-}Fc^{\cdot+}\text{-}P_2{}^{\cdot-})$
3a	Mes	1.90	1.48	−0.42
3e	C_6F_5	1.92	1.22	−0.70
Zn-3a	Mes	2.05	1.62	−0.43
Zn-3e	C_6F_5	2.07	1.35	−0.72
5b	C_6H_5	1.90	1.63	−0.27
5c	4-C_6H_4F	1.90	1.63	−0.27
5d	4-$C_6H_4CF_3$	1.90	1.59	−0.31
5e	C_6F_5	1.91	1.41	−0.50
6b	C_6H_5	1.90	1.68	−0.22
6c	4-C_6H_4F	1.89	1.66	−0.23
Zn-6b	C_6H_5	2.05	1.82[a] / 1.79[b]	−0.23 / −0.26
Zn-6c	4-C_6H_4F	2.08	1.81[a] / 1.78[b]	−0.27 / −0.30

[a] Calculated with the first reduction potential of **Zn-1a** $E_{½}(\text{P,red}^1) = -1.78$ V. [b] Calculated with the first reduction potential $E_{½}(\text{P,red}^1) = -1.75$ V of **Zn-Ac-4b** and **Zn-Ac-4c**.[10]

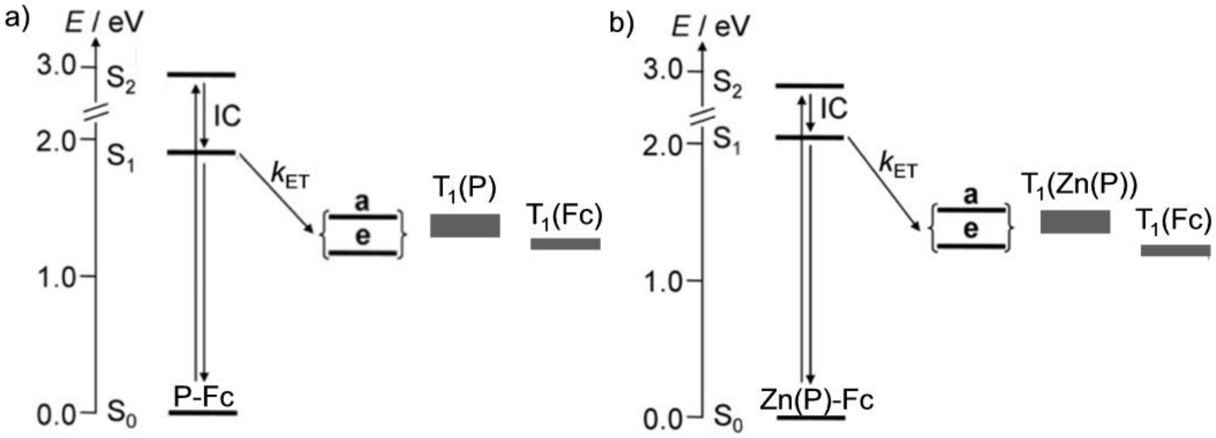

Figure 7. Energy level diagrams of a) **3a**/**3e** and b) **Zn-3a**/**Zn-3e** with the estimated porphyrin triplet state $T_1(P)$ at ca. 1.43 eV[16], the zinc porphyrin triplet state $T_1(Zn(P))$ at ca. 1.53 eV[17] and the ferrocene triplet state $T_1(Fc)$ at ca. 1.16 eV[12]. The energies of triplet states certainly vary with the substituents, as is qualitatively reflected in the diagram by the thicker energy level bars of the triplet states.

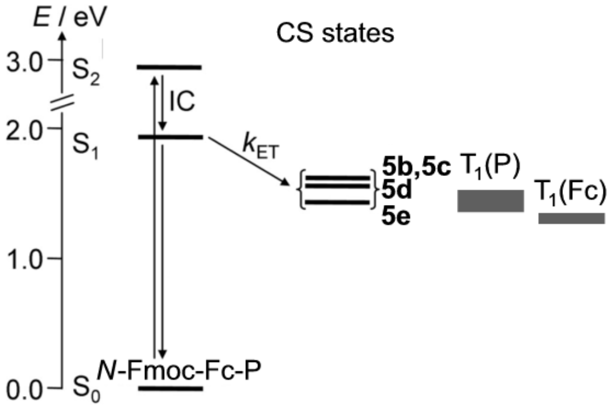

Figure 8. Energy level diagram of **5b** – **5e** with the estimated porphyrin triplet state $T_1(P)$ at ca. 1.43 eV[15] and the ferrocene triplet state $T_1(Fc)$ at ca. 1.16 eV[12]. The energies of triplet states certainly vary with the substituents, as is qualitatively reflected in the diagram by the thicker energy level bars of the triplet states.

The ferrocene-porphyrin centre-to-centre distances in tweezers **6** and **Zn-6** are around $r_{\mathrm{D\text{-}A}}$ = 13.0 Å and the Coulomb term in CH_2Cl_2 is estimated as 0.124 eV. As the first reduction potentials of the different porphyrins in **Zn-6** are not individually resolved in the cyclic voltammograms the energies of the CS states of **Zn-6** were estimated from the first reduction potentials of suitable reference porphyrins **Zn-1a**[10], **Zn-Ac-4b**[1f] and **Zn-Ac-4c**[10]. The estimated energies for *N*- and *C*-terminal CS states of tweezers $\mathrm{M(P^{Mes.-})\text{-}Fc^{\cdot+}\text{-}M(P^{Ar})}$ and $\mathrm{M(P^{Mes})\text{-}Fc^{\cdot+}\text{-}M(P^{Ar.-})}$ (M = 2H, Zn) and the driving forces ΔG_{ET} estimated using the Rehm-Weller equation[14] are essentially identical as expected from the similar optical and redox properties of the constituent porphyrins (Table 4 and Figure 9).

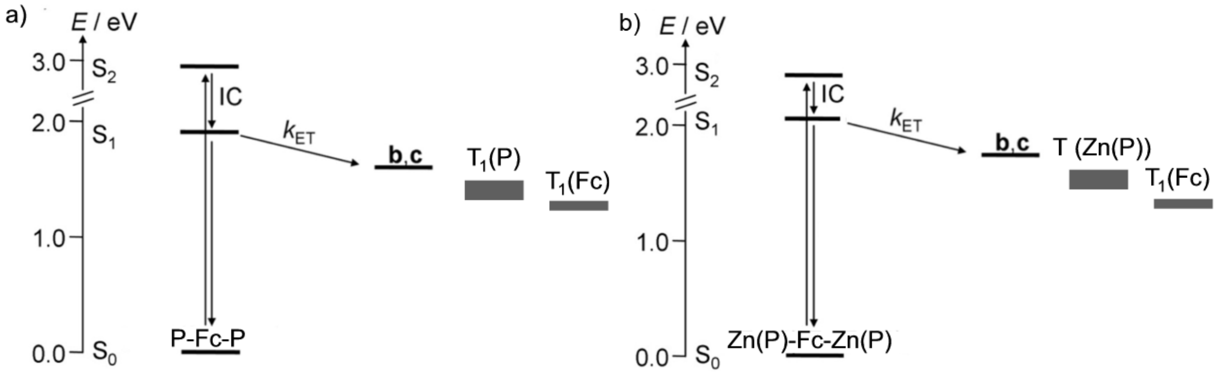

Figure 9. Energy level diagrams of a) **6b**/**6c** and b) **Zn-6b**/**Zn-6c** with the estimated porphyrin triplet state T_1(P) at ca. 1.43 eV[16], the zinc porphyrin triplet state T_1(Zn(P)) at ca. 1.53 eV[17] and the ferrocene triplet state T_1(Fc) at ca. 1.16 eV[12]. The energies of triplet states certainly vary with the substituents, as is qualitatively reflected in the diagram by the thicker energy level bars of the triplet states.

The geometric and electronic structure of the amide-linked dyads and tweezers were studied using DFT (B3LYP, LANL2DZ, IEFPCM CH_2Cl_2)[18] approaches. Although approximate exchange-correlation potentials might not yield orbital energies compatible with the experiment orbital symmetry and the trends imposed by electronic substituent effects will be correctly reproduced. Hence, no attempts to optimize the amount of Hartree-Fock exchange for a better agreement with experiments are pursued and the orbital energies given (especially the relative position of the Fc orbitals with respect to the porphyrin orbitals) shall only be used as a rough guide. Figure 10 shows the typical four Gouterman frontier molecular orbitals of porphyrins[19] and the highest occupied ferrocene based nearly degenerate δ orbitals (d_{xy}, d_{x2-y2}) for dyads **3a** and **3e**. As typically observed the strongly electron withdrawing C_6F_5 substituents lead to a local LUMO orbital inversion with the porphyrin LUMO in **3a** featuring large orbital coefficients at the linking *meso* carbon positions, while in **3e** nodes are observed at the linking *meso* carbon positions.[1f,19,20] The porphyrin HOMOs are located below the ferrocene HOMOs in **3e** while one porphyrin HOMO is found above the ferrocene HOMOs in **3a**. The same picture was observed for zincated dyads **Zn-3a** und **Zn-3e** (see the Supporting Information). In the series **5a** – **5e** the increasing electron withdrawing power of the porphyrin substituents lowers the energy of the porphyrin frontier orbitals (Figure 11) while the ferrocene orbitals remain invariant in energy as expected from the invariant Fc/Fc$^+$ redox potentials (Table 1). Note that the Fc δ orbital energies of **5** are below those of **3**/**Zn-3** due to the electron withdrawing CO substituent at ferrocene consistent with the different Fc/Fc$^+$ redox potentials of **5** and **3**/**Zn-3** (Table 1).

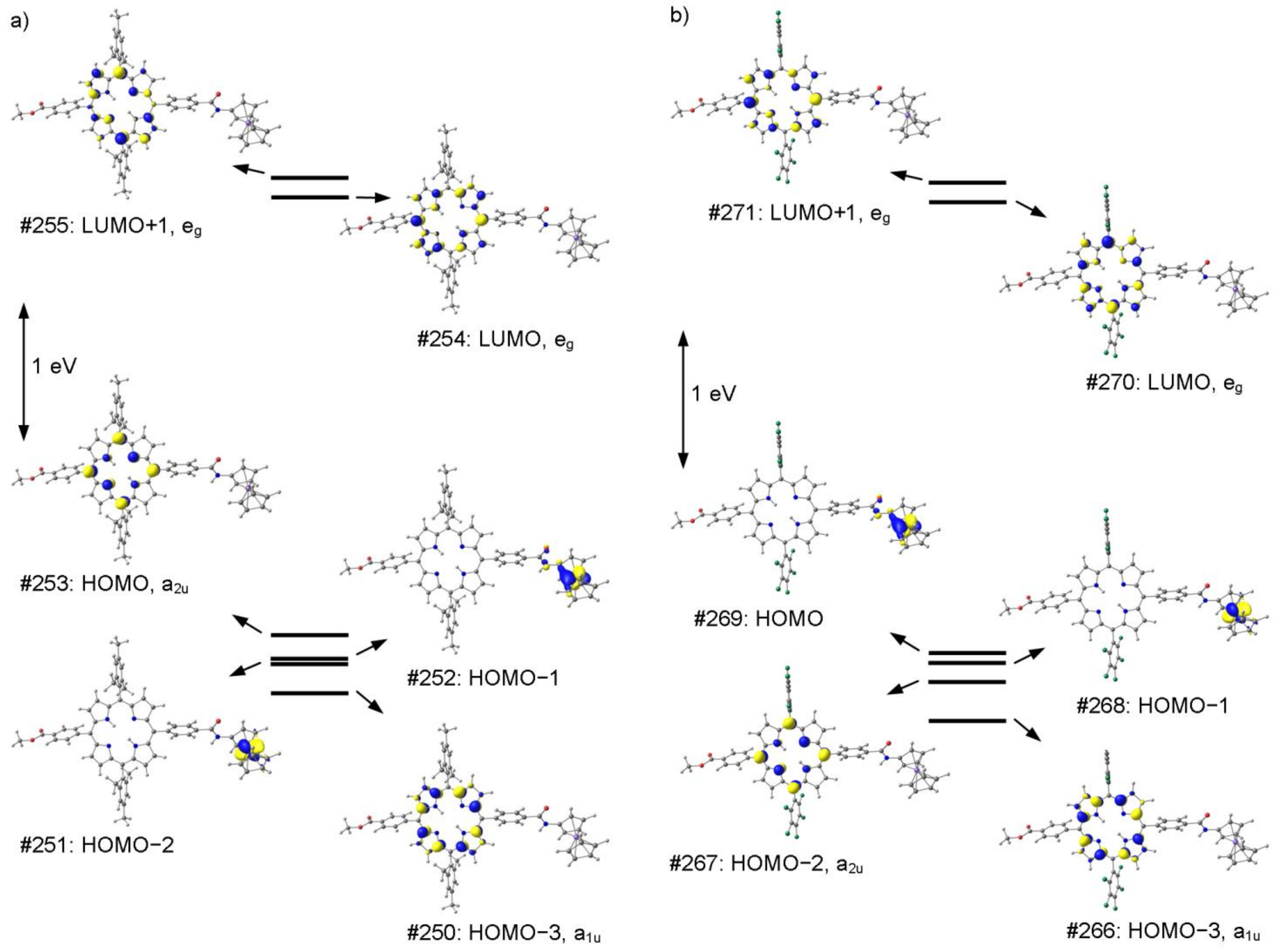

Figure 10. B3LYP/LANL2DZ, IEFPCM calculated frontier orbitals of a) **3a** and b) **3e** (isosurface value 0.05 a.u.).

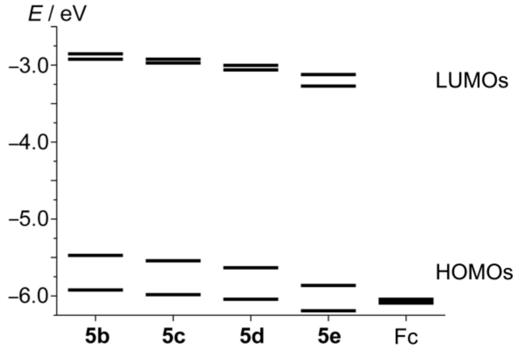

Figure 11. B3LYP/LANL2DZ, IEFPCM calculated molecular orbital energy diagram of dyads **5b** – **5e**. The LUMOs of ferrocene are outside the window shown.

Representatively for all tweezers **6** and **Zn-6** Figure 12 depicts the calculated frontier orbitals of **6b** consisting of a twin set of four Gouterman orbitals[19] and two occupied ferrocene δ orbitals (d_{xy},

d_{x2-y2}). The local porphyrin HOMOs and LUMOs as well as ferrocene δ orbitals are essentially pairwise degenerate (Figure 12). The accidental degeneracy of porphyrin frontier orbitals is caused primarily by cancellation of substituent effects at the different porphyrins (Mes / C_6H_4CONHR *vs.* C_6H_5 / C_6H_4NHCOR or C_6H_4F / C_6H_4NHCOR). In the tweezers the porphyrin local LUMOs feature non-zero orbital coefficients at the *meso* carbon bridging atoms. The porphyrin local HOMOs possess a_{2u} symmetry with large orbital coefficients at the *meso* carbon bridging atoms. This symmetry allows for both reductive PET pathways generating the *N*-terminal $P^{Mes\cdot-}$-$Fc^{\cdot+}$-P^{Ar} or *C*-terminal P^{Mes}-$Fc^{\cdot+}$-$P^{Ar\cdot-}$ charge-separated state depending on the initial local excitation of the *N*-terminal or *C*-terminal porphyrin.

Furthermore, besides the extended tweezers structure as shown in Figure 12 a hydrogen-bonded V-shaped conformer is conceivable for **6** and **Zn-6** (Figure 1b).[5a-d] IR spectra suggested the presence of such V-shaped tweezers in solutions of non-coordinating solvents. In the V-shaped conformers a slight energy decrease of P^{Mes} and a slight energy increase of P^{Ar} frontier orbitals were calculated as expected for a NH···O hydrogen bond from the P^{Ar} porhyrin to the P^{Mes} porphyrin (see the Supporting Information). The hydrogen bond H···O distance amounts to 1.87 Å and the centre-to-centre distance of the porphyrins is calculated around 15 Å. This distance is too large to find evidence for a V-shape structure by optical absorption spectroscopy and indeed no shift of Soret and Q bands due to $\pi - \pi$ interactions between porphyrin macrocycles was observed. However, a through-space singlet-singlet energy transfer in V-shaped **6** and **Zn-6** by a Förster resonance energy transfer mechanism might well occur over this distance.[21] Concerning the emission energies the individual porphyrins in **6** and **Zn-6** are too similar to be distinguished. However, the relative intensities of the Q(0,0) and Q(0,1) emission bands are slightly different in respective reference compounds. With this phenomenological comparison the emission seems to be favoured from the mesityl-substituted porphyrin in all cases **6** and **Zn-6** discussed. This is clearly seen in Figure 4d with the band shape of **Zn-6b** resembling more the band shape of **Zn-1a** than that of **Zn-Ac-4b**. This interpretation also fits to findings obtained for analogous ferrocene-free amide-linked bis(porphyrins) P^{Mes}-P^{Ar}.[10] Further experimental verification of energy transfer between porphyrins within tweezers of type **6** and **Zn-6** must await the synthesis of analogous tweezers featuring more distinct porphyrins such as mixed free-base and metalated porphyrins as has also been unambiguously demonstrated in amide-linked bis(porphyrins).[10]

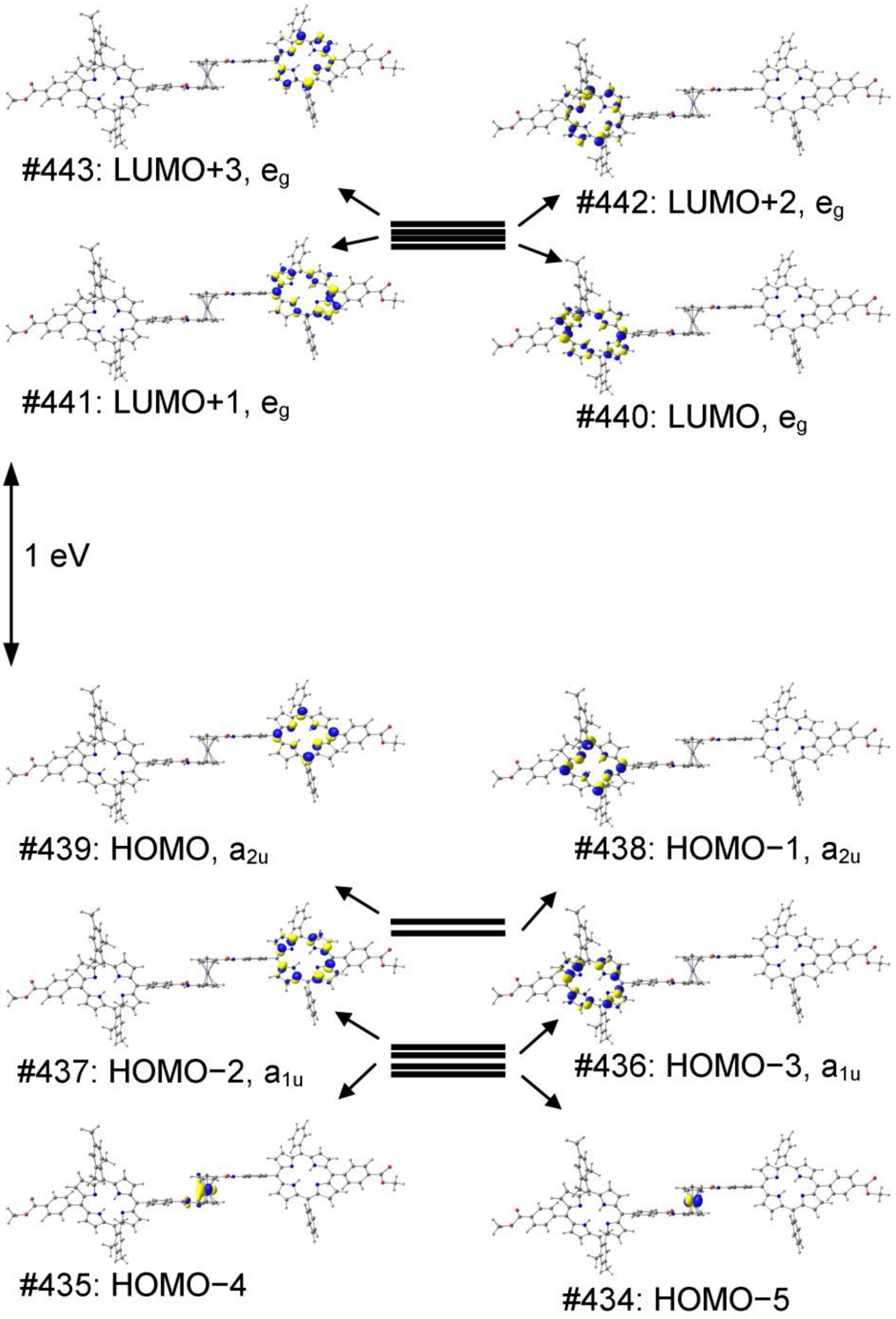

Figure 12. B3LYP/LANL2DZ, IEFPCM calculated frontier orbitals of **6b** (isosurface value 0.05 a.u.).

The proposed V-shape tweezers structure[22] prompted us to attempt to prepare host-guest complexes of **6b** and **Zn-6b** with 7,7,8,8-tetracyanoquinodimethane ($E_{½}$ = –0.30 V in CH_3CN[23]) and *N*-ethyl-anthraquinone-2-carboxylic amide ($E_{½}$ = –1.28 V in CH_2Cl_2[1f]) as electron acceptors. These acceptors could be bound by hydrogen-bonds in the ground state and could give rise to proton-coupled electron transfer in the excited state of the porphyrin.[24] Titration of the tweezers with more than 1000 equivalents of the putative electron acceptors in CH_2Cl_2 did not appreciably change the absorption and emission spectra. Hence, significant electron transfer of the excited porphyrins or the porphyrin radical anions (in the CS state) to the external acceptor is not observed. This might either be based on unfavourable sterical interactions between the potential host and guest or a too rapid excited state decay via ferrocene mediated channels (triplet formation).

Indeed, attempts to calculate $P^{\cdot -}$-$Fc^{\cdot +}$, $Zn(P^{\cdot -})$-$Fc^{\cdot +}$ and *N*-Fmoc-$Fc^{\cdot +}$-$P^{\cdot -}$ CS states by DFT methods lead to ferrocene triplet states as the lowest triplet state with the spin density localised on ferrocene moieties (see the Supporting Information). This fits to the estimated T_1(Fc) energy being similar to or even lower than the CS state energies (Figures 7 – 9).

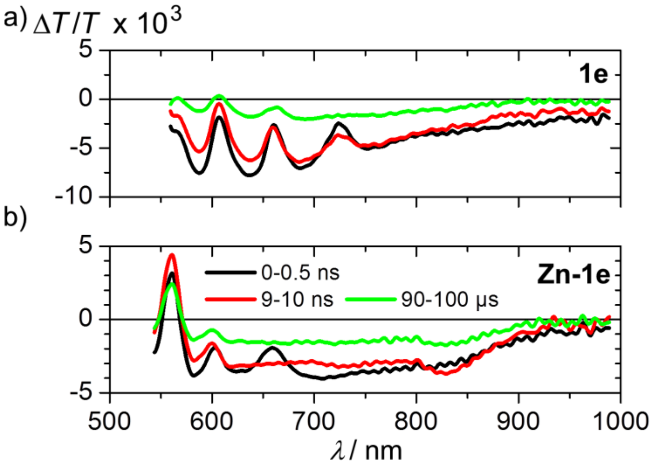

Figure 13. Selected ns-µs TA spectra of (a) **1e** and (b) **Zn-1e** in THF after excitation at 532 nm. The delay times are 500 ps (black), 10 ns (red) and 100 µs (green).

To monitor the excited state and charge transfer kinetics we performed ns-µs transient absorption (TA) pump-probe experiments on porphyrins **1e**, **Zn-1e** and on ferrocenyl porphyrins **3e**, **Zn-3e**. The ns-µs TA spectra of the parent porphyrins **1e** and **Zn-1e** are characterised by a broad excited state absorption covering almost the entire probe wavelength range. However, the porphyrin's ground state bleaching and stimulated emission (Figure 13) can be identified as distinct peaked features superimposing the broad and featureless excited state absorption. The corresponding kinetics tracked at different wavelength regions are shown in Figure 14. The data can be well described by a sum of two exponentials with lifetimes for compound **1e** of τ_1 = 12.5 ns and τ_2 = 105.8 µs, respectively. The short component agrees well with the fluorescence lifetime of about 10 ns[10] as determined by Streak Camera experiments within the experimental uncertainty of the two different measurement techniques. The longer-lived component τ_2 that has a microsecond lifetime can be assigned to the recombination of the porphyrin's triplet state T_1(P), generated by ISC from the S_1 state. In case of compound **Zn-1e** we obtained inverse rate constants of τ_1 = 2.4 ns and τ_2 = 147.5 µs by fitting the experimental data to a sum of two exponentials. Likewise, we assigned the nanosecond lifetime τ_1 to the fluorescence decay and the microsecond lifetime τ_2 to the recombination of the triplet state of the porphyrin. In fact, τ_1 is essentially similar to the experimentally measured fluorescence lifetime of 2 ns. However, we note that here we approach the temporal resolution of our ns-µs TA setup.

Interestingly, a photoinduced absorption (PA) feature emerged after 10 ns in the wavelength range from 800 to 850 nm for compound **Zn-1e**. We assigned this photoinduced absorption to the triplet state of **Zn-1e** T_1(Zn(P)), as similar PA features have been reported for triplet states of metallated porphyrins in the literature.[25] Figure 14b shows the kinetics of this particular wavelength region (green curve). Clearly, the signal grows in at early times and reaches its maximum after about 10 ns. The built up of the porphyrin's triplet state in the first 10 ns is in line with the decay of its S_1 state, which occurs on the same timescale of about 10 ns.

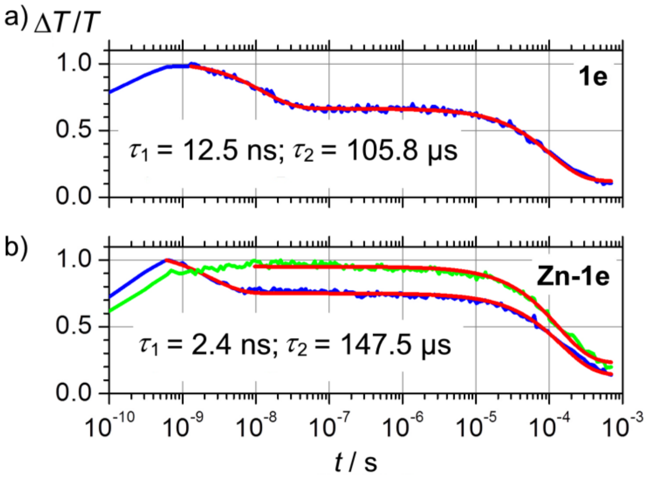

Figure 14. Integrated TA kinetics (750 – 950 nm) of (a) **1e** and (b) **Zn-1e** (blue: 700 – 800 nm; green: 825 – 850 nm). The red curves are exponential or biexponential fits to the experimental data.

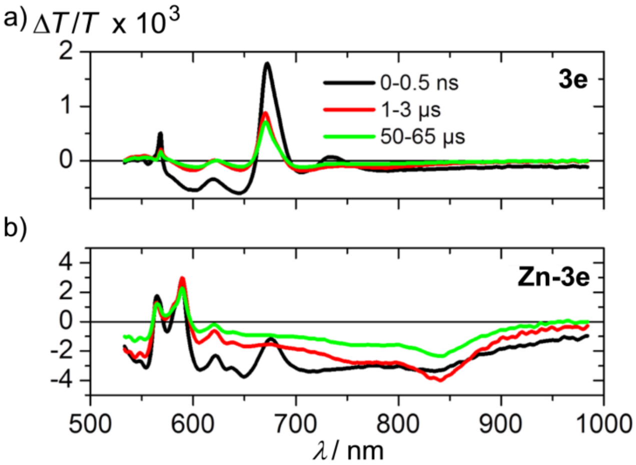

Figure 15. Selected ns-µs TA spectra of (a) **3e** after 0.5 ns, 3 µs and 65 µs and (b) **Zn-3e** after 0.5 ns, 10 ns and 1 µs, respectively in THF solution after excitation at 532 nm.

Figure 15 depicts the ns-µs TA spectra of ferrocenyl-substituted porphyrins **3e** and **Zn-3e**. Since the extinction coefficient of the ferrocenium cation is very small, the TA spectra are dominated by the porphyrin's excited state absorption that extends over the entire spectral range from approximately 500 to 1000 nm. According to reports by M. Kubo et al.[4d] and S. K. Pandey et al.[26] a photoinduced absorption band in the wavelength range from 700 to 900 nm can be assigned to the porphyrin radical anion. In fact, they found radical anion absorption bands in a series of fluorinated porphyrins with maxima between 799 – 813 nm by chemical reduction and steady-state absorption. Figure 16 shows the integrated TA kinetics of the compounds in the wavelength region above 700 nm. A fit of the kinetics found for compound **3e** to a sum of three exponentials yields inverse rate constants of τ_1 = 6 ns, τ_2 = 1.1 µs and τ_3 = 88.1 µs, respectively. The inverse rate constant τ_1 can be attributed to the decay of singlet excitons, which are quenched faster than observed in compound **1e** due to the additional PET decay channel. We attribute τ_2 to the lifetime of the CS state, which appears to undergo ISC to the first triplet excited state T_1(P) on the porphyrin, as the shape of the spectra after 3 µs resembles the spectral shape of the T_1(P) state that we also observed in porphyrin **1e**. Interestingly, the T_1(P) state of **3e** is not as long-lived as the T_1 state of reference porphyrin **1e**. It is well conceivable, that the triplet state on the porphyrin transfers to the triplet excited state of the ferrocene T_1(Fc) or alternatively that the porphyrin's T_1 state is returning faster to the ground state, because of the heavy atom effect induced by the presence of the iron atom in the ferrocene moiety. Figure 16b shows the integrated TA kinetics of compound **Zn-3e** monitored in the wavelength region from 700 – 800 nm (blue curve) and in the region from 825 to 850 nm (green curve), where the main absorption originates from the zinc porphyrin's T_1(Zn(P)) state. For **Zn-3e** the data can be described by a sum of two exponentials. The obtained lifetimes are τ_1 = 1.9 ns and τ_2 = 2.3 µs, respectively. We assume that in case of compound **Zn-3e** we cannot observe the kinetics of the CS state, because the photoinduced absorption signal of the porphyrin radical anion is superimposed by the signal of the zinc porphyrin's T_1(Zn(P)) state, indicating that the latter has a larger cross section than the porphyrin radical anion. The nanosecond component τ_1 describes the kinetics of singlet excitons which transfer into the CS state that is not observed in the TA spectra of compound **Zn-3e**. We assign τ_2 to the decay of the zinc porphyrin's T_1(Zn(P)) state into either the ground state or the ferrocene's T_1(Fc) state, which successively decays to the ground state. The latter however, is a process that we cannot directly observe in our TA experiments. In contrast to the inverse rate constant of τ_3 = 88.1 µs observed in compound **3e**, the inverse rate constant τ_2 = 2.3 µs in compound **Zn-3e** is significantly smaller. Hence, it appears that either of the two processes (or both), namely triplet state decay into the ground state and energy transfer from the porphyrin's T_1(Zn(P)) state to the ferrocene's T_1(Fc) state is facilitated by the zinc atom in compound **Zn-3e**.

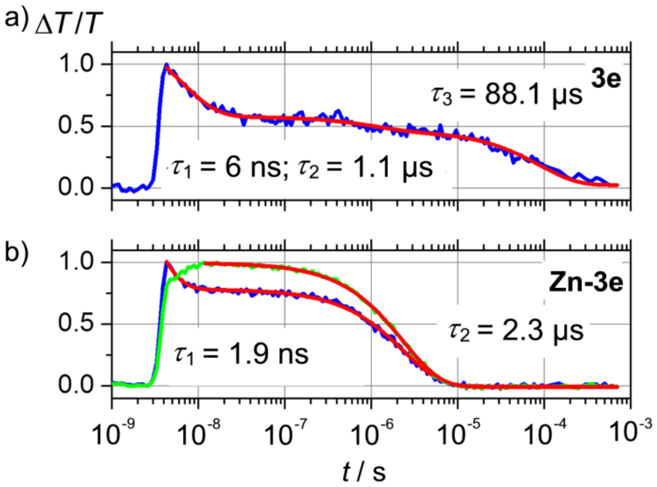

Figure 16. Integrated TA kinetics of (a) **3e** (750 – 950 nm) and (b) **Zn-3e** (blue: 700 – 800 nm; green: 825 – 850 nm). The red curves are fits to the experimental data.

Conclusions

Amide-linked porphyrin-ferrocene dyads P^{Ar}-Fc (**3**), Zn(P^{Ar})-Fc (**Zn-3**) (Ar = Mes, C_6F_5) and *N*-Fmoc-Fc-P^{Ar} (**5**) (Ar = C_6H_5, 4-C_6H_4F, 4-$C_6H_4CF_3$, C_6F_5) were prepared from the corresponding ferrocene and porphyrin building blocks by amide formation. Two *N*-Fmoc-Fc-P^{Ar} dyads (Ar = C_6H_5, 4-C_6H_4F) were further extended to porphyrin-ferrocene-porphyrin tweezers **6**, which were subsequently metallated with zinc(II) to give **Zn-6**.

All dyads and tweezers show only weak interactions between porphyrin and ferrocene moieties in their ground states but a strong fluorescence quenching and excited state lifetime reduction with respect to corresponding ferrocene-free reference compounds. Porphyrin and ferrocene substituent effects as well as low-temperature experiments substantiate a reductive photoinduced electron transfer as major deactivation pathway of the porphyrin S_1 excited state. The final lowest electronically excited states are porphyrin and ferrocene triplet states as shown by DFT calculations and transient absorption measurements. Additionally, hints for a singlet-singlet energy transfer pathway between the different porphyrins in **6** and **Zn-6** are found and suggested to occur via a hydrogen-bonded V-shaped structure of the tweezers.

Experimental Section

Instrumentation. NMR spectra were recorded on a Bruker Avance DRX 400 spectrometer at 400.31 MHz (^{1}H), 100.05 MHz (^{13}C{^{1}H}) and 367.67 MHz (^{19}F). Chemical shifts are reported on the δ scale in ppm relative to the solvent signal as an internal standard: d$_8$-THF (^{1}H: δ = 1.73, 3.58 ppm; ^{13}C: δ = 25.5, 67.7 ppm), $CDCl_3$ (^{1}H: δ = 7.24 ppm; ^{13}C: δ = 77.0 ppm), CD_2Cl_2 (^{1}H: δ = 5.32 ppm; ^{13}C: δ = 54.0 ppm) or versus external $CFCl_3$ (^{19}F: δ = 0 ppm); (s) = singlet, (d) = doublet, (pt) = pseudo triplet (unresolved doublet of doublets), (dd) = doublet of doublets, (ddd) = doublet of doublet of doublets, (br. s) = broad singlet. IR spectra were recorded with a BioRad Excalibur FTS 3100 spectrometer as CsI disks with signal intensity: (vs) = very strong, (s) = strong, (m) = medium, (w) = weak. ESI and HR ESI mass spectra were recorded on a Micromass Q-TOF-Ultima spectrometer. FD mass spectra were obtained on a FD Finnigan MAT95 spectrometer. Cyclic voltammetric (CV) and squarewave voltammetric measurements were carried out with a BioLogic SP-50 voltammetric analyzer in CH_2Cl_2 containing 0.1 M (nBu$_4$N)(PF$_6$) as supporting electrolyte at a glassy carbon working electrode, a platinum wire as the counter electrode and a 0.01 M Ag/AgNO$_3$ electrode as the reference electrode. All cyclic voltammetric measurements were recorded at 100 mV s^{-1} scan speed. Ferrocene was employed as an internal reference redox system. UV/Vis/NIR absorption spectra were measured in CH_2Cl_2 on a Varian Cary 5000 spectrometer in 1.0 cm cells (Hellma, suprasil). Steady-state emission spectra were recorded in CH_2Cl_2 on a Varian Cary Eclipse spectrometer in 1.0 cm cells (Hellma, suprasil). Quantum yields Φ were determined by comparing the areas under the emission spectra on an energy scale [cm^{-1}] recorded for optically matched solutions (absorption intensity under 0.05) of the samples and the reference (Φ(H$_2$TPP) = 0.13 in benzene)[27] using the equation[28] $\Phi = \Phi_{\mathrm{ref}} \times I/I_{\mathrm{ref}} \times \eta^2/\eta^2_{\mathrm{ref}}$ with η(benzene) = 1.5011, η(CH_2Cl_2) = 1.4242 and η(THF) = 1.4070; experimental uncertainty 15%. Fluorescence decay measurements were performed on ca. 1×10^{-5} M solutions by the time correlated single photon counting method using a Hamamatsu Streak Camera system. Two time modes were used for the measurements: one with a resolution down to a few picoseconds and a maximum time range of two nanoseconds (fast sweep, mononuclear zinc(II) porphyrins, P-Fc, Zn(P)-Fc dyads and *N*-Fmoc-Fc-P$^{\mathrm{Ar}}$ with Ar = C_6F_5), and a second time mode with a time resolution down to a few hundred picoseconds and a maximum time range limited by the repetition rate of the excitation source (slow sweep, all free base porphyrins, *N*-Fmoc-Fc-P$^{\mathrm{Ar}}$ dyads, P$^{\mathrm{Mes}}$-Fc-P$^{\mathrm{Ar}}$ and Zn(P$^{\mathrm{Mes}}$)-Fc-Zn(P$^{\mathrm{Ar}}$) tweezers). Excitation was provided depending on the measuring mode. For fast sweep experiments a Ti:sapphire ultrafast laser system (Coherent Mira 900- Dual fs-ps-Oscillator) with a repetition rate of 80 MHz and a pulse length of 100 fs pumped by a diode pumped solid-state laser (Coherent

Verdi V8) was used. The 800 nm output was frequency doubled using a BBO crystal to achieve the excitation wavelength of 400 nm. For the slow sweep measurements, a Fianium fiber laser supercontinuum source (SC450-2) was used, which provides a white laser light (460-2200 nm) with a pulse width of 6 ps and a fundamental repetition rate of 20 MHz, which was typically derated by an implemented pulse picker to 1 MHz. The desired excitation wavelength (550 nm) was filtered out of the white-light using an acousto-optical modulator (AOM, Fianium AOTF).[29] Transient absorption measurements were performed with a home-built pump-probe setup.[29] To measure a time range up to 3 ns with a resolution of ~ 100 fs, the output of a commercial titanium: sapphire amplifier (Coherent LIBRA HE, 3.5 mJ, 1 kHz, 100 fs) was split with one portion used to generate a 515 nm excitation pulse using an optical parametric amplifier (Coherent OPerA Solo), and another used to generate a 1300 nm seed pulse (output of an optical parametric amplifier (Coherent OPerA Solo) for white-light generation in the visible to NIR (500-1000 nm) in a c-cut 3 mm thick sapphire window. The variable delay of up to 3 ns between pump and probe was introduced by a broadband retroreflector mounted on a mechanical delay stage. The excitation pulse was chopped at 500 Hz, while the white light pulses were dispersed onto a linear silicon (Hamamatsu NMOS linear image sensor S3901 photodiode. The array was read out at 1 kHz. Adjacent diode readings corresponding to the transmission of the sample after an excitation pulse and without an excitation pulse were used to calculate $\Delta T/T$. Samples were excited with fluences around 100 µJ cm^{-2}.

Density functional calculations were carried out with the Gaussian09/DFT series[18] of programs. The B3LYP formulation of density functional theory was used employing the LANL2DZ basis set. To include solvent effects the integral equation formalism polarisable continuum model (IEFPCM, CH_2Cl_2) was employed. No symmetry constraints were imposed on the molecules. The presence of energy minima of the ground states was checked by analytical frequency calculations.

Materials. Unless otherwise noted, all chemical reagents were used without any further purification as received from suppliers (Sigma Aldrich, Acros, Alfa Aesar). THF was freshly distilled from sodium. CH_2Cl_2 and 1,2-dichloro-ethanewere freshlydistilled from calcium hydride. Porphyrins **1a**, **2a**, **Zn-1a**, **1e**, **2e**, **4b** − **4e**, **Ac-4b** − **Ac-4e**, **Zn-Ac-4b**, **Zn-Ac-4c**, aminoferrocene and *N*-Fmoc-protected ferrocene amino acidwere prepared by published procedures.[2d, 5a, 8-10,30-33]

General procedure for the preparation of 3a and 3e. Porphyrin 5-(4-carboxyphenyl)-15-(4-carbomethoxyphenyl)-10,20-bis(2,4,6-trimethylphenyl)porphyrin(**2a**) or 5-(4-carboxy-phenyl)-15-(4-carbomethoxyphenyl)-10,20-bis(2,3,4,5,6-pentafluorophenyl) porphyrin (**2e**) (1 eq.) and pyridine (1 mL) were dissolved in anhydrous toluene (20 mL). Thionyl chloride (5 eq.) was added and the reaction mixture was stirred under argon for 3 h at room temperature. Excess of thionyl chloride and solvent were removed under reduced pressure. The residue was redissolved in toluene (20 mL) and pyridine (1 mL) in ultrasonic bath. Aminoferrocene (1.3 eq.) dissolved in toluene (20 mL) and pyridine (1 mL) was added. The mixture was stirred overnight and the solvent was removed by evaporation under reduced pressure. The residue was purified by chromatography [silica, toluene : ethylacetate (20:1)].

General procedure for the preparation of Zn-3a and Zn-3e. Dyad **3a** or **3e** (1 eq.) and zinc(II) acetate dihydrate (5 eq.) were stirred overnight in CH_2Cl_2 (5 mL). After concentration under reduced pressure the product was isolated by column chromatography.

General procedure for the preparation of 5b, 5c, 5d and 5e. *N*-Fmoc protected ferrocene amino acid *N*-Fmoc-Fca-OH (H-Fca-OH= 1-amino-1'-ferrocene carboxylic acid; Fmoc = 9-fluorenylmethoxycarbonyl) and one drop of pyridine were dissolved in anhydrous CH_2Cl_2 (40 mL). Oxalyl chloride was added and the reaction mixture was stirred under nitrogen for 1 h at room temperature. Excess of oxalyl chloride and solvent were removed by evaporation under reduced pressure. The residue was dissolved in CH_2Cl_2 (10 mL) and the solvent was removed under reduced pressure. The acid chloride was dissolved in CH_2Cl_2 (40 mL). To this solution a solution of the porphyrin amino component in CH_2Cl_2 (40 mL with one drop of pyridine) was added. The reaction mixture was stirred for 18 h at room temperature, washed with water and the organic phase was concentrated under reduced pressure. The product was isolated by column chromatography.

General procedure for the preparation of 6b and 6c. 5b or **5c** and tris(2-aminoethyl)amine were dissolved in anhydrous CH_2Cl_2 (20 mL) and the reaction mixture was stirred under nitrogen for 3 h at room temperature, washed with saturated brine (2×10 mL) and phosphate buffer (pH 5.5). After drying with Na_2SO_4 the solvent was removed under reduced pressure. 5-(4-Carboxyphenyl)-15-(4-methoxycarbonylphenyl)-10,20-bis(2,4,6-trimethylphenyl) porphyrin (**2a**) was dissolved in anhydrous CH_2Cl_2 (30 mL), 1-chloro-*N*,*N*,2-trimethylpropenylamine (Ghosez's reagent) was added and the reaction mixture was stirred under nitrogen for 1 h at room temperature. After the acid chloride formed (TLC control) excess of Ghosez's reagent and solvent were removed by evaporation under reduced pressure. In order to remove the *N*,*N*-dimethyl amide byproduct anhydrous CH_2Cl_2 (20 mL) was added and the volatiles were again evaporated. The acid chloride was dissolved in CH_2Cl_2 (30 mL with 0.05 mL of triethylamine) and this solution was added dropwise to a solution of the amino component prepared from **5b** or **5c** in CH_2Cl_2. The reaction mixture was stirred for 18 h at room temperature, washed with water and the organic phase was concentrated under reduced pressure. After column chromatography the **6b** and **6c** were isolated, respectively.

General procedure for the preparation of Zn-6b and Zn-6c. **6b** or **6c** (1 eq.) and zinc(II) acetate dihydrate (12 eq.) were stirred overnight in CH_2Cl_2 (10 mL). After concentration under reduced pressure the product was isolated by column chromatography [silica, toluene : ethyl acetate = 50 : 1].

[10,20-Bis(pentafluorophenyl)-5,15-bis(4-methoxycarbonylphenyl)porphyrinato] zinc(II) (**Zn-1e**)**.** Porphyrin **1e** (50 mg, 0.054 mmol) and zinc(II) acetate dihydrate (61 mg, 0.27 mmol) were stirred overnight in CH_2Cl_2 (10 mL). After concentration under reduced pressure the product was isolated by column chromatography [silica, CH_2Cl_2, $R_f = 0.50$]. Yield 49.9 mg (0.051 mmol, 94%), purple-red powder. $C_{48}H_{22}F_{10}N_4O_4Zn$ (974.1067).

Supporting Information (see footnote on the first page of this article): Complete analytical data; Absorption spectra of **1e** and **3e** in 2-methyltetrahydrofuran at $T = 300 \rightarrow 77$ K; B3LYP/LANL2DZ, IEFPCM calculated frontier orbitals of **Zn-3a**, **Zn-3e**, **5d**, **5e**, **6c**, **Zn-6b**, **Zn-6c**; B3LYP/LANL2DZ, IEFPCM calculated molecular orbital energy diagrams of **3a**, **3e**, **Zn-3a**, **Zn-3e**, **6b**, **6c**, **Zn-6b**, **Zn-6c**; B3LYP/LANL2DZ, IEFPCM calculated spin densities of the lowest triplet state of **3e** and **5e**; Cartesian Coordinates of all DFT optimised geometries.

Acknowledgments

This work was supported by the Deutsche Forschungsgemeinschaft (DFG He 2778-6/1). Julian R. Ochsmann thanks the International Research Training Group (IRTG 1404) Self Organized Materials for Optoelectronics for funding, Michael Meister thanks the Max Planck Graduate Center with the Johannes Gutenberg University (MPGC) for support and Frédéric Laquai (all Max Planck Institute for Polymer Research of Mainz, Germany) thanks the Max Planck Society for funding a Max Planck Research group.

---

[1] a) H. Imahori, D. M. Guldi, K. Tamaki, Y. Yoshida, C. Luo, Y. Sakata, S. Fukuzumi, *J. Am. Chem. Soc.* **2001**, *123*, 6617-6628; b) H. Imahori, K. Tamaki, Y. Araki, Y. Sekiguchi, O. Ito, Y. Sakata, S. Fukuzumi, *J. Am. Chem. Soc.* **2002**, *124*, 5165-5174; c) H. Imahori, Y. Sekiguchi, Y. Kashiwagi, T. Sato, Y. Araki, O. Ito, H. Yamada, S. Fukuzumi, *Chem. Eur. J.* **2004**, *10*, 3184-3196; d) M. U. Winters, E. Dahlstedt, H. E. Blades, C. J. Wilson, M. J. Frampton, H. L. Anderson, B. Albinsson, *J. Am. Chem. Soc.* **2007**, *129*, 4291-4297; e) C. Wijesinghe, M. E. El-Khouly, M. E. Zandler, S. Fukuzumi, F. D'Souza, *Chem. Eur. J.* **2013**, *19*, 9629-9638; f) J. Melomedov, J. R. Ochsmann, M. Meister, F. Laquai, K. Heinze, *Eur. J. Inorg. Chem.* **2014**, 1984-2001.

[2] a) D. Gust, T. A. Moore, A. L. Moore, F. Cao, D. Luttrul, J. M. Degraziano, X. C. Ma, L. R. Makings, S. Lee, T. T. Trier, E. Bittersmann, G. R. Seely, S. Woodward, R. V. Bensasson, M.

Roug, F. C. De Schryver, M. Van der Auweraer, *J. Am. Chem. Soc.* **1991**, *113*, 3638-3649; b) D. Gust, T. A. Moore, A. L. Moore, A. N. Macpherson, A. Lopez, J. M. DeGraziano, I. Gouni, E. Bittersmann, G. R. Seely, F. Gao, R. A. Nieman, X. C. Ma, L. J. Demanche, S. Hung, D. K. Luttrull, S. Lee, P. K. Kerrigan, *J. Am. Chem. Soc.* **1993**, *115*, 11141-11152; c) M. D. Meijer, G. P.M. van Klink, G. van Koten, *Coord. Chem. Rev.* **2002**, *230*, 141-163; d) S. L. Gould, G. Kodis, R. E. Palacios, L. De La Garza, A. Brune, D. Gust, T. A. Moore, A. L. Moore, *J. Phys. Chem. B* **2004**, *108*, 10566-10580.

[3] a) A. M. Brun, A. Harriman, V. Heitz, J.-P. Sauvage, *J. Am. Chem. Soc.* **1991**, *113*, 8657-8663; b) V. Heitz, S. Chardon-Noblat, J.-P. Sauvage, *Tetrahedron Lett.* **1991**, *32*, 197-198; c) E. K. L. Yeow, P. J. Sintic, N. M. Cabral, J. N. H. Reek, M. J. Crossley, K. P. Ghiggino, *Phys. Chem. Chem. Phys.* **2000**, *2*, 4281-4291; d) K. Kilså, J. Kajanus, A. N. Macpherson, J. Mårtensson, B. Albinsson, *J. Am. Chem. Soc.* **2001**, *123*, 3069-3080; e) S. Fukuzumi, K. Ohkubo, W. E, Z. Ou, J. Shao, K. M. Kadish, J. A. Hutchison, K. P. Ghiggino, P. J. Sintic, M. J. Crossley, *J. Am. Chem. Soc.* **2003**, *125*, 14984-14985; f) J. Hee Jang, H. J. Kim, H.-J. Kim, C. H. Kim, T. Joo, D. Won Cho, M. Yoon, *Bull. Korean Chem. Soc.* **2007**, *28*, 1967-1972; g) J. Fortage, J. Boixel, E. Blart, L. Hammarström, H. C. Becker, F. Odobel, *Chem. Eur. J.* **2008**, *14*, 3467-3480; h) J. Fortage, A. Scarpaci, L. Viau, Y. Pellegrin, E. Blart, M. Falkenström, L. Hammarström, I. Asselberghs, R. Kellens, W. Libaers, K. Clays, M. P. Eng, F. Odobel, *Chem. Eur. J.* **2009**, *15*, 9058-9067; i) J. Fortage, J. Boixel, E. Blart, H. C. Becker, F. Odobel, *Inorg. Chem.* **2009**, *48*, 518-526.

[4] a) R. Ciasson, E. J. Lee, X. Zbao, M. S. Wrighton, *J. Phys. Chem.* **1993**, *97*, 2596-2601; b) N. B. Thornton, H. Wojtowicz, T. Netzel, D. W. Dixon, *J. Phys. Chem. B* **1998**, *102*, 2101-2110; c) V. A. Nadtochenko, N. N. Denisov, V. Yu. Gak, N. V. Abramova, N. M. Loim, *Russ. Chem. Bull.* **1999**, 40, 1900-1903; d) M. Kubo, Y. Mori, M. Otani, M. Murakami, Y. Ishibashi, M. Yasuda, K. Hosomizu, H. Miyasaka, H. Imahori, S. Nakashima, *Chem. Phys. Lett.* **2006**, *429*, 91-96; e) H. Mansour, M. E. El-khouly, S. Y. Shaban, O. Ito, N. Jux, *J. Porphyrins Phthalocyanines* **2007**, *10*, 719-728; f) P. K. Poddutoori, A. S. D. Sandanayaka, T. Hasobe, O. Ito, A. van der Est, *J. Phys. Chem. B* **2010**, *114*, 14348–14357; g) M. A. Bakar, N. N. Sergeeva, T. Juillard, M. O. Senge, *Organometallics* **2011**, *30*, 3225-3228; h) B. M. J. M. Suijkerbuijk, R. J. M. Klein Gebbink, *Angew. Chem.* **2008**, *120*, 7506-7532; *Angew. Chem. Int. Ed.* **2008**, *47*, 7396-7421; i) S. J. Dammer, P. V. Solntsev, J. R. Sabin, V. N.Nemykin, , *Inorg. Chem.* **2013**, *52*, 9496-9510; j) L. Lvova, P. Galloni, B. Floris, I. Lundström, R. Paolesse, C. Di Natale, *Sensors* **2013**, *13*, 5841-5856; k) V. N. Nemykin, P. Chen, P. V. Solntsev, A. A. Purchel, K. M. Kadish, *J. Porphyrins Phthalocyanines* **2012**, *16*,

793-801; l) A. Vecchi, E. Gatto, B. Floris, V. Conte, M. Venanzi, V. N. Nemykin, P. Galloni, *Chem. Commun.* **2012**, *48*, 5145-5147; m) V. N. Nemykin, G. T. Rohde, C. D. Barrett, R. G. Hadt, J. R. Sabin, G. Reina, P. Galloni, B. Floris, *Inorg. Chem.* **2010**, *49*, 7497-7509; n) V. N. Nemykin, G. T. Rohde, C. D. Barrett, R. G. Hadt, C. Bizzarri, P. Galloni, B. Floris, I. Nowik, R. H. Herber, A. G. Marrani, R. Zanoni, N. M. Loim, *J. Am. Chem. Soc.* **2009**, *131*, 14969-14978.

[5] a) K. Heinze, M. Schlenker, *Eur. J. Inorg. Chem.* **2004**, 2974–2988; b) K. Heinze, D. Siebler, *Z. Anorg. Allg. Chem.* **2007**, *633*, 2223-2233; c) D. Siebler, M. Linseis, T.Gasi, L. M. Carrella, R. F. Winter, C. Förster, K. Heinze, *Chem. Eur. J.* **2011**, *17*, 4540-4551; d) D. Siebler, C. Förster, K. Heinze, *Dalton Trans.* **2011**, *40*, 3558-3575; e) H. Huesmann, C. Förster, D. Siebler, T. Gasi, K. Heinze, *Organometallics* **2012**, *31*, 413-427.

[6] A. K. Burrell, W. Campbell, D. L. Officer, *Tetrahedron Lett.* **1997**, *38*, 1249-1252.

[7] K. Heinze, K. Hempel, M. Beckmann, *Eur. J. Inorg. Chem.* **2006**, 2040-2050.

[8] C. M. Carcel, J. K. Laha, R. S. Loewe, P. Thamyongkit, K. Schweikart, V. Misra, D. F. Bocian, J. S. Lindsey, N. Carolina, *J. Org. Chem.* **2004**, *69*, 6739-6750.

[9] K. Heinze, A. Reinhart, *Dalton Trans.* **2008**, 469-480.

[10] J. Melomedov, A. Wünsche von Leupoldt, M. Meister, F. Laquai, K. Heinze, *Dalton Trans.* **2013**, *42*, 9727-9739.

[11] A. Devos, J. Remiona, A-M. Frisque-Hesbain, A. Colens, L. Ghosez, *Chem. Comm.* **1979**, 1180-1181.

[12] Y. Araki, Y. Yasumura, O. Ito, *J. Phys. Chem. B* **2005**, *109*, 9843-9848.

[13] E. D. German, A. M. Kuznetso, *Electrochim. Acta* **1981**, *26*, 1595-1608.

[14] A. Weller, *Z. Phys. Chem.* **1982**, *133*, 93-98.

[15] a) R. A. Marcus, *J. Chem. Phys.* **1956**, *24*, 979-989; b) R. A. Marcus, *Annu. Rev. Phys. Chem.* **1964**, *15*, 155-196; c) R. A. Marcus, *Angew. Chem.* **1996**, *105*, 1161-1172; *Angew. Chem. Int. Ed.* **1993**, *32*, 1111-1121.

[16] J. A. Schmidt, A. R. McIntosh, A. C. Weedon, J. R. Bolton, J. S. Connolly, J. K. Hurley, M. R. Wasielewski, *J. Am. Chem. Soc.* **1988**, *110*, 1733-1740.

[17] C. Luo, D. M. Guldi, H. Imahori, K. Tamaki, Y. Sakata, *J. Am. Chem. Soc.* **2000**, *122*, 6535-6551.

[18] M. J. Frisch, G. W. Trucks, H. B. Schlegel, G. E. Scuseria, M. A. Robb, J. R. Cheeseman, G. Scalmani, V. Barone, B. Mennucci, G. A. Petersson, H. Nakatsuji, M. Caricato, X. Li, H. P. Hratchian, A. F. Izmaylov, J. Bloino, G. Zheng, J. L. Sonnenberg, M. Hada, M. Ehara, K. Toyota, R. Fukuda, J. Hasegawa, M. Ishida, T. Nakajima, Y. Honda, O. Kitao, H. Nakai, T.

Vreven, J. A. Montgomery Jr., J. E. Peralta, F. Ogliaro, M. Bearpark, J. J. Heyd, E. Brothers, K. N. Kudin, V. N. Staroverov, R. Kobayashi, J. Normand, K. Raghavachari, A. Rendell, J. C. Burant, S. S. Iyengar, J. Tomasi, M. Cossi, N. Rega, J. M. Millam, M. Klene, J. E. Knox, J. B. Cross, V. Bakken, C. Adamo, J. Jaramillo, R. Gomperts, R. E. Stratmann, O. Yazyev, A. J. Austin, R. Cammi, C. Pomelli, J. W. Ochterski, R. L. Martin, K. Morokuma, V. G. Zakrzewski, G. A. Voth, P. Salvador, J. J. Dannenberg, S. Dapprich, A. D. Daniels, O. Farkas, J. B. Foresman, J. V. Ortiz, J. Cioslowski, D. J. Fox, Gaussian 09 (Revision A.02), Gaussian, Inc., Wallingford CT, **2009**.

[19] M. Gouterman, *J. Chem. Phys.* **1959**, *30*, 1139-1161.

[20] D. Holten, D. F. Bocian, J. S. Lindsey, *Acc. Chem. Res.* **2002**, *35*, 57-69.

[21] J.-M. Camus, S. M. Aly, C. Stern, R. Guilard, P. D. Harvey, *Chem. Commun.* **2011**, *47*, 8817-8819.

[22] a) S. Brahma, S. A. Ikbal, S. P. Rath, *Inorg. Chem.* **2014**, *53*, 49-62; b) H. Yoon, C.-H. Lee, W.-D. Jang, *Chem. Eur. J.***2012**, *18*, 12479-12486; c) A. Chaudhary, S. P. Rath, *Chem. Eur. J.* **2012**, *18*, 7404-7417; d) A. Chaudhary, S. P. Rath, *Chem. Eur. J.* **2011**, *17*, 11478-11487; e) B. Habermeyer, A. Takai, C. P. Gros, M. El Ojaimi, J.-M. Barbe, S. Fukuzumi, *Chem. Eur. J.* **2011**, *17*, 10670-10681; f) J.-M. Barbe, B. Habermeyer, T. Khoury, C. P. Gros, P. Richard, P. Chen, K. M. Kadish, *Inorg. Chem.* **2010**, *49*, 8929-8940.

[23] N. G. Connelly, W. E. Geiger, *Chem. Rev.* **1996**, *96*, 877-910.

[24] O. S. Wenger, *Chem. Eur. J.* **2011**, *17*, 11692-11702.

[25] J. Rodriguez, C. Kirmaier, D. Holten, *J. Am. Chem. Soc.* **1989**, *111*, 6500-6506.

[26] S. K. Pandey, A. L. Gryshuk, A. Graham, K. Ohkubo, S. Fukuzumi, M. P. Dobhal, G. Zheng, Z. Ou, R. Zhan, K. M. Kadish, A. Oseroff, S. Ramaprasade, R. K. Pandey, *Tetrahedron* **2003**, *59*, 10059-10073.

[27] A. Rosa, G. Ricciardi, E. J. Baerends, A. Romeo, L. Monsu, *J. Phys. Chem. A* **2003**, *107*, 11468-11482.

[28] J. R. Lakowicz, *Principles of Fluorescence Spectroscopy*, Springer, 3rd edn, **2006**.

[29] F. Etzold, I. A. Howard, N. Forler, D. M. Cho, M. Meister, H. Mangold, J. Shu, M. R. Hansen, K. Müllen, F. Laquai, *J. Am. Chem. Soc.* **2012**, *134*, 10569-10583.

[30] D. T. Gryko, M. Tasior, B. Koszarna, *J. Porphyrins Phthalocyanines* **2003**, *7*, 239-248.

[31] T. Rohand, E. Dolusic, T. H. Ngo, W. Maes, W. Dehaen, *ARKIVOC* **2007** (x), 307-324.

[32] B. J. Littler, Y. Ciringh, J. S. Lindsey, *J. Org. Chem.* **1999**, *64*, 2864-2872.

[33] K. Heinze, A. Reinhart, *Z. Naturforsch.* **2005**, *60b*, 758-762.

7 Supporting Informations and Experimental Section

7.1 Supporting Informations and Experimental Section of Publication 6.1

Porphyrin Amino Acids – Amide Coupling, Redox and Photophysical Properties of Bis(porphyrin) amides

Jascha Melomedov[a], Anica Wünsche von Leupoldt[a], Michael Meister[b], Frédéric Laquai[b] and Katja Heinze*[,a]

Supporting Information

Experimental Section

Porphyrins **1a**, **2a**, **Boc-3a** and **3a** were prepared by published procedures and characterised as follows.[S1][S2]

10,20-Bis(2,4,6-trimethylphenyl)-5,15-bis[4-(methoxycarbonyl)] porphyrin (1a)[S1][S2]

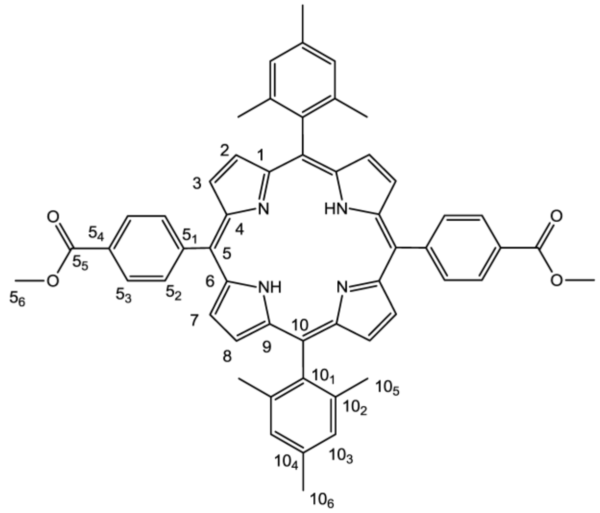

^{1}H-NMR (CDCl$_3$): δ = –2.63 (s, 2 H, $H^{pyrrole\text{-}NH}$), 1.83 (s, 12 H, $H^{10}{}_5$), 2.63 (s, 6 H, $H^{10}{}_6$), 4.11 (s, 6 H, $H^5{}_6$), 8.31 (d, $^3J_{HH}$ = 8.1 Hz, 4 H, $H^5{}_2$), 8.43 (d, $^3J_{HH}$ = 8.1 Hz, 4 H, $H^5{}_3$), 8.71 (d, $^3J_{HH}$ = 4.7 Hz, 4 H, $H^{pyrrole}$), 8.74 (d, $^3J_{HH}$ = 4.7 Hz, 4 H, $H^{pyrrole}$) ppm.

IR (KBr): $\tilde{\nu}$ [cm^{-1}] = 3425 (b, NH), 2922 (w, CH), 2850 (w, CH), 1722 (vs, CO), 1608 (s), 1386 (vs), 1278 (vs, C-O-C), 1114 (s), 800 (w).

UV/Vis (CH$_2$Cl$_2$): λ [nm] (ε / [10^4 M^{-1}cm^{-1}]) = 419 (36.88), 516 (1.99), 548 (1.13), 593 (0.82), 651 (1.38).

Fluorescence (CH$_2$Cl$_2$): λ [nm] (relative intensity) = 654 (1.00), 716 (0.20).

Quantum yield: Φ = 0.0774.

Lifetime: τ [ns] = 9.87 (100%).

CV (Fc/Fc$^+$, 100 mV s^{-1}, CH$_2$Cl$_2$): $E_{½}$[V] = –2.020, –1.670, 0.600, 1.030.

5-(4-Carboxyphenyl)-15-(4-carbomethoxyphenyl)-10,20-bis(2,4,6-trimethylphenyl) porphyrin (2a)[S1][S2]

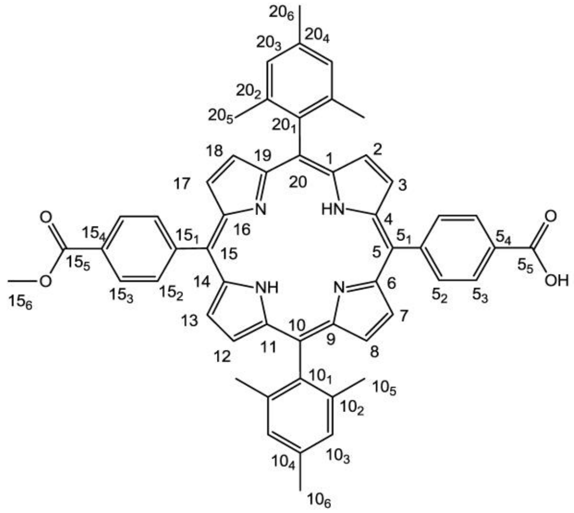

UV/Vis (CH_2Cl_2): λ [nm] (ε / [10^4 $M^{-1}cm^{-1}$]) = 419 (13.58), 515 (0.70), 549 (0.34), 592 (0.24), 650 (0.30).

Fluorescence (CH_2Cl_2): λ [nm] (relative intensity) = 652 (1.00), 716 (0.26).

Quantum yield: Φ = 0.1187.

CV (Fc/Fc$^+$, 100 mV s^{-1}, CH_2Cl_2): $E_{½}$[V] = –2.090, –1.705, 0.600, 1.060.

15-(4-Carbomethoxyphenyl)-5-(*N-tert*-butoxycarbonyl-4-aminophenyl)-10,20-bis(2,3,4,5,6-pentafluorophenyl) porphyrin (Boc-3a)[S1][S2]

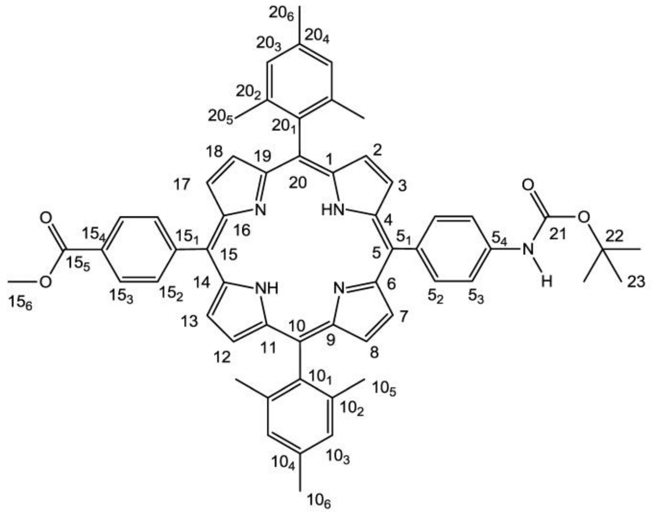

UV/Vis (CH_2Cl_2): λ [nm] (ε / [10^4 $M^{-1}cm^{-1}$]) = 420 (68.60), 516 (3.48), 550 (1.91), 594 (1.36), 651 (2.25).

Fluorescence (CH_2Cl_2): λ [nm] (relative intensity) = 654 (1.00), 719 (0.20).

Quantum yield: Φ = 0.1112.

CV (Fc/Fc$^+$, 100 mV s^{-1}, CH_2Cl_2): $E_{½}$[V] = –2.130, –1.745, 0.535, 0.945.

15-(4-Carbomethoxyphenyl)-5-(4-aminophenyl)-10,20-bis(2,4,6-trimethylphenyl) porphyrin (3a)[S1][S2]

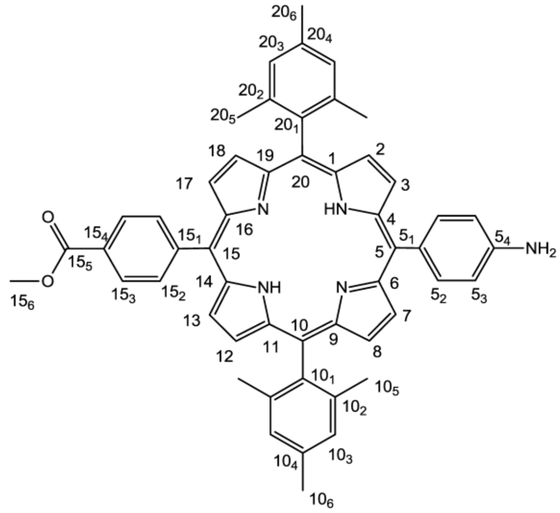

UV/Vis (CH_2Cl_2): λ [nm] (ε / [10^4 $M^{-1}cm^{-1}$]) = 421 (34.07), 517 (1.91), 552 (1.10), 593 (0.74), 651 (1.01).

Fluorescence (CH_2Cl_2): λ [nm] (relative intensity) = 654 (1.00), 719 (0.21).

Quantum yield: Φ = 0.0882.

CV (Fc/Fc$^+$, 100 mV s^{-1}, CH_2Cl_2): $E_{½}$[V] = –2.100, –1.760, 0.455, 0.600.

10,20-Bis(2,3,4,5,6-pentafluorophenyl)-5,15-bis[4-(methoxycarbonylphenyl)] porphyrin (1b). Following a standard procedure[S3] a solution of pentafluorophenyldipyrromethane (2.00 g, 6.4 mmol) and methyl 4-formylbenzoate (1.02 g, 6.4 mmol) in CH_2Cl_2 (700 mL) was treated with TFA (1.2 mL, 15.6 mmol) at room temperature. After 40 min, DDQ (2.1 g, 9.57 mmol) was added and after further 60 min TEA (1.2 mL) was added. The reaction mixture was concentrated under reduced pressure and chromatographed [silica, CH_2Cl_2/petroleum ether b.p. 40/60 (5:1), $R_f = 0.32$] affording a purple powder (200 mg, 0.22 mmol, 7%). $C_{48}H_{24}F_{10}N_4O_4$ (910.71).

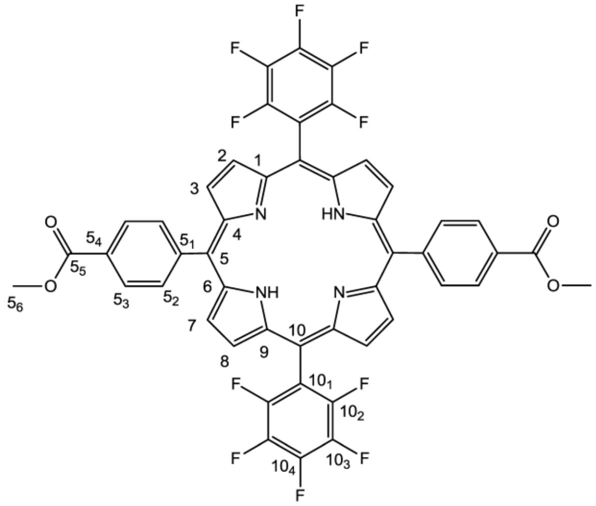

^{1}H-NMR ($CDCl_3$): $\delta = -2.86$ (s, 2 H, $H^{\text{pyrrole-NH}}$), 4.13 (s, 6 H, $H^5{}_6$), 8.31 (d, $^3J_{HH} = 8.2$ Hz, 4 H, $H^5{}_2$), 8.47 (d, $^3J_{HH} = 8.2$ Hz, 4 H, $H^5{}_3$), 8.83 (d, $^3J_{HH} = 4.7$ Hz, 4 H, H^{pyrrole}), 8.90 (d, $^3J_{HH} = 4.8$ Hz, 4 H, H^{pyrrole}) ppm.

^{1}H-NMR (d_8-THF): $\delta = -2.80$ (s, 2 H, $H^{\text{pyrrole-NH}}$), 4.07 (s, 6 H, $H^5{}_6$), 8.37 (d, $^3J_{HH} = 8.2$ Hz, 4 H, $H^5{}_2$), 8.47 (d, $^3J_{HH} = 8.2$ Hz, 4 H, $H^5{}_3$), 8.93 (d, $^3J_{HH} = 4.7$ Hz, 4 H, H^{pyrrole}), 9.05 (d, $^3J_{HH} = 4.8$ Hz, 4 H, H^{pyrrole}) ppm.

^{13}C{^{1}H}-NMR (d_8-THF): $\delta = 52.7$ (s, $C^5{}_6$), 121.4 (s, C^5), 129.1 (s, $C^5{}_3$), 131.4 (s, $C^5{}_4$), 131.4, 133.3 (m, $C^{2,3,7,8,12,13,17,18}$), 135.6 (s, $C^5{}_2$), 147.1 (s, $C^5{}_1$), 167.3 (s, $C^5{}_5$) ppm. $C^{10}{}_1 - C^{10}{}_4$ are not observed.

^{19}F-NMR (d_8-THF): $\delta = -162.9$ (ddd, $^3J_{FF} = 23$ Hz, $^3J_{FF} = 21$ Hz, $^5J_{FF} = 8$ Hz, 4 F, $F^{10/20}{}_{3/3,}$), -153.4 (t, $^3J_{FF} = 21$ Hz, 2 F, $F^{10/20}{}_{4/4}$), -138.0 (dd, $^3J_{FF} = 24$ Hz, $^5J_{FF} = 8$ Hz, 4 F, $F^{10/20}{}_{2/2}$) ppm.

IR (KBr): $\tilde{\nu}$ [cm^{-1}] = 3435 (w, crystal water), 3327 (w, NH), 2923 (w, CH), 2850 (w, CH), 1718 (s, CO), 1605 (w), 1519 (vs), 1496 (m), 1281 (s, C-O-C), 1114 (m, CF), 987 (s), 804 (w).

MS (FD): m/z (%) = 909.7 (100), 910.7 (55) $[M]^+$.

MS (ESI): m/z (%) = 911.17 (100) $[M+H]^+$.

HR-MS (ESI): obs. m/z = 911.1700; calcd. for $[M+H]^+$ 911.1716.

UV/Vis (CH_2Cl_2): λ [nm] (ε / [10^4 $M^{-1}cm^{-1}$]) = 415 (55.69), 510 (3.09), 543 (0.73), 587 (0.95), 641 (0.34).

Fluorescence (CH_2Cl_2): λ [nm] (relative intensity) = 645 (1.00), 711 (0.62).

Quantum yield: $\Phi = 0.0520$.

Lifetime: τ [ns] = 10.05 (100%).

CV (Fc/Fc$^+$, 100 mV s^{-1}, CH_2Cl_2): $E_{½}$[V] = –1.750, –1.350, 0.890, 1.140.

5-(4-Carboxyphenyl)-15-(4-carbomethoxyphenyl)-10,20-bis(2,3,4,5,6-pentafluorophenyl) porphyrin (2b). Porphyrin **1b** (400 mg, 0.447 mmol) was dissolved in 80 mL TFA and 160 mL concentrated HCl_{aq}. The mixture was heated to 60°C. When TLC indicated beginning formation of the diacid the reaction was cooled down, diluted with CH_2Cl_2 (100 mL) and neutralised with a saturated aqueous solution of $NaHCO_3$. The organic layer was washed with water (3×), dried over Na_2SO_4 and concentrated under reduced pressure. Porphyrins **1b** (289 mg) and **2b** (101 mg, 25% yield, purple powder, $C_{47}H_{22}F_{10}N_4O_4$ (896.69)) were isolated by column chromatography [silica, CH_2Cl_2/MeOH (20:1), $R_f = 1.0$ (**1b**) and $R_f = 0.29$ (**2b**)].

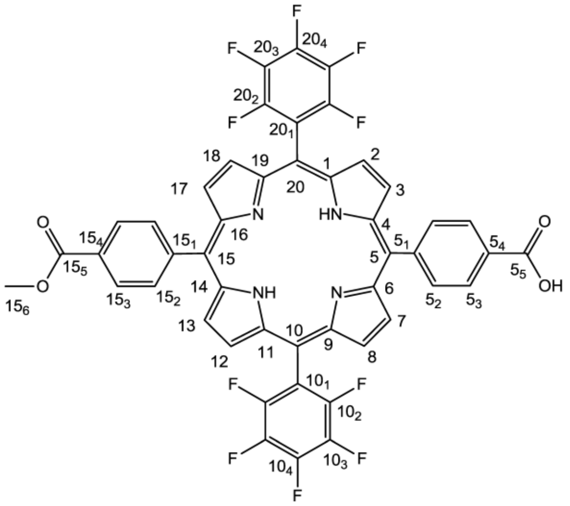

^{1}H-NMR (CD_2Cl_2 + 1 drop MeOD): $\delta = -2.94$ (s, 2 H, $H^{pyrrole\text{-}NH}$), 4.07 (s, 3 H, $H^{15}{}_{6}$), 8.29 (d, $^3J_{HH} = 8.1$ Hz, 2 H, $H^{15}{}_{2}$), 8.30 (d, $^3J_{HH} = 8.1$ Hz, 2 H, $H^{5}{}_{2}$), 8.43 (d, $^3J_{HH} = 8.2$ Hz, 2 H, $H^{15}{}_{3}$), 8.44 (d, $^3J_{HH} = 8.2$ Hz, 2 H, $H^{5}{}_{3}$), 8.86 (br. s, 4 H, $H^{pyrrole}$), 8.91 (br. s, 4 H, $H^{pyrrole}$) ppm.

^{13}C{^{1}H}-NMR (CD_2Cl_2 + 1 drop MeOD): $\delta = 52.6$ (s, $C^{15}{}_{6}$), 120.6 (s, C^{5}), 120.8 (s, C^{15}), 128.2 (s, $C^{15}{}_{3}$), 128.5 (s, $C^{5}{}_{3}$), 130.3 (s, $C^{15}{}_{4}$), 130.7 (s, $C^{5}{}_{4}$), 134.8 (s, $C^{15}{}_{2}$), 134.8 (s, $C^{5}{}_{2}$), 136.3, 138.8, 145.3, 147.8 (m, $C^{10,20}$, $^{10,20/10,20/10,20/10,20}{}_{1/2/3/4}$), 145.9 (s, $C^{15}{}_{1}$), 146.0 (s, $C^{5}{}_{1}$), 167.5 (s, $C^{15}{}_{5}$), 168.8 (s, $C^{5}{}_{5}$) ppm.

^{19}F-NMR (CD_2Cl_2 + 1 drop MeOD): $\delta = -162.1$ (ddd, $^3J_{FF} = 23$ Hz, $^3J_{FF} = 21$ Hz, $^5J_{FF} = 8$ Hz, 4 F, $F^{10/20}{}_{3/3,}$), –153.3 (t, $^3J_{FF} = 21$ Hz, 2 F, $F^{10/20}{}_{4/4}$), –137.2 (dd, $^3J_{FF} = 24$ Hz, $^5J_{FF} = 8$ Hz, 4 F, $F^{10/20}{}_{2/2}$) ppm.

IR (KBr): $\tilde{\nu}$ [cm^{-1}] = 3431 (b, OH), 3314 (w, NH), 2925 (w, CH), 2856 (w, CH), 1725 (s, CO), 1698 (s, CO), 1524 (m), 1489 (vs), 1281 (m, C-O-C), 1108 (s, CF), 990 (s), 920 (s).

MS (FD): m/z (%) = 895.58 (100) $[M]^+$.

MS (ESI): m/z (%) = 897.17 (100) $[M+H]^+$.

HR-MS (ESI): obs. m/z = 897.1547; calcd. for $[M+H]^+$ 897.1560.

UV/Vis (CH_2Cl_2): λ [nm] (ε / [10^4 $M^{-1}cm^{-1}$]) = 415 (13.74), 510 (0.83), 543 (0.25), 587 (0.30), 641 (0.15).

Fluorescence (CH_2Cl_2): λ [nm] (relative intensity) = 645 (1.00), 712 (0.63).

Quantum yield: $\Phi = 0.0604$.

CV (Fc/Fc$^+$, 100 mV s^{-1}, CH_2Cl_2): $E_{½}$[V] = –1.810, –1.380, 0.890, 1.120.

15-(4-Carbomethoxyphenyl)-5-(*N-tert*-butoxycarbonyl-4-aminophenyl)-10,20-bis(2,3,4,5,6-pentafluorophenyl) porphyrin (Boc-3b). Porphyrin **2b** (100 mg, 0.11 mmol) was dissolved in 15 mL of dry *tert*-butyl alcohol and 22 µL (0.16 mmol) TEA. Diphenylphosphoryl azide (DPPA) (29 µL (0.14 mmol)) was added and this solution was heated to 80°C for two days. The mixture was diluted with 50 mL CH_2Cl_2, washed with diluted aqueous citric acid, a saturated solution of $NaHCO_3$, and water (3×). After drying with Na_2SO_4 the solvent was evaporated under reduced pressure and the product isolated by column chromatography as purple powder [silica, toluene/ethyl acetate (20:1), $R_f = 0.47$]. Yield 40% (43.2 mg, 0.045 mmol). $C_{51}H_{31}F_{10}N_5O_4$ (967.81).

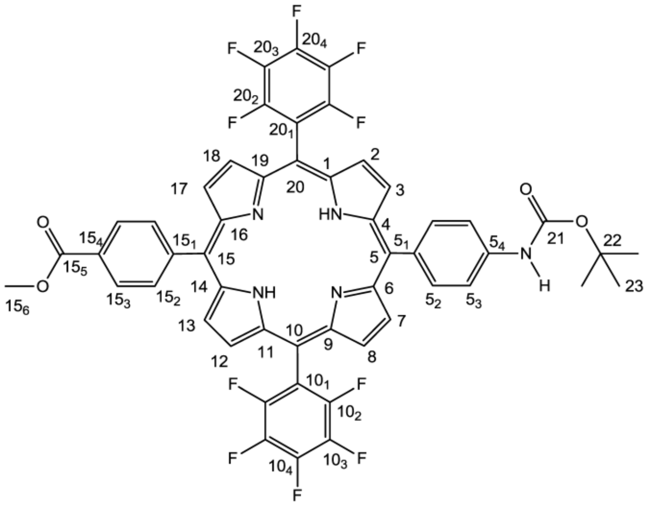

^{1}H-NMR ($CDCl_3$): δ = –2.84 (s, 2 H, $H^{pyrrole\text{-}NH}$), 1.65 (s, 9 H, H^{23}), 4.13 (s, 3 H, $H^{15}{}_6$), 6.86 (s, 1 H, $H^{Boc\text{-}NH}$), 7.81 (d, $^3J_{HH}$ = 8.3 Hz, 2 H, $H^5{}_3$), 8.14 (d, $^3J_{HH}$ = 8.3 Hz, 2 H, $H^5{}_2$), 8.30 (d, $^3J_{HH}$ = 8.1 Hz, 2 H, $H^{15}{}_2$), 8.47 (d, $^3J_{HH}$ = 8.1 Hz, 2 H, $H^{15}{}_3$), 8.81 (pt, $^3J_{HH}$ = 4.5 Hz, 4 H, $H^{pyrrole}$), 8.89 (d, $^3J_{HH}$ = 4.8 Hz, 2 H, $H^{pyrrole}$), 9.00 (d, $^3J_{HH}$ = 4.8 Hz, 2 H, $H^{pyrrole}$) ppm.

^{13}C{^{1}H}-NMR ($CDCl_3$): δ = 28.5 (s, C^{23}), 52.6 (s, $C^{15}{}_6$), 81.1 (s, C^{22}), 116.9 (s, $C^5{}_3$), 119.8 (s, C^{15}), 121.5 (s, C^5), 128.1 (s, $C^{15}{}_3$), 129.8, 132.3, 132.5 ($C^{2,3,7,8,12,13,17,18}$), 130.0 (s, $C^{15}{}_4$), 134.6 (s, $C^{15}{}_2$), 135.2 (s, $C^5{}_2$), 136.3, 138.8, 145.3, 147.8 (4 C), (m, $C^{10}{}_1$, $C^{10}{}_2$, $C^{10}{}_3$, $C^{10}{}_4$), 135.7 (s, $C^5{}_1$), 138.6 (s, $C^5{}_2$), 146.0 (s, $C^{15}{}_1$), 153.0 (s, C^{21}), 167.2 (s, $C^{15}{}_5$) ppm.

^{19}F-NMR ($CDCl_3$): δ = –162.3 (ddd, $^3J_{FF}$ = 23 Hz, $^3J_{FF}$ = 21 Hz, $^5J_{FF}$ = 7 Hz, 4 F, $F^{10/20}{}_{3/3,}$), –152.6 (t, $^3J_{FF}$ = 21 Hz, 2 F, $F^{10/20}{}_{4/4}$), –137.19 (dd, $^3J_{FF}$ = 24 Hz, $^5J_{FF}$ = 8 Hz, 4 F, $F^{10/20}{}_{2/2}$) ppm.

IR (KBr): $\tilde{\nu}$ [cm^{-1}] = 3435 (b w,NH^{Boc}), 3320 (w, $NH^{pyrrole}$), 2928 (w, CH), 2862 (w, CH), 1724 (m, CO), 1708 (m, CO), 1520 (m), 1494 (m), 1282 (m, C-O-C), 1151 (s, CF), 807 (vs).

MS (FD): *m/z* (%) = 866.8 (12) $[M–COOC(CH_3)_3]^+$, 966.7 (100) $[M]^+$.

MS (ESI): *m/z* (%) = 968.24 (100) $[M+H]^+$, 1936.49 (4) $[2M+H]^+$.

HR-MS (ESI): obs. *m/z* = 968.2295; calcd. for $[M+H]^+$ 968.2336.

UV/Vis (CH_2Cl_2): λ [nm] (ε / [10^4 $M^{-1}cm^{-1}$]) = 417 (62.07), 511 (1.56), 545 (1.01), 588 (1.46), 643 (0.68).

Fluorescence (CH_2Cl_2): λ [nm] (relative intensity) = 648 (1.00), 713 (0.50).

Quantum yield: Φ = 0.0377.

CV (Fc/Fc$^+$, 100 mV s^{-1}, CH_2Cl_2): $E_{½}$[V] = –1.820, –1.410, 0.820, 1.020.

15-(4-Carbomethoxyphenyl)-5-(4-aminophenyl)-10,20-bis(2,3,4,5,6-pentafluorophenyl) porphyrin (**3b**). Porphyrin **Boc-3b** (40 mg, 0.041 mmol) was dissolved in 10 mL of CH_2Cl_2 and 10 mL of TFA was added. The solution was stirred at room temperature for 40 min. The solution was neutralised with saturated solution of $NaHCO_3$ and diluted with 10 mL CH_2Cl_2. The organic layer was separated, washed with water (3×), dried with Na_2SO_4 and concentrated under reduced pressure. The yield of **3b** was 95% (33.8 mg, 0.039 mmol, purple powder). $C_{46}H_{23}F_{10}N_5O_2$ (867.69).

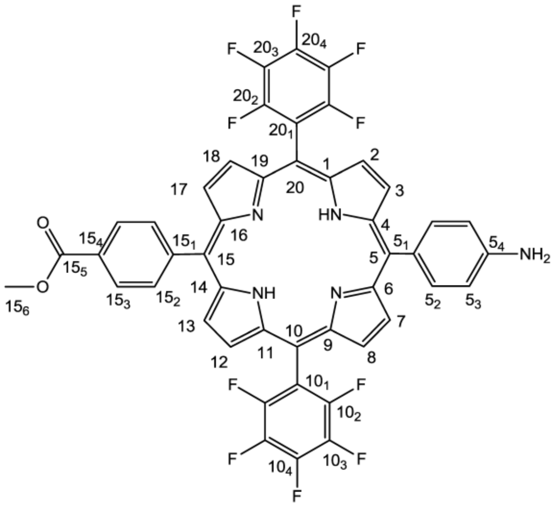

^{1}H-NMR (CDCl$_3$): δ = –2.82 (s, 2 H, $H^{\text{pyrrole-NH}}$), 4.06 (s, 2 H, $H^{\text{amine-NH}}$), 4.10 (s, 3 H, $H^{15}{}_{6}$), 7.08 (d, $^3J_{HH}$ = 8.1 Hz, 2 H, $H^{5}{}_{3}$), 7.97 (d, $^3J_{HH}$ = 8.1 Hz, 2 H, $H^{5}{}_{2}$), 8.28 (d, $^3J_{HH}$ = 8.0 Hz, 2 H, $H^{15}{}_{2}$), 8.44 (d, $^3J_{HH}$ = 8.0 Hz, 2 H, $H^{15}{}_{3}$), 8.76 (pt, $^3J_{HH}$ = 4.5 Hz, 4 H, H^{pyrrole}), 8.85 (d, $^3J_{HH}$ = 4.8 Hz, 2 H, H^{pyrrole}), 9.04 (d, $^3J_{HH}$ = 4.8 Hz, 2 H, H^{pyrrole}) ppm.

^{13}C{^{1}H}-NMR (CDCl$_3$): δ = 113.6 (s, $C^{5}{}_{3}$), 52.5 (s, $C^{15}{}_{6}$), 122.7 (s, C^{5}), 119.5 (s, C^{15}), 128.1 (s, $C^{15}{}_{3}$), 129.6, 132.2, 133.1 ($C^{2,3,7,8,12,13,17,18}$), 130.0 (s, $C^{15}{}_{4}$), 131.2 (s, $C^{5}{}_{1}$), 134.6 (s, $C^{15}{}_{2}$), 135.9 (s, $C^{5}{}_{2}$), 146.1 (s, , $C^{15}{}_{1}$), 146.5 (s, $C^{5}{}_{4}$), 167.2 (s, $C^{15}{}_{5}$) ppm.

^{19}F-NMR (CDCl$_3$): δ = –162.0 (ddd, $^3J_{FF}$ = 23 Hz, $^3J_{FF}$ = 21 Hz, $^5J_{FF}$ = 8 Hz, $F^{10/20}{}_{3/3}$), –152.3 (t, $^3J_{FF}$ = 21 Hz, 2 F, $F^{10/20}{}_{4/4}$), –137.19 (dd, $^3J_{FF}$ = 24 Hz, $^5J_{FF}$ = 8 Hz, 4 F, $F^{10/20}{}_{2/2}$) ppm.

IR (KBr): $\tilde{\nu}$ [cm^{-1}] = 3417 (b m, NH^{amine}), 3314 (w, NH^{pyrrole}), 2919 (w, CH), 2849 (w, CH), 1725 (m, CO), 1614 (m), 1517 (vs), 1496 (vs), 1274 (s, C-O-C), 1108 (s, CF), 990 (vs), 920 (m), 802 (m).

MS (FD): *m/z* (%) = 867.27 (100) $[M]^+$.

MS (ESI): *m/z* (%) = 868.17 (100) $[M+H]^+$.

HR-MS (ESI): obs. *m/z* = 868.1777; calcd. for $[M+H]^+$ 868.1770.

UV/Vis (CH$_2$Cl$_2$): λ [nm] (ε / [10^4 M^{-1}cm^{-1}]) = 419 (73.13), 513 (2.59), 549 (0.95), 590 (0.98), 645 (0.43).

Fluorescence (CH$_2$Cl$_2$): λ [nm] (relative intensity) = 654 (1.00), 717 (0.42).

Quantum yield: Φ = 0.0802.

CV (Fc/Fc$^+$, 100 mV s^{-1}, CH$_2$Cl$_2$): $E_{½}$[V] = –1.82 (qrev.), –1.39 (qrev.), 0.65 (irr.), 0.79 (irr.).

***N*-(4-trifluoromethylbenzoyl)morpholine** was prepared according to the literature.[S4]

***N*-(4-fluorobenzoyl)morpholine** was synthesised according to a general procedure for the preparation of *N*-arylmorpholines[S4]. 33.6 g (0.24 mol) of 4-fluorobenzoic acid was dissolved in 38 mL (0.48 mol) thionyl chloride and heated under reflux overnight. The excess of thionyl chloride was removed under reduced pressure. The residue was dissolved in 100 mL dry CH_2Cl_2 and cooled down to 0°C. A solution of morpholine (60.00 g, 0.70 mol) in 70 ml CH_2Cl_2 was added slowly to the acid chloride solution, so that the temperature remains below 5°C. The colourless suspension was warmed to room temperature and stirred for 10 min. The mixture was washed with water (3×), 2M HCl (3×) and again with water (3×). The organic layer was dried with Na_2SO_4 and the solvent was removed under reduced pressure giving the product as yellow liquid (28.3 g, 0.135 mol, 56%). $C_{11}H_{12}FNO_2$ (209.22).

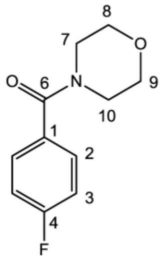

^{1}H-NMR (CDCl$_3$): δ = 3.63 (br. m, 2 H, $H^{7,8,9,10}$), 7.03 (m, $^3J_{HH/FH}$ = 8.6 Hz, 2 H, H^3), 7.69 (dd, $^3J_{HH}$ = 8.4 Hz, $^3J_{FH}$ = 5.4 Hz, 2 H, H^2) ppm.

^{13}C{^{1}H}-NMR (CDCl$_3$): δ = 66.6 (s, $C^{7,8,9,10}$), 115.4 (d, $^2J_{FH}$ = 21.8 Hz, C^3), 129.2 (d, $^3J_{FH}$ = 8.5 Hz, C^2), 131.1 (d, $^4J_{FH}$ = 3.4 Hz, C^1), 163.2 (d, $^1J_{FH}$ = 250.0 Hz, C^4), 169.2 (s, C^6) ppm.

^{19}F-NMR (CDCl$_3$): δ = –110.0 (tt, $^3J_{FH}$ = 8.6 Hz, $^4J_{FH}$ = 5.4 Hz) ppm.

IR (KBr): $\tilde{\nu}$ [cm^{-1}] = 3064 (w, CH), 2967 (w, CH), 2918 (w, CH), 2856 (w, CH), 1635 (vs, CO), 1510 (w), 1433 (s), 1281 (s, C-O-C), 1121 (s), 1108 (s, CF), 837 (s), 754 (s).

MS (FD): *m*/*z* (%) = 209.3 (100) $[M]^+$.

MS (ESI): *m*/*z* (%) = 210.09 (21, $[M]^+$), 210.09 (100, $[M+H]^+$).

HR-MS (ESI): obs. *m*/*z* = 210.0930; calcd. for $[M+H]^+$ 210.0930.

General procedure for the preparation of 1,9-diacyldipyrromethanes.[S4] *N*-aroylmorpholine (1 eq.) and phosphorous oxytrichloride (2 eq.) were heated at 65°C under nitrogen for 3 h. The dark solution was cooled to room temperature and diluted with 1,2-dichloroethane. 5-(4-nitrophenyl)dipyromethane[S6] (0.25 eq.) was added and the solution was stirred under reflux for 2 h and quenched by addition of a saturated aqueous solution of sodium acetate and heated to reflux for 1 h. After cooling to room temperature the mixture was diluted with CH_2Cl_2 and the organic layer was separated. After washing with water (3×) and drying with Na_2SO_4 and the solvent was removed under reduced pressure. The residue was purified by chromatography [silica, CH_2Cl_2/ethyl acetate (15:1), $R_f = 0.60$].

1,9-bis(4-fluorobenzoyl)-5-(4-nitrophenyl)dipyrromethane. 28.30 g, (0.14 mol) *N*-(4-fluorobenzoyl)morpholine, 41.5 g, (0.28 mol) phosphorous oxytrichloride, 200 mL 1,2-dichloroethane, 18.70 (0.07 mol) 5-(4-nitrophenyl)dipyromethane[S6], 150 mL CH_2Cl_2 and 360 mL saturated aqueous solution of sodium acetate. Yield 16.90 g (0.033 mol, 47%), red-brown solid. $C_{29}H_{21}F_2N_3O_4$ (511.49).

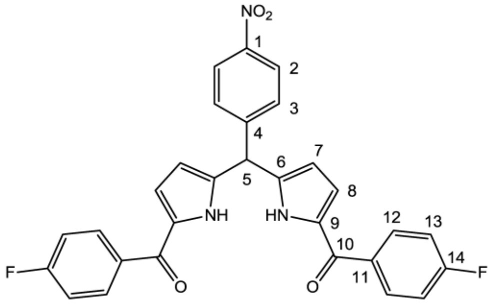

^{1}H-NMR (CDCl$_3$): δ = 5.83 (s, 1H, H^5), 5.93 (ps. t, $^3J_{HH}$ = 3.0 Hz, 2 H, H^7), 6.48 (dd, $^3J_{HH}$ = 3.8 Hz, $^4J_{HH}$ = 2.3 Hz, 2 H, H^8), 7.08 (t, $^3J_{HH}$ = 8.6 Hz, 4 H, H^{13}), 7.74 (dd, $^3J_{HH}$ = 8.8 Hz, $^3J_{HF}$ = 5.4 Hz, 4 H, H^{12}), 7.80 (d, $^3J_{HH}$ = 8.7 Hz, 2 H, H^3), 8.24 (d, $^3J_{HH}$ = 8.7 Hz, 2 H, H^2), 12.18 (br. s, 2 H, NH) ppm.

^{13}C{^{1}H}-NMR (CDCl$_3$): δ = 44.8 (s, C^5), 111.5 (s, C^7), 115.3 (d, $^2J_{FH}$ = 21.7 Hz, C^{13}), 120.8 (s, C^8), 124.1 (s, C^2), 129.8 (s, C^3), 131.1 (s, C^9), 132.0 (d, $^2J_{FH}$ = 9.0 Hz, C^{12}), 133.9 (d, $^4J_{FH}$ = 2.9 Hz, C^{11}), 139.6 (s, C^6), 147.4 (s, C^4), 147.6 (s, C^1), 165.4 (d, $^1J_{FH}$ = 253.9 Hz, C^{14}), 183.2 (s, C^{10}) ppm.

^{19}F-NMR (CDCl$_3$): δ = –106.6 (tt, $^3J_{FH}$ = 8.6 Hz, $^4J_{FH}$ = 5.4 Hz) ppm.

IR (KBr): $\tilde{\nu}$ [cm^{-1}] = 3230 (b, NH), 3099 (w, CH), 1611 (vs), 1600 (vs), 1517 (m, NO), 1476 (vs), 1344 (vs, NO), 1232 (s, C-O-C), 1149 (s, CF), 886 (m), 754 (m).

MS (FD): *m*/*z* (%) = 511.3 (100) [M]$^+$, 255.8 (1.07) [M]$^{2+}$.

MS (ESI): *m*/*z* (%) = 512.14 (16, [M+H]$^+$), 1023.30 (5) [2M+H]$^+$.

HR-MS (ESI): obs. *m*/*z* = 512.1406; calcd. for [M+H]$^+$ 512.1422.

1,9-bis(4-trifluoromethylbenzoyl)-5-(4-nitrophenyl)dipyrromethane. 50.0 g, (0.24 mol) *N*-(4-trifluoromethylbenzoyl)morpholine, 76.7 g, (0.58 mol) phosphorous oxytrichloride, 350 mL 1,2-dichloroethane, 16.0 (0.06 mol) 5-(4-nitrophenyl)dipyromethane[S6], 150 mL CH_2Cl_2 and 360 mL saturated aqueous solution of sodium acetate. Yield 27.0 g (0.044 mol, 74%), red-brown solid. $C_{31}H_{19}F_6N_3O_4$ (611.49).

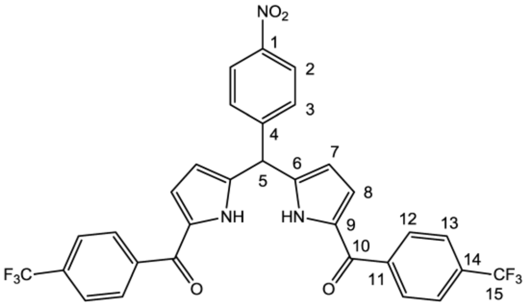

^{1}H-NMR (CDCl$_3$): δ = 5.86 (s, 1H, H^5), 6.03 (m, 2 H, H^7), 6.57 (m, 2 H, H^8), 7.68 (d, $^3J_{HH}$ = 8.0 Hz, 4 H, H^{12}), 7.80 (m, 6 H, $H^{3/13}$), 8.28 (d, $^3J_{HH}$ = 8.5 Hz, 2 H, H^2), 12.09 (s, 2 H, NH) ppm.

^{13}C{^{1}H}-NMR (CDCl$_3$): δ = 44.8 (s, C^5), 112.0 (s, C^7), 121.5 (s, C^8), 122.1 (s, C^{11}), 124.3 (s, C^2), 125.3 (s, C^{12}), 129.8 (s, $C^{3/13}$), 131.1 (s, C^9), 133.6 (q, $^1J_{CF}$ = 32.7 Hz, C^{15}), 140.1 (s, C^6), 140.6 (s, C^{14}), 147.0 (s, C^4), 147.6 (s, C^1), 183.4 (s, C^{10}) ppm.

^{19}F-NMR (CDCl$_3$): δ = –62.9 (s) ppm.

IR (KBr): $\tilde{\nu}$ [cm^{-1}] = 3255 (b, NH), 3107 (w, CH), 1708 (w, CO), 1618 (s), 1528 (m, NO), 1331 (vs, NO), 1249 (w, C-O-C), 1169 (m, CF), 889 (m), 767 (m).

MS (FD): *m*/*z* (%) = 611.22 (100) $[M]^+$.

MS (ESI): *m*/*z* (%) = 610.15 (9, $[M–H]^+$).

HR-MS (ESI): obs. *m*/*z* = 610.1175; calcd. for $[M–H]^+$ 610.1166.

General procedure for the preparation of porphyrins 2c and 2d.[S5] To a stirred solution of 1,9-diacyldipyrromethane in THF/methanol (10 : 1) $NaBH_4$ (20 eq.) was added under nitrogen at room temperature and the mixture was stirred until TLC indicated consumption of starting material. The reaction was quenched with a saturated solution of NH_4Cl_{aq} and diluted with CH_2Cl_2. The organic layer was separated, washed with water (3×) and dried with $NaSO_4$. After removing the solvent the dipyrromethane-dicarbinol was obtained as a foamlike solid. To this brown residue was added 5-(4-benzoic acid methylester)dipyrromethane[S6] (1.2 eq.) and acetonitrile. The suspension was dipped in an ultrasonic bath to dissolve the compounds. This solution was added to a pre-cooled solution of DMF and TFA in acetonitrile (0°C) in small portions over 30 min. After stirring for 10 min 2,3-dicyano-5,6-dichloro-1,4-benzoquinone (DDQ) was added and the mixture was stirred for 1 h. TEA was added to quench the reaction and the mixture was concentrated under reduced pressure. The products were purified by column chromatography [silica, CH_2Cl_2].

4-[15-(4-nitro-phenyl)-10,20-di-(4-fluoro)phenylporphyrin-5-yl]methyl benzoate (2c). 6.81 g (180 mmol) $NaBH_4$, 440 mL THF/methanol (10:1), 9.37 g (0.033 mol) 1,9-bis(4-fluorobenzoyl)-5-(4-nitrophenyl)dipyrromethane, 17.09 g (0.040 mol) 5-(4-methyl benzoate)dipyrromethane, 2 L acetonitrile, 22 mL DMF, 30.8 mL TFA, 28.60 g (0.13 mol) DDQ, 31 mL TEA. [silica, CH_2Cl_2, $R_f = 0.78$]. Yield 2.37 g (3.14 mmol, 9.5%), purple powder. $C_{46}H_{29}F_2N_5O_4$ (753.75).

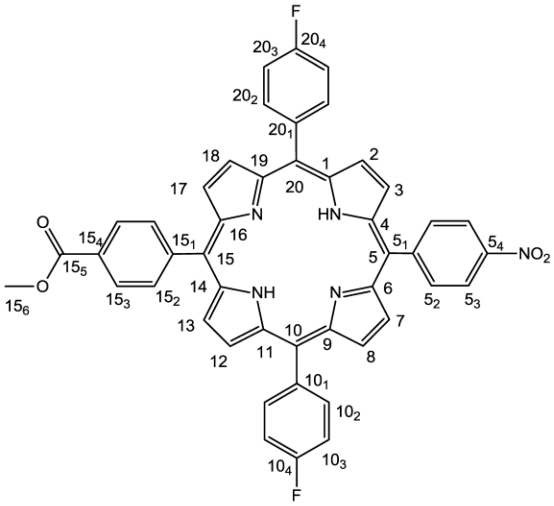

^{1}H-NMR (CDCl$_3$): δ = –2.81 (s, 2 H, $H^{pyrrole\text{-}NH}$), 4.12 (s, 3 H, $H^{15}{}_6$), 7.47 (t, $^3J_{HH}$ = 8.6 Hz, 4 H, $H^{10/20}{}_{3/3}$), 8.17 (dd, $^3J_{HH}$ = 8.4 Hz, $^3J_{HF}$ = 3.1 Hz, 4 H, $H^{10/20}{}_{2/2}$), 8.30 (d, $^3J_{HH}$ = 8.1 Hz, 2 H, $H^{15}{}_2$), 8.39 (d, $^3J_{HH}$ = 8.5 Hz, 2 H, $H^5{}_2$), 8.46 (d, $^3J_{HH}$ = 8.1 Hz, 2 H, $H^{15}{}_3$), 8.65 (d, $^3J_{HH}$ = 8.6 Hz, 2 H, $H^5{}_3$), 8.76 (d, $^3J_{HH}$ = 4.7 Hz, 2 H, $H^{pyrrole}$), 8.85 (m, 6 H, $H^{pyrrole}$) ppm.

^{13}C{^{1}H}-NMR (CDCl$_3$): δ = 52.5 (s, $C^{15}{}_6$), 113.9 (d, $^2J_{CF}$ = 21.3 Hz , $C^{10/20}{}_{3/3}$), 117.4 (s, C^5), 119.6 (s, $C^{10/20}$), 119.6 (s, C^{15}) 121.9 (s, $C^5{}_3$), 128.0 (s, $C^{15}{}_3$), 129.8 (s, $C^{15}{}_4$), 134.5 (s, $C^{15}{}_2$), 131.8 (br. S, $C^{pyrrole}$), 135.1 (s, $C^5{}_2$), 135.7 (d, $^3J_{CF}$ = 8.8 Hz , $C^{10/20}{}_{2/2}$), 137.6 (d, $^4J_{CF}$ = 3.4 Hz, $C^{10/20}{}_{1/1}$), 146.6 (s, $C^{15}{}_1$), 147.4 (s, $C^5{}_1$), 147.8 (s, $C^5{}_4$), 148.9 (s, $C^{pyrrole}$), 165.7 (d, $^1J_{FH}$ = 248.1 Hz, $C^{10/20}{}_{4/4}$), 167.2 (s, $C^{15}{}_5$) ppm.

^{19}F-NMR (CDCl$_3$): δ = –114.2 (tt, $^3J_{FH}$ = 8.6 Hz, $^4J_{FH}$ = 5.4 Hz).

IR (KBr): $\tilde{\nu}$ [cm^{-1}] = 3433 (w, NH), 3315 (w, CH), 1724 (s, CO), 1504 (s), 1525 (s, NO), 1348 (vs, NO), 1282 (s, C-O-C), 1105 (s, CF), 798 (vs).

MS (FD): *m*/*z* (%) = 753.4 (100) [M]$^+$.

MS (ESI): *m*/*z* (%) = 754.25 (100) [M+H]$^+$.

HR-MS (ESI): obs. *m*/*z* = 754.2260; calcd. for [M+H]$^+$ 754.2266.

UV/Vis (CH$_2$Cl$_2$): λ [nm] (ε / [10^4 M^{-1}cm^{-1}]) = 421 (29.55), 517 (1.35),553 (0.58), 592 (0.41), 648 (0.32).

Fluorescence (CH$_2$Cl$_2$): λ [nm] (relative intensity) = 652 (1.00), 716 (0.36).

Quantum yield: Φ = 0.1024.

CV (Fc/Fc$^+$, 100 mV s^{-1}, CH$_2$Cl$_2$): $E_{½}$[V] = –2.150, –1.445 (2e), 0.690, 0.950.

4-[15-(4-nitro-phenyl)-10,20-di-(4-trifluoromethyl)phenylporphyrin-5-yl]methyl benzoate (2d). 1.96 g, (51.80 mmol) NaBH$_4$, 30.8 mL THF/methanol (10:1), 1.00 g (1.64 mmol) 1,9-bis(4- trifluoromethylbenzoyl)-5-(4-nitrophenyl)dipyrromethane, 21.22 g (2.38 mmol) 5-(4-methyl benzoate)dipyrromethane, 568 mL acetonitrile, 2.4 mL DMF, 3.4 mL TFA, 3.12 g (13.74 mmol) DDQ, 3.6 mL TEA. [silica, CH$_2$Cl$_2$, R_f = 0.68]. Yield 308 mg (0.37 mmol, 22%), purple powder. $C_{48}H_{29}F_6N_5O_4$ (853.77).

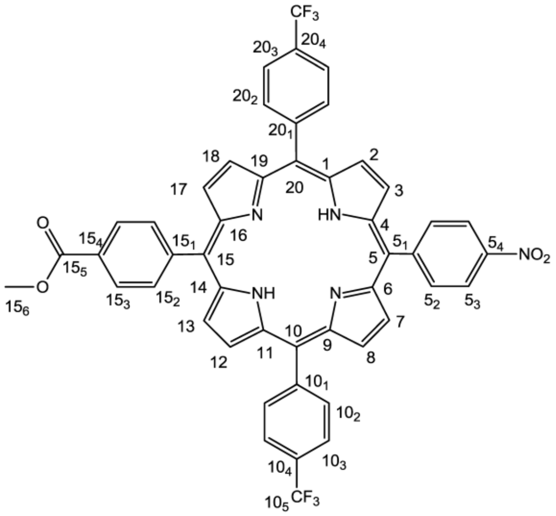

^{1}H-NMR (CDCl$_3$): δ = –2.82 (s, 2 H, $\mathrm{H}^{\text{pyrrole-NH}}$), 4.13 (s, 3 H, $\mathrm{H}^{15}{}_{6}$), 8.05 (d, $^3J_{\mathrm{HH}}$ = 8.0 Hz, 4 H, $\mathrm{H}^{10/20}{}_{3/3}$), 8.30 (d, $^3J_{\mathrm{HH}}$ = 8.1 Hz, 2 H, $\mathrm{H}^{15}{}_{2}$), 8.34 (d, $^3J_{\mathrm{HH}}$ = 8.3 Hz, 4 H, $\mathrm{H}^{10/20}{}_{2/2}$), 8.41 (d, $^3J_{\mathrm{HH}}$ = 8.4 Hz, 2 H, $\mathrm{H}^{5}{}_{2}$), 8.47 (d, $^3J_{\mathrm{HH}}$ = 8.1 Hz, 2 H, $\mathrm{H}^{15}{}_{3}$), 8.66 (d, $^3J_{\mathrm{HH}}$ = 8.5 Hz, 4 H, $\mathrm{H}^{5}{}_{3}$), 8.78 (s, $^3J_{\mathrm{HH}}$ = 4.6 Hz, 2 H, $\mathrm{H}^{\text{pyrrole}}$), 8.91 (m, 4 H, $\mathrm{H}^{\text{pyrrole}}$) ppm.

^{13}C{^{1}H}-NMR (CDCl$_3$): δ = 52.5 (s, $\mathrm{C}^{15}{}_{6}$), 117.6 (d, C^{5}), 119.2 (s, $\mathrm{C}^{10/20}$), 120.0 (s, C^{15}), 122.0 (s, $\mathrm{C}^{5}{}_{3}$), 123.9 (d, $^4J_{\mathrm{CF}}$ = 3.3 Hz, $\mathrm{C}^{10/20}{}_{3/3}$), 125.9 (s, $\mathrm{C}^{10/20}{}_{4/4}$), 128.1 (s, $\mathrm{C}^{15}{}_{3}$), 129.9 (s, $\mathrm{C}^{15}{}_{4}$), 130.6 (q, $^1J_{\mathrm{CF}}$ = 32.6 Hz, $\mathrm{C}^{10/20}{}_{5/5}$), 131.5 (br. s, $\mathrm{C}^{\text{pyrrole 2,3,7,8,12,13,17,18}}$), 134.5 (s, $\mathrm{C}^{15}{}_{2}$), 134.6 (s, $\mathrm{C}^{10/20}{}_{2/2}$), 135.1 (s, $\mathrm{C}^{5}{}_{2}$), 145.4 (s, $\mathrm{C}^{10/20}{}_{1/1}$), 146.4 (s, $\mathrm{C}^{15}{}_{1}$), 147.9 (s, $\mathrm{C}^{5}{}_{4}$), 148.7 (s, $\mathrm{C}^{5}{}_{1}$), 167.2 (s, $\mathrm{C}^{15}{}_{5}$) ppm.

^{19}F-NMR (CDCl$_3$): δ = –62.0 (s) ppm.

IR (KBr): $\tilde{\nu}$ [cm^{-1}] = 3433 (w, NH), 3320 (w, CH), 2925 (w, CH), 2849 (w, CH), 1718 (w, CO), 1504 (s), 1524 (w, NO), 1322 (vs, NO), 1274 (w, C-O-C), 1164 (w, CF), 1066 (s), 796 (vs).

MS (FD): m/z (%) = 853.4 (100) [M$^+$].

MS (ESI): m/z (%) = 854.25 (100) [M+H]$^+$.

HR-MS (ESI): obs. m/z = 854.2200; calcd. for [M+H]$^+$ 854.2202.

UV/Vis (CH$_2$Cl$_2$): λ [nm] (ε / [10^4 M^{-1}cm^{-1}]) = 419 (15.1), 515 (0.42), 549 (0.17), 589 (0.13), 644 (0.07).

Fluorescence (CH$_2$Cl$_2$): λ [nm] (relative intensity) = 650 (1.00), 715 (0.44).

Quantum yield: Φ = 0.0608

CV (Fc/Fc$^+$, 100 mV s^{-1}, CH$_2$Cl$_2$): $E_{½}$[V] = –2.020, –1.470 (2e), 0.750, 1.030.

General procedure for the prepation of porphyrins 3c and 3d[S5]**.** Under nitrogen 1 eq. nitro-porphyrin **2c** or **2d** was suspended in conc. aqueous HCl and $SnCl_2$ (14 eq.) was added. The mixture was stirred under reflux for 1 – 2 h until TLC indicated consumption of starting material. After cooling to room temperature the solution was neutralised with conc. aqueous ammonia and extracted with ethyl acetate. The combined organic phases ware dried with $NaSO_4$ and the solvent was removed under reduced pressure. The products were purified by column chromatography [silica, toluene : ethyl acetate = 20 : 1].

15-(4-Carbomethoxyphenyl)-5-(4-aminophenyl)-10,20-bis-(4-fluorophenyl)porphyrin (3c). 1.00 g (1.33 mmol) porphyrin **1c**, 424 mL conc. aquaeous HCl, 4.33 g (0.019 mol) $SnCl_2$. [silica, toluene : ethyl acetate = 20 : 1, $R_f = 0.36$]. Yield 470 mg (0.65 mmol, 49%), purple powder. $C_{46}H_{31}F_2N_5O_2$ (723.77).

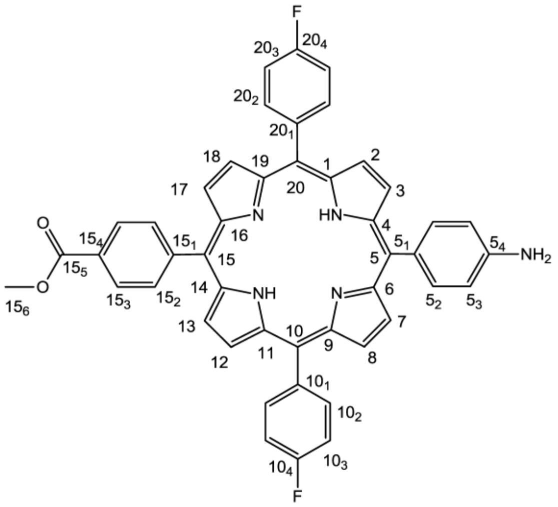

^{1}H-NMR ($CDCl_3$): δ = –2.79 (s, 2 H, $\mathrm{H}^{\text{pyrrole-NH}}$), 4.11 (s, 3 H, $\mathrm{H}^{15}{}_{6}$), 7.02 (d, $^3J_{HH}$ = 8.2 Hz, 2 H, $\mathrm{H}^{5}{}_{3}$), 7.44 (ps. t, $^3J_{HH}$ = 8.6 Hz, 4 H, $\mathrm{H}^{10/20}{}_{3/3}$), 7.99 (d, $^3J_{HH}$ = 8.2 Hz, 2 H, $\mathrm{H}^{5}{}_{2}$), 8.17 (dd, $^3J_{HH}$ = 8.3 Hz, $^3J_{HF}$ = 5.4 Hz, 4 H, $\mathrm{H}^{10/20}{}_{2/2}$), 8.29 (d, $^3J_{HH}$ = 8.1 Hz, 2 H, $\mathrm{H}^{15}{}_{2}$), 8.44 (d, $^3J_{HH}$ = 8.1 Hz, 2 H, $\mathrm{H}^{15}{}_{3}$), 8.80 (m, 6 H, $\mathrm{H}^{\text{pyrrole}}$), 8.96 (d, $^3J_{HH}$ = 8.1 Hz, 2 H, $\mathrm{H}^{\text{pyrrole}}$) ppm.

^{13}C{^{1}H}-NMR ($CDCl_3$): δ = 52.4 (s, $\mathrm{C}^{15}{}_{6}$), 113.5 (s, $\mathrm{C}^{5}{}_{3}$), 113.7 (d, $^2J_{CF}$ = 21.4 Hz , $\mathrm{C}^{10/20}{}_{3/3}$), 118.3 (s, C^{15}), 118.9 (s, $\mathrm{C}^{10/20}$), 121.5 (s, C^{5}), 127.9 (s, $\mathrm{C}^{15}{}_{3}$), 128.5 (s, $\mathrm{C}^{\text{pyrrole}}$), 129.6 (s, $\mathrm{C}^{15}{}_{4}$), 131.0 (br. s, $\mathrm{C}^{\text{pyrrole}}$), 132.1 (s, $\mathrm{C}^{5}{}_{1}$), 134.6 (s, $\mathrm{C}^{15}{}_{2}$), 135.7 (d, $^3J_{CF}$ = 8.8 Hz , $\mathrm{C}^{10/20}{}_{2/2}$), 135.7 (s, $\mathrm{C}^{5}{}_{2}$), 138.0 (d, $^4J_{CF}$ = 3.2 Hz, $\mathrm{C}^{10/20}{}_{1/1}$), 146.2 (s, $\mathrm{C}^{5}{}_{4}$), 146.9 (s, $\mathrm{C}^{15}{}_{1}$), 162.9 (d, $^1J_{FH}$ = 247.3 Hz, $\mathrm{C}^{10/20}{}_{4/4}$), 167.3 (s, $\mathrm{C}^{15}{}_{5}$) ppm.

^{19}F-NMR ($CDCl_3$): δ = –114.7 (tt, $^3J_{FH}$=8.6 Hz, $^4J_{FH}$=5.4 Hz) ppm.

IR (KBr): $\tilde{\nu}$ [cm^{-1}] = 3452 (b, $\mathrm{NH}^{\text{amine}}$), 3386 (b, $\mathrm{NH}^{\text{amine}}$), 3315 (b, $\mathrm{NH}^{\text{pyrrole}}$), 1724 (s, CO), 1504 (s), 1280 (vs, C-O-C), 1155 (s, CF), 802 (vs).

MS (FD): m/z (%) = 723.4 (100) $[M]^+$.

MS (ESI): m/z (%) = 724.2 (100) $[M+H]^+$, 1448.5 (1) $[2M+H]^+$.

HR-MS (ESI): obs. m/z = 724.2522; calcd. for $[M+H]^+$ 724.2524.

UV/Vis (CH_2Cl_2): λ [nm] (ε / [10^4 M^{-1}cm^{-1}]) = 421 (30.42), 517 (1.54), 554 (0.90), 593 (0.51), 649 (0.44).

Fluorescence (CH_2Cl_2): λ [nm] (relative intensity) = 656 (1.00), 719 (0.29).

Quantum yield: Φ = 0.1405.

CV (Fc/Fc$^+$, 100 mV s^{-1}, CH_2Cl_2): $E_{½}$[V] = –1.980, –1.650, 0.51 (irr.).

15-(4-carbomethoxyphenyl)-5-(4-aminophenyl)-10,20-bis-(4-trifluoromethylphenyl) porphyrin (3d). 0.66 g (0.77 mmol) porphyrin **2d**, 100 mL conc. aqueous HCl, 3.00 g (13.2 mmol) $SnCl_2$. [silica, toluene : ethyl acetate = 20 : 1, $R_f = 0.41$]. Yield 310 mg (0.38 mmol, 49%), purple powder. $C_{48}H_{31}F_6N_5O_2$ (823.75).

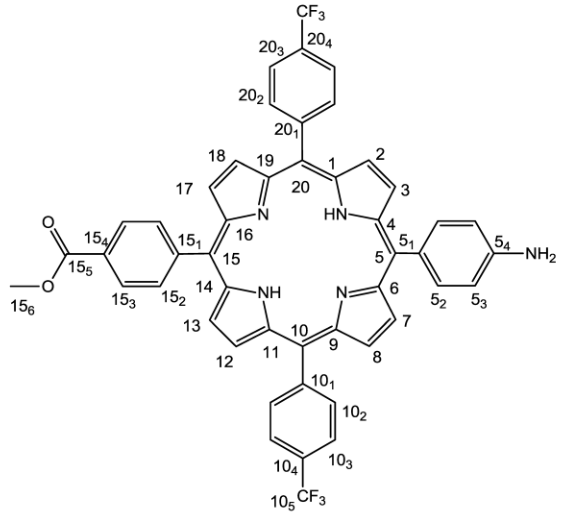

^{1}H-NMR ($CDCl_3$): $\delta = -2.78$ (s, 2 H, $H^{pyrrole\text{-}NH}$), 4.07 (br. s, 2 H, $H^{amine\text{-}NH}$), 4.12 (s, 3 H, $H^{15}{}_6$), 7.09 (d, $^3J_{HH}$ = 8.2 Hz, 2 H, $H^5{}_3$), 7.99 (d, $^3J_{HH}$ = 8.2 Hz, 2 H, $H^5{}_2$), 8.03 (d, $^3J_{HH}$ = 8.0 Hz, 4 H, $H^{10/20}{}_{3/3}$), 8.29 (d, $^3J_{HH}$ = 8.1 Hz, 2 H, $H^{15}{}_2$), 8.34 (d, $^3J_{HH}$ = 7.8 Hz, 4 H, $H^{10/20}{}_{2/2}$), 8.45 (d, $^3J_{HH}$ = 8.1 Hz, 2 H, $H^{15}{}_3$), 8.78 (m, 6 H, $H^{pyrrole}$), 8.98 (d, $^3J_{HH}$ = 4.7 Hz, 2 H, $H^{pyrrole}$) ppm.

^{13}C{^{1}H}-NMR ($CDCl_3$): $\delta = 52.5$ (s, $C^{15}{}_6$), 113.5 (s, $C^5{}_3$), 118.5 (d, $C^{10/20}$), 118.7 (s, C^{15}), 121.9 (s, C^5), 123.7 (d, $^4J_{CF}$ = 3.2 Hz, $C^{10/20}{}_{3/3}$), 125.9 (s, $C^{10/20}{}_{4/4}$), 128.0 (s, $C^{15}{}_3$), 129.7 (s, $C^{15}{}_4$), 130.1 (q, $^1J_{CF}$ = 32.6 Hz, $C^{10/20}{}_{5/5}$), 130.9 (br.s, $C^{2,3,7,8,12,13,17,18}$), 131.9 (s, $C^5{}_1$), 134.6 (s, $C^{10/20/15}{}_{2/2/2}$), 135.7 (s, $C^5{}_2$), 145.8 (s, $C^{10/20}{}_{1/1}$), 146.3 (s, $C^5{}_4$), 146.7 (s, $C^{15}{}_1$), 167.3 (s, $C^{15}{}_5$) ppm.

^{19}F-NMR ($CDCl_3$): $\delta = -62.0$ (s) ppm.

IR (KBr): $\tilde{\nu}$ [cm^{-1}] = 3460 (b, NH^{amine}), 3386 (b, NH^{amine}), 3321 (b, $NH^{pyrrole}$), 1724 (s, CO), 1609 (s), 1315 (vs), 1274 (vs, C-O-C), 1167 (s, CF), 807 (vs).

MS (FD): *m*/*z* (%) = 823.4 (100) $[M]^+$.

MS (ESI): *m*/*z* (%) = 824.30 (100) $[M+H]^+$.

HR-MS (ESI): obs. *m*/*z* = 824.2468; calcd. for $[M+H]^+$ 824.2460.

UV/Vis (CH_2Cl_2): λ [nm] (ε / [10^4 $M^{-1}cm^{-1}$]) = 421 (19.9), 517 (0.38), 553 (0.20), 592 (0.11), 650 (0.10).

Fluorescence (CH_2Cl_2): λ [nm] (relative intensity) = 656 (1.00), 719 (0.28).

Quantum yield: $\Phi = 0.1189$.

CV (Fc/Fc$^+$, 100 mV s^{-1}, CH_2Cl_2): $E_{½}$[V] = –1.900, –1.560, 0.53 (irr.).

[15-(4-Carbomethoxyphenyl)-5-(4-aminophenyl)-10,20-bis-(4-fluorophenyl) porphyrinato]zinc(II) (**Zn-3c**). Porphyrin **3c** (94 mg, 0.13 mmol) and zinc acetate dihydrate (110.2 mg, 0.65 mmol) were stirred overnight in of CH_2Cl_2 (10 mL). After concentration under reduced pressure the product was isolated by column chromatography [silica, toluene : ethyl acetate = 20 : 1, $R_f = 0.36$]. Yield 102 mg (0.13 mmol, 97%), purple powder. $C_{46}H_{29}F_2N_5O_2Zn$ (787.16).

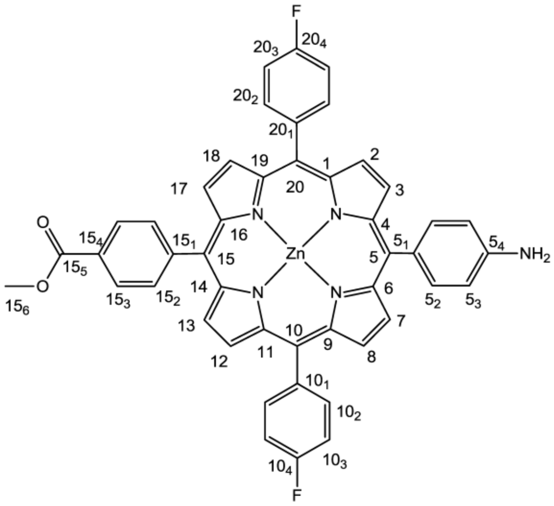

^{1}H-NMR (d$_8$-THF): $\delta = 4.05$ (s, 3 H, $H^{15}{}_6$), 4.90 (s, 2 H, NH_2), 6.96 (d, $^3J_{HH} = 8.1$ Hz, 4 H, $H^5{}_3$), 7.48 (ps. t, $^3J_{HH} = 8.6$ Hz, 4 H, $H^{10/20}{}_{3/3}$), 7.86 (d, $^3J_{HH} = 8.1$ Hz, 2 H, $H^5{}_2$), 8.20 (dd, $^3J_{HH} = 8.1$ Hz, $^3J_{HF} = 5.6$ Hz, 4 H, $H^{10/20}{}_{2/2}$), 8.30 (d, $^3J_{HH} = 8.0$ Hz, 2 H, $H^{15}{}_2$), 8.41 (d, $^3J_{HH} = 8.0$ Hz, 2 H, $H^{15}{}_3$), 8.82 (m, 6 H, $H^{pyrrole}$), 9.00 (d, 2 H, $^3J_{HH} = 4.6$ Hz $H^{pyrrole}$) ppm.

^{13}C{^{1}H}-NMR (d$_8$-THF): $\delta = 52.5$ (s, $C^{15}{}_6$), 113.3 (s, $C^5{}_3$), 114.2 (d, $^2J_{CF} = 21.4$ Hz , $C^{10/20}{}_{3/3}$), 119.7 (s, C^{15}), 120.3 (s, $C^{10/20}$), 123.9 (C^5), 128.5 (s, $C^{15}{}_3$), 130.5 (s, $C^{15}{}_4$), 131.9, 131.9, 132.4, 133.2, (8 C), (s, $C^{pyrrole}{}_{2,3,7,8,12,13,17,18}$), 132.3 (s, $C^5{}_1$), 135.6 (s, $C^{15}{}_2$), 136.5 (s, $C^5{}_2$), 136.8 (d, $^3J_{CF} = 7.9$ Hz, $C^{10/20}{}_{2/2}$), 140.8 (d, $^4J_{CF} = 3.2$ Hz, $C^{10/20}{}_{1/1}$), 149.2 (s, $C^5{}_4$), 149.5 (s, $C^{15}{}_1$), 150.6, 151.0, 151.3, 152.2 (8 C), (s, $C^{1,4,6,9,11,14,16,19}$), 163.9 (d, $^1J_{FH} = 245.6$ Hz, $C^{10/20}{}_{4/4}$), 167.5 (s, $C^{15}{}_5$) ppm.

^{19}F-NMR (d$_8$-THF): $\delta = -118.7$ (m, $^3J_{FH}$=8.6 Hz, $^4J_{FH}$=5.4 Hz).

IR (KBr): $\tilde{\nu}$ [cm^{-1}] = 3438 (b, NH^{amine}), 3386 (b, NH^{amine}), 2918 (w, CH), 2849 (w, CH), 1725 (vs, CO), 1607 1503 (m), 1274 (vs, C-O-C), 1156 (s, CF), 1109 (m), 802 (s).

MS (FD): m/z (%) = 785.4 (100) $[M]^+$.

MS (ESI): m/z (%) = 785.17 (100) $[M]^+$.

HR-MS (ESI): obs. m/z = 785.1579; calcd. for $[M]^+$ 785.1581.

UV/Vis (CH_2Cl_2): λ [nm] (ε / [10^4 M^{-1}cm^{-1}]) = 424 (38.11), 551 (2.00), 593 (0.53).

Fluorescence (CH_2Cl_2): λ [nm] (relative intensity) = 606 (1.00), 652 (0.63).

Quantum yield: $\Phi = 0.0194$.

CV (Fc/Fc$^+$, 100 mV s^{-1}, CH_2Cl_2): $E_{½}$[V] = –2.060, –1.730, 0.415 (irr.).

[10,20-Bis(2,4,6-trimethylphenyl)-5,15-bis[4-(methoxycarbonyl)] porphyrinato]zinc(II) (Zn-1a). Porphyrin **1a** (35 mg, 0.042 mmol) and zinc acetate dihydrate (46.67 mg, 0.21 mmol) were stirred overnight in CH_2Cl_2 (5 mL). After concentration under reduced pressure the product was isolated by column chromatography [silica, CH_2Cl_2, $R_f = 0.80$]. Yield 30 mg (0.034 mmol, 81%), purple powder. $C_{54}H_{44}N_4O_4Zn$ (878.35).

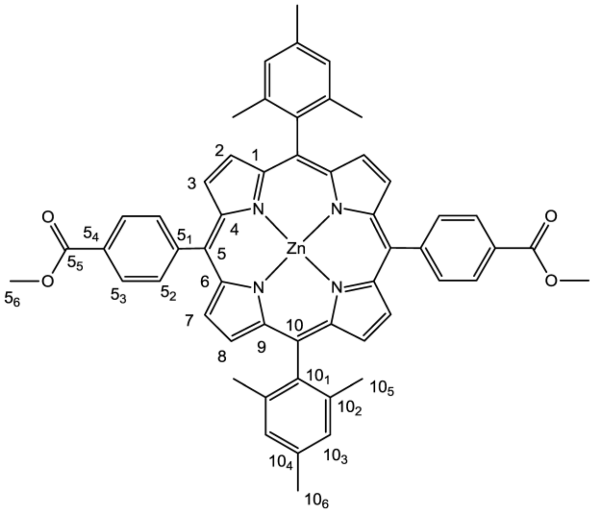

^{1}H-NMR (d_8-THF): δ = 1.84 (s, 12 H, $H^{10}{}_{5}$), 2.61 (s, 6 H, $H^{10}{}_{6}$), 4.04 (s, 6 H, $H^{5}{}_{6}$), 7.30 (s, 4 H, $H^{10/20}{}_{3/3}$), 8.31 (d, $^3J_{HH}$ = 6.8 Hz, 4 H, $H^{5}{}_{2}$), 8.39 (d, $^3J_{HH}$ = 7.9 Hz, 4 H, $H^{5}{}_{3}$), 8.68 (d, $^3J_{HH}$ = 4.4 Hz, 4 H, $H^{pyrrole}$), 8.75 (d, $^3J_{HH}$ = 4.3 Hz, 4 H, $H^{pyrrole}$) ppm.

^{13}C{^{1}H}-NMR (d_8-THF): δ = 21.7 (s, $C^{10/20}{}_{6/6}$), 22.1 (s, $C^{10/20}{}_{5/5}$), 52.5 (s, $C^{5}{}_{6}$), 119.9 (s, C^{5}), 128.4 (s, $C^{5}{}_{3}$), 128.7 (s, $C^{10/20}{}_{3/3}$), 130.5 ($C^{5}{}_{4}$), 131.3, 132.6 ($C^{2,3,7,8,12,13,17,18}$), 135.5 (s, $C^{5}{}_{2}$), 138.4 ($C^{10/20}{}_{4/4}$), 140.0 ($C^{10/20}{}_{2/2}$), 140.7 ($C^{10/20}{}_{1/1}$), 149.4 ($C^{5}{}_{1}$), 150.5, 150.9 ($C^{1,4,6,9,11,14,16,19}$), 167.5 (s, $C^{5}{}_{5}$) ppm.

IR (KBr): $\tilde{\nu}$ [cm^{-1}] = 3425 (b, NH^{pyrrole}), 2922 (w, CH), 2850 (w, CH), 1722 (vs, CO), 1608 (s), 1386 (vs), 1278 (vs, C-O-C), 1114 (s), 800 (w).

MS (ESI): *m*/*z* (%) = 877.33 (29) [M+H]$^+$.

HR-MS (ESI): obs. *m*/*z* = 877.2725; calcd. for [M]$^+$ 877.2732.

UV/Vis (CH_2Cl_2): λ [nm] (ε / [10^4 M^{-1}cm^{-1}]) = 421 (44.4), 548 (1.88), 590 (0.36).

Fluorescence (CH_2Cl_2): λ [nm] (relative intensity) = 598 (0.97), 647(1.00).

Quantum yield: Φ = 0.1001.

Lifetime: τ [ns] = 2.53 (100%).

CV (Fc/Fc$^+$, 100 mV s^{-1}, CH_2Cl_2): $E_{½}$[V] = –2.150, –1.780, 0.439, 0.739.

General procedure for *N*-acylation[S7]**:** To a mixture of the amino porphyrin (1 eq.) and acetyl chloride (35 eq.) iodine (1 eq.) was added and the mixture was stirred at room temperature over night. The iodine was destroyed by addition of a saturated aqueous $Na_2S_2O_3$ solution. CH_2Cl_2 was added and the organic phase was separated, washed with saturated aqueous $NaHCO_3$ solution (2×), brine (1×), water (2×) and dried with Na_2SO_4. The solvent was removed under reduced pressure and the residue was filtered over a silica pad.

5-(4-(*N*-Acetylaminophenyl))-10,20-bis(2,4,6-trimethylphenyl)-15-(4-(methoxycarbonyl-phenyl)) porphyrin (Ac-3a). 40.0 mg (0.052 mmol) Porphyrin **3a**, 12.9 mL (0.182 mol) acetyl chloride, 13.1 mg (0.052 mmol) iodine. [silica, toluene : ethyl acetate = 1 : 1, R_f = 0.38]. Yield: 34 mg (0.042 mmol, 81%), purple powder. $C_{54}H_{47}N_5O_3$ (813.98).

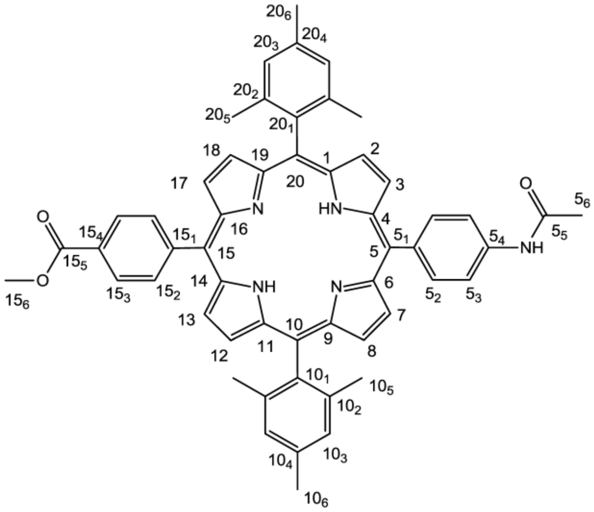

^{1}H-NMR (d_8-THF): δ = –2.50 (s, 2 H, $H^{\text{pyrrole-NH}}$), 1.83 (s, 12 H, $H^{10/20}{}_{5/5}$), 2.19 (s 3H, $H^{5}{}_{6}$), 2.59 (s, 6 H, $H^{10/20}{}_{6/6}$), 4.04 (s, 3 H, $H^{15}{}_{6}$), 7.30 (s, 4 H, $H^{10/20}{}_{3/3}$), 8.03 (d, $^3J_{HH}$ = 8.4 Hz, 2 H, $H^{5}{}_{3}$), 8.10 (d, 2 H, $^3J_{HH}$ = 8.4 Hz, $H^{5}{}_{2}$), 8.32 (d, $^3J_{HH}$ = 8.2 Hz, 2 H, $H^{15}{}_{2}$), 8.41 (d, $^3J_{HH}$ = 8.1 Hz, 2 H, $H^{15}{}_{3}$), 8.66 (ps. t, $^3J_{HH}$ = 4.5 Hz, 4 H, H^{pyrrole}), 8.74 (d, $^3J_{HH}$ = 4.6 Hz, 2 H, H^{pyrrole}), 8.84 (d, $^3J_{HH}$ = 4.6 Hz, 2 H, H^{pyrrole}), 9.40 (s, 1 H, $H^{\text{amide-NH}}$) ppm.

^{13}C{^{1}H}-NMR (d_8-THF): δ = 21.2 (s, $C^{10/20}{}_{5/5}$), 21.7 (s, $C^{10/20}{}_{6/6}$), 24.4 (s, $C^{5}{}_{6}$), 52.5 (s, $C^{15}{}_{6}$), 118.2 (s, $C^{5}{}_{3}$), 119.0 (s, C^{15}), 119.3 (s, $C^{10/20}$), 121.1 (C^{5}), 128.8 (s, $C^{15}{}_{3}$), 128.9 (s, $C^{10/20}{}_{3/3}$), 130.9 ($C^{15}{}_{4}$), 135.6 ($C^{5}{}_{2}$), 135.7 (s, $C^{15}{}_{2}$), 137.4, ($C^{5}{}_{1}$), 138.8 (s, $C^{10/20}{}_{4/4}$), 139.6 (s, $C^{10/20}{}_{2/2}$), 140.1 (s, $C^{10/20}{}_{1/1}$), 141.0 ($C^{5}{}_{4}$) 148.0 (s, $C^{15}{}_{1}$), 167.4 (s, $C^{15}{}_{5}$) 168.8 (s, $C^{5}{}_{5}$) ppm.

IR (KBr): $\tilde{\nu}$ [cm^{-1}] = 3406 (b, NH^{pyrrole}, NH^{amide}), 2954 (m, CH), 2921 (m, CH), 1723 (s, CO), 1702 (s, CO), 1513 (vs), 1381 (m), 1276 (vs, C-O-C), 968 (m).

MS (FD): *m*/*z* (%) = 814.2 (100) $[M]^+$.

MS (ESI): *m*/*z* (%) = 407.69 (2) $[M+H]^{2+}$, 814.37 (100) $[M]^+$.

HR-MS (ESI): obs. *m*/*z* = 814.3725; calcd. for $[M+H]^+$ 814.3757.

UV/Vis (CH_2Cl_2): λ [nm] (ε / [10^4 M^{-1}cm^{-1}]) = 420 (36.29), 516 (1.24), 550 (0.37), 593 (0.28), 652 (0.55).

Fluorescence (CH_2Cl_2): λ [nm] (relative intensity) = 654 (1.00), 718 (0.21).

Quantum yield: Φ = 0.0778.

Lifetime: τ [ns] = 10.90 (100%).

CV (Fc/Fc$^+$, 100 mV s^{-1}, CH_2Cl_2): $E_{½}$[V] = –2.060, –1.710, 0.540, 0.960.

5-(4-(*N*-Acetylaminophenyl))- 10,20-bis(2,3,4,5,6-pentafluorophenyl)-15-(4-(methoxycarbonyl-phenyl)) porphyrin (Ac-3b). 27.5 mg (0.046 mmol) Porphyrin **3b**, 11.4 mL (0.159 mol) acetyl chloride, 5.8 mg (0.046 mmol) iodine. [silica, toluene : ethyl acetate = 1 : 1, R_f = 0.32]. Yield: 27 mg (0.030 mmol, 65%), purple powder. $C_{48}H_{25}F_{10}N_5O_3$ (909.73).

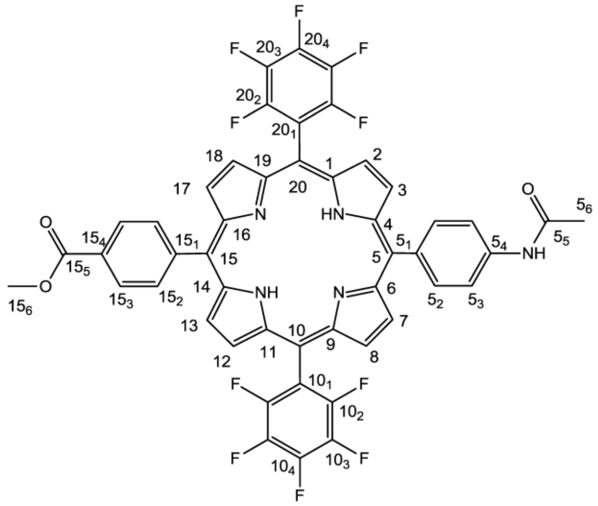

^{1}H-NMR (d_8-THF): δ = –2.78 (s, 2 H, $\mathrm{H^{pyrrole\text{-}NH}}$), 2.21 (s, 3H, $\mathrm{H^{5}{}_{6}}$), 4.05 (s, 3 H, $\mathrm{H^{15}{}_{6}}$), 8.08 (m, 2 H, $^3J_{HH}$ = 8.3 Hz $\mathrm{H^{5}{}_{3}}$), 8.14 (d, 2 H, $^3J_{HH}$ = 8.3 Hz, $\mathrm{H^{5}{}_{2}}$), 8.36 (d, 2 H, $^3J_{HH}$ = 8.0 Hz, $\mathrm{H^{15}{}_{2}}$), 8.46 (d, 2 H, $^3J_{HH}$ = 8.0 Hz, $\mathrm{H^{15}{}_{3}}$), 8.91 (d, 2 H, $^3J_{HH}$ = 4.5 Hz, $\mathrm{H^{pyrrole}}$), 9.01 (m, 6 H, $\mathrm{H^{pyrrole}}$), 9.43 (s, 1 $\mathrm{H^{amide\text{-}NH}}$) ppm.

^{13}C{^{1}H}-NMR (d_8-THF): δ = 24.4 ($\mathrm{C^{5}{}_{6}}$), 52.6 ($\mathrm{C^{15}{}_{6}}$), 118.2 ($\mathrm{C^{5}{}_{3}}$), 120.9 ($\mathrm{C^{15}}$), 122.9 ($\mathrm{C^{5}}$), 129.0 ($\mathrm{C^{15}{}_{3}}$), 131.0 (8 C) (br. s, $\mathrm{C^{2/3/7/8/12/13/17/18}}$), 131.3 ($\mathrm{C^{15}{}_{4}}$), 135.6 ($\mathrm{C^{15}{}_{2}}$), 135.9 ($\mathrm{C^{5}{}_{2}}$), 136.7 ($\mathrm{C^{5}{}_{1}}$),141.4 ($\mathrm{C^{5}{}_{4}}$), 137.7, 140.2, 146.6, 149.1 (m, $\mathrm{C^{10/20}{}_{1/1/2/2/3/3/4/4}}$), 147.2 ($\mathrm{C^{15}{}_{1}}$), 167.3 ($\mathrm{C^{15}{}_{5}}$), 168.9 ($\mathrm{C^{5}{}_{5}}$) ppm.

^{19}F-NMR (d_8-THF): δ = –166.7 (ddd, $^3J_{FF}$ = 23 Hz, $^3J_{FF}$ = 21 Hz, $^5J_{FF}$ = 8 Hz, 4 F, $\mathrm{F^{10/20}{}_{3/3,}}$), –157.8 (t, $^3J_{FF}$ = 21 Hz, 2 F, $\mathrm{F^{10/20}{}_{4/4}}$), –141.3 (dd, $^3J_{FF}$ = 24 Hz, $^5J_{FF}$ = 8 Hz, 4 F, $\mathrm{F^{10/20}{}_{2/2}}$) ppm.

IR (KBr): $\tilde{\nu}$ [cm^{-1}] = 3417 (b, $\mathrm{NH^{amide}}$, $\mathrm{NH^{pyrrole}}$), 2924 (w, CH), 1719 (m, CO), 1699 (m, CO), 1518 (vs), 1496 (vs), 1276 (m), 1109 (w, CF), 1044 (w, CF), 1037 (w, CF), 987 (vs), 918 (s).

MS (FD): *m*/*z* (%) = 909.67 (100) $[M]^+$.

MS (ESI): *m*/*z* (%) = 910.21 (100) $[M]^+$, 1820.41 (49) $[2M+H]^+$.

HR-MS (ESI): obs. *m*/*z* = 910.1898; calcd. for $[M+H]^+$ 910.1876.

UV/Vis (CH_2Cl_2): λ [nm] (ε / [10^4 M^{-1}cm^{-1}]) = 418 (39.31), 512 (2.38), 545 (0.84), 587 (0.93), 642 (0.56).

Fluorescence (CH_2Cl_2): λ [nm] (relative intensity) = 647 (1.00), 713 (0.50).

Quantum yield: Φ = 0.0696.

Lifetime: τ [ns] = 9.83 (100%)

CV (Fc/Fc$^+$, 100 mV s^{-1}, CH_2Cl_2): $E_{1/2}$[V] = –1.810, –1.410, 0.820, 1.030

5-(4-(*N*-Acetylaminophenyl))-10,20-bis(4-fluorophenyl)-15-(4-(methoxycarbonylphenyl)) porphyrin (Ac-3c). 33.0 mg (0.046 mmol) Porphyrin **3c**, 11.4 mL (0.159 mol) acetyl chloride, 5.8 mg (0.046 mmol) iodine. [silica, toluene : ethyl acetate = 1 : 1, $R_f = 0.35$]. Yield: 24 mg (0.031 mmol, 70%), purple powder. $C_{48}H_{33}F_2N_5O_3$ (765.80).

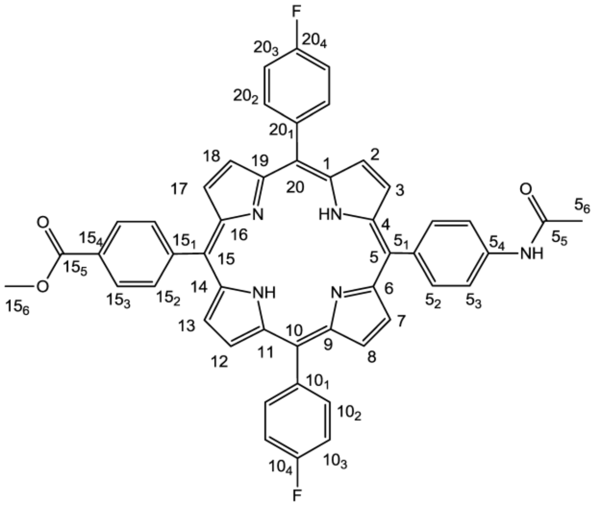

^{1}H-NMR (d$_8$-THF): δ = –2.71 (s, 2 H, $H^{pyrrole\text{-}NH}$), 2.21 (s, 3 H, $H^5{}_6$), 4.05 (s, 3 H, $H^{15}{}_6$), 7.53 (t, $^3J_{HH}$ = 8.6 Hz, 4 H, $H^{10/20}{}_{3/3}$), 8.06 (d, $^3J_{HH}$ = 8.4 Hz, 2 H, $H^5{}_3$), 8.10 (d, $^3J_{HH}$ = 8.4 Hz, 2 H, $H^5{}_2$), 8.21 (dd, $^3J_{HH}$ = 7.9 Hz, $^3J_{HF}$ = 2.3 Hz, 4 H, $H^{10/20}{}_{2/2}$), 8.32 (d, $^3J_{HH}$ = 8.0 Hz, 2 H, $H^{15}{}_2$), 8.44 (d, $^3J_{HH}$ = 7.9 Hz, 2 H, $H^{15}{}_3$), 8.82 (m, 6 H, $H^{pyrrole}$), 8.91(d, $^3J_{HH}$ = 4.3 Hz, 2 H, $H^{pyrrole}$), 9.46 (s, 1 H, $H^{amide\text{-}NH}$) ppm.

^{13}C{^{1}H}-NMR (d$_8$-THF): δ = 24.4 (s, $C^5{}_6$), 52.6 (s, $C^{15}{}_6$), 114.7 (d, $^2J_{CF}$ = 21.6 Hz , $C^{10/20}{}_{3/3}$), 118.1 (s, $C^5{}_3$), 119.7 (s, C^{15}), 120.1 (s, $C^{10/20}$), 121.8 (s, C^5), 128.9 (s, $C^{15}{}_3$), 131.0 (s, $C^{15}{}_4$), 131.9 (br. s $C^{pyrrole}$), 135.6 (s, $C^{15}{}_2$), 135.8 (s, $C^5{}_2$), 136.9 (d, $^3J_{CF}$ = 8.1 Hz, $C^{10/20}{}_{2/2}$), 137.5 (s, $C^5{}_1$), 139.4 (d, $^4J_{CF}$ = 3.1 Hz, $C^{10/20}{}_{1/1}$), 141.1 (s, $C^5{}_4$), 148.0 (s, $C^{15}{}_1$), 164.1(d, $^1J_{FH}$ = 246.5 Hz, $C^{10/20}{}_{4/4}$), 167.4 (s, $C^{15}{}_5$), 168.9 (s, $C^5{}_5$) ppm.

^{19}F-NMR (d$_8$-THF): δ = –117.7 (tt, $^3J_{FH}$ = 8.6 Hz, $^4J_{FH}$ = 5.4 Hz) ppm.

IR (KBr): $\tilde{\nu}$ [cm^{-1}] = 3419 (b, NH^{amide}), 3321 (w, $NH^{pyrrole}$), 2927 (w, CH), 2853 (w, CH), 1715 (m, CO), 1593 (m), 1503 (m), 1282 (m, C-O-C), 1151 (s, CF), 800 (vs).

MS (FD): *m*/*z* (%) = 765.2 (100) $[M]^+$.

MS (ESI): *m*/*z* (%) = 766.26 (100) $[M+H]^+$.

HR-MS (ESI): obs. *m*/*z* = 766.2621; calcd. for $[M+H]^+$ 766.2630.

UV/Vis (CH$_2$Cl$_2$): λ [nm] (ε / [10^4 M^{-1}cm^{-1}]) = 419 (50.42), 515 (2.16), 551 (1.07), 591 (0.72), 647 (0.61).

Fluorescence (CH$_2$Cl$_2$): λ [nm] (relative intensity) = 652 (1.00), 717 (0.32).

Quantum yield: Φ = 0.1003.

Lifetime: τ [ns] = 9.64 (100%).

CV (Fc/Fc$^+$, 100 mV s^{-1}, CH$_2$Cl$_2$): $E_{½}$[V] = –1.920, –1.590, 0.590, 0.870.

5-(4-(*N*-Acetylaminophenyl))-10,20-bis((4-trifluoromethyl)phenyl)-15-(4-(methoxycarbonylphenyl)) porphyrin (Ac-3d). 50.0 mg (0.069 mmol) Porphyrin **3d**, 17.2 mL (0.240 mol) acetyl chloride, 8.8 mg (0.069 mmol) iodine. [silica, toluene : ethyl acetate = 1 : 1, R_f = 0.45]. Yield: 40 mg (0.046 mmol, 67%), purple powder. $C_{50}H_{33}F_6N_5O_3$ (865.82).

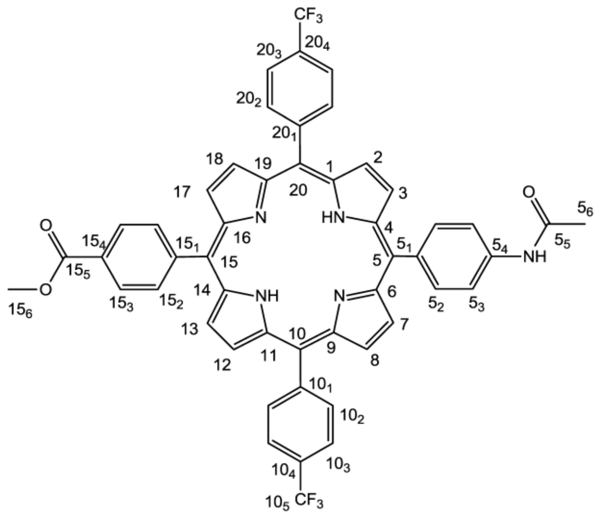

^{1}H-NMR (d$_8$-THF): δ = –2.71 (s, 2 H, $H^{pyrrole\text{-}NH}$), 2.21 (s, 3 H, H^{5}_{6}), 4.05 (s, 3 H, H^{15}_{6}), 8.08 (m, 4 H, $H^{5/5}_{2/3}$), 8.11 (d, $^3J_{HH}$ = 8.1 Hz, 4 H, $H^{10/20}_{3/3}$), 8.32 (d, $^3J_{HH}$ = 8.1 Hz, 2 H, H^{15}_{2}), 8.41 (d, $^3J_{HH}$ = 7.9 Hz, 4 H, $H^{10/20}_{2/2}$), 8.44 (d, $^3J_{HH}$ = 8.1 Hz, 2 H, H^{15}_{3}), 8.81 (m, 6 H, $H^{pyrrole}$), 8.93 (d, $^3J_{HH}$ = 4.5, 2 H, $H^{pyrrole}$), 9.45 (s, 1 H, $H^{amide\text{-}NH}$) ppm.

^{13}C{^{1}H}-NMR (d$_8$-THF): δ = 23.2 (s, C^{5}_{6}), 52.7 (s, C^{15}_{6}), 118.3 (s, C^{5}_{3}), 119.8 (s, $C^{10/20}$), 120.2 (s, C^{15}), 122.3 (s, C^{5}), 124.8 (s, $C^{10/20}_{4/34}$), 124.9 (d, $^4J_{CF}$ = 3.3 Hz, $C^{10/20}_{3/3}$), 127.5 (s, $C^{10/20}_{4/4}$), 129.0 (s, C^{15}_{3}), 130.4 (q, $^1J_{CF}$ = 32.2 Hz, $C^{10/20}_{5/5}$), 131.2 (s, C^{15}_{4}), 132.1 (br. s, $C^{2,3,7,8,12,13,17,18}$), 135.7 (s, C^{15}_{2}), 136.0 (m, $C^{5/10/20}_{2/2/2}$), 137.4 (s, C^{5}_{1}), 141.3 (s, C^{5}_{4}), 147.4 (s, $C^{10/20}_{1/1}$), 147.9 (s, C^{15}_{1}), 167.5 (s, C^{15}_{5}), 169.0 (s, C^{5}_{5}) ppm.

^{19}F-NMR (d$_8$-THF): δ = –65.0 (s).

IR (KBr): $\tilde{\nu}$ [cm^{-1}] = 3419 (b, NH^{amide}), 3321 (w, $NH^{pyrrole}$), 2952 (w, CH), 1724 (s, CO), 1609 (m), 1511 (m), 1282 (s, C-O-C), 1127 (s, CF), 808 (s).

MS (FD): *m*/*z* (%) = 865.6 (100) $[M]^+$.

MS (ESI): *m*/*z* (%) = 866.27 (100) $[M+H]^+$.

HR-MS (ESI): obs. *m*/*z* = 866.2566; calcd. for $[M+H]^+$ 866.2563.

UV/Vis (CH$_2$Cl$_2$): λ [nm] (ε / [10^4 M^{-1}cm^{-1}]) = 419 (41.4), 515 (1.78), 550 (0.79), 590 (0.57), 646 (0.40).

Fluorescence (CH$_2$Cl$_2$): λ [nm] (relative intensity) = 650 (1.00), 716 (0.36).

Quantum yield: Φ = 0.1080.

Lifetime: τ [ns] = 9.98 (100%).

CV (Fc/Fc$^+$, 100 mV s^{-1}, CH$_2$Cl$_2$): $E_{½}$[V] = –1.900, –1.550, 0.640, 0.890.

[5-(4-(*N*-Acetylaminophenyl))-10,20-bis(2,4,6-trimethylphenyl)-15-(4-(methoxycarbonyl-phenyl)) porphyrinato]zinc(II) (Zn-Ac-3a). Porphyrin **Ac-3a** (25 mg, 0.031 mmol) and zinc acetate dihydrate (34 mg, 0.15 mmol) were stirred overnight in CH_2Cl_2 (5 mL). After concentration under reduced pressure the product was isolated by column chromatography [silica, toluene : ethyl acetate = 1 : 1, R_f = 0.50]. Yield 23 mg (0.026 mmol, 85%), purple powder. $C_{54}H_{45}N_5O_3Zn$ (877.35).

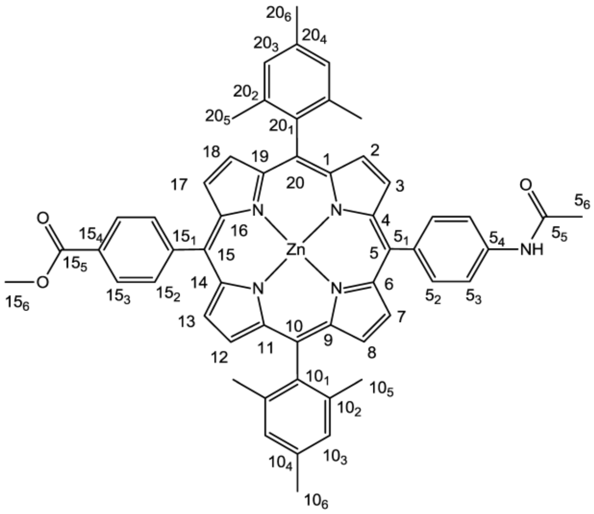

^{1}H-NMR (d$_8$-THF): δ = 1.85 (s, 12 H, H$^{10/20}_{5/5}$), 2.20 (s 3H, H$^{5}_{6}$), 2.61 (s, 6 H, H$^{10/20}_{6/6}$), 4.04 (s, 3 H, H$^{15}_{6}$), 7.29 (s, 4 H, H$^{10/20}_{3/3}$), 8.00 (d, $^{3}J_{HH}$ = 8.2 Hz, 2 H, H$^{5}_{3}$), 8.10 (d, 2 H, $^{3}J_{HH}$ = 8.4 Hz, H$^{5}_{2}$), 8.31 (d, $^{3}J_{HH}$ = 8.2 Hz, 2 H, H$^{15}_{2}$), 8.39 (d, $^{3}J_{HH}$ = 8.0 Hz, 2 H, H$^{15}_{3}$), 8.66 (ps. t, $^{3}J_{HH}$ = 4.6 Hz, 4 H, H^{pyrrole}), 8.74 (d, $^{3}J_{HH}$ = 4.6 Hz, 2 H, H^{pyrrole}), 8.84 (d, $^{3}J_{HH}$ = 4.6 Hz, 2 H, H^{pyrrole}), 9.38 (s, 1 H, H$^{amide\text{-}NH}$) ppm.

^{13}C{^{1}H}-NMR (d$_8$-THF): δ = 21.7 (s, C$^{10/20}_{6/6}$), 22.1 (s, C$^{10/20}_{5/5}$), 24.4 (s, C$^{5}_{6}$), 52.5 (s, C$^{15}_{6}$), 117.6 (C$^{5}_{3}$), 119.4 (s, C^{15}) 119.6 (C$^{10/20}$), 121.4 (s, C^{5}), 128.4 (s, C$^{15}_{3}$), 128.7 (s, C$^{10/20}_{3/3}$), 130.4 (s, C$^{15}_{4}$), 130.9, 131.2, 132.4, 133.3 (s, C^{2,3,7,8,12,13,17,18}), 135.6 (s, C$^{15}_{2}$), 135.6 (s, C$^{5}_{2}$), 138.3 (s, C$^{5}_{1}$), 140.0 (s, C$^{10/20}_{2/2}$), 140.6 (s, C$^{5}_{4}$), 140.8 (s, C$^{10/20}_{1/1}$), 149.6 (s, C$^{15}_{1}$), 150.4, 150.7, 150.9, 151.3 (s, C^{1,4,6,9,11,14,16,19}), 167.5 (s, C$^{15}_{5}$), 168.7 (s, C$^{5}_{5}$) ppm.

IR (KBr): $\tilde{\nu}$ [cm^{-1}] = 3404 (b, NH^{amide}), 2922 (w, CH), 2853 (w, CH), 1732 (m, CO), 1668 (m, CO), 1495 (m), 1398 (m), 1278 (s), 995 (vs), 798 (m).

MS (FD): *m*/*z* (%) = 875.79 (100) [M]$^{+}$.

MS (ESI): *m*/*z* (%) = 875.31 (88), 877.31 (100), 879.31 (68), [M]$^{+}$.

HR-MS (ESI): obs. *m*/*z* = 877.2823; calcd. for [M]$^{+}$ 875.2814.

UV/Vis (CH_2Cl_2): λ [nm] (ε / [10^{4} M^{-1}cm^{-1}]) = 423 (45.12), 551 (1.92), 592 (0.45).

Fluorescence (CH_2Cl_2): λ [nm] (relative intensity) = 604 (1.00), 652 (0.99).

Quantum yield: Φ = 0.1343.

Lifetime: τ [ns] = 2.17 (100%).

CV (Fc/Fc^{+}, 100 mV s^{-1}, CH_2Cl_2): $E_{½}$[V] = –1.860, 0.335, 0.750.

[5-(4-(*N*-Acetylaminophenyl))-10,20-bis(2,3,4,5,6-pentafluorophenyl)-15-(4-(methoxycarbonyl-phenyl)) porphyrinato]zinc(II) (Zn-Ac-3b). Porphyrin **Ac-3b** (15 mg, 0.016 mmol) and zinc acetate dihydrate (18 mg, 0.08 mmol) were stirred overnight in $\mathrm{CH_2Cl_2}$ (5 mL). After concentration under reduced pressure the product was isolated by column chromatography [silica, toluene : ethyl acetate = 1 : 1, R_f = 0.48]. Yield 14 mg (0.014 mmol, 87%), purple powder. $\mathrm{C_{48}H_{23}F_{10}N_5O_3Zn}$ (973.09).

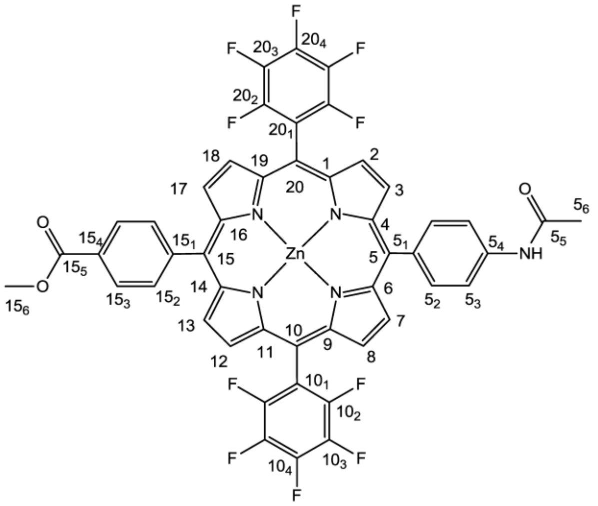

^{1}H-NMR ($\mathbf{d_8}$-THF): δ = 2.21 (s, 3H, $\mathrm{H}^{5}{}_{6}$), 4.06 (s, 3 H, $\mathrm{H}^{15}{}_{6}$), 8.05 (m, 2 H, $^3J_{\mathrm{HH}}$ = 8.3 Hz $\mathrm{H}^{5}{}_{3}$), 8.10(d, 2 H, $^3J_{\mathrm{HH}}$ = 8.3 Hz, $\mathrm{H}^{5}{}_{2}$), 8.33 (d, 2 H, $^3J_{\mathrm{HH}}$ = 8.0 Hz, $\mathrm{H}^{15}{}_{2}$), 8.43 (d, 2 H, $^3J_{\mathrm{HH}}$ = 8.0 Hz, $\mathrm{H}^{15}{}_{3}$), 8.89 (d, 2 H, $^3J_{\mathrm{HH}}$ = 4.6 Hz, $\mathrm{H}^{\mathrm{pyrrole}}$), 8.98 (m, 6 H, $\mathrm{H}^{\mathrm{pyrrole}}$), 9.42 (s, 1 $\mathrm{H}^{\mathrm{amide\text{-}NH}}$) ppm.

^{13}C{^{1}H}-NMR ($\mathbf{d_8}$-THF): δ = 24.4 ($\mathrm{C}^{5}{}_{6}$), 52.6 ($\mathrm{C}^{15}{}_{6}$), 117.8 ($\mathrm{C}^{5}{}_{3}$), 121.3 (C^{15}), 123.2 (C^{5}), 128.6 ($\mathrm{C}^{15}{}_{3}$), 131.0, 131.3, 133.6, 134.3 ($\mathrm{C}^{2,3,7,8,12,13,17,18}$), 130.8 ($\mathrm{C}^{15}{}_{4}$), 135.6 ($\mathrm{C}^{15}{}_{2}$), 135.9 ($\mathrm{C}^{5}{}_{2}$), 138.2 ($\mathrm{C}^{5}{}_{1}$), 140.9 ($\mathrm{C}^{5}{}_{4}$), 137.5, 140.0, 146.6, 149.0 (m, $\mathrm{C}^{10/20}{}_{1/1/2/2/3/3/4/4}$), 148.8 ($\mathrm{C}^{15}{}_{1}$), 150.5, 150.7, 151.3, 152.3 ($\mathrm{C}^{1,4,6,9,11,14,16,19}$), 167.4 ($\mathrm{C}^{15}{}_{5}$), 168.8 ($\mathrm{C}^{5}{}_{5}$) ppm.

^{19}F-NMR ($\mathbf{d_8}$-THF): δ = –167.2 (ddd, $^3J_{\mathrm{FF}}$ = 24 Hz, $^3J_{\mathrm{FF}}$ = 21 Hz, $^5J_{\mathrm{FF}}$ = 8 Hz, 4 F, $\mathrm{F}^{10/20}{}_{3/3,}$), –158.6 (t, $^3J_{\mathrm{FF}}$ = 21 Hz, 2 F, $\mathrm{F}^{10/20}{}_{4/4}$), –141.5 (dd, $^3J_{\mathrm{FF}}$ = 24 Hz, $^5J_{\mathrm{FF}}$ = 8 Hz, 4 F, $\mathrm{F}^{10/20}{}_{2/2}$) ppm.

IR (KBr): $\tilde{\nu}$ [cm^{-1}] = 3442 (b, $\mathrm{NH}^{\mathrm{amide}}$), 2926 (w, CH), 2851 (w, CH), 1720 (m, CO), 1518 (vs), 1493 (vs), 1282 (m), 1114 (w, CF), 1074 (w, CF), 1053 (w, CF), 989 (vs), 918 (vs), 939 (s).

MS (FD): *m*/*z* (%) = 971.35 (100) [M]$^+$.

MS (ESI): *m*/*z* (%) = 971.10 (43) [M]$^+$), 972.11 (100) [M+H]$^+$.

HR-MS (ESI): obs. *m*/*z* = 971.0931; calcd. for [M]$^+$ 971.0933.

UV/Vis ($\mathbf{CH_2Cl_2}$): λ [nm] (ε / [10^4 M^{-1}cm^{-1}]) = 422 (51.09), 552 (2.01), 593 (0.36).

Fluorescence ($\mathbf{CH_2Cl_2}$): λ [nm] (relative intensity) = 602 (1.00), 652 (0.92).

Quantum yield: Φ = 0.0771.

Lifetime: τ [ns] = 1.94 (100%).

CV (Fc/Fc$^+$, 100 mV s^{-1}, $\mathbf{CH_2Cl_2}$): $E_{½}$[V] = –1.980, –1.580, 0.600, 0.940.

[5-(4-(*N*-Acetylaminophenyl))-10,20-bis(4-fluorophenyl)-15-(4-(methoxycarbonyl-phenyl)) porphyrinato]zinc(II) (Zn-Ac-3c). Porphyrin **Ac-3c** (12 mg, 0.016 mmol) and zinc acetate dihydrate (15 mg, 0.15 mmol) were stirred overnight in CH_2Cl_2 (5 mL). After concentration under reduced pressure the product was isolated by column chromatography [silica, toluene : ethyl acetate = 1 : 1, $R_f = 0.50$]. Yield 13 mg (0.015 mmol, 94%), purple powder. $C_{48}H_{31}F_2N_5O_3Zn$ (829.20).

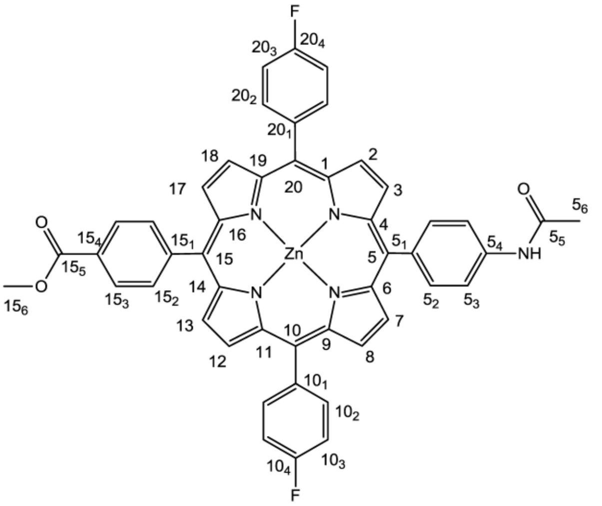

^{1}H-NMR (d$_8$-THF): δ = 2.20 (s, 3 H, $H^5{}_6$), 4.05 (s, 3 H, $H^{15}{}_6$), 7.50 (t, $^3J_{HH}$ = 8.6 Hz, 4 H, $H^{10/20}{}_{3/3}$), 8.03 (d, $^3J_{HH}$ = 8.3 Hz, 2 H, $H^5{}_3$), 8.08 (d, $^3J_{HH}$ = 8.4 Hz, 2 H, $H^5{}_2$), 8.18 (dvd, $^3J_{HH}$ = 8.1 Hz, $^3J_{HF}$ = 2.4 Hz, 4 H, $H^{10/20}{}_{2/2}$), 8.30 (d, $^3J_{HH}$ = 8.0 Hz, 2 H, $H^{15}{}_2$), 8.41 (d, $^3J_{HH}$ = 8.0 Hz, 2 H, $H^{15}{}_3$), 8.83 (m, 6 H, $H^{pyrrole}$), 8.92 (d, $^3J_{HH}$ = 4.6 Hz, 2 H, $H^{pyrrole}$), 9.41 (s, 1 H, $H^{amide\text{-}NH}$) ppm.

^{13}C{^{1}H}-NMR (d$_8$-THF): δ = 24.4 (s, $C^5{}_6$), 52.5 (s, $C^{15}{}_6$), 114.2 (d, $^2J_{CF}$ = 21.4 Hz , $C^{10/20}{}_{3/3}$), 117.8 (s, $C^5{}_3$), 120.2 (s, C^{15}), 120.6 (s, $C^{10/20}$), 122.3 (s, C^5), 128.5 (s, $C^{15}{}_3$), 130.5 (s, $C^{15}{}_4$), 132.1, 132.2, 132.5, 132.8 (s, $C^{pyrrole\ 2,3,7,8,12,13,17,18}$), 135.6 (s, $C^{15}{}_2$), 135.7 (s, $C^5{}_2$), 136.8 (d, $^3J_{CF}$ = 7.9 Hz, $C^{10/20}{}_{2/2}$), 138.8 (s, $C^5{}_1$), 140.7 (d, $^4J_{CF}$ = 2.9 Hz, $C^{10/20}{}_{1/1}$), 140.7 (s, $C^5{}_4$), 149.4 (s, $C^{15}{}_1$), 150.7, 151.2, 151.3, 151.6 (s, $C^{1,4,6,9,11,14,16,19}$), 163.9 (d, $^1J_{FH}$ = 245.7 Hz, $C^{10/20}{}_{4/4}$), 167.5 (s, $C^{15}{}_5$), 168.7 (s, $C^5{}_5$) ppm.

^{19}F-NMR (d$_8$-THF): δ = –118.6 (tt, $^3J_{FH}$ = 8.6 Hz, $^4J_{FH}$=5.4 Hz).

IR (KBr): $\tilde{\nu}$ [cm^{-1}] = 3432 (b, NH^{amide}), 2926 (w, CH), 1698 (m, CO) 1598 (m), 1507 (m), 1283 (m, C-O-C), 1159 (s, CF), 993 (vs), 802 (vs).

MS (FD): *m*/*z* (%) = 827.3 (92) $[M]^+$.

MS (ESI): *m*/*z* (%) = 828.18 (4) $[M+H]^+$.

HR-MS (ESI): obs. *m*/*z* = 827.1695; calcd. for $[M]^+$ 827.1686.

UV/Vis (CH_2Cl_2): λ [nm] (ε / [10^4 M^{-1}cm^{-1}]) = 420 (41.45), 548 (1.87), 587 (0.50).

Fluorescence (CH_2Cl_2): λ [nm] (relative intensity) = 598 (0.97), 646 (1.00).

Quantum yield: Φ = 0.0569.

Lifetime: τ [ns] = 1.85 (100%).

CV (Fc/Fc$^+$, 100 mV s^{-1}, CH_2Cl_2): $E_{½}$[V] = –2.110, –1.750, 0.380, 0.780.

[5-(4-(*N*-Acetylaminophenyl))-10,20-bis((4-trifluoromethyl)phenyl)-15-(4-(methoxycarbonylphenyl)) porphyrinato]zinc(II) (Zn-Ac-3d). Porphyrin **Ac-3d** (20 mg, 0.023 mmol) and zinc acetate dihydrate (25 mg, 0.11 mmol) were stirred overnight in CH_2Cl_2 (10 mL). After concentration under reduced pressure the product was isolated by column chromatography [silica, toluene : ethyl acetate = 1 : 1, $R_f = 0.40$]. Yield 18 mg (0.019 mmol, 82%), purple powder. $C_{50}H_{31}F_6N_5O_3Zn$ (929.18).

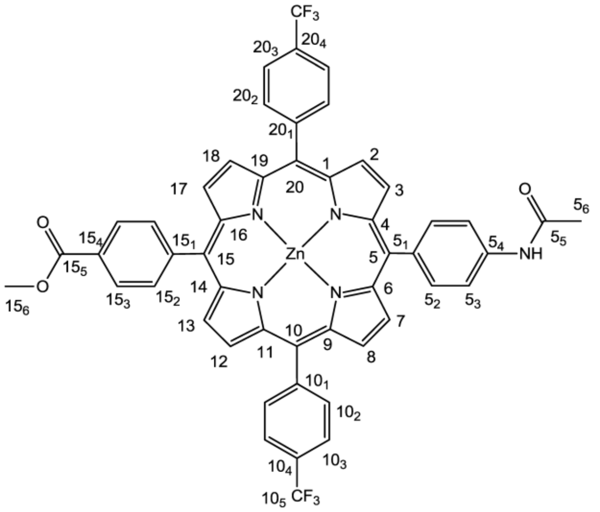

^{1}H-NMR (d_8-THF): δ = 2.19 (s, 3 H, $H^5{}_6$), 4.04 (s, 3 H, $H^{15}{}_6$), 8.02 (d, $^3J_{HH}$ = 8.3 Hz, 2 H, $H^5{}_3$), 8.08 (m, 6 H, $H^{10/20/5}{}_{3/3/2}$), 8.30 (d, $^3J_{HH}$ = 7.99 Hz, 2 H, $H^{15}{}_2$), 8.40 (m, 4 H, $H^{15/10/20}{}_{3/2/2}$), 8.82 (m, 6 H, $H^{pyrrole}$), 8.93 (d, $^3J_{HH}$ = 4.5 Hz, 2 H, $H^{pyrrole}$), 9.40 (s, 1 H, $H^{amide\text{-}NH}$) ppm.

^{13}C{^{1}H}-NMR (d_8-THF): δ = 24.6 (s, $C^5{}_6$), 52.7 (s, $C^{15}{}_6$), 117.9 (s, $C^5{}_3$), 120.3 (s, $C^{10/20}$), 120.7 (s, C^{15}), 122.8 (s, C^5), 124.5 (d, $^4J_{CF}$ = 3.4 Hz, $C^{10/20}{}_{2/2}$), 127.6 (s, $C^{10/20}{}_{4/4}$), 128.7 (s, $C^{15}{}_3$), 130.5 (q, $^1J_{CF}$ = 38.2 Hz, $C^{10/20}{}_{5/5}$), 130.8 (s, $C^5{}_4$), 132.3, 132.6, 132.6, 133.3 (s, $C^{pyrrole\ 2,3,7,8,12,13,17,18}$), 135.7 (s, $C^5{}_2$), 135.9 (s, $C^{15}{}_2$), 136.0 (m, $C^{10/20}{}_{2/2}$), 138.7 (s, $C^5{}_4$) 140.9 (s, $C^5{}_4$), 148.8 (m, $C^{10/20}{}_{1/1}$), 149.3 (s, $C^{15}{}_1$), 150.8, 150.9, 151.0, 151.9 (s, $C^{pyrrole\ 1,4,6,9,11,14,16,19}$), 167.6 (s, $C^{15}{}_5$), 168.9 (s, $C^5{}_5$) ppm.

^{19}F-NMR (d_8-THF): δ = –64.9 (s) ppm.

IR (KBr): $\tilde{\nu}$ [cm^{-1}] = 3433 (b, NH^{amide}), 2929 (w, CH), 2854 (w, CH), 1724 (w, CO), 1703 (w, CO), 1610 (m), 1517 (w), 1387 (w), 1283 (m, C-O-C), 1163 (m, CF), 1126 (s), 997 (s), 792 (s).

MS (FD): *m*/*z* (%) = 927.2 (100) $[M]^+$.

MS (ESI): *m*/*z* (%) = 927.19 (40) $[M]^+$, 950.17 (97) $[M+Na]^+$.

HR-MS (ESI): obs. *m*/*z* = 950.1512; calcd. for $[M+Na]^+$ 950.1512.

UV/Vis (CH_2Cl_2): λ [nm] (ε / [10^4 M^{-1}cm^{-1}]) = 420 (28.3), 548 (1.17), 588 (0.21).

Fluorescence (CH_2Cl_2): λ [nm] (relative intensity) = 597 (0.81), 645 (1.00).

Quantum yield: Φ = 0.0838.

Lifetime: τ [ns] = 2.07 (100%).

CV (Fc/Fc$^+$, 100 mV s^{-1}, CH_2Cl_2): $E_{1/2}$[V] = –2.010, –1.560, 0.420, 0.850.

General synthesis of bis(porphyrins) 4a, 4b, 4c, 4d, Zn^2-4d: The porphyrin acid component was dissolved in anhydrous CH_2Cl_2, 1-chloro-*N*,*N*,2-trimethylpropenylamine (Ghosez' reagent) was added and the reaction mixture was stirred under nitrogen for 3h at room temperature. After the acid chloride formed (TLC control) excess of Ghosez' reagent and solvent were removed by evaporation under reduced pressure. In order to remove the *N*,*N*-dimethyl amide byproduct anhydrous CH_2Cl_2 was added and the volatiles were again evaporated. The acid chloride was dissolved in CH_2Cl_2 (with 1 drop of triethylamine) and the solution was added dropwise to a solution of the porphyrin amino component in CH_2Cl_2 (with 1 drop of triethylamine). The reaction mixture was stirred for 12h at room temperature, washed with water and the organic phase was concentrated under reduced pressure. After column chromatography (silica, CH_2Cl_2/ethyl acetate 100:1) the respective dyad was isolated.

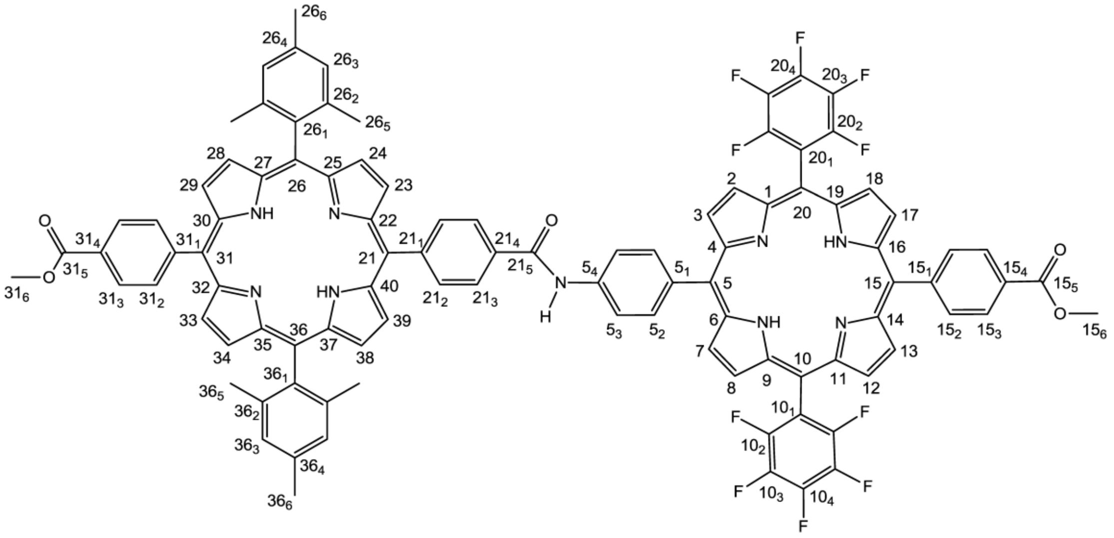

4a: **2a** (10.0 mg, 0.012 mmol), CH_2Cl_2 (3×5 mL), 1-chloro-*N*,*N*,2-trimethylpropenylamine (7 μL, 0.048 mmol), triethylamine (2×1 drop), **3b** (8.7 mg, 0.010 mmol). Yield: 6.1 mg (0.0037 mmol, 37%), purple powder. $C_{99}H_{65}F_{10}N_9O_5$ (1650.61). $R_f = 0.35$ (silica, CH_2Cl_2/ethyl acetate 100:1). ^{1}H NMR ($CDCl_3$): $\delta = -2.80$ (s, 2 H, $H^{C6F5\text{-}pyrroleNH}$), –2.56 (s, 2 H, $H^{Mes\text{-}pyrroleNH}$), 1.87 (s, 12 H, $H^{26/36}{}_{5/5}$), 2.65 (s, 6 H, $H^{26/36}{}_{6/6}$), 4.12 (s, 3 H, $H^{31}{}_6$), 4.14 (s, 3 H, $H^{15}{}_6$), 7.31 (s, 4 H, $H^{26/36}{}_{3/3}$), 8.22 (d, $^3J_{HH}$ = 8.3 Hz, 2 H, $H^5{}_3$), 8.34 (m, 6 H, $H^{5/15/31}{}_{2/2/2}$), 8.44 (d, $^3J_{HH}$ = 8.2 Hz, 2 H, $H^{21}{}_2$), 8.47 (m, 6 H, $H^{15/21/31}{}_{3/3/3}$), 8.72 (d, $^3J_{HH}$ = 4.8 Hz, 2 H, $H^{pyrrole}$), 8.74 (m, 4 H, $H^{pyrrole}$), 8.85 (d, $^3J_{HH}$ = 4.7 Hz, 2 H, $H^{pyrrole}$), 8.89 (d, $^3J_{HH}$ = 4.5 Hz, 2 H, $H^{pyrrole}$), 8.92 (d, $^3J_{HH}$ = 4.7 Hz, 4 H, $H^{pyrrole}$), 9.00 (d, $^3J_{HH}$ = 4.7 Hz, 2 H, $H^{pyrrole}$) ppm; $H^{amide\text{-}NH}$ not observed. $^{13}C\{^1H\}$ NMR ($CDCl_3$): $\delta = 21.5$ ($C^{10/20}{}_{6/6}$), 21.7 ($C^{10/20}{}_{5/5}$), 52.4, 52.5 ($C^{15/31}{}_{6/6}$), 118.6, 119.0, 120.0 ($C^{5/10/15/20/21/26/31/36}$), 118.6 ($C^5{}_3$), 127.8, 127.9, 128.1 ($C^{15/21/31}{}_{3/3/3}$), 127.8 ($C^{26/36}{}_{3/3}$), 130.2, 137.8 ($C^{15/31}{}_{4/4}$), 130.2 ($C^{pyrrole\ 2,3,7,8,12,13,17,18}$), 134.6, 135.0, 135.3, ($C^{5/15/31/21}{}_{2/2/2/2}$), 138.3 ($C^{26/36}{}_{1/1}$), 138.6 ($C^5{}_1$), 139.4 ($C^{26/36}{}_{2/2}$), 145.8 ($C^5{}_4$), 147.0 ($C^{21}{}_4$), 165.9 ($C^{21}{}_5$), 167.1, 167.4 ($C^{15/31}{}_{5/5}$) ppm. ^{19}F NMR ($CDCl_3$): $\delta = -162.0$ (ddd, $^3J_{FF}$ = 23 Hz, $^3J_{FF}$ = 21 Hz, $^5J_{FF}$ = 8 Hz, 4 F, $F^{10/20}{}_{3/3}$), –152.0 (t, $^3J_{FF}$ = 21 Hz, 2 F, $F^{10/20}{}_{4/4}$), –136.7 (dd, $^3J_{FF}$ = 24 Hz, $^5J_{FF}$

= 8 Hz, 4 F, F$^{10/20}{}_{2/2}$) ppm. MS (FD): *m/z* (%) = 1650.1 (100) [M]$^+$. MS (ESI): *m/z* (%) = 825.8 (83) [M+H]$^{2+}$, 1650.1 (87) [M]$^+$, 1651.5 (100) [M+H]$^+$. HR-MS (ESI): obs. *m/z* = 1650.4983; calcd. for [M+H]$^+$ 1650.5027. IR (KBr): $\tilde{\nu}$ [cm^{-1}] = 3439 (b, NH$^{\text{amide}}$/NH$^{\text{pyrrole}}$), 2924 (s, CH), 2850 (m, CH), 1730 (m, CO), 1517 (s), 1281 (m, C-O-C), 1109 (s, CF). UV/Vis (CH$_2$Cl$_2$): λ (ε / M^{-1} cm^{-1}) = 421 (684600), 513 (38500), 549 (14100), 590 (12500), 649 (9500).

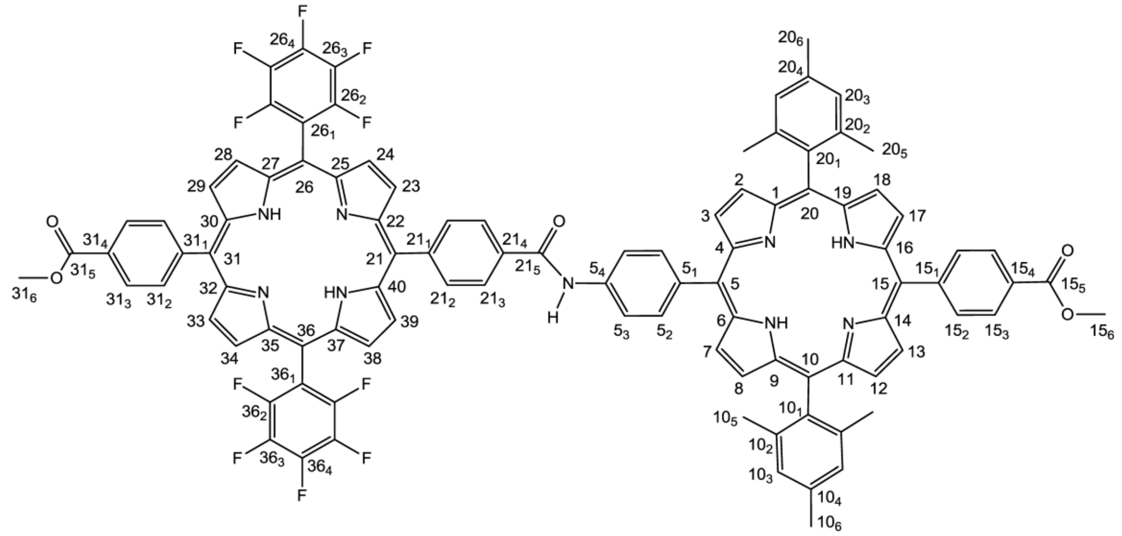

4b: **2b** (35 mg, 0.039 mmol), CH$_2$Cl$_2$ (3×10 mL), 1-chloro-*N*,*N*,2-trimethylpropenylamine (20 µL, 0.156 mmol), triethylamine (2×1 drop), **3a** (27.0 mg, 0.035 mmol). Yield: 28.4 mg (0.017 mmol, 49%), purple powder. C$_{99}$H$_{65}$F$_{10}$N$_9$O$_5$ (1650.61). R_{f} = 0.34 (silica, CH$_2$Cl$_2$/ethyl acetate 100:1). ^{1}H NMR (CDCl$_3$): δ = –2.80 (s, 2 H, H$^{\text{C6F5pyrroleNH}}$), –2.59 (s, 2 H, H$^{\text{MespyrroleNH}}$), 1.87 (s, 12 H, H$^{10/20}{}_{5/5}$), 2.65 (s, 6 H, H$^{10/20}{}_{6/6}$), 4.12 (s, 3 H, H$^{15}{}_6$), 4.14 (s, 3 H, H$^{31}{}_6$), 7.31 (s, 4 H, H$^{10/20}{}_{3/3}$), 8.27 (d, $^3J_{\mathrm{HH}}$ = 8.5 Hz, 2 H, H$^5{}_3$), 8.32 (m, 6 H, H$^{5/15/31}{}_{2/2/2}$), 8.44 (d, $^3J_{\mathrm{HH}}$ = 7.3 Hz, 4 H, H$^{15/21}{}_{3/2}$), 8.48 (d, 4 H, $^3J_{\mathrm{HH}}$ = 7.9 Hz, H$^{21/31}{}_{3/3}$), 8.54 (s, 1 H, H$^{\text{amide-NH}}$), 8.74 (d, $^3J_{\mathrm{HH}}$ = 4.7 Hz, 2 H, H$^{\text{pyrrole}}$), 8.78 (m, 4 H, H$^{\text{pyrrole}}$), 8.84 (d, $^3J_{\mathrm{HH}}$ = 4.3 Hz, 4 H, H$^{\text{pyrrole}}$), 8.87 (d, $^3J_{\mathrm{HH}}$ = 4.5 Hz, 2 H, H$^{\text{pyrrole}}$), 8.91 (d, $^3J_{\mathrm{HH}}$ = 4.7 Hz, 2 H, H$^{\text{pyrrole}}$), 9.09 (d, $^3J_{\mathrm{HH}}$ = 4.7 Hz, 2 H, H$^{\text{pyrrole}}$) ppm. ^{13}C{^{1}H} NMR (CDCl$_3$): δ = 21.5 (C$^{10/20}{}_{6/6}$), 21.7 (C$^{10/20}{}_{5/5}$), 52.4, 52.5 (C$^{15/31}{}_{6/6}$), 117.9, 118.3, 118.8, 118.9, 120.0, 121.2 (C$^{5/10/15/20/21/26/31/36}$), 118.8 (C$^5{}_3$), 125.6, 128.1 (C$^{15/21/31}{}_{3/3/3}$), 127.8 (C$^{10/20}{}_{3/3}$), 127.9, 134.6, 134.6 (C$^{5/15/31}{}_{2/2/2}$), 129.6, 130.0, 135.4, 138.3 (C$^{15/21/31}{}_{4/4/4}$), 134.2, 136.3, 137.9, 146.0 (C$^{15/21/31/26/36}{}_{1/1/1/1/1}$), 135.0 (C$^{21}{}_2$), 137.5 (C$^5{}_1$), 138.2 (C$^{10/20}{}_{1/1}$), 139.4 (C$^{10/20}{}_{2/2}$), 146.2 (C$^5{}_4$), 146.8 (C$^{21}{}_4$), 145.4, 147.7 (C$^{26/36}{}_{2/2}$, C$^{26/36}{}_{3/3}$, C$^{26/36}{}_{4/4}$), 166.2 (C$^{21}{}_5$), 167.2, 167.3 (C$^{15/31}{}_{5/5}$) ppm. ^{19}F NMR (CDCl$_3$): δ = –162.0 (ddd, $^3J_{\mathrm{FF}}$ = 23 Hz, $^3J_{\mathrm{FF}}$ = 21 Hz, $^5J_{\mathrm{FF}}$ = 8 Hz, 4 F, F$^{26/36}{}_{3/3}$), –152.0 (t, $^3J_{\mathrm{FF}}$ = 21 Hz, 2 F, F$^{26/36}{}_{4/4,}$), –136.7 (dd, $^3J_{\mathrm{FF}}$ = 24 Hz, $^5J_{\mathrm{FF}}$ = 8 Hz, 4 F, F$^{26/36}{}_{2/2}$) ppm. MS (FD): *m/z* (%) = 1649.8 (50) [M]$^+$, 1651.9 (100) [M+2H]$^+$. MS (ESI): *m/z* (%) = 826.3 (100) [M+H]$^{2+}$, 1650.5 (50) [M]$^+$, 1651.5 (82) [M+H]$^+$. HR-MS (ESI): obs. *m/z* = 1650.5067; calcd. for [M+H]$^+$ 1650.5027. IR (KBr): $\tilde{\nu}$ [cm^{-1}] = 3441 (b, NH$^{\text{amide}}$), 3324 (w, NH$^{\text{pyrrole}}$), 2926 (s, CH), 2860 (m, CH), 1723 (m, CO), 1515 (m), 1503 (m), 1266 (m, C-O-C), 1109 (s, CF). UV/Vis (CH_2Cl_2): λ (ε / M^{-1} cm^{-1}) = 420 (787000), 513 (46700), 549 (18000), 590 (15500), 649 (11200).

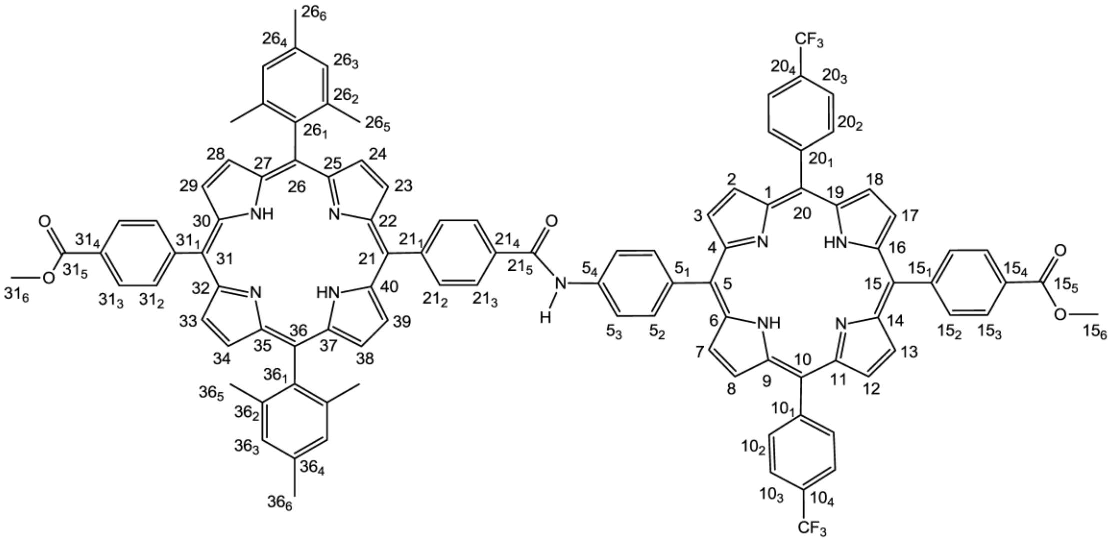

4c: 2a (23.4 mg, 0.026 mmol), CH_2Cl_2 (3 × 10 mL), 1-chloro-*N*,*N*,2-trimethylpropenylamine (14 µL, 0.104 mmol), triethylamine (2×1 drop), **3d** (17.2 mg, 0.021 mmol). Yield: 6.1 mg (0.0145 mmol, 69%), purple powder. $C_{95}H_{51}F_{16}N_9O_5$ (1702.45). R_f = 0.32 (silica, CH_2Cl_2/ethyl acetate 100:1). ^1H NMR ($CDCl_3$): δ = –2.81 (s, 2 H, $H^{C6F5pyrroleNH}$), –2.76 (s, 2 H, $H^{CF3pyrroleNH}$), 4.13, 4.14 (2s, 2×3 H, $H^{15/31}{}_{6/6}$), 8.06 (d, $^3J_{HH}$ = 8.0 Hz, 4 H, $H^{10/20}{}_{3/3}$), 8.26 (d, $^3J_{HH}$ = 8.4 Hz, 2 H, $H^5{}_3$), 8.32 (m, 6 H, $H^{5/15/31}{}_{2/2/2}$), 8.37 (d, $^3J_{HH}$ = 8.0, 4 H, $H^{10/20}{}_{2/2}$), 8.48 (m, 8 H, $H^{15/21/21/31}{}_{3/2/3/3}$), 8.54 (s, 1H, $H^{amide\text{-}NH}$), 8.84 (m, 8 H, $H^{pyrrole}$), 8.90 (d, $^3J_{HH}$ = 4.7 Hz, 2 H, $H^{pyrrole}$), 8.93 (d, $^3J_{HH}$ = 4.8 Hz, 2 H, H^{pyrrol}), 9.01 (pt, $^3J_{HH}$ = 6.3 Hz, 4 H, $H^{pyrrole}$) ppm. $^{13}C\{^1H\}$ NMR ($CDCl_3$): δ = 52.5, 52.6 ($C^{15/31}{}_{6/6}$), 118.7 ($C^5{}_3$), 118.8, 119.2, 120.0, 120.4, 123.2 ($C^{5/10/15/20/21/26/31/36}$), 123.8 (d, $^1J_{CF}$ = 3.3 Hz, $C^{10/20}{}_{3/3}$), 134.6 ($C^{10/20}{}_{3/3}$), 125.8 ($C^{10/20}{}_{4/4}$), 125.8, 125.9, 128, 128.2 ($C^{5/15/21/31}{}_{3/3/3/3}$), 130.1 (q, $^1J_{CF}$ = 32.2 Hz, $C^{10/20}{}_{5/5}$), 130.1, 130.9, 131.2 ($C^{2,3,7,8,12,13,17,18}$), 134.6, 135.0, 135.4 ($C^{5/15/21/31}{}_{2/2/2/2}$), 134.6, 134.8, 138.0 ($C^{15/21/31}{}_{4/4/4}$), 136.3, 138.8, 145.4, 147.8 ($C^{26/36}{}_{2/2}$, $C^{26/36}{}_{3/3}$, $C^{26/36}{}_{4/4}$), 138.3 ($C^5{}_1$), 145.2, 145.7, 145.8, 146.6 ($C^{5/10/20/15/21/31}{}_{4/1/1/1/1/1}$), 166.0 ($C^{21}{}_5$), 167.2, 167.3 ($C^{15}{}_5$, $C^{31}{}_5$) ppm. ^{19}F NMR ($CDCl_3$): δ = –162.6 (ddd, $^3J_{FF}$ = 23 Hz, $^3J_{FF}$ = 23 Hz, $^5J_{FF}$ = 8 Hz, 4 F, $F^{10/20}{}_{3/3,}$), –152.32 (t, $^3J_{FF}$ = 21 Hz, 2 F, $F^{10/20}{}_{4/4,}$), –137.19 (dd, $^3J_{FF}$ = 24 Hz, $^5J_{FF}$ = 8 Hz, 4 F, $F^{10/20}{}_{2/2}$), –62.0 (s, 6 F, $F^{10/20}{}_{5/5}$) ppm. MS (FD): *m/z* (%) = 1703.3 (100) $[M+H]^+$. MS (ESI): *m/z* (%) = 851.7 (72) $[M+H]^{2+}$, 1702.4 (75) $[M]^+$, 1703.4 (100) $[M+H]^+$. HR-MS (ESI): obs. *m/z* = 1702.3815; calcd. for $[M+H]^+$ 1702.3836. IR (KBr): $\tilde{\nu}$ [cm^{-1}] = 3443 (b, NH^{amide}), 3320 (w, $NH^{pyrrole}$), 2952 (w, CH), 2927 (w, CH), 2854 (w, CH), 1724 (m, CO), 1609 (w), 1494 (m), 1266 (s, C-O-C), 1102 (s, CF). UV/Vis (CH_2Cl_2): λ (ε / M^{-1} cm^{-1}) = 420 (745000), 512 (16100), 549 (5300), 590 (5000), 645 (2600).

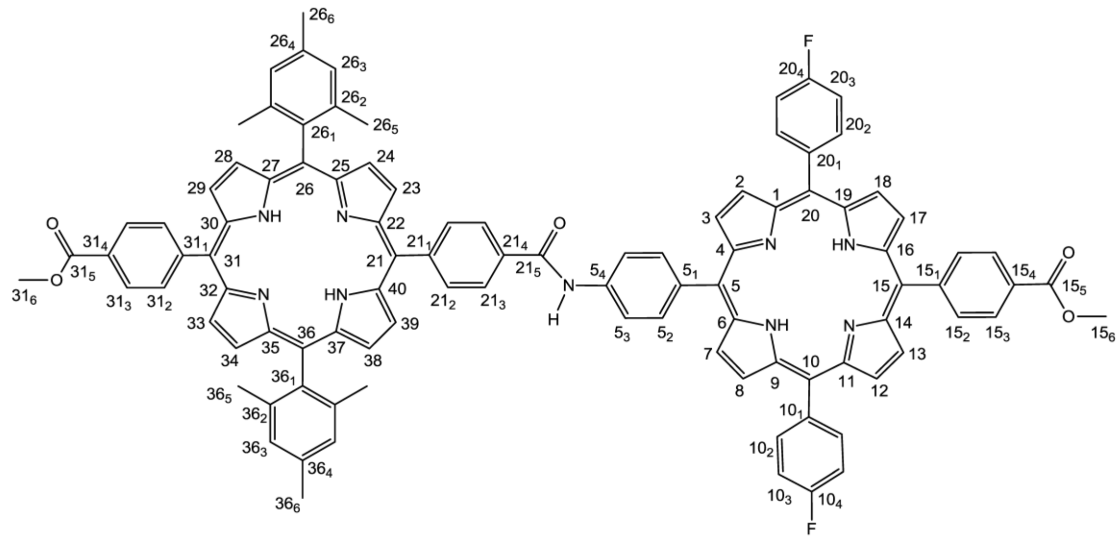

4d: 2a (21.0 mg, 0.029 mmol), CH_2Cl_2 (3×10 mL), 1-chloro-*N*,*N*,2-trimethylpropenylamine (15 µL, 0.116 mmol), triethylamine (2×1 drop), **3c** (20.0 mg, 0.027 mmol). Yield: 25.0 mg (0.017 mmol, 63%), purple powder. $C_{99}H_{73}F_2N_9O_5$ (1506.69). $R_f = 0.41$ (silica, CH_2Cl_2/ethyl acetate 100:1). ^1H NMR ($CDCl_3$): $\delta = -2.76$ (s, 2 H, $H^{PhFpyrroleNH}$), –2.58 (s, 2 H, $H^{MespyrroleNH}$), 1.87 (s, 12 H, $H^{26/36}_{5/5}$), 2.65 (s, 6 H, $H^{26/36}_{6/6}$), 4.12, 4.13 (2 s, 2 × 3 H, $H^{15/36}_{6/6}$), 7.31 (s, 4 H, $H^{26/36}_{3/3}$), 7.47 (t, $^3J = 8.6$ Hz, 4 H, $H^{10/20}_{3/3}$), 8.20 (dd, $^3J = 8.5$ Hz, $^3J = 5.4$ Hz, 4 H, $H^{10/20}_{2/2}$), 8.24 (d, $^3J_{HH} = 8.4$ Hz, 2 H, H^5_3), 8.32 (m, 6 H, $H^{5/15/31}_{2/2/2}$), 8.46 (m, 8 H, $H^{15/21/21/31}_{3/2/3/3}$), 8.52 (s, 1 H, $H^{amide\text{-}NH}$), 8.74 (d, $^3J_{HH} = 4.8$ Hz, 2 H, $H^{pyrrole}$), 8.78 (m, 4 H, $H^{pyrrole}$), 8.82 (d, $^3J_{HH} = 4.7$ Hz, 2 H, $H^{pyrrole}$), 8.85 (m, 4 H, $H^{pyrrole}$), 8.89 (d, $^3J_{HH} = 4.7$ Hz, 2 H, $H^{pyrrole}$), 9.00 (d, $^3J_{HH} = 4.7$ Hz, 4 H, $H^{pyrrole}$) ppm. $^{13}C\{^1H\}$ NMR ($CDCl_3$): $\delta = 52.5$ ($C^{15/31}_{6/6}$), 113.8 (d, $^2J_{CF} = 21.3$ Hz , $C^{10/20}_{3/3}$), 118.6 (C^5_3), 117.9, 118.3, 118.8, 118.9, 119.2, 120.1 ($C^{5/10/15/20/21/26/31/36}$), 125.6, 128.0, 128.0, 135.0 ($C^{15/21/21/31}_{3/2/3/3}$), 127.9 ($C^{26/36}_{3/3}$), 129.7, 134.3, 138.0 ($C^{15/26/36/31}_{4/1/1/4}$), 131.0 ($C^{2,3,7,8,12,13,17,18,23,24,28,29,33,34,38,39}$), 134.6 (d, $^4J_{CF} = 3.2$ Hz, $C^{10/20}_{1/1}$), 134.6, 135.0, 135.4 ($C^{5/15/31}_{2/2/2}$), 135.7 (d, $^3J_{CF} = 8.0$ Hz, $C^{10/20}_{2/2}$), 138.4 (C^5_1), 138.2 ($C^{26/36}_{1/1}$), 139.4, 146.1 146.8, 146.9 ($C^{15/21/21/31}_{1/1/4/1}$), 162.9 (d, $^1J_{CF} = 247.4$ Hz, $C^{10/20}_{4/4}$), 166.2 (C^{21}_5), 167.3, 167.4 (C^{15}_5, C^{31}_5) ppm. ^{19}F NMR ($CDCl_3$): $\delta = -114.5$ (tt, $^3J_{HF} = 8.6$ Hz, $^4J_{HF} = 5.4$ Hz) ppm. MS (FD): *m/z* (%) = 1506.9 (100) $[M]^+$. MS (ESI): *m/z* (%) = 753.8 (90) $[M+H]^{2+}$, 754.3 (100) $[M+2H]^{2+}$, 1506.6 (37) $[M]^+$. HR-MS (ESI): obs. *m/z* = 1506.5826; calcd. for $[M]^+$ 1506.5781. IR (KBr): $\tilde{\nu}$ [cm^{-1}] = 3443 (b, NH^{amide}), 3320 (w, $NH^{pyrrole}$), 2927 (w, CH), 2853 (w, CH), 1724 (m, CO), 1609 (m), 1512 (s), 1274 (s, C-O-C), 1103 (s, CF). UV/Vis (CH_2Cl_2): λ (ε / M^{-1} cm^{-1}) = 421 (459800), 513 (23400), 550 (11600), 592 (73000), 649 (8000).

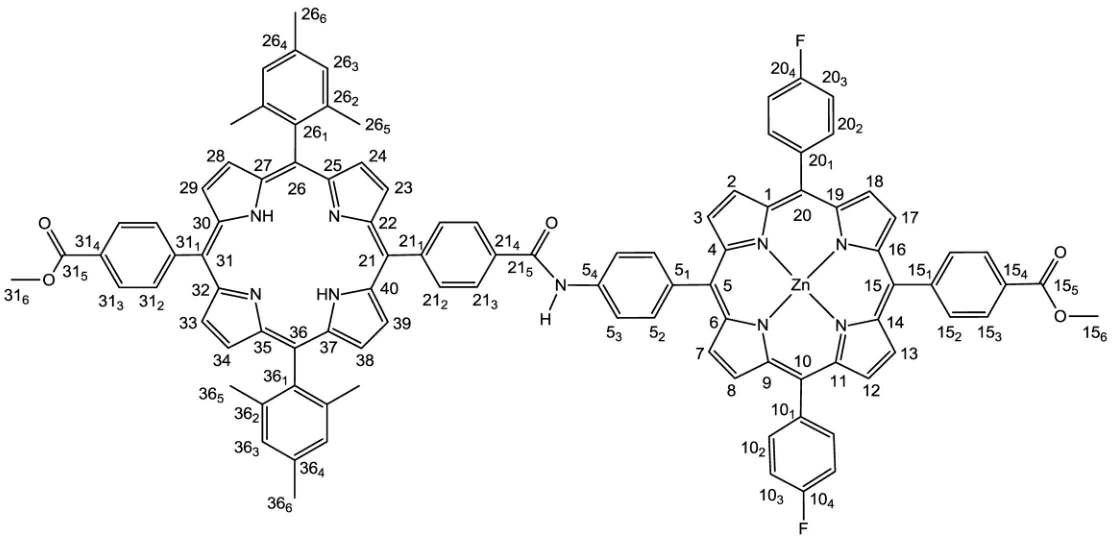

Zn^{2}-4d: 2a (26.0 mg, 0.033 mmol), CH_2Cl_2 (3×10 mL), 1-chloro-*N*,*N*,2-trimethylpropenylamine (17 µL, 0.132 mmol), triethylamine (2×1 drop), **Zn-3c** (22.0 mg, 0.028 mmol). Yield: 17.0 mg (0.011 mmol, 40%), purple powder. $C_{99}H_{71}F_2N_9O_5Zn$ (1570.07). R_f = 0.41 (silica, CH_2Cl_2/ethyl acetate 100:1). ^{1}H NMR (d$_8$-THF): $\delta = -2.47$ (s, 2 H, $H^{MespyrroleNH}$), 1.87 (s, 12 H, $H^{26/36}{}_{5/5}$), 2.63 (s, 6 H, $H^{26/36}{}_{6/6}$), 4.06 (s, 6 H, $H^{15/31}{}_{6/6}$), 7.35 (s, 4 H, $H^{26/36}{}_{3/3}$), 7.52 (t, ^3J = 8.5 Hz, 4 H, $H^{10/20}{}_{3/3}$), 8.22 (dd, ^3J = 8.2 Hz, ^3J = 5.9 Hz, 4 H, $H^{10/20}{}_{2/2}$), 8.25 (d, $^3J_{HH}$ = 8.6 Hz, 2 H, $H^5{}_3$), 8.39 (m) and 8.54 (d, $^3J_{HH}$ = 7.9 Hz, 14 H / 2 H, $H^{5/15/15/21/21/31/31}{}_{2/2/3/2/3/2/3}$), 8.71 (d, $^3J_{HH}$ = 4.6 Hz, 2 H, $H^{pyrrole}$), 8.75 (d, $^3J_{HH}$ = 4.6 Hz, 2 H, $H^{pyrrole}$), 8.78 (d, $^3J_{HH}$ = 4.5, 2 H, $H^{pyrrole}$), 8.84 (d, $^3J_{HH}$ = 4.5 Hz, 2 H, $H^{pyrrole}$), 8.86 (d, $^3J_{HH}$ = 4.7 Hz, 2 H, $H^{pyrrole}$), 8.89 (d, $^3J_{HH}$ = 4.3 Hz, 4 H, $H^{pyrrole}$), 9.03 (d, $^3J_{HH}$ = 4.6 Hz, 2 H, H^{pyrrol}), 10.16 (s, 1 H, $H^{amide\text{-}NH}$) ppm. $^{13}C\{^1H\}$ NMR ($CDCl_3$): δ = 21.7 ($C^{26/36}{}_{6/6}$), 21.9 ($C^{26/36}{}_{5/5}$), 52.5 ($C^{15/31}{}_{6/6}$), 114.2 (d, $^2J_{CF}$ = 21.5 Hz, $C^{10/20}{}_{3/3}$), 119.0 ($C^5{}_3$), 119.6, 119.9, 120.2, 120.6 ($C^{5/10/15/20/21/26/31/36}$), 128.9 (4 C, $C^{26/36}{}_{3/3}$), 136.8 (d, $^3J_{CF}$ = 7.9 Hz, $C^{10/20}{}_{2/2}$), 128.5, 128.8, 128.9, 135.6, 135.9, 136.8, 136.9 ($C^{5/15/15/21/21/31/31}{}_{2/2/3/2/3/2/3}$), 130.6, 131.0, 132.2, 132.3, 132.5, 132.9 ($C^{2,3,7,8,12,13,17,18,23,24,28,29,33,34,38,39}$), 150.7, 151.2, 151.4, 151.6 ($C^{1/4/6/9/11/14/16/19}$), 139.5 ($C^{26/36}{}_{1/1}$), 139.0, 139.8, 136.6, 140.1, 140.7, 146.3, 147.8, 149.4 ($C^{5/5/15/15/21/21/31/31}{}_{1/4/1/4/1/4/1/4}$), 140.7 ($C^{10/20}{}_{1/1}$), 163.9 (d, $^1J_{CF}$ = 245.8 Hz, $C^{10/20}{}_{4/4}$), 166.7 ($C^{21}{}_5$), 167.4, 167.5 ($C^{15/31}{}_{5/5}$) ppm. ^{19}F NMR (d$_8$-THF): $\delta = -114.5$ (m) ppm. MS (FD): *m/z* (%) = 1568.2 (100) $[M]^+$. MS (ESI): *m/z* (%) = 784.8 (34) $[M+H]^{2+}$, 1568.6 (17) $[M]^+$, 1569.6 (21) $[M+H]^+$. HR-MS (ESI): obs. *m/z* = 1568.4926; calcd. for $[M-H]^+$ 1568.4916. IR (KBr): $\tilde{\nu}$ [cm^{-1}] = 3435 (b, $NH^{amide}/NH^{pyrrole}$), 2919 (w, CH), 2853 (w, CH), 1724 (m, CO), 1602 (m), 1511 (m), 1274 (s, C-O-C), 1103 (s, CF). UV/Vis (CH_2Cl_2): λ (ε / M^{-1} cm^{-1}) = 423 (816300), 515 (27000), 549 (32500), 593 (11800), 651 (15300).

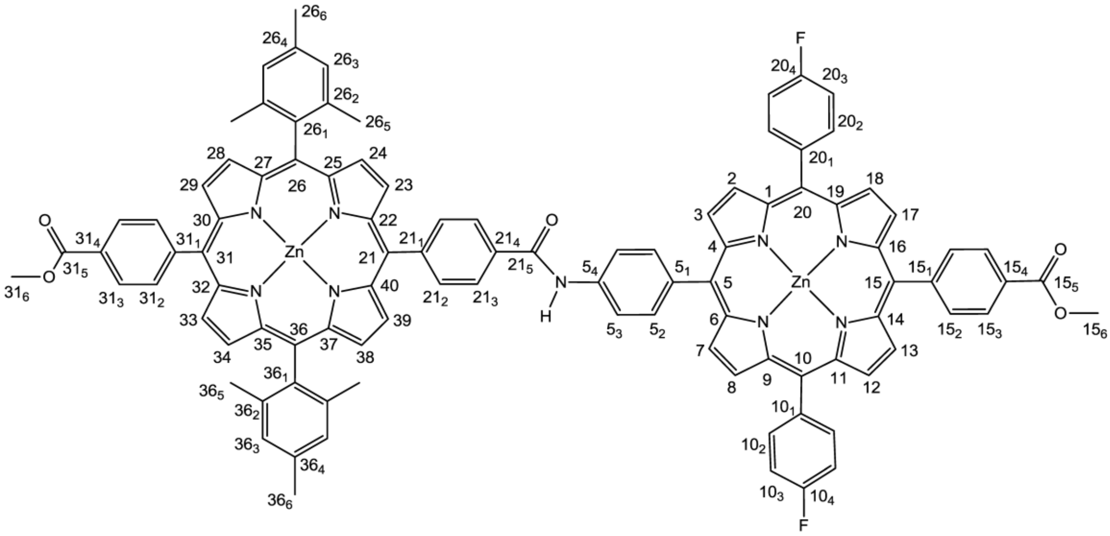

Synthesis of Zn^1Zn^2-4d: To porphyrin **4d** (7.0 mg, 0.0045 mmol) in CH_2Cl_2 (5 mL) was added zinc acetate dihydrate (9.88 mg, 0.045 mmol) and the solution was stirred for 12 h at room temperature. The mixture was concentrated in vacuum. After column chromatography (silica, toluene/ethyl acetate 20:1) **Zn^1Zn^2-4d** was isolated as purple powder. Yield: 6.4 mg (0.0039 mmol, 88%). $C_{99}H_{69}F_2N_9O_5Zn_2$ (1633.44). $R_f = 0.37$ (silica, toluene/ethyl acetate 20:1). ^{1}H NMR (d_8-THF): δ = 1.88 (s, 12 H, $H^{26/36}_{5/5}$), 2.63 (s, 6 H, $H^{26/36}_{6/6}$), 4.05 (s), 4.06 (s, $H^{15/31}_{6/6}$), 7.32 (s, 4 H, $H^{26/36}_{3/3}$), 7.52 (t, ^3J = 8.7 Hz, 4 H, $H^{10/20}_{3/3}$), 8.22 (dd, ^3J = 8.4 Hz, ^3J = 5.6 Hz, 4 H, $H^{10/20}_{2/2}$), 8.25 (d, $^3J_{HH}$ = 8.6 Hz, 2 H, H^5_3), 8.32 (m, 4 H); 8.41 (m, 8 H,); 8.51 (d, $^3J_{HH}$ = 8.1 Hz, 2 H) ($H^{5/15/15/21/2131/31}_{2/2/3/2/3/2/3}$), 8.71 (d, $^3J_{HH}$ = 4.6 Hz, 2 H, $H^{pyrrole}$), 8.74 (d, $^3J_{HH}$ = 4.6 Hz, 2 H, $H^{pyrrole}$), 8.77 (d, $^3J_{HH}$ = 4.6 Hz, 2 H, $H^{pyrrole}$), 8.84 (d, $^3J_{HH}$ = 4.6 Hz, 2 H, $H^{pyrrole}$), 8.87 (d, $^3J_{HH}$ = 4.7 Hz, 2 H, $H^{pyrrole}$), 8.88 (d, $^3J_{HH}$ = 4.6 Hz, 2 H, $H^{pyrrole}$), 8.89 (d, $^3J_{HH}$ = 4.6 Hz, 2 H, $H^{pyrrole}$), 9.04 (d, $^3J_{HH}$ = 4.6 Hz, 2 H, $H^{pyrrole}$), 10.15 (s, 1 H, $H^{amide\text{-}NH}$) ppm. $^{13}C\{^1H\}$ NMR (d_8-THF): δ = 21.8 ($C^{26/36}_{6/6}$), 22.2 ($C^{26/36}_{5/5}$), 52.5 ($C^{15/31}_{6/6}$), 114.2 (d, $^2J_{CF}$ = 21.5 Hz , $C^{10/20}_{3/3}$), 119.0 (s, 1 C, C^5_3), 119.9, 120.3, 120.6, 122.3 ($C^{5/10/15/20/21/26/31/36}$), 126.7, 128.4, 128.5, 135.6, 135.6, 135.9, 138.4, 139.6 ($C^{5/15/15/21/21/31/31}_{2/2/3/2/3/2/3}$), 128.7 ($^{26/36}_{3/3}$), 130.5 (d, $^4J_{CF}$ = 3.2 Hz, $C^{10/20}_{1/1}$), 131.3, 131.3, 140.7, 140.8, 147.9, 149.4 ($C^{5/5/15/15/21/21/31/31}_{1/4/1/4/1/4/1/4}$), 132.2, 132.3, 132.6, 132.7, 132.8, 132.9 ($C^{2,3,7,8,12,13,17,18,23,24,28,29,33,34,38,39}$), 136.9 (d, $^3J_{CF}$ = 7.9 Hz, $C^{10/20}_{2/2}$), 150.6, 150.7, 150.7, 151.0, 151.0, 151.2, 151.4, 151.6 ($C^{1/4/6/9/11/14/16/19/22/25/27/30/32/35/37/40}$), 163.1 (d, $^1J_{CF}$ = 245.2 Hz, $C^{10/20}_{4/4}$), 166.8 (C^{21}_5), 167.5 (C^{15}_5, C^{31}_5) ppm. ^{19}F NMR (d_8-THF): $\delta = -118.7$ (br.s) ppm. MS (FD): *m/z* (%) = 1632.6 (100) $[M]^+$. HR-MS (ESI): obs. *m/z* = 1630.4067; calcd. for $[M+H]^+$ 1630.4051. IR (KBr): $\tilde{\nu}$ [cm^{-1}] = 3425 (b, NH^{amide}), 2925 (s, CH), 2856 (w, CH), 1726 (m, CO), 1602 (m), 1512 (m), 1278 (m, C-O-C), 1101 (s, CF). UV/Vis (CH_2Cl_2): λ (ε / M^{-1} cm^{-1}) = 423 (806700), 549 (45600), 588 (13000).

Discussion of relevant NMR data of bis(porphyrins): The pyrrole NH proton resonances are indicative of the electron withdrawing nature of the porphyrin substituents: $\delta = -2.80$ (C_6F_5), –2.76 (4-$C_6H_4CF_3$), –2.76 (4-C_6H_5F), –2.6 (2,4,6-$C_6H_2(CH_3)_3$). Their correct integral ratio confirms the composition of **4a** – **4d**. The presence of two methyl ester groups is confirmed by the presence of two resonances of the CH_3 groups again in the correct integral ratio at δ = 4.12 – 4.14 ppm. Particularly informative is the ^{19}F NMR spectrum of **4c** which displays the expected ^{19}F resonances of the C_6F_5 and $C_6H_4CF_3$ substituents in the correct intensity ratio (Supporting Information, Figure S1).

The zinc porphyrins **Zn^2-4d** and **Zn^{1}Zn^2-4d** are less soluble in chloroform than their parent free-base bis(porphyrin) **4d**. In tetrahydrofuran their amide protons resonate at δ = 10.1 ppm due to hydrogen-bonding to the solvent. In the bis(metalated) complex **Zn^{1}Zn^2-4d** pyrrole-NH resonances are absent as expected. **Zn^2-4d** shows a single resonance at δ = –2.5 ppm corresponding to the pyrrole-NH nuclei of the mesityl substituted free-base porphyrin proving the presence of the correct isomer **Zn^2-4d**.

References

[S1] C. M. Carcel, J. K. Laha, R. S. Loewe, P. Thamyongkit, K.-H. Schweikart, V. Misra, D. F. Bocian and J. S. Lindsey, *J. Org. Chem.*, 2004, **69**, 6739-6750.

[S2] S. L. Gould, G. Kodis, R. E. Palacios, L. de la Garza, A. Brune, D. Gust, T. A. Moore and A. L. Moore, *J. Phys. Chem. B*, 2004**, 108***,* 10566-10580.

[S3] B. J. Littler, Y. Ciringh and J. S. Lindsey, *J. Org. Chem.*, 1999**, 64***,* 2864-2872.

[S4] D. T Gryko, M. Tasior and B. Koszarna, *J. Porphyrins Phthalocyanines*, 2003, **7**, 239-248.

[S5] K. Heinze and A. Reinhart*, Dalton Trans.*, 2008, 469-480.

[S6] T. Rohand, E. Dolusic, T. H. Ngo, W. Maes and W. Dehaen, *ARKIVOC*, 2007**, (x)**, 307-324.

[S7] P. Kandarpa, G. Mausumi and D. Nirada, *Syn. Comm.*, 2009, **39**, 2694-2701.

Fig. S1 ^{19}F NMR spectrum of bis(porphyrin) **4c** in CDCl$_3$.

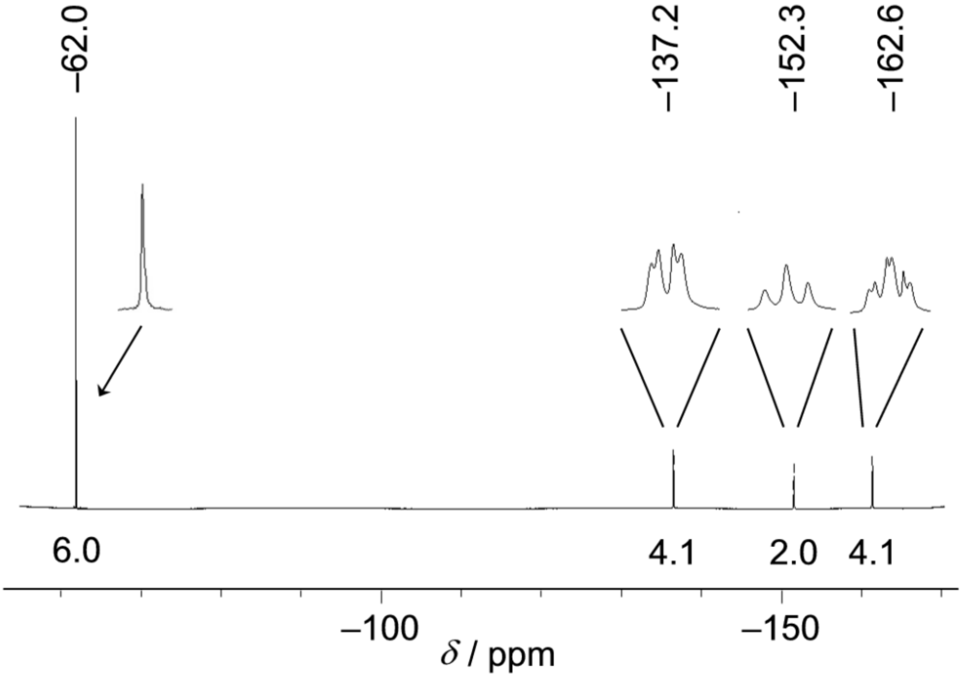

DFT Section

Fig. S2 DFT calculated spin densities of radical ions **4c**$^+$ and **4c**$^-$ (isosurface value at 0.01 a.u.; B3LYP/LANL2DZ, PCM CH_2Cl_2).

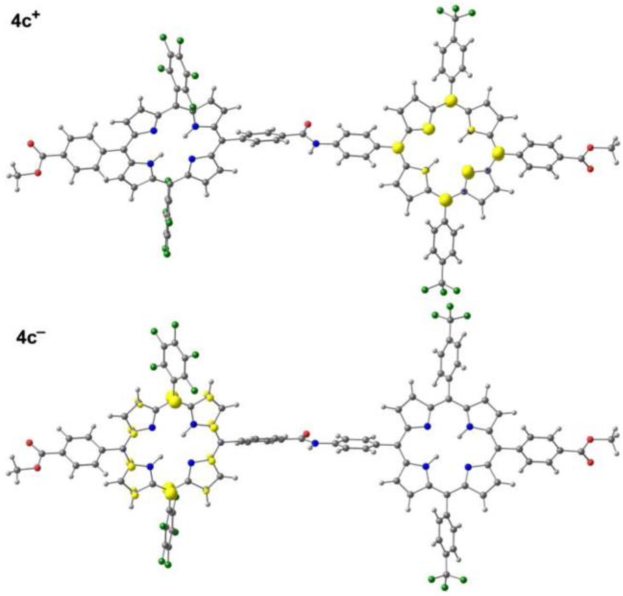

Fig. S3 Frontier orbitals of **4b** isosurface value at 0.05 a.u.; B3LYP/LANL2DZ, PCM CH_2Cl_2.

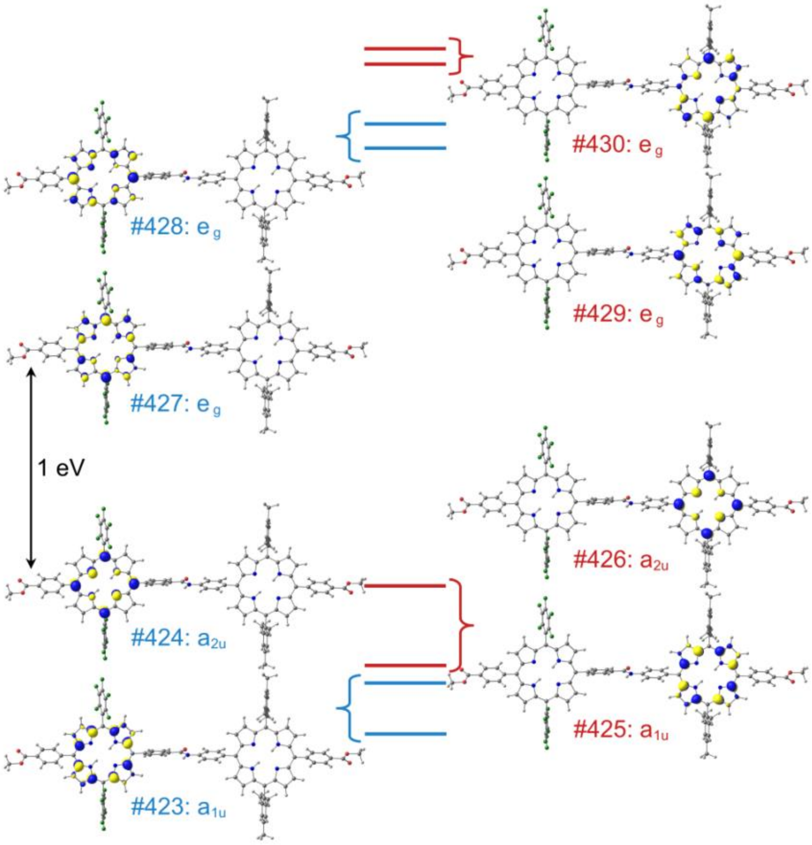

Fig. S4 Frontier orbitals of **4c** isosurface value at 0.05 a.u.; B3LYP/LANL2DZ, PCM CH_2Cl_2.

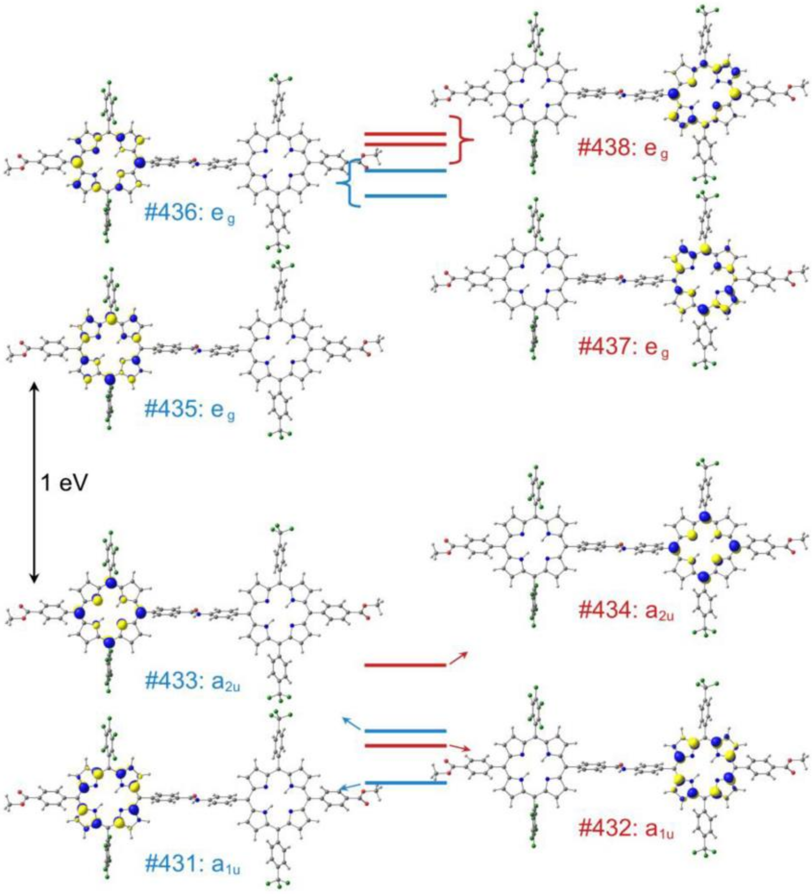

Fig. S5 Frontier orbitals of **Zn^{2}-4d** isosurface value at 0.05 a.u.; B3LYP/LANL2DZ, gasphase.

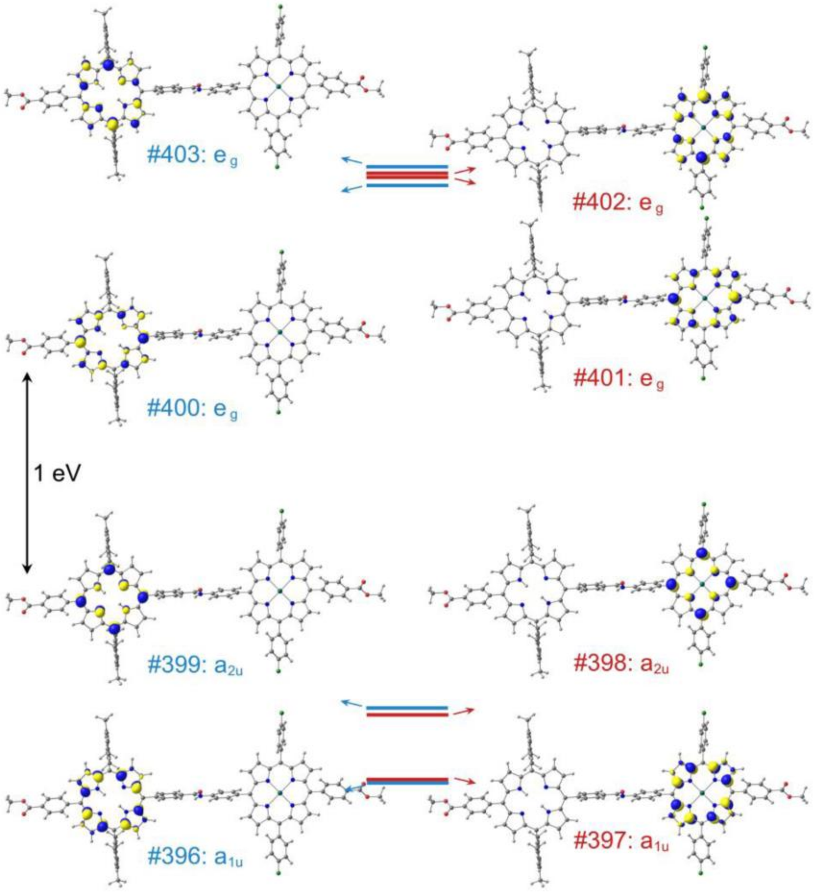

Fig. S6 EPR spectra of **4b**$^{+/-}$, **Zn^2-4d**$^{+/-}$ and their reference compounds in CH_2Cl_2 at 77 K (9.4 GHz).

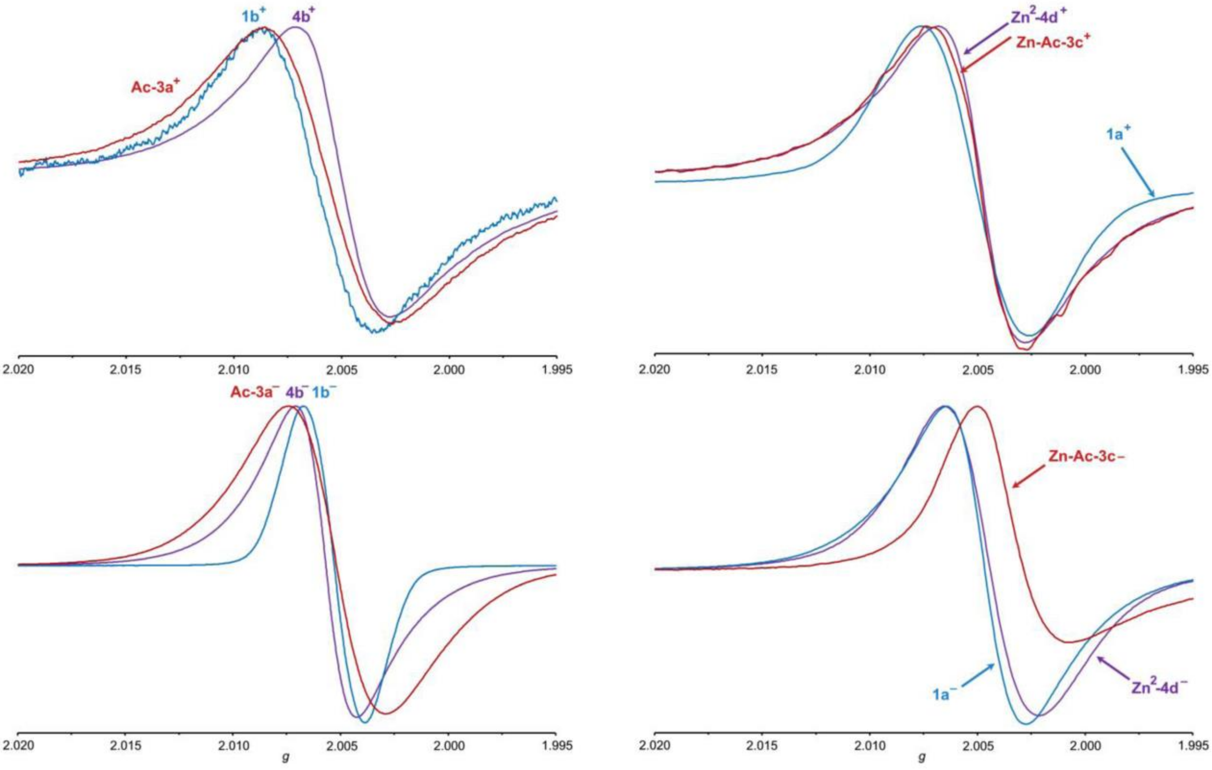

Fig. S7. Normalised Soret bands of **4a** – **4d**, **Zn^2-4d** and **Zn^{1}Zn^2-4d** and their constituent reference porphyrins in CH_2Cl_2.

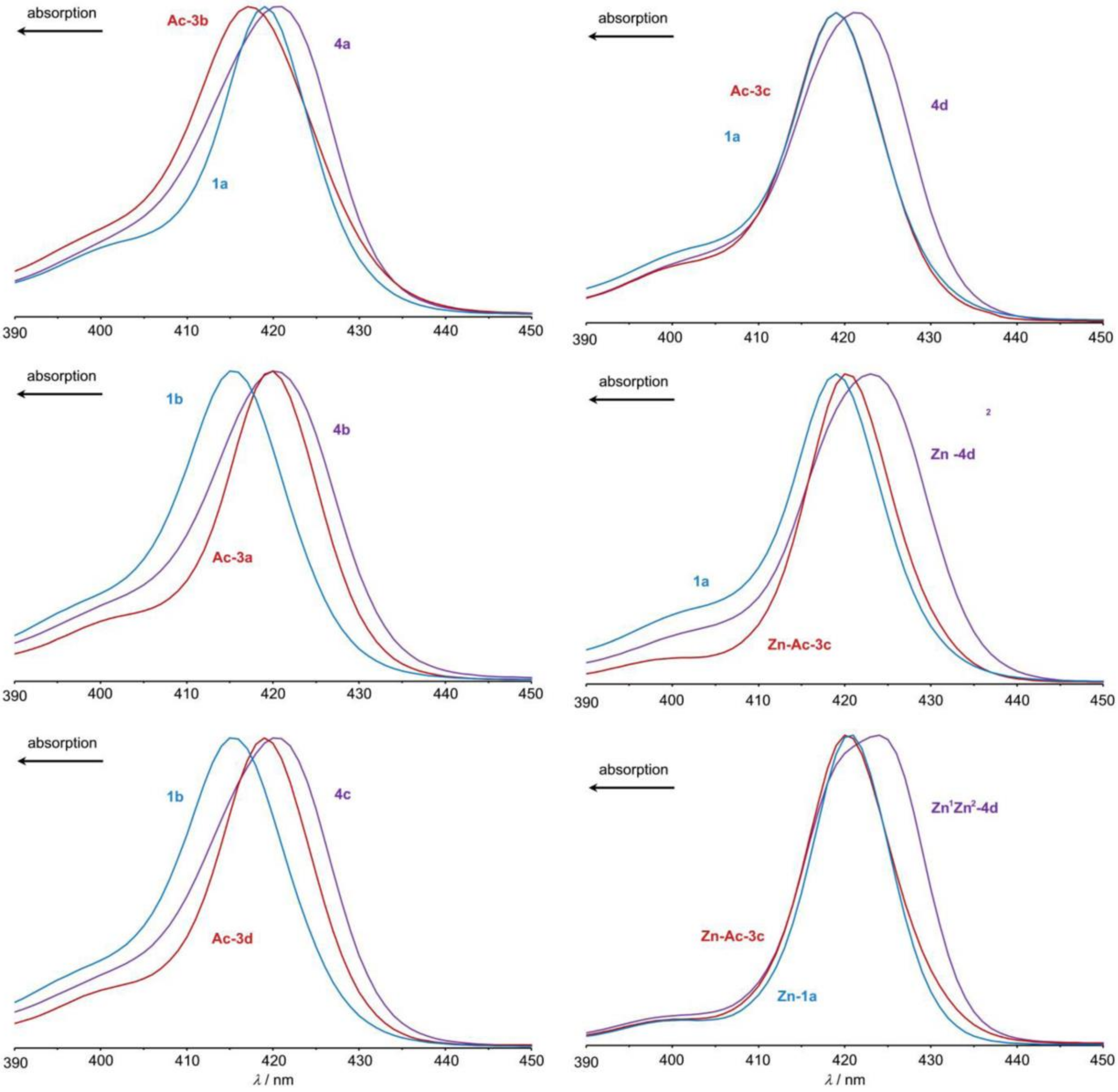

Fig. S8. Normalised (to Q(0,0)) emission spectra of **Ac-3a** – **Ac-3d** in CH_2Cl_2.

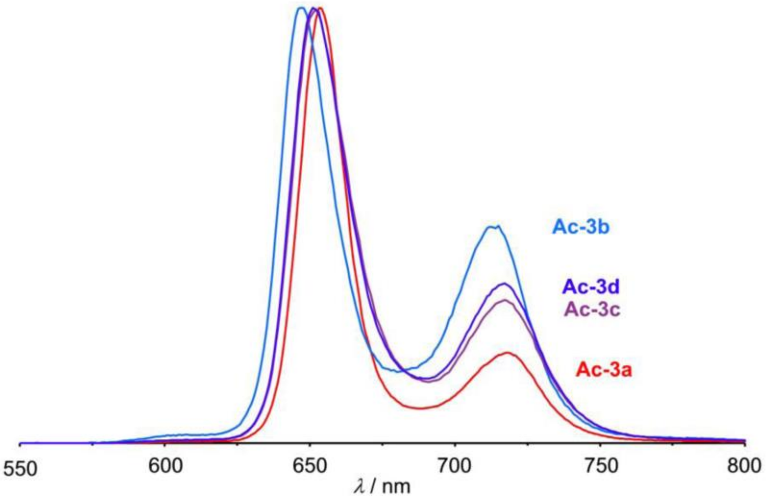

Fig. S9. Normalised (logarithmic) fluorescence decays of **Zn^1Zn^2-4d**, **Zn-1a** and **Zn-Ac-3c** in CH_2Cl_2.

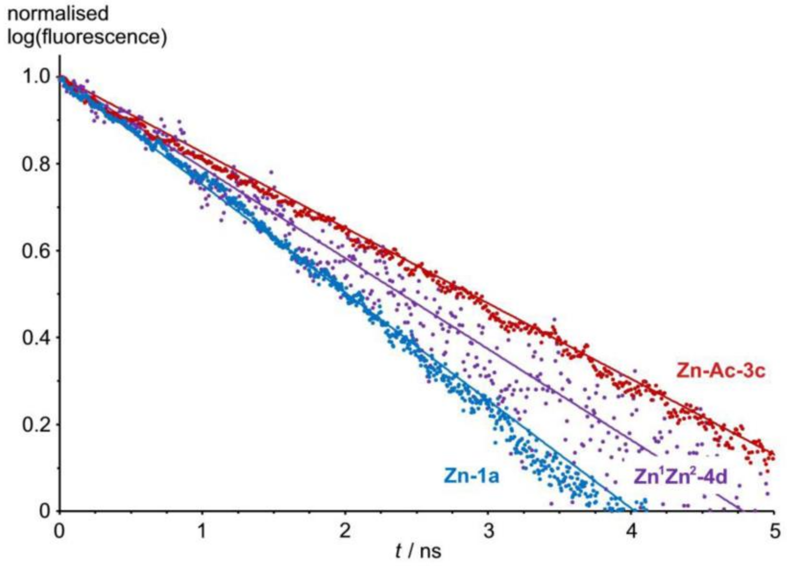

Fig. S10. X-band EPR spectra of radical ions **Zn^1Zn^2-4d$^{+/-}$** and reference radicals in CH_2Cl_2 at 295 K (9.4 GHz).

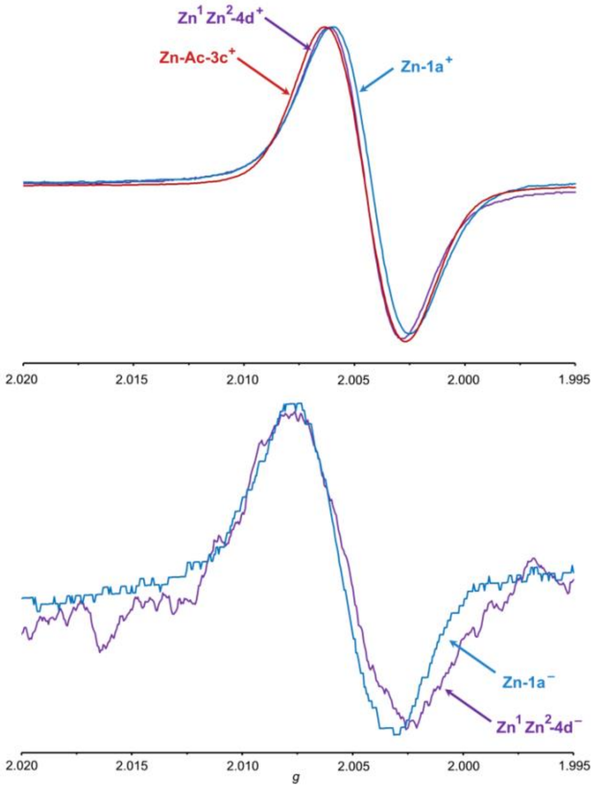

Reproduced by permission of The Royal Society of Chemistry
http://www.rsc.org/suppdata/dt/c3/c3dt50711d/c3dt50711d.pdf (accessed on 24.04.2014)

7.2 Supporting Informations and Experimental Section of Publication 6.2

Eur. J. Inorg. Chem. **2014** · © WILEY-VCH Verlag GmbH & Co. KGaA, 69451 Weinheim, 2014 · ISSN 1099–0682

SUPPORTING INFORMATION

DOI: 10.1002/ejic.201400118
Title: Tuning Reductive and Oxidative Photoinduced Electron Transfer in Amide-Linked Anthraquinone–Porphyrin–Ferrocene Architectures
Author(s): Jascha Melomedov, Julian Robert Ochsmann, Michael Meister, Frédéric Laquai, Katja Heinze*

Experimental Section

Instrumentation. NMR spectra were recorded on a Bruker Avance DRX 400 spectrometer at 400.31 MHz (^{1}H), 100.05 MHz (^{13}C{^{1}H}) and 367.67 MHz (^{19}F). Chemical shifts are reported on the δ scale in ppm relative to the solvent signal as an internal standard: d$_8$-THF (^{1}H: δ = 1.73, 3.58 ppm; ^{13}C: δ = 25.5, 67.7 ppm), CDCl$_3$ (^{1}H: δ = 7.24 ppm; ^{13}C: δ = 77.0 ppm), CD$_2$Cl$_2$ (^{1}H: δ = 5.32 ppm; ^{13}C: δ = 54.0 ppm) or versus external CFCl$_3$ (^{19}F: δ = 0 ppm); (s) = singlet, (d) = doublet, (pt) = pseudo triplet (unresolved doublet of doublets), (dd) = doublet of doublets, (ddd) = doublet of doublet of doublets, (br. s) = broad singlet. IR spectra were recorded with a BioRad Excalibur FTS 3100 spectrometer as CsI disks with signal intensity: (vs) = very strong, (s) = strong, (m) = medium, (w) = weak. ESI and HR ESI mass spectra were recorded on a Micromass Q-TOF-Ultima spectrometer. FD mass spectra were obtained on a FD Finnigan MAT90 spectrometer. Cyclic voltammetric (CV) and squarewave voltammetric measurements were carried out with a BioLogic SP-50 voltammetric analyzer in CH$_2$Cl$_2$ containing 0.1 M (^{n}Bu$_4$N)(PF$_6$) as supporting electrolyte at a glassy carbon working electrode, a platinum wire as the counter electrode and a 0.01 M Ag/AgNO$_3$ electrode as the reference electrode. All cyclic voltammetric measurements were recorded at 100 mV s^{-1} scan speed. Ferrocene was employed as an internal reference redox system. UV/Vis/NIR absorption spectra were measured in CH$_2$Cl$_2$ on a Varian Cary 5000 spectrometer in 1.0 cm cells (Hellma, suprasil). Steady-state emission spectra were recorded in CH$_2$Cl$_2$ or THF on a

Varian Cary Eclipse spectrometer in 1.0 cm cells (Hellma, suprasil). Quantum yields Φ were determined by comparing the areas under the emission spectra on an energy scale [cm^{-1}] recorded for optically matched solutions (absorption intensity below 0.05) of the samples and the reference (Φ(H_2TPP) = 0.13 in benzene)[S1] using the equation[S2] $\Phi = \Phi_{\text{ref}} \times I/I_{\text{ref}} \times \eta^2/\eta^2_{\text{ref}}$ with η(benzene) = 1.5011, η(CH_2Cl_2) = 1.4242 and η(THF) = 1.4070; experimental uncertainty 15%. Fluorescence decay measurements were performed on ca. 10^{-5} M solutions by the time correlated single photon counting method using a Hamamatsu Streak Camera system. Two time modes were used for the measurements: one with a resolution down to a few picoseconds and a maximum time range of two nanoseconds (fast sweep, mononuclear zinc(II) porphyrins, **6a** – **6i**, **Zn-6a** – **Zn-6i** and **9**), and a second time mode with a time resolution down to a few hundred picoseconds and a maximum time range limited by the repetition rate of the excitation source (slow sweep, all free base porphyrins and **4a** – **4h**). Excitation was provided depending on the measuring mode. For fast sweep experiments a Ti:sapphire ultrafast laser system (Coherent Mira 900- Dual fs-ps-Oscillator) with a repetition rate of 80 MHz and a pulse length of 100 fs pumped by a diode pumped solid-state laser (Coherent Verdi V8) was used. The 800 nm output was frequency doubled using a BBO crystal to achieve the excitation wavelength of 400 nm. For the slow sweep measurements a Fianium fiber laser supercontinuum source (SC450-2) was used which provides a white laser light (460 – 2200 nm) with a pulse width of 6 ps and a fundamental repetition rate of 20 MHz, which was typically derated by an implemented pulse picker to 1 MHz. The desired excitation wavelength (550 nm) was filtered out of the white-light using an acousto-optical modulator (AOM, Fianium AOTF).[S3] Transient absorption measurements were performed with a home-built pump-probe setup.[S3] To measure a time range up to 3 ns with a resolution of ~ 100 fs, the output of a commercial titanium: sapphire amplifier (Coherent LIBRA HE, 3.5 mJ, 1 kHz, 100 fs) was split with one portion used to generate a 515 nm excitation pulse using an optical parametric amplifier (Coherent OPerA Solo), and another used to generate a 1300 nm seed pulse (output of an optical parametric amplifier (Coherent OPerA Solo)) for white-light generation in the visible to NIR (500 – 1000 nm) in a c-cut 3 mm thick sapphire window. The variable delay of up to 3 ns between pump and probe was introduced by a broadband retroreflector mounted on a mechanical delay stage. The excitation pulse was chopped at 500 Hz, while the white light pulses were dispersed onto a linear silicon (Hamamatsu NMOS linear image sensor S3901 photodiode. The array was read out at 1 kHz. Adjacent diode readings corresponding to the transmission of the sample after an excitation pulse and without an excitation pulse were used to calculate $\Delta T/T$. Samples were excited with fluences around 100 µJ cm^{-2}.

Density functional calculations were carried out with the Gaussian09/DFT series[S4] of programs. The B3LYP formulation of density functional theory was used employing the LANL2DZ basis set.

To include solvent effects the integral equation formalism polarisable continuum model (IEFPCM, CH_2Cl_2) was employed. No symmetry constraints were imposed on the molecules. The presence of energy minima of the ground states was checked by analytical frequency calculations.

Materials. Unless otherwise noted, all chemical reagents were used without any further purification as received from suppliers (Sigma Aldrich, Acros, Alfa Aesar). Tris(pentafluorophenyl)boron was recrystallized from petroleum ether (40 – 60°C). THF was freshly distilled from sodium. CH_2Cl_2 and 1,2-dichloro-ethane were freshly distilled from calcium hydride. *N*-(4-methylbenzoyl)morpholine,[S5] *N*-(4-(trifluoromethyl)benzoyl)morpholine[S5], 5-(4-Nitrophenyl) dipyrromethane, 5-(pentafluorophenyl)dipyrromethane, 5-(4-(methoxycarbonylphenyl))dipyrromethane,[S6-S8] porphyrins **3c**, **Ac-3c**, **Zn-Ac-3c**[S9-S11] with Ar = 2,4,6-$C_6H_2Me_3$, porphyrin **3e** with Ar = C_6H_5,[S12] porphyrins **3f**, **Ac-3f**, **Zn-Ac-3f**[S9] with Ar = 4-C_6H_4F, porphyrins **3g**, **Ac-3g**, **Zn-Ac-3g**[S9] with Ar = 4-$C_6H_4CF_3$ and porphyrins **3h**, **Ac-3h**, **Zn-Ac-3h**[S9] with Ar = C_6F_5 were prepared by published procedures.

***N*-(4-methylbenzoyl)morpholine** was prepared according to ref S5.

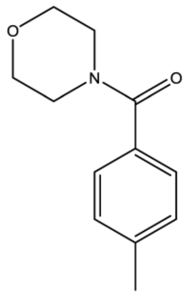

IR (KBr): $\tilde{\nu}$ [cm^{-1}] = 3001 (w), 2952, (CH, w), 2853 (CH, w), 1618 (vs), 1560 (NO, m), 1446 (s), 1348 (w) 1266 (s), 1110 (s), 832 (s), 750 (s).

MS (ESI): *m/z* (%) = 206.11(100) [M+H]$^+$.

***N*-(4-methoxybenzoyl)morpholine and *N*-(4-buthoxybenzoyl)morpholine** were synthesised according to a general procedure for the preparation of *N*-arylmorpholines. 4-methoxybenzoic acid (1 eq.) was dissolved in thionyl chloride (2 eq.) and heated under reflux overnight. The excess of thionyl chloride was removed under reduced pressure. The residue was dissolved in 100 mL dry CH_2Cl_2 and cooled down to 0°C. A solution of morpholine (2 eq.) in 70 ml CH_2Cl_2 was slowly added to the acid chloride solution so that the temperature remains below 5°C. The colourless suspension was warmed to room temperature and stirred for 10 min. The mixture was washed with water (3×), 2M HCl_{aq} (3×) and again with water (3×). The organic layer was dried with Na_2SO_4 and the solvent was removed under reduced pressure.

***N*-(4-butoxybenzoyl)morpholine.** 50 g (0.26 mol) of 4-butoxybenzoic acid, 39 mL (0.52 mol) thionyl chloride, 100 mL dry CH_2Cl_2, 48.00 g (0.54 mol) morpholine in 70 ml CH_2Cl_2. Yield 29.8 g (0.11 mol, 44%), yellow liquid. $C_{15}H_{21}NO_3$ (263.33).

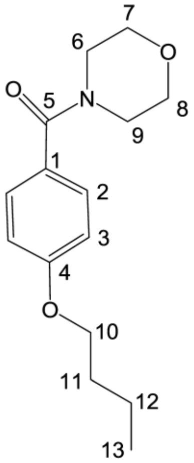

^{1}H-NMR (CDCl$_3$): δ = 0.98 (t, $^3J_{HH}$ = 7.3 Hz, 3 H, H^{13}), 1.50 (m, 2 H, H^{12}), 1.77 (m, 2 H, H^{11}), 3.61 (br. s, 4 H, H^{7,8}), 3.65 (br. s, 4 H, H^{6,9}), 3.97 (t, $^3J_{HH}$ = 6.3 Hz, 3 H, H^{10}), 6.91 (d, $^3J_{HH}$ = 8.4 Hz, 2 H, H^3), 7.38 (d, $^3J_{HH}$ = 8.5 Hz, 2 H, H^2) ppm.

$^{13}C\{^1H\}$-NMR ($CDCl_3$): δ = 13.0 (C^{13}), 18.4 (C^{12}), 30.4 (C^{11}), 66.0 ($C^{6,7,8,9}$), 66.9 (C^{10}), 113.4 (C^3), 126.3 (d, C^2), 128.4(C^1), 159.6 (C^4), 169.4 (C^5) ppm.
IR (KBr) [cm^{-1}]: $\tilde{\nu}$ = 3066 (w), 3042 (w), 2959 (CH, w), 2932 (CH, w), 2866 (CH, w), 1630 (vs), 1512 (m), 1454 (vs), 1423 (vs), 1300 (vs), 1277 (vs), 1247 (C-O-C, vs), 844 (s), 763 (m).
MS (FD): *m/z* (%) = 263.46 (100) $[M]^+$.
MS (ESI): *m/z* (%) = 264.15 (5) $[M+H]^+$), 286.14 (50) $[M+Na]^+$, 549.29 (100) $[2M+Na]^+$.
HR-MS (ESI): obs. *m/z* = 286.1410 $[M+Na]^+$; calcd. for $[M+Na]^+$ 286.1419.

***N*-(4-methoxybenzoyl)morpholine.** 50 g (0.32 mol) 4-methoxybenzoic acid, 48 mL (0.64 mol) thionyl chloride, 100 mL CH_2Cl_2, 59.00 g, (0.67 mol) in 70 ml CH_2Cl_2. Yield 67.2 g (0.30 mol, 95%), yellow liquid. $C_{12}H_{15}NO_3$ (221.25).

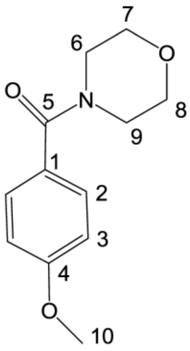

^1H-NMR ($CDCl_3$): δ = 3.61 (br. s, 4 H, $H^{7,8}$), 3.65 (br. s, 4 H, $H^{6,9}$), 3.79 (m, 3 H, H^{10}), 6.91 (m, 2 H, H^3), 7.39 (m, 2 H, H^2) ppm.
$^{13}C\{^1H\}$-NMR ($CDCl_3$): δ = 54.5 (C^{10}), 66.0 ($C^{6,7,8,9}$), 113.0 (C^3), 126.6 (d, C^2), 128.5(C^1), 160.1 (C^4), 169.4 (C^5) ppm.
IR (KBr): $\tilde{\nu}$ [cm^{-1}] = 3070 (w), 2964 (CH, s), 2920 (CH, s), 2854 (CH, s), 1629 (s), 1514 (vs), 1423 (vs), 1454 (vs), 1302 (vs), 1279 (vs), 1247 (C-O-C, vs), 843 (vs), 763 (s).
MS (FD): *m/z* (%) = 221.44 (100) $[M]^+$, 442.57 (1) $[2M]^+$.
MS (ESI): *m/z* (%) = 222.12 (3) $[M+H]^+$, 244.09 (3) $[M+Na]^+$, 465.20 (38) $[2M+Na]^+$.
HR-MS (ESI): obs. *m/z* = 244.0950 $[M+Na]^+$; calcd. for $[M+Na]^+$ 244.0950.

General procedure for the preparation of 1,9-diacyldipyrromethanes.[S6] *N*-aroylmorpholine (1 eq.) and phosphorous oxytrichloride (2 eq.) were heated at 65°C under nitrogen for 3 h. The dark solution was cooled to room temperature and diluted with 1,2-dichloroethane. 5-(4-Nitrophenyl)dipyromethane[S6] (0.25 eq.) was added and the solution was stirred under reflux for 2 h and quenched by addition of a saturated aqueous solution of sodium acetate and heated to reflux for 1 h. After cooling to room temperature the mixture was diluted with CH_2Cl_2 and the organic layer was separated. After washing with water (3×) and drying with Na_2SO_4 and the solvent was removed under reduced pressure. The residue was purified by chromatography on silica using CH_2Cl_2 : ethyl acetate (20:1).

1,9-bis(4-butoxybenzoyl)-5-(4-nitrophenyl)dipyrromethane. 25.0 g, (0.095 mol) *N*-(4-butoxybenzoyl)morpholine, 30.4 g, (0.22 mol) phosphorous oxytrichloride, 175 mL 1,2-dichloroethane, 5.67 g (0.024 mol) 5-(4-nitrophenyl)dipyromethane, 75 mL CH_2Cl_2 and 180 mL saturated aqueous solution of sodium acetate. Silica, CH_2Cl_2 : ethyl acetate (20:1), $R_f = 0.36$. Yield 12.2 g (0.020 mol, 82%), red-brown solid. $C_{37}H_{37}N_3O_6$ (619.71).

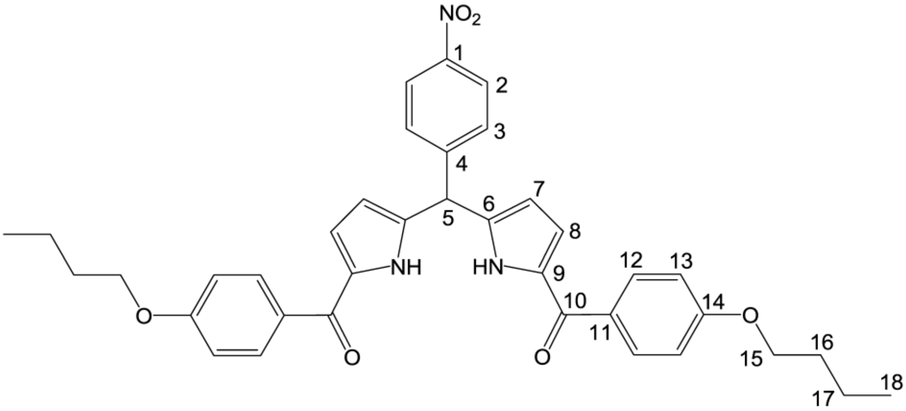

^{1}H-NMR ($CDCl_3$): δ=0.97 (t, $^3J_{HH}$ = 7.4 Hz, 3 H, H^{18}), 1.49 (m, 2 H, H^{17}), 1.78 (m, 2 H, H^{16}), 3.99 (t, $^3J_{HH}$ = 6.3 Hz, 6H, H^{15}), 5.81 (s, 1H, H^5), 5.84 (m, 2 H, H^7), 6.45 (m, 2 H, H^8), 6.86 (d, $^3J_{HH}$ = 8.6 Hz, 4 H, H^{12}), 7.72 (d, $^3J_{HH}$ = 8.6 Hz, 4 H, H^{13}), 7.76 (m, $^3J_{HH}$ = 8.5 Hz, 4 H, H^3), 8.20 (d, $^3J_{HH}$ = 8.5 Hz, 2 H, H^2), 12.19 (s, 2 H, H^{NH}) ppm.

^{13}C{^{1}H}-NMR ($CDCl_3$): δ = 13.8 (C^{18}), 19.2 (C^{17}), 31.1 (C^{16}), 44.7 (C^5), 67.8 (C^{15}), 111.1 (C^7), 113.7 (C^{12}), 120.0 (C^8), 123.9 (C^2), 129.8 (C^3), 130.3 (C^{14}), 131.3 (C^6), 131.8 (C^{13}), 138.9 (C^9), 147.1 (C^{11}), 148.1 (C^4), 162.3 (C^1), 183.5 (C^{10}) ppm.

IR (KBr): $\tilde{\nu}$ [cm^{-1}] = 3244 (NH^{pyrrole}, br, m), 3105 (w), 2959 (CH, s), 2932 (CH, s), 2872 (CH, s), 1605 (s), 1521 (NO, m), 1344 (NO, s) 1252 (C-O-C, s), 887 (m).

MS (FD): *m/z* (%) = 309.96 (2) $[M]^{2+}$, 619.64 (100) $[M]^+$, 1239.4 (1) $[2M]^+$.

MS (ESI): *m/z* (%) = 641.25 (100) $[M–H+Na]^+$.

HR-MS (ESI): obs. *m/z* = 620.2761 $[M+H]^+$; calcd. for $[M+H]^+$ 620.2761.

1,9-bis(4-methoxybenzoyl)-5-(4-nitrophenyl)dipyrromethane. 40.0 g, (0.18 mol) *N*-(4-trifluoromethylbenzoyl)morpholine, 33.4 mL (0.36 mol) phosphorous oxytrichloride, 300 mL 1,2-dichloroethane, 10.2 (0.045 mol) 5-(4-nitrophenyl)dipyromethane, 150 mL CH_2Cl_2 and 300 mL saturated aqueous solution of sodium acetate. Silica, CH_2Cl_2 : ethyl acetate (20:1), $R_f = 0.38$. Yield 12.6 g (0.024 mol, 52%), dark solid. $C_{31}H_{25}N_3O_6$ (535.55).

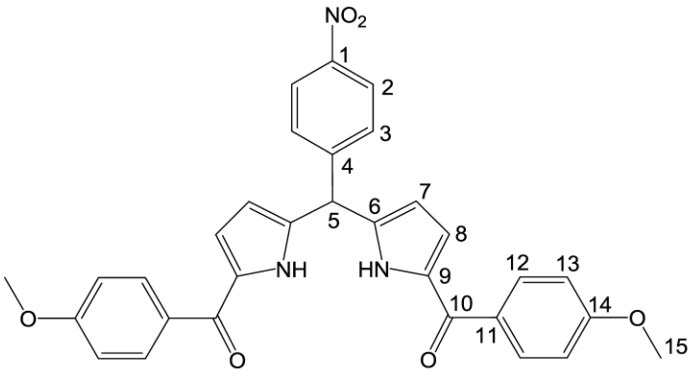

^{1}H-NMR (CDCl$_3$): δ =3.83 (s, 6H, H^{15}), 5.82 (s, 1H, H^5), 5.87 (m, 2 H, H^7), 6.47 (m, 2 H, H^8), 6.87(d, $^3J_{HH}$ = 8.8 Hz, 4 H, H^{12}), 7.73 (m, $^3J_{HH}$ = 8.6 Hz, 6 H, H$^{3/13}$), 8.17 (d, $^3J_{HH}$ = 8.7 Hz, 2 H, H^2), 12.11 (s, 2 H, H^{NH}) ppm.

^{13}C{^{1}H}-NMR (CDCl$_3$): δ = 44.7 (C^5), 55.3 (C^{15}), 111.1 (C^7), 113.3 (C^{12}), 120.2 (C^8), 123.9 (C^2), 129.8 (C^3), 130.4 (C^{14}), 131.3 (C^6), 131.7 (C^{13}), 139.0 (C^9), 147.1 (C^{11}), 148.0 (C^4), 162.7 (C^1), 183.5 (C^{10}) ppm.

IR (KBr): $\tilde{\nu}$ [cm^{-1}] = 3242 (NH^{pyrrole}, br, m), 3107 (w), 2959 (CH, s), 2931 (CH, s), 2839 (CH, s), 1604 (s), 1514 (NO, m), 1346 (NO, s), 1255 (C-O-C, s), 887 (m).

MS (FD): *m/z* (%) = 267.94 (2) [M]$^{2+}$, 535.58 (100) [M]$^+$.

MS (ESI): *m/z* (%) = 536.19 (5) [M+H]$^+$, 558.16 (2) [M+Na]$^+$.

HR-MS (ESI): obs. *m/z* = 536.1806 [M+Na]$^+$; calcd. for [M+Na]$^+$ 536.1822.

1,9-bis(4-methylbenzoyl)-5-(4-nitrophenyl)dipyrromethane. 50.0 g, (0.24 mol) *N*-(4-methylbenzoyl)morpholine, 45.6 mL, (0.50 mol) phosphorous oxytrichloride, 350 mL 1,2-dichloroethane, 16.0 (0.06 mol) 5-(4-nitrophenyl)dipyromethane, 150 mL CH$_2$Cl$_2$ and 360 mL saturated aqueous solution of sodium acetate. Silica, CH$_2$Cl$_2$: ethyl acetate (20:1), R_f = 0.38. Yield 29.6 g (0.059 mol, 99%), red-brown solid. $C_{31}H_{25}N_3O_4$ (503.55).

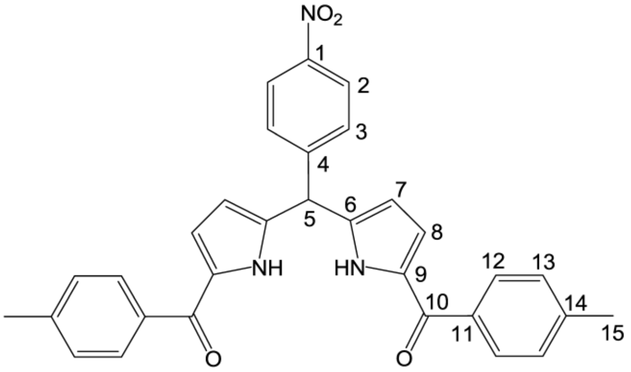

^{1}H-NMR (CDCl$_3$): δ=2.39 (s, 6H, H^{15}), 5.83 (s, 1H, H^5), 5.90 (m, 2 H, H^7), 6.50 (m, 2 H, H^8), 7.19 (d, $^3J_{HH}$ = 7.7 Hz, 4 H, H^{12}), 7.63 (d, $^3J_{HH}$ = 7.9 Hz, 4 H, H^{13}), 7.79 (d, $^3J_{HH}$ = 8.5 Hz, 2 H, H^2), 8.21 (d, $^3J_{HH}$ = 8.5 Hz, 2 H, H^3), 12.17 (s, 2 H, H^{NH}) ppm.

$^{13}C\{^1H\}$-NMR ($CDCl_3$): δ = 21.5 (C^{15}), 44.7 (C^5), 111.3 (C^7), 120.6 (C^8), 123.9 (C^3), 128.7 (C^{12}), 129.8 (C^{13}), 129.8 (C^2), 131.4 (C^6), 135.2 (C^{14}), 139.3 (C^9), 142.5 (C^{11}), 147.1 (C^4), 147.9 (C^1), 184.5 (C^{10}) ppm.
IR (KBr): $\tilde{\nu}$ [cm^{-1}] = 3247 ($NH^{pyrrole}$, br, m), 3107 (w), 2927 (CH, s) 1700 (CO, m), 1602, (s), 1520 (NO, m), 1340 (NO, vs) 1242 (C-O-C, s), 889 (s), 750 (s).
MS (FD): *m/z* (%) = 503.48 (100) $[M]^+$.
MS (ESI): *m/z* (%) = 504.21 (86) $[M+H]^+$, 1007.42 (100) $[2M+H]^+$.
HR-MS (ESI): obs. *m/z* = 504.1927 $[M+H]^+$; calcd. for $[M+H]^+$ 504.1923.

General procedure for the preparation of porphyrins 2a, 2b and 2d. To a stirred solution of 1,9-diacyldipyrromethane in THF/methanol (10:1) $NaBH_4$ (20 eq.) was added under nitrogen at room temperature and the mixture was stirred until TLC indicated consumption of starting material. The reaction was quenched with a saturated solution of NH_4Cl_{aq} and diluted with CH_2Cl_2. The organic layer was separated, washed with water (3×) and dried with Na_2SO_4. After removing the solvent the dipyrromethane-dicarbinol was obtained as a foamlike solid. To this brown residue was added 5-(4-benzoic acid methylester)dipyrromethane[S6] (1.2 eq.) and acetonitrile. The suspension was dipped in an ultrasonic bath to dissolve the compounds. This solution was added to a pre-cooled solution of DMF and TFA in acetonitrile (0°C) in small portions over 30 min. After stirring for 10 min 2,3-dicyano-5,6-dichloro-1,4-benzoquinone (DDQ) was added and the mixture was stirred for 1 h. Triethylamine was added to quench the reaction and the mixture was concentrated under reduced pressure. The products were purified by column chromatography [silica, CH_2Cl_2].

4-[15-(4-nitro-phenyl)-10,20-di-(4-butoxy)phenylporphyrin-5-yl]methyl benzoate (2a). 6.81 g (180 mmol) $NaBH_4$, 440 mL THF/methanol (10:1), 5.58 g (9.0 mmol) 1,9-bis(4-butoxybenzoyl)-5-(4-nitrophenyl)dipyrromethane, 3.02 g (11.3 mmol) 5-(4-methyl benzoate)dipyrromethane, 2 L acetonitrile, 6 mL DMF, 8.4 mL TFA, 7.8 g (0.034 mol) DDQ, 9.0 mL triethylamine. [silica, CH_2Cl_2, R_f = 0.61]. Yield 659 mg (0.76 mmol, 8%), purple powder. $C_{54}H_{47}N_5O_6$ (861.98).

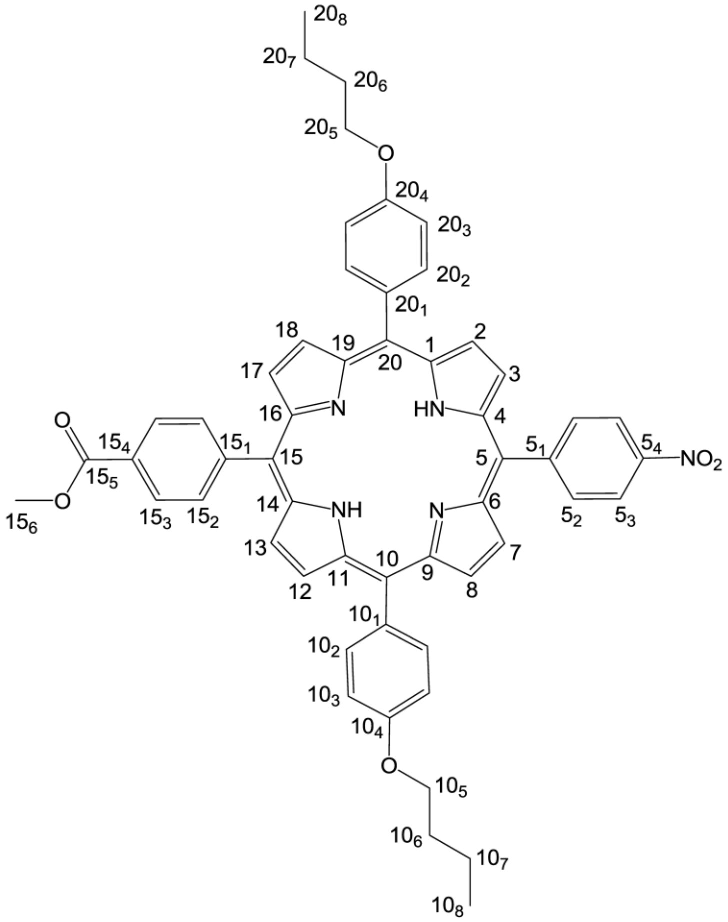

^{1}H-NMR (d$_8$-THF): δ = –2.69 (s, 2 H, $H^{pyrroleNH}$), 1.10 (t, $^3J_{HH}$ = 7.4 Hz, 9 H, $H^{10/20}_{8/8}$), 1.69 (m, 4 H, $H^{10/20}_{7/7}$), 1.95 (m, 4 H, $H^{10/20}_{6/6}$), 4.05 (s, 3 H, H^{15}_{6}), 4.27 (t, $^3J_{HH}$ = 6.3 Hz, 4H, $H^{10/20}_{5/5}$), 7.32 (d, $^3J_{HH}$ = 8.4 Hz, 4 H, $H^{10/20}_{3/3}$), 8.09 (d, $^3J_{HH}$ = 8.4 Hz, 4 H, $H^{10/20}_{2/2}$), 8.32 (d, $^3J_{HH}$ = 8.0 Hz, 2 H, H^{15}_{2}), 8.44 (d, $^3J_{HH}$ = 8.0 Hz, 4 H, H^{15}_{3}), 8.45 (d, $^3J_{HH}$ = 8.5 Hz, 2 H, H^{5}_{2}), 8.66 (d, $^3J_{HH}$ = 8.4 Hz, 2 H, H^{5}_{3}), 8.79 (m, 4 H, $H^{pyrrole}$), 8.91 (m, 4 H, $H^{pyrrole}$) ppm.

^{13}C{^{1}H}-NMR (d$_8$-THF): δ = 14.5 ($C^{10/20}_{8/8}$), 20.5 ($C^{10/20}_{7/7}$), 32.7 ($C^{10/20}_{6/6}$), 52.6 (C^{15}_{6}), 68.8 ($C^{10/20}_{5/5}$), 113.8 ($C^{10/20}_{3/3}$), 118.4 (C^{5}), 120.3 (C^{15}), 121.7 ($C^{10/20}$), 122.8 (C^{5}_{3}), 128.9 (C^{15}_{3}), 131.0 (C^{15}_{4}), 131.8 ($C^{pyrrole\ 2/3/7/8/12/13/17/18}$), 135.0 ($C^{10/20}_{1/1}$), 135.5 ($C^{15}_{2}$), 136.2 ($C^{5}_{2}$), 136.5 ($C^{10/20}_{2/2}$), 148.0 ($C^{5}_{4}$), 149.1 ($C^{15}_{1}$), 150.1 ($C^{5}_{1}$), 160.8 ($C^{10/20}_{4/4}$), 167.2 ($C^{15}_{5}$) ppm.

IR (KBr): $\tilde{\nu}$ [cm^{-1}] = 3317 (NH^{pyrrole},br, m), 2954 (CH, w), 2929 (CH, w), 2866 (CH, w), 1724 (CO, s), 1602 (m), 1512 (NO, m), 1344 (NO, vs), 1278 (vs), 1245 (C-O-C, vs), 1109 (s), 806 (s), 738 (m).

MS (FD): *m/z* (%) = 861.55 (10) [M]$^+$, 862.72 (85) [M]$^+$.

MS (ESI): *m/z* (%) = 431.68 (7) [M+H]$^{2+}$, 862.36 (100) [M+H]$^+$, 1724.71 (6) [2M+H]$^+$.

HR-MS (ESI): obs. *m/z* = 862.3599 [M+H]$^+$; calcd. for [M+H]$^+$ 862.3605.

UV/Vis (CH$_2$Cl$_2$): λ [nm] (ε / [10^4 M^{-1}cm^{-1}]) = 422 (39.16), 518 (1.91), 555 (1.22), 593 (0.61), 649 (0.55).

Fluorescence (CH$_2$Cl$_2$): λ [nm] (relative intensity) = 657 (1.00), 721 (0.27).

Quantum yield: Φ = 0.1245.

CV (Fc/Fc$^+$, 100 mV s^{-1}, CH$_2$Cl$_2$): $E_{1/2}$ [V] = –1.990, –1.440, 0.600, 0.800.

4-[15-(4-nitrophenyl)-10,20-di-(4-methoxy)phenylporphyrin-5-yl]methyl benzoate (2b). 6.81 g (180 mmol) NaBH$_4$, 440 mL THF/methanol (10:1), 4.82 g (9.0 mmol) 1,9-bis(4-methoxybenzoyl)-5-(4-nitrophenyl)dipyrromethane, 3.02 g (11.3 mmol) 5-(4-methyl benzoate)dipyrromethane, 2 L acetonitrile, 6 mL DMF, 8.4 mL TFA, 7.8 g (0.034 mol) DDQ, 9.0 mL triethylamine. [silica, CH$_2$Cl$_2$, R_f = 0.63]. Yield 756 mg (1.0 mmol, 10%), purple powder. $C_{48}H_{35}N_5O_6$ (777.82).

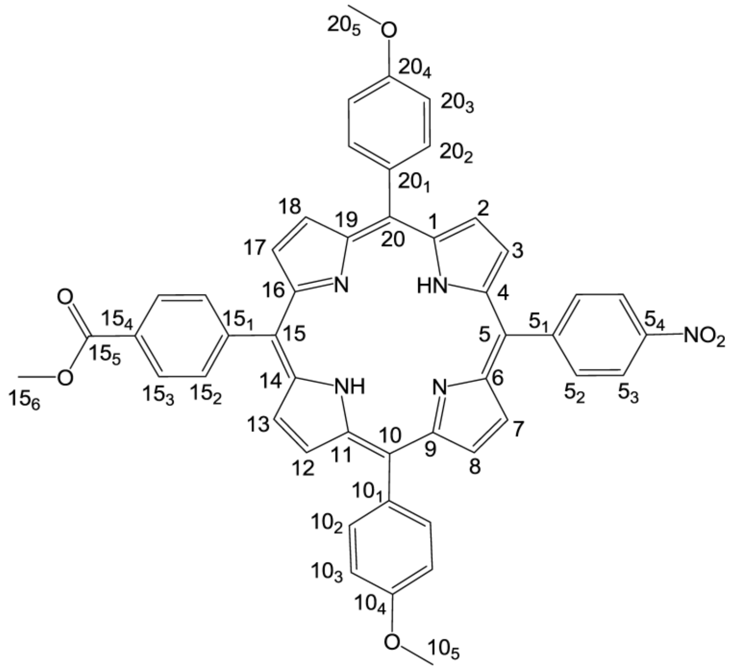

^{1}H-NMR (CD$_2$Cl$_2$): δ = –2.69 (s, 2 H, H$^{\text{pyrroleNH}}$), 4.05 (s, 9 H, H$^{10/20/15}_{5/5/6}$), 7.33 (d, $^3J_{HH}$ = 8.5 Hz, 4 H, H$^{10/20}_{3/3}$), 8.09 (d, $^3J_{HH}$ = 8.5 Hz, 4 H, H$^{10/20}_{2/2}$), 8.31 (d, $^3J_{HH}$ = 8.1 Hz, 2 H, H$^{15}_2$), 8.43 (d, $^3J_{HH}$ = 8.1 Hz, 4 H, H$^{15}_3$), 8.44 (d, $^3J_{HH}$ = 8.5 Hz, 2 H, H$^5_2$), 8.65 (d, $^3J_{HH}$ = 8.5 Hz, 2 H, H$^5_3$), 8.79 (m, 4 H, H$^{\text{pyrrole}}$), 8.90 (m, 4 H, H$^{\text{pyrrole}}$) ppm.

^{13}C{^{1}H}-NMR (CD$_2$Cl$_2$): δ = 52.6 (C$^{15}_6$), 52.9 (C$^{10/20}_{5/5}$), 113.4 (C$^{10/20}_{3/3}$), 118.4 (C^5), 120.3 (C^{15}), 121.7 (C$^{10/20}$), 122.8 (C$^5_3$), 128.8 (C$^{15}_3$), 131.1 (C$^{15}_4$), 132.5 (br. s, C$^{\text{pyrrole 2/3/7/8/12/13/17/18}}$), 135.1 (C$^{10/20}_{1/1}$), 135.5 (C$^{15}_2$), 136.2 (C$^5_2$), 136.5 (C$^{10/20}_{2/2}$), 148.0 (C$^5_4$), 149.1 (C$^{15}_1$), 150.1 (C$^5_1$), 161.1(C$^{10/20}_{4/4}$), 167.4 (C$^{15}_5$) ppm.

IR (KBr): $\tilde{\nu}$ [cm^{-1}] = 3321 (NH$^{\text{pyrrole}}$,br, m), 2949 (CH, w), 2927 (CH, w), 2837 (CH, w), 1722 (CO, s), 1602 (m), 1514 (NO, m), 1346 (NO, vs), 1280 (vs), 1245 (C-O-C, vs), 800 (m), 732 (m).

MS (FD): m/z (%) = 388.95 (4, [M]$^{2+}$), 777.60 (100, [M]$^+$).

MS (ESI): m/z (%) = 389.63 (9) [M^{2+}+H], 778.26 (100) [M+H]$^+$, 1556.52 (2) [2M+H]$^+$.

HR-MS (ESI): obs. m/z = 778.2648 [M+H]$^+$; calcd. for [M+H]$^+$ 778.2666.

UV/Vis ($\mathbf{CH_2Cl_2}$): λ [nm] (ε / [10^4 $\mathrm{M^{-1}cm^{-1}}$]) = 422 (28.18), 517 (1.39), 555 (0.83), 593 (0.42), 649 (0.39).

Fluorescence ($\mathbf{CH_2Cl_2}$): λ [nm] (relative intensity) = 656 (1.00), 720 (0.27).

Quantum yield: Φ = 0.1254.

CV ($\mathbf{Fc/Fc^+}$, 100 mV $\mathbf{s^{-1}}$, $\mathbf{CH_2Cl_2}$): $E_{½}$ [V] = –2.020 (irr.), –1.510, 0.590, 0.800.

4-[15-(4-nitro-phenyl)-10,20-di-(4-methylphenyl) porphyrin-5-yl]methyl benzoate (2d). 6.81g, (180 mmol) $\mathrm{NaBH_4}$, 440 mL THF/methanol (10:1), 4.53 g (9.00 mmol) 1,9-bis(4-methylbenzoyl)-5-(4-nitrophenyl)dipyrromethane, 3.02 g (10.00 mmol) 5-(4-methyl benzoate)dipyrromethane, 2 L acetonitrile, 22 mL DMF, 30.8 mL TFA, 28.60 g (0.13 mol) DDQ, 31 mL triethylamine. [silica, $\mathrm{CH_2Cl_2}$, R_f = 0.69]. Yield 308 mg (2.0 mmol, 22%), purple powder. $\mathrm{C_{48}H_{35}N_5O_4}$ (745.82).

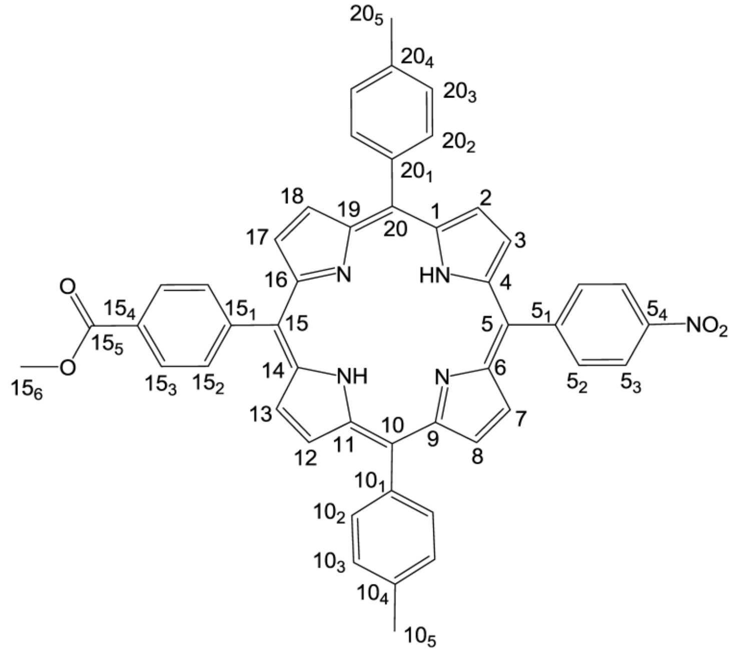

^{1}H-NMR ($\mathbf{CD_2Cl_2}$) δ = –2.82 (s, 2 H, $\mathrm{H^{pyrroleNH}}$), 2.72 (s, 6 H, $\mathrm{H^{10/20}}_{5/5}$), 4.10 (s, 3 H, $\mathrm{H^{15}}_6$), 7.61 (d, $^3J_\mathrm{HH}$ = 7.2 Hz, 4 H, $\mathrm{H^{10/20}}_{3/3}$), 8.11 (d, $^3J_\mathrm{HH}$ = 7.4 Hz, 4 H, $\mathrm{H^{10/20}}_{2/2}$), 8.32 (d, $^3J_\mathrm{HH}$ = 7.6 Hz, 2 H, $\mathrm{H^{15}}_2$), 8.43 (ps.t, $^3J_\mathrm{HH}$ = 7.6 Hz, 4 H, $\mathrm{H^{5/15}}_{2/3}$), 8.64 (d, $^3J_\mathrm{HH}$ = 7.8 Hz, 2 H, $\mathrm{H^5}_3$), 8.80 (d, $^3J_\mathrm{HH}$ = 3.4 Hz, 2 H, $\mathrm{H^{pyrrole}}$), 8.84 (d, $^3J_\mathrm{HH}$ = 3.5 Hz, 2 H, $\mathrm{H^{pyrrole}}$), 8.93 (m, 4 H, $\mathrm{H^{pyrrole}}$) ppm.

^{13}C{^{1}H}-NMR ($\mathbf{CD_2Cl_2}$): δ = 21.8 ($\mathrm{C^{10/20}}_{5/5}$), 52.9 ($\mathrm{C^{15}}_6$), 117.7 ($\mathrm{C^5}$), 119.9 ($\mathrm{C^{15}}$), 121.5 ($\mathrm{C^{10/20}}$), 122.4 ($\mathrm{C^5}_3$), 128.1 ($\mathrm{C^{10/20}}_{3/3}$), 128.4 ($\mathrm{C^{15}}_3$), 130.4 ($\mathrm{C^{15}}_4$), 131.6 (br. s, $\mathrm{C^{pyrrole\ 2/3/7/8/12/13/17/18}}$), 135.1 ($\mathrm{C^{10/20}}_{2/2}$), 135.1 ($\mathrm{C^5}_2$), 135.8 ($\mathrm{C^{15}}_2$), 138.4 ($\mathrm{C^{10/20}}_{4/4}$), 139.3 ($\mathrm{C^{10/20}}_{1/1}$), 147.3 ($\mathrm{C^5}_4$), 148.4 ($\mathrm{C^{15}}_1$), 149.8 ($\mathrm{C^5}_1$), 167.7 ($\mathrm{C^{15}}_5$) ppm.

IR (KBr): $\tilde{\nu}$ [$\mathrm{cm^{-1}}$] = 3423 ($\mathrm{NH^{pyrrole}}$, br, w), 3315 (w), 2939 (CH, w) 1732 (CO, s) 1514 (s), 1521 (NO, s), 1350 (NO, vs), 1274 (s), 793 (vs).

MS (FD): *m/z* (%) = 745.6 (100) $[\mathrm{M}]^+$.

MS (ESI): *m/z* (%) = 746.38 (100) $[M+H]^+$.

HR-MS (ESI): obs. *m/z* = 746.2777 $[M+H]^+$; calcd. for $[M+H]^+$ 746.2767.

UV/Vis (CH_2Cl_2): λ [nm] (ε / [10^4 $M^{-1}cm^{-1}$]) = 420 (21.3), 516 (1.55), 552 (1.09), 591 (0.84), 647 (0.78).

Fluorescence (CH_2Cl_2): λ [nm] (relative intensity) = 654 (1.00), 718 (0.30).

Quantum yield: Φ = 0.0896.

CV (Fc/Fc^+, 100 mV s^{-1}, CH_2Cl_2): $E_{½}$ [V] = −2.180 (q. rev.), −1.530 (2e), 0.610, 0.890.

General procedure for the prepation of porphyrins 3a, 3b and 3d. Under nitrogen 1 eq. nitro-porphyrin **2a, 2b** or **2d** was suspended in conc. aqueous HCl and $SnCl_2$ (14 eq.) was added. The mixture was stirred under reflux for 1 – 2 h until TLC indicated consumption of the starting material. After cooling to room temperature the solution was neutralised with conc. aqueous ammonia and extracted with ethyl acetate. The combined organic phases were dried with Na_2SO_4 and the solvent was removed under reduced pressure. The products were purified by column chromatography [silica, toluene : ethyl acetate (20:1)].

15-(4-Methoxycarbonylphenyl)-5-(4-aminophenyl)-10,20-bis-(4-butoxyphenyl)porphyrin (3b). 185 mg (0.21 mmol) porphyrin **2b**, 65 mL conc. aquaeous HCl, 0.68 g (2.94 mmol) $SnCl_2$. [silica, toluene : ethyl acetate (20:1), R_f = 0.19]. Yield 70.0 mg (0.08 mmol, 40%), purple powder. $C_{54}H_{49}N_5O_4$ (832.00).

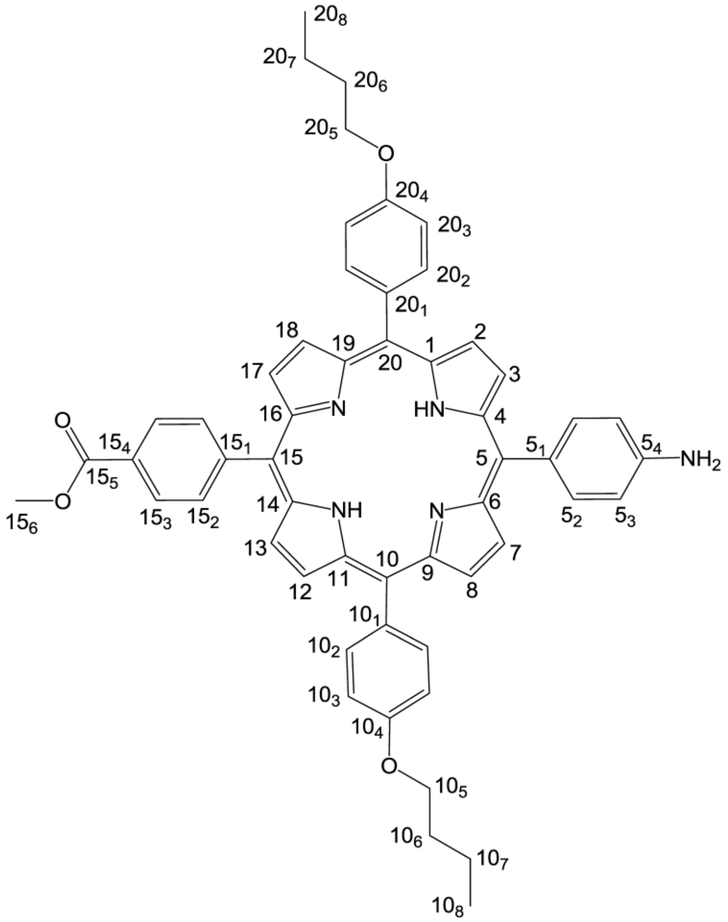

^{1}H-NMR (d$_8$-THF): δ = –2.64 (s, 2 H, $H^{pyrroleNH}$), 1.10 (t, $^3J_{HH}$ = 7.4 Hz, 6 H, $H^{10/20}{}_{8/8}$), 1.68 (m, 4 H, $H^{10/20}{}_{7/7}$), 1.95 (m, 2 H, $H^{10/20}{}_{6/6}$), 4.04 (s, 9 H, $H^{15}{}_{6}$), 4.26 (t, $^3J_{HH}$ = 6.4 Hz, 6H, $H^{10/20}{}_{5/5}$), 4.98 (s, 2H, H^{amine}), 6.99 (d, $^3J_{HH}$ = 8.2 Hz, 2 H, $H^{5}{}_{3}$), 7.31 (d, $^3J_{HH}$ = 8.5 Hz, 4 H, $H^{10/20}{}_{3/3}$), 7.88 (d, $^3J_{HH}$ = 8.2 Hz, 2 H, $H^{5}{}_{2}$), 8.08 (d, $^3J_{HH}$ = 8.4 Hz, 4 H, $H^{10/20}{}_{2/2}$), 8.31 (d, $^3J_{HH}$ = 8.1 Hz, 2 H, $H^{15}{}_{2}$), 8.42 (d, $^3J_{HH}$ = 8.1 Hz, 4 H, $H^{15}{}_{3}$), 8.74 (d, $^3J_{HH}$ = 4.4 Hz, 2 H, $H^{pyrrole}$), 8.82 (d, $^3J_{HH}$ = 4.5 Hz, 2 H, $H^{pyrrole}$), 8.85 (d, $^3J_{HH}$ = 4.6 Hz, 2 H, $H^{pyrrole}$), 8.94 (d, $^3J_{HH}$ = 4.5 Hz, 2 H, $H^{pyrrole}$) ppm.

^{13}C{^{1}H}-NMR (d$_8$-THF): δ = 14.5 ($C^{10/20}{}_{8/8}$), 20.5 ($C^{10/20}{}_{7/7}$), 32.8 ($C^{10/20}{}_{6/6}$), 52.5 ($C^{15}{}_{6}$), 68.7 ($C^{10/20}{}_{5/5}$), 113.5 ($C^{5}{}_{3}$), 113.7 ($C^{10/20}{}_{3/3}$), 118.8 (s, C^{15}), 121.0 ($C^{10/20}$), 123.1 (C^{5}), 128.9 ($C^{15}{}_{3}$), 130.8 ($C^{15}{}_{4}$), 131.2 ($C^{5}{}_{1}$), 131.7 (br. s, $C^{pyrrole\ 2/3/7/8/12/13/17/18}$), 135.4 ($C^{10/20}{}_{1/1}$), 135.5 ($C^{15}{}_{2}$), 136.5 ($C^{10/20}{}_{2/2}$), 136.6 ($C^{5}{}_{2}$), 148.4 ($C^{15}{}_{1}$), 149.7 ($C^{5}{}_{4}$), 160.4 ($C^{10/20}{}_{4/4}$), 167.4 ($C^{15}{}_{5}$) ppm.

IR (KBr): $\tilde{\nu}$ [cm^{-1}] = 3435 (NH^{amine}, br, m), 3317 (NH^{pyrrole}, m), 2957 (CH, m), 2930 (CH, m), 2871 (CH, w), 1722 (CO, s), 1606 (vs), 1510 (m), 1283 (s), 1246 (C-O-C, vs), 1176 (s), 804 (m).

MS (FD): *m/z* (%) = 831.67 (100) [M]$^+$.

MS (ESI): *m/z* (%) = 416.71 (3) [M^{2+}+H], 832.42 (100) [M+H]$^+$, 1664.85 (1) [2M+H]$^+$.

HR-MS (ESI): obs. *m/z* = 832.3826 [M+H]$^+$; calcd. for [M+H]$^+$ 832.3863.

UV/Vis (CH$_2$Cl$_2$): λ [nm] (ε / [10^4 M^{-1}cm^{-1}]) = 423 (42.01), 519 (1.57), 557 (1.12), 594 (0.39), 651 (0.49).

Fluorescence (CH$_2$Cl$_2$): λ [nm] (relative intensity) = 660 (1.00), 723 (0.20).

Quantum yield: $\Phi = 0.1631$.

CV (Fc/Fc$^+$, 100 mV s^{-1}, CH$_2$Cl$_2$): $E_{½}$ [V] = –2.010, –1.660, 0.420 (irr.), 0.590 (irr.).

15-(4-Methoxycarbonylphenyl)-5-(4-aminophenyl)-10,20-bis-(4-methoxyphenyl)porphyrin (3b). 150 mg (0.193 mmol) porphyrin **2b**, 62 mL conc. aqueous HCl, 0.61 g (2.70 mmol) SnCl$_2$. [silica, toluene : ethyl acetate (20:1), $R_f = 0.17$]. Yield 60.0 mg (0.08 mmol, 42%), purple powder. $C_{48}H_{37}N_5O_4$ (747.84).

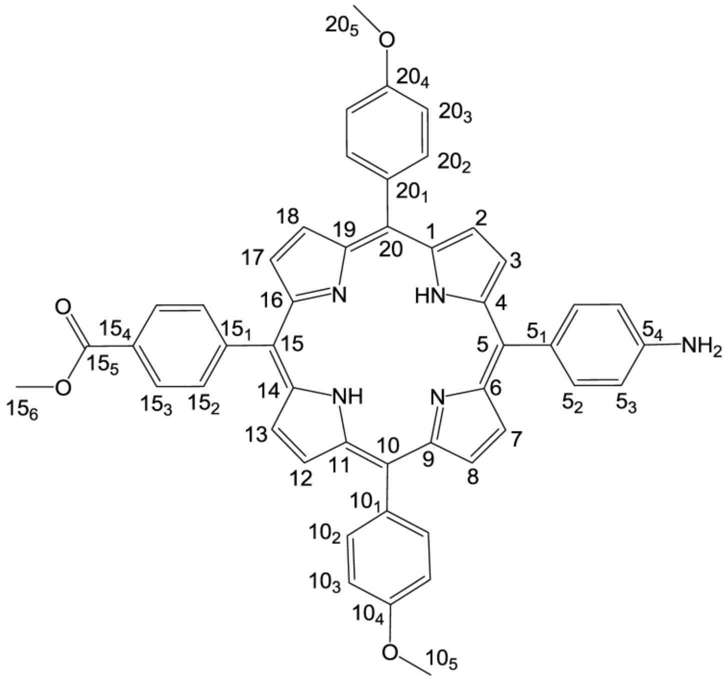

^{1}H-NMR (CD$_2$Cl$_2$): δ = –2.64 (s, 2 H, H$^{\text{pyrroleNH}}$), 4.05 (s, 9 H, H$^{15}{}_6$), 4.06 (s, 9 H, H$^{10/20}{}_{5/5}$), 4.99 (s, 2H, H$^{\text{NH}_2}$), 7.00 (d, $^3J_{\text{HH}}$ = 8.2 Hz, 2 H, H$^5{}_3$), 7.33 (d, $^3J_{\text{HH}}$ = 8.5 Hz, 4 H, H$^{10/20}{}_{3/3}$), 7.88 (d, $^3J_{\text{HH}}$ = 8.2 Hz, 2 H, H$^5{}_2$), 8.10 (d, $^3J_{\text{HH}}$ = 8.5 Hz, 4 H, H$^{10/20}{}_{2/2}$), 8.31 (d, $^3J_{\text{HH}}$ = 8.1 Hz, 2 H, H$^{15}{}_2$), 8.43 (d, $^3J_{\text{HH}}$ = 8.0 Hz, 2 H, H$^{15}{}_3$), 8.75 (d, $^3J_{\text{HH}}$ = 4.4 Hz, 2 H, H$^{\text{pyrrole}}$), 8.83 (d, $^3J_{\text{HH}}$ = 4.5 Hz, 2 H, H$^{\text{pyrrole}}$), 8.85 (d, $^3J_{\text{HH}}$ = 4.6 Hz, 2 H, H$^{\text{pyrrole}}$), 8.95 (d, $^3J_{\text{HH}}$ = 4.4 Hz, 2 H, H$^{\text{pyrrole}}$) ppm.

^{13}C{^{1}H}-NMR (CD$_2$Cl$_2$): δ = 52.5 (C$^{15}{}_6$), 55.9 (C$^{10/20}{}_{5/5}$), 113.2 (C$^{10/20}{}_{3/3}$), 123.1 (C^5), 118.8 (C^{15}), 120.9 (C$^{10/20}$), 113.5 (C$^5{}_3$), 128.8 (C$^{15}{}_3$), 130.8 (C$^{15}{}_4$), 131.1 (C$^5{}_1$), 131.9 (br.s, C$^{\text{pyrrole 2/3/7/8/12/13/17/18}}$), 135.5 (C$^{15}{}_2$), 135.6 (C$^{10/20}{}_{1/1}$), 136.6 (C$^5{}_2$), 136.5 (C$^{10/20}{}_{2/2}$), 149.7 (C$^5{}_4$), 148.4 (C$^{15}{}_1$), 161.0 (C$^{10/20}{}_{4/4}$), 167.4 (C$^{15}{}_6$) ppm.

IR (KBr): $\tilde{\nu}$ [cm^{-1}] = 3443 (NH$^{\text{amide}}$, br, m), 3319 (NH$^{\text{pyrrole}}$, m), 2950 (CH, w), 2928 (CH, w), 1724 (CO, s), 1606 (s), 1510 (s), 1282 (s), 1248 (C-O-C, vs), 1178 (s), 801 (m).

MS (FD): m/z (%) = 374.16 (100) [M]$^{2+}$, 747.59 (100) [M]$^+$.

MS (ESI): m/z (%) = 374.64 (6) [M^{2+}+H], 748.29 (100) [M+H]$^+$, 1496.57 (7) [2M+H]$^+$.

HR-MS (ESI): obs. m/z = 748.2934 [M+H]$^+$; calcd. for [M+H]$^+$ 748.2924.

UV/Vis (CH_2Cl_2): λ [nm] (ε / [10^4 $M^{-1}cm^{-1}$]) = 423 (27.96), 519 (1.09), 557 (0.73), 594 (0.26), 651 (0.28).

Fluorescence (CH_2Cl_2): λ [nm] (relative intensity) = 659 (1.00), 721 (0.24).

Quantum yield: Φ = 0.1448.

CV (Fc/Fc$^+$, 100 mV s^{-1}, CH_2Cl_2): $E_{½}$ [V] = –1.990, –1.660, 0.540 (irr.).

15-(4-Methoxycarbonylphenyl)-5-(4-aminophenyl)-10,20-bis-(4-methylphenyl)porphyrin (3d). 600 mg (0.80 mmol) porphyrin **2d**, 255 mL conc. aqueous HCl, 2.60 g (0.011 mol) $SnCl_2$. [silica, toluene : ethyl acetate (20:1), R_f = 0.32]. Yield 313 mg (0.44 mmol, 55%), purple powder. $C_{48}H_{37}N_5O_2$ (715.84).

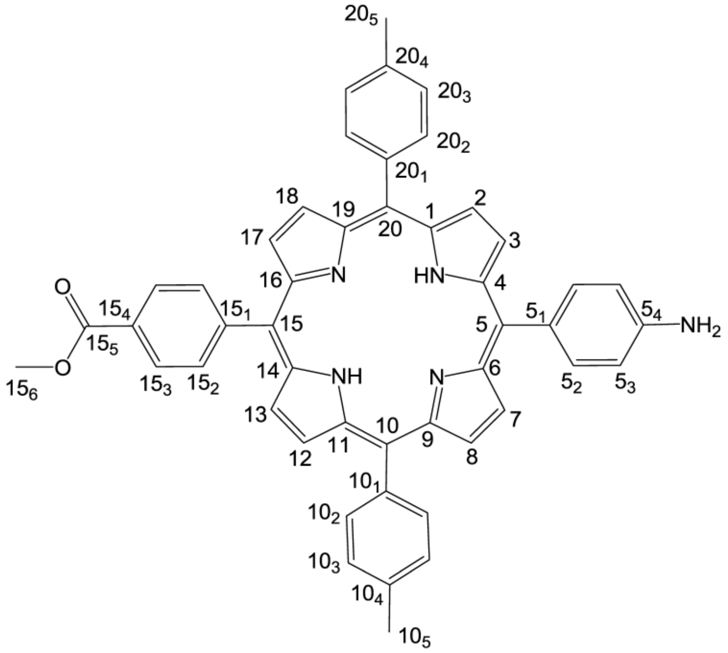

^{1}H-NMR (d_8-THF): δ = -2.64 (s, 2 H, $H^{pyrroleNH}$), 2.66 (s, 6 H, $H^{10/20}_{5/5}$), 4.03 (s, 3 H, H^{15}_{6}), 4.98 (b. s, 2 H, H^{NH}_{2}), 6.97 (d, $^3J_{HH}$ = 8.1 Hz, 2 H, H^5_3), 7.61 (d, $^3J_{HH}$ = 7.6 Hz, 4 H, $H^{10/20}_{3/3}$), 7.87 (d, $^3J_{HH}$ = 8.1 Hz, 2 H, H^5_2), 8.06 (d, $^3J_{HH}$ = 7.7 Hz, 4 H, $H^{10/20}_{2/2}$), 8.30 (d, $^3J_{HH}$ = 8.0 Hz, 2 H, H^{15}_2), 8.41 (d, $^3J_{HH}$ = 8.1 Hz, 2 H, H^{15}_3), 8.74 (d, $^3J_{HH}$ = 4.4 Hz, 2 H, $H^{pyrrole}$), 8.80 (d, $^3J_{HH}$ = 4.8 Hz, 2 H, $H^{pyrrole}$), 8.82 (d, $^3J_{HH}$ = 4.6 Hz, 2 H, $H^{pyrrole}$), 8.95 (d, $^3J_{HH}$ = 4.4 Hz, 2 H, $H^{pyrrole}$) ppm.

^{13}C{^{1}H}-NMR (d_8-THF): δ = 21.8 ($C^{10/20}_{5/5}$), 52.7 (C^{15}_6), 113.7 (C^5_3), 119.0 (C^{15}), 121.3 ($C^{10/20}$), 123.3 (C^5), 128.5 ($C^{10/20}_{3/3}$), 128.9 (C^{15}_3), 131.0 (C^{15}_4), 131.2 (C^5_1), 132.2 (br.s, $C^{pyrrole}_{2/3/7/8/12/13/17/18}$), 135.5 ($C^{10/20}_{2/2}$), 135.7 ($C^{15}_2$), 136.7 ($C^5_2$), 138.5 ($C^{10/20}_{4/4}$), 140.7 ($C^{10/20}_{1/1}$), 148.4 ($C^{15}_1$), 149.8 ($C^5_4$), 167.5 ($C^{15}_5$) ppm.

IR (KBr): $\tilde{\nu}$ [cm^{-1}] = 3431 (NH^{amine}, br, m), 3321 ($NH^{pyrrole}$, b, m), 2928 (CH, w), 1728 (CO, s), 1602 (s), 1278 (vs), 798 (vs).

MS (FD): *m/z* (%) = 715.6 (100) $[M]^+$.

MS (ESI): *m/z* (%) = 716.29 (100) [M+H]$^+$, 1432.63 (8) [2M+H]$^+$.

HR-MS (ESI): obs. *m/z* = 716.3031 [M+H]$^+$; calcd. for [M+H]$^+$ 716.3026.

UV/Vis (CH_2Cl_2): λ [nm] (ε / [10^4 $M^{-1}cm^{-1}$]) = 421 (26.93), 518 (1.39), 555 (0.97), 593(0.57), 650 (0.57).

Fluorescence (CH_2Cl_2): λ [nm] (relative intensity) = 657 (1.00), 721 (0.26).

Quantum yield: Φ = 0.0878.

CV (Fc/Fc$^+$, 100 mV s^{-1}, CH_2Cl_2): $E_{½}$ [V] = −1.980, −1.640, 0.440 (irr.), 0.550 (irr.).

General procedure for the preparation of Q-P-dyads 4

Anthraquinone-2-carboxylic acid (1 eq.) and pyridine (2 mL) were dissolved in anhydrous toluene (20 mL) and thionyl chloride (5 eq.) was added and the reaction mixture was stirred under argon for 3 h at room temperature. Excess of thionyl chloride and solvent were removed under reduced pressure. The residue was redissolved in an ultrasonic bath in toluene (20 mL) and pyridine (1 mL) and porphyrin amine (0.33 eq.), dissolved in toluene (20 mL) and pyridine (1 mL) was added. The mixture was stirred overnight and solvent was removed by evaporation under redeuced pressure. The residue was purified by chromatography [silica, toluene : ethylacetate (20:1)].

4a. 36.3 mg (0.144 mmol) anthraquinone-2-carboxylic acid, 54 µL (0.72 mmol) thionyl chloride, 40 mg (0.048 mmol) porphyrin **3a**. [silica, toluene: ethyl acetate (20:1), R_f = 0.35]. Yield: 436 mg (0.34 mmol, 70%), purple powder. $C_{69}H_{55}N_5O_7$ (1066.20).

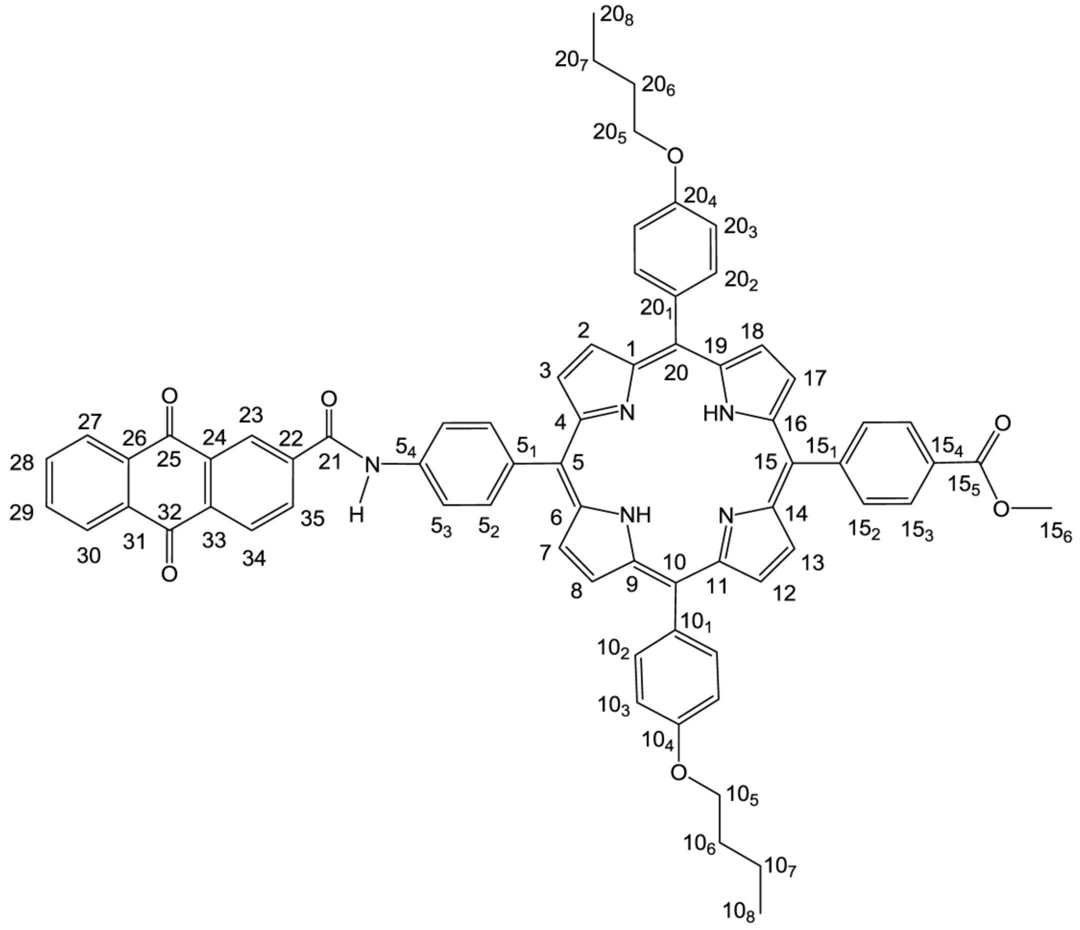

^{1}H-NMR (d$_8$-THF): $\delta = -2.67$ (s, 2 H, H$^{\text{pyrroleNH}}$), 1.10 (t, $^{3}J_{\text{HH}} = 7.4$ Hz, 6 H, H$^{10/20}{}_{8/8}$), 1.68 (m, 4 H, H$^{10/20}{}_{7/7}$), 1.95 (m, 4 H, H$^{10/20}{}_{6/6}$), 4.05 (s, 3 H, H$^{15}{}_{6}$), 4.26 (t, $^{3}J_{\text{HH}} = 6.3$ Hz, 4H, H$^{10/20}{}_{5/5}$), 7.33 (d, $^{3}J_{\text{HH}} = 8.5$ Hz, 4 H, H$^{10/20}{}_{3/3}$), 7.89 (m, 2 H, H$^{28/29}$), 8.10 (d, $^{3}J_{\text{HH}} = 8.4$ Hz, 4 H, H$^{10/20}{}_{2/2}$), 8.22 (d, $^{3}J_{\text{HH}} = 8.4$ Hz, 2 H, H$^{5}{}_{2}$), 8.34 (m, 6 H, H$^{5/15/27/30}{}_{3/2}$), 8.45 (m, 3 H, H$^{15/34}{}_{3}$), 8.56 (dd, $^{3}J_{\text{HH}} = 8.0$ Hz, $^{3}J_{\text{HH}} = 1.5$ Hz, 1 H, H^{35}), 8.77 (d, $^{3}J_{\text{HH}} = 4.4$ Hz, 2 H, H$^{\text{pyrrole}}$), 8.90 (m, 6 H, H$^{\text{pyrrole}}$), 8.98 (d, $^{4}J_{\text{HH}} = 1.3$ Hz, 1 H, H^{23}), 10.32 (s, 1 H, H$^{\text{amideNH}}$) ppm.

^{13}C{^{1}H}-NMR (d$_8$-THF): $\delta = 14.5$ (C$^{10/20}{}_{8/8}$), 20.5 (C$^{10/20}{}_{7/7}$), 32.8 (C$^{10/20}{}_{6/6}$), 68.8 (C$^{10/20}{}_{5/5}$), 113.7 (C$^{10/20}{}_{3/3}$), 119.3 (s, C$^{5}{}_{3}$), 119.5 (C^{15}), 121.2 (C^{5}), 121.3 (C$^{10/20}$), 126.7 (C^{23}), 127.9, 128.0 (C$^{27/30}$), 128.3 (C^{34}), 128.8 (C$^{15}{}_{3}$), 130.9 (C$^{15}{}_{4}$), 131.7 (br. s, C$^{\text{pyrrole 2/3/7/8/12/13/17/18}}$), 134.3 (C^{35}), 134.8 (C^{24}), 136.5 (C$^{10/20/33}{}_{2/2}$), 135.2 (C$^{10/20}{}_{1/1}$), 135.2, 135.3 (C$^{28/29}$), 135.6 (C$^{15}{}_{2}$), 135.9 (C$^{5}{}_{2}$), 138.9 (C$^{5}{}_{1}$), 140.5 (C$^{5}{}_{4}$), 141.8 (C^{22}), 148.3 (C$^{15}{}_{1}$), 160.5 (C$^{10/20}{}_{4/4}$), 165.2 (C^{21}), 167.4 (C$^{15}{}_{5}$), 182.9, 183.1 (C$^{25/32}$) ppm.

IR (KBr): $\tilde{\nu}$ [cm^{-1}] = 3422 (NH$^{\text{amide}}$, NH$^{\text{pyrrole}}$, br, m), 2957 (CH, w), 2928 (CH, w), 2866 (CH, w), 1724 (CO, s), 1676 (CO, s), 1605 (s), 1512 (s), 1471 (s), 1286 (C-O-C, vs), 1244 (C-O-C, vs), 800 (m).

MS (FD): *m/z* (%) = 1065.28 (100) [M]$^{+}$.

MS (ESI): *m/z* (%) = 533.70 (34) [M^{2+}+H], 1066.41 (100) [M+H]$^{+}$.

HR-MS (ESI): obs. *m/z* = 1066.4171 [M+H]$^{+}$; calcd. for [M+H]$^{+}$ 1066.4180.

UV/Vis (CH$_2$Cl$_2$): λ [nm] (ε / [10^4 M^{-1}cm^{-1}]) = 422 (32.44), 518 (1.36), 555 (0.84), 593 (0.49), 649 (0.47).

Fluorescence (CH$_2$Cl$_2$): λ [nm] (relative intensity) = 657 (1.00), 720 (0.25).

Quantum yield: Φ = 0.0125.

Lifetime: τ [ns] = 0.613 (100%).

CV (Fc/Fc$^+$, 100 mV s^{-1}, CH$_2$Cl$_2$): $E_{½}$ [V] = −2.000, −1.640, −1.230, 0.500, 0.750.

4b. 30.3 mg (0.12 mmol) anthraquinone-2-carboxylic acid, 45 µL (0.60 mmol) thionyl chloride, 30.0 mg (0.04 mmol) porphyrin **3b**. [silica, toluene: ethyl acetate (20:1), R_f = 0.19]. Yield: 35.0 mg (0.036 mmol, 89%), purple powder. $\mathrm{C_{63}H_{43}N_5O_7}$ (982.04).

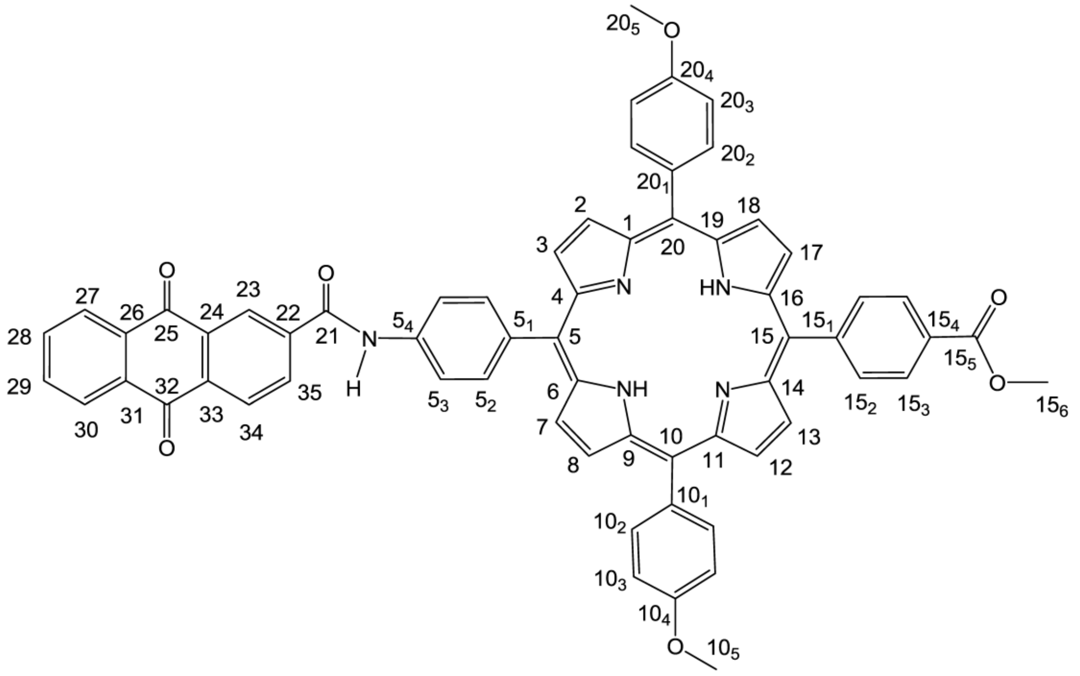

^{1}H-NMR (d$_8$-THF): δ = −2.66 (s, 2 H, $\mathrm{H}^{\mathrm{pyrroleNH}}$), 4.06 (s, 3 H, $\mathrm{H}^{15}{}_{6}$), 4.07 (s, 4H, $\mathrm{H}^{10/20}{}_{5/5}$), 7.35 (d, $^3J_\mathrm{HH}$ = 8.5 Hz, 4 H, $\mathrm{H}^{10/20}{}_{3/3}$), 7.91 (m, 2 H, $\mathrm{H}^{28/29}$), 8.12 (d, $^3J_\mathrm{HH}$ = 8.4 Hz, 4 H, $\mathrm{H}^{10/20}{}_{2/2}$), 8.23 (d, $^3J_\mathrm{HH}$ = 8.3 Hz, 2 H, $\mathrm{H}^{5}{}_{2}$), 8.33 (m, 4 H, $\mathrm{H}^{5/15/}{}_{3/2}$), 8.37 (m, 4 H, $\mathrm{H}^{27/30}$), 8.45 (d, $^3J_\mathrm{HH}$ = 8.1 Hz, 2 H, $\mathrm{H}^{15}{}_{3}$), 8.49 (d, $^3J_\mathrm{HH}$ = 8.0 Hz, 1 H, H^{34}), 8.58 (dd, $^3J_\mathrm{HH}$ = 7.9 Hz, $^3J_\mathrm{HH}$ = 1.4 Hz, 1 H, H^{35}), 8.77 (d, $^3J_\mathrm{HH}$ = 4.0 Hz, 2 H, $\mathrm{H}^{\mathrm{pyrrole}}$), 8.90 (m, 6 H, $\mathrm{H}^{\mathrm{pyrrole}}$), 9.00 (d, $^4J_\mathrm{HH}$ not determinable, 1 H, H^{23}), 10.32 (s, 1 H, $\mathrm{H}^{\mathrm{amideNH}}$) ppm.

^{13}C{^{1}H}–NMR (d$_8$-THF): Poor solubility of **5b** in THF.

IR (KBr): $\tilde{\nu}$ [cm^{-1}] = 3433 (NH$^{\mathrm{amide}}$, NH$^{\mathrm{pyrrole}}$, br, vs), 2924 (CH, w), 2855 (CH, w), 1722 (CO, vs), 1676 (CO, vs), 1512 (s), 1384 (m), 1483 (vs), 1288 (vs), 1247 (C-O-C, vs), 800 (m).

MS (FD): m/z (%) = 981.39 (100) [M]$^+$.

MS (ESI): m/z (%) = 491.66 (12) [M^{2+}+H], 982.33 (100) [M+H]$^+$.

HR-MS (ESI): obs. m/z = 982.3253 [M+H]$^+$; calcd. for [M+H]$^+$ 982.3241.

UV/Vis (CH_2Cl_2): λ [nm] (ε / [10^4 $M^{-1}cm^{-1}$]) = 421 (39.59), 517 (1.40), 554 (0.89), 593 (0.33), 649 (0.35).

Fluorescence (CH_2Cl_2): λ [nm] (relative intensity) = 656 (1.00), 720 (0.26).

Quantum yield: $\Phi = 0.0140$.

Lifetime: τ [ns] = 0.700 (100%).

CV (Fc/Fc$^+$, 100 mV s^{-1}, CH_2Cl_2): $E_{½}$ [V] = −1.990, −1.660, −1.230, 0.500, 0.760.

4d. 200.0 mg (0.63 mmol) anthraquinone-2-carboxylic acid, 0.24 mL (3.15 mmol) thionyl chloride, 150.0 mg (0.21 mmol) porphyrin **3d**. [silica, toluene: ethyl acetate (20:1), $R_f = 0.31$]. Yield: 137.5 mg (0.14 mmol, 69%), purple powder. $C_{63}H_{43}N_5O_5$ (950.05).

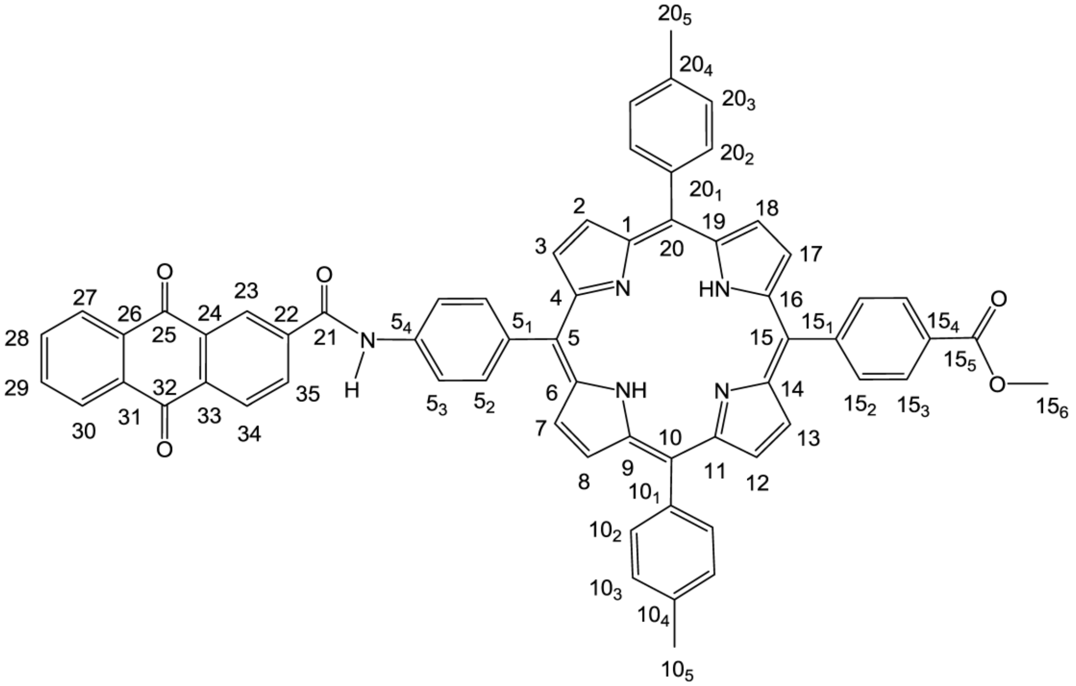

^{1}H-NMR (d_8-THF): $\delta = -2.68$ (s, 2 H, $H^{pyrroleNH}$), 2.69 (s, 6 H, $H^{10/20}{}_{5/5}$), 4.05 (s, 3 H, $H^{15}{}_6$), 7.60 (d, $^3J_{HH}$ = 7.7 Hz, 4 H, $H^{10/20}{}_{3/3}$), 7.90 (m, 2 H, $H^{28/29}$), 8.10 (d, $^3J_{HH}$ = 7.7 Hz, 4 H, $H^{10/20}{}_{2/2}$), 8.22 (d, $^3J_{HH}$ = 8.1 Hz 2 H, $H^5{}_2$), 8.33 (m, 4 H, $H^{5/15}{}_{3/2}$), 8.36 (m, 2 H, $H^{27/30}$), 8.43 (d, $^3J_{HH}$ = 8.0 Hz, 2 H, $H^{15}{}_3$), 8.47 (d, $^3J_{HH}$ = 8.0 Hz, 1 H, H^{34}), 8.57 (dd, $^3J_{HH}$ = 7.9 Hz, $^3J_{HH}$ = 1.2 Hz, 1 H, H^{35}), 8.77 (d, $^3J_{HH}$ = 4.3 Hz, 2 H, $H^{pyrrole}$), 8.86 (d, $^3J_{HH}$ = 4.5 Hz, 4 H, $H^{pyrrole}$), 8.92 (d, $^3J_{HH}$ = 4.3 Hz, 2 H, $H^{pyrrole}$), 8.99 (d, $^4J_{HH}$ = 1.0 Hz, 1 H, H^{23}), 10.31 (s, 1 H, $H^{amideNH}$) ppm.

^{13}C{^{1}H}-NMR (d_8-THF): δ = 21.7 ($C^{10/20}{}_{5/5}$), 52.6 ($C^{15}{}_6$), 119.4 ($C^5{}_3$), 119.5 (C^{15}), 121.2 (C^5), 121.4 ($C^{10/20}$), 126.8 (C^{23}), 128.0 (C^{27}), 128.0 (C^{30}), 128.3 (C^{34}), 128.5 ($C^{10/20}{}_{3/3}$), 128.8 ($C^{15}{}_3$), 130.9 ($C^{15}{}_4$), 134.3 (s, C^{35}), 134.9 (C^{24}), 135.2, 135.3 ($C^{28/29}$), 135.5 ($C^{10/20}{}_{2/2}$), 135.6 ($C^{15}{}_2$), 135.9 ($C^5{}_2$), 136.5 (C^{33}), 138.5 ($C^{10/20}{}_{4/4}$), 138.9 ($C^5{}_1$), 140.4 ($C^{10/20}{}_{1/1}$), 140.5 ($C^5{}_4$), 141.8 (C^{22}), 165.3 (C^{21}), 167.4 ($C^{15}{}_5$), 183.0, 183.2 ($C^{25/32}$) ppm.

IR (KBr): $\tilde{\nu}$ [cm^{-1}] = 3437 (NH^{amide}, br, vs), 3319 (NH^{pyrrole}, m), 2923 (CH, w), 2855 (CH, w), 1730 (CO, m), 1676 (CO, s), 1595 (m), 1515 (m), 1385 (m), 1290 (vs), 800 (m), 708 (m).

MS (FD): *m/z* (%) = 949.7 (100) [M]$^{+}$.

MS (ESI): *m/z* (%) = 950. 34 (100) [M+H]$^{+}$, 1900.68 (9) [2M+H]$^{+}$.

HR-MS (ESI): obs. *m/z* = 950. 3342 [M+H]$^{+}$; calcd. for [M+H]$^{+}$ 950.3342.

UV/Vis (CH_2Cl_2): λ [nm] (ε / [10^{4} M^{-1}cm^{-1}]) = 420 (39.00), 517 (1.93), 552 (1.26), 591 (0.85), 647 (0.82).

Fluorescence (CH_2Cl_2): λ [nm] (relative intensity) = 654 (1.00), 719 (0.28).

Quantum yield: Φ = 0.0161.

Lifetime: τ [ns] = 0.942 (100%).

CV (Fc/Fc^{+}, 100 mV s^{-1}, CH_2Cl_2): $E_{½}$ [V] = −1.980, −1.600, −1.210, 0.540, 0.840.

4e. 160.0 mg (0.63 mmol) anthraquinone-2-carboxylic acid, 0.24 mL (3.15 mmol) thionyl chloride, 144.2 mg (0.21 mmol) porphyrin **3e**. Yield: 106.7 mg (0.12 mmol, 57%), purple powder. R_f = 0.30 [silica, toluene / ethylacetate (20:1)]. $C_{61}H_{39}N_5O_5$ (921.99).

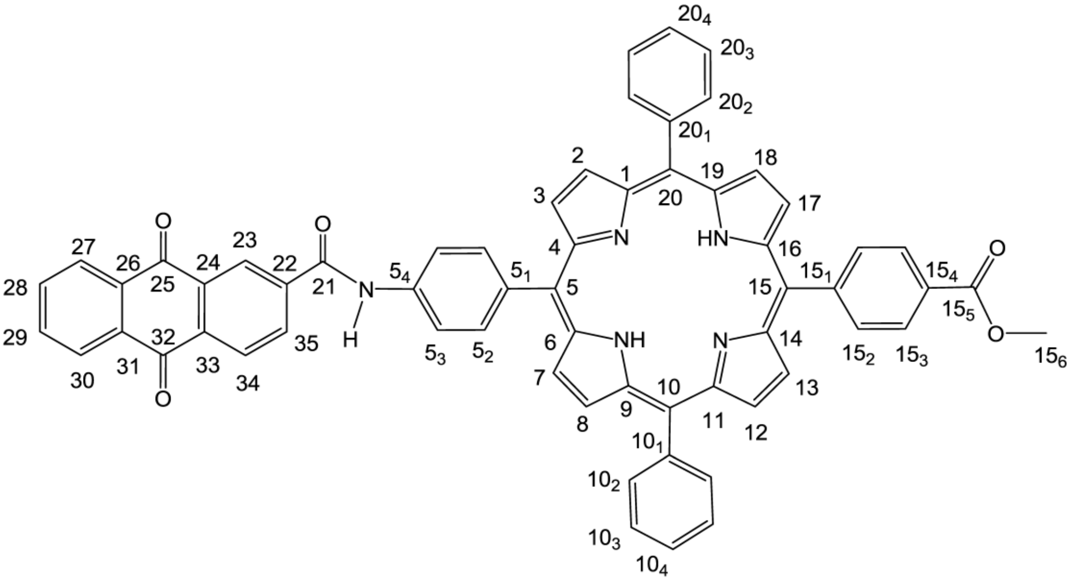

^{1}H-NMR (d_8-THF): δ = -2.67 (s, 2 H, H^{pyrrolNH}), 4.06 (s, 2 H, $\mathrm{H}^{15}{}_{6}$), 7.79 (m, 6 H, $\mathrm{H}^{10/20}{}_{3/4}$), 7.90 (m, 2 H, H$^{28/29}$), 8.23 (m, 6 H, $\mathrm{H}^{10/20/5}{}_{2/2/2}$), 8.33 (d, $^{3}J_{HH}$ = 8.4 Hz, 2 H, $\mathrm{H}^{5}{}_{3}$), 8.35 (d, $^{3}J_{HH}$ = 8.2 Hz 2 H, $\mathrm{H}^{15}{}_{2}$), 8.37 (m, 2 H, H$^{27/30}$), 8.45 (d, $^{3}J_{HH}$ = 8.1 Hz, 2 H, $\mathrm{H}^{15}{}_{3}$), 8.48 (d, $^{3}J_{HH}$ = 8.0 Hz, 1 H, H^{34}), 8.57 (dd, $^{3}J_{HH}$ = 8.0 Hz, $^{4}J_{HH}$ = 1.7 Hz, 1 H, H^{35}), 8.80 (d, $^{3}J_{HH}$ = 4.5 Hz, 2 H, H^{pyrrole}), 8.85 (d, $^{3}J_{HH}$ = 4.7 Hz, 4 H, H^{pyrrole}), 8.93 (d, $^{3}J_{HH}$ = 4.5 Hz, 2 H, H^{pyrrole}), 8.99 (d, $^{4}J_{HH}$ = 1.5 Hz, 1 H, H^{23}), 10.30 (s, 1 H, H^{amideNH}) ppm.

^{13}C{^{1}H}-NMR (d_8-THF): δ = 52.6 (s, 1C, $\mathrm{C}^{15}{}_{6}$), 119.4 ($\mathrm{C}^{5}{}_{3}$), 121.4 (C$^{10/20}$), 126.7 (C^{23}), 127.4 ($\mathrm{C}^{10/20}{}_{3/3}$), 128.0 (C^{27}), 128.0 (C^{30}), 128.3 (C^{34}), 128.9 ($\mathrm{C}^{10/20/15}{}_{4/4/3}$), 131.0 ($\mathrm{C}^{15}{}_{4}$), 132.2 (br. s, C$^{pyrrole\ 2/3/7/8/12/13/17/18}$), 134.5 (C^{35}), 134.9 ($\mathrm{C}^{15}{}_{4}$), 135.2, 135.3 (C$^{28/29}$), 135.5 ($\mathrm{C}^{10/20}{}_{2/2}$), 135.6 ($\mathrm{C}^{15}{}_{2}$), 135.9 ($\mathrm{C}^{5}_{2}$), 136.5 ($\mathrm{C}^{33}$), 138.8 ($\mathrm{C}^{5}_{1}$), 139.1, 140.5 ($\mathrm{C}^{10/20}_{1/1}$, C^{5}_{4}), 141.8 (C^{22}), 148.1 (C^{15}_{1}), 165.2 (C^{22}), 167.4 (C^{15}_{5}), 183.0, 183.2 ($\mathrm{C}^{25/32}$) ppm.

IR (KBr): $\tilde{\nu}$ [cm^{-1}] = 3424 (NH$^{\text{amide}}$, NH$^{\text{pyrrole}}$, br, vs), 2926 (CH, w), 2855 (CH, w), 1722 (CO, m), 1678 (CO, vs), 1607 (m), 1514 (m), 1383 (m), 1288 (vs), 968 (m), 800 (m).

MS (FD): *m/z* (%) = 921.7 (100) [M]$^{+}$.

MS (ESI): *m/z* (%) = 922.30 (100) [M+H]$^{+}$.

HR-MS (ESI): obs. *m/z* = 922.3046 [M+H]$^{+}$; calcd. for [M+H]$^{+}$ 922.3029.

UV/Vis ($\mathbf{CH_2Cl_2}$): λ [nm] (ε / [10^{4} M^{-1}cm^{-1}]) = 419 (32.25), 515 (1.34), 551 (0.69), 591 (0.42), 646 (0.36).

Fluorescence ($\mathbf{CH_2Cl_2}$): λ [nm] (relative intensity) = 651 (1.00), 716 (0.30).

Quantum yield: Φ = 0.0230.

Lifetime: τ [ns] = 1.37 (100%).

CV (Fc/Fc^{+}, 100 mV s^{-1}, $\mathbf{CH_2Cl_2}$): $E_{½}$ [V] = −1.940, −1.560, −1.190, 0.580, 0.870.

4f. 200.0 mg (0.63 mmol) anthraquinone-2-carboxylic acid, 0.24 mL (3.15 mmol) thionyl chloride, 152.3 mg (0.21 mmol) porphyrin **3f**. [silica, toluene: ethyl acetate (20:1), R_{f} = 0.27]. Yield: 150.4 mg (0.16 mmol, 75%), purple powder. $\mathrm{C_{61}H_{37}F_2N_5O_5}$ (957.97).

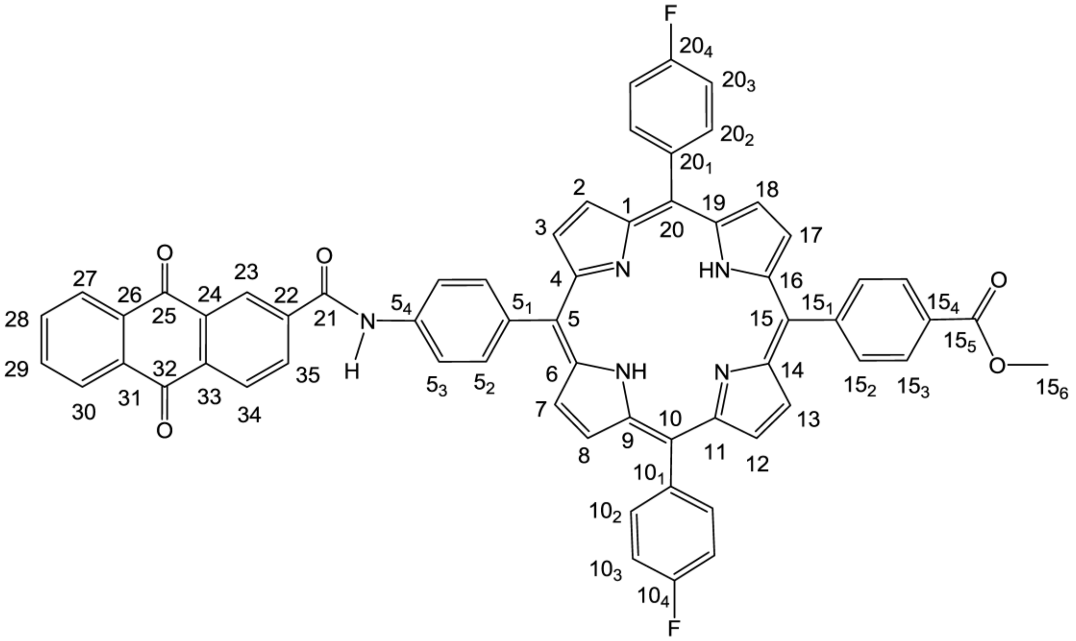

^{1}H-NMR ($\mathbf{CDCl_3}$): δ = -2.80 (s, 2 H, H$^{\text{pyrroleNH}}$), 4.12 (s, 3 H, H^{15}_{6}), 7.47 (ps. t, $^{3}J_{\mathrm{HH}}$ = 8.7 Hz, 4 H, $\mathrm{H}^{10/20}_{3/3}$), 7.90 (m, 2 H, H$^{28/29}$), 8.14 (d, $^{3}J_{\mathrm{HH}}$ = 8.2 Hz, 2 H, H^{5}_{2}), 8.17 (dvd, $^{3}J_{\mathrm{HH}}$ = 8.5 Hz, $^{3}J_{\mathrm{HF}}$ = 5.4 Hz, 4 H, $\mathrm{H}^{10/20}_{2/2}$), 8.27 (d, $^{3}J_{\mathrm{HH}}$ = 8.4 Hz, 2 H, H^{5}_{3}), 8.31 (d, $^{3}J_{\mathrm{HH}}$ = 8.1 Hz, 2 H, H^{15}_{2}), 8.41 (m, 2 H, H^{27,30} and H$^{\text{amideNH}}$), 8.45 (d, $^{3}J_{\mathrm{HH}}$ = 8.2 Hz, 2 H, H^{15}_{3}), 8.51 (m, 1H, H^{34}), 8.52 (d, $^{4}J_{\mathrm{HH}}$ = 1.7 Hz ,2 H, H^{35}), 8.80 (d, 2 H, $^{3}J_{\mathrm{HH}}$ = 4.7 Hz, H$^{\text{pyrrole}}$), 8.83 (d, 2 H, $^{3}J_{\mathrm{HH}}$ = 4.2 Hz, H$^{\text{pyrrole}}$), 8.84 (d, 2

H, $^{3}J_{\mathrm{HH}}$ = 4.6 Hz, $\mathrm{H}^{\mathrm{pyrrole}}$), 8.86 (d, 1 H, $^{4}J_{\mathrm{HH}}$ = 1.1 Hz, H^{23}), 8.92 (d, 2 H, $^{3}J_{\mathrm{HH}}$ = 4.8 Hz $\mathrm{H}^{\mathrm{pyrrole}}$) ppm.

^{13}C{^{1}H}-NMR (CDCl$_3$): δ =52.6 ($\mathrm{C}^{15}{}_{6}$), 113.9 (d, $^{2}J_{\mathrm{CF}}$ = 21.3 Hz , $\mathrm{C}^{10/20}{}_{3/3}$), 118.7 ($\mathrm{C}^{5}{}_{3}$), 118.8 ($\mathrm{C}^{5}$), 119.2, 119.8 ($\mathrm{C}^{10/20/15}$), 124.9 ($\mathrm{C}^{23}$), 127.5 ($\mathrm{C}^{27}$), 127.5 ($\mathrm{C}^{30}$), 128.0 ($\mathrm{C}^{15}{}_{3}$), 128.3 ($\mathrm{C}^{34}$), 129.6 ($\mathrm{C}^{15}{}_{4}$), 131.8 (br. s $\mathrm{C}^{\mathrm{pyrrole}\ 2/3/7/8/12/13/17/18}$), 133.5 (s, C^{35}), 134.5, 134.6, 134.6 ($\mathrm{C}^{28/29/15}{}_{2}$), 135.1 (s, $\mathrm{C}^{5}{}_{2}$), 135.7 (d, $^{3}J_{\mathrm{CF}}$ = 8.8 Hz, $\mathrm{C}^{10/20}{}_{2/2}$), n.o. ($\mathrm{C}^{24/33}$), 137.4 ($\mathrm{C}^{5}{}_{1}$), 137.9 (d, $^{4}J_{\mathrm{CF}}$ = 2.8 Hz, $\mathrm{C}^{10/20}{}_{1/1}$), 138.8 ($\mathrm{C}^{5}{}_{4}$), n.o. ($\mathrm{C}^{22}$), 146.8 ($\mathrm{C}^{15}{}_{1}$), 165.7 (d, $^{1}J_{\mathrm{FH}}$ = 248.1 Hz, $\mathrm{C}^{10/20}{}_{4/4}$), 167.3 ($\mathrm{C}^{15}{}_{5}$), 164.1 ($\mathrm{C}^{21}$), 182.3, 185.5 ($\mathrm{C}^{25/32}$) ppm.

^{19}F-NMR (THF): $\delta = -112.8$ (m, F-$\mathrm{C}^{10/20}{}_{4/4}$) ppm.

IR (KBr): $\tilde{\nu}$ [cm^{-1}] = 3451 ($\mathrm{NH}^{\mathrm{amide}}$, $\mathrm{NH}^{\mathrm{pyrrole}}$, b, vs), 2928 (CH, w), 2862 (CH, w), 1674 (CO, vs), 1592, (s), 1516 (m), 1384 (m), 1317 (m), 1293 (s), 1176 (CF, w), 794 (s).

MS (FD): *m/z* (%) 958.97 (100) [M]$^{+}$.

MS (ESI): *m/z* (%) = 958.34 (100,) [M+H]$^{+}$.

HR-MS (ESI): obs. *m/z* = 958.2840 [M+H]$^{+}$; calcd. for [M+H]$^{+}$ 958.2841.

UV/Vis (CH$_2$Cl$_2$): λ [nm] (ε / [10^{4} M^{-1}cm^{-1}]) = 419 (46.25), 515 (1.96), 551 (0.98), 591 (0.59), 647 (0.45).

Fluorescence (CH$_2$Cl$_2$): λ [nm] (relative intensity) = 652 (1.00), 717 (0.32).

Quantum yield: Φ = 0.0281.

Lifetime: τ [ns] = 2.97 (100%).

CV (Fc/Fc^{+}, 100 mV s^{-1}, CH$_2$Cl$_2$): $E_{½}$ [V] = −1.930, −1.580, −1.210, 0.600, 0.880.

4g. 200.0 mg (0.63 mmol) anthraquinone-2-carboxylic acid, 0.24 mL (3.15 mmol) thionyl chloride, 173.1 mg (0.21 mmol) porphyrin **3g**. [silica, toluene: ethyl acetate (20:1), R_{f} = 0.23]. Yield: 142.2 mg (0.13 mmol, 64%), purple powder. $\mathrm{C_{63}H_{37}F_{6}N_{5}O_{5}}$ (1057.99).

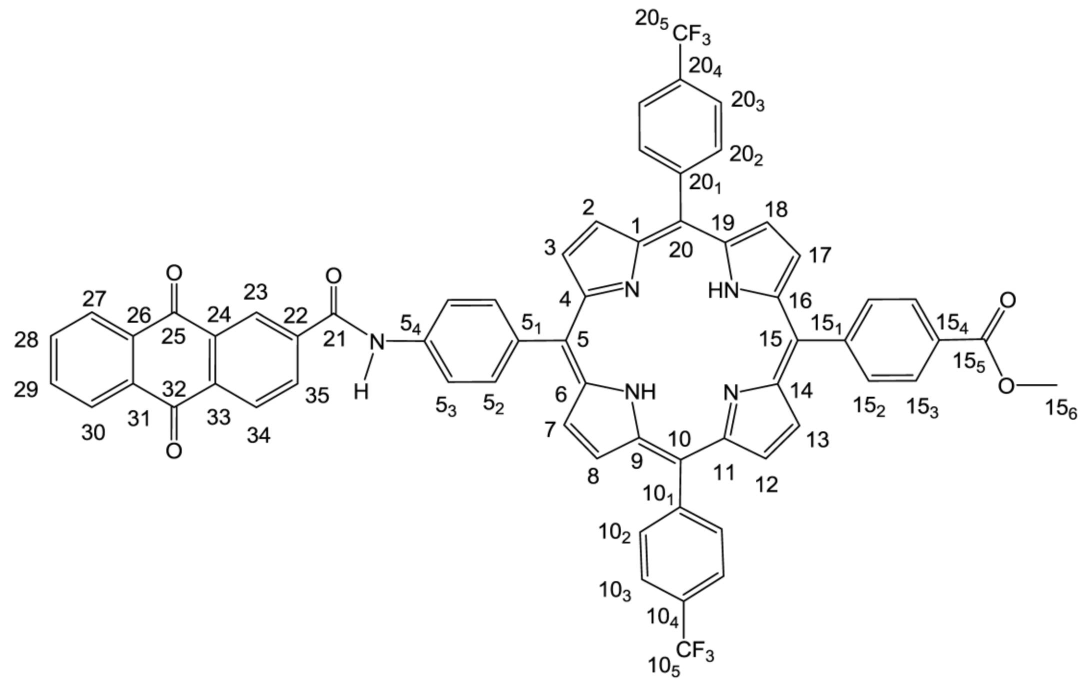

^{1}H-NMR (d_8-THF): $\delta = -2.73$ (s, 2 H, $H^{pyrroleNH}$), 4.05 (s, 3 H, $H^{15}{}_6$), 7.84 (m, 2 H, $H^{28/29}$), 8.12 (d, $^3J_{HH}$ = 8.1 Hz, 4 H, $H^{10/20}{}_{3/3}$), 8.23 (d, $^3J_{HH}$ = 8.4 Hz, 2 H, $H^5{}_2$), 8.26 (m, 2 H, $H^{27/30}$), 8.34 (ps. t, $^3J_{HH}$ = 8.1 Hz, 4 H, $H^{5/15}{}_{3/2}$), 8.41 (m, 5 H, $H^{10/20/34}{}_{2/2}$), 8.45 (d, $^3J_{HH}$ = 8.2 Hz, 2 H, $H^{15}{}_3$), 8.52 (dd, 1 H, $^4J_{HH}$ = 1.8 Hz, $^3J_{HH}$ = 8.0 Hz, H^{35}), 8.83 (m, 6 H, $H^{pyrrole}$), 8.92 (d, 1 H, $^4J_{HH}$ = 1.7 Hz, H^{23}), 8.98 (d, 2 H, $^3J_{HH}$ = 4.6 Hz $H^{pyrrole}$), 10.38 (s, 1H, H^{amide}) ppm.

^{13}C{^{1}H}-NMR (d_8-THF): δ = 52.6 ($C^{15}{}_6$), 119.5 (s, $C^5{}_3$), 119.8 (C^{15}), 121.9 (C^5), 120.2 ($C^{10/20}$), 124.8 (d, $^4J_{CF}$ = 3.3 Hz, $C^{10/20}{}_{3/3}$), 126.7 (C^{23}), 127.5 ($C^{10/20}{}_{4/4}$), 127.9 (C^{27}), 127.9 (C^{30}), 128.2 (s, C^{34}), 128.8 ($C^{15}{}_3$), 131.1 ($C^{15}{}_4$), 131.1 (m, $C^{10/20}{}_{5/5}$), 132.0 ($C^{pyrrole\ 2/3/7/8/12/13/17/18}$), 134.2 (s, C^{35}), 134.7 (C^{24}), 135.1, 135.2 ($C^{28/29}$), 135.6 ($C^{15}{}_2$), 136.0 ($C^5{}_2$), 135.9 ($C^{10/20}{}_{2/2}$), 136.4 (C^{33}), 138.5 ($C^5{}_1$), 140.7 ($C^5{}_4$), 141.6 (C^{22}), 147.3 ($C^{10/20}{}_{1/1}$), 147.8 ($C^{15}{}_1$), 165.3 (C^{21}), 167.4 ($C^{15}{}_5$), 182.8, 183.0 ($C^{25/32}$) ppm.

^{19}F-NMR (THF): $\delta = -64.6$ (s, F-$C^{10/20}{}_{5/5}$) ppm.

IR (KBr): $\tilde{\nu}$ [cm^{-1}] = 3444 (NH^{amide}, $NH^{pyrrole}$, br,vs), 2925 (CH, m), 2850 (CH, m), 1728 (CO, m), 1676, (CO, s), 1517 m), 1384 (m), 1314 (vs) 1279 (s), 1112 (CF, s), 1159 (CF, s), 794(m).

MS (FD): *m/z* (%) = 1057.4 (100) $[M]^+$.

MS (ESI): *m/z* (%) = 529.67 (5) $[M+H]^{2+}$, 1058.34 (100) $[M+H]^+$, 1059.36 (81) $[M+H]^+$, 1191.18 (81) $[M+H]^+$.

HR-MS (ESI): obs. *m/z* = 1058.2773 $[M+H]^+$; calcd. for $[M+H]^+$ 1058.2777.

UV/Vis (CH_2Cl_2): λ [nm] (ε / [10^4 M^{-1}cm^{-1}]) = 419 (31.57), 515 (1.45), 549 (0.69), 591 (0.47), 649 (0.41).

Fluorescence (CH_2Cl_2): λ [nm] (relative intensity) = 652 (1.00), 717 (0.35).

Quantum yield: $\Phi = 0.0548$.

Lifetime: τ [ns] = 4.81 (100%).

CV (Fc/Fc$^+$, 100 mV s^{-1}, CH$_2$Cl$_2$): $E_{½}$ [V] = −1.870, −1.530, −1.200, 0.670, 0.960.

4c. 82.2 mg (0.156 mmol) anthraquinone-2-carboxylic acid, 59.0 µL (0.78 mmol) thionyl chloride, 40 mg (0.052 mmol) porphyrin **3c**. [silica, toluene: ethyl acetate (20:1), R_f = 0.40]. Yield: 37.0 mg (0.037 mmol, 71%), purple powder. $C_{67}H_{51}N_5O_5$ (1006.15).

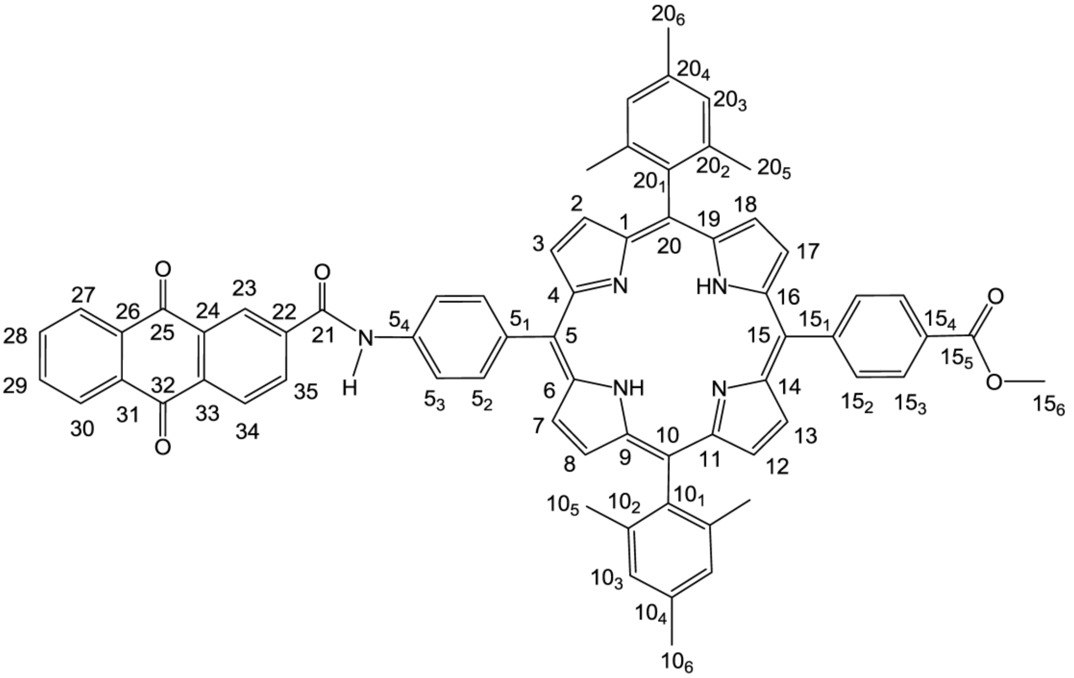

^{1}H-NMR (d$_8$-THF): δ = −2.49 (s, 2 H, $H^{pyrroleNH}$), 1.85 (s, 12 H, $H^{10/20}{}_{5/5}$), 2.61 (s, 6 H, $H^{10/20}{}_{6/6}$), 4.05 (s, 3 H, $H^{15}{}_6$), 7.32 (s, 4 H, $H^{10/20}{}_{3/3}$), 7.91 (m, 2 H, $H^{28/29}$), 8.23 (d, $^3J_{HH}$ = 8.3 Hz, 2 H, $H^5{}_2$), 8.35 (m, 6 H, $H^{5/15/27/30}{}_{3/2}$), 8.43 (d, $^3J_{HH}$ = 8.1 Hz, 2 H, $H^{15}{}_3$), 8.49 (d, $^4J_{HH}$ = 8.0 Hz, 1H, H^{34}), 8.58 (dd, $^3J_{HH}$ = 8.1 Hz, $^4J_{HH}$ = 1.5 Hz, 1 H, H^{35}), 8.69 (m, 4 H, $H^{pyrrole}$), 8.76 (d, 2 H, $^3J_{HH}$ = 4.6 Hz, $H^{pyrrole}$), 8.89 (d, 2 H, $^3J_{HH}$ = 4.6 Hz, $H^{pyrrole}$), 9.00 (d, 1 H, $^4J_{HH}$ = 1.2 Hz, H^{23}), 10.32 (s, 1 H, $H^{amideNH}$) ppm.

^{13}C{^{1}H}-NMR (d$_8$-THF): δ = 21.7 ($C^{10/20}{}_{6/6}$), 21.9 ($C^{10/20}{}_{5/5}$), 52.6 ($C^{15}{}_6$), 119.3 ($C^5{}_3$), 119.1 (C^{15}), n.o. ($C^{10/20}$), 120.8 (C^5), 126.6 (C^{23}), 128.0 (C^{27}), 128.0 (C^{30}), 128.9 ($C^{10/20}{}_{3/3}$), 128.3 (C^{34}), 128.8 ($C^{15}{}_3$), 131.3 (br. s, $C^{pyrrole\ 2/3/7/8/12/13/17/18}$), 131.1 ($C^{15}{}_4$), 134.4 ($C^{35}$), 134.9 ($C^{24}$), 135.2, 135.3 ($C^{28/29}$), 135.6 ($C^{15}{}_2$), 135.9 ($C^5{}_2$), 136.5 ($C^{33}$), 138.6 ($C^5{}_1$), 139.6 ($C^{10/20}{}_{1/1}$), 140.6 ($C^5{}_4$), 141.8 ($C^{22}$), 147.9 ($C^{15}{}_1$), 165.3 ($C^{21}$), 167.4 ($C^{15}{}_5$), 183.0, 183.2 ($C^{25/32}$) ppm.

IR (KBr): $\tilde{\nu}$ [cm^{-1}] = 3427 (NH^{amide}, NH^{pyrrole}, b, vs), 2928 (CH, w), 2851 (CH, w), 1724 (C=O, m), 1678 (C=O, m), 1516 (m), 1285 (vs), 1020 (m).

MS (FD): *m/z* (%) = 1006.13 (100) [M]$^+$.

MS (ESI): *m/z* (%) = 1006.43 (100) [M+H]$^+$.

HR-MS (ESI): obs. *m/z* = 1006.3947 [M+H]$^+$; calcd. for [M+H]$^+$ 1006.3968.

UV/Vis (CH_2Cl_2): λ [nm] (ε / [10^4 $M^{-1}cm^{-1}$]) = 421 (36.33), 516 (1.55), 551 (0.68), 592 (0.34), 651 (0.56).

Fluorescence (CH_2Cl_2): λ [nm] (relative intensity) = 653 (1.00), 719 (0.23).

Quantum yield: Φ = 0.0532.

Lifetime: τ [ns] = 1.82 (100%).

CV (Fc/Fc$^+$, 100 mV s^{-1}, CH_2Cl_2): $E_{½}$ [V] = −2.070, −1.720(2e), −1.230, 0.560, 0.960.

4h. 52.2 mg (0.21 mmol) anthraquinone-2-carboxylic acid, 80 µL (1.05 mmol) thionyl chloride, 60 mg (0.069 mmol) porphyrin **3h**. [silica, toluene: ethyl acetate (20:1), R_f = 0.35]. Yield: 60.5 mg (0.055 mmol, 79%), purple powder. $C_{61}H_{29}F_{10}N_5O_5$ (1101.90).

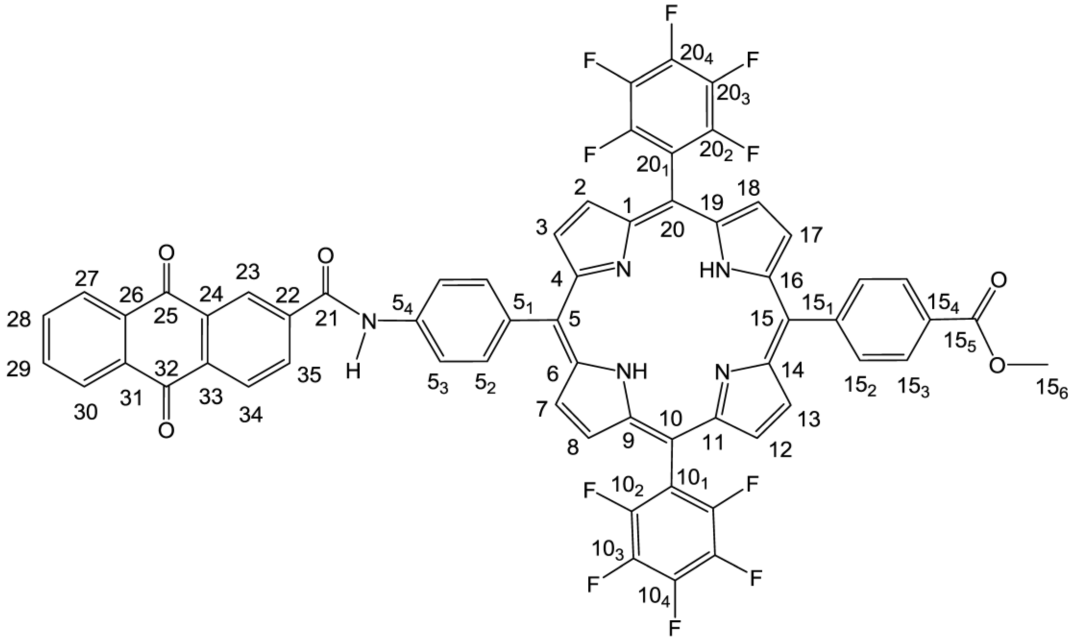

^{1}H-NMR (d$_8$-THF): δ = −2.75 (s, 2 H, $H^{pyrroleNH}$), 4.07 (s, 3 H, $H^{15}{}_6$), 7.92 (m, 2 H, $H^{28/29}$), 8.27 (d, $^3J_{HH}$ = 8.4 Hz, 2 H, $H^5{}_2$), 8.37 (m, 6 H, $H^{5/15/27/30}{}_{3/2}$), 8.50 (d, $^4J_{HH}$ = 8.3 Hz 1H, H^{34}), 8.59 (m, 3 H, $H^{15/35}{}_3$), 8.98 (m, 2 H, $H^{pyrrole}$), 8.86 (d, 1 H, $^4J_{HH}$ not determinable, H^{23}), 9.05 (m, 6 H, $H^{pyrrole}$) 10.37 (s, 1 H, $H^{amideNH}$) ppm.

^{13}C{^{1}H}-NMR (d$_8$-THF): δ = 119.5 ($C^5{}_3$), n.o. ($C^{10/20}$), 122.5 (C^5), 126.8 (C^{23}), 128.0 (C^{27}), 128.0 (C^{30}), 128.3 (C^{34}), 129.4 ($C^{15}{}_3$), 131.0 (br. s, $C^{pyrrole\ 2/3/7/8/12/13/17/18}$), n.o. ($C^{15}{}_4$), 134.4 ($C^{35}$), 134.9 ($C^{24}$), 135.2, 135.3 ($C^{15/28/29}{}_2$), 136.0 ($C^5{}_2$), 136.5 ($C^{33}$), 137.9 ($C^5{}_1$), 140.8 ($C^5{}_4$), n.o. ($C^{15}{}_1$), 141.7 ($C^{22}$), 140.9 ($C^5{}_4$), 140.3, 144.7, 146.6, 149.1 ($C^{10/20}{}_{1/2/3/4}$) 165.3 (C^{21}), n.o. ($C^{15}{}_5$), 183.0, 183.2 ($C^{25/32}$) ppm.

^{19}F-NMR (d$_8$-THF): δ = −166.6 (ddd, $^3J_{FF}$ = 23 Hz, $^3J_{FF}$ = 21 Hz, $^5J_{FF}$ = 8 Hz, 4 F, $F^{10/20}{}_{3/3}$), −157.7 (t, $^3J_{FF}$ = 21 Hz, 2 F, $F^{10/20}{}_{4/4}$), −138.0 (dd, $^3J_{FF}$ = 24 Hz, $^5J_{FF}$ = 8 Hz, 4 F, $F^{10/20}{}_{2/2}$) ppm.

IR (KBr): $\tilde{\nu}$ [cm^{-1}] = 3425 (NH^{amide}, NH^{pyrrole}, br, s), 2928 (CH, w), 2848 (CH, w), 1724 (CO, m), 1680 (CO, m), 1520 (vs), 1498 (vs), 1286 (vs), 1113 (CF, w), 988 (s), 922 (m).

MS (FD): *m/z* (%)=1101.69 (100) [M]$^+$.

MS (ESI): *m/z* (%) = 1102.23 (100) [M+H]$^+$.

HR-MS (ESI): obs. *m/z* = 1102.2074 [M+H]$^+$; calcd. for [M+H]$^+$ 1102.2087.

UV/Vis (CH_2Cl_2): λ [nm] (ε / [10^4 M^{-1}cm^{-1}]) = 418 (34.69), 512 (2.15), 546 (0.70), 588 (0.79), 642 (0.44).

Fluorescence (CH_2Cl_2): λ [nm] (relative intensity) = 647 (1.00), 712 (0.53).

Quantum yield: Φ = 0.0628.

Lifetime: τ [ns] = 9.55 (100%).

CV (Fc/Fc$^+$, 100 mV s^{-1}, CH_2Cl_2): $E_{½}$ [V] = −1.850, −1.420, −1.240, 0.830, 1.050.

General procedure for the preparation of Q-P-dyads 5.

Dyad **4** was dissolved in a mixture of freshly distilled THF and methanol (24 mL, 3:1) and 1 mL of 10% aqueous KOH was added. The mixture was stirred overnight, neutralised with 1 mL of acetic acid and deluted with CH_2Cl_2. The organic layer was separated, washed with water (3x), dried over $MgSO_4$ and the solvent was removed under reduced pressure. The product was used without additional purification.

5a. 33.0 mg (0.031 mmol) **4a**. [TLC, silica, CH_2Cl_2/methanol (20:1), R_f = 0.53]. Yield 32.0 mg (0.030 mmol, 98%), purple powder. $C_{68}H_{53}N_5O_7$ (1052.18).

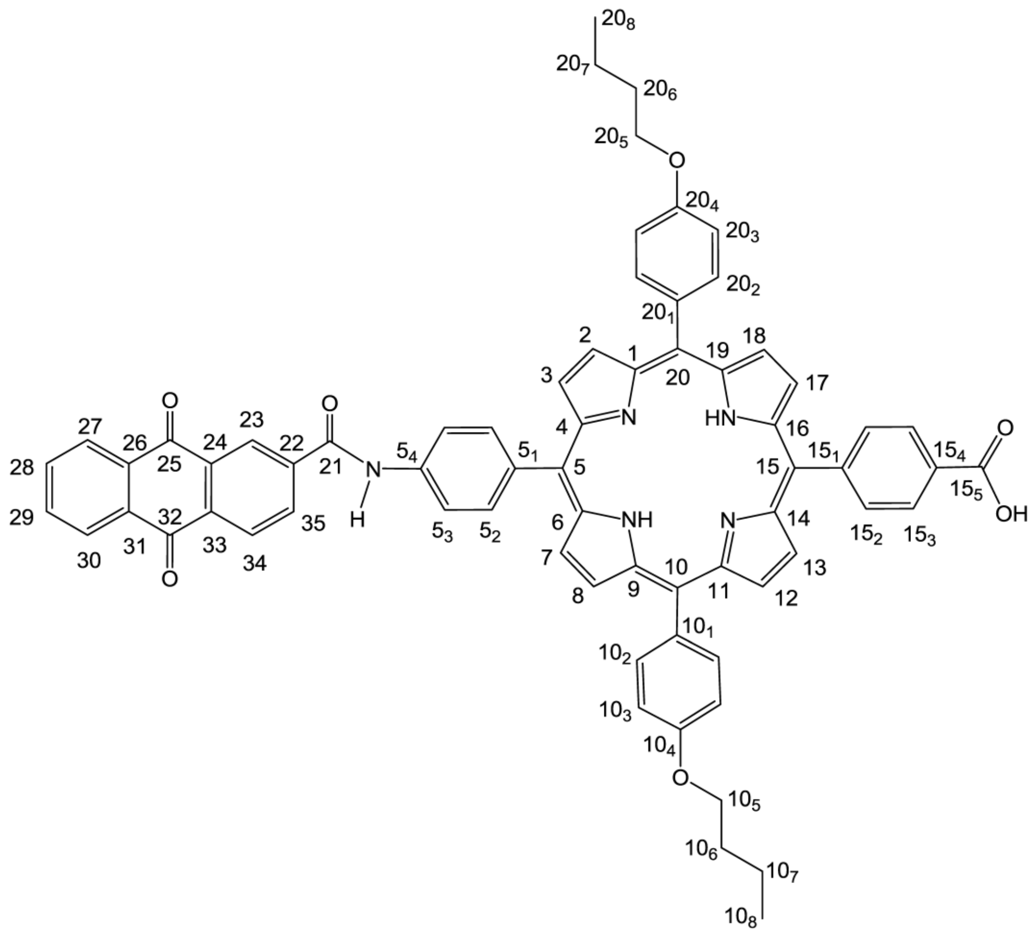

^{1}H-NMR (d$_8$-THF): $\delta = -2.66$ (s, 2 H, $\mathrm{H}^{\text{pyrroleNH}}$), 1.10 (t, $^3J_{\mathrm{HH}}$ = 7.4 Hz, 6 H, $\mathrm{H}^{10/20}_{8/8}$), 1.68 (m, 2 H, $\mathrm{H}^{10/20}_{7/7}$), 1.95 (m, 2 H, $\mathrm{H}^{10/20}_{6/6}$), 4.25 (t, $^3J_{\mathrm{HH}}$ = 6.3 Hz, 4H, $\mathrm{H}^{10/20}_{5/5}$), 7.32 (d, $^3J_{\mathrm{HH}}$ = 8.4 Hz, 4 H, $\mathrm{H}^{10/20}_{3/3}$), 7.89 (m, 2 H, $\mathrm{H}^{28/29}$), 8.10 (d, $^3J_{\mathrm{HH}}$ = 8.3 Hz, 4 H, $\mathrm{H}^{10/20}_{2/2}$), 8.22 (d, $^3J_{\mathrm{HH}}$ = 8.3 Hz, 2 H, H^{5}_{2}), 8.33 (m, 6 H, $\mathrm{H}^{5/15/27/30}_{3/2}$), 8.45 (m, 3 H, $\mathrm{H}^{15/34}_{3}$), 8.57 (br. d, $^3J_{\mathrm{HH}}$ = 8.0 Hz, 1 H, H^{35}), 8.79 (d, $^3J_{\mathrm{HH}}$ = 4.2 Hz, 2 H, $\mathrm{H}^{\text{pyrrole}}$), 8.89 (m, 6 H, $\mathrm{H}^{\text{pyrrole}}$), 8.98 (br. s, 1 H, H^{23}), 10.35 (s, 1 H, $\mathrm{H}^{\text{amideNH}}$) ppm.

^{13}C{^{1}H}-NMR (d$_8$-THF): δ = 14.5 ($\mathrm{C}^{10/20}_{8/8}$), 20.5 ($\mathrm{C}^{10/20}_{7/7}$), 32.8 ($\mathrm{C}^{10/20}_{6/6}$), 68.8 ($\mathrm{C}^{10/20}_{5/5}$), 113.8 ($\mathrm{C}^{10/20}_{3/3}$), 119.4 (s, C^{5}_{3}), 119.7 (C^{15}), 121.1 (C^{5}), 121.3 ($\mathrm{C}^{10/20}$), 126.8 (C^{23}), 128.0, 128.0 ($\mathrm{C}^{27/30}$), 128.3 (C^{34}), 129.1 (C^{15}_{3}), 131.6 (C^{15}_{4}), 131.6 (br. s, $\mathrm{C}^{\text{pyrrole 2/3/7/8/12/13/17/18}}$), 134.3 ($\mathrm{C}^{35}$), 134.8 ($\mathrm{C}^{24}$), 136.5 ($\mathrm{C}^{10/20/33}_{2/2}$), 135.2 ($\mathrm{C}^{10/20}_{1/1}$), 135.2, 135.3 ($\mathrm{C}^{28/29}$), 135.6 ($\mathrm{C}^{15}_{2}$), 135.9 ($\mathrm{C}^{5}_{2}$), 139.0 ($\mathrm{C}^{5}_{1}$), 140.5 ($\mathrm{C}^{5}_{4}$), 141.8 ($\mathrm{C}^{22}$), 147.9 ($\mathrm{C}^{15}_{1}$), 165.3 ($\mathrm{C}^{21}$), 160.5 ($\mathrm{C}^{10/20}_{4/4}$), 183.0 ($\mathrm{C}^{32}$), 183.2 ($\mathrm{C}^{25}$) ppm.

IR (KBr): $\tilde{\nu}$ [cm^{-1}] = 3435 (NH$^{\text{amide}}$, NH$^{\text{pyrrole}}$,COOH, br, w), 2958 (CH, w), 2932 (CH, w), 2872 ((CH, w), 1676 (CO, s), 1604 (s), 1510 (s), 1384 (w), 1288 (C-O-C, vs), 1244 (C-O-C, vs), 800 (m).

MS (FD): *m/z* (%) = 1051.80 (100) [M]$^+$.

MS (ESI): *m/z* (%) = 526.71 (12) [M^{2+}+H], 1052.42 (100) [M+H]$^+$.

HR-MS (ESI): obs. *m/z* = 1052.4028 [M+H]$^+$; calcd. for [M+H]$^+$ 1052.4023.

UV/Vis (CH$_2$Cl$_2$): λ [nm] (ε / [10^4 M^{-1}cm^{-1}]) = 422 (39.35), 518 (1.85), 555 (1.11), 593 (0.53), 650 (0.35).

Fluorescence (CH$_2$Cl$_2$): λ [nm] (relative intensity) = 658 (1.00), 721 (0.26).

Quantum yield: Φ = 0.0146.

5b. 33.0 mg (0.034 mmol) **4b**. [TLC, silica, CH$_2$Cl$_2$/methanol (20:1), R_f = 0.45]. Yield 31 mg (0.32 mmol, 94%), purple powder. $C_{62}H_{41}N_5O_7$ (968.02).

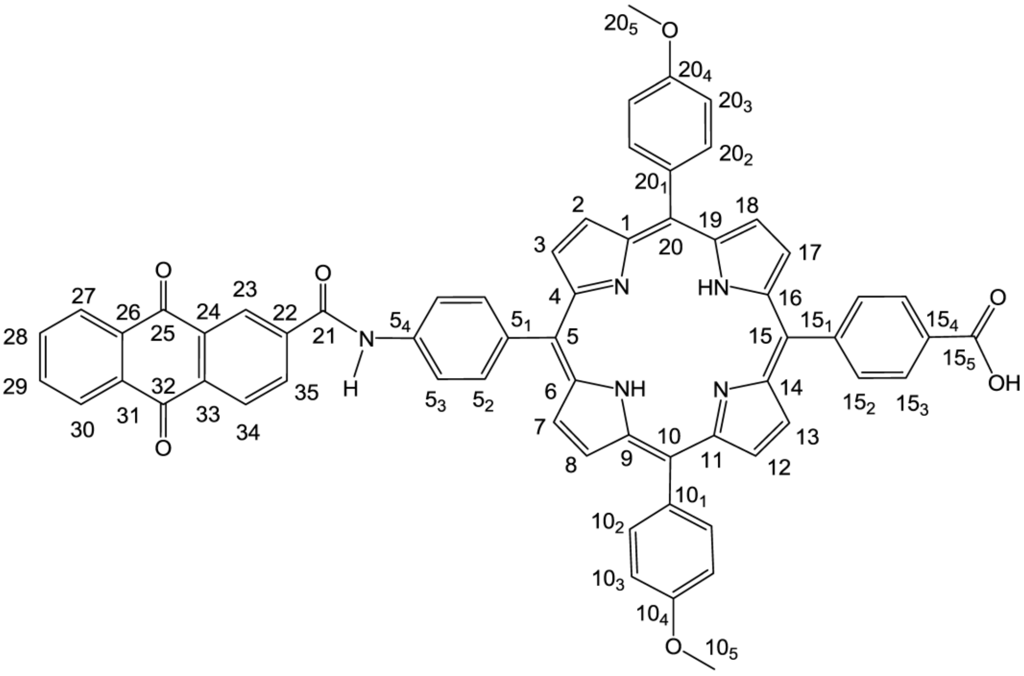

^{1}H-NMR (d$_8$-THF): δ = −2.66 (s, 2 H, H$^{\mathrm{pyrroleNH}}$), 4.07 (s, 4H, H$^{10/20}_{5/5}$), 7.35 (d, $^3J_\mathrm{HH}$ = 8.7 Hz, 4 H, H$^{10/20}_{3/3}$), 7.91 (m, 2 H, H$^{28/29}$), 8.12 (d, $^3J_\mathrm{HH}$ = 7.9 Hz, 4 H, H$^{10/20}_{2/2}$), 8.24 (br. s, 2 H, H$^5_2$), 8.35 (m, 4 H, H$^{5/15/27/30}_{3/2}$), 8.47 (m, 2 H, H$^{15/34}_3$), 8.59 (br. s, 1 H, H^{35}), 8.80 (br. s, 2 H, H$^{\mathrm{pyrrole}}$), 8.91 (m, 6 H, H$^{\mathrm{pyrrole}}$), 9.00 (br. s, 1 H, H^{23}), 10.32 (s, 1 H, H$^{\mathrm{amideNH}}$) ppm.

^{13}C{^{1}H}-NMR (d$_8$-THF). Poor solubility of **5b** in THF.

IR (KBr): $\tilde{\nu}$ [cm^{-1}] = 3431 (NH$^{\mathrm{amine}}$, NH$^{\mathrm{pyrrole}}$, COOH, b, vs), 2954 (CH, w), 2928 (CH, w), 1676 (CO, s), 1602 (s), 1512 (s), 1384 (vs), 1290 (vs), 1247 (C-O-C, vs), 802 (m).

MS (FD): m/z (%) = 967.35 (100) [M]$^+$.

MS (ESI): m/z (%) = 484.65 (24) [M^{2+}+H], 968.29 (100) [M+H]$^+$.

HR-MS (ESI): obs. m/z = 968.3045 [M+H]$^+$; calcd. for [M+H]$^+$ 968.3084.

UV/Vis (CH$_2$Cl$_2$): λ [nm] (ε / [10^4 M^{-1}cm^{-1}]) = 421 (34.49), 519 (1.61), 555 (1.02), 593 (0.44), 650 (0.29).

Fluorescence (CH$_2$Cl$_2$): λ [nm] (relative intensity) = 656 (1.00), 720 (0.27).

Quantum yield: Φ = 0.0168.

5d. 120.0 mg (0.13 mmol) **4d**. [TLC, silica, CH_2Cl_2/methanol (20:1), $R_f = 0.34$]. Yield: 81.2 mg (0.087 mmol, 69 %), purple powder. $C_{62}H_{41}N_5O_5$ (936.02).

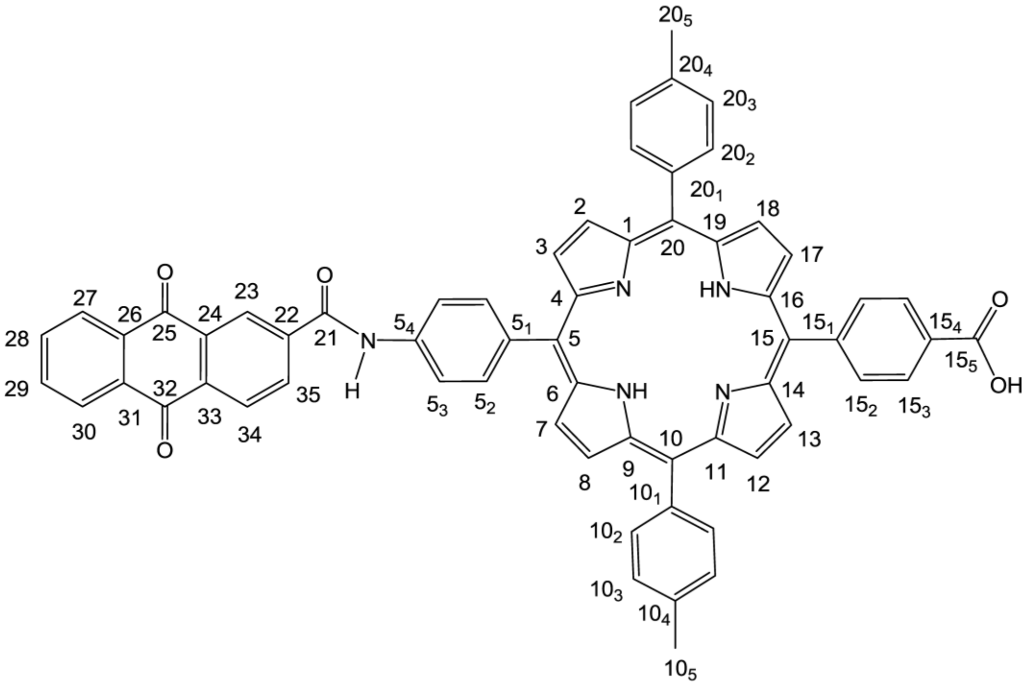

^{1}H-NMR (d_8-THF): δ = n.o. ($H^{pyrroleNH}$), 2.68 (s, 6 H, $H^{10/20}{}_{5/5}$), 7.60 (d, $^3J_{HH}$ = 7.7 Hz, 4 H, $H^{10/20}{}_{3/3}$), 7.92 (m, 2 H, $H^{28/29}$), 8.08 (d, $^3J_{HH}$ = 7.8 Hz, 4 H, $H^{10/20}{}_{2/2}$), 8.15 (d, $^3J_{HH}$ = 7.7 Hz, 2 H, $H^{15}{}_2$), 8.21 (d, $^3J_{HH}$ = 8.3 Hz, 2 H, $H^5{}_2$), 8.30 (d, $^3J_{HH}$ = 8.3 Hz, 2 H, $H^5{}_3$), 8.41 (d, $^3J_{HH}$ = 7.6 Hz, 2 H, $H^{15}{}_3$), 8.47 (d, $^3J_{HH}$ = 7.9 Hz, 1 H, H^{34}), 8.56 (dd, $^3J_{HH}$ = 8.3 Hz, $^4J_{HH}$ = 1.4 Hz, 1 H, H^{35}), 8.84 (m, 8 H, $H^{pyrrole}$), 8.99 (d, $^4J_{HH}$ = 0.9 Hz, 1 H, H^{23}), n.o. ($H^{amideNH}$) ppm.

^{13}C{^{1}H}-NMR (d_8-THF). Poor solubility of **5d** in THF.

IR (KBr): $\tilde{\nu}$ [cm^{-1}] = 3418 (NH^{amide} and COOH, br, vs), 3314 ($NH^{pyrrole}$, m), 2919 (CH, w), 1676 (CO, vs), 1595 (m), 1518 (m), 1385 (m), 1292 (vs), 966 (w), 798(s).

MS (FD): *m/z* (%) = 936.4 (36) $[M]^+$.

MS (ESI): *m/z* (%) = 936.37 (100) $[M]^+$, 937.38 (68) $[M+H]^+$.

HR-MS (ESI): obs. *m/z* = 936.3200 $[M+H]^+$; calcd. for $[M+H]^+$ 936.3186.

UV/Vis (CH_2Cl_2): λ [nm] (ε / [10^4 M^{-1}cm^{-1}]) = 420 (6.38), 516 (0.38), 552 (0.28), 591 (0.20), 648 (0.18).

Fluorescence (CH_2Cl_2): λ [nm] (relative intensity) = 654 (1.00), 719 (0.27).

Quantum yield: Φ = 0.0212.

5e. 100.0 mg (0.11 mmol) **4e**. [TLC, silica, CH_2Cl_2/methanol (20:1), $R_f = 0.44$]. Yield: 94.7 mg (0.12 mmol 95%), purple powder. $C_{60}H_{37}N_5O_5$ (907.97).

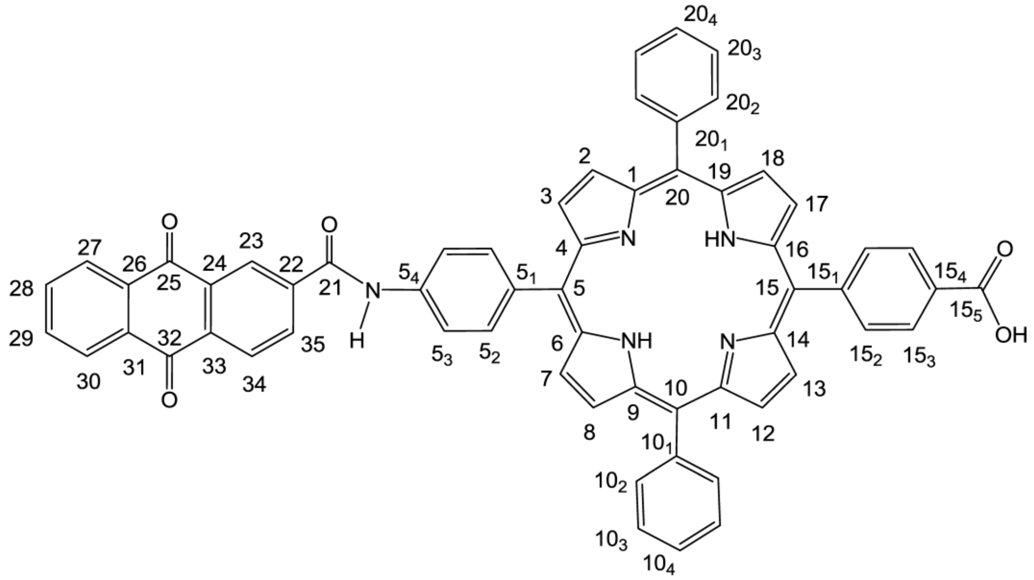

^{1}H-NMR (d$_8$-THF): $\delta = -2.68$ (s, 2 H, $H^{\text{pyrroleNH}}$), 7.79 (m, 6 H, $H^{10/20}{}_{3/4}$), 7.90 (m, 2 H, $H^{28/29}$), 8.24 (m, 6 H, $H^{10/20/5}{}_{2/2/2}$), 8.33 (m, 6 H, $H^{5/15/27/30}{}_{3/2}$), 8.46 (d, $^3J_{\text{HH}} = 8.1$ Hz, 2 H, $H^{15/34}{}_3$), 8.57 (m, 1 H, H^{35}), 8.85 (m, 4 H, H^{pyrrole}), 8.93 (m, 2 H, H^{pyrrole}), 8.99 (s, 1 H, H^{23}), 10.31 (s, 1 H, H^{amideNH}) ppm.

^{13}C{^{1}H}-NMR (d$_8$-THF). Poor solubility of **5e** in THF.

IR (KBr): $\tilde{\nu}$ [cm^{-1}] = 3440 (NH$^{\text{amide}}$ and COOH, br, m), 3315 (NH$^{\text{pyrrole}}$, w), 1678 (CO, vs), 1593 (m), 1515 (m), 1290 (vs), 966 (m), 798 (m).

MS (FD): *m/z* (%) = 907.8 (78) $[\text{M}]^+$.

MS (ESI): *m/z* (%) = 908.29 (62) $[\text{M+H}]^+$.

HR-MS (ESI): obs. *m/z* = 908.2906 $[\text{M+H}]^+$; calcd. for $[\text{M+H}]^+$ 908.2873.

UV/Vis (CH_2Cl_2): λ [nm] (ε / [10^4 M^{-1}cm^{-1}]) = 419 (37.1), 516 (1.58), 551 (0.82), 591 (0.48), 646 (0.39).

Fluorescence (CH_2Cl_2): λ [nm] (relative intensity) = 651 (1.00), 717 (0.30).

Quantum yield: $\Phi = 0.0235$.

5f. 110.0 mg (0.11 mmol) **4f**. [TLC, silica, CH_2Cl_2/methanol (20:1), $R_f = 0.47$]. Yield: 101.3 mg (0.107 mmol, 97%), purple powder. $C_{60}H_{35}F_2N_5O_5$ (943.95).

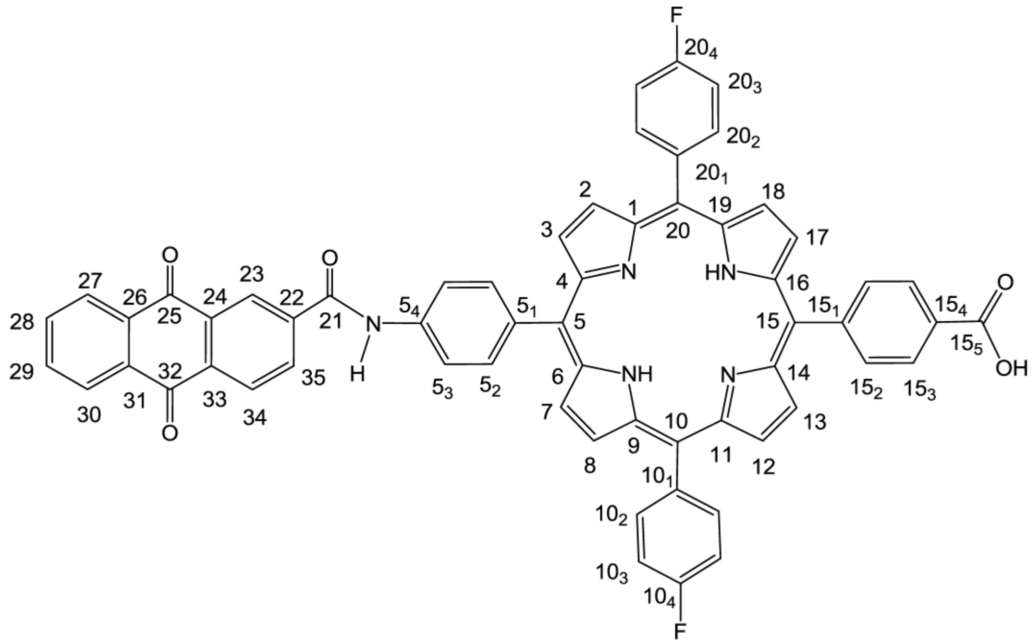

^{1}H-NMR (d$_8$-THF): δ = -2.70 (s, 2 H, H$^{\text{pyrroleNH}}$), 7.54 (ps. t, $^3J_{\text{HH}}$ = 8.7 Hz, 4 H, H$^{10/20}_{3/3}$), 7.89 (m, 2 H, H$^{28/29}$), 8.23 (m, $^3J_{\text{HH}}$ = 8.2 Hz, 6 H, H$^{5/10/20}_{2/2/2}$), 8.32 (ps. t, $^3J_{\text{HH}}$ = 8.1 Hz, 4 H, H$^{5/15}_{3/2}$), 8.35 (m, 2 H, H^{27,30}), 8.46 (d, $^3J_{\text{HH}}$ = 8.0 Hz, 2 H, H$^{15}_{3}$), 8.47 (d, $^3J_{\text{HH}}$ = 7.8 Hz, 1 H, H^{34}), 8.57 (dd, 1 H, $^4J_{\text{HH}}$ = 1.7 Hz, $^3J_{\text{HH}}$ = 8.0 Hz, H^{35}), 8.85 (m, 6 H, H$^{\text{pyrrole}}$), 8.95 (d, $^3J_{\text{HH}}$ = 4.5 Hz, 2 H, H$^{\text{pyrrole}}$), 8.98 (d, 1 H, $^4J_{\text{HH}}$ = 1.6 Hz, H^{23}), 10.31 (s, 1 H, H$^{\text{amideNH}}$). 11.68 (br. s, 1 H, H$^{\text{CO}_2\text{H}}$) ppm.

^{13}C{^{1}H}-NMR (d$_8$-THF). Poor solubility of **5f** in THF.

^{19}F-NMR (THF): $\delta = -115.9$ (m, F-C$^{10/20}_{4/4}$).

IR (KBr) [cm^{-1}]: $\tilde{\nu}$ = 3442 (NH$^{\text{amide}}$ and COOH, br, s), 3317 (NH$^{\text{pyrrole}}$, m), 1733 (CO, m), 1666 (CO, vs), 1591 (m), 1508 (m), 1284 (vs), 1160 (CF, w), 969 (w), 812 (m).

MS (FD): m/z (%) = 943.62 (100) [M]$^+$.

MS (ESI): m/z (%) = 944.26 (100) [M+H]$^+$.

HR-MS (ESI): obs. m/z = 944.2659 [M+H]$^+$; calcd. for [M+H]$^+$ 944.2685.

UV/Vis (CH$_2$Cl$_2$): λ [nm] (ε / [10^4 M^{-1}cm^{-1}]) = 419 (3.88), 515 (0.73), 550 (0.66), 592 (0.63), 651 (0.60).

Fluorescence (CH$_2$Cl$_2$): λ [nm] (relative intensity) = 651 (1.00), 718 (0.34).

Quantum yield: Φ = 0.0133.

5g. 40.0 mg (0.039 mmol) **4g**. [TLC, silica, CH$_2$Cl$_2$/methanol (20:1), R_f = 0.44]. Yield: 37 mg (0.035 mmol, 90%), purple powder. $C_{62}H_{35}F_6N_5O_5$ (1043.96).

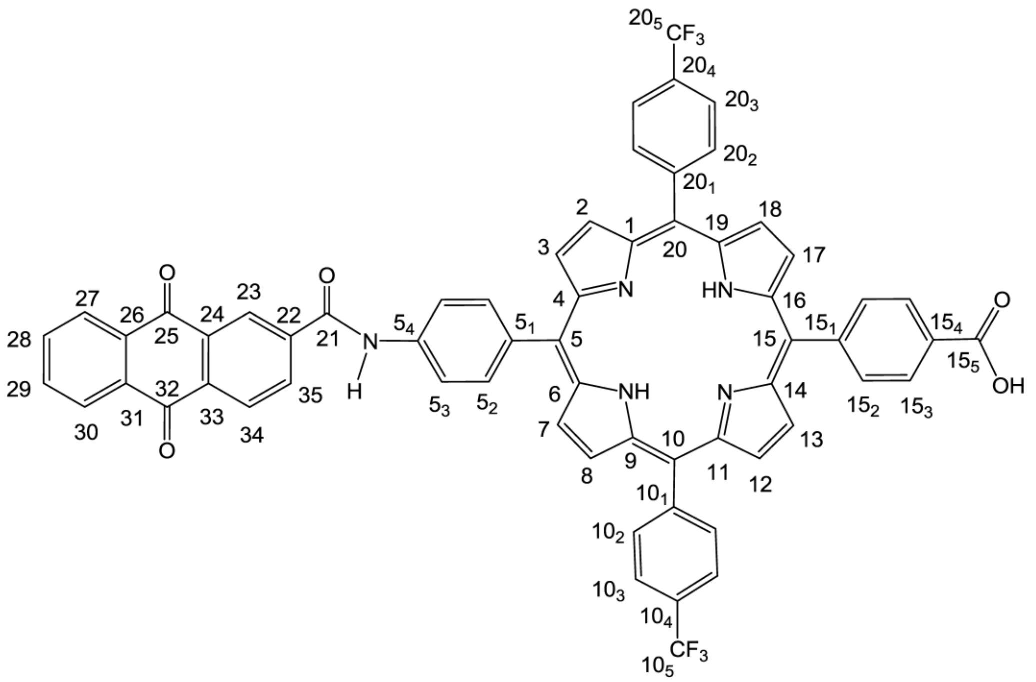

^{1}H-NMR (d^8-THF): $\delta = -2.70$ (s, 2 H, $\mathrm{H}^{\mathrm{pyrroleNH}}$), 7.90 (m, 2 H, $\mathrm{H}^{28/29}$), 8.14 (d, $^3J_{\mathrm{HH}} = 8.1$ Hz, 4 H, $\mathrm{H}^{10/20}{}_{3/3}$), 8.23 (d, $^3J_{\mathrm{HH}} = 8.5$ Hz, 2 H, $\mathrm{H}^{5}{}_{2}$), 8.34 (ps. t, $^3J_{\mathrm{HH}} = 8.1$ Hz, 4 H, $\mathrm{H}^{5/15}{}_{3/2}$), 8.35 (m, 2 H, $\mathrm{H}^{27,30}$), 8.45 (d, $^3J_{\mathrm{HH}} = 8.8$ Hz, 4 H, $\mathrm{H}^{10/20/15}{}_{2/2/3}$), 8.47 (d, $^3J_{\mathrm{HH}} = 7.9$ Hz, 1 H, H^{34}), 8.56 (dd, 1 H, $^4J_{\mathrm{HH}} = 1.7$ Hz, $^3J_{\mathrm{HH}} = 8.0$ Hz, H^{35}), 8.84 (m, 6 H, $\mathrm{H}^{\mathrm{pyrrole}}$), 8.98 (d, 3 H, $^4J_{\mathrm{HH}} = 1.7$ Hz, $\mathrm{H}^{23/\mathrm{pyrrole}}$), 8.98 (2 H, $\mathrm{H}^{\mathrm{pyrrole}}$), 10.32 (s, 1 H, $\mathrm{H}^{\mathrm{amideNH}}$) 11.71 (br. s, 1 H, $\mathrm{H}^{\mathrm{CO_2H}}$) ppm.

^{13}C{^{1}H}-NMR (d$_8$-THF): δ = 119.5 (s, $\mathrm{C}^{5}{}_{3}$), 119.5 (s, $\mathrm{C}^{10/20}$), 118.2 (C^{15}), 121.7 (C^{5}), 124.7 ($\mathrm{C}^{10/20}{}_{3/3}$), 126.9 ($\mathrm{C}^{23}$), 127.5 ($\mathrm{C}^{10/20}{}_{4/4}$), 128.1 ($\mathrm{C}^{27/30}$), 129.0 ($\mathrm{C}^{34}$), 128.1 ($\mathrm{C}^{15}{}_{2}$), 131.0 ($\mathrm{C}^{15}{}_{4}$), 131.6 (m, $\mathrm{C}^{10/20}{}_{5/5}$), 134.4 ($\mathrm{C}^{35}$), 134.7 ($\mathrm{C}^{24}$), 135.3 ($\mathrm{C}^{28/29}$), 135.5 ($\mathrm{C}^{15}{}_{3}$), 135.9 ($\mathrm{C}^{5}{}_{2}$), 135.9 ($\mathrm{C}^{10/20}{}_{2/2}$), 136.4 ($\mathrm{C}^{33}$), 138.4 ($\mathrm{C}^{5}{}_{1}$), 140.5 ($\mathrm{C}^{5}{}_{4}$), 141.5 ($\mathrm{C}^{22}$), 147.0 ($\mathrm{C}^{10/20}{}_{1/1}$), 147.2 ($\mathrm{C}^{15}{}_{1}$), 165.1 ($\mathrm{C}^{21}$), 167.7 ($\mathrm{C}^{15}{}_{5}$), 182.7, 182.9 ($\mathrm{C}^{25/32}$) ppm.

^{19}F-NMR (THF): $\delta = -62.7$ (s, F-$\mathrm{C}^{10/20}{}_{5/5}$) ppm.

IR (KBr): $\tilde{\nu}$ [cm^{-1}] = 3443 ($\mathrm{NH}^{\mathrm{amide}}$, $\mathrm{NH}^{\mathrm{pyrrole}}$, COOH, br, m), 2920 (CH, m), 1676 (CO, m), 1605 (m), 1518 (m), 1394 (m), 1288 (s), 1120 (CF, s), 794(m).

MS (FD): *m/z* (%) = 1043.7 (100) $[\mathrm{M}]^+$.

MS (ESI): *m/z* (%) = 522.63 (1) $[\mathrm{M}^{2+}\mathrm{+H}]$, 1044.26 (100) $[\mathrm{M+H}]^+$.

HR-MS (ESI): obs. *m/z* = 1044.2646 $[\mathrm{M+H}]^+$; calcd. for $[\mathrm{M+H}]^+$ 1044.2621.

UV/Vis (CH_2Cl_2): λ [nm] (ε / [10^4 M^{-1}cm^{-1}]) = 419 (53.69), 515 (2.62) 550 (1.30), 590 (0.91), 649 (0.83).

Fluorescence (CH_2Cl_2): λ [nm] (relative intensity) = 652 (1.00), 716 (0.35).

Quantum yield: $\Phi = 0.0388$.

5c. 25.0 mg (0.025 mmol) **4c**. [TLC, silica, CH_2Cl_2/methanol (20:1), $R_f = 0.60$]. Yield: 22.0 mg (0.022 mmol, 87%), purple powder. $C_{66}H_{49}N_5O_5$ (992.13).

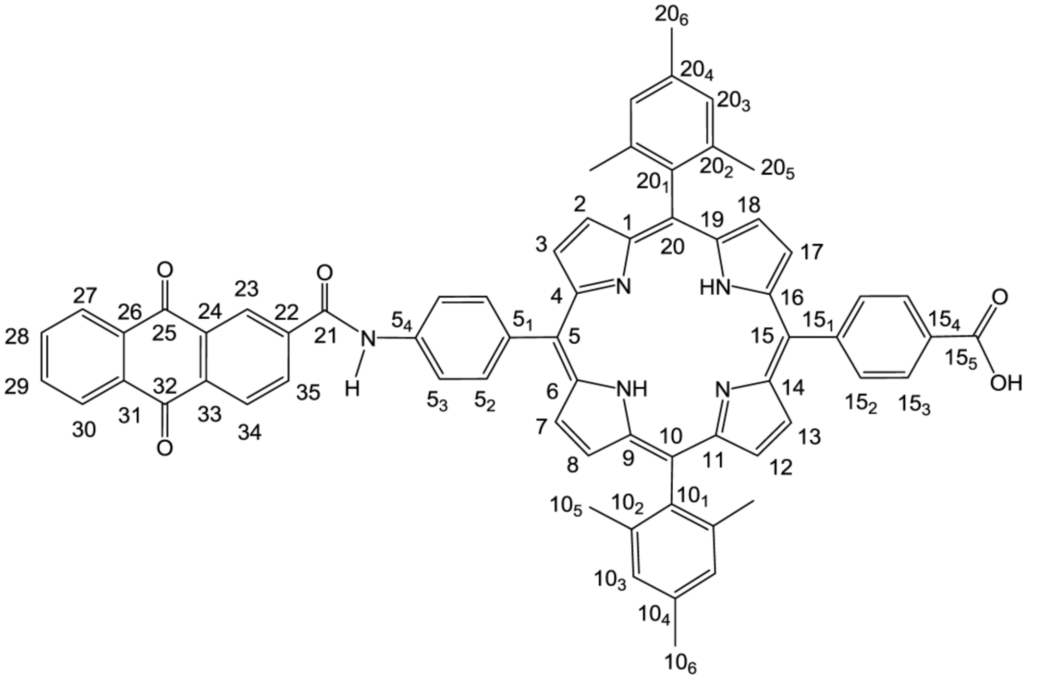

^{1}H-NMR (d_8-THF): $\delta = -2.48$ (s, 2 H, $H^{pyrroleNH}$), 1.85 (s, 12 H, $H^{10/20}{}_{5/5}$), 2.61 (s, 6 H, $H^{10/20}{}_{6/6}$), 7.32 (s, 4 H, $H^{10/20}{}_{3/3}$), 7.91 (m, 2 H, $H^{28/29}$), 8.22 (d, $^3J_{HH}$ = 8.3 Hz, 2 H, $H^5{}_2$), 8.32 (m, 4 H, $H^{5/15}{}_{3/2}$), 8.37 (m, 2 H, $H^{27/30}$), 8.43 (d, $^3J_{HH}$ = 7.9 Hz, 2 H, $H^{15}{}_3$), 8.48 (d, $^4J_{HH}$ = 8.0 Hz 1H, H^{34}), 8.59 (dd, $^3J_{HH}$ = 8.1 Hz, $^4J_{HH}$ = 1.5 Hz, 1 H, H^{35}), 8.67 (d, $^3J_{HH}$ = 3.9 Hz, 4 H, $H^{pyrrole}$), 8.77 (d, 2 H, $^3J_{HH}$ = 4.6 Hz, $H^{pyrrole}$), 8.88 (d, 2 H, $^3J_{HH}$ = 4.5 Hz, $H^{pyrrole}$), 9.01 (br. s, 1 H, H^{23}), 10.37 (1 H, $H^{amideNH}$) ppm.

^{13}C{^{1}H}-NMR (d_8-THF): δ = 21.7 ($C^{10/20}{}_{6/6}$), 21.9 ($C^{10/20}{}_{5/5}$), 119.4 ($C^5{}_3$), 119.3, 119.6 ($C^{5/10/15/20}$), 126.9 (C^{23}), 128.0 (C^{27}), 128.0 (C^{30}), 128.8 ($C^{10/20/34}{}_{3/3}$), 129.0($C^{15}{}_3$), n.o. (br. s, $C^{pyrrole}{}_{2/3/7/8/12/13/17/18}$), 132.3 ($C^{15}{}_4$), 134.4 ($C^{35}$), n.o. ($C^{24}$), 135.2, 135.2 ($C^{28/29}$), 135.4 ($C^{15}{}_2$), 135.9 ($C^5{}_2$), 137.1 ($C^{33}$), 139.6 ($C^5{}_1$), 140.1 ($C^{10/20}{}_{1/1}$), 141.1 ($C^5{}_4$), 142.5 ($C^{22}$), 148.3 ($C^{15}{}_1$), n.o. ($C^{21}$), 168.1 ($C^{15}{}_5$), 183.2, 183.2 ($C^{25/32}$) ppm.

IR (KBr): $\tilde{\nu}$ [cm^{-1}] = 3422 (NH^{amide}, $NH^{pyrrole}$,COOH, br, vs), 2920 (CH, w), 2856 (CH, w), 1680 (CO, vs), 1512 (m), 1382 (m), 1288 (m), 968 (m).

MS (FD): *m/z* (%) = 991.89 (100) $[M]^+$.

MS (ESI): *m/z* (%) = 496.71 (7) $[M^{2+}$+H]), 992.42 (100) $[M+H]^+$.

HR-MS (ESI): obs. *m/z* = 992.3830 $[M+H]^+$; calcd. for $[M+H]^+$ 992.3812.

UV/Vis (CH_2Cl_2): λ [nm] (ε / [10^4 M^{-1}cm^{-1}]) = 420 (19.56), 516 (0.82), 550 (0.34), 592 (0.18), 650 (0.28).

Fluorescence (CH_2Cl_2): λ [nm] (relative intensity) = 652 (1.00), 718 (0.28).

Quantum yield: Φ = 0.0291.

CV (Fc/Fc$^+$, 100 mV s^{-1}, CH$_2$Cl$_2$): $E_{½}$ [V] = −1.310 (q. rev.), 0.900 (q. rev.).

5i. 55 mg (0.050 mmol) **4h**. [TLC, silica, CH$_2$Cl$_2$/methanol (20:1), R_f = 0.46]. Yield: 51.6 mg (0.046 mmol 92%), purple powder. $C_{62}H_{33}F_8N_5O_7$ (1111.94).

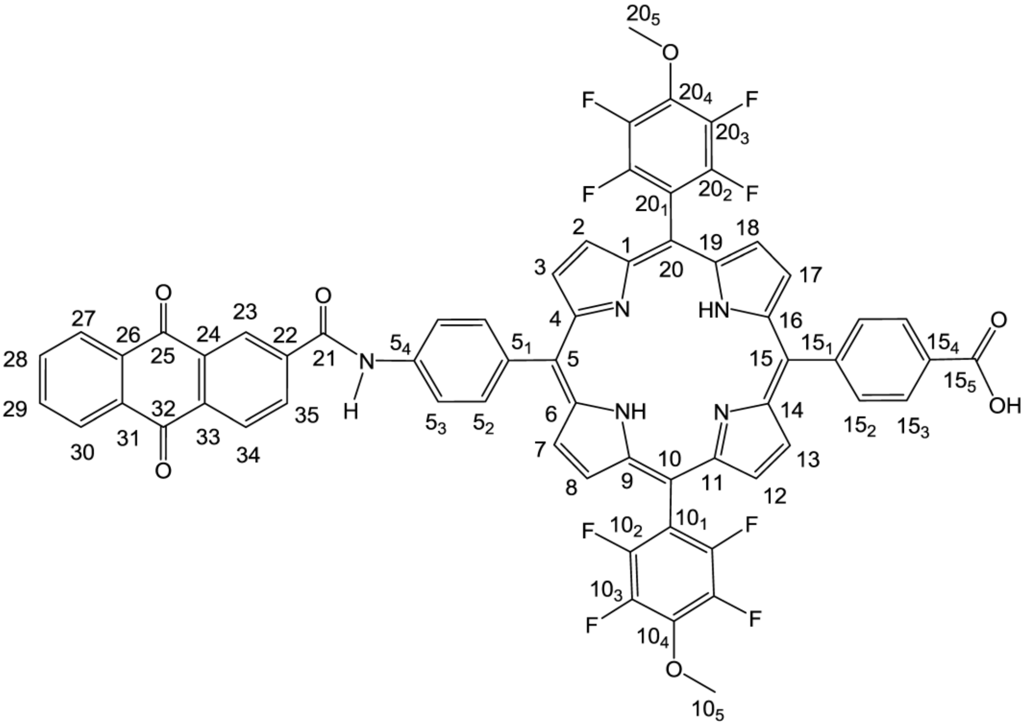

^{1}H-NMR (d$_8$-THF): δ = −2.74 (s, 2 H, H$^{\text{pyrroleNH}}$), 4.39 (s, H$^{10/20}{}_{5/5}$) 7.90 (m, 2 H, H$^{28/29}$), 8.25 (d, $^3J_{\text{HH}}$ = 8.4 Hz, 2 H, H$^5{}_2$), 8.37 (m, 4 H, H$^{15}{}_2{}^{/27/30}$), 8.40 (d, $^3J_{\text{HH}}$ = 8.4 Hz, 2 H, H$^5{}_3$), 8.47 (m, 3H, H$^{15}{}_3{}^{/34}$), 8.65 (dd, $^3J_{\text{HH}}$ = 8.1 Hz, $^4J_{\text{HH}}$ = 1.2 Hz, 1 H, H^{35}), 8.91 (d, 2 H, $^3J_{\text{HH}}$ = 4.5 Hz, H$^{\text{pyrrole}}$), 9.02 (m, 7 H, H$^{\text{pyrrole/23}}$), 10.49 (s, 1 H, H$^{\text{amideNH}}$) ppm.

^{13}C{^{1}H}-NMR (d$_8$-THF): δ = 63.1 (C$^{10/20}{}_{5/5}$), 119.5 (s, C$^5{}_3$), n.o. (C$^{10/20}$), 121.2 (C^{15}), 122.7 (C^5), 126.7 (C^{23}), 128.0 (C^{27}), 128.0 (C^{30}), 128.3 (C^{34}), 129.2 (C$^{15}{}_3$), 131.1 (br. s, C$^{\text{pyrrole 2/3/7/8/12/13/17/18}}$), 132.8 (C$^{15}{}_4$), 134.4 (C^{35}), 134.9 (C^{24}), 135.2, 135.3 (C$^{28/29}$), 135.4 (C$^{15}{}_2$), 136.0 (C$^5{}_2$), 136.5 (C^{33}), 138.1 (C$^5{}_1$), 140.9 (C$^5{}_4$), 141.7 (C^{22}), 146.7 (C$^{15}{}_1$), 143.3, 146.8 149.3 (C$^{10/20}{}_{2/3/4}$), 165.3 (C^{21}), 168.4 (C$^{15}{}_5$), 183.0, 183.2 (C$^{25/32}$) ppm.

^{19}F-NMR (d$_8$-THF): δ = −161.8 (dd, $^3J_{\text{FF}}$ = 23 Hz, $^5J_{\text{FF}}$ = 8 Hz, 4 F, F$^{10/20}{}_{3/3}$), −143.2 (dd, $^3J_{\text{FF}}$ = 22 Hz, $^5J_{\text{FF}}$ = 8 Hz, 4 F, F$^{10/20}{}_{2/2}$) ppm.

IR (KBr): $\tilde{\nu}$ [cm^{-1}] = 3421 (NH$^{\text{amide}}$, NH$^{\text{pyrrole}}$, COOH, br, vs), 2924 (CH, w), 2851 (CH, w), 1680 (CO, s), 1506 (vs), 1483 (vs), 1288 (vs), 1082 (CF, w), 1060 (CF, w), 988 (s).

MS (FD): *m/z* (%) = 606.62 (61) [M]$^{2+}$,1111.34 (100) [M]$^+$.

MS (ESI): *m/z* (%) = 1112.27 (100) [M+H]$^+$.

HR-MS (ESI): obs. *m/z* = 1112.2338 [M+H]$^+$; calcd. for [M+H]$^+$ 1112.2330.

UV/Vis (CH_2Cl_2): λ [nm] (ε / [10^4 $M^{-1}cm^{-1}$]) = 418 (21.41), 513 (2.07), 545 (0.64), 590 (0.60), 647 (0.64).

Fluorescence (CH_2Cl_2): λ [nm] (relative intensity) = 649 (1.00), 713 (0.34).

Quantum yield: Φ = 0.0856.

CV (Fc/Fc$^+$, 100 mV s^{-1}, CH_2Cl_2): $E_{½}$ [V] = −1.910 (q. rev.), −1.465 (q. rev.), −1.230 (q. rev), 0.770 (irr.), 1.000 (irr.).

5h. Dyad **4h** (40 mg, 0.036 mmol) was dissolved in TFA (30 mL) and conc. HCl aq (60 mL). The mixture was heated to 60°C. After 28 h TLC indicated beginning formation of byproducts and the reaction was cooled down, neutralised with a saturated aqueous solution of $NaHCO_3$ and diluted with CH_2Cl_2 (100 mL). The organic layer was washed with water (3×), dried over $MgSO_4$ and concentrated under reduced pressure. The residue was purified by column chromatography [silica, CH_2Cl_2/MeOH (20:1), R_f = 0.50]. Yield: 34.0 mg (0.031 mmol, 89%), purple powder. $C_{60}H_{27}F_{10}N_5O_5$ (1087.87).

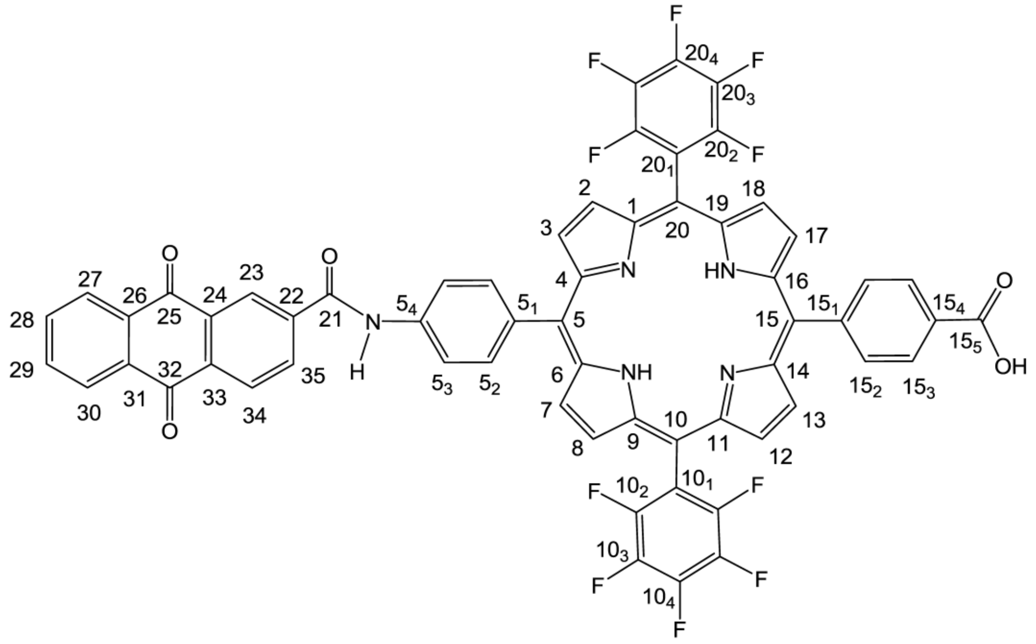

^{1}H-NMR (d_8-THF): δ = –2.74 (s, 2 H, $H^{pyrroleNH}$), 7.92 (m, 2 H, $H^{28/29}$), 8.27 (d, $^3J_{HH}$ = 8.3 Hz, 2 H, $H^5{}_2$), 8.35 (m, 6 H, $H^{5/15/27/30}{}_{2/2}$), 8.49 (d, $^3J_{HH}$ = 8.0 Hz, 1 H, H^{34}), 8.58 (m, 3H, $H^{15}{}_3{}^{/35}$), 8.98 (m, 2 H, $H^{pyrrole}$), 9.01 (br. s, 1 H, H^{23}), 9.05 (m, 6 H, $H^{pyrrole}$), 10.40 (s, 1 H, $H^{amideNH}$) ppm.

^{13}C{^{1}H}-NMR (d_8-THF): δ = 119.5 ($C^5{}_3$), n.o. ($C^{10/20}$), 122.5 (C^5), 126.8 (C^{23}), 128.0 (C^{27}), 128.0 (C^{30}), 128.3 (C^{34}), 129.4 ($C^{15}{}_3$), 131.0 (br.s, $C^{pyrrole\ 2/3/7/8/12/13/17/18}$), n.o. ($C^{15}{}_4$), 134.4 ($C^{35}$), 134.9 ($C^{24}$), 135.2 ($C^{28/29}$), 135.3 ($C^{15}{}_2$), 136.0 ($C^5{}_2$), 136.5 ($C^{33}$), 137.9 ($C^5{}_1$), 140.8 ($C^5{}_4$), n.o. ($C^{15}{}_1$), 141.7 ($C^{22}$), 140.9 ($C^5{}_4$), 141.7 ($C^{15}{}_1$), 140.3, 144.7, 146.6, 149.1 ($C^{10/20}{}_{1/1/2/2/3/3/4/4}$) 165.3 ($C^{21}$), n.o. ($C^{15}{}_5$), 183.0, 183.2 ($C^{25/32}$) ppm.

^{19}F-NMR (d_8-THF): $\delta = -166.6$ (ddd, $^3J_{FF} = 23$ Hz, $^3J_{FF} = 20$ Hz, $^5J_{FF} = 8$ Hz, 4 F, $F^{10/20}{}_{3/3}$), -157.8 (t, $^3J_{FF} = 20$ Hz, 2 F, $F^{10/20}{}_{4/4}$), -141.3 (dd, $^3J_{FF} = 24$ Hz, $^5J_{FF} = 8$ Hz, 4 F, $F^{10/20}{}_{2/2}$) ppm.
IR (KBr): $\tilde{\nu}$ [cm^{-1}] = 3442 (NH^{amide}, NH^{pyrrole}, COOH, b, vs), 1674 (CO, w), 1649 (CO, w), 1520 (m), 1497 (m), 1382 (vs), 1290 (m), 1112 (CF, w), 988 (s), 922 (m).
MS (FD): *m/z* (%) = 1086.84 (100) [M]$^+$.
MS (ESI): *m/z* (%) = 1088.23 (100) [M+H]$^+$, 2176.44 (2) [2M+H]$^+$.
HR-MS (ESI): obs. *m/z* = 1088.1907 [M+H]$^+$; calcd. for [M+H]$^+$ 1088.1931.
UV/Vis (CH_2Cl_2): λ [nm] (ε / [10^4 M^{-1}cm^{-1}]) = 417 (9.59), 512 (0.068), 544 (0.027), 588 (0.026), 643 (0.012).
Fluorescence (CH_2Cl_2): λ [nm] (relative intensity) = 647 (1.00), 713 (0.53).
Quantum yield: $\Phi = 0.0835$.

General procedure for the preparation of Q-P-Fc dyads 6a – 6i.
Carboxylic acid **5** (1 eq.) and pyridine (1 mL) were dissolved in anhydrous toluene (20 mL), thionyl chloride (5 eq.) was added and the reaction mixture was stirred under argon for 3h at room temperature. Excess of thionyl chloride and solvent were removed under reduced pressure. The residue was redesolved in an ultrasonic bath in toluene (20 mL) and pyridine (1 mL) and ferrocenylamine (1.3 eq.), dissolved in toluene (10 mL) and pyridine (1 mL) was added. The mixture was stirred overnight and solvent was removed by evaporation under reduced pressure. The residue was purified by chromatography.

6a. 26.9 mg (0.026 mmol) **5a**, 10 µL (0.13 mmol) thionyl chloride, 6.8 mg (0.034) ferrocenylamine. [silica, CH_2Cl_2, R_f = 0.35]. Yield: 13.3 mg (0.001 mmol, 41%), purple powder. $C_{78}H_{62}FeN_6O_6$ (1235.21).

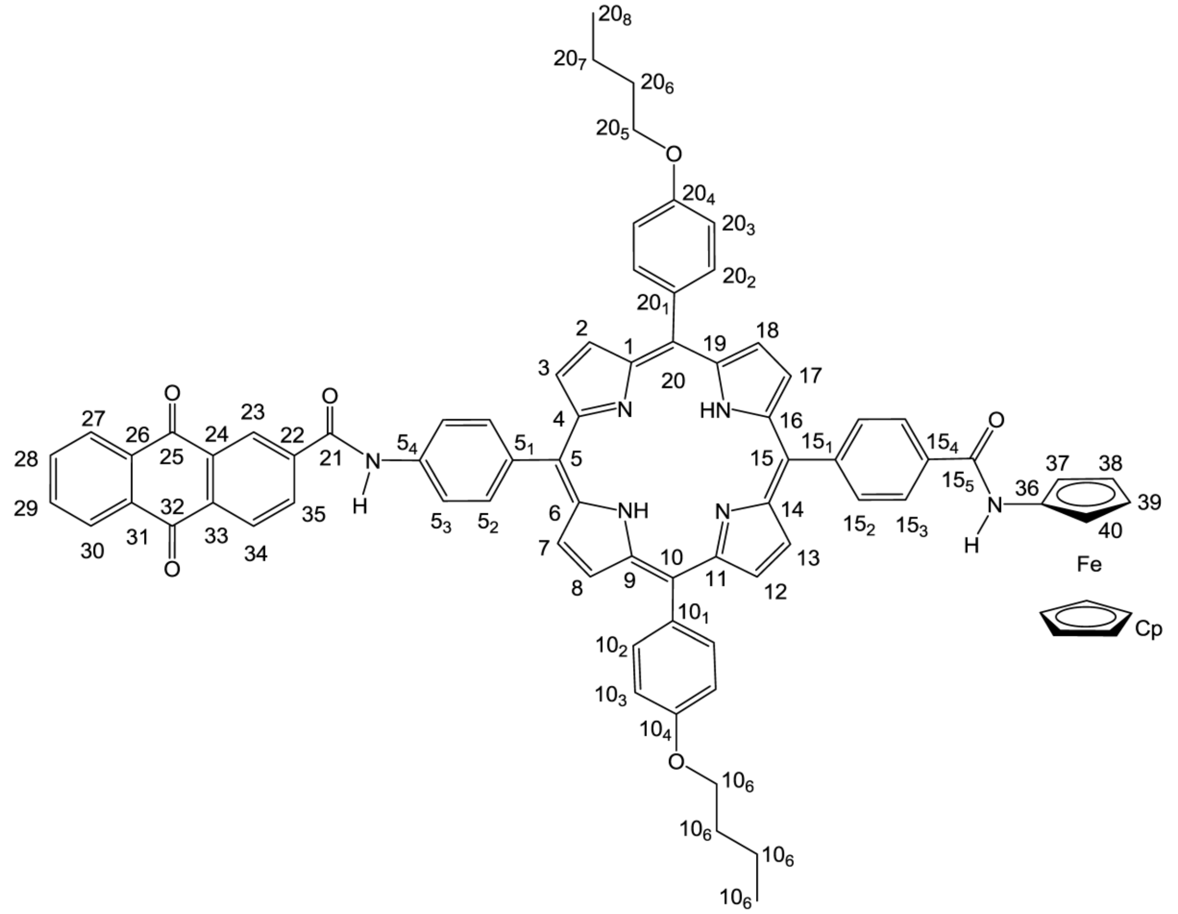

^{1}H-NMR (d$_8$-THF): δ = –2.65 (s, 2 H, $H^{pyrroleNH}$), 1.10 (t, $^{3}J_{HH}$ = 7.4 Hz, 6 H, $H^{10/20}{}_{8/8}$), 1.67 (m, 4 H, $H^{10/20}{}_{7/7}$), 1.96 (m, 4 H, $H^{10/20}{}_{6/6}$), 4.05 (s, 2 H, $H^{38/39}$), 4.24 (s, 5 H, H^{41}), 4.28 (t, $^{3}J_{HH}$ = 6.3 Hz, 4 H, $H^{10/20}{}_{5/5}$), 4.95 (s, 2 H, $H^{37/40}$), 7.33 (d, $^{3}J_{HH}$ = 8.4 Hz, 4 H, $H^{10/20}{}_{3/3}$), 7.91 (m, 2 H, $H^{28/29}$), 8.11 (d, $^{3}J_{HH}$ = 8.4 Hz, 4 H, $H^{10/20}{}_{2/2}$), 8.22 (d, $^{3}J_{HH}$ = 8.4 Hz, 2 H, $H^{5}{}_{2}$), 8.34 (m, 8 H, $H^{5/15/15/27/30}{}_{2/3/3}$), 8.47 (d, $^{3}J_{HH}$ = 8.0 Hz, 1 H, H^{34}), 8.58 (dd, $^{3}J_{HH}$ = 8.0 Hz, $^{4}J_{HH}$ = 1.5 Hz, 1 H, H^{35}), 8.82 (d, $^{3}J_{HH}$ = 4.6 Hz, 2 H, $H^{pyrrole}$), 8.90 (m, 6 H, $H^{pyrrole}$), 8.99 (br. s, 1 H, H^{23}), 9.20 (s, 1H, $H^{amideFcNH}$), 10.33 (s, 1 H, $H^{amidePorphNH}$) ppm.

^{13}C{^{1}H}-NMR (d$_8$-THF): δ = 14.5 ($C^{10/20}{}_{8/8}$), 20.5 ($C^{10/20}{}_{7/7}$), 32.8 ($C^{10/20}{}_{6/6}$), 68.3 ($C^{10/20}{}_{5/5}$), 61.9 ($C^{38/39}$), 69.5 (C^{Cp}), 113.5 ($C^{10/20}{}_{3/3}$), 119.1 ($C^{5}{}_{3}$), 126.0 ($C^{15}{}_{3}$), 126.5 (C^{23}), 127.7 ($C^{27/30}$), 134.0 (C^{35}), 135.0 ($C^{28/29}$), 135.0 ($C^{15}{}_{2}$). 135.5 ($C^{5}{}_{2}$), 136.2 ($C^{10/20}{}_{2/2}$) ppm. Because of the poor solubility of **6a** in THF not all ^{13}C resonances could be observed.

IR (KBr): $\tilde{\nu}$ [cm^{-1}] = 3416 (NH^{amide}, br, w), 3317 ($NH^{pyrrole}$, b, w), 2955 (CH, m), 2924 (CH, m), 2864 (CH, m), 1676(CO, vs), 1512 (vs), 1387 (s), 1288 (m), 1245 (C-O-C, s), 802 (m).

MS (FD): *m/z* (%) = 617.70 (1) $[M]^{2+}$, 1234.69 (100) $[M]^{+}$, 2468.4 (1) $[2M]^{+}$.

MS (ESI): *m/z* (%) = 618.22 (66) $[M+H]^{2+}$, 1235.47 (100) $[M+H]^{+}$.

HR-MS (ESI): obs. *m/z* = 1235.4115 $[M+H]^{+}$; calcd. for $[M+H]^{+}$ 1235.4124.

UV/Vis (CH$_2$Cl$_2$): λ [nm] (ε / [10^{4} M^{-1}cm^{-1}]) = 422 (36.31), 518 (1.35), 555 (0.89), 593 (0.36), 650 (0.39).

Fluorescence (CH_2Cl_2): λ [nm] (relative intensity) = 656 (1.00), 720 (0.24).

Quantum yield: $\Phi = 0.0042$.

Lifetime: τ [ps] = 214.99 (100%).

CV (Fc/Fc$^+$, 100 mV s^{-1}, CH_2Cl_2): $E_{½}$ [V] = −2.010 (irr.), −1.650, −1.210, −0.070, 0.510, 0.770.

6b. 17.0 mg (0.018 mmol) **5b**, 7 µL (0.089 mmol) thionyl chloride, 4.6 mg (0.023) ferrocenylamine. [silica, CH_2Cl_2, $R_f = 0.29$]. Yield: 10.3 mg (0.009 mmol, 50%), purple powder. $C_{72}H_{50}FeN_6O_6$ (1151.05).

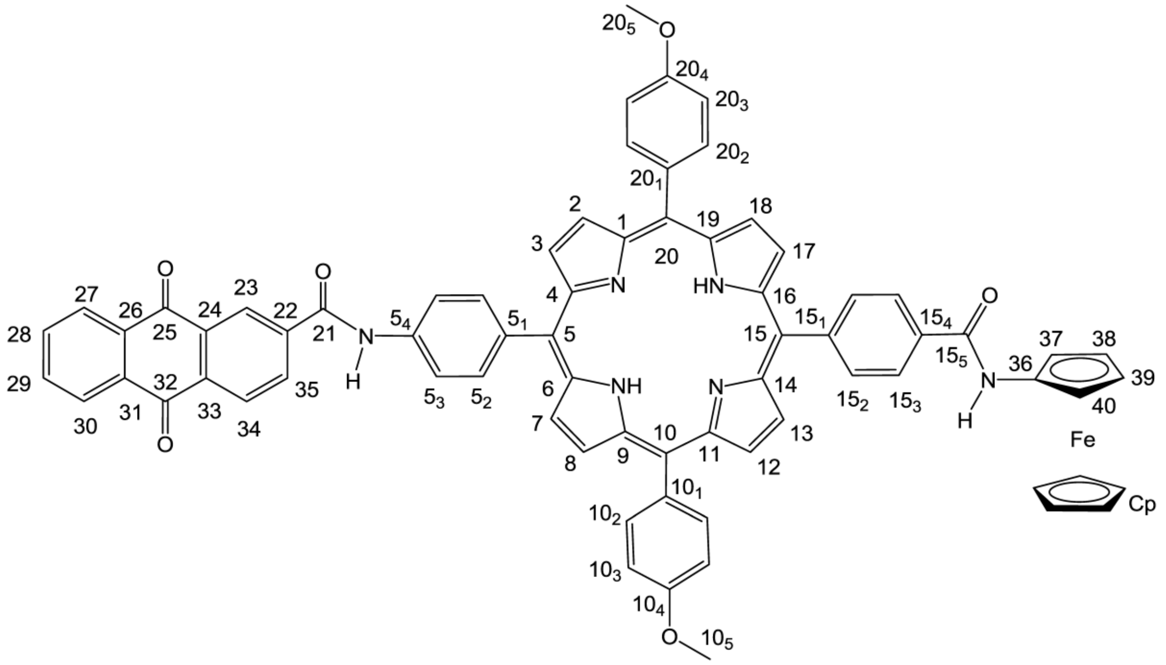

^{1}H-NMR (d_8-THF): $\delta = -2.65$ (s, 2 H, H$^{\text{pyrroleNH}}$), 4.05 (s, 2 H, H$^{39/38}$), 4.07 (s, 6 H, H$^{10/20}{}_{5/5}$), 4.24 (s, 5 H, H$^{\text{Cp}}$), 4.95 (s, 2 H, H$^{37/40}$), 7.34 (d, $^3J_{\text{HH}} = 8.4$ Hz, 4 H, H$^{10/20}{}_{3/3}$), 7.91 (m, 2 H, H$^{28/29}$), 8.12 (d, $^3J_{\text{HH}} = 8.2$ Hz, 4 H, H$^{10/20}{}_{2/2}$), 8.22 (d, $^3J_{\text{HH}} = 8.6$ Hz, 2 H, H$^5{}_2$), 8.36 (m, 8 H, H$^{5/15/15/27/30}{}_{2/3/3}$), 8.48 (d, $^3J_{\text{HH}} = 8.3$ Hz, 1 H, H^{34}), 8.58 (dd, $^3J_{\text{HH}} = 8.4$ Hz, $^4J_{\text{HH}} = 1.4$ Hz, 1 H, H^{35}), 8.82 (d, $^3J_{\text{HH}} = 4.5$ Hz, 2 H, H$^{\text{pyrrole}}$), 8.90 (m, 6 H, H$^{\text{pyrrole}}$), 9.00 (br. s, 1 H, H^{23}), 9.19 (s, 1H, H$^{\text{amideFcNH}}$), 10.31 (s, 1 H, H$^{\text{amidePorphNH}}$) ppm.

^{13}C{^{1}H}-NMR (d_8-THF): δ = 55.9 (C$^{10/20}{}_{5/5}$), 61.9 (C$^{37/40}$), 64.9 (C$^{39/38}$), 69.5 (C$^{\text{Cp}}$), 113.3 (C$^{10/20}{}_{3/3}$), 119.1 (C$^5{}_3$), 126.7 (C^{23}), 127.8 (C$^{27/30}$), 128.2 (C^{34}), 134.8 (C$^{28/29}$), 135.5 (C$^{15}{}_2$), 135.7 (C$^5{}_2$), 136.5 (C$^{10/20}{}_{2/2}$), 139.3 (C$^5{}_1$), 140.6 (C$^5{}_4$), 142.2 (C^{22}), 161.3 (C$^{10/20}{}_{4/4}$) ppm. Because of the poor solubility of **6b** in THF not all ^{13}C resonances could be observed.

IR (KBr): $\tilde{\nu}$ [cm^{-1}] = 3420 (NH$^{\text{amide}}$, NH$^{\text{pyrrole}}$, br, s), 2924 (CH, m), 1674(CO, s), 1607 (m), 1520 (s), 1382 (vs), 1473 (s), 1290 (m), 1247 (C-O-C, s), 802 (m).

MS (FD): *m/z* (%) = 1151.70 (100) [M+H]$^+$.

MS (ESI): *m/z* (%) = 575.68 (100) [M+H]$^{2+}$, 1151.36 (52) [M+H]$^+$.

HR-MS (ESI): obs. *m/z* = 1151.3256 [M+H]$^+$; calcd. for [M+H]$^+$ 1151.3219.

UV/Vis (CH$_2$Cl$_2$): λ [nm] (ε / [10^4 M^{-1}cm^{-1}]) = 422 (39.19), 518 (1.67), 554 (1.11), 593 (0.69), 649 (0.53).

Fluorescence (CH$_2$Cl$_2$): λ [nm] (relative intensity) = 657 (1.00), 722 (0.26).

Quantum yield: Φ = 0.0034.

Lifetime: τ [ps] = 240.54 (100%).

CV (Fc/Fc$^+$, 100 mV s^{-1}, CH$_2$Cl$_2$): $E_{1/2}$ [V] = −2.010 (irr.), −1.650, −1.220, −0.079, 0.500, 0.770.

6c. 20.0 mg (0.020 mmol) **5c**, 8.0 µL (0.10 mmol) thionyl chloride, 5.2 mg (0.026) ferrocenylamine. [silica, CH$_2$Cl$_2$, R_f = 0.49)]. Yield: 17.6 mg (0.015 mmol, 75%), purple powder. $C_{76}H_{58}FeN_6O_4$ (1175.16).

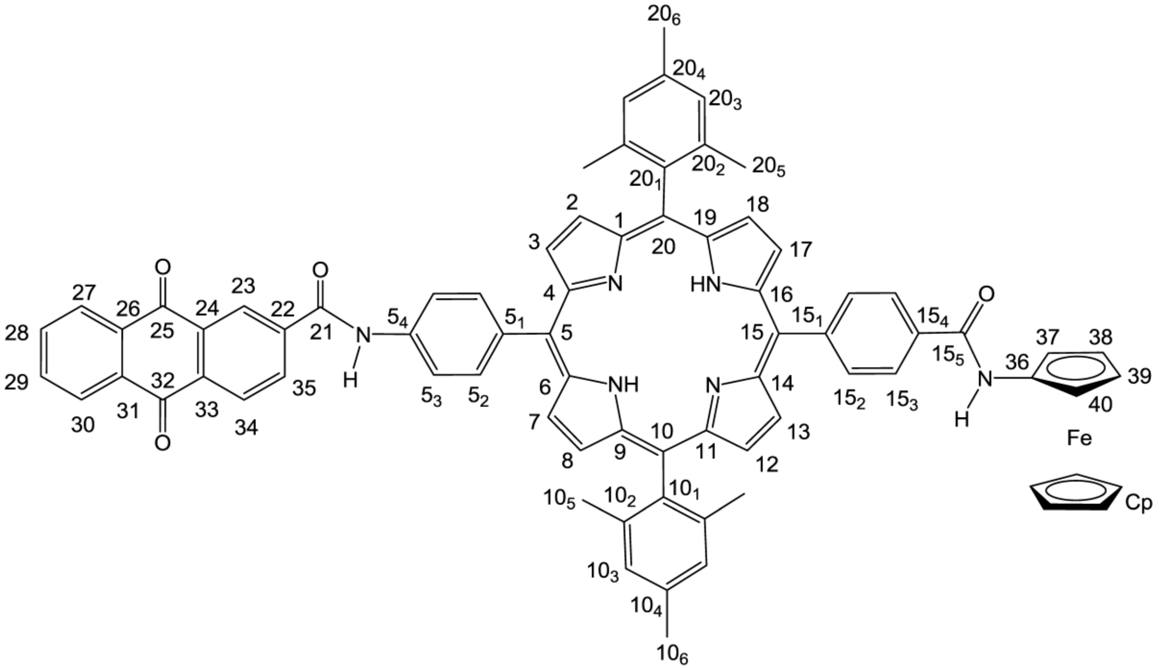

^{1}H-NMR (d$_8$-THF): δ = –2.47 (s, 2 H, $\mathrm{H}^{\text{pyrroleNH}}$), 1.86 (s, 12 H, $\mathrm{H}^{10/20}{}_{5/5}$), 2.62 (s, 6 H, $\mathrm{H}^{10/20}{}_{6/6}$), 4.05 (br. s, 2 H, $\mathrm{H}^{39/38}$), 4.24 (s, 5 H, H^{Cp}), 4.95 (br. s, 2 H, $\mathrm{H}^{37/40}$), 7.33 (s, 4 H, $\mathrm{H}^{10/20}{}_{3/3}$), 7.91 (m, 2 H, $\mathrm{H}^{28/29}$), 8.23 (d, $^3J_{\mathrm{HH}}$ = 8.4 Hz, 2 H, $\mathrm{H}^{5}{}_{2}$), 8.31 (m, 6 H, $\mathrm{H}^{5/15/15}{}_{3/2/3}$), 8.37 (m, 2H, $\mathrm{H}^{27/30}$), 8.49 (d, $^4J_{\mathrm{HH}}$ = 7.9 Hz, 1H, H^{34}), 8.58 (dd, $^3J_{\mathrm{HH}}$ = 8.6 Hz, $^4J_{\mathrm{HH}}$ = 1.3 Hz, 1 H, H^{35}), 8.69 (d, $^3J_{\mathrm{HH}}$ = 3.9 Hz, 4 H, $\mathrm{H}^{\text{pyrrole}}$), 8.81 (d, 2 H, $^3J_{\mathrm{HH}}$ = 4.5 Hz, $\mathrm{H}^{\text{pyrrole}}$), 8.89 (d, 2 H, $^3J_{\mathrm{HH}}$ = 4.8 Hz, $\mathrm{H}^{\text{pyrrole}}$), 9.00 (br.s, 1 H, H^{23}), 9.21 (br. s, 1 H, $\mathrm{H}^{\text{amideFcNH}}$), 10.32 (1 H, $\mathrm{H}^{\text{amidePorphNH}}$) ppm.

^{13}C{^{1}H}-NMR (d$_8$-THF): δ = 21.7 ($\mathrm{C}^{10/20}{}_{6/6}$), 21.9 ($\mathrm{C}^{10/20}{}_{5/5}$), 62.2 ($\mathrm{C}^{37/40}$), 65.1 ($\mathrm{C}^{38/39}$), 70.0 ($\mathrm{C}^{\mathrm{Cp}}$), 119.3 ($\mathrm{C}^{5}{}_{3}$), 119.3. ($\mathrm{C}^{15}$), n.o ($\mathrm{C}^{10/20}$), 120.7 ($\mathrm{C}^{5}$), 126.8 ($\mathrm{C}^{15}{}_{3}$),126.6 ($\mathrm{C}^{23}$), 128.0 ($\mathrm{C}^{27}$), 128.0 ($\mathrm{C}^{30}$), 128.3 ($\mathrm{C}^{34}$), 128.9 ($\mathrm{C}^{10/20}{}_{3/3}$), 130.9 (br. s, $\mathrm{C}^{\text{pyrrole 2/3/7/8/12/13/17/18}}$), 130.7 ($\mathrm{C}^{15}{}_{4}$), 134.4 ($\mathrm{C}^{35}$), 134.9 ($\mathrm{C}^{24}$), 135.2, 135.3 ($\mathrm{C}^{28/29}$), 135.6 ($\mathrm{C}^{15}{}_{2}$), 135.9 ($\mathrm{C}^{5}{}_{2}$), 136.5 ($\mathrm{C}^{33}$), 138.9 ($\mathrm{C}^{5}{}_{1}$), 139.6 ($\mathrm{C}^{10/20}{}_{1/1}$), 140.6 ($\mathrm{C}^{5}{}_{4}$), 141.8 ($\mathrm{C}^{22}$), 146.0 ($\mathrm{C}^{15}{}_{1}$), 165.2 ($\mathrm{C}^{21}$), 167.7 ($\mathrm{C}^{15}{}_{5}$), 183.0, 183.2 ($\mathrm{C}^{25/32}$) ppm.

IR (KBr): $\tilde{\nu}$ [cm^{-1}] = 3433 (NH$^{\text{amide}}$, NH$^{\text{pyrrole}}$, br, vs), 2918 (CH, w), 2856 (CH, w), 1676 (CO, vs), 1522 (m), 1384 (vs), 1290 (vs), 970 (m).

MS (FD): *m/z* (%) = 646.80 (100) [M]$^{2+}$, 1174.92 (49) [M]$^{+}$.

MS (ESI): *m/z* (%) = 588.15 (23) [M+H]$^{2+}$, 1175.36 (100) [M+H]$^{+}$.

HR-MS (ESI): obs. *m/z* = 1174.3833 [M]$^{+}$; calcd. for [M+H]$^{+}$ 1174.3869.

UV/Vis (CH_2Cl_2): λ [nm] (ε / [10^4 M^{-1}cm^{-1}]) = 421 (36.18), 516 (1.51), 552 (0.60), 592 (0.30), 648 (0.25).

Fluorescence (CH_2Cl_2): λ [nm] (relative intensity) = 652 (1.00), 718 (0.32).

Quantum yield: Φ = 0.0041.

Lifetime: τ [ps] = 272.83 (100%).

CV (Fc/Fc$^+$, 100 mV s^{-1}, CH_2Cl_2): $E_{½}$ [V] = −2.070, −1.710, −1.230, −0.070, 0.560, 0.990.

6d. 45.0 mg (0.048 mmol) **5d**, 18 µL (0.24 mmol) thionyl chloride, 12.6 mg (0.062 mmol) ferrocenylamine. [silica, CH_2Cl_2, R_f = 0.73]. Yield: 26.0 mg (0.023 mmol, 49%), purple powder. $C_{72}H_{50}FeN_6O_4$ (1119.05).

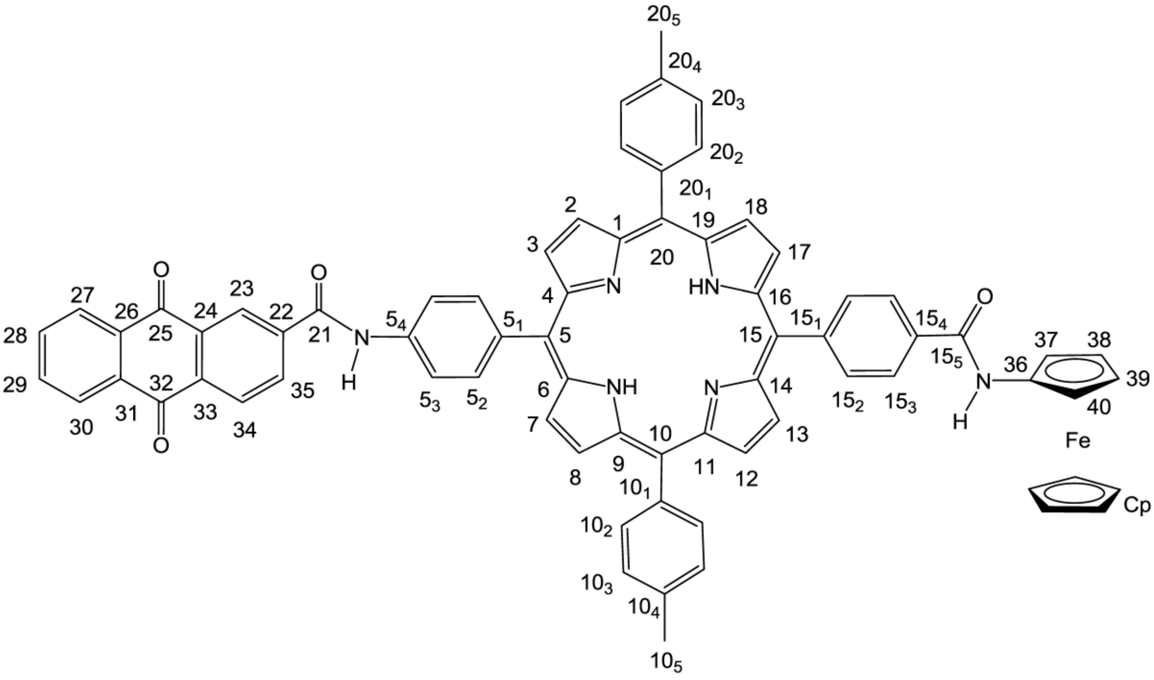

^{1}H-NMR (d_8-THF): δ = –2.67 (s, 2 H, H$^{\text{pyrroleNH}}$), 2.70 (s, 6 H, H$^{10/20}{}_{5/5}$), 4.06 (s, 2 H, H$^{39/38}$), 4.24 (s, 5 H, H^{41}) 4.96 (s, 2 H, H$^{37/40}$), 7.60 (d, $^3J_{\text{HH}}$ = 7.7 Hz, 4 H, H$^{10/20}{}_{3/3}$), 7.90 (m, 2 H, H$^{28/29}$), 8.11 (d, $^3J_{\text{HH}}$ = 7.8 Hz, 4 H, H$^{10/20}{}_{2/2}$), 8.23 (d, $^3J_{\text{HH}}$ = 8.4 Hz, 2 H, H$^{5}{}_{2}$), 8.34 (m, 8 H, H$^{5/15/15/27/30}{}_{3/3/3}$), 8.47 (d, $^3J_{\text{HH}}$ = 8.0 Hz, 1 H, H^{34}), 8.57 (dd, $^3J_{\text{HH}}$ = 7.9 Hz, $^4J_{\text{HH}}$ = 1.2 Hz, 1 H, H^{35}), 8.83 (d, $^3J_{\text{HH}}$ = 4.5 Hz, 2 H, H$^{\text{pyrrole}}$), 8.87 (d, $^3J_{\text{HH}}$ = 3.6 Hz, 4 H, H$^{\text{pyrrole}}$), 8.92 (d, $^3J_{\text{HH}}$ = 4.4 Hz, 2 H, H$^{\text{pyrrole}}$), 8.99 (d, $^4J_{\text{HH}}$ = 1.3 Hz, 1 H, H^{23}), 9.21 (s, 1H, H$^{\text{amideFcNH}}$), 10.32 (s, 1 H, H$^{\text{amidePorphNH}}$) ppm.

$^{13}C\{^1H\}$-NMR (d_8-THF): δ = 21.7 ($\mathrm{C}^{10/20}{}_{5/5}$), 62.2 ($\mathrm{C}^{37/40}$), 65.1 ($\mathrm{C}^{38/39}$), 70.0 ($\mathrm{C}^{Cp}$), 97.8 ($\mathrm{C}^{36}$), 119.4 ($\mathrm{C}^{5}{}_{3}$), 121.4 ($\mathrm{C}^{10/20}$), 126.7 ($\mathrm{C}^{23}$), 126.7 ($^{15}{}_{3}$), 128.0 ($\mathrm{C}^{27}$), 128.0 ($\mathrm{C}^{30}$), 128.3 ($\mathrm{C}^{34}$), 128.5 ($\mathrm{C}^{10/20}{}_{3/3}$), 132.0 (br. s, $\mathrm{C}^{\text{pyrrole } 2/3/7/8/12/13/17/18}$), 134.3 ($\mathrm{C}^{35}$), 134.8 ($\mathrm{C}^{24}$), 135.2, 135.2 ($\mathrm{C}^{28/29}$), 135.4 ($\mathrm{C}^{5}{}_{2}$), 135.5 ($\mathrm{C}^{10/20}{}_{2/2}$), 135.9 ($\mathrm{C}^{15}{}_{2}$), 136.5 ($\mathrm{C}^{33}$), 138.5 ($\mathrm{C}^{10/20}{}_{4/4}$), 138.8 ($\mathrm{C}^{5}{}_{1}$), 146.2 ($\mathrm{C}^{15}{}_{1}$), 140.5 ($\mathrm{C}^{10/20}{}_{1/1}$), 141.8 ($\mathrm{C}^{22}$), 165.2, 165.8 ($\mathrm{C}^{15/21}{}_{5}$), 183.0, 183.2 ($\mathrm{C}^{25/32}$) ppm.

IR (KBr): $\tilde{\nu}$ [cm^{-1}] = 3443 ($\mathrm{NH}^{\text{amide}}$, br, vs), 3319 ($\mathrm{NH}^{\text{pyrrole}}$, m), 2924 (CH, w), 1674 (CO, vs), 1595 (m), 1520 (m), 1385 (m), 1321 (w), 1288 (vs), 800 (s).

MS (FD): *m/z* (%) = 1119.06 (100) $[\mathrm{M}]^+$.

MS (ESI): *m/z* (%) = 559.71 (100) $[\mathrm{M+H}]^{2+}$, 1119.44 (95) $[\mathrm{M+H}]^+$.

HR-MS (ESI): obs. *m/z* = 1118.3243 $[\mathrm{M+H}]^+$; calcd. for $[\mathrm{M+H}]^+$ 1118.3254.

UV/Vis (CH_2Cl_2): λ [nm] (ε / [10^4 $\mathrm{M^{-1}cm^{-1}}$]) = 420 (44.69), 517 (1.72), 553 (1.57), 591 (1.12), 647 (0.61).

Fluorescence (CH_2Cl_2): λ [nm] (relative intensity) = 655 (1.00), 720 (0.28).

Quantum yield: Φ = 0.0036.

Lifetime: τ [ps] = 229.37 (100%).

CV (Fc/Fc$^+$, 100 mV s^{-1}, CH_2Cl_2): $E_{½}$ [V] = −1.965, −1.605, −1.190, −0.075, 0.550, 0.855.

6e. 60.0 mg (0.066 mmol) **5e**, 25 µL (0.33 mmol) thionyl chloride, 17.3 mg (0.086) ferrocenylamine. [silica, CH_2Cl_2, R_f = 0.78]. Yield: 47.4 mg (0.043 mmol, 65%), purple powder. $C_{70}H_{46}FeN_6O_4$ (1091.00).

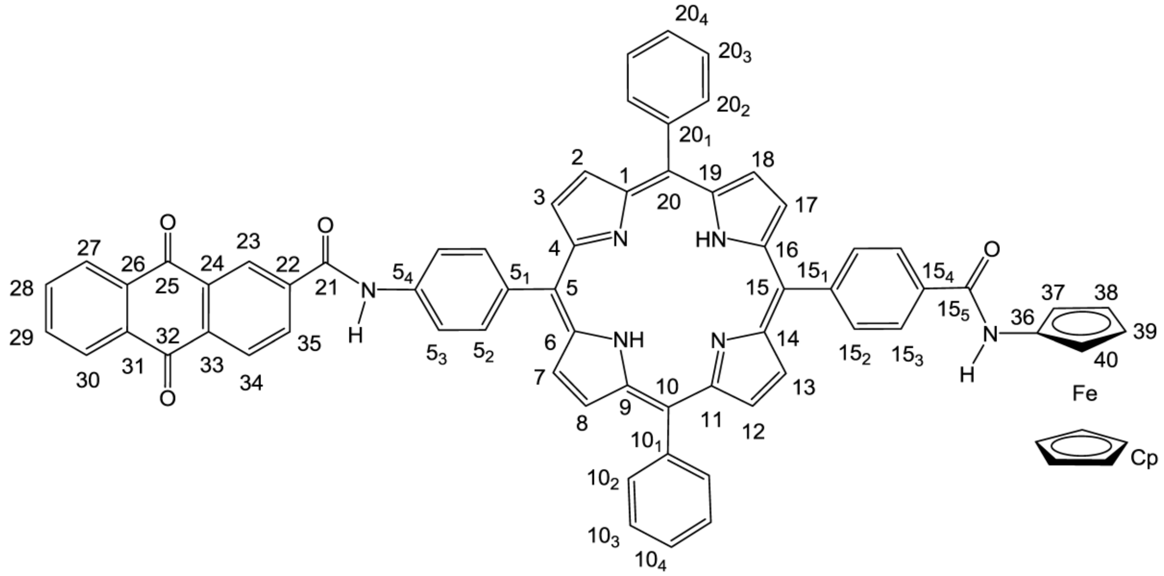

^1H-NMR (d_8-THF): δ = –2.76 (s, 2 H, $\mathrm{H}^{\text{pyrroleNH}}$), 4.05 (s, 2 H, $\mathrm{H}^{39/38}$), 4.24 (s, 5 H, H^{Cp}) 4.95 (s, 2 H, $\mathrm{H}^{37/40}$), 7.79 (m, 6 H, $\mathrm{H}^{10/20}{}_{3/4}$), 7.91 (m, 2 H, $\mathrm{H}^{28/29}$), 8.23 (m, 6 H, $\mathrm{H}^{5/10/20}{}_{2/2/2}$), 8.33 (m, 6 H, $\mathrm{H}^{5/15/15}{}_{3/2/3}$), 8.37 (m, 2 H, $\mathrm{H}^{27/30}$), 8.48 (d, $^3J_{HH}$ = 8.0 Hz, 1 H, H^{34}), 8.58 (dd, $^3J_{HH}$ = 7.9 Hz, $^4J_{HH}$ =

1.7 Hz, 1 H, H^{35}), 8.85 (m, 6 H, H$^{\text{pyrrole}}$), 8.94 (d, $^{3}J_{\text{HH}}$ = 4.5 Hz, 2 H, H$^{\text{pyrrole}}$), 8.99 (d, $^{4}J_{\text{HH}}$ = 1.5 Hz, 1 H, H^{23}), 9.18 (s, 1 H, H$^{\text{amideFcNH}}$), 10.31 (s, 1 H, H$^{\text{amidePorphNH}}$) ppm.

^{13}C{^{1}H}-NMR (d$_{8}$-THF): δ = 62.2 (C$^{37/40}$), 65.1 (C$^{38/39}$), 70.0 (C$^{\text{Cp}}$), 119.4 ($\mathrm{C}^{5}{}_{3}$), 126.7 ($\mathrm{C}^{15}{}_{3}$), 128.0, 128.0 (C$^{27/30}$), 121.3 (C$^{10/20}$), 126.7 (C^{23}), 127.8 ($\mathrm{C}^{10/20}{}_{3/3}$), 128.3 (C^{34}), 128.9 ($\mathrm{C}^{10/20}{}_{4/4}$) 132.1 (br. s, C$^{\text{pyrrole 2/3/7/8/12/13/17/18}}$), 134.3 (C^{35}), 134.9 (C^{24}), 135.2, 135.3 (C$^{28/29}$), 135.4, 135.9 ($\mathrm{C}^{5/15}{}_{2/2}$), 135.5 ($\mathrm{C}^{10/20}{}_{2/2}$), 136.5 (C^{33}), 138.8 ($\mathrm{C}^{5}{}_{1}$), 140.5 ($\mathrm{C}^{5}{}_{4}$), 141.7 (C^{22}), 143.4 ($\mathrm{C}^{10/20}{}_{1/1}$), 165.2, 165.8 ($\mathrm{C}^{15/21}{}_{5}$), 182.9, 183.2 (C$^{25/32}$) ppm.

IR (KBr): $\tilde{\nu}$ [cm^{-1}] = 3444 (NH$^{\text{amide}}$, NH$^{\text{pyrrole}}$, br, vs), 2926 (CH, w), 2854 (CH, w), 1728 (CO, w), 1674 (CO, vs), 1522 (vs), 1593 (m), 1290 (vs), 1161 (CF, w), 800 (s).

MS (FD): *m/z* (%) = 1090.6 (100) [M]$^{+}$.

MS (ESI): *m/z* (%) = 545.64 (100) [M^{2+}+H], 1091.31 (62) [M+H]$^{+}$.

HR-MS (ESI): obs. *m/z* = 1091.3037 [M+H]$^{+}$; calcd. for [M+H]$^{+}$ 1091.3008.

UV/Vis (CH$_2$Cl$_2$): λ [nm] (ε / [10^{4} M^{-1}cm^{-1}]) = 419 (35.06), 516 (1.56), 551 (0.84), 591 (0.49), 646 (0.42).

Fluorescence (CH$_2$Cl$_2$): λ [nm] (relative intensity) = 651 (1.00), 717 (0.30).

Quantum yield: Φ = 0.0030.

Lifetime: τ [ps] = 644.23 (14%), 164.02 (86%).

CV (Fc/Fc^{+}, 100 mV s^{-1}, CH$_2$Cl$_2$): $E_{½}$ [V] = −2.060, −1.670, −1.260, −0.090, 0.560, 0.925.

6f. 60.0 mg (0.064 mmol) **5f**, 24 µL (0.32 mmol) thionyl chloride, 16.7 mg (0.083 mmol) ferrocenylamine. [silica, CH$_2$Cl$_2$, R_{f} = 0.71]. Yield: 33.0 mg (0.029 mmol, 46%), purple powder. $\mathrm{C_{70}H_{44}F_2FeN_6O_4}$ (1126.98).

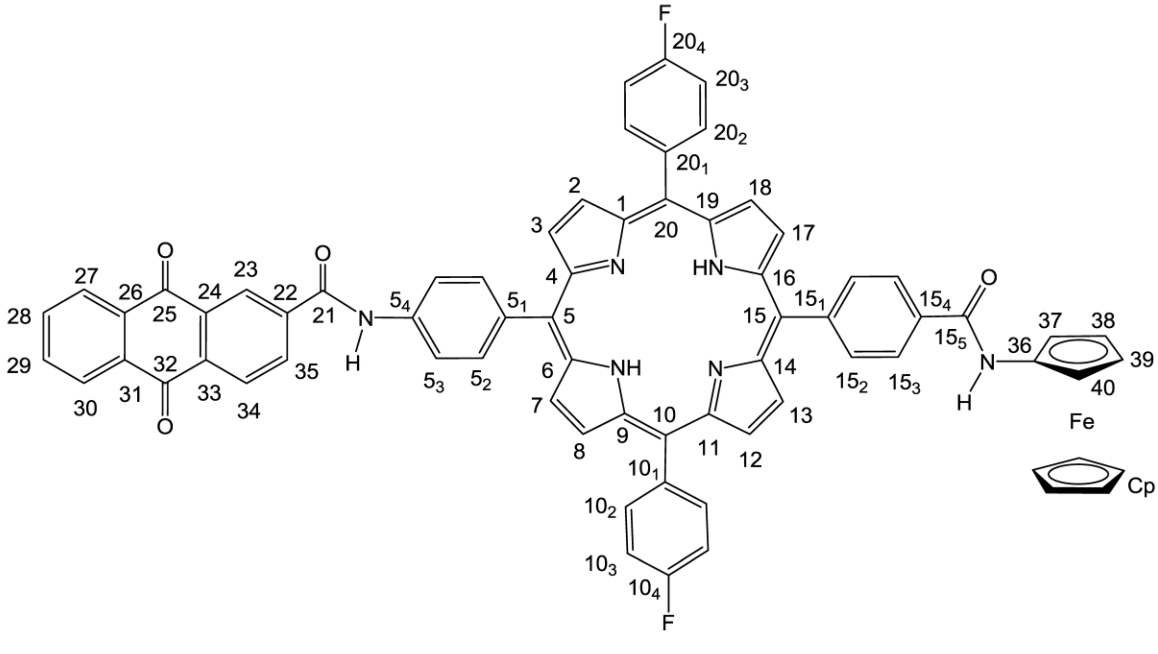

^{1}H-NMR (d_8-THF): δ = –2.70 (s, 2 H, H$^{\text{pyrroleNH}}$), 4.06 (br. s, 2 H, H$^{39/38}$), 4.24 (s, 5 H, H$^{\text{Cp}}$), 4.96 (br. s, 2 H, H$^{37/40}$), 7.55 (ps. t, $^{3}J_{\text{HH}}$ = 8.7 Hz, 4 H, H$^{10/20}_{3/3}$), 7.89 (m, 2 H, H$^{28/29}$), 8.22 (m, 6 H, H$^{5/10/20}_{2/2/2}$), 8.33 (m, 8 H, H$^{27/30/5/15/15}_{3/2/3}$), 8.46 (d, $^{3}J_{\text{HH}}$ = 8.0 Hz, H^{34}), 8.56 (dd, 1 H, $^{4}J_{\text{HH}}$ = 1.7 Hz, $^{3}J_{\text{HH}}$ = 7.9 Hz, H^{35}), 8.86 (m, 6 H, H$^{\text{pyrrole}}$), 8.96 (d, 2 H, $^{3}J_{\text{HH}}$ = 4.6 Hz, H$^{\text{pyrrole}}$), 8.98 (d, 1 H, $^{4}J_{\text{HH}}$ = 1.6 Hz, H^{23}), 9.25 (br. s, 1 H, H$^{\text{amideFcNH}}$), 10.36 (br. s, 1 H, H$^{\text{amidePorphNH}}$) ppm.

^{13}C{^{1}H}-NMR (d_8-THF): δ = 62.2 (C$^{37/40}$), 65.1 (C$^{38/39}$), 70.0 (C$^{\text{Cp}}$), 114.7 (d, $^{2}J_{\text{CF}}$ = 21.6 Hz, C$^{10/20}_{3/3}$), 119.4 (C$^{5}_{3}$), 120.1, 120.3, 121.5 (C$^{5/15/10/20}$), 126.7 (C$^{15}_{3}$), 126.8 (C^{23}), 127.9, 128.0 (C$^{27/30}$), 128.3 (C^{34}), 131.9 (br. s, C$^{\text{pyrrole 2/3/7/8/12/13/17/18}}$), 134.3 (C^{35}), 135.2, 135.2 (C$^{28/29}$), 135.9 (C$^{5}_{2}$), 136.9 (d, $^{2}J_{\text{CF}}$ = 7.9 Hz, C$^{10/20}_{2/2}$), 135.4 (C$^{15}_{2}$), 136.2 (C^{24}), 136.5 (C^{33}), 138.7 (C$^{5}_{1}$), 139.5 (d, $^{4}J_{\text{CF}}$ = 3.2 Hz, C$^{10/20}_{1/1}$), 140.6 (C$^{5}_{4}$), 141.7 (C^{22}), 145.9 (C$^{15}_{1}$) 162.8 (d, $^{1}J_{\text{FH}}$ = 249.2 Hz, C$^{10/20}_{4/4}$), 165.3, 165.8 (C$^{15/21}_{5}$), 182.9, 183.1 (C$^{25/32}$) ppm.

^{19}F-NMR (d_8-THF): δ = −114.2 (tt, $^{3}\text{J}_{\text{FH}}$=8.6 Hz, $^{4}J_{\text{FH}}$=5.4 Hz, F-C$^{10/20}_{4/4}$) ppm.

IR (KBr): $\tilde{\nu}$ [cm^{-1}] = 3433 (NH$^{\text{amide}}$, NH$^{\text{pyrrole}}$, br, vs), 1676 (CO, vs), 1659 (CO, vs), 1596 (m), 1508 (vs), 1290 (s), 1158 (CF, m), 966 (m), 800 (s).

MS (FD): *m/z* (%) = 1126.99 (100) [M]$^{+}$.

MS (ESI): *m/z* (%) = 563.64 (100) [M^{2+}+H], 1127.29 (77) [M+H]$^{+}$.

HR-MS (ESI): obs. *m/z* = 1126.2767 [M]$^{+}$; calcd. for [M+H]$^{+}$ 1126.2742.

UV/Vis (CH_2Cl_2): λ [nm] (ε / [10^{4} M^{-1}cm^{-1}]) = 419 (41.79), 515 (2.22), 551 (1.38), 589 (1.00), 646 (0.86).

Fluorescence (CH_2Cl_2): λ [nm] (relative intensity) = 652 (1.00), 718 (0.32).

Quantum yield: Φ = 0.0025.

Lifetime: τ [ps] = 586.62 (6%), 148.07 (94%).

CV (Fc/Fc^{+}, 100 mV s^{-1}, CH_2Cl_2): $E_{½}$ [V] = −2.015, −1.625, −1.235, −0.085, 0.585, 0.945 (irr.).

6g. 40 mg (0.038 mmol) **5g**, 15 µL (0.19 mmol) thionyl chloride, 10.0 mg (0.049) ferrocenylamine. [silica, CH_2Cl_2, R_f = 0.70]. Yield: 29.2 mg (0.024 mmol, 63%), purple powder. $C_{72}H_{44}F_6FeN_6O_4$ (1226.99).

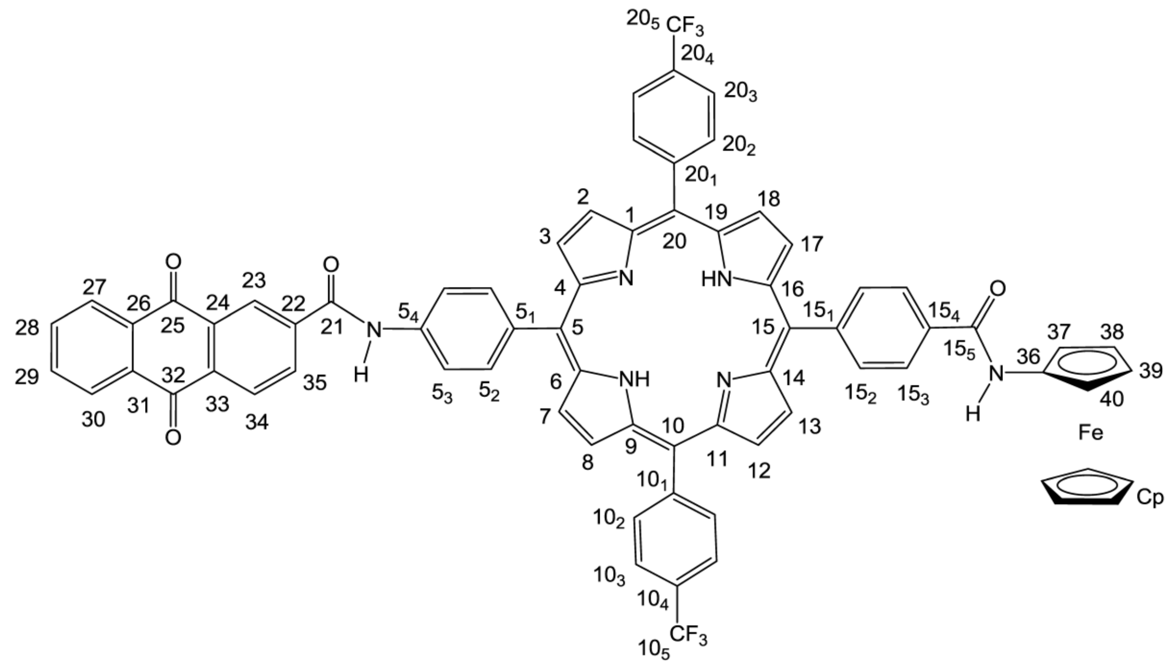

^{1}H-NMR (d$_8$-THF): δ = –2.68 (s, 2 H, $H^{pyrroleNH}$), 4.06 (br. s, 2 H, $H^{39/38}$), 4.24 (s, 5 H, H^{Cp}), 4.95 (br. s, 2 H, $H^{37/40}$), 7.91 (m, 2 H, $H^{28/29}$), 8.14 (d, $^3J_{HH}$ = 8.1 Hz, 4 H, $H^{10/20}{}_{2/2}$), 8.23 (d, $^3J_{HH}$ = 8.4 Hz, 2 H, $H^{5}{}_{2}$), 8.35 (m, 8 H, $H^{27,30,\ 5/15/15}{}_{3/2/3}$), 8.44 (d, $^3J_{HH}$ = 8.0 Hz, 4 H, $H^{10/20}{}_{3/3}$), 8.48 (d, $^3J_{HH}$ = 8.0 Hz, 1 H, H^{34}), 8.52 (dd, 1 H, $^4J_{HH}$ = 1.7 Hz, $^3J_{HH}$ = 8.1 Hz, H^{35}), 8.84 (d, 4 H, $^3J_{HH}$ = 4.6 Hz, $H^{pyrrole}$), 8.89 (d, 2 H, $^3J_{HH}$ = 4.51 Hz, $H^{pyrrole}$), 8.98 (d, 1 H, $^4J_{HH}$ = 1.8 Hz, H^{23}), 8.98 (m, 2 H $H^{pyrrole}$), 9.19 (br. s, 1 H, $H^{amideFcNH}$), 10.32 (s, 1H, $H^{amidePorphNH}$) ppm.

^{13}C{^{1}H}-NMR (d$_8$-THF): δ = 62.2 ($C^{37/40}$), 65.1 ($C^{38/39}$), 70.0 (C^{Cp}), 119.4 (C^{15}), 119.4 ($C^{5}{}_{3}$), 119.7 ($C^{10/20}$), 121.8 (C^{5}), 126.6 (C^{23}), 124.8 (d, $^4J_{CF}$ = 3.4 Hz, $C^{10/20}{}_{3/3}$), 126.8 ($^{15}{}_{3}$), 127.3 ($C^{10/20}{}_{4/4}$), 127.9, 128.0 ($C^{27/30}$), 128.3 (C^{34}), 131.1 (m, $C^{10/20}{}_{5/5}$), 132.0 (br. s, $C^{pyrrole\ 2/3/7/8/12/13/17/18}$), 134.3 ($C^{35}$), 134.8 ($C^{24}$), 135.2, 135.2 ($C^{28/29}$), 135.4 ($C^{15}{}_{2}$), 135.9 ($C^{5}{}_{2}$), 135.9 ($C^{10/20}{}_{2/2}$), 136.5 ($C^{33}$), 140.7 ($C^{10/20}{}_{1/1}$), 138.5 ($C^{5}{}_{1}$), 140.7 ($C^{5}{}_{4}$), 141.7 ($C^{22}$), 145.8 ($C^{15}{}_{1}$), 147.3 ($C^{10/20}{}_{1/1}$), 165.3 ($C^{21}$), 165.5 ($C^{5}{}_{5}$), 182.9, 183.1 ($C^{25/32}$) ppm.

^{19}F-NMR (d$_8$-THF): δ = −64.6 (s, F-$C^{10/20}{}_{5/5}$) ppm.

IR (KBr): $\tilde{\nu}$ [cm^{-1}] = 3440 (NH^{amide}, br, m), 3317 ($NH^{pyrrole}$, w), 2928 (CH, w), 2849 (CH, w), 1676 (CO, m), 1614 (m), 1517 (m), 1394 (w), 1324 (vs) 1297 (s), 1120 (CF, s), 794(m).

MS (FD): *m/z* (%) = 1226.7 (100) [M]$^+$.

MS (ESI): *m/z* (%) = 613.62 (100) [M^{2+}+H], 1227.27 (62) [M+H]$^+$.

HR-MS (ESI): obs. *m/z* = 1227.2649 [M+H]$^+$; calcd. for [M+H]$^+$ 1227.2756.

UV/Vis (CH$_2$Cl$_2$): λ [nm] (ε / [10^4 M^{-1}cm^{-1}]) = 419 (32.42), 515 (1.54), 551 (0.78), 590 (0.53), 646 (0.41).

Fluorescence (CH$_2$Cl$_2$): λ [nm] (relative intensity) = 652 (1.00), 717 (0.34).

Quantum yield: Φ = 0.0063.

Lifetime: τ [ps] = 467.65 (14%), 94.96 (86%).

CV (Fc/Fc$^+$, 100 mV s^{-1}, CH$_2$Cl$_2$): $E_{1/2}$ [V] = −1.930, −1.570, −1.230, −0.080, 0.640, 0.990 (irr.).

6h. 60.0 mg (0.055 mmol) **5h**, 21.0 µL (0.28 mmol) thionyl chloride, 14.4 mg (0.072) ferrocenylamine. [silica, CH$_2$Cl$_2$, R_f = 0.32]. Yield: 33.2 mg (0.026 mmol, 47%), purple powder. $C_{70}H_{36}F_{10}FeN_6O_4$ (1270.90).

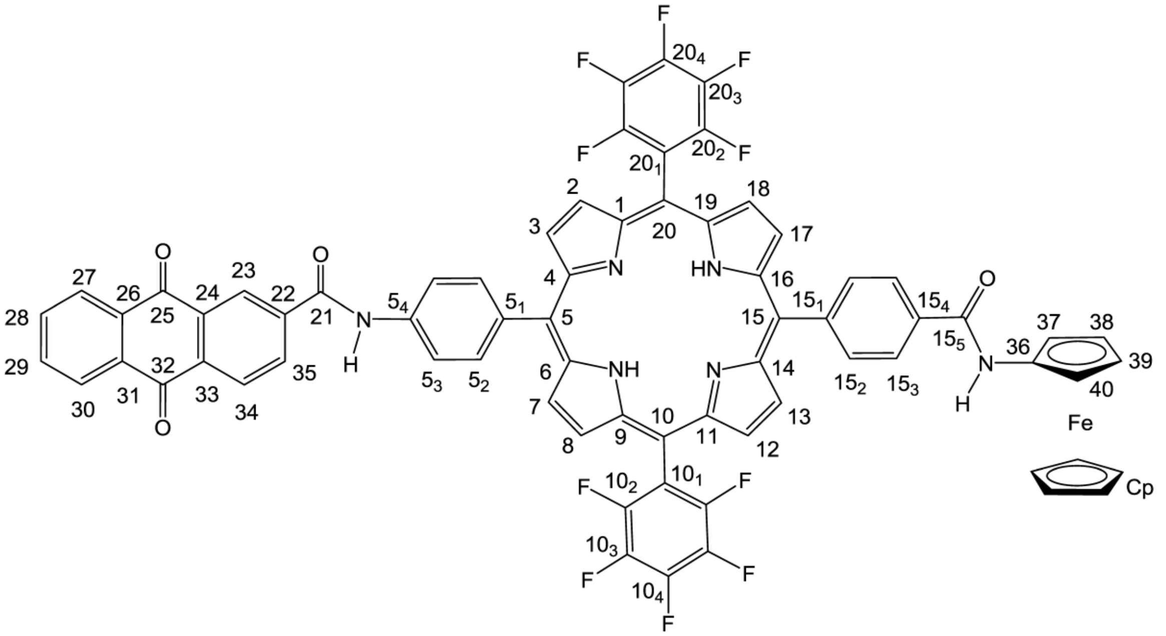

^{1}H-NMR (d$_8$-THF): δ = –2.74 (s, 2 H, H$^{\text{pyrroleNH}}$), 4.06 (s, 2 H, H$^{39/38}$), 4.25 (s, 5 H, H$^{\text{Cp}}$), 4.96 (s, 2 H, H$^{37/40}$), 7.92 (m, 2 H, H$^{28/29}$), 8.27 (d, $^3J_{\text{HH}}$ = 8.2 Hz, 2 H, H$^5{}_2$), 8.36 (m, 8 H, H$^{5/15/15/27/30}{}_{3/2/3}$), 8.49 (d, $^4J_{\text{HH}}$ = 7.9 Hz, 1H, H^{34}), 8.59 (dd, $^3J_{\text{HH}}$ = 7.9 Hz, $^4J_{\text{HH}}$ = 1.1 Hz ,1 H, H^{35}), 8.97 (d, 2 H, $^3J_{\text{HH}}$ = 4.2 Hz, H$^{\text{pyrrole}}$), 9.01 (br. s, 1 H, H^{23}), 9.05 (m, 6 H, H$^{\text{pyrrole}}$), 9.29 (s, 1 H, H$^{\text{amideFcNH}}$), 10.42 (s, 1 H, H$^{\text{amidePorphNH}}$) ppm.

^{13}C{^{1}H}-NMR (d$_8$-THF): δ = 62.2 (C$^{37/40}$), 65.1 (C$^{39/38}$), 70.0 (C$^{\text{Cp}}$), 97.7 (C^{36}), 119.5 (C$^5{}_3$), 121.4 (C^{15}), 122.6 (C^5), n.o. (C$^{10/20}$), 128.0 (C^{27}), 128.0 (C^{30}), 128.3 (C^{34}), 126.8 (C^{23}), 127.0 (C$^{15}{}_3$), 131.1 (br. s, C$^{\text{pyrrole 2/3/7/8/12/13/17/18}}$), 134.3 (C^{35}), 134.9 (C^{22}), 135.2, 135.3 (C$^{28/29}$), 135.5 (C$^{15}{}_2$), 136.0 (s, C$^5{}_2$), 136.4 (C$^{15}{}_4$), 136.5 (C^{33}), 137.9 (C$^5{}_1$), 140.9 (C$^5{}_4$), 141.7 (C^{24}), 145.2 (C$^{15}{}_1$), 140.2, 144.6, 146.6, 149.1 (m, C$^{10/20}{}_{1/1/2/2/23/3/4/4}$), 165.4 (C^{21}), 165.7 (C$^{15}{}_5$), 183.0, 183.2 (C$^{25/32}$) ppm.

^{19}F-NMR (d$_8$-THF): δ = −166.6 (ddd, $^3J_{\text{FF}}$ = 23 Hz, $^3J_{\text{FF}}$ = 21 Hz, $^5J_{\text{FF}}$ = 8 Hz, 4 F, F$^{10/20}{}_{3/3}$), −157.7 (t, $^3J_{\text{FF}}$ = 20 Hz, 2 F, F$^{10/20}{}_{4/4}$), −141.3 (dd, $^3J_{\text{FF}}$ = 24 Hz, $^5J_{\text{FF}}$ = 7 Hz, 4 F, F$^{10/20}{}_{2/2}$) ppm.

IR (KBr): $\tilde{\nu}$ [cm^{-1}] = 3433 (NH$^{\text{pyrrole}}$, NH$^{\text{pyrrole}}$, br, s), 2930 (CH, w), 1676 (CO, vs), 1506 (vs), 1483 (vs), 1290 (vs), 1082 (CF, w), 1061 (CF, w), 989 (s).

MS (FD): m/z (%) = 1269.55 (100) [M]$^+$, 1270.56 (32) [M]$^+$, 12771.62 (15) [2M]$^+$.

MS (ESI): m/z (%) = 636.10 (54) [M+H]$^{2+}$, 1270.21 (73) [M]$^+$, 1271.22 (100) [M+H]$^+$.

HR-MS (ESI): obs. m/z = 1270.2029 [M]$^+$; calcd. for [M]$^+$ 1270.1988.

UV/Vis (CH_2Cl_2): λ [nm] (ε / [10^4 $M^{-1}cm^{-1}$]) = 417 (41.02), 511 (2.20), 545 (0.42), 588 (0.49), 642 (0.48).

Fluorescence (CH_2Cl_2): λ [nm] (relative intensity) = 648 (1.00), 712(0.58).

Quantum yield: Φ = 0.0029.

Lifetime: τ [ps] = 274.57 (4%); 26.39 (96%).

CV (Fc/Fc$^+$, 100 mV s^{-1}, CH_2Cl_2): $E_{½}$ [V] = −1.900, −1.430, −1.270, −0.010, 0.800, 1.040.

6i. 40 mg (0.035 mmol) **5i**, 13.0 µL (0.18 mmol) thionyl chloride, 9.1 mg (0.046) ferrocenyl amine. [silica, CH_2Cl_2 : ethylacetate = 40:1, R_f = 0.43]. Yield: 38.7 mg (0.030 mmol, 85%), purple powder. $C_{72}H_{42}F_8FeN_6O_6$ (1294.97).

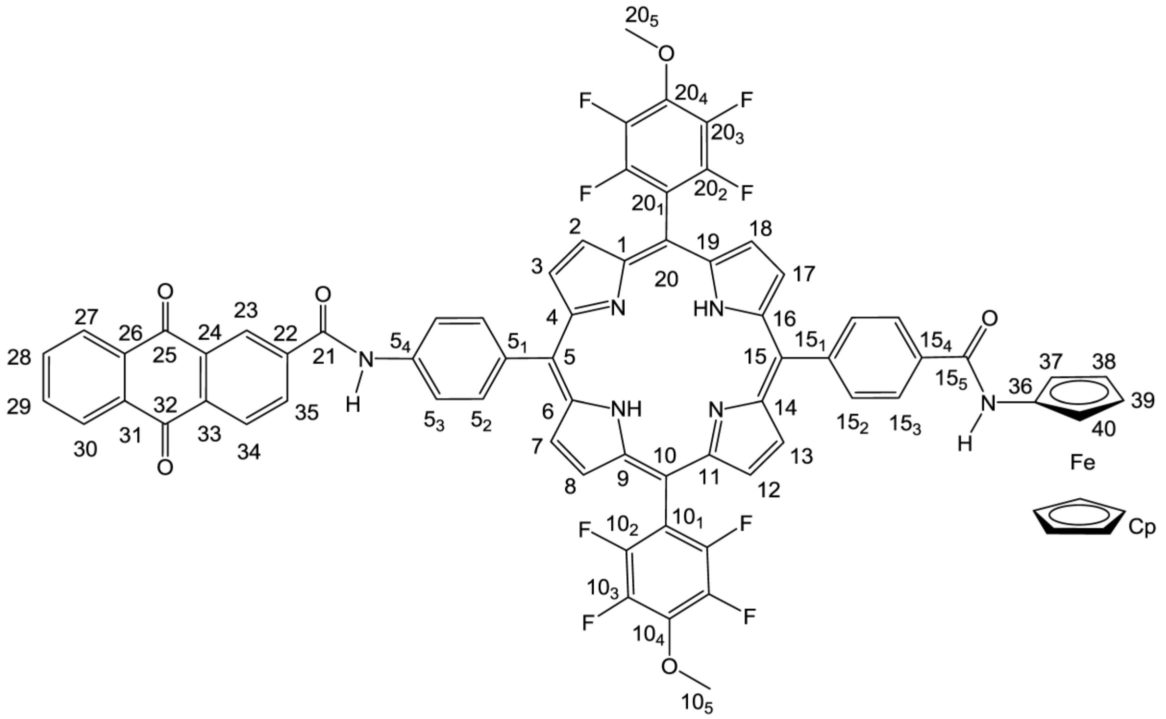

^{1}H-NMR (d_8-THF): δ = –2.73 (s, 2 H, $H^{pyrroleNH}$), 4.06 (ps. t, 2 H, $H^{39/38}$), 4.25 (s, 5 H, H^{Cp}), 4.40 (s, 6 H, $H^{10/20}{}_{5/5}$) 4.96 (s, 2 H, $H^{37/40}$), 7.92 (m, 2 H, $H^{28/29}$), 8.27 (d, $^3J_{HH}$ = 8.4 Hz, 2 H, $H^5{}_2$), 8.37 (m, 8 H, $H^{5/15/15/27/30}{}_{3/2/3}$), 8.50 (d, $^4J_{HH}$ = 8.0 Hz, 1H, H^{34}), 8.59 (dd, $^3J_{HH}$ = 8.1 Hz, $^4J_{HH}$ = 1.8 Hz ,1 H, H^{35}), 8.95 (d, 2 H, $^3J_{HH}$ = 4.7 Hz, $H^{pyrrole}$), 9.03 (m, 7 H, $H^{pyrrole/23}$), 9.29 (s, 1 H, $H^{amideFcNH}$), 10.40 (s, 1 H, $H^{amidePorphNH}$) ppm.

^{13}C{^{1}H}-NMR (d_8-THF): δ = 62.2 ($C^{37/40}$), 63.1 ($C^{10/20}{}_{5/5}$), 65.1 ($C^{39/38}$), 70.0 (C^{Cp}), 97.7 (C^{36}), 119.5 ($C^5{}_3$), n.o. ($C^{10/20}$), 121.2 (s, C^{15}), 122.3 (C^5), 126.8 (C^{23}), 126.9 ($C^{15}{}_3$), 128.0 (C^{27}), 128.0 (C^{30}), 128.3 (C^{34}), 131.2 (br. s, $C^{pyrrole\ 2/3/7/8/12/13/17/18}$), 134.4 ($C^{35}$), 134.9 ($C^{24}$), 135.2, 135.3 ($C^{28/29}$), 135.5 ($C^{15}{}_2$), 136.0 ($C^5{}_2$), 136.3 ($C^{15}{}_4$), 136.5 ($C^{33}$), 138.1 ($C^5{}_1$), 140.8 ($C^5{}_4$), 141.7 ($C^{22}$), 145.4 ($C^{15}{}_1$), 143.4, 146.8, 149.3 (m, $C^{10/20}{}_{2/3/4}$) 165.3 (C^{21}), 165.7 ($C^{15}{}_5$), 183.0, 183.2 ($C^{25/32}$) ppm.

^{19}F-NMR (d_8-THF): $\delta = -161.9$ (dd, $^3J_{FF} = 23$ Hz, $^5J_{FF} = 8$ Hz, 4 F, $F^{10/20}{}_{3/3}$), -143.2 (dd, $^3J_{FF} = 22$ Hz, $^5J_{FF} = 8$ Hz, 4 F, $F^{10/20}{}_{2/2}$) ppm.

IR (KBr): $\tilde{\nu}$ [cm^{-1}] = 3433 (NH^{amide}, NH^{pyrrole}, br, s), 2930 (CH, w), 1676 (CO, vs), 1506 (vs), 1483 (vs), 1290 (vs), 1082 (CF, w), 1061 (CF, w), 989 (s).

MS (FD): *m/z* (%) = 646.80 (65) [M]$^{2+}$, 1294.67 (100) [2M]$^{+}$.

MS (ESI): *m/z* (%) = 647.63 (40) [M+H]$^{2+}$, 1295.26 (100) [M+H]$^{+}$.

HR-MS (ESI): obs. *m/z* = 1295.2449 [M+H]$^{+}$; calcd. for [M+H]$^{+}$ 1295.2466.

UV/Vis (CH_2Cl_2): λ [nm] (ε / [10^4 M^{-1}cm^{-1}]) = 419 (37.03), 512 (1.87), 546 (0.45), 589 (0.48), 644 (0.11).

Fluorescence (CH_2Cl_2): λ [nm] (relative intensity) = 650 (1.00), 714 (0.44).

Quantum yield: $\Phi = 0.0006$.

Lifetime: τ [ps] = 398.03 (7%); 39.30 (93%).

CV (Fc/Fc$^+$, 100 mV s^{-1}, CH_2Cl_2): $E_{½}$ [V] = −1.890, −1.420, −1.240, −0.050, 0.770, 1.075.

General procedure for the preparation of Zn-6a − Zn-6i.

Triad **6a − 6i** (1 eq.) and zinc(II) acetate dihydrate (5 eq.) were stirred overnight in CH_2Cl_2 (5 mL). After concentration under reduced pressure the product was isolated by column chromatography

Zn-6a. 7.0 mg (0.0057 mmol) **6a**, 11.1 mg (0.028 mmol) zinc(II) acetate dihydrate. [silica, CH_2Cl_2 : ethylacetate = 40:1, R_f = 0.59]. Yield: 6.7 mg (0.0052 mmol, 91%), purple powder. $C_{78}H_{60}FeN_6O_6Zn$ (1298.57).

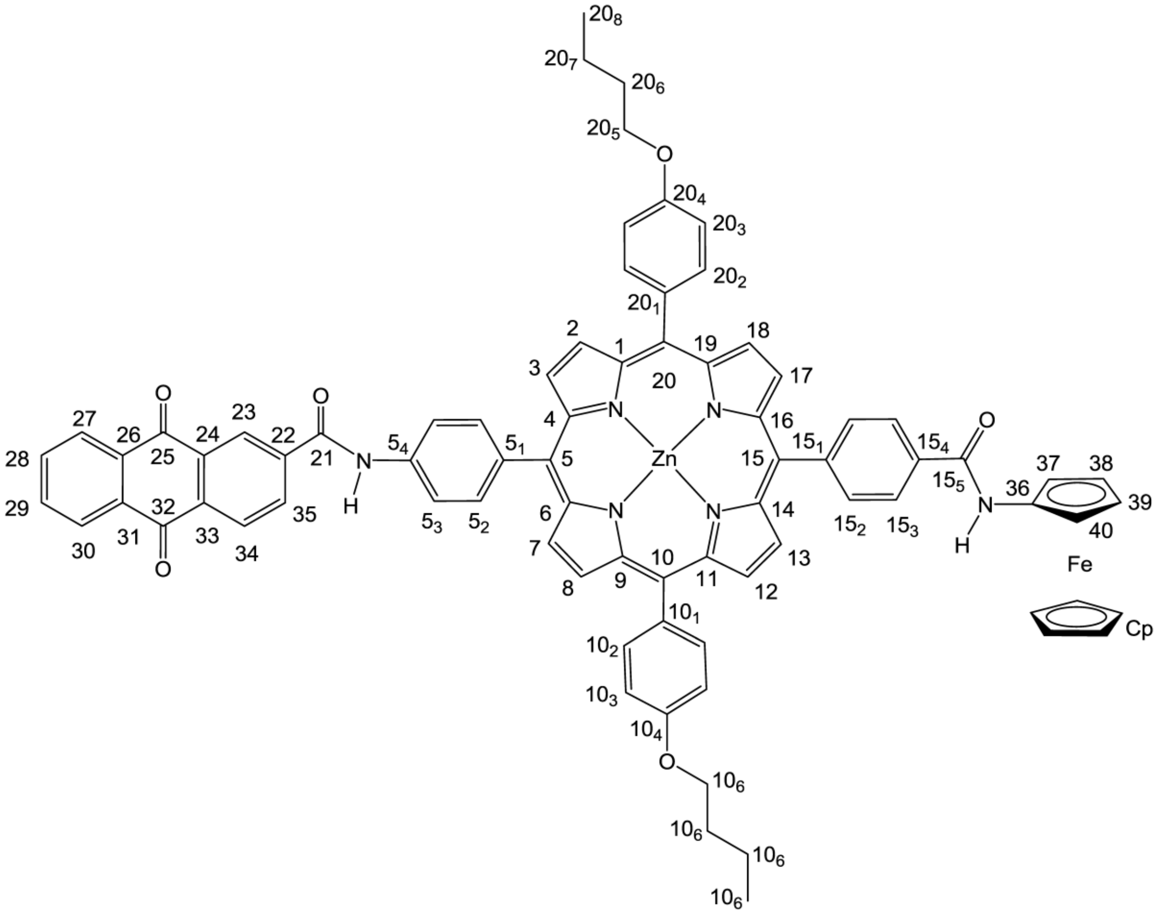

^{1}H-NMR (d$_8$-THF): δ = 1.10 (t, $^{3}J_{\text{HH}}$ = 7.4 Hz, 6 H, $\text{H}^{10/20}{}_{8/8}$), 1.68 (m, 4 H, $\text{H}^{10/20}{}_{7/7}$), 1.96 (m, 4 H, $\text{H}^{10/20}{}_{6/6}$), 4.05 (s, 2 H, $\text{H}^{38/39}$), 4.25 (s, 5 H, H^{41}), 4.28 (t, $^{3}J_{\text{HH}}$ = 6.3 Hz, 4 H, $\text{H}^{10/20}{}_{5/5}$), 4.96 (s, 2 H, $\text{H}^{37/40}$), 7.30 (d, $^{3}J_{\text{HH}}$ = 8.5 Hz, 4 H, $\text{H}^{10/20}{}_{3/3}$), 7.91 (m, 2 H, $\text{H}^{28/29}$), 8.09 (d, $^{3}J_{\text{HH}}$ = 8.4 Hz, 4 H, $\text{H}^{10/20}{}_{2/2}$), 8.21 (d, $^{3}J_{\text{HH}}$ = 8.3 Hz, 2 H, $\text{H}^{5}{}_{2}$), 8.30 (m, 6 H, $\text{H}^{5/15/15}{}_{3/2/3}$), 8.37 (m, 2 H, $\text{H}^{27/30}$), 8.49 (d, $^{3}J_{\text{HH}}$ = 8.0 Hz, 1 H, H^{34}), 8.58 (dd, $^{3}J_{\text{HH}}$ = 8.2 Hz, $^{4}J_{\text{HH}}$ = 1.3 Hz, 1 H, H^{35}), 8.84 (d, $^{3}J_{\text{HH}}$ = 4.6 Hz, 2 H, $\text{H}^{\text{pyrrole}}$), 8.92 (m, 6 H, $\text{H}^{\text{pyrrole}}$), 9.01 (br. s, 1 H, H^{23}), 9.19 (s, 1H, $\text{H}^{\text{amideFcNH}}$), 10.29 (s, 1 H, $\text{H}^{\text{amidePorphNH}}$) ppm.

^{13}C{^{1}H}-NMR (d$_8$-THF): δ = 14.5 ($\text{C}^{10/20}{}_{8/8}$), 20.5 ($\text{C}^{10/20}{}_{7/7}$), 32.8 ($\text{C}^{10/20}{}_{6/6}$), 61.7 ($\text{C}^{37/40}$), 68.7 ($\text{C}^{10/20}{}_{5/5}$), 65.2 ($\text{C}^{38/39}$), 68.4 (C^{Cp}), 113.3 ($\text{C}^{10/20}{}_{3/3}$), 119.0 ($\text{C}^{5}{}_{3}$), 120.4 ($\text{C}^{5/15}$), 121.2 ($\text{C}^{10/20}$), 126.0 ($\text{C}^{15}{}_{3}$), 126.8 (C^{23}), 128.0, 128.0 ($\text{C}^{27/30}$), 128.3 (H^{34}), 132.4, 132.4, 132.7, 132.8 ($\text{C}^{\text{pyrrole}}{}_{2/3/7/8/12/13/17/18}$), 134.3 ($\text{C}^{35}$), 134.9 ($\text{C}^{24}$), 135.2, 135.3 ($\text{C}^{28/29}$), 136.4 ($\text{C}^{10/20}{}_{2/2}$), 136.5 ($\text{C}^{33}$), 135, 3, 135.8 ($\text{C}^{5/15}{}_{2/2}$), 140.1 ($\text{C}^{5}{}_{4}$), 140.1 ($\text{C}^{5}{}_{1}$), 141.8 ($\text{C}^{22}$), n.o. ($\text{C}^{15}{}_{1}$), 151.3, 151.3, 151.6, 151.7 ($\text{C}^{\text{pyrrole}}{}_{1/4/6/9/11/14/16/19}$) 160.2 ($\text{C}^{10/20}{}_{4/4}$), n.o. ($\text{C}^{25/32}$) ppm.

IR (KBr): $\tilde{\nu}$ [cm^{-1}] = 3429 (NH$^{\text{amide}}$, br, m), 2959 (CH, w), 2928 (CH, w), 2868 (CH, w), 1674 (CO, vs),1604 (vs), 1523 (vs), 1384 (vs), 1288 (vs), 1244 (C-O-C, vs), 999 (s), 798 (m).

MS (FD): *m/z* (%) = 1298.79 (100) [M]$^{+}$.

MS (ESI): *m/z* (%) = 648.48 (1) [M^{2+}]), 1297.32 (4) [M]$^{+}$, 1298.32 (4) [M]$^{+}$.

HR-MS (ESI): obs. *m/z* = 1296.3210 [M]$^{+}$; calcd. for [M+H]$^{+}$ 1296.3215.

UV/Vis (CH_2Cl_2): λ [nm] (ε / [10^4 $M^{-1}cm^{-1}$]) = 425 (47.78), 552 (1.33), 594 (0.78).

Fluorescence (CH_2Cl_2): λ [nm] (relative intensity) = 607 (1.00), 652 (0.79).

Quantum yield: Φ = 0.0011.

Lifetime: τ [ps] = 139.15 (13%), 23.04 (87%).

CV (Fc/Fc$^+$, 100 mV s^{-1}, CH_2Cl_2): $E_{\frac{1}{2}}$ [V] = −2.200 (irr.), −1.620, −1.170, −0.070, 0.370, 0.670.

Zn-6b. 2.0 mg (0.0017 mmol) **6b**, 2.0 mg (0.0087 mmol) zinc(II) acetate dihydrate. [silica, CH_2Cl_2 : ethylacetate = 40:1, R_f = 0.48]. Yield: 1.9 mg (0.0016 mmol, 90%), purple powder. $C_{72}H_{48}FeN_6O_6Zn$ (1214.41).

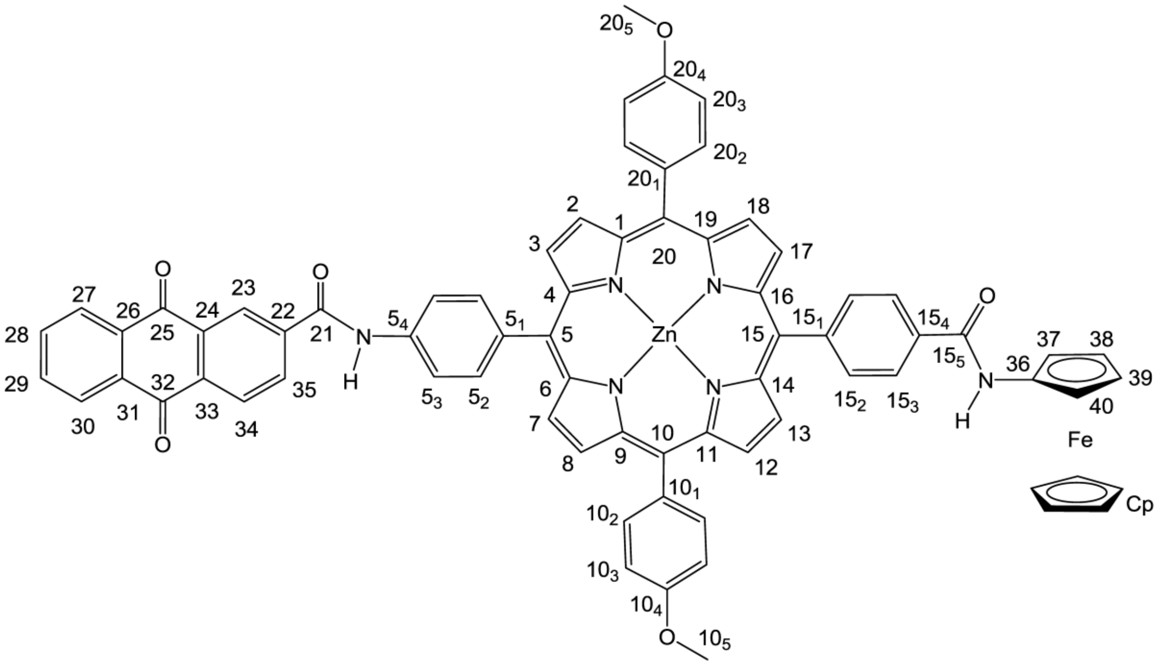

^{1}H-NMR (d_8-THF): δ = 4.07 (s, 8 H, $H^{10/20/38/39}_{5/5}$), 4.25 (s, 5 H, H^{41}), 4.96 (s, 2 H, $H^{37/40}$), 7.32 (d, $^3J_{HH}$ = 8.5 Hz, 4 H, $H^{10/20}_{3/3}$), 7.92 (m, 2 H, $H^{28/29}$), 8.11 (d, $^3J_{HH}$ = 8.5 Hz, 4 H, $H^{10/20}_{2/2}$), 8.21 (d, $^3J_{HH}$ = 8.6 Hz, 2 H, H^5_2), 8.30 (m, 6 H, $H^{5/15/15}_{3/2/3}$), 8.36 (m, 2 H, $H^{27/30}$) 8.49 (d, $^3J_{HH}$ = 8.0 Hz, 1 H, H^{34}), 8.59 (dd, $^3J_{HH}$ = 8.0 Hz, $^4J_{HH}$ = 1.6 Hz, 1 H, H^{35}), 8.84 (d, $^3J_{HH}$ = 4.7 Hz, 2 H, $H^{pyrrole}$), 8.90 (m, 4 H, $H^{pyrrole}$), 8.93 (d, $^3J_{HH}$ = 4.6 Hz, 2 H, $H^{pyrrole}$), 9.01 (d, $^4J_{HH}$ = 1.3 Hz, 1 H, H^{23}), 9.22 (s, 1H, $H^{amideFcNH}$), 10.32 (s, 1 H, $H^{amidePorphNH}$) ppm.

^{13}C{^{1}H}-NMR (d_8-THF): δ = 55.9 ($C^{10/20}_{5/5}$), 112.9 ($C^{10/20}_{3/3}$), 119.0 (C^5_3), 128.0 (C^{30}), 128.0 (C^{34}), 135.3, 135.3 ($C^{28/29}$), 135.8 (C^5_2), 136.4 ($C^{10/20}_{2/2}$) ppm. Because of the poor solubility of **Zn-6b** in THF not all ^{13}C resonances could be observed.

IR (KBr): $\tilde{\nu}$ [cm^{-1}] = 3433 (NH^{amide}, br, vs), 2924 (CH, w), 2854 (CH, w), 1742 (CO, w), 1670 (CO, s), 1637 (vs), 1510 (m), 1384 (vs), 1290 (m), 1248 (s), 1032 (m), 800 (m).

MS (FD): *m/z* (%) = 1212.55 (100) [M]$^+$.

MS (ESI): *m/z* (%) = 1214.24 (6) [M]$^+$, 1215.24 (4) [M]$^+$.

HR-MS (ESI): obs. *m/z* = 1213.2328 $[M+H]^+$; calcd. for $[M+H]^+$ 1213.2354.

UV/Vis (CH_2Cl_2): λ [nm] (ε / [10^4 $M^{-1}cm^{-1}$]) = 424 (51.07), 552 (1.96), 594 (0.73).

Fluorescence (CH_2Cl_2): λ [nm] (relative intensity) = 606 (1.00), 651 (0.71).

Quantum yield: $\Phi = 0.0005$.

Lifetime: τ [ps] = 182.80 (8%), 33.34 (92%).

CV (Fc/Fc^+, 100 mV s^{-1}, CH_2Cl_2): $E_{½}$ [V] = −1.590 (irr.), −1.150, −0.080, 0.360, 0.670.

Zn-6c. 10.0 mg (0.0085 mmol) **6c**, 9.3 mg (0.043 mmol) and zinc(II) acetate dihydrate. [silica, CH_2Cl_2 : ethylacetate = 40:1, R_f = 0.46]. Yield: 9.9 mg (0.0080 mmol, 94%), purple powder. $C_{76}H_{56}FeN_6O_4Zn$ (1238.55).

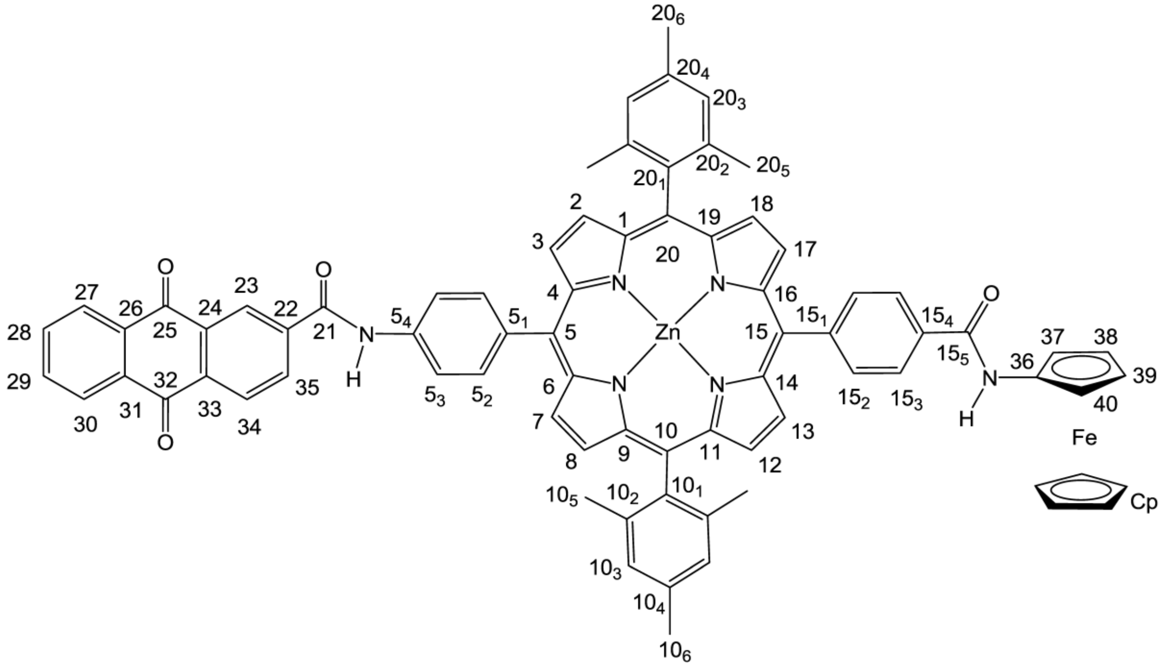

^{1}H-NMR (d_8-THF): δ = 1.86 (s, 12 H, $H^{10/20}_{5/5}$), 2.61 (s, 6 H, $H^{10/20}_{6/6}$), 4.05 (br. s, 2 H, $H^{38/39}$), 4.24 (s, 5 H, HCp), 4.95 (br. s, 2 H, $H^{37/40}$), 7.30 (s, 4 H, $H^{10/20}_{3/3}$), 7.91 (m, 2 H, $H^{28/29}$), 8.19 (d, $^3J_{HH}$ = 8.5 Hz, 2 H, $H^5{}_2$), 8. 28 (m, 6 H, $H^{5/15/15}_{3/2/3}$), 8.37 (m, 2H, $H^{27/30}$), 8.49 (d, $^4J_{HH}$ = 8.0 Hz, 1H, H^{34}), 8.58 (dd, $^3J_{HH}$ = 8.0 Hz, $^4J_{HH}$ = 1.7 Hz, 1 H, H^{35}), 8.68 (d, $^3J_{HH}$ = 4.6 Hz, 2 H, $H^{pyrrole}$), 8.69 (d, $^3J_{HH}$ = 4.5 Hz, 2 H, $H^{pyrrole}$), 8.80 (d, 2 H, $^3J_{HH}$ = 4.6 Hz, $H^{pyrrole}$), 8.88 (d, 2 H, $^3J_{HH}$ = 4.6 Hz, $H^{pyrrole}$), 9.00 (d, $^4J_{HH}$ = 1.5 Hz, 1 H, H^{23}), 9.18 (br. s, 1 H, $H^{amideFcNH}$), 10.27 (1 H, $H^{amidePorphNH}$) ppm.

^{13}C{^{1}H}-NMR (d_8-THF): δ = 21.7 ($C^{10/20}_{6/6}$), 21.9 ($C^{10/20}_{5/5}$), 62.1 ($C^{37/40}$), 65.0 ($C^{38/39}$), 70.0 (C^{Cp}), 119.3 ($C^5{}_3$), 119.3. (C^{15}), n.o ($C^{10/20}$), 120.7 (C^5), 126.3 ($C^{15}{}_3$), 126.6 (s, C^{23}), 128.0 (C^{27}), 128.0 (C^{30}), 128.9 ($C^{10/20}_{3/3}$), 128.3 (C^{34}), 130.7, 130.9, 132.6, 133.1 ($C^{pyrrole\ 2/3/7/8/12/13/17/18}$), 134.4 ($C^{35}$), 134.9 ($C^{24}$), 135.2, 135.3 ($C^{28/29}$), 135.4 ($C^{15}{}_2$), 135.9 ($C^5{}_2$), 136.5 ($C^{33}$), 138.9 ($C^5{}_1$), 139.6

(C$^{10/20}{}_{1/1}$), 140.5 (C$^{5}{}_{4}$), 141.8 (C^{22}), 146.7 (C$^{15}{}_{1}$), n.o. (C$^{\mathrm{pyrrole}\ 1/4/6/9/11/14/16/19}$), 165.2 (C^{21}), 165.8 (C$^{15}{}_{5}$), 183.0, 183.2 (C$^{25/32}$) ppm.

IR (KBr): $\tilde{\nu}$ [cm^{-1}] = 3425 (NH$^{\mathrm{amide}}$, br. vs), 2918 (CH, w), 2854 (CH, w), 1676 (CO, vs), 1524 (s), 1384 (w), 1288 (s), 999 (vs), 797 (m).

MS (FD): *m/z* (%) = 1237.8 (100) [M]$^{+}$.

MS (ESI): *m/z* (%) = 1236.31 (12) [M]$^{+}$.

HR-MS (ESI): obs. *m/z* = 1236.2971 [M]$^{+}$; calcd. for [M]$^{+}$ 1236.3004.

UV/Vis (CH_2Cl_2): λ [nm] (ε / [10^4 M^{-1}cm^{-1}]) = 424 (49.71), 552 (1.88), 594 (0.18).

Fluorescence (CH_2Cl_2): λ [nm] (relative intensity) = 604 (1.00), 653 (0.80).

Quantum yield: Φ = 0.0014.

Lifetime: τ [ps] = 184.51 (13%), 25.92 (77%).

CV (Fc/Fc^{+}, 100 mV s^{-1}, CH_2Cl_2): $E_{½}$ [V] = −2.220 (irr.), −1.830 (irr.), −1.180 (q. rev.), −0.060, 0.410, 0.750.

Zn-6d. 10.0 mg (0.0089 mmol) triad **7d**, 9.8 mg (0.045 mmol) zinc(II) acetate dihydrate. [silica, CH_2Cl_2, R_f = 0.70]. Yield: 9.2 mg (0.0078 mmol, 87%), purple powder. $C_{72}H_{48}FeN_6O_4Zn$ (1182.44).

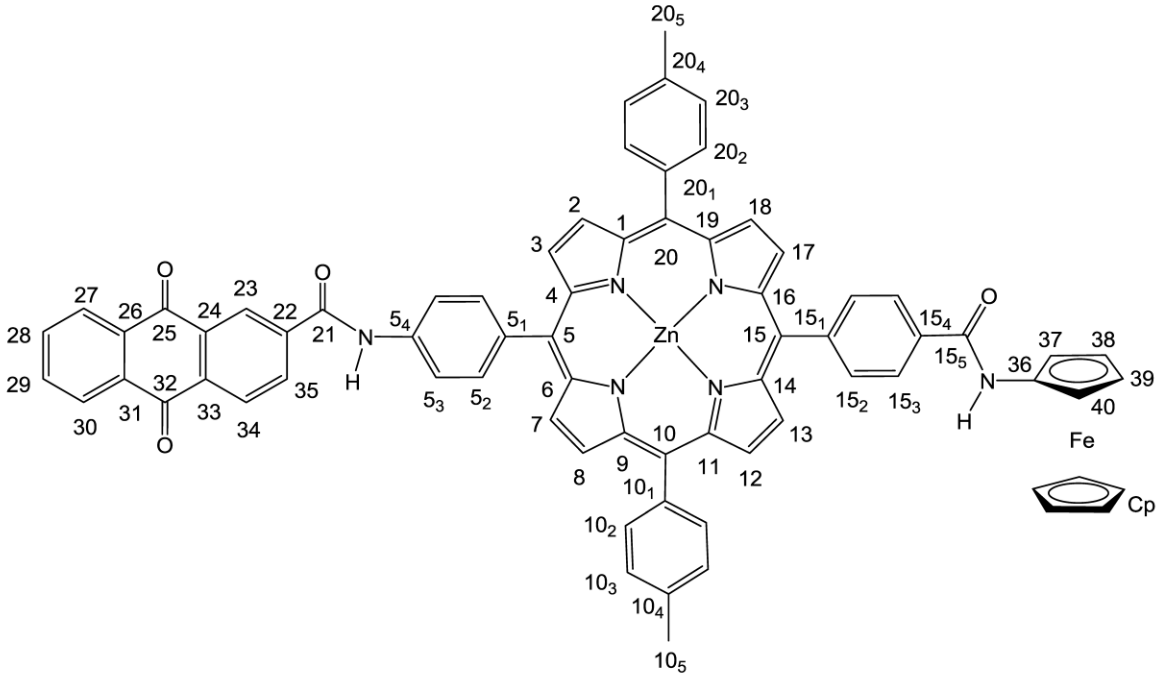

^{1}H-NMR (d_8-THF): δ = 2.69 (s, 6 H, H$^{10/20}{}_{5/5}$), 4.05 (s, 2 H, H$^{39/38}$), 4.24 (s, 5 H, H^{41}) 4.95 (s, 2 H, H$^{37/40}$), 7.56 (d, $^3J_{\mathrm{HH}}$ = 7.7 Hz, 4 H, H$^{10/20}{}_{3/3}$), 7.90 (m, 2 H, H$^{28/29}$), 8.08 (d, $^3J_{\mathrm{HH}}$ = 7.7 Hz, 4 H, H$^{10/20}{}_{2/2}$), 8.20 (d, $^3J_{\mathrm{HH}}$ = 8.3 Hz, 2 H, H$^{5}{}_{2}$), 8.30 (m, 6 H, H$^{5/15/15}{}_{2/3/3}$), 8.35 (m, 2 H, H$^{27/30}$), 8.48 (d, $^3J_{\mathrm{HH}}$ = 8.0 Hz, 1 H, H^{34}), 8.57 (dd, $^3J_{\mathrm{HH}}$ = 8.1 Hz, $^3J_{\mathrm{HH}}$ = 1.5 Hz, 1 H, H^{35}), 8.83 (d, $^3J_{\mathrm{HH}}$ = 4.6 Hz, 2

H, $H^{pyrrole}$), 8.88 (d, $^{3}J_{HH}$ = 3.8 Hz, 4 H, $H^{pyrrole}$), 8.92 (d, $^{3}J_{HH}$ = 4.6 Hz, 2 H, $H^{pyrrole}$), 9.00 (br. s, 1 H, H^{23}), 9.17 (s, 1H, $H^{amideFcNH}$), 10.28 (s, 1 H, $H^{amidePorphNH}$) ppm.

$^{13}C\{^{1}H\}$-NMR (d_8-THF): δ = 21.7 ($C^{10/20}_{5/5}$), 62.1 ($C^{37/40}$), 64.8 ($C^{38/39}$), 70.0 (C^{Cp}), 118.9 (C^{5}_{3}), 121.9 (s, $C^{10/20}$), 126.6 ($C^{23/15}_{3}$), 127.9, 127.9 ($C^{27/30}$), 128.0 ($C^{10/20}_{3/3}$), 128.2 (C^{34}), 131.8, 131.9, 132.3, 132.4, 132.5, 132.6, 132.6 ($C^{pyrrole\ 2/3/7/8/12/13/17/18}$), 134.2 (s, C^{35}), 134.8 (C^{24}), 135.1, 135.2 ($C^{28/29}$), 135.4 ($C^{5/10/20}_{2/2/2}$), 135.7 (C^{15}_{2}), 136.4 (s, C^{33}), 137.9 ($C^{10/20}_{4/4}$), 140.0 (C^{5}_{4}), 141.7 ($C^{10/20}_{1/1}$), 141.8 (C^{22}), 151.3, 151.4 ($C^{pyrrole\ 1/4/6/9/11/14/16/19}$), 165.1, 166.4 ($C^{15/21}_{5}$), 182.9, 183.1 ($C^{25/32}$) ppm.

IR (KBr): $\tilde{\nu}$ [cm^{-1}] = 3406 (NH^{amide}, br, m), 2926 (CH, w), 1676 (CO, vs), 1595 (m), 1524 (s), 1387 (m), 1333 (w), 1290 (vs), 900 (w), 800 (m), 710 (m).

MS (FD): *m/z* (%) 1180.96 (100) $[M]^{+}$, 1182.05 (86) $[M]^{+}$, 1183.03 (87) $[M]^{+}$.

MS (ESI): *m/z* (%) = 590.11 (3) $[M]^{2+}$, 1180.24 (36) $[M]^{+}$.

HR-MS (ESI): obs. *m/z* = 1180.2378 $[M+H]^{+}$; calcd. for $[M+H]^{+}$ 1180.2378.

UV/Vis (CH_2Cl_2): λ [nm] (ε / [10^{4} $M^{-1}cm^{-1}$]) = 423 (47.02), 551 (2.02), 593 (0.75).

Fluorescence (CH_2Cl_2): λ [nm] (relative intensity) = 607 (0.89), 653 (1.00).

Quantum yield: Φ = 0.0012.

Lifetime: τ [ps] = 189.38 (17%), 27.13 (83%).

CV (Fc/Fc^{+}, 100 mV s^{-1}, CH_2Cl_2): $E_{½}$ [V] = −2.230 (irr.), −1.630 (irr.), −1.190 (q. rev.), −0.090, 0.390, 0.710.

Zn-6e. 12.0 mg (0.010 mmol) **6e**, 11.1 mg (0.050 mmol) zinc(II) acetate dihydrate. [silica, CH_2Cl_2, R_f = 0.73]. Yield: 11.0 mg (0.0095 mmol, 95%), purple powder. $C_{70}H_{44}FeN_6O_4Zn$ (1154.39).

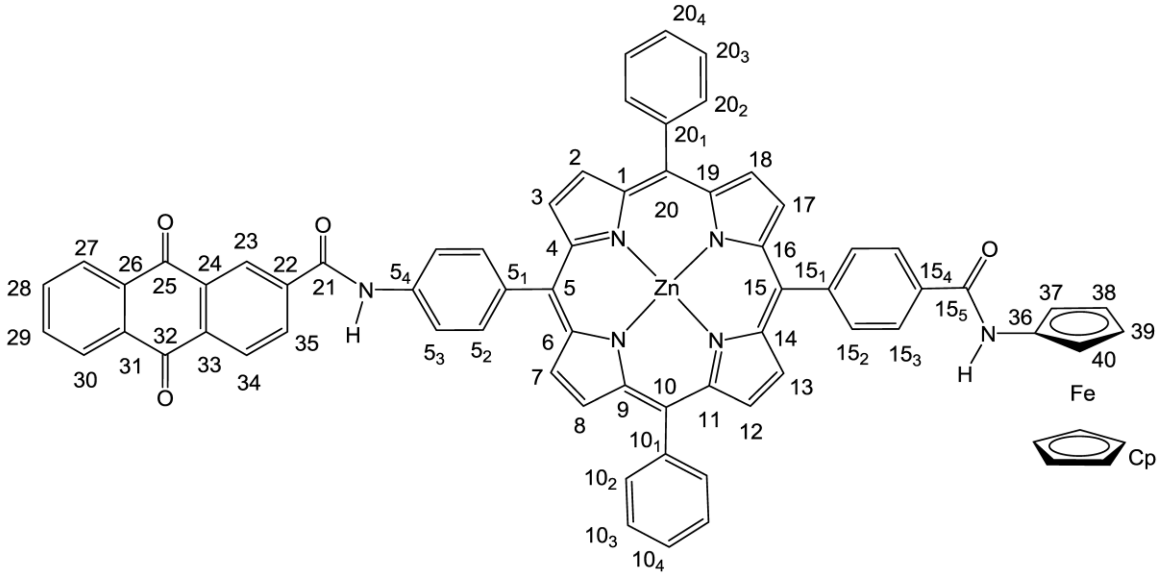

^{1}H-NMR (d_8-THF): δ = 4.05 (s, 2 H, $H^{38/39}$), 4.24 (s, 5 H, H^{41}) 4.95 (s, 2 H, $H^{37/40}$), 7.76 (m, 6 H, $H^{10/20}_{3/4}$), 7.91 (m, 2 H, $H^{28/29}$), 8.21 (m, 6 H, $H^{5/10/20}_{2/2/2}$), 8.30 (m, 6 H, $H^{5/15/15}_{3/2/3}$), 8.36 (m, 2 H,

$\mathrm{H}^{27/30}$), 8.49 (d, $^{3}J_{\mathrm{HH}}$ = 8.0 Hz, 1 H, H^{34}), 8.58 (dd, $^{3}J_{\mathrm{HH}}$ = 8.1 Hz, $^{4}J_{\mathrm{HH}}$ = 1.7 Hz, 1 H, H^{35}), 8.87 (m, 6 H, $\mathrm{H}^{\mathrm{pyrrole}}$), 8.95 (d, $^{3}J_{\mathrm{HH}}$ = 4.6 Hz, 2 H, $\mathrm{H}^{\mathrm{pyrrole}}$), 9.00 (d, $^{4}J_{\mathrm{HH}}$ = 1.6 Hz, 1 H, H^{23}), 9.20 (s, 1 H, $\mathrm{H}^{\mathrm{amideFcNH}}$), 10.30 (s, 1 H, $\mathrm{H}^{\mathrm{amidePorphNH}}$) ppm.

^{13}C{^{1}H}-NMR (d_8-THF): δ = 62.2 ($\mathrm{C}^{37/40}$), 65.0 ($\mathrm{C}^{38/39}$) 70.0 (C^{Cp}), 97.9 (C^{36}), 119.0 ($\mathrm{C}^{5}{}_{3}$), 120.6 (C^{15}), 121.7 (C^{5}), 121.8 ($\mathrm{C}^{10/20}$), 126.4 ($\mathrm{C}^{15}{}_{3}$), 126.7 (C^{23}), 127.4 ($\mathrm{C}^{10/20}{}_{3/3}$), 128.0, 128.0 ($\mathrm{C}^{27/30}$), 128.3 ($\mathrm{C}^{10/20}{}_{4/4}$), 128.3 ($\mathrm{C}^{34}$), 132.1, 132.5, 132.5, 132.6 ($\mathrm{C}^{\mathrm{pyrrole}\ 2/3/7/8/12/13/17/18}$), 134.3 ($\mathrm{C}^{35}$), 134.9, ($\mathrm{C}^{24}$), 135.2, 135.3 ($\mathrm{C}^{28/29}$), 135.5 ($\mathrm{C}^{10/20}{}_{2/2}$) 135.4, 135.8 ($\mathrm{C}^{5/15}{}_{2/2}$), 136.5 ($\mathrm{C}^{33}$), 140.1 ($\mathrm{C}^{5}{}_{4}$), 140.2 ($\mathrm{C}^{15}{}_{4}$), 141.9 ($\mathrm{C}^{22}$), 144.7 ($\mathrm{C}^{10/20}{}_{1/1}$), 147.6 ($\mathrm{C}^{15}{}_{1}$), 150.8, 151.2, 151.3, 151.4 ($\mathrm{C}^{\mathrm{pyrrole}\ 1/4/6/9/11/14/16/19}$), 165.2 ($\mathrm{C}^{21}$), 165.9 ($\mathrm{C}^{15}{}_{5}$) 183.0, 183.2 ($\mathrm{C}^{25/32}$) ppm.

IR (KBr): $\tilde{\nu}$ [cm^{-1}] = 3443 (NH$^{\mathrm{amide}}$, br, vs), 1676 (CO, s), 1598 (m), 1524 (-NH, m), 1289 (s), 1279 (s), 1000 (s), 797 (w).

MS (FD): *m/z* (%) = 1153.12 (100) [M]$^{+}$, 1154.09 (82) [M]$^{+}$, 1155.08 (92) [M]$^{+}$.

MS (ESI): *m/z* (%) = 1152.26 (6) [M]$^{+}$.

HR-MS (ESI): obs. *m/z* = 1152.2076 [M+H]$^{+}$; calcd. for [M+H]$^{+}$ 1152.2065.

UV/Vis (CH_2Cl_2): λ [nm] (ε / [10^{4} M^{-1}cm^{-1}]) = 423 (38.89), 551 (1.63), 592 (0.46).

Fluorescence (CH_2Cl_2): λ [nm] (relative intensity) = 601 (1.00), 647 (0.82).

Quantum yield: Φ = 0.0009.

Lifetime: τ [ps] = 107.63 (12%), 29.53 (88%).

CV (Fc/Fc^{+}, 100 mV s^{-1}, CH_2Cl_2): $E_{½}$ [V] = −2.190 (irr.), −1.580 (irr.), −1.120, −0.080, 0.430, 0.740.

Zn-6f. 10.0 mg (0.0089 mmol) **6f**, 10.0 mg (0.044 mmol) zinc(II) acetate dihydrate. [silica, CH_2Cl_2, R_f = 0.64]. Yield: 10.2 mg (0.0086 mmol, 97%), purple powder. $C_{70}H_{42}F_2FeN_6O_4Zn$ (1190.37).

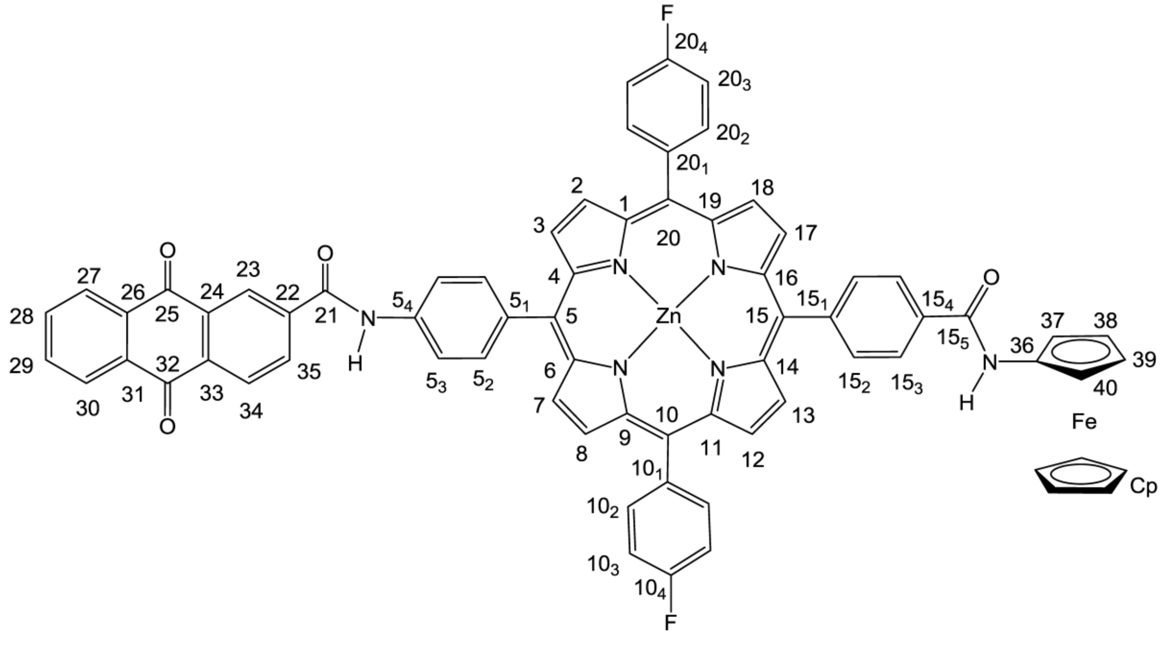

^{1}H-NMR (d^{8}-THF): δ = 4.06 (br. s, 2 H, H$^{39/38}$), 4.25 (s, 5 H, H$^{\mathrm{Cp}}$), 4.96 (br. s, 2 H, H$^{37/40}$), 7.51 (ps. t, $^{3}J_{\mathrm{HH}}$ = 8.7 Hz, 4 H, H$^{10/20}_{3/3}$), 7.90 (m, 2 H, H$^{28/29}$), 8.21 (m, 6 H, H$^{5/10/20}_{2/2/2}$), 8.31 (m, 6 H, H$^{5/15/15}_{3/2/3}$), 8.36 (m, 2 H, H$^{27/30}$), 8.48 (d, $^{3}J_{\mathrm{HH}}$ = 8.0 Hz, H^{34}), 8.58 (dd, 1 H, $^{4}J_{\mathrm{HH}}$ = 1.8 Hz, $^{3}J_{\mathrm{HH}}$ = 8.0 Hz, H^{35}), 8.87 (m, 6 H, H$^{\mathrm{pyrrole}}$), 8.97 (d, 2 H, $^{3}J_{\mathrm{HH}}$ = 4.6 Hz, H$^{\mathrm{pyrrole}}$), 9.00 (d, 1 H, $^{4}J_{\mathrm{HH}}$ = 1.6 Hz, H^{23}), 9.19 (br. s, 1 H, H$^{\mathrm{amideFcNH}}$). 10.30 (br. s, 1 H, H$^{\mathrm{amidePorphNH}}$) ppm.

^{13}C{^{1}H}-NMR (d$_{8}$-THF): δ = 61.9 (C$^{37/40}$), 64.8 (C$^{38/39}$), 70.2 (C$^{\mathrm{Cp}}$), 113.6 (d, $^{2}J_{\mathrm{CF}}$ = 24.6 Hz, C$^{10/20}_{3/3}$), 118.8 (C$^{5}_{3}$), 120.3, 120.5, 121.6 (C$^{5/15/10/20}$), 126.4 (C$^{15}_{3}$), 126.6 (C^{23}), 127.6, 127.8 (C$^{27/30}$), 128.1 (C^{34}), 132.2, 132.4, 132.4 (C$^{\mathrm{pyrrole}\ 2/3/7/8/12/13/17/18}$), 134.2 (C^{35}), 135.2, 135.2 (C$^{28/29}$), 136.5 (C$^{5}_{2}$), 136.0 (d, $^{2}J_{\mathrm{CF}}$ = 7.6 Hz, C$^{10/20}_{2/2}$), 135.2 (C$^{15}_{2}$), 136.2 (C^{24}), 136.5 (C^{33}), 140.2 (C$^{5}_{1}$), 140.7 (d, $^{4}J_{\mathrm{CF}}$ = 4.7 Hz, C$^{10/20}_{1/1}$), 140.1 (C$^{5}_{4}$), 141.8 (C^{22}), n.o. (C$^{15}_{1}$), 150.9, 151.2, 151.4, 151.5 (C$^{\mathrm{pyrrole}\ 1/4/6/9/11/14/16/19}$), 163.9 (d, $^{1}J_{\mathrm{FH}}$ = 250.2 Hz, C$^{10/20}_{4/4}$), 165.2 (C$^{15/21}_{5}$), 183.0, 183.2 (C$^{25/32}$) ppm.

^{19}F-NMR (d$_{8}$-THF): δ = −118.6 (m, F-C$^{10/20}_{5/5}$) ppm.

IR (KBr): $\tilde{\nu}$ [cm^{-1}] = 3435 (NH$^{\mathrm{amide}}$, br, vs), 1676 (CO, vs), 1599, (m), 1524 (vs), 1290 (s), 1159 (CF, w), 999 (s) 806 (w).

MS (FD): *m/z* (%) = 1189.13 (100) [M]$^{+}$, 1190.15 (86) [M]$^{+}$, 1191.12 (84) [M]$^{+}$.

MS (ESI): *m/z* (%) = 1188.17 (100) [M+H]$^{+}$, 1190.18 (81) [M+H]$^{+}$, 1191.18 (54) [M+H]$^{+}$.

HR-MS (ESI): obs. *m/z* = 1188.1869 [M+H]$^{+}$; calcd. for [M+H]$^{+}$ 1188.1842.

UV/Vis (CH_2Cl_2): λ [nm] (ε / [10^{4} M^{-1}cm^{-1}]) = 422 (47.69), 551 (2.05), 593 (0.63).

Fluorescence (CH_2Cl_2): λ [nm] (relative intensity) = 602 (1.00), 649 (0.92).

Quantum yield: Φ = 0.0049.

Lifetime: τ [ps] = 281.39 (27%), 133.53 (73%).

CV (Fc/Fc^{+}, 100 mV s^{-1}, CH_2Cl_2): $E_{½}$ [V] = −2.180 (irr.), −1.590, −1.120, −0.080, 0.440, 0.750.

Zn-6g. 10.0 mg (0.0082 mmol) **6g**, 8.9 mg (0.041 mmol) zinc(II) acetate dihydrate. [silica, CH_2Cl_2, R_f = 0.72]. Yield: 9.4 mg (0.0073 mmol, 89%), purple powder. $C_{72}H_{42}F_6FeN_6O_4Zn$ (1290.36).

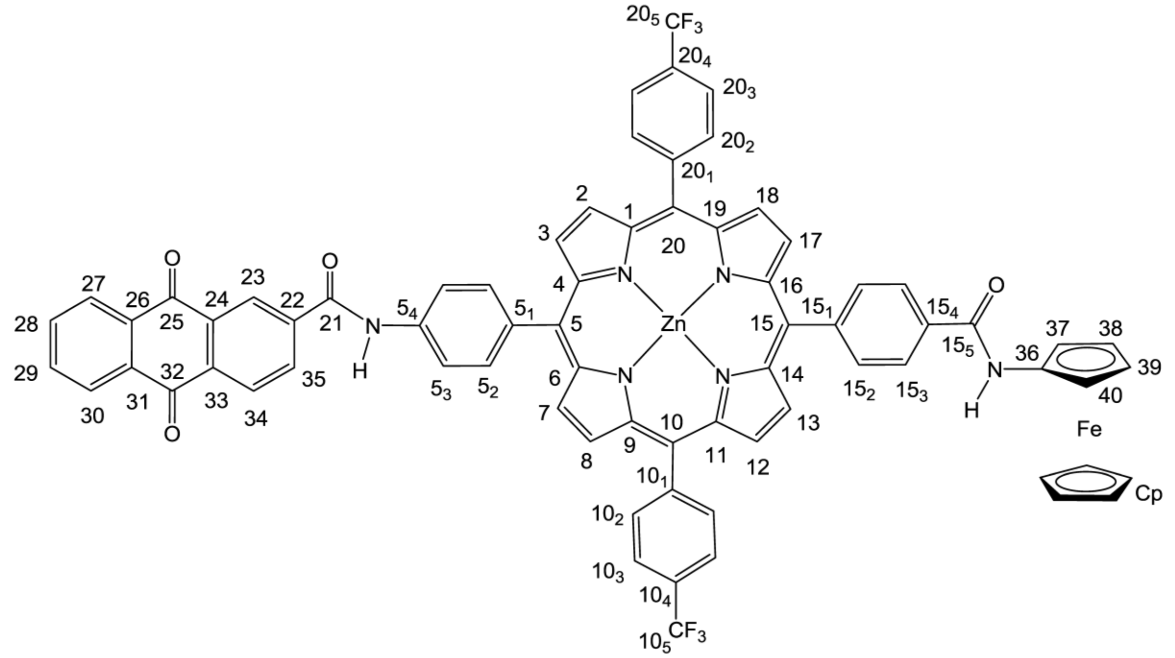

^{1}H-NMR (d$_8$-THF): δ = 4.06 (br. s, 2 H, H$^{39/38}$), 4.24 (s, 5 H, H^{Cp}), 4.95 (br. s, 2 H, H$^{37/40}$), 7.91 (m, 2 H, H$^{28/29}$), 8.11 (d, $^3J_{HH}$ = 7.6 Hz, 4 H, H$^{10/20}_{2/2}$), 8.21 (d, $^3J_{HH}$ = 8.2 Hz, 2 H, H$^5_2$), 8.31 (m, 6 H, H$^{5/15/15}_{3/2/3}$), 8.36 (m, 2 H, H^{27,30}), 8.41 (d, $^3J_{HH}$ = 7.8 Hz, 4 H, H$^{10/20}_{3/3}$), 8.48 (d, $^3J_{HH}$ = 8.0 Hz, 1 H, H^{34}), 8.58 (d, 1 H, $^3J_{HH}$ = 7.8 Hz, H^{35}), 8.84 (d, 4 H, $^3J_{HH}$ = 4.5 Hz, H^{pyrrole}), 8.89 (d, 2 H, $^3J_{HH}$ = 4.5 Hz, H^{pyrrole}), 8.98 (m, 3 H, H$^{23/pyrrole}$), 9.20 (br. s, 1 H, H^{amideFcNH}), 10.31 (s, 1H, H^{amidePorphNH}) ppm.

^{13}C{^{1}H}-NMR (d$_8$-THF): δ = 61.4 (C$^{37/40}$), 64.7 (C$^{38/39}$), 69.7 (C^{Cp}), 119.1 (C$^5_3$), 119.4 (C$^{5/10/20}$), 126.7 (C^{23}), 124.4 (d, $^4J_{CF}$ = 2.7 Hz, C$^{10/20}_{3/3}$), 126.7 (C$^{15}_3$), 128.3 (C$^{10/20}_{4/4}$), 128.0, 128.0 (C$^{27/30}$), 128.3 (C^{34}), n.o. (C$^{10/20}_{5/5}$), 132.2 (C$^{pyrrole\ 2/3/7/8/12/13/17/18}$), 134.3 (C^{35}), n.o. (C^{24}), 135.2, 135.3, 135.3 (C$^{28/29/15}_2$), 135.9 (C$^5_2$), 135.9 (C$^{10/20}_{2/2}$), 136.4 (C^{33}), n.o. (C$^{10/20}_{4/4}$), n.o (C$^5_1$), 141.1 (C$^5_4$), n.o. (C^{22}), n.o. (C$^{15}_1$), 149.6 (C$^{10/20}_{1/1}$), 150.7, 150.8, 150.9, 151.6, 151.7, 151.8 132.2 (C$^{pyrrole\ 1/4/6/9/11/14/16/19}$), 165.2 (C$^{21/15}_5$), 181.6, 183.2 (C$^{25/32}$) ppm.

^{19}F-NMR (d$_8$-THF): δ = −64.5 (s, F-C$^{10/20}_{5/5}$) ppm.

IR (KBr): $\tilde{\nu}$ [cm^{-1}] = 3440 (NH^{amide}, br, m), 2928 (CH, w), 2849 (CH, w), 1729 (CO, m), 1676 (CO, m), 1614 (m), 1518 (m), 1384 (m), 1314 (vs), 1279 (s), 1120 (CF, s), 794(w).

MS (FD): *m/z* (%) = 1289.22 (91) [M]$^+$, 1290.15 (68) [M]$^+$, 1291.18 (100) [M]$^+$.

MS (ESI): *m/z* (%) = 1288.20 (7) [M]$^+$, 1289.20 (6) [M]$^+$.

HR-MS (ESI): obs. *m/z* = 1288.1791 [M]$^+$; calcd. for [M]$^+$ 1288.1813.

UV/Vis (CH$_2$Cl$_2$): λ [nm] (ε / [10^4 M^{-1}cm^{-1}]) = 423 (34.13), 552 (1.59), 593 (0.48).

Fluorescence (CH$_2$Cl$_2$): λ [nm] (relative intensity) = 605 (1.00), 653 (0.27).

Quantum yield: Φ = 0.0028.

Lifetime: τ [ps] = 285.80 (25%), 35.20 (75%).

CV (Fc/Fc$^+$, 100 mV s^{-1}, CH$_2$Cl$_2$): $E_{½}$ [V] = −1.610 (irr.), −1.240 (irr.), −0.100, 0.480, 0.770.

Zn-6h. 15.0 mg (0.012 mmol) **6h**, 13.0 mg (0.059 mmol) zinc(II) acetate dihydrate. [silica, CH$_2$Cl$_2$, R_f = 0.42]. Yield: 14.7 mg (0.011 mmol, 92%), purple powder. $C_{70}H_{34}F_{10}FeN_6O_4Zn$ (1334.27).

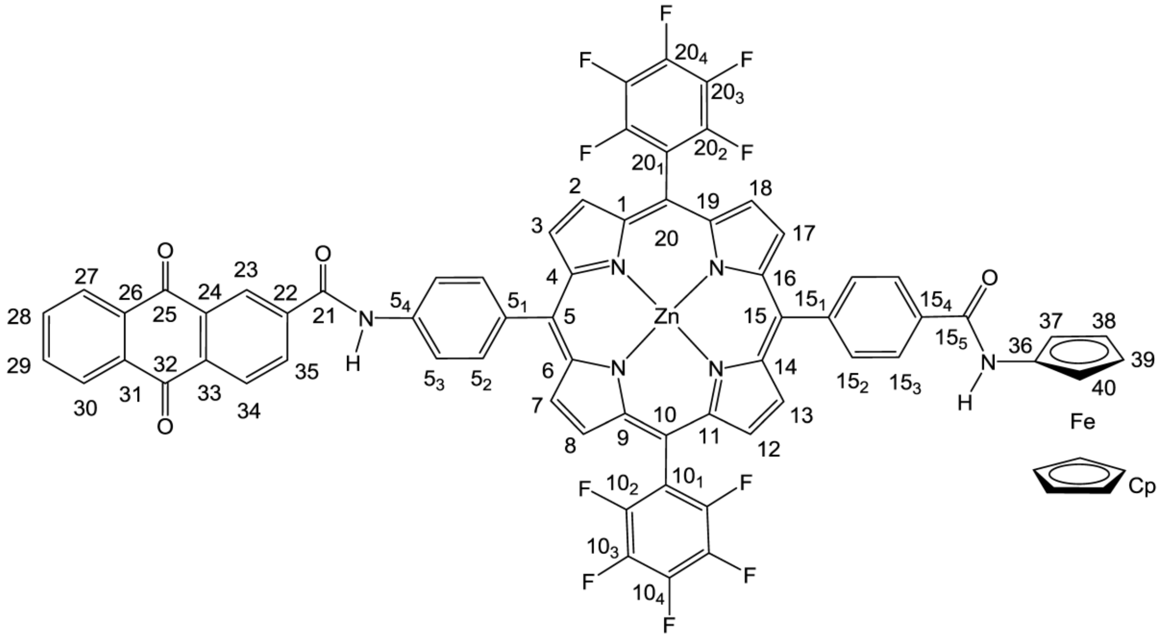

^{1}H-NMR (d$_8$-THF): δ = 4.08 (s, 2 H, H$^{39/38}$), 4.27 (s, 5 H, H^{Cp}), 4.97 (s, 2 H, H$^{37/40}$), 7.92 (m, 2 H, H$^{28/29}$), 8.23 (d, $^3J_{HH}$ = 8.3 Hz, 2 H, H$^5{}_2$), 8.33 (m, 6 H, H$^{5/15/15}{}_{3/2/3}$), 8.37 (m, 2 H, H$^{27/30}$), 8.50 (d, $^4J_{HH}$ = 8.0 Hz, 1H, H^{34}), 8.59 (dd, $^3J_{HH}$ = 8.0 Hz, $^4J_{HH}$ = 1.3 Hz ,1 H, H^{35}), 8.95 (d, 2 H, $^3J_{HH}$ = 4.6 Hz, H^{pyrrole}), 9.00 (m, 5 H, H$^{23/pyrrole}$), 9.05 (d, 2 H, $^3J_{HH}$ = 4.6 Hz, H^{pyrrole}), 9.21 (s, 1 H, H^{amideFcNH}), 10.33 (s, 1 H, H^{amidePorphNH}) ppm.

^{13}C{^{1}H}-NMR (d$_8$-THF): δ = 62.1 (C$^{37/40}$), 65.3 (C$^{38/39}$), 70.1 (C^{Cp}), n.o. (C^{36}), 119.1 (C$^5{}_3$), n.o. (C$^{5/15/10/20}$), 128.0 (C^{27}), 128.0 (C^{30}), 128.3 (C^{34}), 126.7 (C$^{23/15}{}_3$), 131.1, 131.2, 131.3, 131.3, 134.2 (C$^{pyrrole\ 2/3/7/8/12/13/17/18}$), 134.3 (C^{35}), 134.9 (C^{24}), 135.2, 135.3 (C$^{28/29}$), 135.5 (C$^{15}{}_2$), 135.9 (s, C$^5{}_2$), 136.5 (C^{33}), 139.4 (C$^5{}_1$ or C$^{15}{}_4$), 140.4 (C$^5{}_4$), 141.8 (C^{22}), 146.6 (C$^{15}{}_1$), 140.0, 146.6, 149.0 (m, C$^{10/20}{}_{1/2/3/4}$), 150.6, 150.7, 151.6, 152.2 (C$^{pyrrole\ 1/4/6/9/11/14/16/19}$), 165.2 (C^{22}), 165.6 (C$^{15}{}_5$), 183.0, 183.2 (C$^{25/32}$) ppm.

^{19}F-NMR (d$_8$-THF): δ = −167.2 (ddd, $^3J_{FF}$ = 24 Hz, $^3J_{FF}$ = 21 Hz, $^5J_{FF}$ = 8 Hz, 4 F, F$^{10/20}{}_{3/3}$), −158.6 (t, $^3J_{FF}$ = 21 Hz, 2 F, F$^{10/20}{}_{4/4}$), −141.4 (dd, $^3J_{FF}$ = 24 Hz, $^5J_{FF}$ = 8 Hz, 4 F, F$^{10/20}{}_{2/2}$) ppm.

IR (KBr): $\tilde{\nu}$ [cm^{-1}] = 3429 (NH^{amide}, br, vs), 1674 (CO, m), 1652 (CO, m), 1520 (s), 1288 (vs),1107 (CF, w), 991 (ws), 937 (m).

MS (FD): m/z (%) = 1331.21 (94) [M]$^+$, 1333.20 (100) [M]$^+$, 1334.12 (79) [M]$^+$.

MS (ESI): m/z (%) = 1332.12 (31) [M$^+$], 1333.13 (25) [M$^+$], 1334.12 (27) [M]$^+$.

HR-MS (ESI): obs. m/z = 1332.1123 [M]$^+$; calcd. for [M]$^+$ 1332.1138.

UV/Vis (CH$_2$Cl$_2$): λ [nm] (ε / [10^4 M^{-1}cm^{-1}]) = 422 (47.51), 551 (1.68), 594 (0.65).

Fluorescence (CH_2Cl_2): λ [nm] (relative intensity) = 602 (1.00), 654 (0.98).

Quantum yield: Φ = 0.0025.

Lifetime: τ [ps] = 215.88 (6%), 20.65 (94%).

CV (Fc/Fc$^+$, 100 mV s^{-1}, CH_2Cl_2): $E_{½}$ [V] = −2.000 (irr.), −1.180, −0.090, 0.630, 0.910.

Zn-6i. 12.0 mg (0.0093 mmol) **6i**, 10.2 mg (0.046 mmol) zinc(II) acetate dihydrate. [silica, CH_2Cl_2 : ethylacetate = 40:1, R_f = 0.40]. Yield: 10.1 mg (0.0074 mmol, 80%), purple powder. $C_{72}H_{40}F_8FeN_6O_6Zn$ (1358.34).

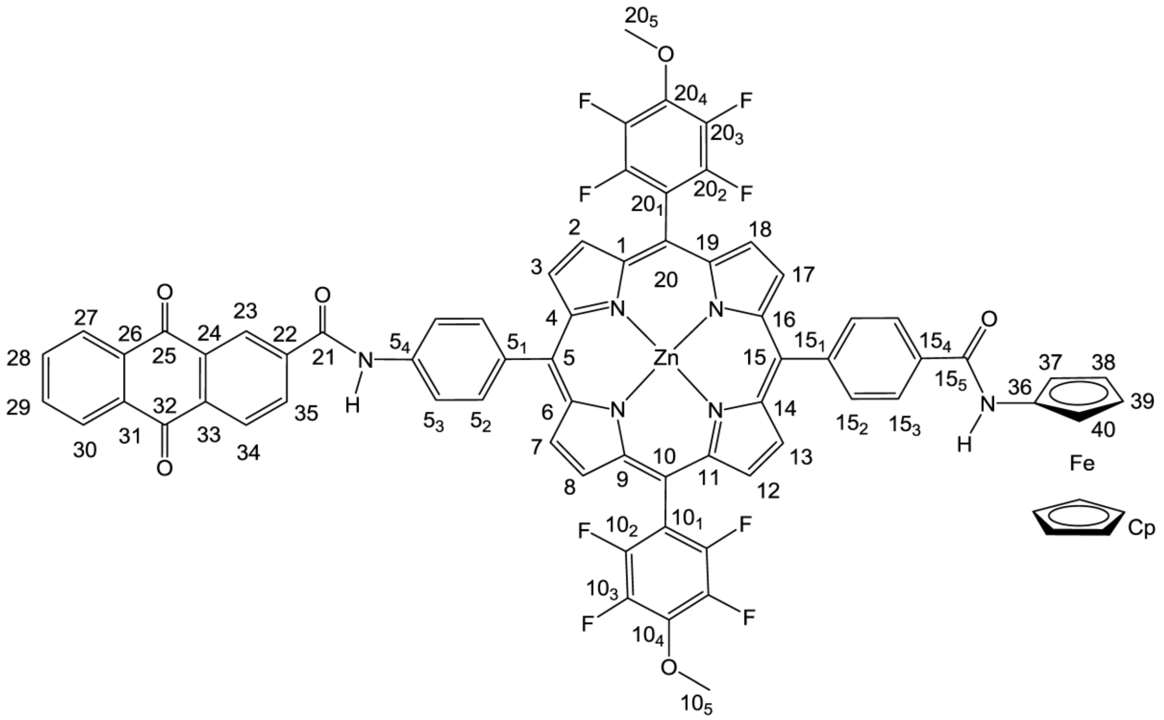

^{1}H-NMR (d$_8$-THF): δ = 4.06 (ps. t, 2 H, $H^{39/38}$), 4.25 (s, 5 H, H^{Cp}), 4.40 (s, 6 H, $H^{10/20}{}_{5/5}$) 4.96 (s, 2 H, $H^{37/40}$), 7.92 (m, 2 H, $H^{28/29}$), 8.23 (d, $^3J_{HH}$ = 8.0 Hz, 2 H, $H^{5}{}_{2}$), 8.33 (m, 6 H, $H^{5/15/15}{}_{3/2/3}$), 8.38 (m, 2 H, $H^{27/30}$), 8.50 (d, $^4J_{HH}$ = 8.0 Hz, 1H, H^{34}), 8.60 (dd, $^3J_{HH}$ = 7.7 Hz, $^4J_{HH}$ = 1.2 Hz ,1 H, H^{35}), 8.94 (m, 2 H, $H^{pyrrole}$), 8.98 (m, 4 H, $H^{pyrrole}$), 8.98 (m, 3 H, $H^{pyrrole/23}$), 9.26 (s, 1 H, $H^{amideFcNH}$), 10.35 (s, 1 H, $H^{amidePorphNH}$) ppm.

^{13}C{^{1}H}-NMR (d$_8$-THF): δ = 62.2 ($C^{37/40}$), 63.1 ($C^{10/20}{}_{5/5}$), 65.1 ($C^{39/38}$), 70.0 (C^{Cp}), 98.0 (C^{36}), 119.1 ($C^{5}{}_{3}$), n.o. ($C^{10/20}$), n.o. (C^{15}), n.o (C^{5}), 126.5 ($C^{15}{}_{3}$), 126.7 (C^{23}), 128.0 (C^{27}), 128.0 (C^{30}), 128.3 (C^{34}), 131.2, 131.3, 133.5, 133.9 ($C^{pyrrole\ 2/3/7/8/12/13/17/18}$), 134.4 ($C^{35}$), 134.9 ($C^{24}$), 135.2, 135.3 (s, $C^{28/29}$), 135.4 ($C^{15}{}_{2}$), 135.9 ($C^{5}{}_{2}$), 135.8 ($C^{15}{}_{4}$), 136.5 (C^{33}), 139.6 ($C^{5}{}_{1}$), 140.3 ($C^{5}{}_{4}$), 141.8 (C^{22}), 146.9 ($C^{15}{}_{1}$), 143.4, 146.8, 149.3 (m, $C^{10/20}{}_{1/1/2/2/3/3/4/4}$), 150.8, 150.9, 151.4, 152.0 ($C^{pyrrole\ 1/4/6/9/11/14/16/19}$), 165.2 ($C^{21}$), 165.8 ($C^{15}{}_{5}$), 183.0, 183.2 ($C^{25/32}$) ppm.

^{19}F-NMR (d$_8$-THF): δ = −162.3 (dd, $^3J_{FF}$ = 22 Hz, $^5J_{FF}$ = 7 Hz, 4 F, $F^{10/20}{}_{3/3}$), −143.2 (dd, $^3J_{FF}$ = 23 Hz, $^5J_{FF}$ = 7 Hz, 4 F, $F^{10/20}{}_{2/2}$) ppm.

IR (KBr): $\tilde{\nu}$ [cm^{-1}] = 3429 (NH^{amide}, br, vs), 2930 (CH, w), 1676 (CO, s), 1650 (CO, s), 1502 (vs), 1483 (vs), 1384 (s), 1288 (s), 1078 (CF, m), 995 (vs).

MS (FD): *m/z* (%) = 1356.58 (94) $[M]^+$, 1357.72 (90) $[M]^+$, 1358.60 (100) $[M]^+$.

MS (ESI): *m/z* (%) = 1356.19 (26) $[M]^+$.

HR-MS (ESI): obs. *m/z* = 1356.1545 $[M+H]^+$; calcd. for $[M]^+$ 1356.1522.

UV/Vis (CH_2Cl_2): λ [nm] (ε / [10^4 M^{-1}cm^{-1}]) = 423 (43.97), 552 (1.86), 592 (0.32).

Fluorescence (CH_2Cl_2): λ [nm] (relative intensity) = 602 (1.00), 651 (0.98).

Quantum yield: Φ = 0.0020.

Lifetime: τ [ps] = 142.73 (10), 15.33 (90%).

CV (Fc/Fc$^+$, 100 mV s^{-1}, CH_2Cl_2): $E_{½}$ [V] = −2.040 (irr.), −1.160, −0.090, 0.600, 0.880.

Triad 7. Dyad **5e** (70 mg, 0.077 mmol) and pyridine (2 mL) were dissolved in anhydrous toluene (20 mL). Thionyl chloride (30 μL, 0.39 mmol) was added and the reaction mixture was stirred under argon for 3h at room temperature. Excess of thionyl chloride and solvent were removed under reduced pressure. The residue was redissolved in an ultrasonic bath in toluene (20 mL) and pyridine (1 mL). Porphyrin **3d** (55.1 mg, 0.077 mmol) was dissolved in toluene (20 mL) and pyridine (1 mL) was added. The mixture was stirred overnight and the solvent was removed by evaporation under reduced pressure. The residue was purified by chromatography [silica, CH_2Cl_2 : ethylacetate (80:1), R_f = 0.43]. Yield: 48 mg (0.030 mmol, 39%), purple powder. $C_{108}H_{72}N_{10}O_6$ (1605.79).

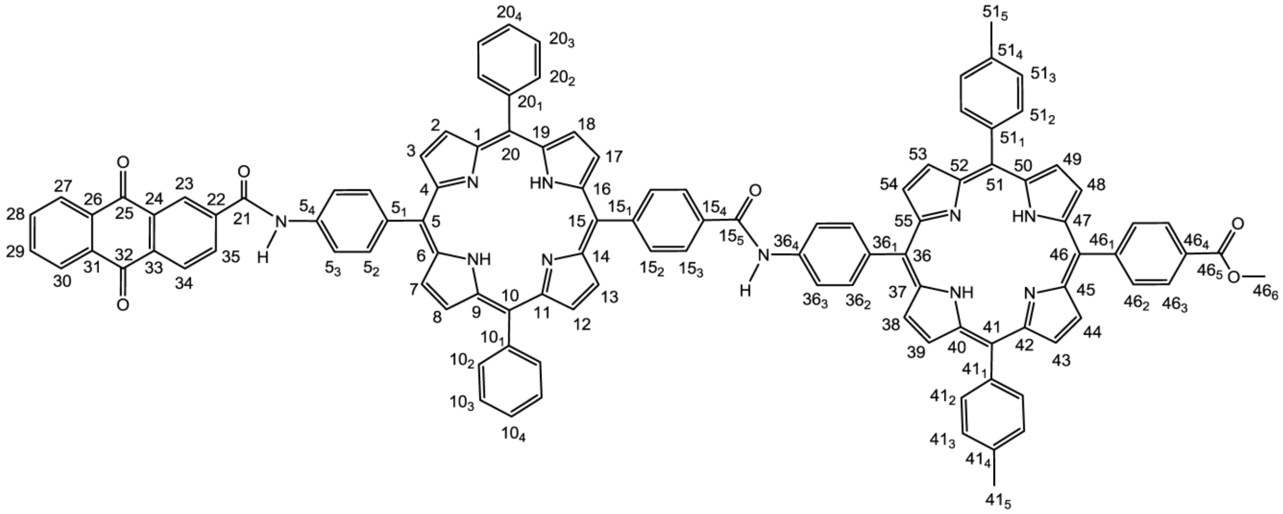

^{1}H-NMR (d_8-THF): δ = –2.65 (s, 2 H, $H^{pyrroleNH}$), –2.62 (s, 2 H, $H^{pyrroleNH}$), 2.71 (s, 6 H, $H^{41/51}_{5/5}$), 4.06 (s, 3 H, H^{46}_{6}), 7.62 (d, $^3J_{HH}$ = 7.7 Hz, 4 H, $H^{41/51}_{3/3}$), 7.81 (m, 6 H, $H^{10/20}_{3/4}$), 7.91 (m, 2 H, $H^{28/29}$), 8.12 (d, $^3J_{HH}$ = 7.8 Hz, 4 H, $H^{41/51}_{2/2}$), 8.26 (m, 8 H, $H^{5/10/20/36}_{2/2/2/2}$), 8.34 (d, $^3J_{HH}$ = 7.2 Hz, 4 H, $H^{15/36}_{2/3}$), 8.37 (m, 2 H, $H^{27/30}$), 8.44 (m, 6 H, $H^{5/15/46}_{3/3/2}$), 8.48 (d, $^3J_{HH}$ = 8.2 Hz, 1 H, H^{34}), 8.55 (d, $^3J_{HH}$ = 7.7 Hz, 2 H, H^{46}_{3}), 8.58 (dd, $^3J_{HH}$ = 8.7 Hz, $^4J_{HH}$ = 1.6 Hz, 1 H, H^{35}), 8.79 (d, $^3J_{HH}$ = 4.2

Hz, 2 H, $\mathrm{H}^{\mathrm{pyrrole}}$), 8.89 (m, 10 H, $\mathrm{H}^{\mathrm{pyrrole}}$), 8.96 (d, $^3J_{\mathrm{HH}}$ = 4.4 Hz, 2 H, $\mathrm{H}^{\mathrm{pyrrole}}$), 8.99 (m, 3 H, $\mathrm{H}^{23/\mathrm{Pyrrole}}$), 10.21 (s, 1 H, $\mathrm{H}^{\mathrm{amideNH}}$), 10.34 (s, 1 H, $\mathrm{H}^{\mathrm{amideNH}}$) ppm.

^{13}C{^{1}H}-NMR (d_8-THF): δ = 21.7 ($\mathrm{C}^{10/20}_{5/5}$), 52.6 (C^{46}_{6}), 119.4 (C^{36}_{3}), 119.3 (C^{5}_{3}), 121.5 ($\mathrm{C}^{41/51}$), n.o. ($\mathrm{C}^{10/20}$), 126.6 (C^{23}), 127.3 (C^{46}_{3}), 127.8 ($\mathrm{C}^{10/20}_{3/3}$), 128.0 (C^{27}), 128.0 (C^{30}), 128.6 ($\mathrm{C}^{41/51/34}_{3/3}$), 128.8 ($\mathrm{C}^{15/10/20}_{3/4/4}$), 131.0 ($\mathrm{C}^{15}_{4}$), 134.4 ($\mathrm{C}^{35}$), 135.2 ($\mathrm{C}^{28/29}$), 135.5, 135.5, 135.6, 135.6, 135.9 ($\mathrm{C}^{5/10/20/15/36/41/51}_{2/2/2/2/2/2/2}$), 136.6 ($\mathrm{C}^{33}$), 138.6 ($\mathrm{C}^{41/51}_{4/4}$), 138.8 ($\mathrm{C}^{36}_{1}$), 140.5 ($\mathrm{C}^{41/51}_{1/1}$), 140.7 ($\mathrm{C}^{5}_{4}$), n.o. ($\mathrm{C}^{22}$), n.o. ($\mathrm{C}^{21}$), n.o. ($\mathrm{C}^{15}_{5}$), n.o. ($\mathrm{C}^{25/32}$) ppm. Because of the poor solubility of **7** in THF not all ^{13}C resonances could be observed.

IR (KBr): $\tilde{\nu}$ [cm^{-1}] = 3451 ($\mathrm{NH}^{\mathrm{amide}}$, br, vs), 2927 (CH, w), 2851 (CH, w), 1746 (CO, m), 1678 (CO, s), 1650 (w), 1601 (s), 1517 (m), 1387 (s), 1317 (m), 1288 (m), 970 (w), 800 (m).

MS (FD): *m/z* (%) = 1605.5 (100) $[\mathrm{M}]^+$.

MS (ESI): *m/z* (%) = 803.79 (100) $[\mathrm{M+H}]^{2+}$, 1605.59 (8) $[\mathrm{M}]^+$.

HR-MS (ESI): obs. *m/z* = 1605.5693 $[\mathrm{M}]^+$; calcd. for $[\mathrm{M}]^+$ 1605.5667.

UV/Vis (CH_2Cl_2): λ [nm] (ε / [10^4 M^{-1}cm^{-1}]) = 422 (76.62), 516 (3.57), 552 (2.06), 591 (1.15), 647 (1.04).

Fluorescence (CH_2Cl_2): λ [nm] (relative intensity) = 653 (1.00), 718 (0.28).

Quantum yield: Φ = 0.0458.

Lifetime: τ [ns] = 4.07 (100%).

CV (Fc/Fc$^+$, 100 mV s^{-1}, CH_2Cl_2): $E_{½}$ [V] = −1.970, −1.590 (2e), −1.200, 0.560 (2e), 0.890.

Triad 8. Triad **7** (35 mg, 0.022 mmol) was dissolved in a mixture of freshly distilled THF and methanol (24 mL, 3:1) and 10% aqueous KOH (1 mL) was added. The mixture was stirred overnight, neutralised with acetic acid (1 mL) and diluted with CH_2Cl_2. The organic layer was separated, washed with water (3×), dried over $MgSO_4$ and the solvent was removed under reduced pressure. The product was used without additional purification [TLC, CH_2Cl_2 : methanol = 40:1, R_{f} = 0.57]. Yield: 34 mg (0.021 mmol, 97%), purple powder. $C_{107}H_{70}N_{10}O_6$ (1591.76).

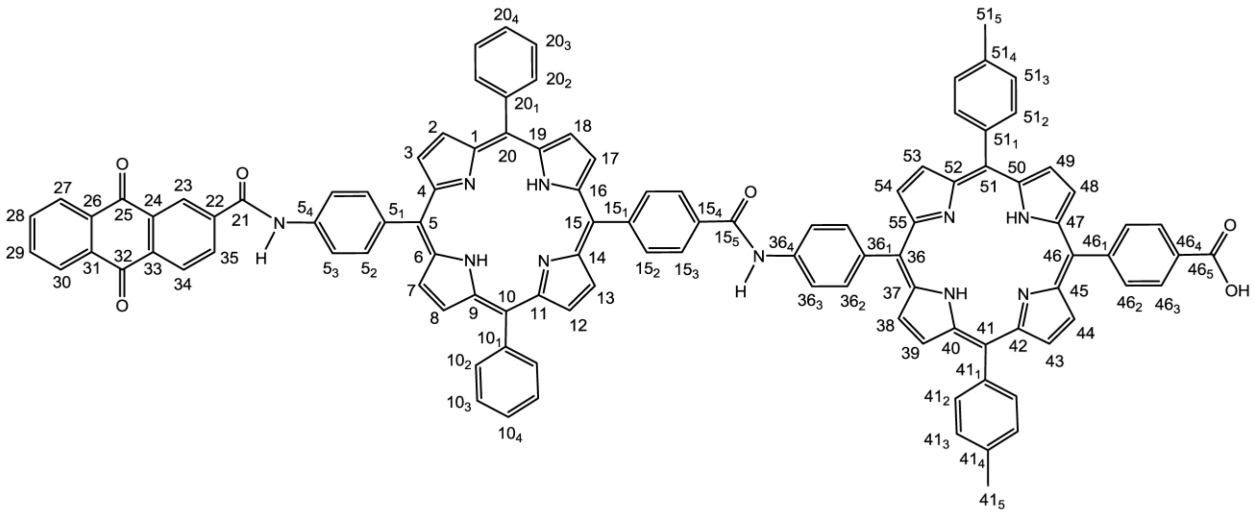

^{1}H-NMR (d_8-THF): δ = –2.64 (s, 2 H, $H^{pyrroleNH}$), –2.62 (s, 2 H, $H^{pyrroleNH}$), 2.71 (s, 6 H, $H^{41/51}{}_{5/5}$), 7.62 (d, $^3J_{HH}$ = 7.8 Hz, 4 H, $H^{41/51}{}_{3/3}$), 7.81 (m, 6 H, $H^{10/20}{}_{3/4}$), 7.92 (m, 2 H, $H^{28/29}$), 8.12 (d, $^3J_{HH}$ = 7.9 Hz, 4 H, $H^{41/51}{}_{2/2}$), 8.26 (m, 8 H, $H^{5/10/20/36}{}_{2/2/2/2}$), 8.34 (d, $^3J_{HH}$ = 7.2 Hz, 6 H, $H^{15/36/27/30}{}_{2/3}$), 8.44 (m, 6 H, $H^{5/15/46}{}_{3/3/2}$), 8.49 ($^3J_{HH}$ = 8.0 Hz, 1 H, H^{34}), 8.56 (d, $^3J_{HH}$ = 8.2 Hz, 2 H, $H^{46}{}_3$), 8.59 (dd, $^3J_{HH}$ = 7.9 Hz, $^4J_{HH}$ = 1.7 Hz, 1 H, H^{35}), 8.81 (d, $^3J_{HH}$ = 4.7 Hz, 2 H, $H^{pyrrolee}$), 8.91 (m, 10 H, $H^{pyrrole}$), 8.96 (d, $^3J_{HH}$ = 4.6 Hz, 2 H, $H^{pyrrole}$), 8.99 (m, 3 H, $H^{23/Pyrrole}$), 10.28 (s, 1 H, H^{amide}), 10.40 (s, 1 H, H^{amide}) ppm.

^{13}C{^{1}H}-NMR (d_8-THF): Poor solubility of **8** in THF.

IR (KBr): $\tilde{\nu}$ [cm^{-1}] = 3424 (NH^{amide}, br, s), 3321 ($NH^{pyrrole}$, s) 2928 (CH, w), 2860 (CH, w), 1742 (CO, w), 1676 (CO, s), 1595 (s), 1517 (s), 1384 (m), 1319 (m), 1290 (m), 966 (m), 790 (vs).

MS (FD): *m/z* (%) = 1592.6 (100) $[M+H]^+$.

MS (ESI): *m/z* (%) = 796.79 (99) $[M+H]^{2+}$, 1592.58 (5) $[M+H]^+$.

HR-MS (ESI): obs. *m/z* = 1591.5562 $[M+H]^+$; calcd. for $[M+H]^+$ 1591.5558.

UV/Vis (CH_2Cl_2): λ [nm] (ε / [10^4 M^{-1}cm^{-1}]) = 422 (20.63), 516 (1.30), 552 (0.91), 590 (0.66), 647 (0.59).

Fluorescence (CH_2Cl_2): λ [nm] (relative intensity) = 653 (1.00), 718 (0.28).

Quantum yield: Φ = 0.0497.

Tetrad 9. Triad **8** (30 mg, 0.019 mmol) and pyridine (1 mL) were dissolved in anhydrous toluene (30 mL) and thionyl chloride (7.0 µL, 0.095 mmol) was added. The reaction mixture was stirred under argon for 3h at room temperature. Excess of thionyl chloride and solvent were removed under reduced pressure. The residue was redisolved in an ultrasonic bath in toluene (30 mL) and pyridine (1 mL). Ferrocenylamine (5.0 mg, 0.025) dissolved in toluene (10 mL) and pyridine (1 mL) was added. The mixture was stirred overnight and solvent was removed under reduced pressure. The residue was purified by chromatography [silica, CH_2Cl_2, $R_f = 0.60$]. Yield: 7.7 mg (0.0043 mmol, 23%). $C_{117}H_{79}FeN_{11}O_5$ (1774.79).

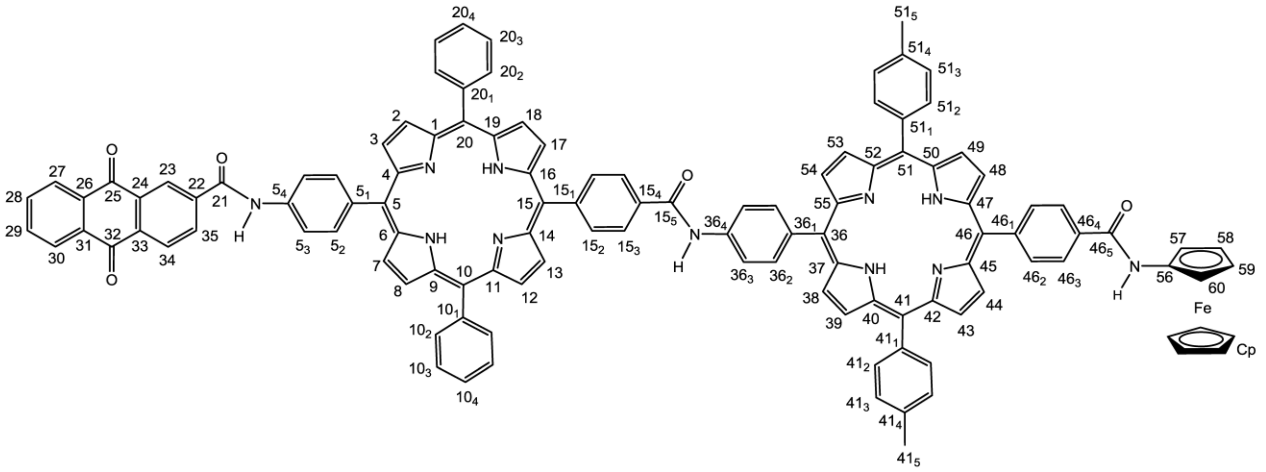

^{1}H-NMR (d_8-THF): $\delta = -2.63$ (s, 2 H, $H^{pyrroleNH}$), -2.62 (s, 2 H, $H^{pyrroleNH}$), 2.71 (s, 6 H, $H^{41/51}{}_{5/5}$), 4.06 (br. s, 2 H, $H^{58/59}$), 4.25 (s, 5 H, H^{Cp}), 4.96 (br. s, 2 H, $H^{57/60}$), 7.62 (d, $^3J_{HH} = 7.5$ Hz, 4 H, $H^{41/51}{}_{3/3}$), 7.81 (m, 6 H, $H^{10/20}{}_{3/4}$), 7.91 (m, 2 H, $H^{28/29}$), 8.13 (d, $^3J_{HH} = 7.7$ Hz, 4 H, $H^{41/51}{}_{2/2}$), 8.27 (m, 8 H, $H^{5/10/20/36}{}_{2/2/2/2}$), 8.36 (m, 6 H, $H^{15/36/27/30}{}_{2/3}$), 8.46 (m, 7 H, $H^{5/15/46/34}{}_{3/3/2}$), 8.55 (d, $^3J_{HH} = 8.1$ Hz, 2 H, $H^{46}{}_3$), 8.58 (d, $^3J_{HH} = 8.4$ Hz, 1 H, H^{35}), 8.84 (m, 2 H, $H^{pyrrole}$), 8.91 (m, 10 H, $H^{pyrrole}$), 8.96 (d, $^3J_{HH} = 4.5$ Hz, 2 H, $H^{pyrrole}$), 9.00 (m, 3 H, $H^{23/pyrrole}$), 9.21 (s, 1H, $H^{amideFcNH}$), 10.21 (s, 1 H, H^{amide}), 10.33 (s, 1 H, H^{amide}) ppm.

^{13}C{^{1}H}-NMR (d_8-THF): Poor solubility of **9** in THF.

IR (KBr): $\tilde{\nu}$ [cm^{-1}] = 3438 (NH^{amide}, $NH^{pyrrole}$, br, vs), 2923 (CH, w), 2855 (CH, w), 1676 (CO, vs), 1637 (vs), 1516 (s), 1382 (vs), 1319 (m), 1290 (s), 802 (m).

MS (FD): *m/z* (%) = 1774.0 (100) $[M]^+$.

MS (ESI): *m/z* (%) = 887.79 (53) $[M+H]^{2+}$, 1774.61 (5) $[M]^+$.

HR-MS (ESI): obs. *m/z* = 1774.5693 $[M]^+$; calcd. for $[M]^+$ 1774.5614.

UV/Vis (CH_2Cl_2): λ [nm] (ε / [10^4 M^{-1}cm^{-1}]) = 422 (77.48), 517 (3.74), 553 (2.14), 591 (1.14), 647 (1.02).

Fluorescence (CH_2Cl_2): λ [nm] (relative intensity) = 654 (1.00), 718 (0.28).

Quantum yield: $\Phi = 0.0145$.

Lifetime: τ [ps] = 2152.55 (33%), 361.77 (67%).

CV (Fc/Fc$^+$, 100 mV s^{-1}, CH_2Cl_2): $E_{½}$ [V] = −1.980, −1.600(2e), −1.190, −0.050, 0.590 (2e), 0.930.

***N*-ethyl-anthraquinone-2-carboxylic acid amide (10).** 60.0 mg (0.24 mmol) anthraquinone-2-carboxylic acid and pyridine (2 mL) were dissolved in anhydrous toluene (50 mL) and 90 µL (1.20 mmol) thionyl chloride was added. The reaction mixture was stirred under argon for 1h at room temperature. Excess of thionyl chloride and solvent were removed under reduced pressure. The residue was redisolved in an ultrasonic bath in toluene (40 mL) and pyridine (2 mL). Ethylamine (2 M solution in THF, 12 mL, 0.24 mmol) was added. The mixture was stirred for 1 h and quenched with water. The solution was dried with $MgSO_4$ and solvent was removed under reduced pressure. The residue was purified by chromatography [silica, toluene : ethylacetate (1:2), R_f = 0.63]. Yield 55.0 mg (0.20 mol, 82%), colorless solid. $C_{17}H_{13}NO_3$ (279.29).

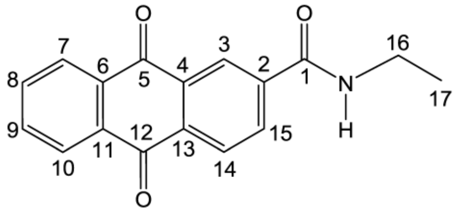

^{1}H-NMR (d_8-THF): δ = 1.23 (t, $^3J_{HH}$ = 7.3 Hz, 3 H, H^{17}), 3.45 (m, 2 H, H^{16}), 7.86 (m, 2 H, H$^{8/9}$), 8.12 (br. s, 1 H, H^{NH}), 8.30 (m, 2 H, H$^{7/10}$), 8.32 (m, 2 H, H$^{15/14}$), 8.67 (br. s, 1 H, H^3) ppm.

^{13}C{^{1}H}-NMR (d_8-THF): δ = 15.4 (C^{17}), 35.7 (C^{16}), 126.1 (C^3), 127.9, 127.9 (C$^{7/10}$), 128.0 (C^{14}), 133.9 (C^{15}), 134.6 (C^4), 134.8, 134.8 (C$^{6/11}$), 135.1, 135.1 (C$^{8/9}$), 136.1 (C^{13}), 141.4 (C^2), 165.5 (C^1), 183.0, 183.2 (C$^{5/12}$) ppm.

IR (KBr): $\tilde{\nu}$ [cm^{-1}] = 3276 (NH^{amide}, b, vs), 3076 (CH, w), 2974 (CH, w), 2934 (CH, w), 1676(CO, vs), 1637 (vs), 1593 (m), 1547 (s), 1288 (CN, vs), 976 (m), 932 (m), 873 (m).

MS (FD): *m/z* (%) = 139.96 (9) [M]$^{2+}$, 279.45 (100) [M]$^+$, 559.69 (1) [2M]$^+$.

MS (ESI): *m/z* (%) = 279.13 (2) [M]$^+$, 280.09 (100) [M+H]$^+$, 302.07 (41) [M+Na]$^+$, 581.17 (31) [2M+Na]$^+$.

HR-MS (ESI): obs. *m/z* = 302.0805 [M+Na]$^+$; calcd. for [M+Na]$^+$ 302.0793.

Elemental analysis calcd. (%) for $C_{17}H_{13}NO_3$ (279.29): C, 73.11; H, 4.69; N, 5.02. Found: C, 72.41; H, 4.90; N, 5.04.

UV/Vis (CH_2Cl_2): λ [nm] (ε / [10^4 M^{-1}cm^{-1}]) = 328 (0.53).

CV (Fc/Fc$^+$, 100 mV s^{-1}, CH_2Cl_2): $E_{½}$ [V] = −1.805, −1.275.

General procedure for *N*-acylation: To a mixture of the amino porphyrin (1 eq.) and acetyl chloride (35 eq.) was added iodine (1 eq.) and the mixture was stirred at room temperature overnight. The iodine was destroyed by addition of a saturated aqueous $Na_2S_2O_3$ solution. CH_2Cl_2 was added and the organic phase was separated, washed with saturated aqueous $NaHCO_3$ solution (2×), brine (1×), water (2×) and dried with Na_2SO_4. The solvent was removed under reduced pressure and the residue was filtered over a silica pad.

5-(4-(*N*-Acetylaminophenyl))-10,20-bis((4-butoxy)phenyl)-15-(4-(methoxycarbonylphenyl)) porphyrin (Ac-3a). 19.5 mg (0.023 mmol) **3a**, 5.3 mL (0.074 mmol) acetyl chloride, 5.3 mg (0.021

mmol) iodine. [silica, toluene : ethyl acetate (1:1), $R_f = 0.32$]. Yield: 17.2 mg (0.020 mmol, 86%), purple powder. $C_{56}H_{51}N_5O_5$ (874.03).

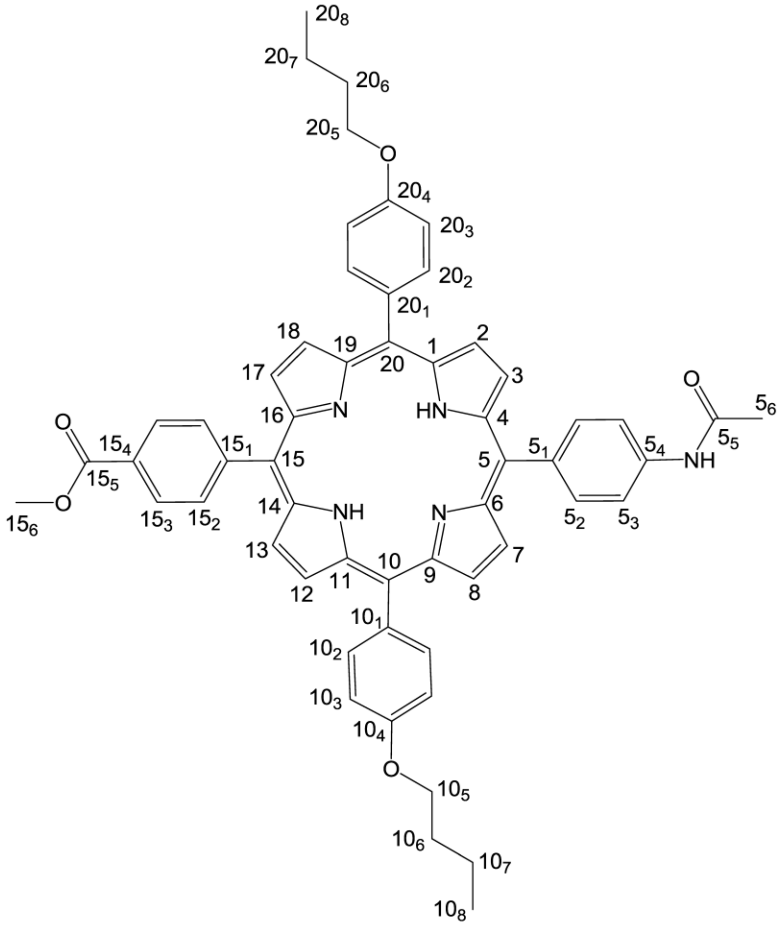

^{1}H-NMR (d$_8$-THF): $\delta = -2.68$ (s, 2 H, $H^{pyrroleNH}$), 1.10 (t, $^3J_{HH} = 7.4$ Hz, 6 H, $H^{10/20}{}_{8/8}$), 1.69 (m, 4 H, $H^{10/20}{}_{7/7}$), 1.95 (m, 4 H, $H^{10/20}{}_{6/6}$), 2.21 (s, 3 H, $H^5{}_6$), 4.05 (s, 3 H, $H^{15}{}_6$), 4.27 (t, $^3J_{HH} = 6.3$ Hz, 4 H, $H^{10/20}{}_{5/5}$), 7.32 (d, $^3J_{HH} = 8.4$ Hz, 4 H, $H^{10/20}{}_{3/3}$), 8.07 (m, 8 H, $H^{5/5/10/20}{}_{2/3/2/2}$), 8.32 (d, $^3J_{HH} = 8.0$ Hz, 2 H, $H^{15}{}_2$), 8.43 (d, $^3J_{HH} = 8.0$ Hz, 4 H, $H^{15}{}_3$), 8.76 (d, $^3J_{HH} = 4.2$ Hz, 2 H, $H^{pyrrole}$), 8.86 (m, 6 H, $H^{pyrrole}$), 9.48 (s, 1 H, $H^{amideNH}$) ppm.

^{13}C{^{1}H}-NMR (d$_8$-THF): $\delta = 14.4$ ($C^{10/20}{}_{8/8}$), 20.4 ($C^{10/20}{}_{7/7}$), 24.3 ($C^5{}_6$), 32.6 ($C^{10/20}{}_{6/6}$), 52.4 ($C^{15}{}_6$), 68.6 ($C^{10/20}{}_{5/5}$), 113.6 ($C^{10/20}{}_{3/3}$), 117.9 ($C^5{}_3$), 119.2 (C^{15}), 121.1 ($C^{10/20}$), 121.3 (C^5), 128.7 ($C^{15}{}_3$), 130.8 ($C^{15}{}_4$), 131.7 (br. s, $C^{pyrrole\ 2/3/7/8/12/13/17/18}$), 135.2 ($C^{10/20}{}_{1/1}$), 135.4 ($C^{15}{}_2$), 135.6 ($C^5{}_2$) 136.4 ($C^{10/20}{}_{2/2}$), 137.6 ($C^5{}_1$), 140.9 ($C^5{}_4$), 148.2 ($C^{15}{}_1$), 160.4 ($C^{10/20}{}_{4/4}$), 167.3 ($C^{15}{}_5$), 168.7 ($C^5{}_5$) ppm.

IR (KBr): $\tilde{\nu}$ [cm^{-1}] = 3431 (NH^{amine}, $NH^{pyrrole}$, br, vs), 2959 (CH, w), 2928 (CH, w), 2864 (CH, w), 1722 (CO, m), 1606 (s), 1512 (s), 1468 (w), 1283 (s), 1245 (C-O-C, vs), 800 (m).

MS (FD): *m/z* (%) = 873.74 (100) $[M]^+$.

MS (ESI): *m/z* (%) = 437.70 (6) $[M^{2+}+H]$, 874.39 (100) $[M+H]^+$, 1748.79 (2) $[2M+H]^+$.

HR-MS (ESI): obs. *m/z* = 874.3967 $[M+H]^+$; calcd. for $[M+H]^+$ 874.3968.

UV/Vis ($\mathrm{CH_2Cl_2}$): λ [nm] (ε / [10^4 $\mathrm{M^{-1}cm^{-1}}$]) = 422 (30.03), 517 (1.14), 555 (0.73), 593 (0.63), 649 (0.65).

Fluorescence ($\mathrm{CH_2Cl_2}$): λ [nm] (relative intensity) = 657 (1.00), 720 (0.25).

Quantum yield: $\Phi = 0.1594$.

Lifetime: τ [ns] = 9.28 (100%).

CV (Fc/Fc$^+$, 100 mV s^{-1}, $\mathrm{CH_2Cl_2}$): $E_{½}$ [V] = –1.980, –1.640, 0.480, 0.730.

5-(4-(*N*-Acetylaminophenyl))-10,20-bis((4-methoxy)phenyl)-15-(4-(methoxycarbonylphenyl)) porphyrin (Ac-3b). 13.0 mg (0.017 mmol) porphyrin **3b**, 4.0 mL (0.054 mmol) acetyl chloride, 4.0 mg (0.016 mmol) iodine. [silica, toluene : ethyl acetate (1:1), R_f = 0.28]. Yield: 11.0 mg (0.014 mmol, 82%), purple powder. $\mathrm{C_{50}H_{39}N_5O_5}$ (789.88).

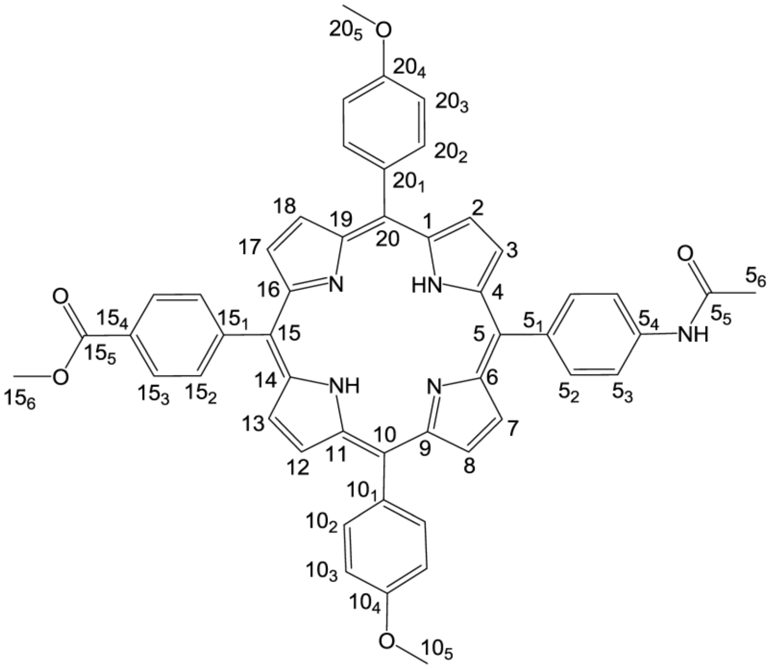

^{1}H-NMR (d$_8$-THF): δ = –2.68 (s, 2 H, $\mathrm{H^{pyrroleNH}}$), 2.20 (s, 3 H, $\mathrm{H}^{5}{}_{6}$), 4.05 (s, 3 H, $\mathrm{H}^{15}{}_{6}$), 4.06 (s, 6 H, $\mathrm{H}^{10/20}{}_{5/5}$), 7.33 (d, $^3J_\mathrm{HH}$ = 8.5 Hz, 4 H, $\mathrm{H}^{10/20}{}_{3/3}$), 8.05 (d, $^3J_\mathrm{HH}$ = 8.4 Hz, 2 H, $\mathrm{H}^{5}{}_{3}$), 8.10 (d, $^3J_\mathrm{HH}$ = 8.5 Hz, 6 H, $\mathrm{H}^{5/10/20/}{}_{2/2/2}$), 8.31 (d, $^3J_\mathrm{HH}$ = 8.1 Hz, 4 H, $\mathrm{H}^{15}{}_{2}$), 8.44 (d, $^3J_\mathrm{HH}$ = 8.5 Hz, 2 H, $\mathrm{H}^{15}{}_{3}$), 8.76 (d, $^3J_\mathrm{HH}$ = 4.3 Hz, 2 H, $\mathrm{H^{pyrrole}}$), 8.86 (m, 6 H, $\mathrm{H^{pyrrole}}$), 9.45 (s, 1 H, $\mathrm{H^{amideNH}}$) ppm.

^{13}C{^{1}H}-NMR (d$_8$-THF): δ = 24.4 ($\mathrm{C}^{5}{}_{6}$), 52.5 ($\mathrm{C}^{15}{}_{6}$), 52.9 ($\mathrm{C}^{10/20}{}_{5/5}$), 113.3 ($\mathrm{C}^{10/20}{}_{3/3}$), 118.1 ($\mathrm{C}^{5}{}_{3}$), 119.3 (s, C^{15}), 121.2 ($\mathrm{C}^{10/20}$), 121.5 (C^{5}), 128.8 ($\mathrm{C}^{15}{}_{3}$), 130.9 ($\mathrm{C}^{15}{}_{4}$), 131.9 (br. s, $\mathrm{C}^{\mathrm{pyrrole}}{}_{2/3/7/8/12/13/17/18}$), 135.4 ($\mathrm{C}^{10/20}{}_{1/1}$), 135.5 ($\mathrm{C}^{5}{}_{2}$), 135.8 ($\mathrm{C}^{15}{}_{2}$), 136.5 ($\mathrm{C}^{10/20}{}_{2/2}$), 137.7 ($\mathrm{C}^{5}{}_{1}$), 141.0 ($\mathrm{C}^{5}{}_{4}$), 148.3 (s, $\mathrm{C}^{15}{}_{1}$), 161.0 ($\mathrm{C}^{10/20}{}_{4/4}$), 167.4 ($\mathrm{C}^{15}{}_{5}$), 168.8 ($\mathrm{C}^{5}{}_{5}$) ppm.

IR (KBr): $\tilde{\nu}$ [cm^{-1}] = 3433 ($\mathrm{NH^{amide}}$, $\mathrm{NH^{pyrrole}}$, br, s), 2926 (CH, w), 2855 (CH, w), 1722 (CO, m), 1605 (s), 1510 (s), 1468 (w), 1385 (m), 1286 (s), 1248 (C-O-C, vs), 802 (m).

MS (FD): *m/z* (%) = 789.80 (100) [M]$^+$.

MS (ESI): *m/z* (%) = 395.65 (15) $[M+H]^{2+}$, 790.22 (100) $[M+H]^+$, 1580.45 (2) $[2M+H]^+$.

HR-MS (ESI): obs. *m/z* = 790.3032 $[M+H]^+$; calcd. for $[M+H]^+$ 790.3029.

UV/Vis (CH_2Cl_2): λ [nm] (ε / [10^4 $M^{-1}cm^{-1}$]) = 421 (35.40), 517 (1.38), 554 (0.87), 593 (0.45), 648 (0.42).

Fluorescence (CH_2Cl_2): λ [nm] (relative intensity) = 657 (1.00), 719 (0.26).

Quantum yield: Φ = 0.1348.

Lifetime: τ [ns] = 9.49 (100%).

CV (Fc/Fc$^+$, 100 mV s^{-1}, CH_2Cl_2): $E_{½}$ [V] = –1.970, –1.630, 0.510, 0.750.

5-(4-(*N*-Acetylaminophenyl))-10,20-bis(4-methylphenyl)-15-(4-(methoxycarbonyl-phenyl)) porphyrin (Ac-3d). 54.0 mg (0.076 mmol) porphyrin **3d**, 17.2 mL (0.240 mmol) acetyl chloride, 18.0 mg (0.071 mmol) iodine. [silica, toluene : ethyl acetate (1:1), R_f = 0.48]. Yield: 52.0 mg (0.069 mmol, 91%), purple powder. $C_{50}H_{39}N_5O_3$ (757.87).

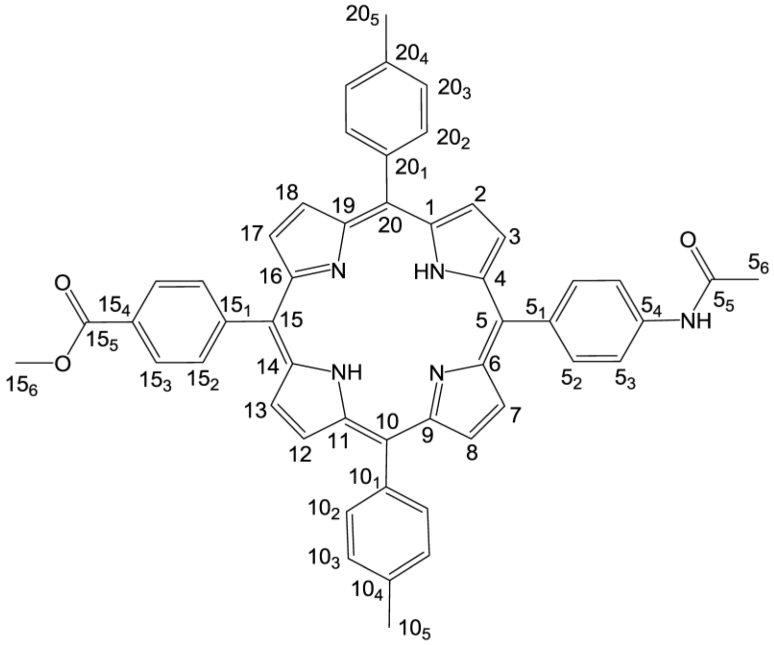

^{1}H-NMR (d_8-THF): δ = –2.70 (s, 2 H, $H^{pyrroleNH}$), 2.20 (s, 3 H, $H^5{}_6$), 2.68 (s, 6 H, $H^{10/20}{}_{5/5}$), 4.05 (s, 3 H, $H^{15}{}_6$), 7.58 (d, $^3J_{HH}$ = 7.6 Hz, 4 H, $H^{10/20}{}_{3/3}$), 8.07 (m, 8 H, $H^{10/20/5/5}{}_{2/2/2/3}$), 8.31 (d, $^3J_{HH}$ = 7.9 Hz, 2 H, $H^{15}{}_2$), 8.43 (d, $^3J_{HH}$ = 8.0 Hz, 2 H, $H^{15}{}_3$), 8.76 (d, $^3J_{HH}$ = 4.2 Hz, 2 H, $H^{pyrrole}$), 8.84 (m, 6 H, $H^{pyrrole}$), 9.44 (s, 1 H, $H^{amideNH}$) ppm.

^{13}C{^{1}H}-NMR (d_8-THF): δ = 21.8 ($C^{10/20}{}_{5/5}$), 24.6 ($C^5{}_6$) 52.7 ($C^{15}{}_6$), 118.2 ($C^5{}_3$), 119.5 (C^{15}), 121.5 ($C^{10/20}$), 121.6 (C^5), 128.6 ($C^{10/20}{}_{3/3}$), 128.9 ($C^{15}{}_3$), 131.0 ($C^{15}{}_4$), 132.1 (br. s, $C^{pyrrole\ 2/3/7/8/12/13/17/18}$), 135.6 ($C^{10/20}{}_{2/2}$), 135.7 ($C^{15}{}_2$), 135.9 ($C^5{}_2$), 137.8 ($C^5{}_1$), 138.6 ($C^{10/20}{}_{4/4}$), 141.2 ($C^5{}_4$), 140.6 ($C^{10/20}{}_{1/1}$), 148.3 ($C^{15}{}_1$), 167.5 ($C^{15}{}_5$), 168.9 ($C^5{}_5$) ppm.

IR (KBr): $\tilde{\nu}$ [cm^{-1}] = 3402 (NH^{amide}, br, s), 3320 (NH^{pyrrole}, w), 3025 (CH, w), 2919 (CH, w), 1733 (CO, vs), 1609 (m), 1511 (m), 1274 (C-O-C, vs), 800 (s), 734 (s).

MS (FD): *m/z* (%) = 757.3 (100) [M]$^+$.

MS (ESI): *m/z* (%) = 758.32 (100) [M+H]$^+$.

HR-MS (ESI): obs. *m/z* = 758.3128 [M+H]$^+$; calcd. for [M+H]$^+$ 758.3131.

UV/Vis (CH_2Cl_2): λ [nm] (ε / [10^4 M^{-1}cm^{-1}]) = 420 (33.60), 516 (1.27), 552 (0.71), 592 (0.39), 647 (0.35).

Fluorescence (CH_2Cl_2): λ [nm] (relative intensity) = 654 (1.00), 719 (0.29).

Quantum yield: Φ = 0.1311.

Lifetime: τ [ns] = 9.69 (100%).

CV (Fc/Fc$^+$, 100 mV s^{-1}, CH_2Cl_2): $E_{½}$ [V] = –1.950, –1.610, 0.520, 0.830.

5-(4-(*N*-Acetylaminophenyl))-10,20-bis(phenyl)-15-(4-(methoxycarbonylphenyl)) porphyrin (Ac-3e). 40.0 mg (0.058 mmol) porphyrin **3e**, 13.1 mL (0.180 mmol) acetyl chloride, 13.7 mg (0.054 mmol) iodine. [silica, toluene : ethyl acetate (1:1), R_f = 0.60]. Yield: 38.9 mg (0.053 mmol, 92%), purple powder. $C_{48}H_{35}N_5O_3$ (729.82).

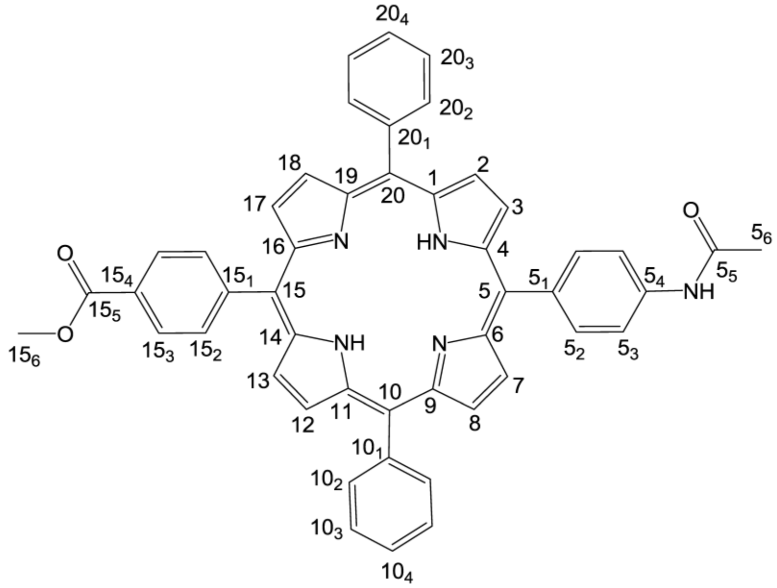

^{1}H-NMR (d^8-THF): δ = –2.69 (s, 2 H, H^{pyrroleNH}), 2.20 (s, 3 H, H$^5{}_6$), 4.04 (s, 3 H, H$^{15}{}_6$), 7.77 (m, 6 H, H$^{10/20}{}_{3/4}$), 8.06 (d, $^3J_{HH}$ = 8.4 Hz, 2 H, H$^5{}_3$), 8.11 (d, $^3J_{HH}$ = 8.4 Hz, 2 H, H$^5{}_2$), 8.20 (m, 2 H, H$^{10/20}{}_{2/2}$), 8.32 (d, $^3J_{HH}$ = 8.1 Hz, 2 H, H$^{15}{}_2$), 8.43 (d, $^3J_{HH}$ = 8.0 Hz, 2 H, H$^{15}{}_3$), 8.78 (d, $^3J_{HH}$ = 4.5 Hz, 2 H, H^{pyrrole}), 8.82 (m, 4 H, H^{pyrrole}), 8.89 (d, $^3J_{HH}$ = 4.3 Hz, 2 H, H^{pyrrole}), 9.49 (s, 1 H, H^{amideNH}) ppm.

^{13}C{^{1}H}-NMR (d$_8$-THF): δ = 24.4 (C$^5{}_6$) 52.5 (C$^{15}{}_6$), 118.1 (C$^5{}_3$), 119.5 (C^{15}), 121.3 (C$^{10/20}$), 121.7 (C^5) 127.8 (C$^{10/20}{}_{3/3}$), 128.8 (C$^{10/20}{}_{4/4}$), 128.8 (C$^{15}{}_3$), 130.9 (C$^{15}{}_4$), 132.0 (br. s, C$^{pyrrole\ 2/3/7/8/12/13/17/18}$), 135.5 ($C^{10/20}{}_{2/2}$), 135.6 ($C^{15}{}_{2}$), 135.8 ($C^{5}{}_{2}$), 137.6 ($C^{5}{}_{1}$), 141.1 ($C^{5}{}_{4}$), 143.4 ($C^{10/20}{}_{1/1}$), 148.1 ($C^{15}{}_{1}$), 167.4 ($C^{15}{}_{5}$), 168.8 ($C^{5}{}_{5}$) ppm.

IR (KBr): $\tilde{\nu}$ [cm^{-1}] = 3404 (NH^{amide}, br, w), 3314 (NH^{pyrrole}, br, w), 2947 (CH, w), 2924 (CH, w), 1708 (CO, vs), 1511 (vs), 1600 (s), 1394 (m), 1282 (C-O-C, vs), 798 (s).

MS (FD): *m/z* (%) = 729.3 (100) [M]$^+$.

MS (ESI): *m/z* (%) = 730.33 (62) [M+H]$^+$.

HR-MS (ESI): obs. *m/z* = 730.2808 [M+H]$^+$; calcd. for [M+H]$^+$ 730.2818.

UV/Vis (CH_2Cl_2): λ [nm] (ε / [10^4 M^{-1}cm^{-1}]) = 419 (32.6), 515 (1.34), 551 (0.68), 591 (0.43), 646 (0.34).

Fluorescence (CH_2Cl_2): λ [nm] (relative intensity) = 652 (1.00), 717 (0.31).

Quantum yield: Φ = 0.1167.

Lifetime: τ [ns] = 9.88 (100%).

CV (Fc/Fc$^+$, 100 mV s^{-1}, CH_2Cl_2): $E_{½}$ [V] = –2.000, –1.630, 0.550, 0.840.

General procedure for zinc(II) porphyrin complexes. Porphyrin (1 eq.) and zinc acetate dihydrate (5 eq.) were stirred overnight in CH_2Cl_2 (10 mL). After concentration under reduced pressure the product was isolated by column chromatography.

[5-(4-(*N*-Acetylaminophenyl))-10,20-bis((4-butoxy)phenyl)-15-(4-(methoxycarbonylphenyl)) porphyrinato]zinc(II) (Zn-Ac-3a). Ac-3a (8.9 mg, 0.010 mmol), zinc acetate dehydrate (11.2 mg, 0.051 mmol). [silica, toluene : ethyl acetate (1:1), R_f = 0.50]. Yield: 8.7 mg (0.0093 mmol, 93%), purple powder. $C_{56}H_{49}N_5O_5Zn$ (937.43).

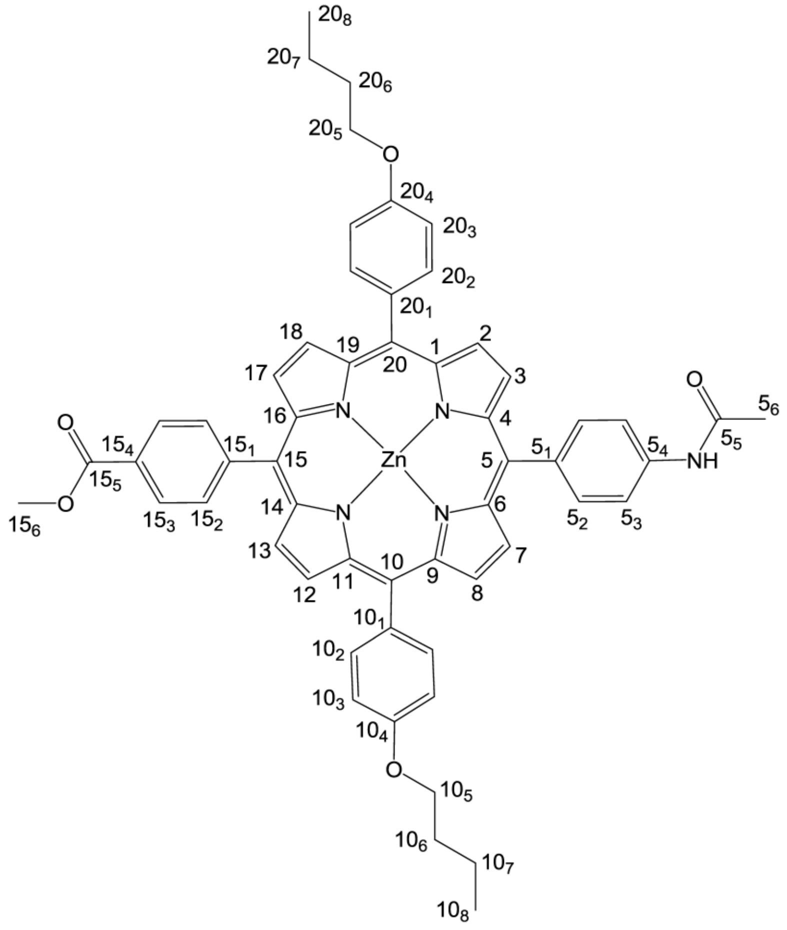

^{1}H-NMR (d_8-THF): δ = 1.11 (t, $^3J_{HH}$ = 7.4 Hz, 6 H, $H^{10/20}{}_{8/8}$), 1.70 (m, 4 H, $H^{10/20}{}_{7/7}$), 1.96 (m, 4 H, $H^{10/20}{}_{6/6}$), 2.21 (s, 3 H, $H^5{}_6$), 4.05 (s, 3 H, $H^{15}{}_6$), 4.27 (t, $^3J_{HH}$ = 6.3 Hz, 4 H, $H^{10/20}{}_{5/5}$), 7.29 (d, $^3J_{HH}$ = 8.4 Hz, 4 H, $H^{10/20}{}_{3/3}$), 8.02 (d, $^3J_{HH}$ = 8.3 Hz, 4 H, $H^5{}_3$), 8.07 (m, 4 H, $H^{10/20/5}{}_{2/2/2}$), 8.30 (d, $^3J_{HH}$ = 8.0 Hz, 2 H, $H^{15}{}_2$), 8.43 (d, $^3J_{HH}$ = 8.0 Hz, 4 H, $H^{15}{}_3$), 8.78 (d, $^3J_{HH}$ = 4.6 Hz, 2 H, $H^{pyrrole}$), 8.89 (m, 6 H, $H^{pyrrole}$), 9.43 (s, 1 H, $H^{amideNH}$) ppm.

^{13}C{^{1}H}-NMR (d_8-THF): δ = 14.5 ($C^{10/20}{}_{8/8}$), 20.5 ($C^{10/20}{}_{7/7}$), 24.4 ($C^5{}_6$) 32.8 ($C^{10/20}{}_{6/6}$), 52.5 ($C^{15}{}_6$), 68.7 ($C^{10/20}{}_{5/5}$), 113.3 ($C^{10/20}{}_{3/3}$), 117.7 ($C^5{}_3$), 119.8 (s, C^{15}), 121.7 ($C^{10/20}$), 121.9 (C^5), 128.4 ($C^{15}{}_3$), 130.4 ($C^{15}{}_4$), 131.7, 132.4, 132.7 ($C^{pyrrole\ 2/3/7/8/12/13/17/18}$), 135.6 ($C^5{}_2$), 135.7 ($C^{15}{}_2$), 136.4 ($C^{10/20}{}_{2/2}$), 136.6 ($C^{10/20}{}_{1/1}$), 139.1 ($C^5{}_1$), 140.6 ($C^5{}_4$), 149.7 ($C^{15}{}_1$), 150.5, 151.4, 151.5, 151.7 ($C^{pyrrole\ 1/4/6/9/11/14/16/19}$), 160.2 ($C^{10/20}{}_{4/4}$), 167.5 ($C^{15}{}_5$), 168.7 ($C^5{}_5$) ppm.

IR (KBr): $\tilde{\nu}$ [cm^{-1}] = 3411 (NH^{amide}, br, w), 2957 (CH, m), 2928 (CH, m), 2870 (CH, m), 1701, 1650 (CO, s), 1604 (s), 1516 (vs), 1385 (s), 1280 (C-O-C, s), 1246 (C-O-C, s), 997 (m), 800 (m).

MS (FD): *m/z* (%) = 935.72 (100) [M]$^+$, 936.69 (57) [M]$^+$, 937.70 (79) [M]$^+$.

MS (ESI): *m/z* (%) = 935.32 (58) [M]$^+$, 936.32 (39) [M]$^+$, 937.32 (45) [M]$^+$.

HR-MS (ESI): obs. *m/z* = 935.3068 [M]$^+$; calcd. for [M]$^+$ 935.3025.

UV/Vis (CH_2Cl_2): λ [nm] (ε / [10^4 M^{-1}cm^{-1}]) = 424 (40.10), 552 (1.75), 594 (0.65).

Fluorescence (CH_2Cl_2): λ [nm] (relative intensity) = 606 (1.00), 651(0.60).

Quantum yield: $\Phi = 0.1003$.

Lifetime: τ [ns] = 1.71 (100%).

CV (Fc/Fc$^+$, 100 mV s^{-1}, CH_2Cl_2): $E_{½}$ [V] = −2.160, −1.790, 0.300, 0.720 (irr).

[5-(4-(*N*-Acetylaminophenyl))-10,20-bis((4-methoxy)phenyl)-15-(4-(methoxycarbonylphenyl)) porphyrinato]zinc(II) (Zn-Ac-3b). Ac-3b (5 mg, 0.0063 mmol), zinc acetate dihydrate (7.0 mg, 0.032 mmol). [silica, toluene : ethyl acetate (1:1), $R_f = 0.32$]. Yield 5.1 mg (0.0060 mmol, 94%), purple powder. $C_{50}H_{37}N_5O_5Zn$ (853.27).

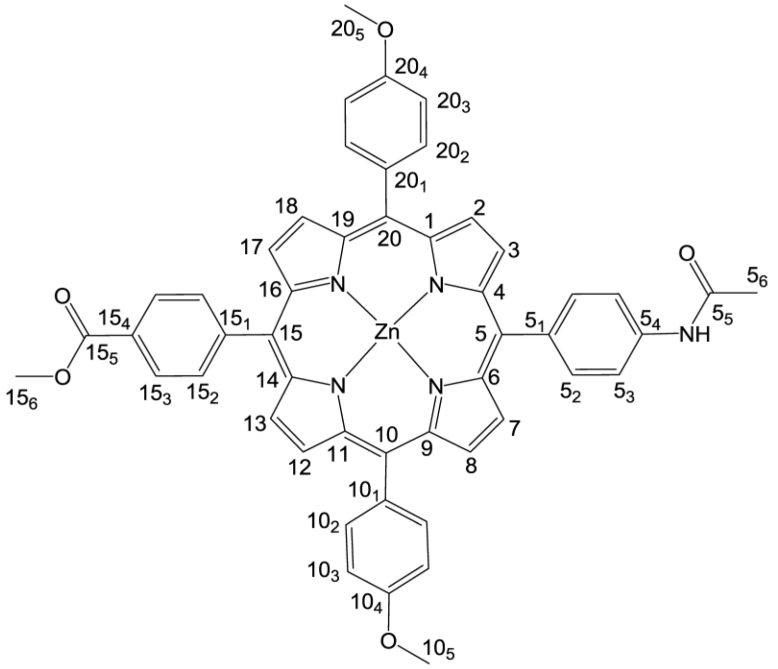

^{1}H-NMR (d$_8$-THF): δ = 2.20 (s, 3 H, $H^5{}_6$), 4.04 (s, 3 H, $H^{15}{}_6$), 4.06 (s, 9 H, $H^{10/20}{}_{5/5}$), 7.29 (d, $^3J_{HH}$ = 8.3 Hz, 4 H, $H^{10/20}{}_{3/3}$), 8.01 (d, $^3J_{HH}$ = 8.2 Hz, 2 H, $H^5{}_3$), 8.07 (d, $^3J_{HH}$ = 8.2 Hz, 6 H, $H^{5/10/20}{}_{2/2/2}$), 8.29 (d, $^3J_{HH}$ = 8.0 Hz, 2 H, $H^{15}{}_2$), 8.40 (d, $^3J_{HH}$ = 8.0 Hz, 4 H, $H^{15}{}_3$), 8.77 (d, $^3J_{HH}$ = 4.5 Hz, 2 H, $H^{pyrrole}$), 8.88 (m, 6 H, $H^{pyrrole}$), 9.42 (s, 1 H, $H^{amideNH}$) ppm.

^{13}C{^{1}H}-NMR (d$_8$-THF): δ = 24.4 ($C^5{}_6$), 52.5 ($C^{15}{}_6$), 55.9 ($C^{10/20}{}_{5/5}$), 112.9 ($C^{10/20}{}_{3/3}$), 117.7 ($C^5{}_3$), 119.8 (C^{15}), 121.6 ($C^{10/20}$), 121.9 (C^5), 128.4 ($C^{15}{}_3$), 130.4 ($C^{15}{}_4$), 131.7, 132.4, 132.4, 132.7 ($C^{pyrrole\ 2/3/7/8/12/13/17/18}$), 135.6 ($C^5{}_2$), 135.7 ($C^{15}{}_2$), 136.4 ($C^{10/20}{}_{2/2}$), 136.7 ($C^{10/20}{}_{1/1}$), 139.0 ($C^5{}_1$), 140.6 ($C^5{}_4$), 149.7 ($C^{15}{}_1$), 150.5, 151.4, 151.5, 151.7 ($C^{pyrrole\ 1/4/6/9/11/14/16/19}$), 160.7 ($C^{10/20}{}_{4/4}$), 167.5 ($C^{15}{}_5$), 168.7 ($C^5{}_5$) ppm.

IR (KBr): $\tilde{\nu}$ [cm^{-1}] = 3420 (NH^{amide}, br, w), 2924 (CH, m), 2853 (CH, m), 1703 (CO, s), 1653 (s), 1514 (vs), 1384 (vs), 1280 (C-O-C, m), 1246 (C-O-C, s), 999 (s), 802 (m).

MS (FD): m/z (%) = 851.28 (100) $[M]^+$.

MS (ESI): m/z (%) = 852.23 (3) $[M]^+$, 853.23 (2) $[M]^+$.

HR-MS (ESI): obs. m/z = 851.2092 $[M]^+$; calcd. for $[M]^+$ 851.2086.

UV/Vis (CH_2Cl_2): λ [nm] (ε / [10^4 $M^{-1}cm^{-1}$]) = 424 (48.62), 551 (1.90), 593 (0.63).

Fluorescence (CH_2Cl_2): λ [nm] (relative intensity) = 606 (1.00), 651(0.61).

Quantum yield: Φ = 0.0940.

Lifetime: τ [ns] = 1.81 (100%).

CV (Fc/Fc$^+$, 100 mV s^{-1}, CH_2Cl_2): $E_{½}$ [V] = –1.780, 0.310, 0.710.

[5-(4-(*N*-Acetylaminophenyl))-10,20-bis((4-methyl)phenyl)-15-(4-(methoxycarbonylphenyl)) porphyrinato]zinc(II) (Zn-Ac-3d). Ac-3d (20 mg, 0.024 mmol), zinc acetate dihydrate (26 mg, 0.12 mmol). [silica, toluene : ethyl acetate (1:1), R_f = 0.42]. Yield 20.0 mg (0.024 mmol, 100%), purple powder. $C_{50}H_{37}N_5O_3Zn$ (821.27).

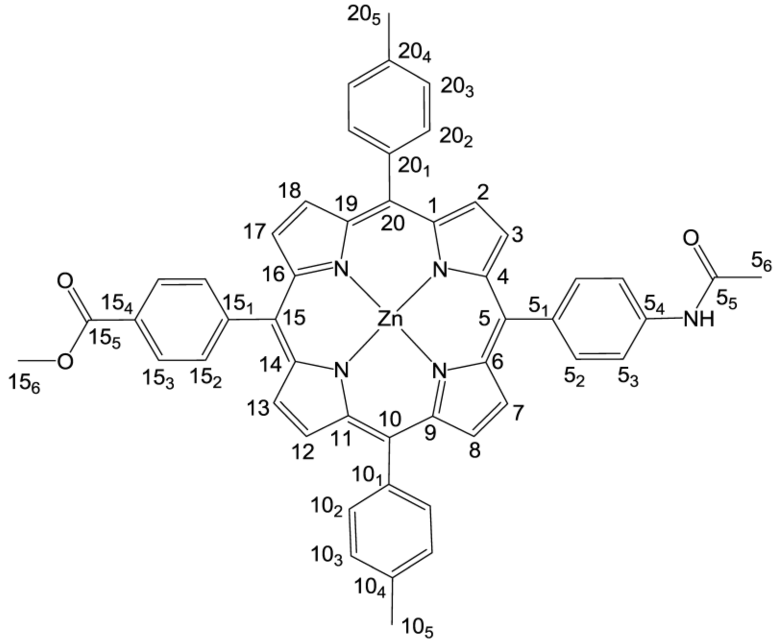

^{1}H-NMR (d_8-THF): δ = 2.20 (s, 3 H, $H^5{}_6$), 2.68 (s, 6 H, $H^{10/20}{}_{5/5}$), 4.05 (s, 3 H, $H^{15}{}_6$), 7.55 (d, $^3J_{HH}$ = 7.7 Hz, 4 H, $H^{10/20}{}_{3/3}$), 8.02 (d, $^3J_{HH}$ = 8.3 Hz, 2 H, $H^5{}_3$), 8.07 (d, $^3J_{HH}$ = 7.7 Hz, 2 H, $H^{10/20}{}_{2/2}$), 8.08 (d, $^3J_{HH}$ = 8.2 Hz, 2 H, $H^5{}_2$), 8.30 (d, $^3J_{HH}$ = 8.1 Hz, 2 H, $H^{15}{}_2$), 8.41 (d, $^3J_{HH}$ = 8.1 Hz, 2 H, $H^{15}{}_3$), 8.77 (d, $^3J_{HH}$ = 4.6 Hz, 2 H, $H^{pyrrole}$), 8.86 (m, 6 H, $H^{pyrrole}$), 9.39 (s, 1 H, $H^{amideNH}$) ppm.

^{13}C{^{1}H}-NMR (d_8-THF): δ = 21.8 ($C^{10/20}{}_{5/5}$), 24.6 ($C^5{}_6$), 52.6 ($C^{15}{}_6$), 117.8 ($C^5{}_3$), 120.0 (C^{15}), 122.0 ($C^{10/20}$), 122.1 (C^5), 128.2 ($C^{10/20}{}_{3/3}$), 128.6 ($C^{15}{}_3$), 130.6 ($C^{15}{}_4$), 131.9, 132.5, 132.6, 132.8 ($C^{pyrrole}{}_{2/3/7/8/12/13/17/18}$), 135.6 ($C^{10/20}{}_{2/2}$), 135.7 ($C^{15}{}_2$), 135.8 ($C^5{}_2$), 138.0 ($C^{10/20}{}_{4/4}$), 139.1 ($C^5{}_1$), 140.7 ($C^5{}_4$), 141.9 ($C^{10/20}{}_{1/1}$), 149.8 ($C^{15}{}_1$), 150.6, 151.4, 151.6 ($C^{pyrrole\ 1/4/6/9/11/14/16/19}$), 167.6 ($C^{15}{}_5$), 168.8 ($C^5{}_5$) ppm.

IR (KBr): $\tilde{\nu}$ [cm^{-1}] = 3427 (NH^{amide}, br, s), 2960 (CH, w), 2927 (CH, w), 1728 (CO, m), 1603 (m), 1525 (m), 1386 (w), 1284 (C-O-C, s), 997 (vs), 794 (s).

MS (FD): *m/z* (%) = 819.3 (100) $[M]^+$.

MS (ESI): *m/z* (%) = 819.28 (100) [M]$^+$, 820.29 (97) [M+H]$^+$.

HR-MS (ESI): obs. *m/z* = 820.2256 [M+H]$^+$; calcd. for [M+H]$^+$ 820.2266.

UV/Vis (CH_2Cl_2): λ [nm] (ε / [10^4 $M^{-1}cm^{-1}$]) = 421 (45.15), 549 (1.82), 588 (0.46).

Fluorescence (CH_2Cl_2): λ [nm] (relative intensity) = 600 (1.00), 646 (0.83).

Quantum yield: Φ = 0.0884.

Lifetime: τ [ns] = 1.91 (100%).

CV (Fc/Fc$^+$, 100 mV s^{-1}, CH_2Cl_2): $E_{½}$ [V] = –2.090, –1.720, 0.360, 0.800.

[5-(4-(*N*-Acetylaminophenyl))-10,20-bis(phenyl)-15-(4-(methoxycarbonylphenyl)) porphyrinato]zinc(II) (Zn-Ac-3e). Ac-3e (25 mg, 0.034 mmol), zinc acetate dihydrate (37.6 mg, 0.17 mmol). [silica, toluene : ethyl acetate (1:1), R_f = 0.60]. Yield 23.0 mg (0.029 mmol, 85%), purple powder. $C_{48}H_{33}N_5O_3Zn$ (793.22).

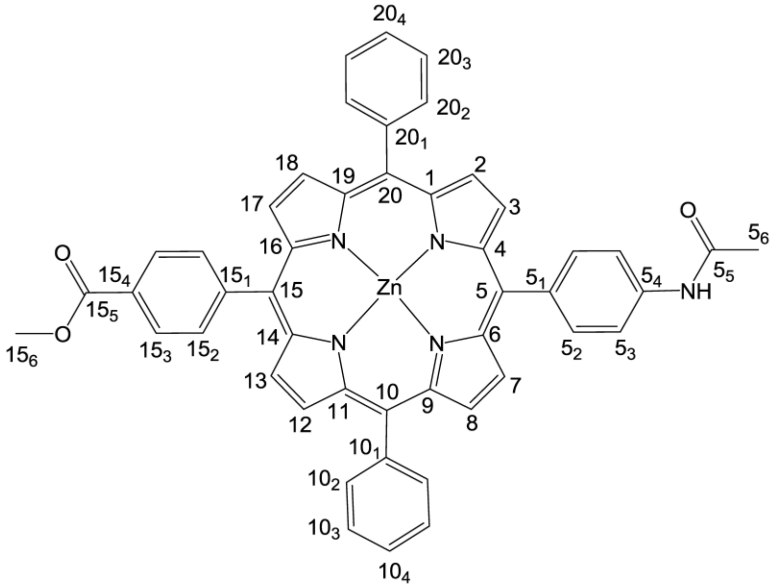

^{1}H-NMR (d^8-THF): δ = 2.20 (s, 3 H, H^{5}_{6}), 2.20 (s, 3 H, H^{5}_{6}), 4.04 (s, 3 H, H^{15}_{6}), 7.74 (m, 6 H, $H^{10/20}_{3/4}$), 8.02 (d, $^3J_{HH}$ = 8.4 Hz, 2 H, H^{5}_{3}), 8.08 (d, $^3J_{HH}$ = 8.4 Hz, 2 H, H^{5}_{2}), 8.19 (d, $^3J_{HH}$ = 7.7 Hz, 2 H, $H^{10/20}_{2/2}$), 8.30 (d, $^3J_{HH}$ = 8.1 Hz, 2 H, H^{15}_{2}), 8.41 (d, $^3J_{HH}$ = 8.1 Hz, 2 H, H^{15}_{3}), 8.79 (d, $^3J_{HH}$ = 4.6 Hz, 2 H, $H^{pyrrole}$), 8.83 (d, $^3J_{HH}$ = 4.8 Hz, 2 H, $H^{pyrrole}$), 8.84 (d, $^3J_{HH}$ = 4.8 Hz, 2 H, $H^{pyrrole}$), 8.89 (d, $^3J_{HH}$ = 4.6 Hz, 2 H, $H^{pyrrole}$), 9.41 (s, 1 H, $H^{amideNH}$) ppm.

^{13}C{^{1}H}-NMR (d$_8$-THF): δ = 24.4 (C^{5}_{6}), 52.5 (C^{15}_{6}), 117.7 (C^{5}_{3}), 120.0 (C^{15}), 121.8 ($C^{10/20}$), 122.1 (C^{5}) 127.4 ($C^{10/20}_{3/3}$), 128.3 ($C^{10/20}_{4/4}$), 128.5 (C^{15}_{3}), 130.6 (C^{15}_{4}), 131.9, 132.4, 132.6, 132.7 ($C^{pyrrole\ 2/3/7/8/12/13/17/18}$), 135.5 ($C^{10/20}_{2/2}$), 135.6 ($C^{15}_{2}$), 135.7 ($C^{5}_{2}$), 139.0 ($C^{5}_{1}$), 140.6 ($C^{5}_{4}$), 144.7 ($C^{10/20}_{1/1}$), 149.6 ($C^{15}_{1}$), 150.6, 151.4, 151.3, 151.5 ($C^{pyrrole\ 1/4/6/9/11/14/16/19}$), 167.5 ($C^{15}_{5}$), 168.7 ($C^{5}_{5}$) ppm.

IR (KBr): $\tilde{\nu}$ [cm^{-1}] = 3418 ($NH^{pyrrole}$ br, w), 3366 (NH^{amide}, br, w), 2947 (CH, w), 2928 (CH, w), 1724 (CO, s), 1650 (s), 1518 (vs), 1387 (vs), 1281 (C-O-C, vs), 999 (vs), 798 (m).

MS (FD): *m/z* (%) = 791.80 (100) $[M]^+$, 792.78 (61) $[M]^+$, 793.78 (78) $[M]^+$.

MS (ESI): *m/z* (%) = 791.22 (100) $[M+H]^+$, 792.22 (54) $[M+H]^+$, 793.22 (68) $[M+H]^+$, 794.22 (39) $[M+H]^+$, 795.22. (47) $[M+H]^+$.

HR-MS (ESI): obs. *m/z* = 814.1756 $[M+Na]^+$; calcd. for $[M+Na]^+$ 814.1773.

UV/Vis (CH_2Cl_2): λ [nm] (ε / [10^4 $M^{-1}cm^{-1}$]) = 420 (36.10), 549 (1.63), 589 (0.48).

Fluorescence (CH_2Cl_2): λ [nm] (relative intensity) = 597 (1.00), 645 (0.96).

Quantum yield: Φ = 0.1037.

Lifetime: τ [ns] = 1.99 (100%).

CV (Fc/Fc$^+$, 100 mV s^{-1}, CH_2Cl_2) [V]: –2.110, –1.750, 0.360, 0.779.

5-(4-(*N*-Acetylaminophenyl))-15-(4-carboxyphenyl)-10,20-bis(phenyl) porphyrin (Ac-3j). Porphyrin **Ac-3e** (65.0 mg, 0.089 mmol) was dissolved in a mixture of freshly distilled THF and methanol (24 mL, 3:1) and 10% aqueous KOH (1 mL) was added. The mixture was stirred overnight, neutralised with acetic acid (1 mL) and diluted with CH_2Cl_2. The organic layer was separated, washed with water (3×), dried over $MgSO_4$ and the solvent was removed under reduced pressure. The product was used without additional purification. [TLC, CH_2Cl_2 : methanol = 20:1, R_f = 0.34]. Yield: 59.0 mg (0.082 mmol, 93%), purple powder. $C_{47}H_{33}N_5O_3$ (715.80).

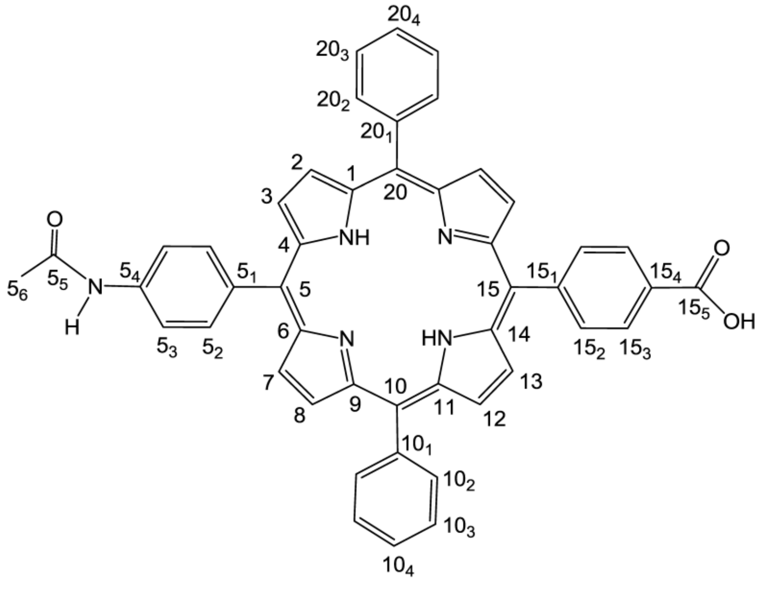

^{1}H-NMR (d_8-THF): δ = –2.69 (s, 2 H, $H^{pyrroleNH}$), 2.20 (s, 3 H, $H^5{}_6$), 7.77 (m, 6 H, $H^{10/20}{}_{3/4}$), 8.05 (d, $^3J_{HH}$ = 8.4 Hz, 2 H, $H^5{}_3$), 8.11 (d, $^3J_{HH}$ = 8.5 Hz, 2 H, $H^5{}_2$), 8.21 (m, 2 H, $H^{10/20}{}_{2/2}$), 8.31 (d, $^3J_{HH}$ = 8.0 Hz, 2 H, $H^5{}_2$), 8.44 (d, $^3J_{HH}$ = 8.0 Hz, 2 H, $H^5{}_3$), 8.81 (m, 6 H, $H^{pyrrole}$), 8.88 (d, $^3J_{HH}$ = 4.5 Hz, 2 H, $H^{pyrrole}$), 9.43 (s, 1 H, $H^{amideNH}$), 11.67 (s, 1 H, H^{COOH}) ppm.

^{13}C{^{1}H}-NMR (d_8-THF): δ = 24.4 ($C^5{}_6$), 118.1 ($C^5{}_3$), 119.5 (C^{15}), 121.3 ($C^{10/20}$), 121.6 (C^5) 127.8 ($C^{10/20}{}_{3/3}$), 128.8 ($C^{10/20}{}_{4/4}$), 129.1 ($C^{15}{}_3$), 131.6 ($C^{15}{}_4$), 132.0 (br. s, $C^{pyrrole\ 2/3/7/8/12/13/17/18}$), 135.5

($\mathrm{C}^{10/20/15}_{2/2/2}$), 135.8 ($\mathrm{C}^{5}_{2}$), 137.6 ($\mathrm{C}^{5}_{1}$), 141.1 ($\mathrm{C}^{5}_{4}$), 143.4 ($\mathrm{C}^{10/20}_{1/1}$), 147.8 ($\mathrm{C}^{15}_{1}$), 168.0 ($\mathrm{C}^{5}_{5}$), 168.8 ($\mathrm{C}^{15}_{5}$) ppm.

IR (KBr): $\tilde{\nu}$ [cm^{-1}] = 3421 (NH$^{\text{amide}}$, NH$^{\text{pyrrole}}$,COOH, br, s), 2924 (CH, w), 2853 (CH, w), 1740 (CO, w), 1690 (CO, w), 1601 (m), 1514 (m), 1386 (w), 1283 (m), 966 (m).

MS (FD): *m/z* (%) = 715.54 (100) [M]$^{+}$.

MS (ESI): *m/z* (%) = 358.63 (7) [M+H]$^{2+}$, 716.29 (100) [M+H]$^{+}$.

HR-MS (ESI): obs. *m/z* = 716.2659 [M+H]$^{+}$; calcd. for [M+H]$^{+}$ 716.2662.

UV/Vis ($\mathbf{CH_2Cl_2}$): λ [nm] (ε / [10^{4} M^{-1}cm^{-1}]) = 419 (33.33), 515 (1.37), 551 (0.69), 590 (0.44), 646 (0.35).

Fluorescence ($\mathbf{CH_2Cl_2}$): λ [nm] (relative intensity) = 652 (1.00), 718 (0.32).

Quantum yield: Φ = 0.1124.

Bisporphyrin 11. Porphyrin **Ac-3j** (22.0 mg, 0.031 mmol) and pyridine (2 mL) were dissolved in anhydrous toluene (20 mL). Thionyl chloride (12 µL, 0.155 mmol) was added and the reaction mixture was stirred under argon for 3h at room temperature. Excess of thionyl chloride and solvent were removed under reduced pressure. The residue was redisolved in an ultrasonic bath in toluene (20 mL) and pyridine (1 mL). Porphyrin **3e** (22.0 mg, 0.031) dissolved in toluene (20 mL) and pyridine (1 mL) was added. The mixture was stirred overnight and the solvent was removed under redeuced pressure. The residue was purified by chromatography [silica, toluene : ethylacetate (2:1), R_{f} = 0.58]. Yield: 13.0 mg (0.0092 mmol, 30%). $\mathrm{C_{95}H_{68}N_{10}O_4}$ (1413.62).

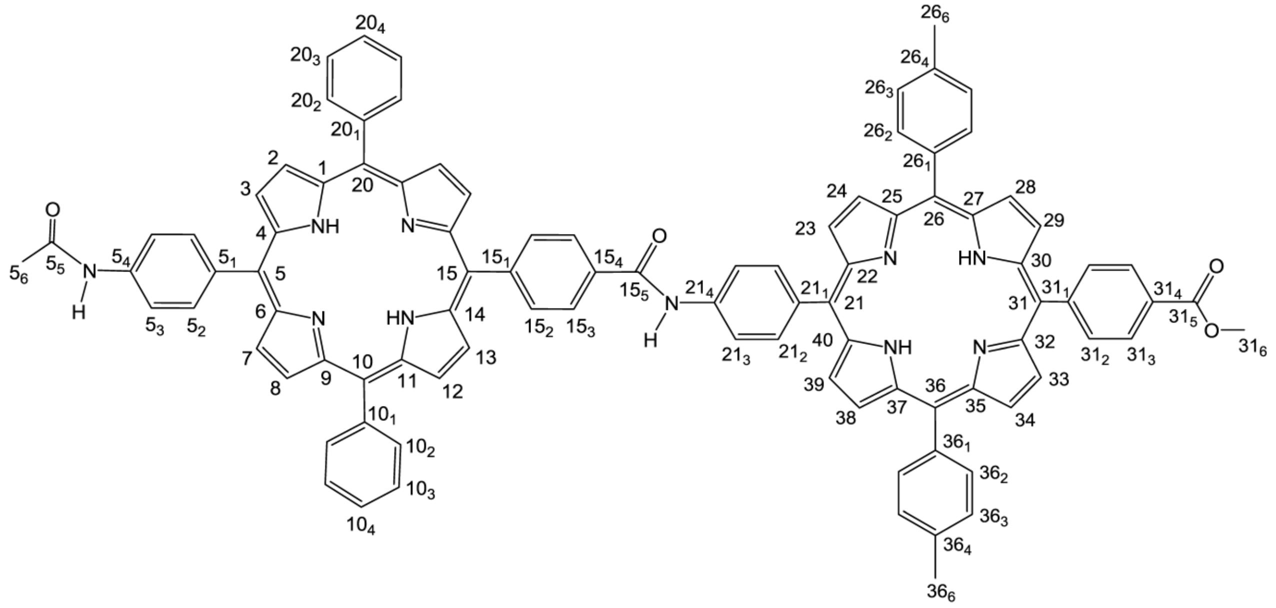

¹H-NMR (d₈-THF): δ = –2.64 (s, 4 H, H$^{\text{pyrroleNH}}$), 2.21 (s, 3 H, H^{15}_{6}), 2.70 (s, 6 H, $\mathrm{H}^{26/36}_{6/6}$), 4.06 (s, 2 H, H^{31}_{6}), 7.61 (d, $^{3}J_{\mathrm{HH}}$ = 7.8 Hz, 4 H, $\mathrm{H}^{26/36}_{3/3}$), 7.80 (m, 6 H, $\mathrm{H}^{10/20}_{3/4}$), 8.07 (d, $^{3}J_{\mathrm{HH}}$ = 8.3 Hz, 2 H, H^{15}_{3}), 8.12 (m, 6 H, $\mathrm{H}^{15/26/36}_{2/2/2}$), 8.24 (m, 4 H, $\mathrm{H}^{10/20}_{2/2}$), 8.27 (d, $^{3}J_{\mathrm{HH}}$ = 8.3 Hz, 2 H, H^{21}_{2}), 8.34

(d, $^{3}J_{\mathrm{HH}}$ = 8.0 Hz, 2 H, $\mathrm{H}^{31}{}_{2}$), 8.43 (ps. t, $^{3}J_{\mathrm{HH}}$ = 7.1 Hz, 6 H, $\mathrm{H}^{5/21/31}{}_{2/3/3}$), 8.53 (d, $^{3}J_{\mathrm{HH}}$ = 8.0 Hz, 2 H, $\mathrm{H}^{5}{}_{3}$), 8.79 (d, $^{3}J_{\mathrm{HH}}$ = 4.4 Hz, 2 H, $\mathrm{H}^{\mathrm{pyrrol}}$), 8.84 (d, $^{3}J_{\mathrm{HH}}$ = 4.5 Hz, 2 H, $\mathrm{H}^{\mathrm{pyrrole}}$), 8.89 (m, 10 H, $\mathrm{H}^{\mathrm{pyrrole}}$), 8.99 (d, $^{3}J_{\mathrm{HH}}$ = 4.4 Hz, 2 H, $\mathrm{H}^{\mathrm{pyrrole}}$), 9.44 (s, 1H, $\mathrm{H}^{\mathrm{amideAcCONH}}$), 10.19 (s, 1 H, $\mathrm{H}^{\mathrm{amidePorphCONHPorph}}$) ppm.

^{13}C{^{1}H}-NMR (d$_{8}$-THF): δ = 24.4 ($\mathrm{C}^{15}{}_{6}$), 21.7 ($\mathrm{C}^{26/36}{}_{6/6}$), 52.6 ($\mathrm{C}^{31}{}_{6}$), 118.1 ($\mathrm{C}^{15}{}_{3}$), 119.2 ($\mathrm{C}^{21}{}_{3}$), 119.5, 121.3, 121.4, 121.6 ($\mathrm{C}^{5/10/15/20/21/26/31/36}$), 127.1 ($\mathrm{C}^{31}{}_{3}$), 127.8 ($\mathrm{C}^{10/20}{}_{3/3}$), 128.5 ($\mathrm{C}^{26/36}{}_{3/3}$), 128.8 ($\mathrm{C}^{5/10/20}{}_{3/4/4}$), 130.9 ($\mathrm{C}^{31}{}_{4}$), 135.5, 135,5 135.6 ($\mathrm{C}^{5/10/20/15/26/36}{}_{2/2/2/2/2/2}$), 136.4, 136.5 ($\mathrm{C}^{5/21/36}{}_{4/1}$), 138.5, 138.5 ($\mathrm{C}^{15/26/36}{}_{4/4/4}$), 140.5 ($\mathrm{C}^{26/26}{}_{1/1}$), 141.0, 141.1 ($\mathrm{C}^{10/20/21}{}_{1/1/4}$), 146.7 ($\mathrm{C}^{15}{}_{1}$), 148.0 ($\mathrm{C}^{31}{}_{1}$), 167.9 ($\mathrm{C}^{31}{}_{5}$), 169.4 ($\mathrm{C}^{15}{}_{5}$), n.o. ($\mathrm{C}^{5}{}_{5}$), 167.4 ($\mathrm{C}^{31}{}_{5}$), 168.9 ($\mathrm{C}^{15}{}_{5}$) ppm.

IR (KBr): $\tilde{\nu}$ [cm^{-1}] = 3433 (NH$^{\mathrm{amide}}$, NH$^{\mathrm{pyrrole}}$, br, vs), 2923 (CH, w), 2855 (CH, w), 1726 (CO, w), 1678 (CO, w), 1605 (m), 1514 (m), 1385 (m), 1283 (m), 966 (m).

MS (FD): *m/z* (%) = 706.66 (20) $[\mathrm{M}]^{2+}$, 1413.85 (100) $[\mathrm{M}]^{+}$.

MS (ESI): *m/z* (%) = 707.86 (100) $[\mathrm{M}^{2+}\mathrm{+H}]$, 1413.73 (3) $[\mathrm{M}]^{+}$.

HR-MS (ESI): obs. *m/z* = 1413.5442 $[\mathrm{M+H}]^{+}$; calcd. for $[\mathrm{M+H}]^{+}$ 1413.5503.

UV/Vis (CH$_2$Cl$_2$): λ [nm] (ε / [10^{4} M^{-1}cm^{-1}]) = 422 (73.50), 516 (3.53), 552 (2.05), 591 (1.19), 647 (1.06).

Fluorescence (CH$_2$Cl$_2$): λ [nm] (relative intensity) = 654 (1.00), 718 (0.28).

Quantum yield: Φ = 0.1284.

Lifetime: τ [ns] = 9.70 (100%).

CV (Fc/Fc^{+}, 100 mV s^{-1}, CH$_2$Cl$_2$): $E_{½}$ [V] = −2.010, −1.660 (2e), 0.540 (2e), 0.860.

Figure S1. Normalized absorption and emission spectra of selected Q-P dyads, Q-P-Fc triads and reference porphyrins in CH_2Cl_2.

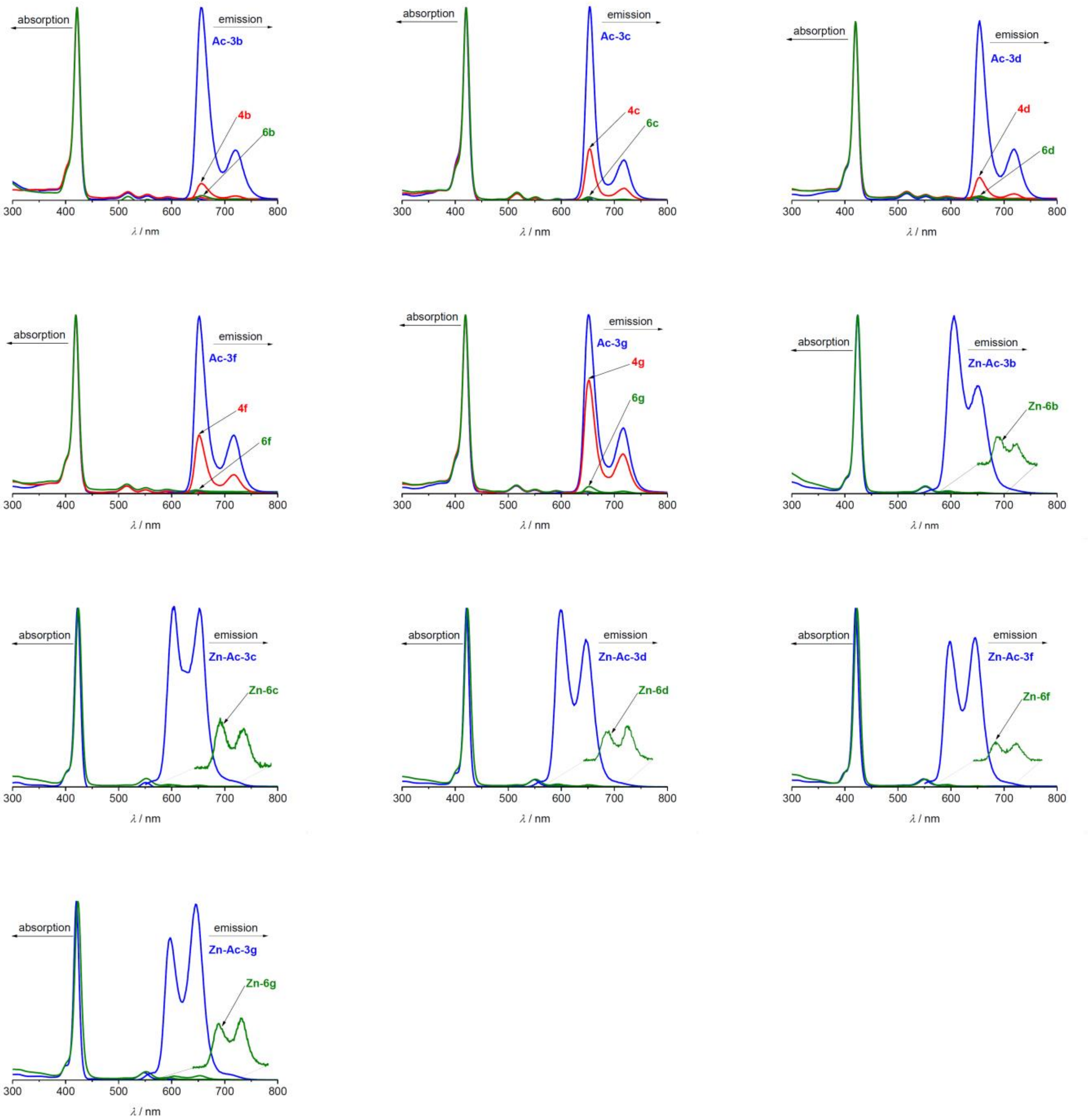

Figure S2. DFT (B3LYP/LANL2DZ, PCM) calculated frontier orbitals of **Zn-6b**.

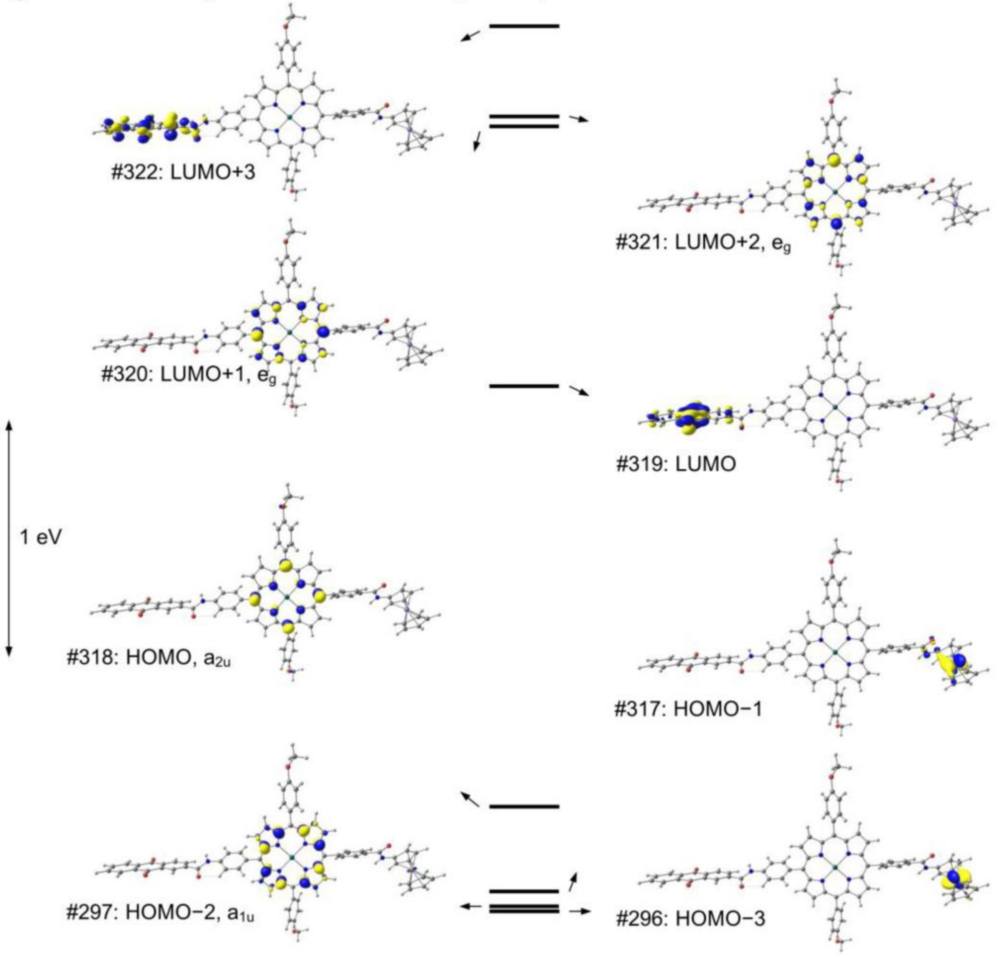

Figure S3. DFT (B3LYP/LANL2DZ, PCM) calculated frontier orbitals of **Zn-6g**.

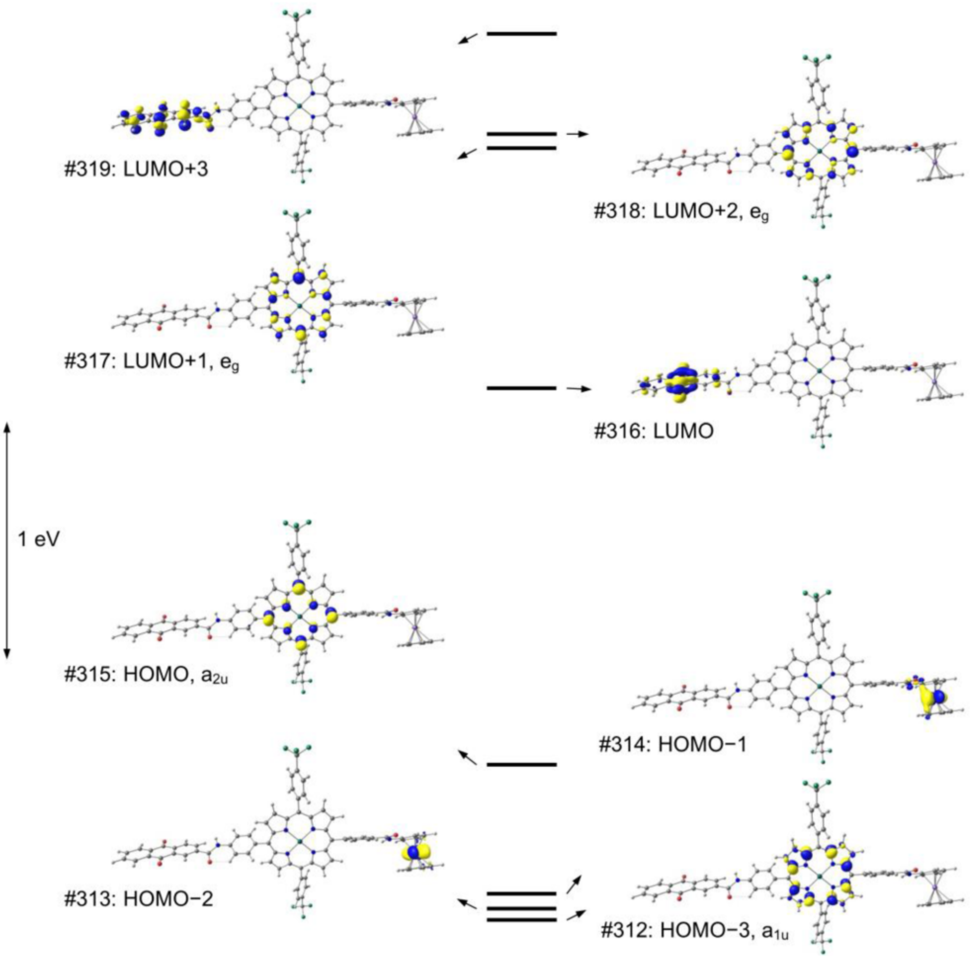

Figure S4. DFT (B3LYP/LANL2DZ, PCM) calculated frontier orbitals of **Zn-6h**.

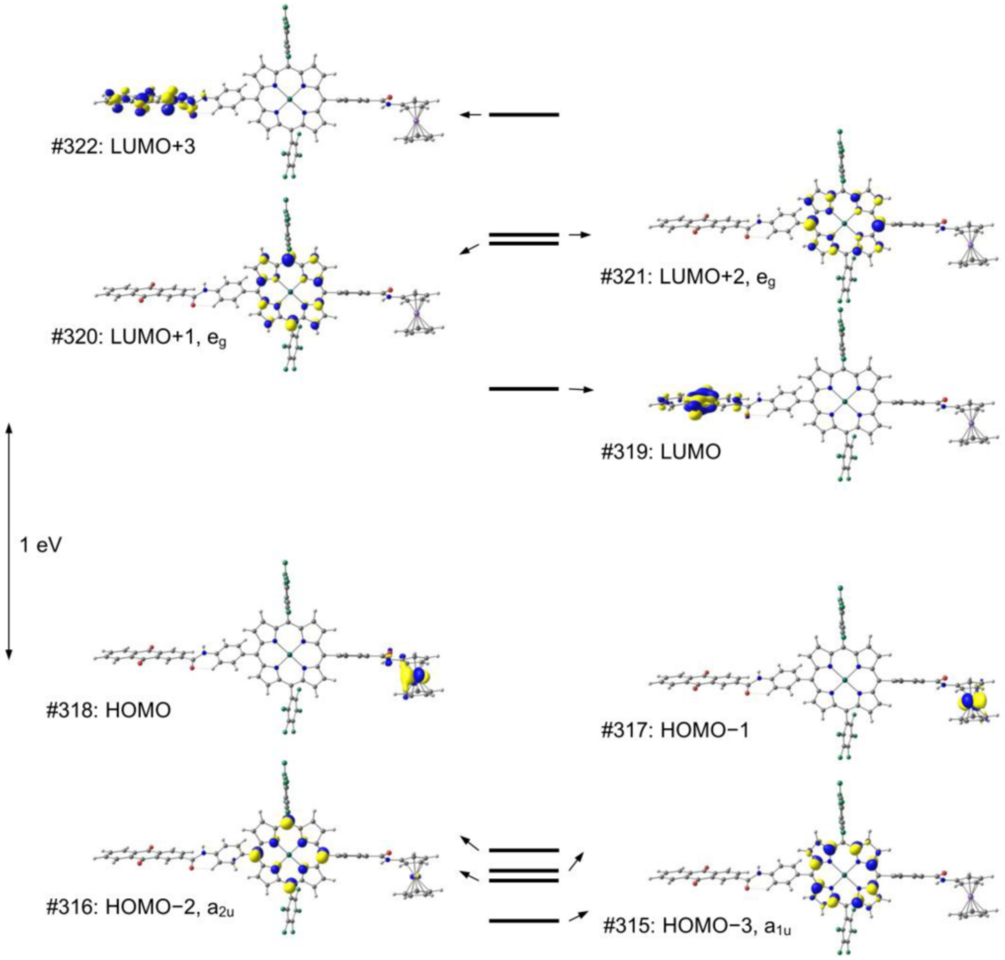

Figure S5. DFT (B3LYP/LANL2DZ, PCM) calculated frontier orbitals of **9**.

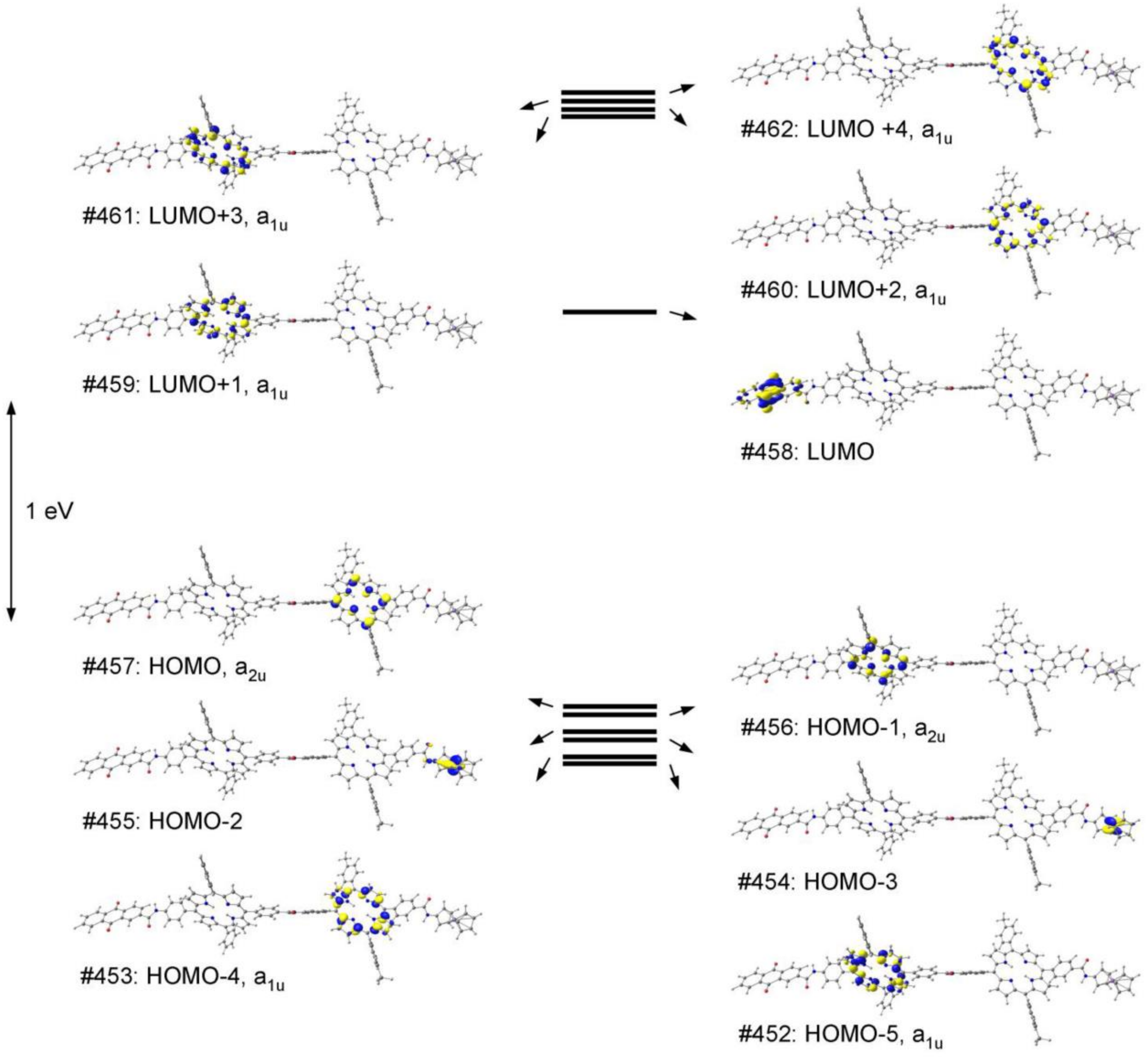

Figure S6. Absorption spectra of *N*-ethyl-anthraquinone-2-carboxylic acid amide treated with $CoCp^*_2$ in THF.

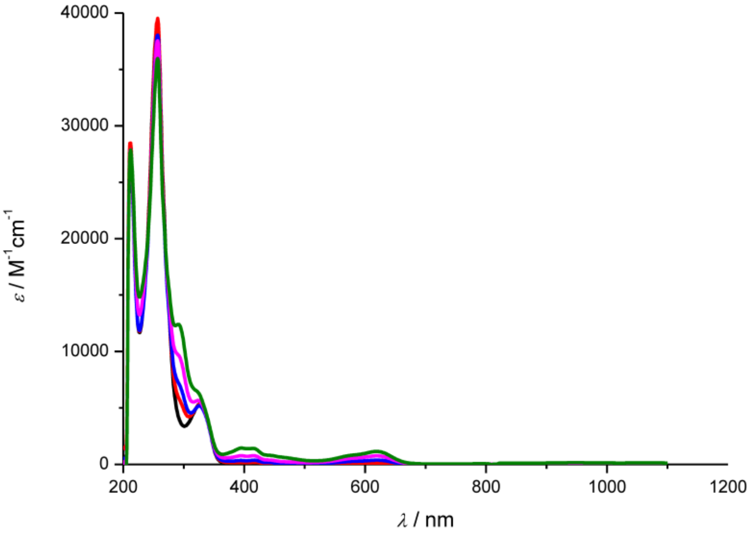

Figure S7. ns-µs transient absorption spectra of a) **Ac-3a**, b) **4a** c) **4a**+$B(C_6F_5)_3$, d) **6a** and e) **6a**+$B(C_6F_5)_3$ in THF; after excitation at λ_{exc} = 532 nm.

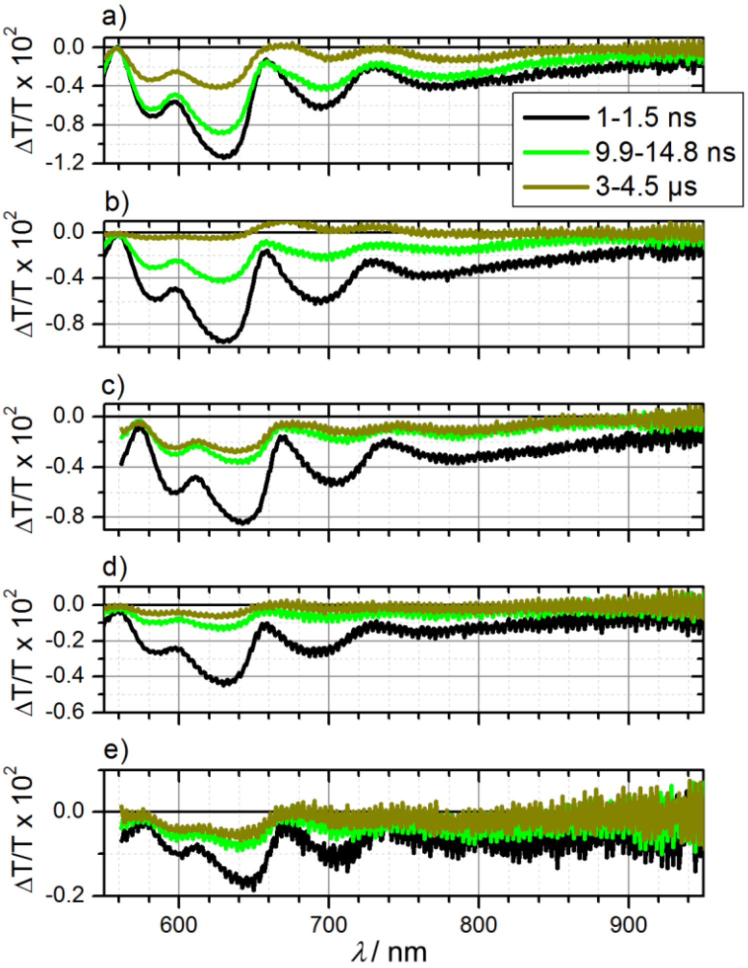

Table S1 Energies (eV) of relevant frontier molecular orbitals of the Q-P dyads **4a** – **4h** determined by DFT (B3LYP/LANL2DZ, PCM).

	Ar^1	HOMO−2	HOMO−1	HOMO	LUMO	LUMO+1	LUMO+2	LUMO+3
4a	$C_6H_4O^nBu$	−6.28	−5.82	−5.33	−3.55	−2.82	−2.74	−2.32
4b	C_6H_4OMe	−6.30	−5.83	−5.34	−3.55	−2.82	−2.75	−2.32
4c	Mes	−6.51	−5.81	−5.41	−3.55	−2.80	−2.73	−2.32
4d	C_6H_4Me	−6.52	−5.82	−5.37	−3.55	−2.82	−2.75	−2.32
4e	C_6H_5	−6.54	−5.84	−5.41	−3.55	−2.84	−2.77	−2.32
4f	C_6H_4F	−6.56	−5.91	−5.48	−3.56	−2.90	−2.84	−2.33
4g	$C_6H_4CF_3$	−6.58	−5.97	−5.57	−3.56	−2.97	−2.93	−2.33
4h	C_6F_5	−6.63	−6.11	−5.82	−3.56	−3.19	−3.05	−2.34

Table S2 Energies (eV) of relevant frontier molecular orbitals of the Q-P-Fc triads (**6a** – **6i**) and Q-P-Fc triads **Zn-6a** – **Zn-6i** determined by DFT (B3LYP/LANL2DZ, PCM).

	Ar^1	HOMO−3	HOMO−2	HOMO−1	HOMO	LUMO	LUMO+1	LUMO+2	LUMO+3
6a	$C_6H_4O^nBu$	−5.82	−5.67	−5.60	−5.33	−3.55	−2.82	−2.74	−2.32
6b	C_6H_4OMe	−5.82	−5.67	−5.60	−5.33	−3.55	−2.82	−2.74	−2.32
6c	Mes	−5.81	−5.67	−5.60	−5.41	−3.55	−2.80	−2.72	−2.32
6d	C_6H_4Me	−5.82	−5.67	−5.60	−5.37	−3.55	−2.81	−2.75	−2.32
6e	C_6H_5	−5.84	−5.67	−5.60	−5.41	−3.55	−2.83	−2.77	−2.32
6f	C_6H_4F	−5.91	−5.68	−5.61	−5.49	−3.56	−2.89	−2.84	−2.33
6g	$C_6H_4CF_3$	−5.97	−5.68	−5.61	−5.57	−3.56	−2.97	−2.92	−2.33
6i	C_6F_4OMe	−6.03	−5.73	−5.67	−5.60	−3.56	−3.09	−2.98	−2.33
6h	C_6F_5	−6.11	−5.81	−5.68	−5.61	−3.56	−3.19	−3.04	−2.34
Zn-6a	$C_6H_4O^nBu$	−5.67	−5.66	−5.59	−5.23	−3.55	−2.64	−2.59	−2.31
Zn-6b	C_6H_4OMe	−5.66	−5.66	−5.60	−5.23	−3.55	−2.65	−2.60	−2.31
Zn-6c	Mes	−5.67	−5.64	−5.59	−5.30	−3.55	−2.62	−2.57	−2.32
Zn-6d	C_6H_4Me	−5.67	−5.66	−5.59	−5.26	−3.55	−2.64	−2.60	−2.31
Zn-6e	C_6H_5	−5.68	−5.67	−5.59	−5.30	−3.55	−2.66	−2.63	−2.32
Zn-6f	C_6H_4F	−5.74	−5.67	−5.60	−5.37	−3.55	−2.72	−2.70	−2.32
Zn-6g	$C_6H_4CF_3$	−5.80	−5.68	−5.61	−5.46	−3.56	−2.81	−2.77	−2.33
Zn-6i	C_6F_4OMe	−5.86	−5.67	−5.63	−5.59	−3.55	−2.93	−2.80	−2.33
Zn-6h	C_6F_5	−5.93	−5.71	−5.68	−5.60	−3.56	−3.03	−2.87	−2.33

References

[S1] A. Rosa, G. Ricciardi, E. J. Baerends, A. Romeo, L. Monsu, *J. Phys. Chem. A* **2003**, *107*, 11468-11482.

[S2] J. R. Lakowicz, *Principles of Fluorescence Spectroscopy*, Springer, 3rd edn, **2006**.

[S3] F. Etzold, I. A. Howard, N. Forler, D. M. Cho, M. Meister, H. Mangold, J. Shu, M. R. Hansen, K. Müller, F. Laquai, *J. Am. Chem. Soc.* **2012**, *134*, 10569-10583.

[S4] M. J. Frisch, G. W. Trucks, H. B. Schlegel, G. E. Scuseria, M. A. Robb, J. R. Cheeseman, G. Scalmani, V. Barone, B. Mennucci, G. A. Petersson, H. Nakatsuji, M. Caricato, X. Li, H. P. Hratchian, A. F. Izmaylov, J. Bloino, G. Zheng, J. L. Sonnenberg, M. Hada, M. Ehara, K. Toyota, R. Fukuda, J. Hasegawa, M. Ishida, T. Nakajima, Y. Honda, O. Kitao, H. Nakai, T. Vreven, J. A. Montgomery Jr., J. E. Peralta, F. Ogliaro, M. Bearpark, J. J. Heyd, E. Brothers, K. N. Kudin, V. N. Staroverov, R. Kobayashi, J. Normand, K. Raghavachari, A. Rendell, J. C. Burant, S. S. Iyengar, J. Tomasi, M. Cossi, N. Rega, J. M. Millam, M. Klene, J. E. Knox, J. B. Cross, V. Bakken, C. Adamo, J. Jaramillo, R. Gomperts, R. E. Stratmann, O. Yazyev, A. J. Austin, R. Cammi, C. Pomelli, J. W. Ochterski, R. L. Martin, K. Morokuma, V. G. Zakrzewski, G. A. Voth, P. Salvador, J. J. Dannenberg, S. Dapprich, A. D. Daniels, O. Farkas, J. B. Foresman, J. V. Ortiz, J. Cioslowski, D. J. Fox, Gaussian 09 (Revision A.02), Gaussian, Inc., Wallingford CT, **2009**.

[S5] D. T. Gryko, M. Tasior, B. Koszarna, *J. Porphyrins Phthalocyanines* **2003**, *7*, 239-248.

[S6] T. Rohand, E. Dolusic, T. H. Ngo, W. Maes, W. Dehaen, *ARKIVOC* **2007** (x), 307-324.

[S7] B. J. Littler, Y. Ciringh, J. S. Lindsey, *J. Org. Chem.* **1999**, *64*, 2864-2872.

[S8] K. Heinze and A. Reinhart, *Z. Naturforsch.* **2005**, *60b*, 758-762.

[S9] J. Melomedov, A. Wünsche Von Leupoldt, M. Meister, F. Laquai, K. Heinze, *Dalton Trans.* **2013**, *42*, 9727-9739.

[S10] S. L. Gould, G. Kodis, R. E. Palacios, L. De La Garza, A. Brune, D. Gust, T. A. Moore, A. L. Moore, *J. Phys. Chem. B* **2004**, *108***,** 10566-10580.

[S11] C. M. Carcel, J. K. Laha, R. S. Loewe, P. Thamyongkit, K. Schweikart, V. Misra, D. F. Bocian, J. S. Lindsey, N. Carolina, *J. Org. Chem.* **2004**, *69*, 6739-6750.

[S12] K. Heinze, A. Reinhart, *Dalton Trans.* **2008**, 469-480.

http://onlinelibrary.wiley.com/store/10.1002/ejic.201400118/asset/supinfo/ejic_201400118_sm_miscellaneous_information.pdf?v=1&s=ff4ed03d6ca9d37b6f40fd0a10e45b47f5009f0d (accessed on 24.04.2014)

7.3 Supporting Informations and Experimental Section of Publication 6.3

Aminoferrocene and Ferrocene Amino Acid as Electron Donors in Modular Porphyrin-Ferrocene and Porphyrin-Ferrocene-Porphyrin Conjugates

J. Melomedov, J. R. Ochsmann, M. Meister, F. Laquai and K. Heinze, *Eur. J. Inorg. Chem.* **2014**, accepted (ejic.201402138).

Analytical data:

3a. 5-(4-Carboxyphenyl)-15-(4-methoxycarbonylphenyl)-10,20-bis(2,4,6-trimethyllphenyl) porphyrin (**2a**) (31.2 mg, 0.039 mmol), 15 µL (0.20 mmol) thionyl chloride, 10.2 mg (0.051) aminoferrocene. [silica, toluene : ethylacetate (20:1), R_f = 0.58]. Yield: 26.0 mg (0.026 mmol, 68%), purple powder. $C_{63}H_{53}FeN_5O_3$ (983.97).

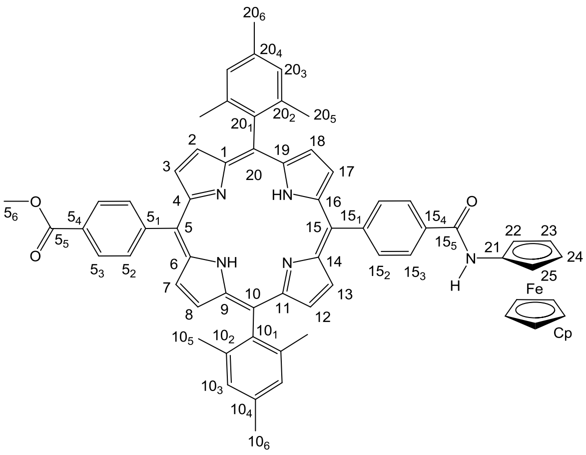

^{1}H-NMR (d$_8$-THF): δ = −2.50 (s, 2 H, $\mathrm{H}^{NHpyrrole}$), 1.84 (s, 12 H, $\mathrm{H}^{10/20}{}_{5/5}$), 2.61 (s, 6 H, $\mathrm{H}^{10/20}{}_{6/6}$), 4.05 (s, 5 H, $\mathrm{H}^{5}{}_{6}{}^{/23/24}$), 4.24 (s, 5 H, H^{Cp}), 4.95 (br. s, 2 H, $\mathrm{H}^{22/25}$), 7.32 (s, 4 H, $\mathrm{H}^{10/20}{}_{3/3}$), 8.33 (m, 6 H, $\mathrm{H}^{5/15/15}{}_{2/2/3}$), 8.42 (d, $^3J_{HH}$ = 7.9 Hz 2 H, $\mathrm{H}^{5}{}_{3}$), 8.70 (pt, $^3J_{HH}$ = 3.7 Hz, 4 H, $\mathrm{H}^{pyrrole}$), 8.76 (d, 2 H, $^3J_{HH}$ = 4.4 Hz, $\mathrm{H}^{pyrrole}$), 8.82 (d, 2 H, $^3J_{HH}$ = 4.3 Hz, $\mathrm{H}^{pyrrole}$), 9.20 (br. s, 1 H, $\mathrm{H}^{NHamide}$) ppm.

^{13}C{^{1}H}-NMR (d$_8$-THF): δ = 21.7 ($\mathrm{C}^{10/20}{}_{6/6}$), 21.9 ($\mathrm{C}^{10/20}{}_{5/5}$), 52.5 ($\mathrm{C}^{5}{}_{6}$), 62.1 ($\mathrm{C}^{22/25}$), 65.1 ($\mathrm{C}^{23/24}$), 70.1 ($\mathrm{C}^{Cp}$), 119.5, 119.5 ($\mathrm{C}^{5/15}$), 120.0 ($\mathrm{C}^{10/20}$), 126.8 ($\mathrm{C}^{15}{}_{3}$), 128.8 ($\mathrm{C}^{5}{}_{3}$), 128.9 ($\mathrm{C}^{10/20}{}_{3/3}$), 131.2 (br. s, $\mathrm{C}^{2/3/7/8/12/13/17/18}$), 131.0 ($\mathrm{C}^{5}{}_{4}$), 135.4, 135.5 ($\mathrm{C}^{5/15}{}_{2/2}$), 136.1 ($\mathrm{C}^{15}{}_{4}$), 139.5 ($\mathrm{C}^{10/20}{}_{1/1}$), 145.8 ($\mathrm{C}^{5}{}_{1}$), 147.8 ($\mathrm{C}^{15}{}_{1}$), 165.7 ($\mathrm{C}^{15}{}_{5}$), 167.4 ($\mathrm{C}^{5/15}{}_{5/5}$) ppm.

IR (KBr): $\tilde{\nu}$ [cm^{-1}] = 3433 (br, $\mathrm{NH}^{amide,}$, $\mathrm{NH}^{pyrrole}$), 2922 (w, CH), 2856 (w, CH), 1726 (s, CO^{ester}), 1678 (m, CO^{amide}), 1535 (m), 1499 (vs), 1383 (m), 1277 (vs), 968 (m).

MS (FD): *m/z* (%) = 984.07 (100) $[\mathrm{M+H}]^+$.

MS (ESI): *m/z* (%) = 984.30 (100) $[\mathrm{M+H}]^+$, 1968.58 (1) $[\mathrm{2M+H}]^+$.

HR-MS (ESI): obs. *m/z* (%) = 983.3497; calcd. for $[\mathrm{M}]^+$ 983.3498.

UV/Vis (CH_2Cl_2): λ [nm] (ε / [10^4 $M^{-1}cm^{-1}$]) = 420 (44.69), 550 (1.77), 591 (0.61), 587 (0.35), 647 (0.27).

Fluorescence (CH_2Cl_2): λ [nm] (relative intensity) = 653 (1.00), 717 (0.26).

Quantum yield: $\Phi = 0.0122$.

Lifetime: τ [ps] = 3518.78 (20%), 200.53 (80%).

CV (Fc/Fc$^+$, 100 mV s^{-1}, CH_2Cl_2): $E_{½}$ [V] = −2.060, −1.700, −0.090, 0.590, 1.040.

3e. 5-(4-Carboxyphenyl)-15-(4-methoxycarbonylphenyl)-10,20-bis(2,3,4,5,6-pentafluorophenyl) porphyrin (**2e**) 35 mg (0.039 mmol), 15 μL (0.20 mmol) thionyl chloride, 10.2 mg (0.051) aminoferrocene. [silica, toluene : ethylacetate, R_f = 0.53]. Yield: 32.5 mg (0.030 mmol, 77%), purple powder. $C_{57}H_{31}F_{10}FeN_5O_3$ (1079.72).

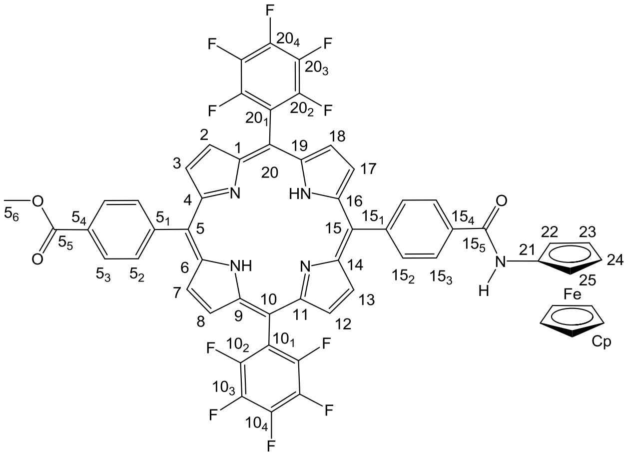

^{1}H-NMR (d_8-THF): δ = −2.78 (s, 2 H, $H^{NHpyrrole}$), 4.07 (s, 5 H, $H^{5}_{6}{}^{/23/24}$), 4.25 (s, 5 H, H^{Cp}), 4.96 (pt, 2 H, $H^{22/25}$), 8.37 (m, 6 H, $H^{5/15/15}_{2/3/3}$), 8.47 (d, 2 H, $^3J_{HH}$ = 8.0 Hz, H^5_3), 8.94 (d, 2 H, $^3J_{HH}$ = 4.6 Hz, $H^{pyrrole}$), 8.98 (d, 2 H, $^3J_{HH}$ = 4.6 Hz, $H^{pyrrole}$), 9.05 (m, 4 H, $H^{pyrrole}$), 9.22 (s, 1 H, $H^{NHamide}$) ppm.

^{13}C{^{1}H}-NMR (d_8-THF): δ = 52.6 (C^5_6), 62.2 ($C^{22/25}$), 65.1 ($C^{23/24}$), 70.1 (C^{Cp}), 117.4 (m, $C^{10/20}$), 121.3, 121.8 ($C^{5/15}$), 126.9 (C^{15}_3), 129.0 (C^5_3), 131.2 (br. s, $C^{2/3/7/8/12/13/17/18}$), 131.4 (C^5_4), 145.1, 147.1 ($C^{5/15}_{1/1}$), 135.5, 135.6 ($C^{5/15}_{2/2}$), 136.4 (C^{15}_4), 137.7, 140.2, 146.7, 149.1 (m, $C^{10/20}_{1/1/2/2/3/3/4/4}$), 165.6 ($C^{15}_5$), 167.3 ($C^5_5$) ppm.

^{19}F-NMR (d_8-THF): δ = −167.2 (ddd, $^3J_{FF}$ = 24 Hz, $^3J_{FF}$ = 21 Hz, $^5J_{FF}$ = 8 Hz, 4 F, $F^{10/20}_{3/3}$), −158.5 (t, $^3J_{FF}$ = 21 Hz, 2 F, $F^{10/20}_{4/4}$), −141.5 (dd, $^3J_{FF}$ = 24 Hz, $^5J_{FF}$ = 8 Hz, 4 F, $F^{10/20}_{2/2}$) ppm.

IR (KBr): $\tilde{\nu}$ [cm^{-1}] = 3433 (br, NH^{amide}, $NH^{pyrrole}$), 2930 (w, CH), 1720 (m, CO^{ester}), 1522 (vs), 1499 (vs), 1281 (m), 1109 (w, CF), 1042 (w, CF), 1024 (w, CF), 989 (vs), 922 (s).

MS (FD): *m/z* (%) = 1079.76 (100) $[\mathrm{M}]^{+}$.

MS (ESI): *m/z* (%) = 540.05 (3) $[\mathrm{M}]^{2+}$, 1079.10 (100) $[\mathrm{M}]^{+}$.

HR-MS (ESI): obs. *m/z* (%) = 1080.1730; calcd. for $[\mathrm{M+H}]^{+}$ 1080.1695.

UV/Vis (CH_2Cl_2): λ [nm] (ε / $[10^{4}\ \mathrm{M}^{-1}\mathrm{cm}^{-1}]$) = 416 (33.50), 511 (1.69), 544 (0.30), 587 (0.42), 642 (0.054).

Fluorescence (CH_2Cl_2): λ [nm] (relative intensity) = 646 (1.00), 714 (0.57).

Quantum yield: Φ = 0.0014.

Lifetime: τ [ps] = 1990.85 (9%), 21.64 (91%).

CV ($\mathrm{Fc/Fc}^{+}$, 100 mV s^{-1}, CH_2Cl_2): $E_{½}$ [V] = −1.820, −1.430, −0.090, 0.890.

Zn-3a. 3a (10.0 mg, 0.010 mmol), 11.1 mg (0.051 mmol) zinc(II) acetate dihydrate. [silica, CH_2Cl_2, R_f = 0.21]. Yield: 10 mg (0.0096 mmol, 96%), purple powder. $C_{63}H_{51}FeN_5O_3Zn$ (1047.37).

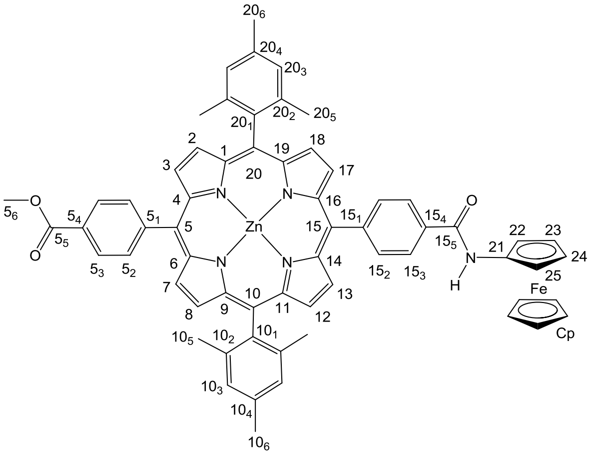

^{1}H-NMR (d_8-THF): δ = 1.85 (s, 12 H, $\mathrm{H}^{10/20}{}_{5/5}$), 2.61 (s, 6 H, $\mathrm{H}^{10/20}{}_{6/6}$), 4.04 (s, 5 H, $\mathrm{H}^{5}{}_{6}{}^{/23/24}$), 4.24 (s, 5 H, H^{Cp}), 4.94 (br. s, 2 H, $\mathrm{H}^{22/25}$), 7.30 (s, 4 H, $\mathrm{H}^{10/20}{}_{3/3}$), 8.30 (m, 6 H, $\mathrm{H}^{5/15/15}{}_{2/2/3}$), 8.40 (d, $^{3}J_\mathrm{HH}$ = 8.1 Hz, 2 H, $\mathrm{H}^{5}{}_{3}$), 8.68 (pt, $^{3}J_\mathrm{HH}$ = 4.4 Hz, 4 H, $\mathrm{H}^{\mathrm{pyrrole}}$), 8.75 (d, 2 H, $^{3}J_\mathrm{HH}$ = 4.6 Hz, $\mathrm{H}^{\mathrm{pyrrole}}$), 8.81 (d, 2 H, $^{3}J_\mathrm{HH}$ = 4.6 Hz, $\mathrm{H}^{\mathrm{pyrrole}}$), 9.21 (br. s, 1 H, $\mathrm{H}^{\mathrm{NHamide}}$) ppm.

^{13}C{^{1}H}-NMR (d_8-THF): δ = 21.7 ($\mathrm{C}^{10/20}{}_{6/6}$), 22.1 ($\mathrm{C}^{10/20}{}_{5/5}$), 52.5 ($\mathrm{C}^{5}{}_{6}$), 62.1 ($\mathrm{C}^{22/25}$), 65.0 ($\mathrm{C}^{23/24}$), 70.0 ($\mathrm{C}^{\mathrm{Cp}}$), 97.9 ($\mathrm{C}^{21}$), 119.8, 119.9 ($\mathrm{C}^{5/15}$), 120.4 ($\mathrm{C}^{10/20}$), 126.3 ($\mathrm{C}^{15}{}_{3}$), 128.4 ($\mathrm{C}^{5}{}_{3}$), 128.7 ($\mathrm{C}^{10/20}{}_{3/3}$), 131.2, 131.3, 132.6, 132.8 ($\mathrm{C}^{2/3/7/8/12/13/17/18}$), 130.5 ($\mathrm{C}^{5}{}_{4}$), 135.4, 135.5 ($\mathrm{C}^{5/15/15}{}_{2/2/4}$), 138.3 ($\mathrm{C}^{10/20}{}_{2/2}$), 140.7 ($\mathrm{C}^{10/20}{}_{1/1}$), 147.4 ($\mathrm{C}^{15}{}_{1}$), 149.4 ($\mathrm{C}^{5}{}_{1}$), 150.5, 150.7, 150.9, 150.9 ($\mathrm{C}^{1/4/6/9/11/14/16/19}$), 167.4 ($\mathrm{C}^{15}{}_{5}$), 167.4 ($\mathrm{C}^{5}{}_{5}$) ppm.

IR (KBr): $\tilde{\nu}$ [cm^{-1}] = 3433 (br, NH$^{\mathrm{amide}}$, NH$^{\mathrm{pyrrole}}$), 2954 (w, CH), 2918 (w, CH), 1726 (s, CO$^{\mathrm{ester}}$), 1523 (m), 1499 (vs), 1384 (m), 1278 (vs), 999 (vs).

MS (FD): *m/z* (%) = 1045.83 (97) [M]$^+$.

MS (ESI): *m/z* (%) = 1045.28 (100) [M]$^+$.

HR-MS (ESI): obs. *m/z* (%) = 1045.2622; calcd. for [M]$^+$ 1045.2633.

UV/Vis (CH_2Cl_2): λ [nm] (ε / [10^4 M^{-1}cm^{-1}]) = 424 (30.18), 552 (1.03), 594 (0.38).

Fluorescence (CH_2Cl_2): λ [nm] (relative intensity) = 605 (1.00), 651 (0.89).

Quantum yield: Φ = 0.0096.

Lifetime: τ [ps] = 1563.23 (18%), 139.16 (82%).

CV (Fc/Fc$^+$, 100 mV s^{-1}, CH_2Cl_2): $E_{½}$ [V] = −2.230, −1.830, −0.090, 0.440, 0.730.

Zn-3e. 3e (15.0 mg, 0.014 mmol), 15.2 mg (0.069 mmol) zinc(II) acetate dihydrate. [silica, CH_2Cl_2 : ethylacetate = 40 : 1, R_f = 0.44]. Yield: 15.0 mg (0.013 mmol, 94%), purple powder. $C_{57}H_{29}F_{10}FeN_5O_3Zn$ (1143.08).

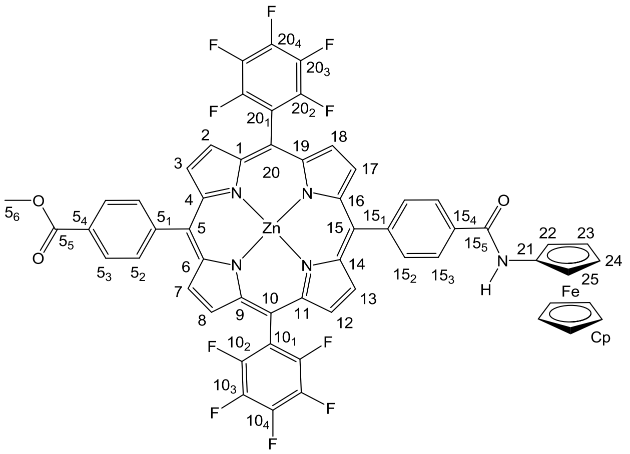

^{1}H-NMR (d_8-THF): δ = 4.07 (s, 5 H, $\mathrm{H}^{5}_{6}{}^{/23/24}$), 4.25 (s, 5 H, H$^{\mathrm{Cp}}$), 4.96 (pt, 2 H, H$^{22/25}$), 8.33 (m, 6 H, $\mathrm{H}^{5/15/15}_{2/2/3}$), 8.44 (d, 2 H, $^3J_{\mathrm{HH}}$ = 7.9 Hz, H^5_3), 8.91 (d, 2 H, $^3J_{\mathrm{HH}}$ = 4.6 Hz, H$^{\mathrm{pyrrole}}$), 8.96 (d, 2 H, $^3J_{\mathrm{HH}}$ = 4.6 Hz, H$^{\mathrm{pyrrole}}$), 9.00 (m, 4 H, H$^{\mathrm{pyrrole}}$), 9.22 (s, 1 H$^{\mathrm{NHamide}}$) ppm.

^{13}C{^{1}H}-NMR (d_8-THF): δ = 52.6 (C^5_6), 62.2 (C$^{22/25}$), 65.1 (C$^{23/24}$), 70.1 (C$^{\mathrm{Cp}}$), 118.7 (m, C$^{10/20}$), 121.6, 121.7 (C$^{5/15}$), 126.5 (C^{15}_3), 128.6 (C^5_3), 131.4, 131.4, 133.8, 133.9 (C$^{2/3/7/8/12/13/17/18}$), 130.9 (C^5_4), 135.5, 135.6 ($\mathrm{C}^{5/15}_{2/2}$), 137.6, 139.9, 141.8, 149.1 (m, $\mathrm{C}^{10/20}_{1/1/2/2/3/3/4/4}$), 146.7 ($\mathrm{C}^{15}_1$), 148.7 ($\mathrm{C}^5_1$), 150.7, 151.4, 151.6 (C$^{1/4/6/9/11/14/16/19}$), 166.9 (C^{15}_5), 167.4 (C^5_5) ppm (C^{15}_4 not observed).

^{19}F-NMR (d_8-THF): δ = −167.2 (ddd, $^3J_{\mathrm{FF}}$ = 24 Hz, $^3J_{\mathrm{FF}}$ = 21 Hz, $^5J_{\mathrm{FF}}$ = 8 Hz, 4 F, $\mathrm{F}^{10/20}_{3/3}$), −158.5 (t, $^3J_{\mathrm{FF}}$ = 21 Hz, 2 F, $\mathrm{F}^{10/20}_{4/4}$), −141.5 (dd, $^3J_{\mathrm{FF}}$ = 24 Hz, $^5J_{\mathrm{FF}}$ = 8 Hz, 4 F, $\mathrm{F}^{10/20}_{2/2}$) ppm.

IR (KBr): $\tilde{\nu}$ [cm^{-1}] = 3433 (br, N^{amide}, $NH^{pyrrole}$), 2930 (w, CH), 1716 (m, CO^{ester}), 1643 (vs, CO^{amide}), 1518 (vs), 1491 (vs), 1385 (vs), 1278 (m), 1112 (w, CF), 1011 (w, CF), 991 (s).

MS (FD): *m/z* (%) = 1141.59 (100) $[M]^+$.

MS (ESI): *m/z* (%) = 1141.10 (100) $[M]^+$.

HR-MS (ESI): obs. *m/z* (%) = 1141.0787; calcd. for $[M]^+$ 1141.0752.

UV/Vis (CH_2Cl_2): λ [nm] (ε / [10^4 $M^{-1}cm^{-1}$]) = 421 (50.0), 552 (2.65), 583(1.03).

Fluorescence (CH_2Cl_2): λ [nm] (relative intensity) = 598 (0.91), 649 (1.00).

Quantum yield: $\Phi = 6.342\times10^{-4}$.

Lifetime: τ [ps] = 1112.17 (16%), 12.73 (84%).

CV (Fc/Fc$^+$, 100 mV s^{-1}, CH_2Cl_2): $E_{½}$ [V] = −1.980, −1.570, −0.010, 0.680, 0.920.

5b. *N*-Fmoc-Fca-OH (139.0 mg, 0.297 mmol), 15-(4-methoxycarbonylphenyl)-5-(4-aminophenyl)-10,20-bis-(phenyl)porphyrin (**4b**) (100.0 mg, 0.145 mmol), oxalyl chloride (0.10 mL, 1.21 mmol), pyridine (2 mL). [silica, CH_2Cl_2; a few drops NEt_3, R_f = 0.10]. Yield: 64.5 mg (0.087 mmol, 39%), purple powder. $C_{72}H_{52}FeN_6O_5$ (1137.07).

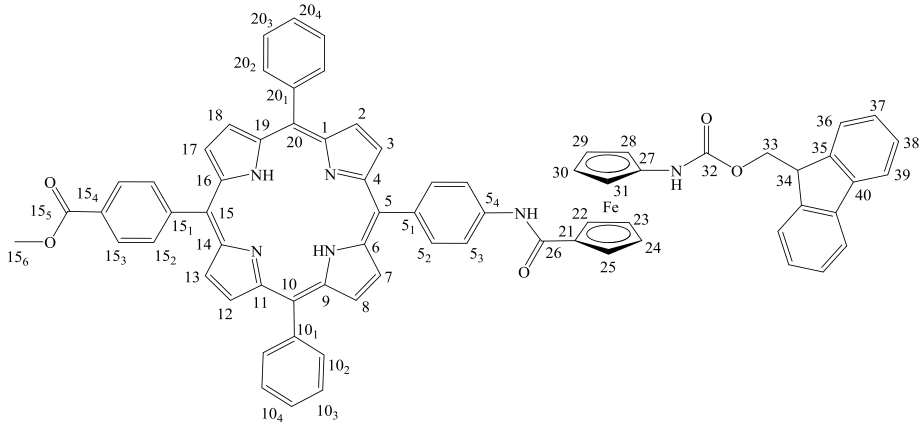

^{1}H-NMR ($CDCl_3$): δ = −2.78 (s, 2 H, $H^{NHpyrrole}$), 4.11 (s, 3 H, $H^{15}{}_6$), 4.21 (b. s, 2 H, $H^{29/30}$), 4.30 (t, 1 H, $^3J_{HH}$ = 6.4 Hz, H^{34}), 4.48 (b.s, 2 H, $H^{23/24}$), 4.53 (b. s, 2 H, $H^{28/31}$), 4.65 (d, $^3J_{HH}$ = 6.5 Hz, 2 H, H^{33}), 4.84 (b. s, 2 H, $H^{22/25}$), 6.28 (s, 1 H, H^{NHFmoc}), 7.28 (m, 4 H, $H^{37/38}$), 7.65 (t, $^3J_{HH}$ = 6.2 Hz, 4 H, $H^{36/39}$), 7.78 (m, 6 H, $H^{10/20}{}_{3/4}$), 8.15 (m, 4 H, $H^{5/5}{}_{2/3}$), 8.21 (dd, $^3J_{HH}$ = 7.8 Hz, $^4J_{HH}$ = 1.7 Hz, 4 H, $H^{10/20}{}_{2/2}$), 8.31 (d, $^3J_{HH}$ = 8.2 Hz, 2 H, $H^{15}{}_2$), 8.44 (d, $^3J_{HH}$ = 8.2 Hz, 2 H, $H^{15}{}_3$), 8.78 (d, $^3J_{HH}$ = 4.2 Hz, 4 H, $H^{pyrrole}$), 8.86 (d, $^3J_{HH}$ = 4.9 Hz, 2 H, $H^{pyrrole}$), 8.88 (d, $^3J_{HH}$ = 4.8 Hz, 2 H, $H^{pyrrole}$), 9.18 (b. s, 1 H, $H^{NHamide}$) ppm.

^{13}C{^{1}H}-NMR ($CDCl_3$): δ = 47.3 (C^{34}), 52.4 ($C^{15}{}_6$), 62.9 ($C^{28/31}$), 66.0 ($C^{29/30}$), 67.1 (C^{33}), 69.9 ($C^{22/25}$), 71.2 ($C^{23/24}$), 79.0 (C^{21}), 96.0 (C^{27}), 117.9 ($C^5{}_3$), 118.4 (C^{15}), 120.0 (C^{36}), 120.1 ($C^{10/20}$), 120.3 (C^5), 124.9 (C^{39}), 126.7 ($C^{10/20}{}_{3/3}$), 127.1 (C^{38}), 127.8 ($C^{10/20}{}_{4/4}$), 127.8 ($C^{15}{}_3$), 127.9 (C^{37}), 129.5 ($C^{15}{}_4$), 131.2 (b. s, $C^{2,3,7,8,12,13,17,18}$), 134.5 ($C^{10/20}{}_{2/2}$), 134.6 ($C^{15}{}_2$), 135.2 ($C^5{}_2$), 138.7 ($C^5{}_4$), 141.4 (C^{40}), 142.1 ($C^{10/20}{}_{1/1}$),143.5 (C^{35}), 147.1 ($C^{15}{}_1$), 154.3 (C^{32}), 167.4 ($C^{15}{}_5$) ppm (C^{26} not observed).

IR (KBr): $\tilde{\nu}$ [cm^{-1}] = 3424, 3323 (br, NH^{amide}, NH^{Fmoc}), 2926 (w, CH), 2855 (w, CH), 1720 (vs, CO^{ester}), 1514 (s), 1384 (ws), 1281 (s, C-O-C), 800 (m), 734 (m).

MS (FD): *m/z* (%) = 569.32 (1) $[M]^{2+}$, 1136.82 (100) $[M]^+$.

MS (ESI): *m/z* (%) = 569.17 (18) $[M]^{2+}$, 1137.35 (100) $[M+H]^+$.

HR-MS (ESI): obs. *m/z* (%) = 1137.3403; calcd. for $[M+H]^+$ 1137.3427.

UV/Vis (CH_2Cl_2): λ [nm] (ε / [10^4 $M^{-1}cm^{-1}$]) = 420 (38.93), 516 (1.68), 552 (0.88), 591 (0.53), 647 (0.43).

Fluorescence (CH_2Cl_2): λ [nm] (relative intensity) = 652 (1.00), 717 (0.31).

Quantum yield: Φ = 0.0416.

Lifetime: τ [ns] = 5.97 (25%), 2.00 (75%).

CV (Fc/Fc^{+}, 100 mV s^{-1}, CH$_2$Cl$_2$): $E_{½}$ [V] = −1.980, −1.610, 0.140, 0.580, 0.890.

5c. *N*-Fmoc-Fca-OH (187.0 mg, 0.4×10^{-3} mol), 15-(4-methoxycarbonylphenyl)-5-(4-aminophenyl)-10,20-bis-(4-fluorophenyl)porphyrin (**4c**) (100.0 mg, 0.138 mmol), oxalyl chloride (0.10 mL, 1.17 mmol), pyridine (0.5 mL). [silica, CH$_2$Cl$_2$/ethylacetate = 5 : 1; a few drops NEt$_3$, R_f = 0.85]. Yield: 102.0 mg (0.087 mmol, 63%), purple powder. $C_{72}H_{50}F_2FeN_6O_5$ (1173.05).

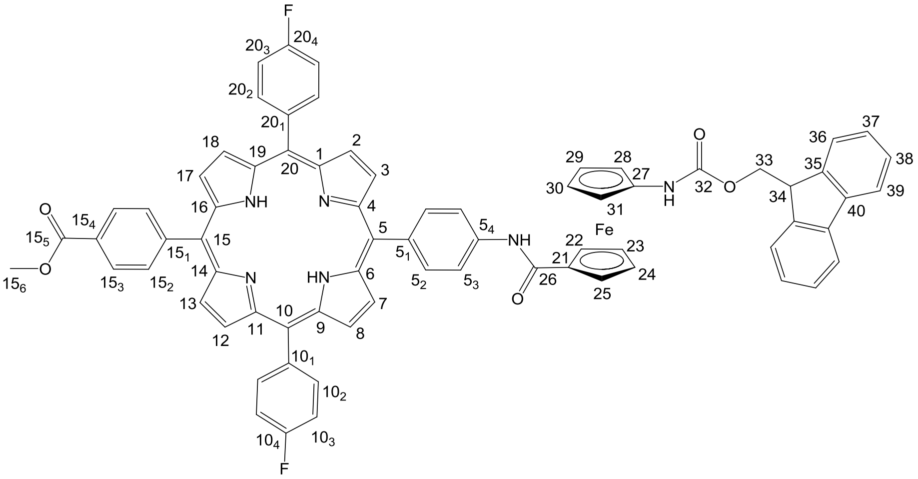

^{1}H-NMR (CDCl$_3$): δ = −2.81 (s, 2 H, $H^{NHpyrrole}$), 4.13 (s, 3 H, $H^{15}{}_{6}$), 4.22 (b. s, 2 H, $H^{29/30}$), 4.31 (t, 1 H, $^3J_{HH}$ = 6.4 Hz, H^{34}), 4.49 (s, 2 H, $H^{23/24}$), 4.52 (s, 2 H, $H^{28/31}$), 4.65 (d, $^3J_{HH}$ = 6.5 Hz, 2 H, H^{33}), 4.84 (s, 2 H, $H^{22/25}$), 6.26 (s, 1 H, H^{NHFmoc}), 7.28 (m, 4 H, $H^{37/38}$), 7.46 (t, $^3J_{HH}$ = 8.7 Hz, 4 H, $H^{10/20}{}_{3/3}$), 7.66 (d, $^3J_{HH}$ = 7.4 Hz, 4 H, $H^{36/39}$), 8.16 (m, 8 H, $H^{5/5/10/20}{}_{2/3/2/2}$), 8.30 (d, $^3J_{HH}$ = 8.1 Hz, 2 H, $H^{15}{}_{2}$), 8.45 (d, $^3J_{HH}$ = 8.0 Hz, 2 H, $H^{15}{}_{3}$), 8.76 (d, $^3J_{HH}$ = 4.7 Hz, 2 H, $H^{pyrrole}$), 8.79 (d, $^3J_{HH}$ = 4.7 Hz, 2 H, $H^{pyrrole}$), 8.83 (d, $^3J_{HH}$ = 4.7 Hz, 2 H, $H^{pyrrole}$), 8.90 (d, $^3J_{HH}$ = 4.8 Hz, 2 H, $H^{pyrrole}$), 9.22 (b. s, 1 H, $H^{NHamide}$) ppm.

^{13}C{^{1}H}-NMR (CDCl$_3$): δ = 47.3 (C^{34}), 52.4 ($C^{15}{}_{6}$), 63.0 ($C^{28/31}$), 66.0 ($C^{29/30}$), 67.0 (C^{33}), 69.9 ($C^{22/25}$), 71.2 ($C^{23/24}$), 78.9 (C^{21}), 96.1 (C^{27}), 113.7 (d, $^2J_{CF}$ = 21.4 Hz, $C^{10/20}{}_{3/3}$), 117.9 ($C^{5}{}_{3}$), 118.6 (C^{15}), 119.0 ($C^{10/20}$), 120.1($C^{36/39}$), 124.9 ($C^{36/39}$), 127.1 ($C^{37/38}$), 127.8 ($C^{37/38}$), 127.8 ($C^{15}{}_{3}$), 129.6 ($C^{15}{}_{4}$), 131.0 (b. s, $C^{2,3,7,8,12,13,17,18}$), 134.5 ($C^{15}{}_{2}$), 135.2 ($C^{5}{}_{2}$), 135.7 (d, $^3J_{CF}$ = 7.9 Hz, $C^{10/20}{}_{2/2}$), 138.0 (d, $^4J_{CF}$ = 3.3 Hz, $C^{10/20}{}_{1/1}$), 138.8 ($C^{5}{}_{4}$), 141.4 (C^{40}), 143.5 (C^{35}), 146.9 ($C^{15}{}_{1}$), 154.3 (C^{32}), 162.9 (d, $^1J_{FH}$ = 247.2 Hz, $C^{10/20}{}_{4/4}$), 167.3 (s, $C^{15}{}_{5}$) ppm (C^5, C^{26} not observed).

^{19}F-NMR (CDCl$_3$): δ = −114.6 (m, F-$C^{10/20}{}_{4/4}$) ppm.

IR (KBr): $\tilde{\nu}$ [cm^{-1}] = 3423, 3217 (br, NH$^{\text{amide}}$, NH$^{\text{Fmoc}}$), 2927 (w, CH), 2854 (w, CH), 1720 (ws, CO), 1602 (w), 1510 (ws), 1385 (ws), 1323 (s, C-O-C), 1157 (w, C-F), 800 (m), 734 (m).

MS (FD): *m/z* (%) = 1173.0 (100) [M$^+$].

MS (ESI): *m/z* (%) = 587.16 (13) [M]$^{2+}$, 1173.32 (100) [M]$^+$.

HR-MS (ESI): obs. *m/z* (%) = 1173.3224; calcd. for [M]$^+$ 1173.3238.

UV/Vis (CH_2Cl_2): λ [nm] (ε / [10^4 M^{-1}cm^{-1}]) = 420 (39.89), 516 (1.56), 552 (0.97), 591 (0.56), 647 (0.46).

Fluorescence (CH_2Cl_2): λ [nm] (relative intensity) = 652 (1.00), 717 (0.32).

Quantum yield: Φ = 0.0449.

Lifetime: τ [ns] = 4.66 (60%), 1.79 (40%).

CV (Fc/Fc$^+$, 100 mV s^{-1}, CH_2Cl_2): $E_{½}$ [V] = −1.960, −1.620, 0.130, 0.590, 0.880.

5d. *N*-Fmoc-Fca-OH (130.0 mg, 0.278 mmol), 15-(4-methoxycarbonylphenyl)-5-(4-aminophenyl)-10,20-bis-(4-trifluoromethylphenyl) porphyrin (**4d**) (104.0 mg, 0.126 mmol), oxalyl chloride (0.10 mL, 1.17 mmol), pyridine (1.0 mL). [silica, CH_2Cl_2; a few drops NEt_3, R_f = 0.27]. Yield: 59.2 mg (0.047 mmol, 37%), purple powder. $C_{74}H_{50}F_6FeN_6O_5$ (1273.06).

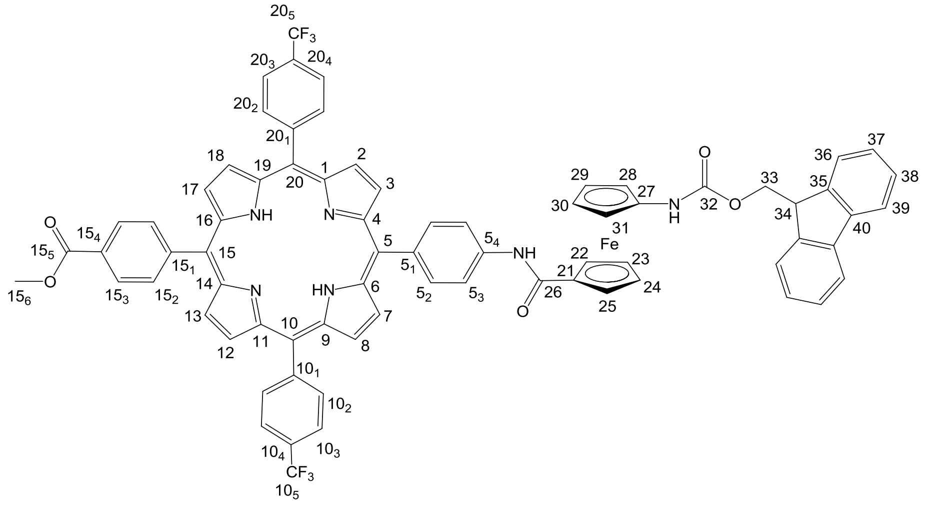

^{1}H-NMR ($CDCl_3$): δ = −2.81 (s, 2 H, H$^{\text{NHpyrrole}}$), 4.12 (s, 3 H, H$^{15}{}_6$), 4.23 (br. s, 2 H, H$^{29/30}$), 4.30 (t, 1 H, $^3J_{\text{HH}}$ = 6.5 Hz, H^{34}), 4.49 (b.s, 2 H, H$^{23/24}$), 4.53 (b. s, 2 H, H$^{28/31}$), 4.64 (d, $^3J_{\text{HH}}$ = 6.6 Hz, 2 H, H^{33}), 4.85 (b. s, 2 H, H$^{22/25}$), 6.31 (s, 2 H, H$^{\text{NHFmoc}}$), 7.27 (m, 4 H, H$^{37/38}$), 7.65 (t, $^3J_{\text{HH}}$ = 6.2 Hz, 4 H, H$^{36/39}$), 8.04 (d, $^3J_{\text{HH}}$ = 8.0 Hz, H$^{10/20}{}_{3/3}$), 8.14 (d, $^3J_{\text{HH}}$ = 8.3 Hz, 2 H, H$^5{}_3$), 8.21 (d, $^3J_{\text{HH}}$ = 8.0 Hz 2 H, H$^5{}_2$), 8.31 (d, $^3J_{\text{HH}}$ = 8.5 Hz, 2 H, H$^{15}{}_2$), 8.33 (d, $^3J_{\text{HH}}$ = 8.1 Hz, 4 H, H$^{10/20}{}_{2/2}$), 8.46 (d, $^3J_{\text{HH}}$ =

8.1, 2 H, $H^{15}{}_{3}$), 8.70 (d, $^{3}J_{HH}$ = 4.7 Hz, 2 H, $H^{pyrrole}$), 8.79 (d, $^{3}J_{HH}$ = 4.7 Hz, 2 H, $H^{pyrrole}$), 8.82 (d, $^{3}J_{HH}$ = 4.8 Hz, 2 H, $H^{pyrrole}$), 8.82 (d, $^{3}J_{HH}$ = 4.7 Hz, 2 H, $H^{pyrrole}$), 9.24 (b. s, 1 H, $H^{NHamide}$) ppm.

^{13}C{^{1}H}-NMR ($CDCl_3$): δ = 47.3 (C^{34}), 52.5 (s, $C^{15}{}_{6}$), 62.9 (s, $C^{28/31}$), 66.0 (s, $C^{29/30}$), 67.1 (s, C^{33}), 69.9 (s, $C^{22/25}$), 71.2 (s, $C^{23/24}$), 78.9 (C^{21}), 96.1 (C^{27}), 117.9 ($C^{5}{}_{3}$), 118.0 (C^{15}), 118.6 ($C^{10/20}$), 119.9 (C^{5}), 120.0 ($C^{36/39}$), 121.0 (C^{5}), 123.7 (d, $^{3}J_{CF}$ = 3.1 Hz, $C^{10/20}{}_{3/3}$), 124.9 ($C^{36/39}$), 127.1 ($C^{37/38}$), 128.0 ($C^{15}{}_{3}$), 127.8 ($C^{37/38}$), 129.7 ($C^{15}{}_{4}$), 130.0 (q, $^{1}J_{CF}$ = 32.2 Hz, $C^{10/20}{}_{5/5}$), 131.1 (b. s, $C^{2,3,7,8,12,13,17,18}$), 134.6 (s, $C^{10/20/15}{}_{2/2}$), 135.2 ($C^{5}{}_{2}$), 136.8 ($C^{5}{}_{1}$), 138.9 ($C^{5}{}_{4}$), 141.4 (C^{40}), 143.5 (C^{35}), 145.7 ($C^{10/20}{}_{1/1}$), 146.7 ($C^{15}{}_{1}$), 154.3 (C^{32}), 167.3 (s, $C^{15}{}_{5}$) ppm (C^{26} not observed).

^{19}F-NMR ($CDCl_3$): $\delta = -64.6$ (s, F-$C^{10/20}{}_{5/5}$) ppm.

IR (KBr): $\tilde{\nu}$ [cm^{-1}] = 3418, 3213 (br, NH^{amide}, NH^{Fmoc}), 2924 (w, CH), 2856 (w, CH), 1662, (vs, CO^{amide}), 1612 (m), 1323 (s, C-O-C), 1168 (w, C-F), 1124 (s, C-O-C), 1045 (s), 800 (s).

MS (FD): *m/z* (%) = 1273.50 (100) $[M]^{+}$.

MS (ESI): *m/z* (%) = 637.15 (22) $[M]^{2+}$, 1273.31 (100) $[M]^{+}$.

HR-MS (ESI): obs. *m/z* (%) = 1273.3209; calcd. for $[M]^{+}$ 1273.3175.

UV/Vis (CH_2Cl_2): λ [nm] (ε / [10^{4} $M^{-1}cm^{-1}$]) = 420 (29.1), 516 (1.46), 551 (0.77), 592 (0.51), 649 (0.43).

Fluorescence (CH_2Cl_2): λ [nm] (relative intensity) = 655 (1.00), 716 (0.25).

Quantum yield: $\Phi = 0.0255$.

Lifetime: τ [ns] = 1.87 (100%).

CV (Fc/Fc^{+}, 100 mV s^{-1}, CH_2Cl_2): $E_{½}$ [V] = −1.900, −1.570, 0.140, 0.660, 0.940.

5e. *N*-Fmoc-Fca-OH (21.5 mg, 0.046 mmol), 15-(4-methoxycarbonylphenyl)-5-(4-aminophenyl)-10,20-bis(2,3,4,5,6-pentafluorophenyl) porphyrin (**4e**) (20.0 mg, 0.023 mmol), oxalyl chloride (16 μL, 0.184 mmol), pyridine (0.5 mL). [silica, CH_2Cl_2/ethylacetate (50:1); a few drops NEt_3, R_f = 0.50]. Yield: 9.0 mg (0.0068 mmol, 30%), red powder. $C_{72}H_{42}F_{10}FeN_6O_5$ (1316.97).

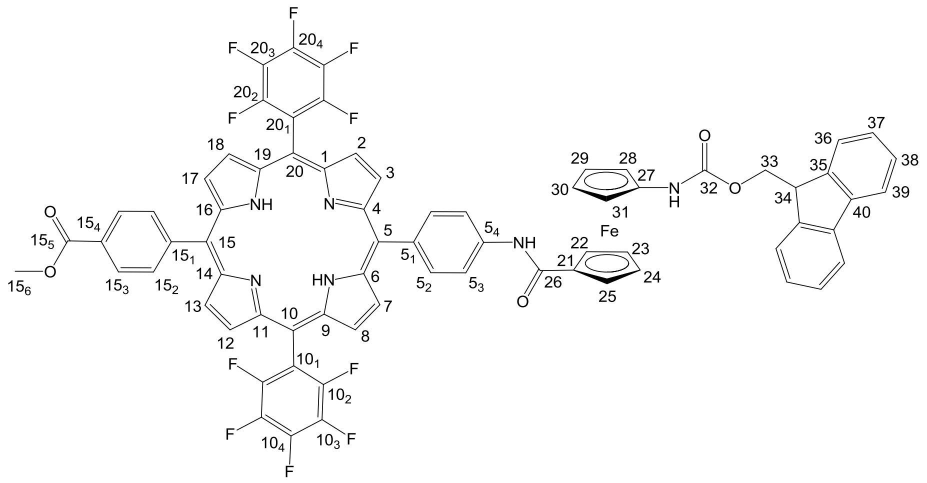

^{1}H-NMR (CDCl$_3$): $\delta = -2.85$ (s, 2 H, H$^{\text{NHpyrrole}}$), 4.13 (s, 3 H, H$^{15}{}_{6}$), 4.23 (br. s, 2 H, H$^{29/30}$), 4.31 (t, 1 H, $^3J_{\text{HH}}$ = 6.6 Hz, H^{34}), 4.50 (br. s, 2 H, H$^{23/24}$), 4.53 (br. s, 2 H, H$^{28/31}$), 4.65 (d, $^3J_{\text{HH}}$ = 6.6 Hz, 2 H, H^{33}), 4.85 (s, 2 H, H$^{22/25}$), 6.31 (b. s, 1 H, H$^{\text{NHFmoc}}$), 7.27 (m, 2 H, H$^{37/38}$), 7.53 (m, 2 H, H$^{36/39}$), 7.66 (d, $^3J_{\text{HH}}$ = 6.4 Hz, 2 H, H$^{37/38}$), 7.72 (m, 2 H, H$^{36/39}$), 8.13 (d, $^3J_{\text{HH}}$ = 7.9, 2 H, H$^{5}{}_{3}$), 8.22 (d, $^3J_{\text{HH}}$ = 7.6 Hz, 2 H, H$^{5}{}_{2}$), 8.31 (d, $^3J_{\text{HH}}$ = 7.6 Hz, 2 H, H$^{15}{}_{2}$), 8.47 (d, $^3J_{\text{HH}}$ = 8.0 Hz, 2 H, H$^{15}{}_{3}$), 8.73 (d, $^3J_{\text{HH}}$ = 4.3 Hz, 2 H, H$^{\text{pyrrole}}$), 8.82 (d, $^3J_{\text{HH}}$ = 4.7 Hz, 2 H, H$^{\text{pyrrole}}$), 8.89 (d, $^3J_{\text{HH}}$ = 4.7 Hz, 2 H, H$^{\text{pyrrole}}$), 8.98 (d, $^3J_{\text{HH}}$ = 4.7 Hz, 2 H, H$^{\text{pyrrole}}$), 9.26 (br. s, 1 H, H$^{\text{NHamide}}$) ppm.

^{13}C{^{1}H}-NMR (d$_8$-THF): Solubility too low for 13C NMR spectra data acquisition.

^{19}F-NMR (d$_8$-THF): $\delta = -162.9$ (ddd, $^3J_{\text{FF}}$ = 24 Hz, $^3J_{\text{FF}}$ = 21 Hz, $^5J_{\text{FF}}$ = 8 Hz, 4 F , F$^{10/20}{}_{3/3,}$), -152.3 (t, $^3J_{\text{FF}}$ = 21 Hz, 2 F, F$^{10/20}{}_{4/4,}$), -136.7 (dd, $^3J_{\text{FF}}$ = 24 Hz, $^5J_{\text{FF}}$ = 8 Hz, 4 F, F$^{10/20}{}_{2/2}$) ppm.

IR (KBr): $\tilde{\nu}$ [cm^{-1}] = 3437, 3217 (br, NH$^{\text{amide}}$, NH$^{\text{Fmoc}}$), 2926 (w, CH), 2855 (w, CH), 1722 (m, CO$^{\text{ester}}$), 1517(vs), 1498 (vs), 1282 (w, C-O-C), 1112 (w, CF), 987 (m), 807 (w).

MS (FD): *m/z* (%) = 1316.44 (100) [M]$^+$.

MS (ESI): *m/z* (%) = 658.62 (8) [M+H]$^{2+}$, 1317.26 (100) [M+H]$^+$.

HR-MS (ESI): obs. *m/z* (%) = 1317.2505; calcd. for [M+H]$^+$ 1317.2485.

UV/Vis (CH$_2$Cl$_2$): λ [nm] (ε / [10^4 M^{-1}cm^{-1}]) = 417 (66.6), 512 (4.26), 546(1.37), 588 (1.45), 643 (0.73).

Fluorescence (CH$_2$Cl$_2$): λ [nm] (relative intensity) = 649 (1.00), 716 (0.50).

Quantum yield: Φ = 0.0094.

Lifetime: τ [ps] = 1488.61 (28%), 331.66 (72%).

CV (Fc/Fc$^+$, 100 mV s^{-1}, CH$_2$Cl$_2$): $E_{½}$ [V] = -1.820, -1.400, 0.130, 0.820, 1.050.

6b. **5b** (30.0 mg, 2.64×10^{-5} mol), tris(2-aminoethyl)amine (187.0 mg, 1.28 mmol), 5-(4-carboxyphenyl)-15-(4-methoxycarbonylphenyl)-10,20-bis(2,4,6-trimethylphenyl) porphyrin (**2a**) (35.7 mg, 4.46×10^{-5} mol), 1-chloro-*N*,*N*,2-trimethylpropenylamine (10 μL, 7.13×10^{-5} mol). [silica, CH_2Cl_2/ethylacetate = 40:1, R_f = 0.50]. Yield: 25.0 mg (1.47×10^{-5} mol, 56 %), purple powder. $C_{110}H_{84}FeN_{10}O_6$ (1697.75).

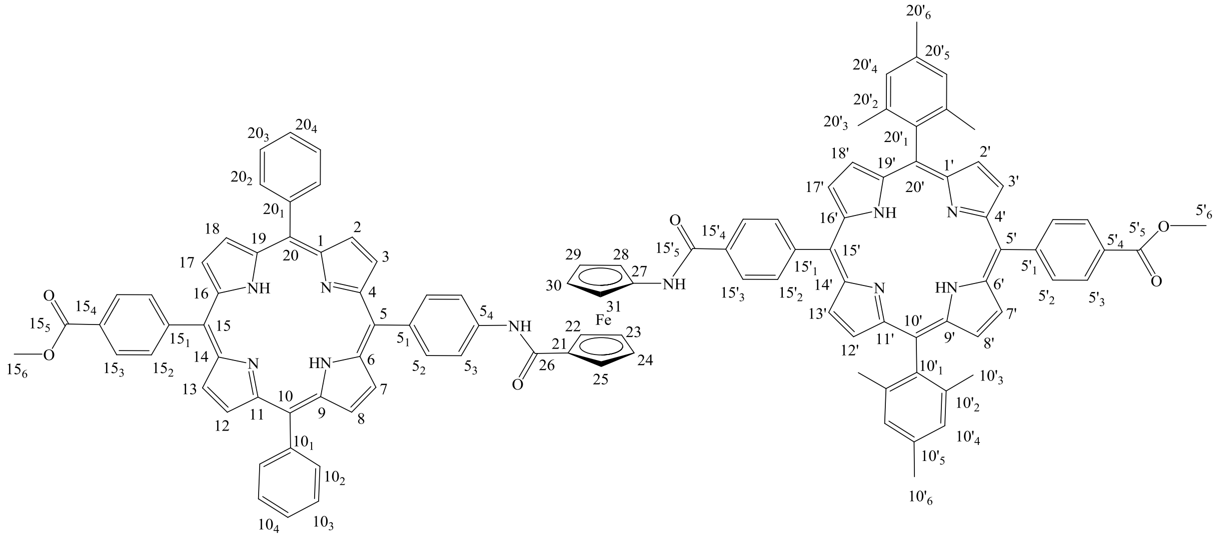

^{1}H-NMR (d_8-THF): δ = −2.73 (s, 2 H, $\mathrm{H}^{\mathrm{NHpyrrole}}$), −2.53 (s, 2 H, $\mathrm{H}^{\mathrm{NHpyrrole}}$), 1.63 (s, 12 H, $\mathrm{H}^{10'/20'}_{3/3}$), 4.03, 4.04 (2 × s, 3 H / 3 H, $\mathrm{H}^{5'/15}_{6/6}$), 4.34 (pt, 2 H, $\mathrm{H}^{29/30}$), 4.58 (pt, 2 H, $\mathrm{H}^{23/24}$), 4.98 (pt, 2 H, $\mathrm{H}^{28/31}$), 5.08 (pt, 2 H, $\mathrm{H}^{22/25}$), 7.13 (s, 4 H, $\mathrm{H}^{10'/20'}_{4/4}$), 7.53 (t, $^3J_{\mathrm{HH}}$ = 7.53 Hz, 4 H, $\mathrm{H}^{10/20}_{3/3}$), 7.61 (d, $^3J_{\mathrm{HH}}$ = 7.61 Hz, 2 H, $\mathrm{H}^{10/20}_{4/4}$), 8.01 (d, $^3J_{\mathrm{HH}}$ = 6.9 Hz, 4 H, $\mathrm{H}^{10/20}_{2/2}$), 8.21 (d, $^3J_{\mathrm{HH}}$ = 8.4 Hz, 2 H, H^{5}_{2}), 8.30 (m, 6 H), 8.41 (m, 6 H), 8.52 (m, 4 H) $\mathrm{H}^{5'/5'/5/15'/15'15/15}_{2/3/3/2/3/2/3}$, $\mathrm{H}^{\mathrm{pyrrole}}$), 8.59 (d, $^3J_{\mathrm{HH}}$ = 4.6 Hz, 2 H, $\mathrm{H}^{\mathrm{pyrrole}}$), 8.68 (d, $^3J_{\mathrm{HH}}$ = 4.7 Hz, 2 H, $\mathrm{H}^{\mathrm{pyrrole}}$), 8.72 (d, $^3J_{\mathrm{HH}}$ = 4.7 Hz, 2 H, $\mathrm{H}^{\mathrm{pyrrole}}$), 8.75 (m, 4 H, $\mathrm{H}^{\mathrm{pyrrole}}$), 8.80 (d, $^3J_{\mathrm{HH}}$ = 4.8 Hz, 2 H, $\mathrm{H}^{\mathrm{pyrrole}}$), 8.96 (d, $^3J_{\mathrm{HH}}$ = 4.4 Hz, 2 H, $\mathrm{H}^{\mathrm{pyrrole}}$), 9.72 (s, 1H, $\mathrm{H}^{\mathrm{FcNHamide}}$), 10.21 (s, 1 H, $\mathrm{H}^{\mathrm{PorphNHamide}}$) ppm ($\mathrm{H}^{10'/20'}_{6/6}$ hidden under solvent resonance).

^{1}H-NMR ($CDCl_3$): δ= −2.69 (s, 2 H, $\mathrm{H}^{\mathrm{NHpyrrole}}$), −2.80 (s, 2 H, $\mathrm{H}^{\mathrm{NHpyrrole}}$), 1.68 (s, 12 H, $\mathrm{H}^{10'/20'}_{3/3}$), 2.53 (s, 6 H, $\mathrm{H}^{10'/20'}_{6/6}$), 4.10, 4.10 (2 × s, 3 H / 3 H, $\mathrm{H}^{5'/15}_{6/6}$), 4.42 (s, 2 H, $\mathrm{H}^{29/30}$), 4.63 (s, 2 H, $\mathrm{H}^{23/24}$), 4.86 (s, 2 H, $\mathrm{H}^{28/31}$), 5.07 (s, 2 H, $\mathrm{H}^{22/25}$), 7.14 (s, 4 H, $\mathrm{H}^{10'/20'}_{4/4}$), 7.64 (m, 6 H, $\mathrm{H}^{10/20}_{3/3/4/4}$), 8.05 (s, 1H, $\mathrm{H}^{\mathrm{NHamide}}$), 8.10 (d, $^3J_{\mathrm{HH}}$ = 6.7 Hz, 4 H, $\mathrm{H}^{10/20}_{2/2}$), 8.27 (m, 6 H, $\mathrm{H}^{5/5'/15'}_{2/3/2}$), 8.41 (m, 10 H, $\mathrm{H}^{5'/5/15'/15/15}_{2/3/3/2/3}$), 8.58 (d, $^3J_{\mathrm{HH}}$ = 4.7 Hz, 2 H, $\mathrm{H}^{\mathrm{pyrrole}}$), 8.64 (d, $^3J_{\mathrm{HH}}$ = 4.7 Hz, 2 H, $\mathrm{H}^{\mathrm{pyrrole}}$), 8.70 (d, $^3J_{\mathrm{HH}}$ = 4.7 Hz, 2 H, $\mathrm{H}^{\mathrm{pyrrole}}$), 8.75 (m, 6 H, $\mathrm{H}^{\mathrm{pyrrole}}$), 8.80 (d, $^3J_{\mathrm{HH}}$ = 4.7 Hz, 2 H, $\mathrm{H}^{\mathrm{pyrrole}}$), 8.97 (d, $^3J_{\mathrm{HH}}$ = 4.6 Hz, 2 H, $\mathrm{H}^{\mathrm{pyrrole}}$), 9.94 (b. s, 1 H, $\mathrm{H}^{\mathrm{NHamide}}$) ppm.

^{13}C{^{1}H}-NMR ($CDCl_3$): δ = 21.4 ($\mathrm{C}^{10'/20'}_{4/4}$), 21.5 ($\mathrm{C}^{10'/20'}_{3/3}$), 52.4 ($\mathrm{C}^{5'/15}_{6/6}$), 64.5 ($\mathrm{C}^{28/31}$), 66.6 ($\mathrm{C}^{29/30}$), 70.1 ($\mathrm{C}^{22/25}$), 71.3 ($\mathrm{C}^{23/24}$), 95.0 ($\mathrm{C}^{27}$), 117.8, 118.0, 118.3, 118.8, 120.5 ($\mathrm{C}^{5/15/5'/15'/10'/20'}$), 120.3 ($\mathrm{C}^{10/20}$), 125.6, 127.9, 135.0, 135.3 ($\mathrm{C}^{15/15/15'/15'}_{2/3/2/3}$), 126.6 ($\mathrm{C}^{10/20}_{3/3}$), 127.6, 127.7

($C^{10/20/10'/20'}_{4/4/4/4}$), 129.5, 129.5, 139.2 ($C^{15/5/5'}_{1/4/4}$), 131.2 (br. s, $C^{2,3,7,8,12,13,17,18,2',3',7',8',12',13',17',18'}$), 134.5 ($C^{10/20}_{2/2}$), 134.6 ($C^{5}_{3}$), 135.0 ($C^{5'}_{2}$), 135.3 ($C^{5}_{2}$), 137.8 ($C^{10'/20'}_{5/5}$), 139.1 ($C^{5}_{4}$), 142.0 ($C^{10/20}_{1/1}$), 146.2, 146.7, 147.1 ($C^{5'/5'/15'}_{1/4/4}$), 167.3 ($C^{15/5'}_{5/5}$), 166.2, 169.7 ($C^{26/15'}_{5}$) ppm.

IR (KBr): $\tilde{\nu}$ [cm^{-1}] = 3421, 3321 (br, NH^{amide}), 2924 (w, CH), 2852 (w, CH), 1720 (vs, CO^{ester}), 1514 (s), 1384 (vs), 1281 (s, C-O-C), 800 (m), 737 (m).

MS (FD): *m/z* (%) = 849.2 (19) [M]$^{2+}$, 1698.7 (100) [M+H]$^{+}$.

MS (ESI): *m/z* (%) = 849.81 (88) [M+H]$^{2+}$, 1698.61 (100) [M+H]$^{+}$.

HR-MS (ESI): obs. *m/z* (%) = 1697.5977; calcd. for [M]$^{+}$ 1697.6003.

UV/Vis (CH_2Cl_2): λ [nm] (ε / [10^4 M^{-1}cm^{-1}]) = 419 (78.60), 516 (3.99), 551 (2.09), 592 (1.30), 650 (1.46).

Fluorescence (CH_2Cl_2): λ [nm] (relative intensity) = 654 (1.00), 717 (0.20).

Quantum yield: Φ = 0.0475.

Lifetime: τ [ns] = 4.19 (42%), 1.76 (58%).

CV (Fc/Fc^{+}, 100 mV s^{-1}, CH_2Cl_2): $E_{½}$ [V] = −2.000, −1.640 (2e), 0.160, 0.600 (2e), 0.880, 1.070.

6c. **5c** (15.0 mg, 1.30×10^{-5} mol), tris(2-aminoethyl)amine (93.5 mg, 0.64 mmol), 5-(4-carboxyphenyl)-15-(4-methoxycarbonylphenyl)-10,20-bis(2,4,6-trimethylphenyl) porphyrin (**2a**) (37.9 mg, 4.73×10^{-5} mol), 1-chloro-*N*,*N*,2-trimethylpropenylamine (25 μL, 18.9×10^{-5} mol). [silica, CH_2Cl_2/ethylacetate = 10:1, R_f = 0.75]. Yield: 11.0 mg (0.63×10^{-5} mol, 48 %), purple powder. $C_{110}H_{82}F_2FeN_{10}O_6$ (1733.73).

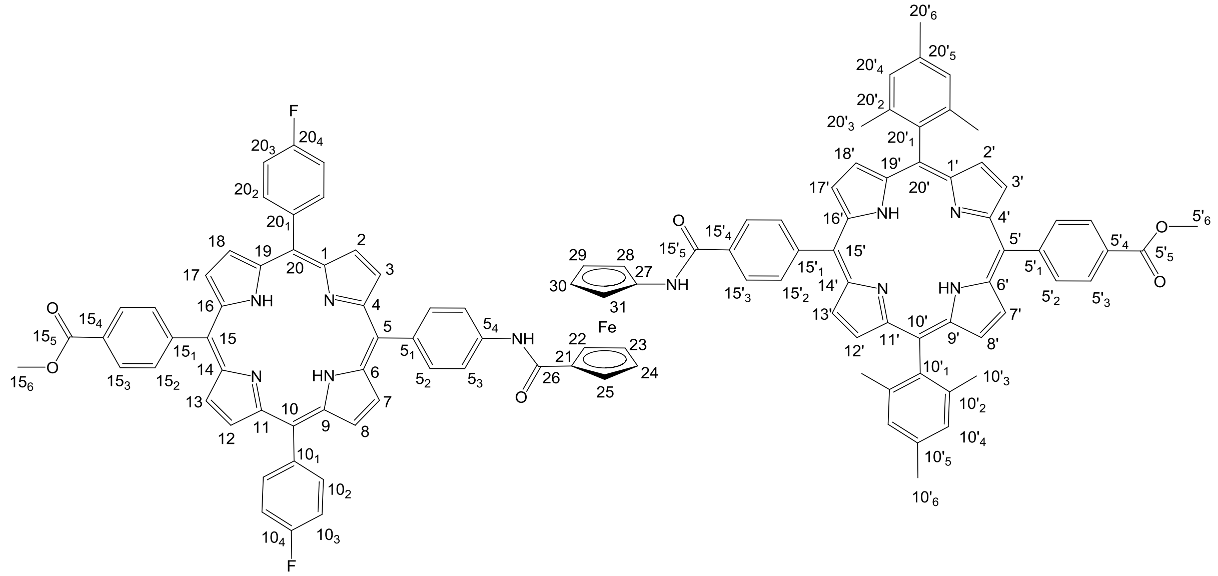

^{1}H-NMR (d_8-THF): δ = −2.75 (s, 2 H, H^{NHpyrrole}), −2.57 (s, 2 H, H^{NHpyrrole}), 1.61 (s, 12 H, $H^{10'/20'}_{3/3}$), 4.03, 4.04 (s, 3 H / 3 H, $H^{5'}_{6}$ and H^{15}_{6}), 4.35 (pt, 2 H, H$^{29/30}$), 4.58 (b.s, 2 H, H$^{23/24}$), 4.99 (b. s, 2 H, H$^{28/31}$), 5.08 (b. s, 2 H, H$^{22/25}$), 7.11 (s, 4 H, $H^{10'/20'}_{4/4}$), 7.28 (t, $^3J_{HH}$ = 8.3 Hz, 4 H, H$^{10/20}_{3/3}$), 7.97 (m, 4 H, H$^{10/20}_{2/2}$), 8.20 (d, $^{3}J_{\mathrm{HH}}$ = 8.4 Hz, 2 H, H$^{5}_{2}$), 8.30 (m, 4 H), 8.41 (m, 6 H), 8.53 (d, $^{3}J_{\mathrm{HH}}$ = 8.3 Hz, 2 H), 8.53 (d, $^{3}J_{\mathrm{HH}}$ = 8.4 Hz, 2 H) (H$^{5/15/15/5'/5'/15'/15'}_{3/2/3/2/3/2/3}$), 8.49 (d, $^{3}J_{\mathrm{HH}}$ = 4.7 Hz, 2 H, H$^{\mathrm{pyrrole}}$), 8.66 (d, $^{3}J_{\mathrm{HH}}$ = 5.0 Hz, 2 H, H$^{\mathrm{pyrrole}}$), 8.71 (d, $^{3}J_{\mathrm{HH}}$ = 4.5 Hz, 2 H, H$^{\mathrm{pyrrole}}$), 8.76 (m, 4 H, H$^{\mathrm{pyrrole}}$), 8.79 (d, $^{3}J_{\mathrm{HH}}$ = 4.7 Hz, 2 H, H$^{\mathrm{pyrrole}}$), 8.97 (d, $^{3}J_{\mathrm{HH}}$ = 4.7 Hz, 2 H, H$^{\mathrm{pyrrol}}$), 9.72 (s, 1H, H$^{\mathrm{FcNHamide}}$), 10.21 (s, 1 H, H$^{\mathrm{PorphNHamide}}$) ppm (H$^{10'/20'}_{6/6}$ hidden under solvent resonance).

^{1}H-NMR (CDCl$_3$): δ = −2.83 (s, 2 H, H$^{\mathrm{NHpyrrole}}$), −2.69 (s, 2 H, H$^{\mathrm{NHpyrrole}}$), 1.67 (s, 12 H, H$^{10'/20'}_{3/3}$), 2.53 (s, 6 H, H$^{10'/20'}_{4/4}$), 4.10 (s, 3 H, H$^{5'}_{6}$), 4.11 (s, 3 H, H$^{15}_{6}$), 4.42 (pt, 2 H, $^{3}J_{\mathrm{HH}}$ = 1.7 Hz, H$^{29/30}$), 4.63 (pt, 2 H, $^{3}J_{\mathrm{HH}}$ = 1.5 Hz, H$^{23/24}$), 4.87 (pt, 2 H, $^{3}J_{\mathrm{HH}}$ = 1.7 Hz, H$^{28/31}$), 5.07 (pt, 2 H, $^{3}J_{\mathrm{HH}}$ = 1.7 Hz, H$^{22/25}$), 7.14 (s, 2 H, H$^{10'/20'}_{4/4}$), 7.32 (t, ^{3}J = 8.6 Hz, 4 H, H$^{10/20}_{3/3}$), 8.04 (dd, ^{3}J = 8.3 Hz, ^{3}J = 5.4 Hz, 4 H, 4 H, H$^{10/20}_{2/2}$), 8.09 (s, 1H, H$^{\mathrm{NHamide}}$), 8.26 (m, 2 H, H$^{5/15'}_{3/2}$), 8.29 (d, 2 H, H$^{15}_{2}$) 8.43 (m, 10 H, H$^{5/15/5'/5'/15'}_{2/2/3/2/3/2}$), 8.58 (d, $^{3}J_{\mathrm{HH}}$ = 4.8 Hz, 2 H, H$^{\mathrm{pyrrole}}$), 8.64 (d, $^{3}J_{\mathrm{HH}}$ = 4.7 Hz, 2 H, H$^{\mathrm{pyrrole}}$), 8.71 (d, $^{3}J_{\mathrm{HH}}$ = 4.8 Hz, 2 H, H$^{\mathrm{pyrrole}}$), 8.73 (d, $^{3}J_{\mathrm{HH}}$ = 4.8 Hz, 2 H, H$^{\mathrm{pyrrole}}$), 8.76 (d, $^{3}J_{\mathrm{HH}}$ = 4.8 Hz, 2 H, H$^{\mathrm{pyrrole}}$), 8.78 (m, 4 H, H$^{\mathrm{pyrrole}}$), 8.99 (d, $^{3}J_{\mathrm{HH}}$ = 4.7 Hz, 2 H, H$^{\mathrm{pyrrole}}$), 9.99 (s, 1 H, H$^{\mathrm{NHamide}}$) ppm.

^{13}C{^{1}H}-NMR (CDCl$_3$): δ = 21.4 (C$^{10'/20'}_{6/6}$), 21.5 (C$^{10'/20'}_{3/3}$), 52.4 (C$^{5'/15}_{6/6}$), 64.5 (C$^{28/31}$), 66.6 (C$^{29/30}$), 70.1(C$^{22/25}$), 71.3 (s, C$^{23/24}$), 79.5 (s, C^{21}), 95.0 (s, C^{27}), 113.6 (d, $^{2}J_{\mathrm{CF}}$ = 21.4 Hz, C$^{10/20}_{3/3}$), 117.8, 118.2, 118.5, 119.0, 120.8 (C$^{5/15/5'/15'/10'/20'}$), 118.1, 125.6, 127.9, 127.9, 134.5, 135.0, 137.0 (C$^{5/15/15/5'/5'/15'}_{2/2/2/3/2/3/2}$), 118.8 (C$^{10/20}$), 127.7 (C$^{10'/20'}_{4/4}$), 129.6 (C$^{15}_{4}$), 130.9 (b. s, C$^{2,3,7,8,12,13,17,18,2',3',7',8',12',13',17',18'}$), 133.1 (C$_{\mathrm{q}}$), 134.5, 135.3 (C$^{5/15'}_{3/2}$), 135.6 (d, $^{2}J_{\mathrm{CF}}$ = 8.1 Hz, C$^{10/20}_{2/2}$), 137.8 (C$_{\mathrm{q}}$), 137.9 (d, $^{4}J_{\mathrm{CF}}$ = 3.0 Hz, C$^{10/20}_{1/1}$), 138.0 (C$^{10'/20'}_{5/5}$), 139.2 (C$^{10'/20'}_{2/2}$), 146.2, 146.7, 146.9 (C$^{5/15/5'}_{4/1/1}$), 162.8 (d, $^{1}J_{\mathrm{FH}}$ = 247.5 Hz, C$^{10/20}_{4/4}$), 166.3, 169.7 (C$^{26/\ 15'}_{5}$), 167.3 (C$^{15/5'}_{5/5}$), ppm.

^{19}F-NMR (CDCl$_3$): δ = −114.7 (m, F-C^{4}) ppm.

IR (KBr): $\tilde{\nu}$ [cm^{-1}] = 3435, 3223 (br, NH$^{\mathrm{amide}}$), 2923 (w, CH), 2855 (w, CH), 1724 (m, CO$^{\mathrm{ester}}$), 1653 (m, CO$^{\mathrm{amide}}$), 1606 (m), 1506 (m), 1383 (vs), 1277 (m, C-O-C), 1155 (w, C-F), 800 (m), 727 (m).

MS (FD): *m/z* (%)= 1735.32 (100) [M+H]$^{+}$.

MS (ESI): *m/z* (%) = 866.82 (100) [M]$^{2+}$, 1733.58 (13) [M]$^{+}$.

HR-MS (ESI): obs. *m/z* (%) = 1733.5856; calcd. for [M]$^{+}$ 1733.5815.

UV/Vis (CH$_2$Cl$_2$): λ [nm] (ε / [10^{4} M^{-1}cm^{-1}]) = 420 (53.00), 516 (2.83), 552 (1.44), 591 (0.94), 647 (0.97).

Fluorescence (CH$_2$Cl$_2$): λ [nm] (relative intensity) = 655 (1.00), 718 (0.20).

Quantum yield: Φ = 0.0451.

Lifetime: τ [ns] = 3.07 (100%).

CV (Fc/Fc$^+$, 100 mV s^{-1}, CH$_2$Cl$_2$): $E_{½}$ [V] = −1.960, −1.630 (2e), 0.150, 0.610 (2e), 0.880, 1.080.

Zn-6b. **6b** (10.0 mg, 5.89×10^{-6} mol), zinc(II) acetate dihydrate (13.0 mg, 70.63×10^{-6} mol). [silica, toluene : ethyl acetate = 50 : 1, R_f = 0.20]. Yield 7.2 mg (3.95×10^{-6} mol, 67%), purple powder. $C_{110}H_{80}FeN_{10}O_6Zn_2$ (1824.54).

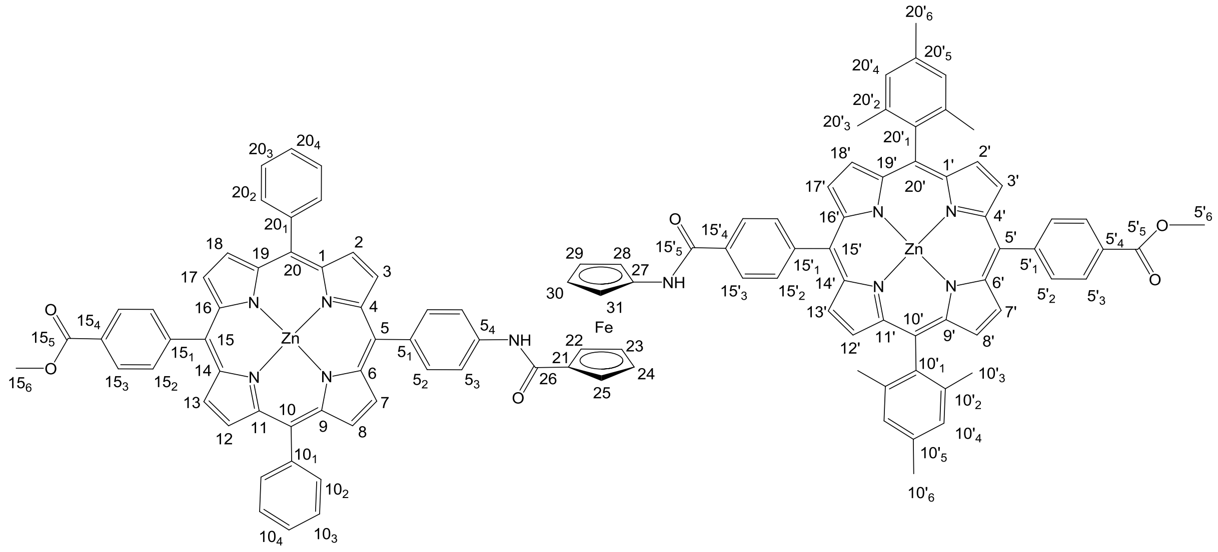

^{1}H-NMR (d$_8$-THF): δ = 4.03, 4.04 (2 × s, 3 H / 3 H, $H^{5'/15}_{6/6}$), 4.37 (s, 2 H, $H^{29/30}$), 4.58 (s, 2 H, $H^{23/24}$), 4.94 (s, 2 H, $H^{28/31}$), 5.04 (s, 2 H, $H^{22/25}$), 7.21 (s, 4 H, $H^{10'/20'}_{4/4}$), 7.68 (m, 6 H, $H^{10/20}_{3/3/4/4}$), 8.13 (m, 4 H, $H^{10/20}_{2/2}$), (d, $^3J_{HH}$ = 8.2 Hz, 2 H, H^{5}_{2}), 8.27 (m, 4 H), 8.37 (m, 6 H), 8.51 (m, 4 H) ($H^{5/5'/5'/15/15/15'/15'}_{3/2/3/2/3/2/3}$ and $H^{pyrrole}$), 8.62 (m, 4 H, $H^{pyrrole}$), 8.71 (d $^3J_{HH}$ = 4.7 Hz, 4 H, $H^{pyrrole}$), 8.78 (m, 8 H, $H^{pyrrole}$), 8.99 (d, $^3J_{HH}$ = 4.5 Hz, 2 H, $H^{pyrrole}$), 9.75 (s, 1H, $H^{FcNHamide}$), 10.37 (s, 1 H, $H^{PorphNHamide}$) ppm ($H^{10'/20'}_{3/3}{}^{10'/20'}_{6/6}$ hidden under solvent resonance).

^{1}H-NMR (CDCl$_3$): δ = 1.63 (s, 12 H, $H^{10'/20'}_{3/3}$), 2.51 (s, 6 H, $H^{10'/20'}_{6/6}$), 4.06, 4.07 (2 × s, 3 H / 3 H, $H^{5'/15}_{6/6}$), 4.53 (s, 2 H, $H^{29/30}$), 4.65 (s, 2 H, $H^{23/24}$), 4.80 (s, 2 H, $H^{28/31}$), 5.13 (s, 2 H, $H^{22/25}$), 7.11 (s, 4 H, $H^{10'/20'}_{4/4}$), 7.52 (m, 6 H, $H^{10/20}_{3/3/4/4}$), 8.00 (m, 5 H, $H^{10/20}_{2/2}$, $H^{NHamide}$), 8.18 (m, 6 H, $H^{5/5'/15'}_{2/3/2}$), 8.26, 8.41 (m, 10 H, $H^{5'/5/15'/15/15}_{2/3/3/2/3}$), 8.61 (d, $^3J_{HH}$ = 4.6 Hz, 2 H, $H^{pyrrole}$), 8.70 (pt, 4 H, $H^{pyrrole}$), 8.76 (d, $^3J_{HH}$ = 4.5 Hz, 2 H, $H^{pyrrole}$), 8.80 (m, 4 H, $H^{pyrrole}$), 8.84 (d, $^3J_{HH}$ = 4.6 Hz, 2 H, $H^{pyrrole}$), 9.00 (d, $^3J_{HH}$ = 4.6 Hz, 2 H, $H^{pyrrole}$), 9.43 (b. s, 1 H, $H^{NHamide}$) ppm.

^{13}C{^{1}H}-NMR (CDCl$_3$): δ = 21.4 ($C^{10'/20'}_{4/4}$), 21.4 ($C^{10'/20'}_{3/3}$), 52.3 ($C^{5'/15}_{6/6}$), 64.1 ($C^{28/31}$), 66.4 ($C^{29/30}$), 69.8 ($C^{22/25}$), 71.2 ($C^{23/24}$), 95.0 (C^{27}), 117.1, 117.6.0, 118.7, 119.5, 121.1 ($C^{5/15/5'/15'/10/20/10'/20'}$), 126.3 ($C^{10/20}_{3/3}$), 127.5 ($C^{10/20}_{4/4}$), 127.6 ($C^{10'/20'}_{4/4}$), 129.1, 132.7, 134.7, 138.6 ($C^{5/15/5'/15'}_{1/4/4/4}$), 130.9, 131.0, 131.0, 131.3, 131.9, 131.9, 132.0, 132.0, 132.1, 132.3, 132.3 ($C^{2,3,7,8,12,13,17,18,2',3',7',8',12',13',17',18'}$), 134.3 ($C^{10/20}_{2/2}$), 134.3, 134.4, 134.4, 134.8 ($C^{5'/5/15'/15/15}_{2/3/3/2/3}$), 127.7, 134.3, 134.4, 134.4, 134.8 ($C^{5/15/15/5'/5'/15'/15'}_{2/2/3/2/3/2/3}$), 139.1 ($C^{10'/20'}_{5/5}$), 142.6 ($C^{10/20}_{1/1}$), 147.7, 147.9 ($C^{15/5'}_{1/1}$), 149.4, 149.5, 149.9, 150.0, 150.2 150.4 ($C^{1,4,6,9,11,14,16,19,1',4',6',9',11',14',16',19'}$), 167.4, 167.7 ($C^{15/5'}_{5/5}$), 166.1, 169.2 ($C^{26/15'}_{5}$) ppm.

IR (KBr): $\tilde{\nu}$ [cm^{-1}] = 3446 (br, NH^{amide}), 2924 (w, CH), 2851 (w, CH), 1727 (m, CO^{ester}), 1645 (m, CO^{amide}), 1517 (m), 1382 (vs) 1280 (m, C-O-C), 1000 (m), 797 (m).

MS (FD): *m/z* (%) = 913.3 (7) $[M]^{2+}$, 1824.4 (100) $[M]^{+}$.

MS (ESI): *m/z* (%) = 910.25 (3) $[M]^{2+}$, 1822.48 (1) $[M]^{+}$.

HR-MS (ESI): obs. *m/z* (%) = 910.2098; calcd. for $[M]^{2+}$ 910.2098.

UV/Vis (CH_2Cl_2): λ [nm] (ε / [10^4 $M^{-1}cm^{-1}$]) = 422 (109.44), 551 (5.48), 593 (1.62).

Fluorescence (CH_2Cl_2): λ [nm] (relative intensity) = 603 (0.66), 655 (1.00).

Quantum yield: Φ = 0.0198.

Lifetime: τ [ns] = 1.87 (16%), 0.63 (84%).

CV (Fc/Fc^{+}, 100 mV s^{-1}, CH_2Cl_2): $E_{½}$ [V] = −1.820, 0.160, 0.420 (2e), 0.740 (2e).

Zn-6c. **6c** (8.0 mg, 4.63×10^{-6} mol), zinc(II) acetate dihydrate (12.2 mg, 55.56×10^{-6} mol) were stirred overnight in CH_2Cl_2 (10 mL). [silica, toluene : ethyl acetate = 50 : 1, R_f = 0.22]. Yield 7.1 mg (3.82×10^{-6} mol, 82%), purple powder. $C_{110}H_{78}F_2FeN_{10}O_6Zn_2$ (1860.52).

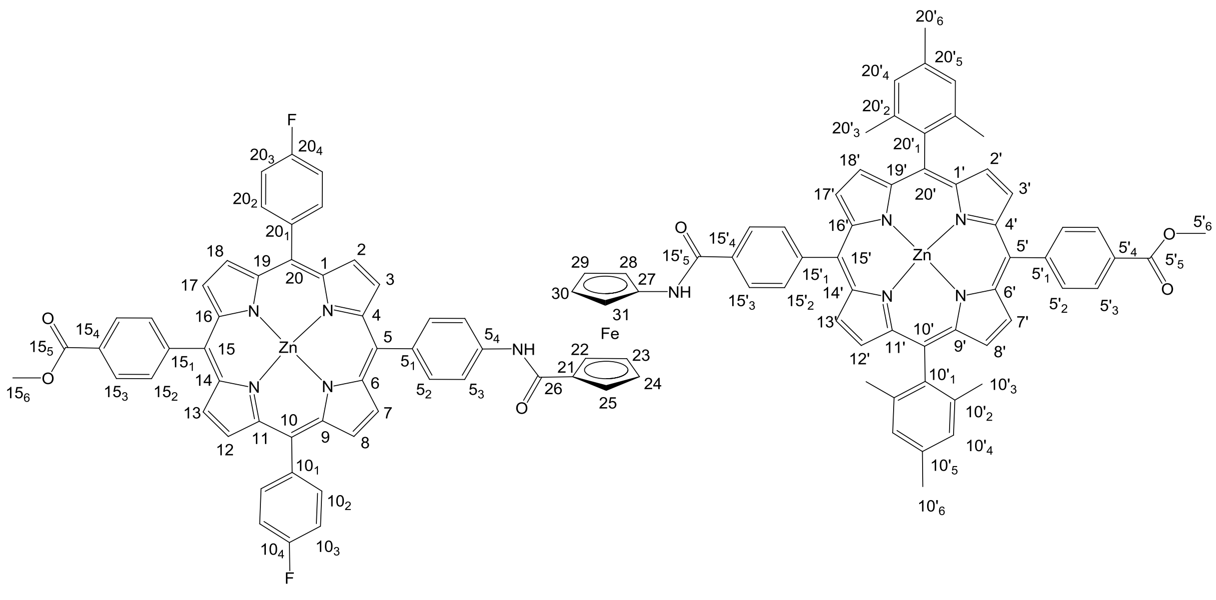

^{1}H-NMR (d_8-THF): δ =1.75 (s, 12 H, $H^{10'/20'}_{3/3}$), 2.54 (s, 6 H, $H^{10'/20'}_{6/6}$), 4.03, 4.04 (s, 3 H/ 3 H, $H^{5'}_{6}$ and H^{15}_{6}), 4.42 (b. s, 2 H, $H^{29/30}$), 4.58 (b.s, 2 H, $H^{23/24}$), 4.93 (b. s, 2 H, $H^{28/31}$), 5.04 (b. s, 2 H, $H^{22/25}$), 7.22 (s, 4 H, $H^{10'/20'}_{4/4}$), 7.43 (t, $^3J_{HH}$ = 8.7 Hz, 4 H, $H^{10/20}_{3/3}$), 8.13 (m, 4 H, $H^{10/20}_{2/2}$), 8.18 (d, $^3J_{HH}$ = 8.2 Hz, 2 H, H^{5}_{2}), 8.27 (m, 4 H), 8.37 (d, $^3J_{HH}$ = 7.9 Hz, 4 H), 8.40 (d, $^3J_{HH}$ = 8.0 Hz, 2 H), 8.50 (d, ${}^{3}J_{HH}$ = 8.0 Hz, 2 H)($H^{15/15/5'/5'/15'/15'}_{2/3/2/3/2/3}$), 8.55 (d, ${}^{3}J_{HH}$ = 8.4 Hz, 2 H, H^{5}_{3}), 8.62 (d, ${}^{3}J_{HH}$ = 4.5 Hz, 2 H, $H^{pyrrole}$), 8.62 (d, ${}^{3}J_{HH}$ = 4.6 Hz, 2 H, $H^{pyrrole}$), 8.71 (d, ${}^{3}J_{HH}$ = 4.6 Hz, 2 H, $H^{pyrrole}$), 8.80 (m, 8 H, $H^{pyrrole}$), 9.02 (d, ${}^{3}J_{HH}$ = 4.6 Hz, 2 H, $H^{pyrrole}$), 9.71 (s, 1H, $H^{FcNHamide}$), 10.42 (s, 1 H, $H^{PorphNHamide}$) ppm.

^{1}H-NMR (CDCl$_3$): δ = 1.65 (s, 12 H, $H^{10'/20'}_{3/3}$), 2.52 (s, 6 H, $H^{10'/20'}_{6/6}$), 4.09, 4.10 (2 × s, 3 H / 3 H, $H^{5'/15}_{6/6}$), 4.41 (pt, 2 H, $H^{29/30}$), 4.63 (pt, 2 H, $H^{23/24}$), 4.86 (b.s, 2 H, $H^{28/31}$), 5.04 (b. s, 2 H, $H^{22/25}$), 7.12 (s, 4 H, $H^{10'/20'}_{4/4}$), 7.32 (t, ${}^{3}J_{HH}$ = 8.7 Hz, 4 H, $H^{10/20}_{3/3}$), 8.04 (m, 5 H, $H^{10/20}_{2/2}$, $H^{NHamide}$), 8.25 (d, ${}^{3}J_{HH}$ = 8.7 Hz, 2H, H^{5}_{2}), 8.27 (d, ${}^{3}J_{HH}$ = 8.1 Hz, 4 H), 8.41 (m, 10 H, $H^{5/15/15/5'/5'/15'/15'}_{3/2/3/2/3/2/3}$), 8.64 (d, ${}^{3}J_{HH}$ = 4.6 Hz, 2 H, $H^{pyrrole}$), 8.70 (d, ${}^{3}J_{HH}$ = 4.7 Hz, 2 H, $H^{pyrrole}$), 8.77 (d, ${}^{3}J_{HH}$ = 4.6 Hz, 2 H, $H^{pyrrole}$), 8.81 (d, ${}^{3}J_{HH}$ = 4.5 Hz, 2 H, $H^{pyrrole}$), 8.82 (m, 2 H, $H^{pyrrole}$), 9.08 (d, ${}^{3}J_{HH}$ = 4.6 Hz, 2 H, $H^{pyrrole}$), 9.89 (b. s, 1 H, $H^{NHamide}$) ppm.

^{13}C{^{1}H}-NMR (d$_8$-THF): δ = 21.7 (s, 2C, $C^{10'/20'}_{6/6}$), 22.1 (s, 4C, $C^{10'/20'}_{3/3}$), 52.5 (s, 2C, $C^{5'/15}_{6/6}$), 64.8 ($C^{28/31}$), 67.2 ($C^{29/30}$), 70.9($C^{22/25}$), 71.9 (s, $C^{23/24}$), 114.2 (d, ${}^{2}J_{CF}$ = 21.5 Hz, $C^{10/20}_{3/3}$), 119.9, 120.5, 120.6 ($C^{5/15/10/20/5'/15'/10'/20'}$), 118.4 ($C^{5}_{3}$), 128.7 ($C^{10'/20'}_{4/4}$), 130.5, 132.1 132.2, 132.5, 138.7 (C_q) ($C^{5/15/5'}_{1/4/4}$), 126.7,128.4, 128.5, 135.5, 135.6, 135.7, 137.4 ($C^{5/15/15/15/5'/5'/15'/15'}_{2/2/3/1/2/3/2/3}$), 131.3 (b. s, $C^{2,3,7,8,12,13,17,18,2',3',7',8',12',13',17',18'}$), 140.0 ($C^{10/20}_{1/1}$), 140.6 ($C^{10'/20'}_{1/1}$), 140.7 (d, ${}^{4}J_{CF}$ = 3.0 Hz, $C^{10/20}_{1/1}$), 144.6, 144.9, 149.4 ($C^{5/15/5'}_{4/1/1}$), 150.5, 150.7, 150.9, 151.0, 151.2, 151.4 ($C^{1,4,6,9,11,14,16,19,1',4',6',9',11',14',16',19'}$), 136.8 (d, ${}^{2}J_{CF}$ = 8.1 Hz, $C^{10/20}_{2/2}$), 164.3 (d, ${}^{1}J_{FH}$ = 246.0 Hz, $C^{10/20}_{4/4}$), 167.5 ($C^{15/5'}_{5/5}$) ppm ($C^{26/15'}_{5}$ not observed).

^{19}F-NMR (d$_8$-THF): δ = −118.7 (m, F-C^4) ppm.

IR (KBr): $\tilde{\nu}$ [cm^{-1}] = 3427 (br, NH^{amide}), 2926 (w, CH), 2855 (m, CH), 1741 (w, CO), 1666 (m, CO), 1521 (m), 1384 (vs), 1279 (m, C-O-C), 1159 (w, C-F), 997 (m).

MS (FD): *m/z* (%) = 930.66 (9) [M]$^{2+}$, 1860.42(100) [M]$^{+}$.

MS (ESI): *m/z* (%) = 1858.41 (3) [M]$^{+}$, 1860.41 (5) [M]$^{+}$.

HR-MS (ESI): obs. *m/z* (%) = 1857.4043; calcd. for [M]$^{+}$ 1857.4084.

UV/Vis (CH$_2$Cl$_2$): λ [nm] (ε / [10^4 M^{-1}cm^{-1}]) = 420 (82.95), 549 (5.68), 588 (2.81).

Fluorescence (CH$_2$Cl$_2$): λ [nm] (relative intensity) = 597 (0.77), 653 (1.00).

Quantum yield: Φ = 0.0173.

Lifetime: τ [ns] = 3.23 (27%), 0.74 (73%).

CV (Fc/Fc^{+}, 100 mV s^{-1}, CH$_2$Cl$_2$): $E_{½}$ [V] = −1.910, 0.150, 0.400 (2e), 0.730 (2e).

Zn-1e.

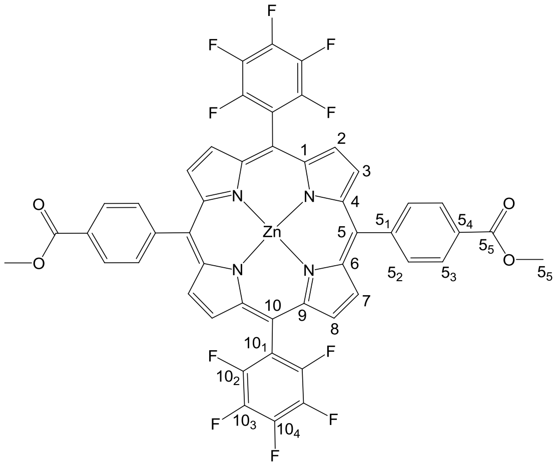

^{1}H-NMR (d$_8$-THF): δ = 4.07 (s, 6 H, H$^5{}_6$), 8.33 (d, $^3J_{HH}$ = 8.1 Hz, 4 H, H$^5{}_2$), 8.44 (d, $^3J_{HH}$ = 8.0 Hz, 4 H, H$^5{}_3$), 8.91 (d, $^3J_{HH}$ = 4.6 Hz, 4 H, H^{pyrrole}), 9.00 (d, $^3J_{HH}$ = 4.6 Hz, 4 H, H^{pyrrole}) ppm.

^{13}C{^{1}H}-NMR (d$_8$-THF): δ = 52.6 (C$^5{}_6$), 121.7 (C^5), 128.6 (C$^5{}_3$), 130.9 (C$^5{}_4$), 131.5, 133.8 (C^{2,3,7,8}), 135.6 (C$^5{}_2$), 137.5, 140.0, 141.8, 144.3, 146.6, 149.0 (m, C^{10} and C$^{10}{}_{1/2/3/4}$), 148.6 (C$^5{}_1$), 150.7, 151.4 (C^{1,4,6,9}), 167.4 (C$^5{}_5$) ppm.

^{19}F-NMR (d$_8$-THF): δ = −167.2 (ddd, $^3J_{FF}$ = 24 Hz, $^3J_{FF}$ = 21 Hz, $^5J_{FF}$ = 8 Hz, 4 F , F$^{10/20}{}_{3/3}$), −158.5 (t, $^3J_{FF}$ = 21 Hz, 2 F, F$^{10/20}{}_{4/4}$), −141.5 (dd, $^3J_{FF}$ = 24 Hz, $^5J_{FF}$ = 8 Hz, 4 F, F$^{10/20}{}_{2/2}$) ppm.

IR (KBr): $\tilde{\nu}$ [cm^{-1}] = 2923 (w, CH), 2852 (w, CH) 1724 (s, CO^{ester}), 1607 (w), 1518 (s), 1489 (vs), 1279 (vs, C-O-C), 1114 (m, C-F), 991 (s).

UV/Vis (CH$_2$Cl$_2$): λ [nm] (ε / [10^4 M^{-1}cm^{-1}]) = 421 (50.39), 551 (2.07), 591 (0.35).

Fluorescence (CH$_2$Cl$_2$): λ [nm] (relative intensity) = 599 (1.00), 650 (1.16).

Quantum yield: Φ = 0.0788.

Lifetime [ns]: τ = 1.95 (100%).

MS (FD): *m/z* (%) = 974.55 (100) [M]$^+$.

MS (ESI): *m/z* (%) = 972.10 (90) [M]$^+$.

HR-MS (ESI): obs. *m/z* (%) = 972.0780; calcd. for [M]$^+$ 972.0773.

CV (Fc/Fc$^+$, 100 mV s^{-1}, CH$_2$Cl$_2$): $E_{½}$ [V] = –2.000, –1.580, 0.920, 0.680.

Figure S1. Absorption spectra of **1e** and **3e** in 2-methyltetrahydrofuran at $T = 300 - 77$ K.

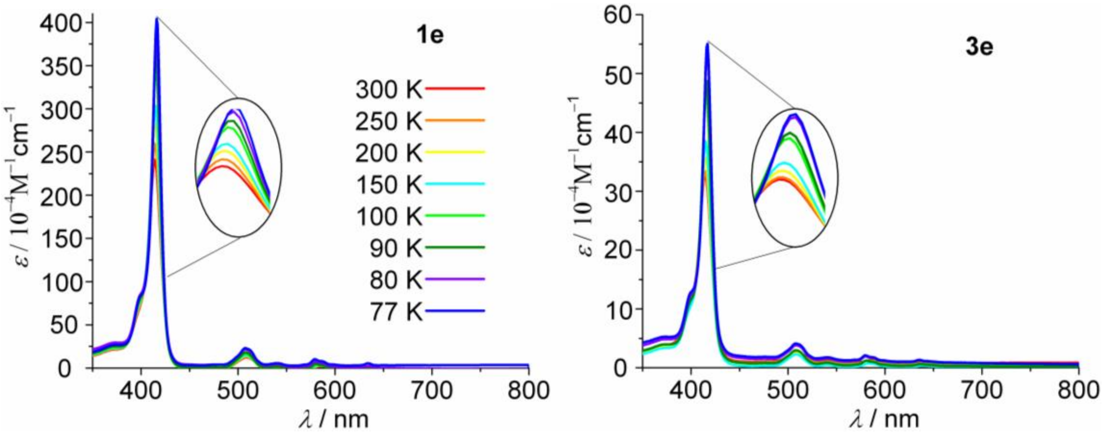

Figure S2. B3LYP/LANL2DZ, IEFPCM calculated frontier orbitals of a) **Zn-3a** and b) **Zn-3e** (isosurface value 0.05 a.u.).

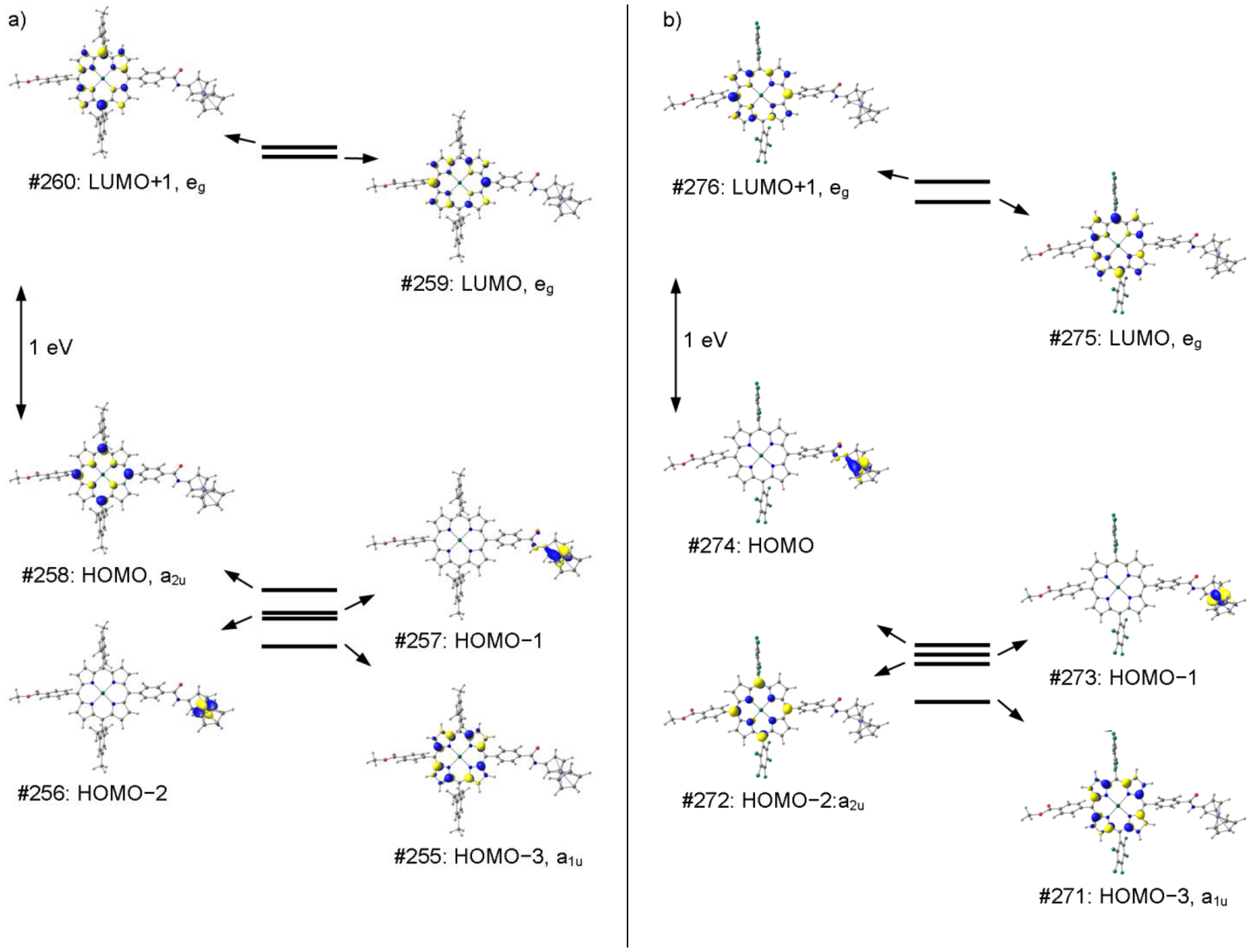

Figure S3. B3LYP/LANL2DZ, IEFPCM calculated frontier orbitals of a) **5d** and b) **5e** (isosurface value 0.05 a.u.).

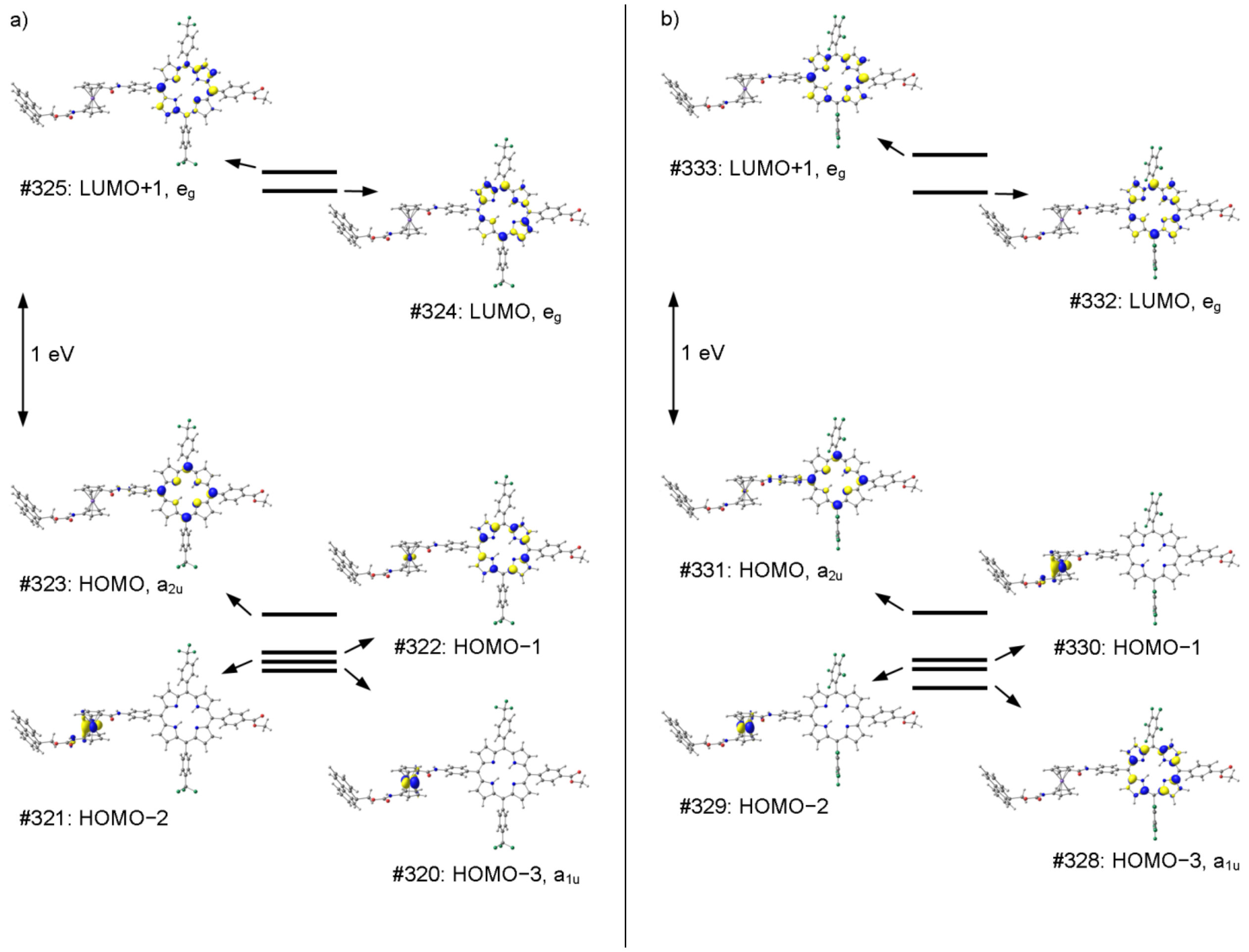

Figure S4. B3LYP/LANL2DZ, IEFPCM calculated frontier orbitals of **6c** (isosurface value 0.05 a.u.).

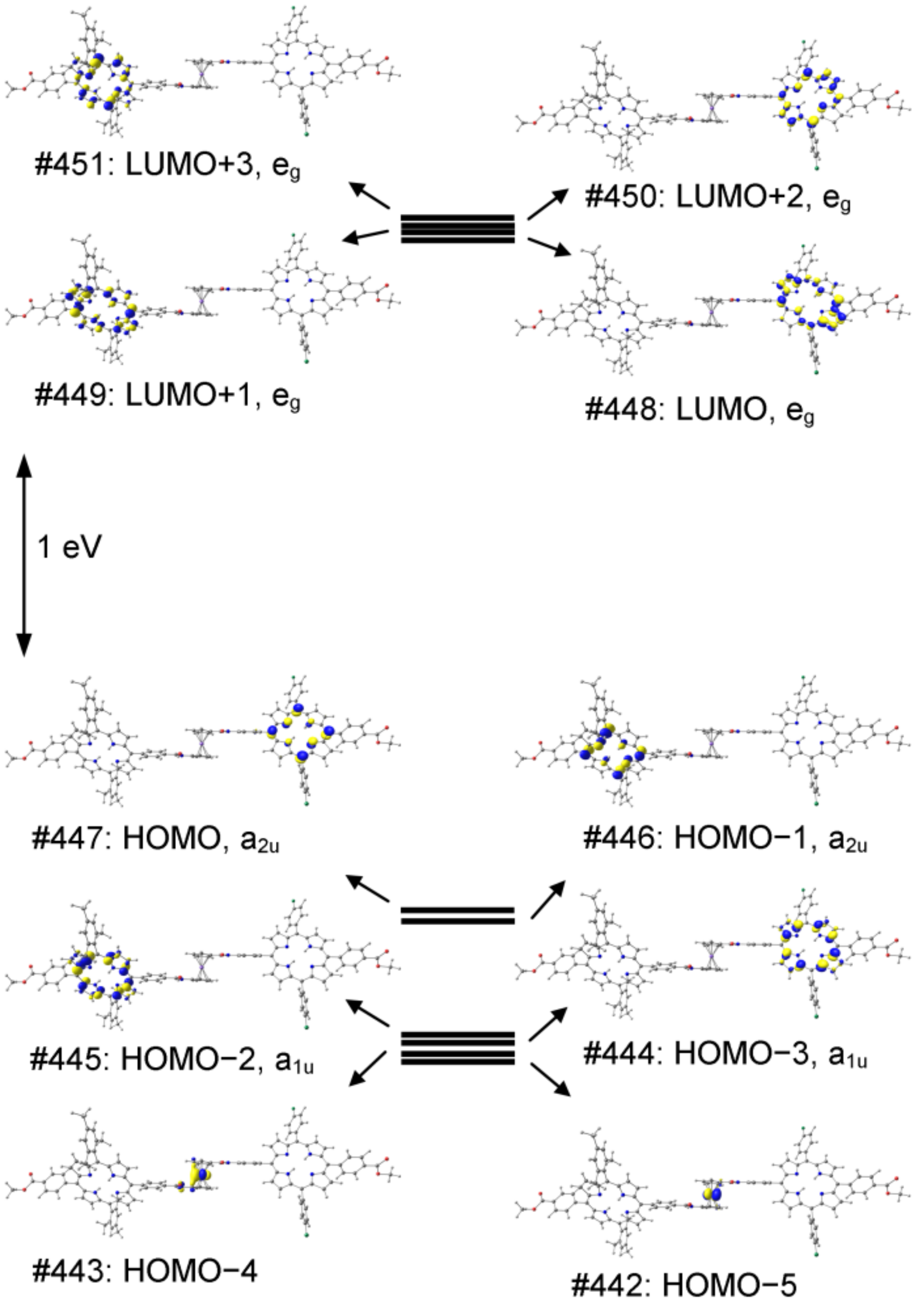

Figure S5. B3LYP/LANL2DZ, IEFPCM calculated frontier orbitals of **Zn-6b** (isosurface value 0.05 a.u.).

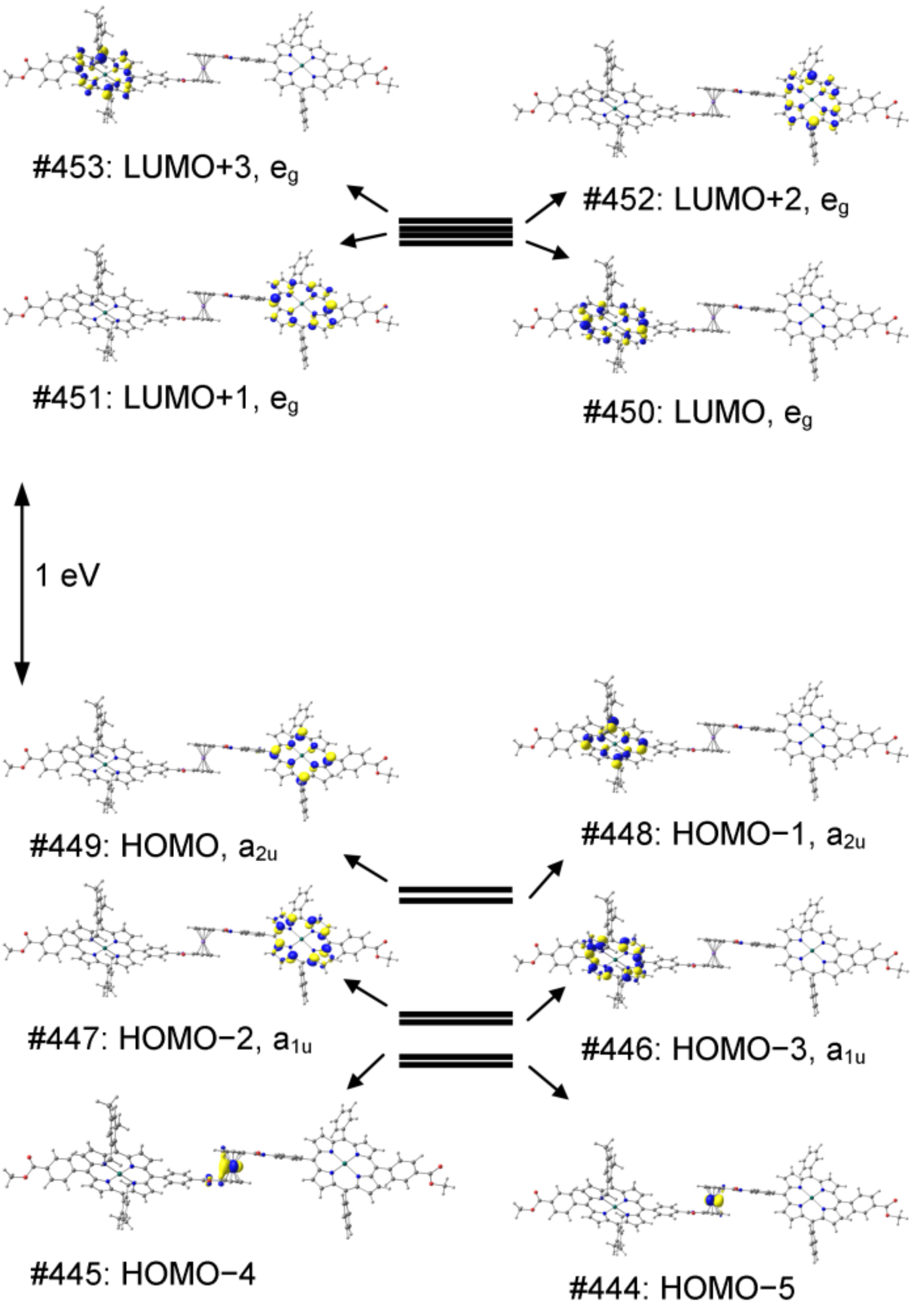

Figure S6. B3LYP/LANL2DZ, IEFPCM calculated frontier orbitals of **Zn-6c** (isosurface value 0.05 a.u.).

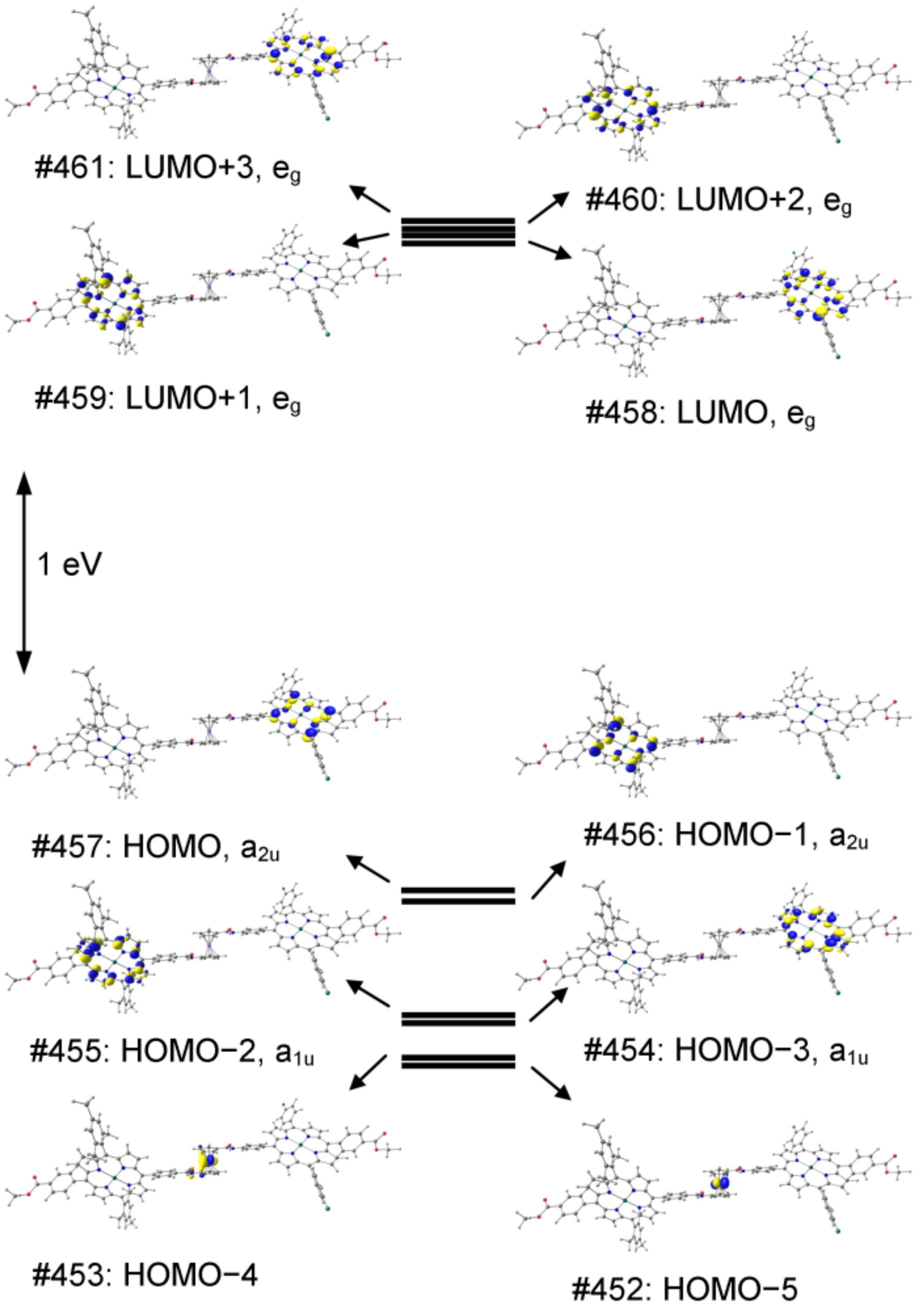

Figure S7. B3LYP/LANL2DZ, IEFPCM calculated molecular orbital energy diagram of **3a** and **3e**. The LUMOs of ferrocene are outside the window shown.

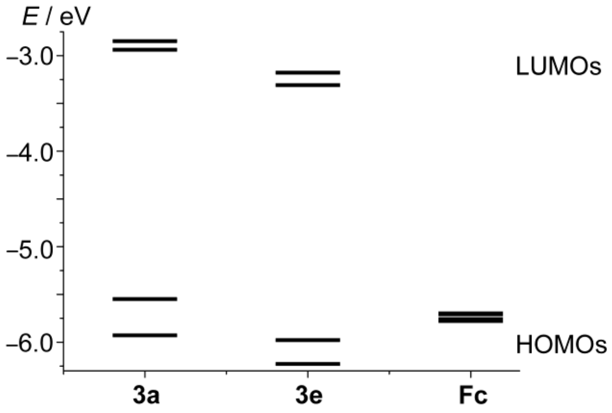

Figure S8. B3LYP/LANL2DZ, IEFPCM calculated molecular orbital energy diagram of **Zn-3a** and **Zn-3e**. The LUMOs of ferrocene are outside the window shown.

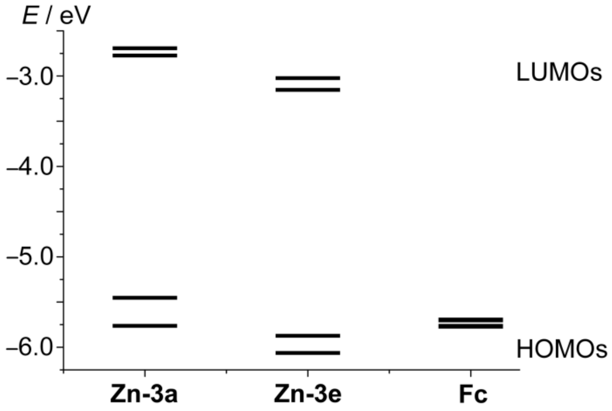

Figure S9. B3LYP/LANL2DZ, IEFPCM calculated molecular orbital energy diagram of **6b** (extended and V-shape conformations). The LUMOs of ferrocene are outside the window shown.

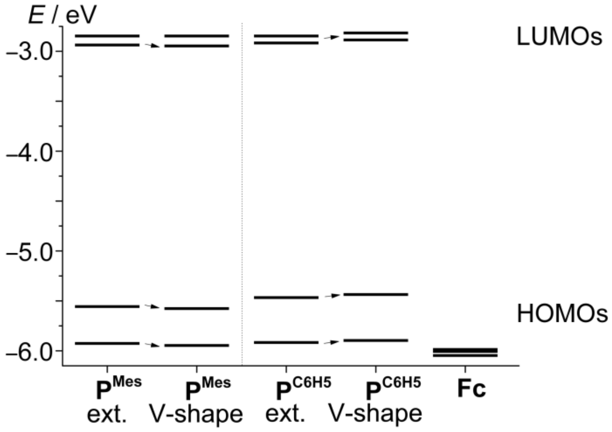

Figure S10. B3LYP/LANL2DZ, IEFPCM calculated molecular orbital energy diagram of **6c** (extended and V-shape conformations). The LUMOs of ferrocene are outside the window shown.

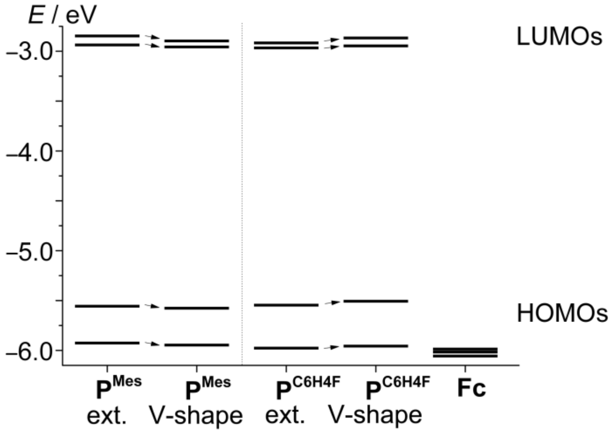

Figure S11. B3LYP/LANL2DZ, IEFPCM calculated molecular orbital energy diagram of **Zn-6b** (extended and V-shape conformations). The LUMOs of ferrocene are outside the window shown.

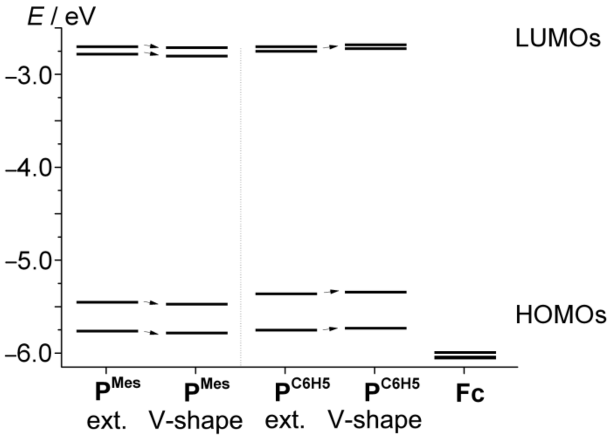

Figure S12. B3LYP/LANL2DZ, IEFPCM calculated molecular orbital energy diagram of **Zn-6c** (extended and V-shape conformations). The LUMOs of ferrocene are outside the window shown.

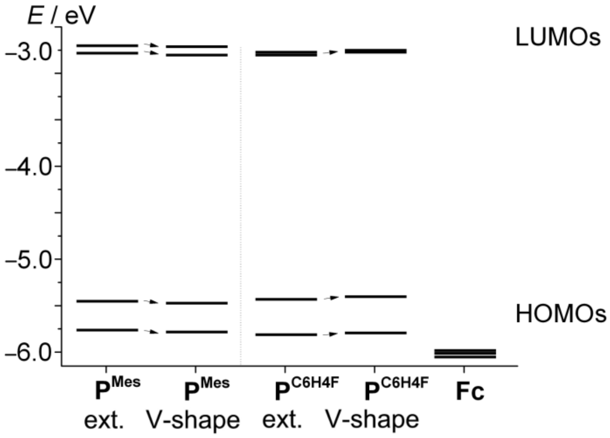

Figure S13. B3LYP/LANL2DZ, IEFPCM calculated spin density of the lowest triplet state of **3e** (isosurface value 0.01 a.u.).

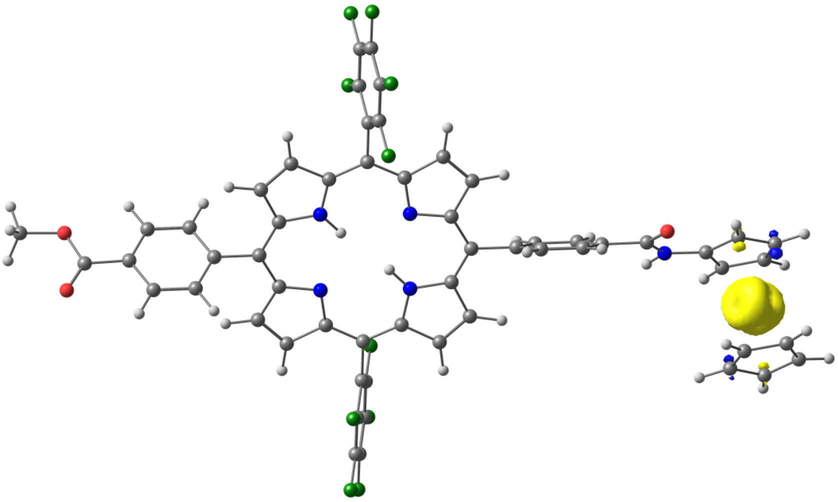

Figure S14. B3LYP/LANL2DZ, IEFPCM calculated spin density of the lowest triplet state of **5e** (isosurface value 0.01 a.u.).

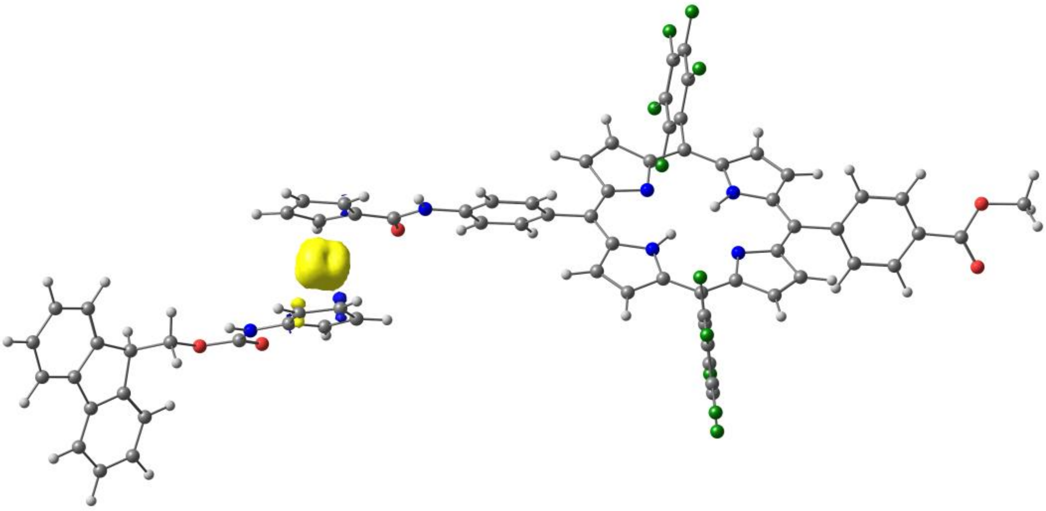

8 List of Publications

In the following the publications that contribute to this PhD work are given:

6.1. J. Melomedov, A. Wünsche von Leupoldt, M. Meister, F. Laquai, K. Heinze, *Dalton. Trans.* **2013**, *42*, 9727-9739. Porphyrin Amino Acids – Amide Coupling, Redox and Photophysical Properties of Bis(porphyrin) amides
[DOI: 10.1039/c3dt50711d]

6.2. J. Melomedov, J. R. Ochsmann, M. Meister, F. Laquai, K. Heinze, *Eur. J. Inorg. Chem.* **2014**, 1984-2001. Tuning Reductive and Oxidative Photoinduced Electron Transfer in Amide Linked Anthraquinone-Porphyrin-Ferrocene Architectures
[DOI: 10.1002/ejic.201400118]

6.3. J. Melomedov, J. R. Ochsmann, M. Meister, F. Laquai, K. Heinze, *Eur. J. Inorg. Chem.* **2014**, accepted. Aminoferrocene and Ferrocene Amino Acid as Electron Donors in Modular Porphyrin-Ferrocene and Porphyrin-Ferrocene-Porphyrin Conjugates
DOI: 10.1002/ejic.201402138

6.4. V. Gierz, J. Melomedov, C. Förster, C. Deißler, F. Rominger, D. Kunz, K. Heinze, *Chem. Eur. J.* **2012**, *18*, 10677-10688. Consequences of the one-electron reduction and photoexcitation of unsymmetric bisimidazolium salts
[DOI: 10.1002/chem.201200323]

Contributed Oral and Poster Presentations

Oral Presentation

„Lichtsammlung und Ladungstrennung mit neuartigen (Metallo)-Porphyrinen“
8. Koordinationschemie-Treffen at the TU Dortmund University
26.02.2012

Poster Presentations

„Neue Porphyrin-Aminosäuren mit einstellbaren elektronischen Eigenschaften zur Unter-suchung photoinduzierter Elektronentransfer- und Energietransfer-Prozesse“
6. Koordinationschemie-Treffen at the Johannes Gutenberg University Mainz
23.02.2010

“Artificial Photosynthetic Reaction Centers with Ferrocene as Primary Electron Donor”
10th Ferrocene Colloquiumat the Chemnitz University of Technology
14.02.2011

“Sequential photoinduced electron transfer: reductive versus oxidative initial electron transfer”
9. Koordinationschemie-Treffen at the Bayreuth University
24.02.2013

9 Acknowledgments

The presented research work for this thesis was carried out at the Department of Inorganic and Analytical Chemistry at the Johannes Gutenberg University Mainz during the years 2009 – 2014.

First of all, I want to express my gratitude to [redacted] for giving me the opportunity to work in the field of bioinorganic chemistry and introducing me to very interesting interdisciplinary research topics. I am certainly grateful for her reviews, suggestions and improving the manuscript of this thesis and publications and for giving me the chance to present my work results at various conferences.

I thank [redacted], [redacted], [redacted] and [redacted] (MPI-P, Mainz) for the fruitful collaboration.

I warmly thank the scientific staff members of the analytic department: [redacted] and [redacted] for support of NMR measurements; [redacted], [redacted] and [redacted] for mass spectrometry measurements; [redacted] for IR measurements.

I like to thank all of my present and former colleagues of the AK [redacted]: [redacted], [redacted], [redacted], [redacted], [redacted], [redacted], [redacted], [redacted], [redacted], [redacted], [redacted], [redacted], [redacted], [redacted], [redacted] and [redacted] for the great time and extraordinary atmosphere during my PhD work. I particularly thank [redacted] for reading the Introduction of my thesis and suggesting corrections.

I thank my students [redacted], [redacted], [redacted], [redacted], [redacted] and [redacted] for preparative assistance.

[redacted], [redacted], [redacted] and [redacted] I want to express my special thanks for reading parts of this work and the common sportive experience.

I warmly thank our secretaries [redacted] and [redacted] for their kindness and dealing with many important things.

I thank **Deutsche Forschung Gemeinschaft** (**DFG)** for financial support (He 2778 / 6-1).

I am deeply grateful for my family, especially [redacted] [redacted] [redacted] and [redacted] for their immense care and unlimited support.

Lebenslauf

The CV is only contained in the printed original.